Stratégies d'acquisition des ressources en proies et coût du transport chez l'éléphant de mer austral

Joffrey Jouma'A

UNIVERSITÉ DE LA ROCHELLE

ÉCOLE DOCTORALE GAY LUSSAC

LABORATOIRE : Centre d'Études Biologiques de Chizé

THÈSE présentée par :

Joffrey JOUMA'A

soutenue le : **29 novembre 2016**
pour obtenir le grade de : **Docteur de l'université de La Rochelle**
Discipline : **Biologie de l'Environnement, des Populations, Écologie**

Stratégies d'acquisition des ressources en proies et coût du transport chez l'éléphant de mer austral

---

JURY :

Andrew TRITES	Professeur, University of British Columbia, Rapporteur
Jean-Benoît CHARRASSIN	Professeur, Muséum National d'Histoire Naturelle, Rapporteur
Cécile VINCENT	Maître de conférences, Université de La Rochelle, Examinateur
Christophe THÉBAUD	Professeur, Université Paul Sabatier - Toulouse III, Examinateur
Odile GÉRARD	Ingénieur Ph.D, DGA Techniques Navales, Examinateur
Christophe GUINET	Directeur de recherche, Université de La Rochelle, Directeur de thèse
Patrick MILLER	Senior lecturer, St Andrews University, Co-directeur de thèse

Table des matières

Remerciements

- Je tiens tout d'abord à remercier mon directeur de thèse, Christophe Guinet, qui il y a 5 ans m'a donné l'opportunité de découvrir le *monde Chizéen*, au moment où j'en avais sûrement le plus besoin. Merci de m'avoir fait confiance tout au long de ces années et d'avoir été présent lorsque j'en avais besoin, malgré ton emploi du temps... chargé ! Merci enfin de m'avoir donné l'opportunité de découvrir les Terres Australes, l'une des expériences les plus dingues de ma thèse !

- Merci à Patrick Miller, mon co-directeur de thèse, pour m'avoir accueilli au Sea Mammal Research Unit lors de mes deux séjours en Écosse. Tes conseils et commentaires avisés ont grandement contribué à l'écriture de ce manuscrit.

- Je remercie tout particulièrement la Direction Générale de l'Armement en la personne de Carole Nahum, d'avoir financé cette thèse. Justifier d'un tel financement n'a pas toujours été facile, mais cela témoigne d'une ouverture d'esprit qui laisse présager de belles collaborations. Merci également à Duncan Williams pour sa disponibilité.

- Merci à Xavier Bonnet et Henri Weimerskirch de m'avoir permis de réaliser ce travail de thèse au sein du CEBC et de l'équipe Prédateurs Marins.

- Merci également à Andrew Trites, Jean-Benoît Charrassin, Cécile Vincent, Christophe Thébaud et Odile Gérard d'avoir accepté de faire partie de mon jury.

- Je remercie également Julien Bonnel, Dorian Cazau, Yves Le Bras, Baptiste Picard, Florian Orgeret, Gaëtan Richard, Alexandre Génin, Nathan Pacoureau, Rémi Fay et Philippine Chambault pour vos échanges, conseils et collaborations durant ces trois années. Je remercie aussi tous les stagiaires de l'équipe éléphants de mer qui ont contribué de près ou de loin à ce travail : Charles Rhodes, Louise Day, Julie Mestre et Adèle Rémazeilles.

- Merci à Sara Labrousse pour sa bonne humeur et ses moments de folies qui ont ponctué notre séjour à Ker. Merci également à Florian Orgeret et Elie Gaget de nous avoir supportés durant tout ce temps. Une grosse pensée à Antoine Protin qui a payé de sa personne pour nous aider à récupérer nos balises.

- Je tiens à remercier comme il se doit Marine Desprez, Adéle Rémazeilles et bien évidemment Philippine Chambault pour leurs relectures, leurs remarques et leurs commentaires sur ce manuscrit.

- Merci également à toutes les personnes qui font, ou qui ont fait de Chizé, un endroit dont je me souviendrai longtemps : Andéaz Dupoué, Pierre Blévin, Gaëtan Richard,

Laurie Thiers, Baptiste Picard, Yves Le Bras, Sophie de Grissac, Aurélien Prudor, Anaïs Janc, Gaëtane Le Provost, Nathan Pacoureau, Meumeu, Gaspard Bernard, Cécile Bon, Alizée Meillere, Julien Collet ou encore Alice Carravieri.

- Avant de terminer par les habituels remerciements pour la famille, je tiens à particulièrement remercier mes collègues de bureau Nathan Pacoureau, Yves Le Bras et Baptiste Picard, sans qui l'atmosphère dans le bureau n'aurait pas été aussi *phosphorante*. Merci à vous pour ces grosses marades qui ont marqué ces trois années, et qui ont parfois pris le pas sur le travail.

- Je souhaite donc enfin terminer par remercier ma famille et plus particulièrement mes parents et Philippine pour m'avoir toujours soutenu et encouragé jusqu'à la fin.

Avant-Propos

Démarrée en Octobre 2013, cette thèse s'inscrit dans la continuité des travaux de thèses de Frédéric Bailleul (2006), Matthieu Authier (2011), Anne-Cécile Dragon (2011) et plus récemment de Jade Vacquié-Garcia (2014), réalisés sous la direction de Christophe Guinet, sur l'écologie de l'éléphant de mer austral, au laboratoire de Chizé (CEBC-CNRS UMR 7372, Université de La Rochelle). Elle fait suite à l'ANR TOPP-PATCHES[1] achevée en 2013, qui visait à évaluer la distribution des poissons mésopélagiques par la modélisation des zones d'alimentation des éléphants de mer, ainsi qu'à l'ANR IPSOS-SEAL[2], qui visait à étudier les variations du comportement d'alimentation des éléphants de mer en lien avec les variations environnementales. L'obtention d'un financement de la Direction Générale de l'Armement dans le carde d'une collaboration franco-britannique pour étudier les stratégies de chasse de l'éléphant de mer a permis la mise en place de collaborations (ENSTA Bretagne, SMRU St Andrews) qui ont abouti au document présenté ici.

Le dynamisme de l'équipe dont j'ai pu faire partie durant ces trois années, m'a permis d'être impliqué dans de nombreuses études abordées dans la thèse et présentées en annexes. Je vais ici détailler ma contribution personnelle à chacune d'entre elles, par ordre chronologique :

- Annexe A : *Variation in body condition during the post-moult foraging trip of southern elephant seals and its consequences on diving behaviour.*
  J'ai dans cette étude participé au développement de la méthode caractérisant l'effort de nage. J'ai également été impliqué dans les analyses statistiques lors du processus de révision du papier.

- Annexe B : *Characterization of postdive recovery using sound recordings and its relationship to dive duration, exertion and foraging effort of southern elephant seals (Mirounga leonina).*
  Pour cette étude, j'ai également été impliqué dans le calcul de l'effort de nage ainsi que sur le traitement des données d'accélération.

- Annexe C : *Measuring the marine soundscape of the Indian Ocean with Southern Elephant Seals used as acoustic gliders of opportunity.*
  Pour cette collaboration avec l'ENSTA Bretagne, j'ai participé aux pré-traitements des données issues des Acousondes™.

- Annexe D : *How elephant seals (Mirounga leonina) adjust their fine scale horizontal movement and diving behaviour in relation to local prey encounter rate.*

[1] TOPP-PATCHES pour Temperature, dissolved Oxygen and Predator-Prey interactions - Prey distribution Assessment Through Characterization of feeding Habitats of Elephant Seals

[2] IPSOS-SEAL pour Investigation of the vulnerability of the biological Productivity of the Southern Ocean Subsystems to climate change : the Southern Elephant seal Assessment from mid to high Latitudes

Pour ce travail, j'ai collaboré avec mon collègue Yves Le Bras sur la structure de l'étude.

- Annexe E : *Acoustic measurements of post-dive cardiac responses in southern elephant seals (Mirounga leonina) during surfacing at sea.*
  Ici, j'ai contribué à l'orientation de l'étude de Louise Day, de passage à Chizé dans le cadre d'un stage de césure. J'ai contribué à la conception, aux analyses, ainsi qu'au travail de relecture du papier.

- Annexe F : *Usage of the three-dimensional space at the bottom of the southern elephant seals' dives.*
  Pour cette dernière étude, j'ai participé au travail de relecture, ainsi qu'aux techniques de reconstruction 3D employées.

Concernant ma contribution aux trois chapitres qui constituent le corps de cette thèse, ma contribution personnelle a été la suivante :

- Chapitre 3 : *Three-dimensional assessment of hunting strategies in a deep diving predator.*
  Ici, j'ai participé aux traitements des données d'accélération, de magnétométrie et de plongée. J'ai ensuite réalisé l'ensemble des analyses statistiques et rédigé la totalité de l'article.

- Chapitre 4 : *Adjustment of diving behaviour with prey encounters and body condition in a deep diving predator: the Southern Elephant Seal.*
  Dans cette étude, j'ai contribué aux traitements des données d'accélération et réalisé l'ensemble des analyses statistiques. J'ai également rédigé la totalité de l'article.

- Chapitre 5 : *Spatio-Temporal Variations in Field Metabolic Rate of Post-Moulting Southern Elephant Seals.*
  Dans cette dernière partie, j'ai modestement participé à la récolte des données sur le terrain en 2014. J'ai ensuite contribué aux traitement des données d'accélération et réalisé l'ensemble des analyses statistiques. J'ai enfin rédigé la totalité de l'article.

Publications

Partie	Titre	Statut
Chapitre 4	**Jouma'a, Joffrey**, Yves, Le Bras, Richard, Gaëtan, Vacquié-Garcia, Jade, El Ksabi, Nory, Picard, Baptiste & Guinet Christophe. (2016) Adjustment of diving behaviour with prey encounters and body condition in a deep diving predator: the Southern Elephant Seal. *Functional Ecology*, **30**(4), 636-648	Publié
Chapitre 3	**Jouma'a, Joffrey**, Yves, Le Bras, Picard, Baptiste & Guinet, Christophe, Three-dimensional assessment of hunting strategies in a deep diving predator. *Marine Ecology Progress Series*	Sous presse
Chapitre 5	**Jouma'a, Joffrey**, Yves, Le Bras, Picard, Baptiste & Guinet, Christophe. Spatio-Temporal Variations in Field Metabolic Rate of Post-Moulting Southern Elephant Seals	En préparation
Annexe A	Richard, Gaëtan, Vacquié-Garcia, Jade, **Jouma'a, Joffrey**, Picard, Baptiste, Génin, Alexandre, Arnould, John, Bailleul, Frédéric & Guinet, Christophe, (2014) Variation in body condition during the post-moult foraging trip of southern elephant seals and its consequences on diving behaviour. *Journal of Experimental Biology*, **217**, 2609-2619	Publié
Annexe B	Génin, Alexandre, Richard, Gaëtan, **Jouma'a, Joffrey**, Picard, Baptiste, El Ksabi, Nory, Vacquié-Garcia, Jade & Guinet Christophe, (2015) Characterization of postdive recovery using sound recordings and its relationship to dive duration, exertion and foraging effort of southern elephant seals (*Mirounga leonina*). *Marine Mammal Science*, 1748-7692	Publié
Annexe C	Cazau, Dorian, Bonnel, Julien, **Joffrey, Jouma'a**, Yves, Le Bras & Guinet Christophe, (2016) Measuring the marine soundscape of the Indian Ocean with Southern Elephant Seals used as acoustic gliders of opportunity. *Journal of Atmospheric and Oceanic Technology*, **34**, 207-223	Publié
Annexe D	Yves, Le Bras, **Jouma'a, Joffrey**, Picard, Baptiste & Guinet Christophe, (2016) How elephant seals (*Mirounga leonina*) adjust their fine scale horizontal movement and diving behaviour in relation to local prey encounter rate. *PLoS One*, **11**(12)	Publié

Annexe E	Day, Louise, **Jouma'a, Joffrey**, Bonnel, Julien & Guinet Christophe, (2017) Acoustic measurements of post-dive cardiac responses in southern elephant seals (*Mirounga leonina*) during surfacing at sea. *Journal of Experimental Biology*, **220**(9), 1626-1633	Publié
Annexe F	Yves, Le Bras, **Jouma'a, Joffrey**, & Guinet Christophe, Usage of the three-dimensional space at the bottom of the southern elephant seals' dives. *Movement Ecology*	En révision

Conférences, Workshops & Formations

Conférences & Workshop

Les conférences auxquelles j'ai donné un oral sont en gras :

- "Adjustment of diving behaviour with prey encounters and body condition in a deep diving predator: the Southern Elephant Seal" Bio-Logging Symposium 5 – Septembre 2014
- "Adjustment of diving behaviour with prey encounters and body condition in a deep diving predator: the Southern Elephant Seal" Ecology and Behaviour 2015 – Starsbourg en mai 2015
- **"Austral elephant seal: optimization of transport cost, for a stealth deep diving predator" Université de La Rochelle en mai 2015**
- **"Adjustment of diving behaviour with prey encounters and body condition in a deep diving predator: the Southern Elephant Seal" 21st Biennial Conference on the Biology of Marine Mammals – San Francisco en septembre 2015**
- "Wikipedia as a tool for teaching, outreach and open access science" San Francisco en septembre 2015
- **"Insight of the hunting behaviours of females Southern Elephant Seals" Seminar lunch, Sea Mammal Research Unit – St Andrews University en mars 2016**
- **"Comportement de chasse à fine échelle et bioénergétique de l'éléphant de mer austral", 5ème Journéées Éléphants de Mer Chizé en avril 2016**
- **"Insight of the hunting behaviours of females Southern Elephant Seals" International Society on Biotelemetry 2016 – Leuven en mai 2016**

Formations

- "Introduction au traitement du signal", à l'ENSTA Bretagne en mai 2014
- "Initiation aux Systèmes d'Information Géographique", au CEBC en juin 2015

CHAPITRE 1

Introduction Générale

Sommaire

1.1 De l'Écosystème Marin aux Stratégies d'Approvisionnements

1.1.1 Liens entre Variabilité Environnementale et Disponibilité des Ressources

Malgré les polémiques, le changement climatique, et plus particulièrement le réchauffement des océans, est aujourd'hui accepté par la très grande majorité de la communauté scientifique (Melillo *et al.*, 1993; Rosenzweig & Parry, 1994; Levitus *et al.*, 2005; Moss *et al.*, 2010). Selon le dernier rapport de synthèse du groupe d'experts intergouvernemental sur l'évolution du climat (GIEC, 2014), les écosystèmes polaires, au même titre que les écosystèmes des récifs coralliens, sont considérés comme extrêmement vulnérables face à l'évolution actuelle du climat. L'une des conséquences de l'accroissement du dioxyde de carbone d'origine anthropique relargué dans l'atmosphère est l'acidification croissante des océans. Ce mécanisme qui impacte toute la chaîne trophique de l'écosystème marin (Fabry *et al.*, 2008), interagit également avec le réchauffement des masses d'eaux (Kroeker *et al.*, 2013), la baisse progressive des concentrations en dioxygène dissous (Hofmann & Schellnhuber, 2009; Melzner *et al.*, 2012) ou plus localement, avec le phénomène d'eutrophisation (Cai *et al.*, 2011; Wallace *et al.*, 2014). Déterminer et comprendre les liens entre la réponse comportementale d'une espèce à l'impact de ces variations environnementales, et notamment climatiques, est une problématique majeure en écologie, puisqu'elle permet *in fine* de mieux prévoir l'évolution d'un écosystème (Walther *et al.*, 2002; Weimerskirch *et al.*, 2003; Ozgul *et al.*, 2010; Bost *et al.*, 2015).

Dans ce contexte, l'océan Austral joue un rôle particulier à l'échelle de l'océan mondial, puisque situé à la confluence de tous les autres océans, il est la principale zone de formation d'eaux denses qui alimentent la circulation globale de l'océan (Talley *et al.*, 2011). La complexité des interactions physiques du système océan-atmosphère mises en jeu dans cette zone a des conséquences importantes sur les processus océanographiques de l'océan mondial et sur le climat. Prédire quelles seront les conséquences de ces variations sur les processus biologiques n'est pas simple (Mayewski *et al.*, 2009). Les sorties des modèles climatiques prévoient une forte hétérogénéité spatio-temporelle car les différents forçages n'agissent pas de la même façon selon les saisons et les régions concernées. Le cas du phénomène *El Niño Southern Oscillation* (ENSO) mesuré à l'aide du *Southern Oscillation Index* (SOI) en est le parfait exemple. Lors d'une année à SOI négatif, ENSO est responsable de fortes anomalies de pression atmosphérique au-dessus de la mer d'Amundsen et de Bellingshsen (Jacobs & Comiso, 1997). Cela a pour effet de réduire l'étendue de glace de mer dans ces régions, et de l'augmenter en mer de Weddell. Lors des années

à SOI négatif, la relation inverse est observée. L'ensemble des études qui tentent de comprendre les relations entre les processus physico-chimiques et biologiques s'accorde sur le rôle prépondérant de la glace de mer dans l'écosystème austral, puisqu'un changement de sa dynamique semble avoir des conséquences sur l'ensemble de l'écosystème austral (Atkinson *et al.*, 2004; Clarke *et al.*, 2007; Labrousse *et al.*, 2015).

L'augmentation des températures consécutives à l'émission de gaz à effet de serre pourrait conduire à une diminution significative de l'étendue de glace de mer au cours du XXI^{ème}, ainsi qu'à une augmentation de son amplitude saisonnière (Arzel *et al.*, 2006). Bien qu'encore débattue par les climatologues, cette augmentation de la température devrait également jouer sur la circulation thermohaline (Gregory *et al.*, 2005; Toggweiler & Russell, 2008), ainsi que sur l'intensité et la trajectoire du courant circumpolaire antarctique (Fyfe *et al.*, 2007). La fréquence des phénomènes à SOI négatif[1] devrait augmenter (Timmermann *et al.*, 1999) et d'autres variations climatiques comme l'oscillation antarctique, mesurée à l'aide du SAM (*Southern Annular Mode*), devraient également voir leur amplitude et leur fréquence modifier (Thompson & Solomon, 2002; Miller *et al.*, 2006).

Selon les niveaux trophiques, la réponse à ces fluctuations environnementales n'est pas la même (Inchausti *et al.*, 2003). Pour la production primaire, un réchauffement des températures induit un changement des paramètres physiques qui peuvent *in fine* altérer les niveaux de production. La fonte des glaces va par exemple favoriser l'apparition d'une couche de plus faible densité en surface, à cause de son apport en eaux douces, ce qui va augmenter la stratification et réduire l'épaisseur de la couche de mélange aboutissant à une diminution de la production primaire (Behrenfeld *et al.*, 2006). Pour les échelons trophiques intermédiaires, peu d'information sont disponibles dans l'océan Austral du fait des difficultés d'échantillonnage. Atkinson *et al.* (2004) a toutefois montré que la réduction du stock de krill observée dans les années 1970 en mer de Scotia pouvait être reliée au réchauffement des masses d'eaux ainsi qu'à des modifications de la dynamique de glace de mer. L'impact de ces variations environnementales sur les échelons trophiques supérieurs est mieux documenté grâce aux suivis à long terme de nombreuses espèces de prédateurs marins dans l'océan Austral. Il a par exemple été montré que certaines populations d'oiseaux marins ont vu leur abondance diminuée dans les années 1970 suite à l'augmentation des températures (Weimerskirch *et al.*, 2003). Reid & Croxall (2001) ont ainsi montré que de nombreuses populations d'oiseaux et de mammifères marins se nourrissant de krill ont vu leur population déclinée. Cet exemple illustre comment des changements dans l'abondance, mais aussi l'accessibilité des ressources en proies, dus aux fluctuations climatiques, peuvent affecter la trajectoire démographique d'une espèce. Ces changements dans la disponibilité des ressources alimentaires vont conditionner les

[1] Également connus sous le nom d'*El Niño*

adaptations comportementales des prédateurs plongeurs en terme de distribution en mer, d'effort de pêche et de comportement de plongée. L'étude des comportements de recherche alimentaire de ces prédateurs et de leurs variations au cours du temps, sont susceptibles de nous renseigner sur les changements affectant leur milieu de pêche. Cela permet alors d'utiliser les prédateurs plongeurs comme des indicateurs des changements affectant leur environnement physique et d'évaluer leurs conséquences écologiques.

1.1.2 Quels sont les Apports d'une Étude Comportementale ?

Comprendre quelles sont les adaptations mises en jeu par les prédateurs marins pour faire face à ces changements dans l'abondance et la distribution des ressources en proies nous aide à mieux prévoir et anticiper l'impact potentiel du changement climatique à l'échelle de l'écosystème marin. *In fine*, il s'agit de mieux prévoir l'évolution de ces adaptations, qu'elles soient physiologiques, morphologiques ou bien comportementales, avec les variations du milieu. Dans le cas d'une étude comportementale, ces stratégies correspondent à un ensemble de décisions par lesquelles l'individu cherche à répondre à un besoin, ou réagir à une situation. L'intérêt d'une étude comportementale est donc multiple puisque :

- Ces études permettent dans un premier temps de mieux comprendre les mécanismes globaux et proximaux qui existent entre l'environnement et les populations d'organisme. L'étude des stratégies d'approvisionnement fait partie intégrante de ces études comportementales. Elles visent notamment à mieux comprendre les relations entre la distribution, la qualité et l'abondance des ressources, avec la trajectoire démographique des populations.

- De telles études peuvent également permettre de mettre en évidence des variations environnementales encore inconnues. Il s'agit ici d'utiliser les changements comportementaux comme un indicateur des tendances environnementales, on parle alors d'éco-indicateur ou d'espèce sentinelle. L'exemple le plus connu est certainement celui des abeilles, couramment utilisées pour surveiller le niveau de pollution et la qualité de l'environnement globale (Tong *et al.*, 1975; Conti & Botrè, 2001; Ponikvar *et al.*, 2005). Mais l'étude comportementale de prédateurs supérieurs apporte une vision plus globale des conséquences écologiques de ces variations environnementales, puisque des changements dans les processus populationnels d'un prédateur supérieur reflètent les influences directes et indirectes de l'interaction entre les processus biologiques et physiques d'un écosystème (Furness & Greenwood, 1993; Croxall *et al.*, 2002).

- Enfin, compte tenu de la compréhension des stratégies mises en jeu, l'étude comportementale d'une espèce doit pouvoir permettre la prévision des comportements et

des adaptations futurs, face aux fluctuations climatiques. Il s'agit ici de mesurer la plasticité comportementale d'une espèce afin d'anticiper son pouvoir d'adaptation aux changements de l'environnement (Morris *et al.*, 2009).

1.1.3 Rôle de l'Écologie Alimentaire

L'étude de l'écologie alimentaire est l'un des moyens permettant de mieux comprendre les adaptations comportementales aux contraintes environnementales. En effet, dans un environnement où les ressources sont limitées, la sélection naturelle doit tendre à favoriser les individus adoptant la stratégie d'acquisition des ressources la plus efficace (Charnov, 1976). L'activité d'alimentation d'un individu consiste donc à mettre en place des stratégies d'approvisionnement en se focalisant sur la répartition spatio-temporelle de la recherche alimentaire ou sur le choix de la proie à capturer (Stephens & Krebs, 1986). En ajustant leur comportement d'alimentation en fonction de la présence de prédateurs ou de compétiteurs, du choix et de la quantité de proies ingérées ou bien de l'effort de prospection, les individus maximisent leurs chances de survie et de reproduction. L'écologie alimentaire vise donc à étudier et comprendre ces adaptations comportementales qui tendent à maximiser le gain net d'énergie dans un environnement où l'abondance et la distribution des ressources peuvent être affectées par les variations climatiques.

1.2 Théorie de l'Approvisionnement Optimal

1.2.1 Modèle Général

En écologie alimentaire, l'ensemble des choix qu'un individu devrait faire pour maximiser sa fitness est développé par plusieurs modèles formant ce que l'on appelle *la théorie de l'approvisionnement optimal*. Pour un individu évoluant dans un environnement où la ressource est limitée, cette théorie décrit l'ensemble des choix attendus afin de s'assurer une descendance viable, selon des contraintes temporelles et énergétiques qui lui sont propres. Cette théorie offre donc un cadre conceptuel permettant de décrire et comprendre les comportements d'un individu cherchant à optimiser l'acquisition d'une ressource dans un environnement donné. Ce postulat permet alors de confronter les comportements d'approvisionnement réels, c'est-à-dire ceux observés en milieu naturel, à un idéal comportemental qui aurait été sélectionné au cours de l'évolution, car maximisant la survie et la reproduction.

Les questions abordées dans le cadre de la théorie de l'approvisionnement optimal couvrent des domaines allant de l'étude de la composition quantitative et qualitative du régime alimentaire, à ceux de la répartition spatio-temporelle de la recherche alimentaire.

À l'aide de modèles d'optimalité, MacArthur & Pianka (1966) ont par exemple tenté de comprendre les compromis impliqués dans le choix lié à la sélection d'une proie plutôt qu'une autre. Ils ont ainsi montré qu'une espèce aux comportements d'alimentation plus flexibles persistera plus facilement qu'une espèce plus spécialisée dans un environnement où la disponibilité et l'abondance des ressources varient. En effet, plus une espèce diversifie son régime alimentaire et moins elle aura de chance de subir les conséquences des variations en disponibilité d'une ressource en particulier. L'aspect spatio-temporel de cette recherche alimentaire a également beaucoup été étudié depuis la formalisation du *théorème de la valeur marginale* de Charnov (1976). Ce théorème est énoncé dans le cas d'un environnement où la ressource est distribuée sous forme de parcelles, et cherche à comprendre quelles sont les décisions qui vont conduire l'individu à changer de parcelle. Pour ce faire, Charnov présuppose plusieurs points :

1. L'individu est considéré comme omniscient, c'est-à-dire qu'il connaît *a priori* tous les paramètres du modèle. Il a donc une connaissance parfaite de son environnement.

2. La ressource est distribuée sous forme de parcelles uniquement. Charnov considérait que l'espace séparant deux parcelles était vide.

3. Puisque le prédateur épuise la ressource à mesure qu'il évolue au sein d'une parcelle, le gain net de nourriture au sein de cette parcelle est fonction de la durée d'exploitation de celle-ci.

4. Le prédateur doit prendre des décisions qui vont maximiser son gain net d'apport énergétique à long terme.

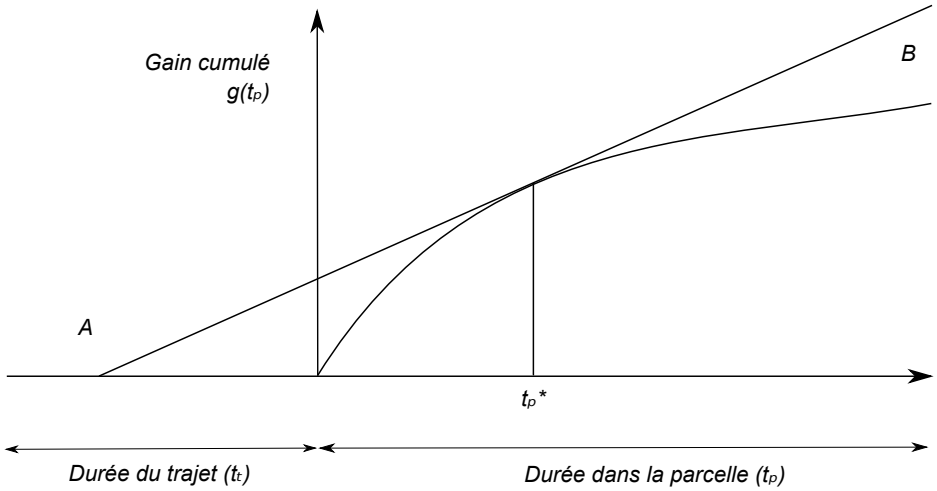

FIGURE 1.1 – Représentation du *théorème de la valeur marginale* et de la détermination du temps optimal passé dans une parcelle (Charnov, 1976).

Ce modèle permet de décrire le gain net d'énergie cumulée ($g(t_p)$) pour un prédateur exploitant une parcelle de nourriture, en tenant en compte de la réduction de la disponibilité en proies dans chaque parcelle visitée (Figure 1.1). Cette réduction de la ressource au

sein d'une parcelle est modélisée par une courbe croissante du gain net d'énergie par unité de temps passé dans la parcelle. À mesure que la ressource s'épuise, le gain net d'énergie va diminuer, entraînant un ralentissement du gain net d'énergie cumulée, caractérisé par une pente plus faible qu'au début. La droite AB est la tangente à la courbe d'acquisition, ayant pour origine le temps de transit considéré (t_t). La valeur marginale, c'est-à-dire le temps optimal (t_p^*) que l'individu doit passer dans la parcelle est déterminée en prenant le projeté du point où la droite AB touche la courbe d'acquisition sur l'axe x. D'après le *théorème de la valeur marginale*, il existe donc un moment optimal où l'animal doit quitter la parcelle : lorsque la valeur marginale est atteinte, c'est-à-dire lorsque la vitesse instantanée d'acquisition d'énergie diminue jusqu'à devenir égale à la vitesse moyenne d'acquisition d'énergie du milieu.

Ce théorème a depuis été utilisé pour examiner l'exploitation de proies distribuées sous forme de parcelle sur bien des espèces, comme l'otarie à fourrure antarctique, *Arctocephalus gazella* (Staniland & Boyd, 2003) ou encore la mésange charbonnière, *Parus major* (Cowie, 1977). Cependant, les hypothèses que présuppose le modèle de Charnov ne sont pas toujours valides *in situ*. L'hypothèse d'omniscience est la plus souvent critiquée, puisqu'un animal ne connaît généralement pas tous les paramètres du milieu dans lequel il évolue. Dans cette configuration, il devient difficile de quantifier la vitesse d'acquisition d'énergie au sein d'une parcelle, puisque l'animal passera très certainement un peu plus de temps à appréhender la qualité de celle-ci (Stephens & Krebs, 1986; Bouskila & Blumstein, 1992; Nonacs, 2001; Thompson & Fedak, 2001), rendant plus difficile la détermination du temps efficace d'alimentation. D'autres critiques portent sur la notion même de parcelle. Certaines ressources ne sont en effet pas distribuées sous forme parcellaire, mais plutôt sous la forme d'un continuum, dont la densité locale varie en fonction de la localisation (Cezilly & Benhamou, 1996). Pour ces ressources, une parcelle de proies peut donc se définir comme une zone où la densité locale de proies est supérieure à la densité moyenne dans l'environnement (Pielou, 1969). Seulement pour un prédateur évoluant dans un tel milieu, il devient difficile de déterminer s'il se trouve bien dans une parcelle et donc une zone favorable. Pour être efficace, il devrait ajuster localement ses déplacements après la détection d'une proie, compte tenu de la forte probabilité de trouver d'autres proies aux alentours (Pyke, 1978).

1.2.2 Notion d'Optimisation : l'Écologie Alimentaire par une Approche Économétrique

La théorie de l'approvisionnement optimal, au même titre que de nombreuses autres théories développées en écologie, est issue de concepts déjà éprouvés en économie. Cette ap-

proche qui consiste à trouver les meilleurs compromis entre les coûts et les bénéfices d'une action offre un outil puissant pour la compréhension des adaptations comportementales. Seulement les choix comportementaux d'un animal ne sont pas directement dictés par la sélection naturelle. Il s'agit ici de comprendre que la maximisation de la valeur sélective d'un individu n'implique pas nécessairement un choix conscient de celui-ci vers la meilleure stratégie. Son choix est donc plutôt le résultat de l'analyse d'un ensemble d'informations par lesquelles l'individu associe un coût et un bénéfice qui lui sont propres, et qui ne seront pas forcément les mêmes pour un conspécifique. Il résulte de ce cheminement, que le comportement observé n'est pas forcément le comportement attendu ou prédit. Ainsi, si l'on considère la sélection naturelle comme un processus de maximisation de la survie et du succès reproducteur, l'efficacité d'alimentation d'un prédateur devrait dépendre de sa capacité à maximiser son rendement de chasse. Or il a été montré chez de nombreuses espèces que ce rendement n'augmente pas indéfiniment, car cet effort de chasse peut être contraint temporellement, par le temps alloué à la prospection par exemple (Houston & Carbone, 1992), ou bien énergétiquement, comme l'énergie liée à la capture d'une proie (Houston, 1995).

Ici, la notion d'optimisation n'intervient que lorsque l'on parle de maximisation sous contraintes. Un prédateur aquatique à respiration aérienne va par exemple chercher à maximiser le nombre de proies qu'il capture, compte tenu du temps qu'il est capable de passer sous l'eau sans respirer. Dès lors apparaît la notion de compromis, ou comment tirer le meilleur avantage d'une situation compte tenu d'un coût. La compréhension du rôle de ces coûts ou contraintes est importante en écologie comportementale, car elle est fortement liée aux processus de décisions. C'est notamment le cas du temps et de l'énergie qui sont deux paramètres généralement pris en compte dans les modèles d'optimalité, pour leur rôle essentiel dans la prise de décision (Cuthill & Houston, 1997).

1.2.3 Prédateurs à Place Centrale

De nombreux animaux sont contraints de retourner à une place centrale entre deux périodes d'alimentation, souvent pour nourrir leur petit ou se reproduire. Cette particularité, qui est une composante importante de la théorie générale, est l'objet principal de la théorie de l'approvisionnement optimal à partir d'une place centrale (Orians & Pearson, 1979; Schoener, 1979). Cette théorie a initialement été développée pour le carouge à épaulettes, *Agelaius phoeniceus* (Orians & Pearson, 1979), afin de comprendre pourquoi la population de l'état du Washington ramenait de nombreuses proies, tandis que celle du Costa Rica ramenait des insectes plus grands. Cette différence fut attribuée aux coûts de manipulation des proies et au temps de prospection plus important pour la population du

Costa Rica. Par la suite, cette théorie fut appliquée à d'autres oiseaux reproducteurs ayant besoin de retourner à leur nid pour nourrir leur petits (Andersson, 1981; Carrete & Donázar, 2005), ainsi qu'à certains pinnipèdes (Costa, 1991). Par extension, cette théorie tente de comprendre l'ajustement des règles de décisions quant au temps de résidence dans une parcelle, ainsi qu'au temps de transit entre la place centrale et la parcelle de proie, sous certaines contraintes comme la distance aux parcelles, la présence de prédateurs, la compétition ou la qualité des parcelles et des proies (Bowen *et al.*, 2002; Ropert-Coudert *et al.*, 2004; Staniland *et al.*, 2007).

1.3 Théorie de la Plongée Optimale : Cas particulier des Prédateurs Plongeurs à Respiration Aérienne

1.3.1 Modèle Général

Dans le règne animal, le cas des prédateurs plongeurs à respiration aérienne est un peu particulier. En effet, certains de ces animaux peuvent être considérés comme des prédateurs à place centrale sur deux niveaux. Le premier correspond à la définition donnée plus haut, c'est-à-dire à des animaux qui reviennent à une place centrale pour nourrir leurs petits, comme chez la plupart des oiseaux marins, ou bien pour se reproduire, comme c'est le cas chez la plupart des pinnipèdes lorsqu'ils reviennent à terre. Une fois en mer, ces animaux doivent s'alimenter sur des ressources présentent en profondeur, entraînant des aller-retours entre la zone d'alimentation en profondeur et la surface pour respirer. La surface apparaît donc comme une "seconde" place centrale qui va en partie régir les règles de décisions permettant à l'individu d'optimiser sa quête alimentaire.

Cette quête alimentaire et plus largement le temps de plongée, sont contraints par la nécessité de l'individu à renouveler ses réserves en dioxygène. C'est notamment pour cela que la plupart des modèles développés dans le cadre de la *théorie de la plongée optimale* sont basés sur la limitation en dioxygène (Kramer, 1988; Houston & Carbone, 1992). Cette limitation est généralement associée à la limite de plongée aérobie (ADL ; *Aerobic Dive Limit*), qui détermine la durée maximum qu'un individu plongeur peut passer sous l'eau, compte tenu de ses capacités physiologiques. Cette limite est définie comme la durée de plongée à partir de laquelle toutes les réserves en dioxygènes que l'animal peut stocker ont été consommées (Houston, 2011). Au-delà, la concentration en acide lactique augmente significativement (Kooyman *et al.*, 1983), entraînant une augmentation du temps de récupération à la surface. La limite de plongée aérobie calculée (cADL, *calculated Aerocbic Dive Limit*), est obtenue en divisant la quantité estimée de dioxygène stockée utilisable, par le taux estimé de consommation de dioxygène durant la plongée (Costa *et al.*, 2001;

Butler, 2006). La limite comportementale de plongée aérobie (bADL ; *behavioural Aerobic Dive Limit*) est quant à elle définie comme le temps de plongée au-delà duquel on observe une brusque augmentation du temps de surface (Kooyman *et al.*, 1980; Cook *et al.*, 2008; Elliott *et al.*, 2015). Elle permet d'obtenir plus facilement une approximation de la vraie valeur d'ADL.

Il est également important de noter que le taux de consommation de dioxygène pendant la plongée dépend d'un ensemble d'éléments comme la physiologie, la morphologie ainsi que le comportement de l'animal. L'ADL n'est en effet pas une mesure constante, elle peut varier selon les plongées en fonction de paramètres intrinsèques à l'individu comme la flottabilité de l'animal (les stratégies de nage ou de chasse, Grémillet & Wilson 1999; Williams *et al.* 2000; Green *et al.* 2007; Halsey *et al.* 2007a), et extrinsèques comme la température de l'eau (Fuster *et al.*, 1997).

1.3.2 Un Premier Modèle Basé sur les Réserves en Dioxygène

C'est ainsi que le premier modèle de plongée optimale fut proposé par Kramer (1988), en étant uniquement basé sur les réserves en dioxygène de l'animal plongeur. L'idée était de considérer le trajet surface-profondeur, de la même manière que la théorie de l'approvisionnement optimal avait traité le problème des prédateurs à place centrale par optimisation de l'énergie acquise, sauf qu'ici le paramètre à optimiser était le taux d'acquisition du dioxygène. Kramer parlait même de *théorie de la respiration optimale*, puisqu'il s'agit de maximiser le rapport entre l'acquisition de dioxygène et le temps passé en surface (Figure 1.2). Cela permet de maximiser l'apport en dioxygène lors des plongées et donc de maximiser le temps passé à s'alimenter en profondeur. Pour un temps de trajet en profondeur donné (t_t), l'animal arrive à la surface avec une certaine quantité de dioxygène m_t. C'est le temps qu'il va passer à la surface qui va conditionner les réserves en dioxygène qu'il pourra allouer à la prochaine plongée. Le temps optimal t_s^* que l'animal devrait passer à la surface pour maximiser son taux d'acquisition en dioxygène est déterminé par la tangente à la courbe d'acquisition en dioxygène à la surface, et au temps de trajet. Houston & Carbone (1992) ont par la suite montré que le taux d'acquisition de dioxygène était décroissant avec le temps passé à la surface, ce qui explique la phase plateau entre la quantité de dioxygène acquise et le temps passé à la surface.

Dans le modèle de Kramer, c'est la quantité de dioxygène utilisée et donc disponible par un individu au cours de sa plongée qui est considérée. En prenant en compte la quantité maximale qu'un animal plongeur peut utiliser s'il renouvelle 100 % de ses réserves, Houston & Carbone (1992) ont également pu montrer que le temps passé dans une parcelle

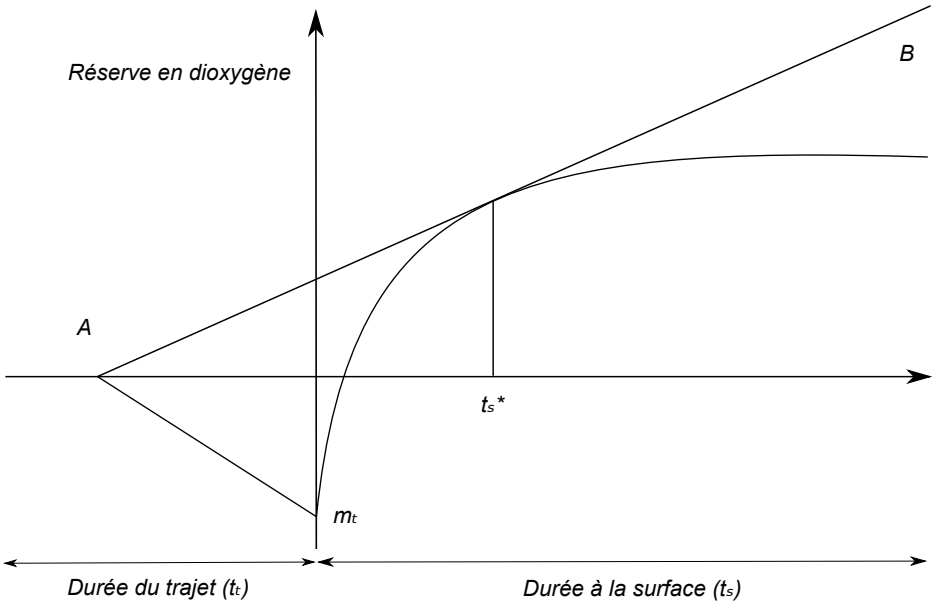

FIGURE 1.2 – Représentation de la *théorie de la plongée optimale* et de la détermination du temps optimal passé en surface selon Kramer (1988).

augmente bien avec le temps de trajet dans un premier temps, puis diminue dans un second temps lorsque l'animal atteint son ADL à mesure que le temps de trajet continue d'augmenter.

1.3.3 Modèle Basé sur le Temps d'Allocation

Suivant le modèle de Kramer, de nombreux autres modèles ont été formulés sur la base des temps d'allocation aux différentes phases de la plongée (Houston & Carbone, 1992; Carbone & Houston, 1996; Mori, 1999; Thompson & Fedak, 2001). Dans ces modèles, le cycle d'une plongée est bien souvent divisé en quatre phases : la phase de descente, la phase de fond, la phase de remontée et la phase de surface entre deux plongées (Figure 1.3).

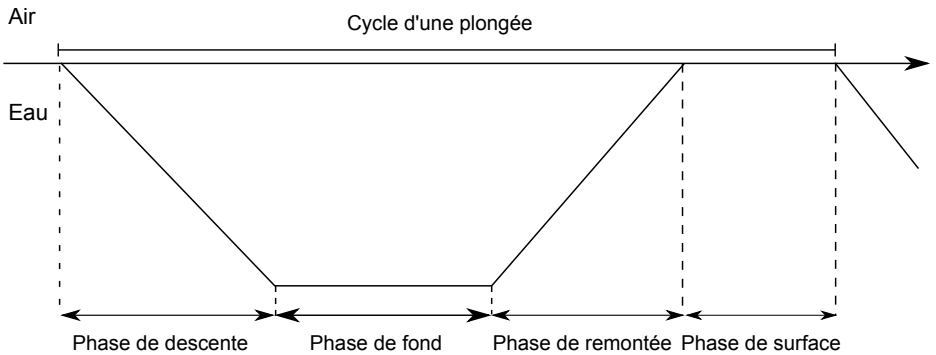

FIGURE 1.3 – Un cycle de plongée est défini par quatre phases : la phase de descente, la phase de fond, la phase de remontée et la phase de surface.

L'optimisation des stratégies d'approvisionnement étant basée sur une maximisation du gain net d'énergie, les modèles développés dans le cadre de la théorie de la plongée optimale prévoient une maximisation de la phase d'alimentation aux dépens des phases de transits et de récupération. Les modèles basés sur le temps d'allocation aux différentes phases d'une plongée consistent donc à comprendre les règles de décisions comportementales prises par un animal plongeur au cours des différentes phases de la plongée.

Temps de Résidence

Comme le temps passé au fond d'une plongée correspond au moment où l'animal plongeur accède aux ressources en proies, cette phase est généralement considérée comme la phase de recherche alimentaire (Carbone & Houston, 1996; Mori, 1998; Thompson & Fedak, 2001; Guinet *et al.*, 2014). De nombreuses études confirment que cette phase est la phase principale d'alimentation chez des prédateurs plongeurs (Tremblay & Cherel, 2000; Doniol-Valcroze *et al.*, 2011). Fossette *et al.* (2008) ont par exemple montré chez les tortues luths (*Dermochelys coriacea*) que les événements de mouvement de bec, probablement lié au comportement d'alimentation, ont majoritairement lieu au fond, avec une présence respective de 71 %, 55 % et 84,8 % de ces événements durant la phase de fond de plongée en "U", "V" et "W".

L'ajustement du temps de résidence chez un prédateur plongeur va donc notamment dépendre de la distance à la parcelle, *i.e.* la profondeur de plongée, et de la qualité de celle-ci, *i.e.* la densité du champ de proies. Houston & Carbone (1992) ont par exemple montré que le temps passé dans la parcelle augmentait avec la profondeur à mesure que l'animal s'approche de sa limite aérobie. Une fois l'ADL atteinte, le temps de résidence diminue à mesure que la profondeur augmente pour compenser le coût d'accès à la ressource. Cette augmentation du temps de résidence avec la profondeur à été montré chez de nombreuses espèces comme le fuligule milouin, *Aythya ferina* (Carbone & Houston, 1994), l'otarie de Kerguelen, *Arctocephalus gazella* (Viviant *et al.*, 2016), le phoque commun, *Phoca vitulina* (Heaslip *et al.*, 2014) ou encore la baleine bleue, *Balaenoptera musculus* (Doniol-Valcroze *et al.*, 2011). Mais très peu d'études ont réussi à mettre en évidence une diminution du temps de résidence au-delà d'une certaine profondeur (Cook *et al.*, 2008).

Par la suite, Thompson & Fedak (2001) ont développé un modèle tenant également compte de la qualité de la parcelle visitée. Ils montrent ainsi que pour des plongées à faibles profondeurs, l'animal plongeur devrait toujours terminer sa plongée plus tôt s'il ne rencontre aucune proie au début de sa plongée. Qui plus est, le bénéfice de cette stratégie serait plus important pour des parcelles de faible qualité. À mesure que la profondeur augmente et que l'animal atteint son ADL, cette stratégie n'apporterait plus d'avantage

: il n'y aurait donc plus de bénéfices à terminer sa plongée plus tôt si aucune proie n'est rencontrée. Testé en captivité chez les lions de mer de Steller, *Eumetopias jubatus*, Cornick & Horning (2003) ont montré que le temps passé à s'alimenter augmentait avec le nombre de proies rencontrées, validant ainsi certaines des hypothèses du modèle de Thompson & Fedak (2001).

Temps de Transit

Comme vu précédemment, maximiser le gain net d'énergie au cours d'un cycle de plongée peut se faire en maximisant le temps passé dans la parcelle, et donc le temps passé au fond, ou bien en minimisant les phases de transits que sont les phases de descente, de remontée et de surface. De la même façon que pour le temps de résidence, les temps de transit peuvent être affectés par la distance entre la parcelle et la place centrale, mais également par la qualité de la parcelle. Thompson *et al.* (1993) ont ainsi proposé un modèle dans lequel ils explorent le comportement qu'un plongeur devrait adopter durant ces phases de transits afin d'augmenter la proportion de temps passé au fond. Ils montrent qu'un animal plongeur devrait nager au coût de transport minimal (Miller *et al.*, 2012) durant les phases de transits pour des plongées à grandes profondeurs. À de plus faibles profondeurs, ils s'attendent à ce que l'animal augmente sa vitesse de nage pour augmenter le temps passé dans la parcelle. Selon leur modèle, cette vitesse de nage serait également dépendante de la qualité de la parcelle visitée, avec des vitesses de nage plus importantes pour des qualités de parcelles plus élevées. Les prédateurs plongeurs devraient donc trouver le meilleur compromis entre l'énergie allouée aux mouvements de nage et donc aux coûts du transport, et la quantité de dioxygène disponible restante pour la phase de fond. Hassrick *et al.* (2007) ont par exemple montré que chez l'éléphant de mer du nord, *Mirounga angustirostris*, la vitesse de nage augmentait avec la distance à la parcelle. Ce résultat également retrouvé chez l'éléphant de mer du sud, *Mirounga leonina* (Hindell & Lea, 1998), le lion de mer de Nouvelle-Zélande, *Phocarctos hookeri* (Crocker *et al.*, 2001) ou encore chez l'otarie de Kerguelen, *Arctocephalus gazella* (Boyd *et al.*, 1995), est interprété par Hassrick *et al.* (2007) comme étant la preuve d'ajustements physiologiques chez l'éléphant de mer, puisque leurs données suggèrent également une relation négative entre le temps passé au fond et la vitesse de nage.

1.3.4 Limites de la Théorie

Tester les prédictions de ces modèles permet de mettre en exergue les limites de la théorie et donc d'améliorer notre compréhension du comportement de plongée des prédateurs plongeurs à respirations aérienne. Halsey *et al.* (2003) ont par exemple montré chez le

fuligule morillon, *Aythya fuligula*, que le temps passé à s'alimenter augmente lorsque les coûts associés augmentent également. Ce résultat contraire aux prédictions de Houston & Carbone (1992), a permis de mettre en évidence chez cette espèce que la courbe d'absorption du dioxygène à la surface n'est pas fixe, comme présupposée par Houston & Carbone (1992), mais que la moyenne du taux d'absorption à la surface augmente avec l'augmentation des coûts liés à la plongée.

À l'image de cet exemple, il existe de nombreux cas pour lesquels les prédictions diffèrent des observations (Boyd *et al.*, 1995; Hindell & Lea, 1998; Crocker *et al.*, 2001; Hassrick *et al.*, 2007). Un modèle va par définition tenter de représenter la réalité en approximant de nombreux paramètres, quitte à omettre certaines variables se révélant essentielles pour la compréhension des comportements de plongée. C'est notamment le cas de la flottabilité qui est liée à la densité corporelle et donc à la proportion en lipides des tissus qui composent l'animal plongeur. Il existe aujourd'hui de nombreuses études qui attestent du rôle prépondérant de la flottabilité dans l'ajustement du comportement de plongée chez l'éléphant de mer (Webb *et al.*, 1998; Richard *et al.*, 2014), le phoque gris, *Halichoerus grypus* (Beck *et al.*, 2000), le cormoran des Kerguelen, *Phalacrocorax verrucosus* (Cook *et al.*, 2010), la tortue luth, *Dermochelys coriacea* (Fossette *et al.*, 2010) ou encore le cachalot, *Physeter macrocephalus* (Miller *et al.*, 2004a). La flottabilité jouant sur le coût du transport, un animal plongeur aura tout intérêt à se rapprocher d'une flottabilité neutre s'il souhaite minimiser le coût du transport pour accéder à une parcelle en profondeur (Sato *et al.*, 2013; Adachi *et al.*, 2014).

L'autre limitation de ce genre de modèle concerne l'estimation de la qualité de la parcelle visitée. Accéder à cette information *in situ* se révèle en pratique compliqué, c'est pourquoi un certain nombre de méthodes alternatives ont été développées. L'utilisation d'appareils embarqués tels que les accéléromètres (Gallon *et al.*, 2013) ou les capteurs à effet Hall (Viviant *et al.*, 2010) permettent d'avoir une idée du taux de rencontre de proies, sans que l'on sache si l'animal a réellement réussi à capturer une proie. Les sondes œsophagiennes peuvent quant à elles donner une idée du nombre d'événements d'ingestion (Charrassin *et al.*, 2001). Cependant, beaucoup d'études n'ayant pas les moyens de mesurer les tentatives de prises alimentaires à l'aide de ces appareils font alors l'hypothèse que le temps que l'animal passe au fond d'une plongée est proportionnel à la qualité de la parcelle visitée (Wilson *et al.*, 2002; Watanabe *et al.*, 2003; Fossette *et al.*, 2008).

1.4 Problématiques et Structure de la Thèse

L'objectif de ma thèse est donc d'étudier les comportements d'approvisionnement d'un prédateur plongeur en milieu naturel, afin de mieux comprendre les contraintes temporelles

et énergétiques auxquelles ces animaux peuvent être soumis. Il s'agit ici de comprendre comment ces animaux ajustent leur comportement en fonction des contraintes qui leur sont propres, mais également en fonction des environnements qu'ils rencontrent. Pour ce faire, cette thèse s'est intéressée à la population d'éléphant de mer de l'hémisphère sud, *Mirounga leonina*, située sur l'archipel des Kerguelen. Facile d'accès depuis la station technique et scientifique de Port-aux-Français, cette espèce permet de par sa taille, son cycle de vie et ses performances de plongées d'étudier le comportement de prédateurs plongeurs habituellement difficile d'accès. L'essentiel des travaux présenté dans la suite de ce manuscrit a été réalisé sur des femelles équipées d'appareils de mesure permettant le suivi de leur comportement de plongée au cours des plusieurs mois de trajet en mer. Ce travail de thèse s'articule autour de trois hypothèses, dont chacune fait l'objet d'un article scientifique, constituant le corps du manuscrit :

1. Chapitre 3 : Nous testerons ici, l'hypothèse que l'éléphant de mer augmente son effort de prospection dans des zones où le taux de rencontre de proie est plus important qu'ailleurs. L'hypothèse d'une multitude de proies chassées sera également testée. À l'échelle des plongées, il s'agira d'identifier des zones en recherche restreinte et d'en étudier les propriétés. À l'échelle d'une tentative de capture, il s'agira de déterminer si différentes stratégies de chasse sont mises en place, potentiellement indicatrices de différentes espèces de proies chassées. Pour cette partie, l'utilisation d'un ensemble de capteurs sera nécessaire pour reconstruire la trajectoire en trois dimensions de l'animal sous l'eau. L'étude à fine échelle de la cinématique du mouvement de l'animal lors de l'approche d'une proie devrait nous permettre d'avoir un nouvel éclairage sur les relations proie-prédateur.

   Jouma'a, Joffrey, Yves, Le Bras, Picard, Baptiste & Guinet, Christophe, Three-dimensional assessment of hunting strategies in a deep diving predator. *Marine Ecology Progress Series* (in press)

2. Chapitre 4 : Dans ce chapitre nous testerons si l'éléphant de mer ajuste son comportement de plongée pour maximiser le temps qu'il passe au fond. Il s'agira ici de déterminer et comprendre les ajustements comportementaux mis en place par l'éléphant de mer pour passer plus de temps en recherche alimentaire. Cette partie consistera également à tester si l'éléphant de mer se conforme à la théorie de la plongée optimale et notamment s'il module son comportement de plongée en fonction du nombre de proies rencontrées, de la profondeur ciblée et de l'évolution de sa flottabilité au cours de son trajet en mer.

   Jouma'a, Joffrey, Yves, Le Bras, Richard, Gaëtan, Vacquié-Garcia, Jade, El Ksabi, Nory, Picard, Baptiste & Guinet Christophe. (2016) Adjustment of diving behaviour

with prey encounters and body condition in a deep diving predator: the Southern Elephant Seal. *Functional Ecology*

3. Chapitre 5 : Ici, nous testerons si la dépense énergétique moyenne de l'éléphant de mer au cours d'une plongée varie selon le sexe, l'année et l'environnement prospecté. Dans ce chapitre, nous étudierons donc les variations de la dépense énergétique obtenues à partir du comportement de plongée et de la flottabilité des animaux, sur des individus post-mues sur une période de 11 ans (2004 à 2015). Il s'agira dans un premier temps de construire un modèle prédictif de la dépense énergétique réalisé sur des données hautes résolutions (individus post-reproducteurs), pour ensuite prédire sur un ensemble plus important de plongées basses résolutions (individus post-mues), les variations de cet indice de la dépense énergétique et d'en étudier les variations spatio-temporelles.

   Jouma'a, Joffrey, Yves, Le Bras, Picard, Baptiste & Guinet, Christophe. Spatio-Temporal Variations in Field Metabolic Rate of Post-Moulting Southern Elephant Seals (En préparation)

CHAPITRE 2

Modèle Biologique, Site d'Étude & Jeux de Données

Sommaire

2.1 L'Éléphant de Mer du Sud: un Prédateur Supérieur de l'Océan Austral

2.1.1 Situation du Plus Imposant Phocidé au Monde

Parmi les nombreux prédateurs qui peuplent les eaux australes, l'éléphant de mer austral, *Mirounga leonina*, est le représentant le plus imposant de la famille des Phocidés regroupant pas moins de 18 espèces différentes. On trouve parmi cette famille deux espèces d'éléphants de mer qui constituent le genre *Mirounga* : l'éléphant de mer du nord, *Mirounga angustirostris*, situé principalement sur la côte nord-est américaine et l'éléphant de mer du sud, ou éléphant de mer austral, que l'on retrouve de l'Antarctique jusqu'aux îles subantarctiques et qui constitue le modèle biologique de cette thèse. Cette espèce, plus massive que sa cousine nord américaine, est notamment caractérisée par un important dimorphisme sexuel. En effet, on estime que les mâles peuvent peser plus de 3 tonnes et mesurer jusqu'à 6 mètres de long, mais en général le poids moyen d'un adulte mâle est de 2 tonnes pour une longueur moyenne de 4 mètres (Slip *et al.*, 1994). Les femelles sont quant à elles 4 à 6 fois moins imposantes, puisqu'elles ne pèsent en moyenne que 500 kilogrammes pour 2,5 mètres de long (Figure 2.1).

FIGURE 2.1 – Représentation d'éléphant de mer du sud, *Mirounga leonina*. Du premier au dernier plan: un juvénile, une femelle adulte et un mâle adulte. Illustration par P. Folkens.

De la fin du XIX^{ème} jusqu'à la moitié du XX^{ème} siècle, la chasse aux phoques a décimé la population d'éléphant de mer du sud (Guinet *et al.*, 1999; McMahon *et al.*, 2009; Authier *et al.*, 2011). Après l'arrêt de la chasse dans les années 50, les différentes sous-populations d'individu des îles subantarctiques et antarctiques auraient dû se reconstituer.

Seulement avec un déclin marqué depuis la fin de la chasse aux phoques pour certaines colonies, comme pour celle de l'île Marion qui a connu une diminution de près 87 % de sa population d'éléphant de mer jusque dans les années 2000 (McMahon *et al.*, 2009), de nombreux scientifiques se sont intéressés à cette espèce.

Il existe quatre sous-populations génétiquement différentes d'éléphants de mer australs que sont la Géorgie du Sud (400 000 individus), l'archipel des Kerguelen (220 000 individus), l'île Macquarie (76 000 individus) et la péninsule de Valdès en Argentine (42 000 individus). Au début des années 2000, McMahon *et al.* (2005) estima la taille totale de la population à plus de 700 000 individus, avec près de 220 000 individus pour l'archipel des Kerguelen, représentant le deuxième plus gros site de reproduction après la Géorgie du Sud.

2.1.2 Cycle Biologique

Les éléphants de mer sont des mammifères marins qui ont la particularité de revenir deux fois dans l'année à terre pour se reproduire et pour renouveler leur fourrure. Durant ces deux périodes à terre déjà coûteuse en énergie, les éléphants de mer jeûnent, ce qui accroît d'autant plus leurs dépenses énergétiques (Boyd *et al.*, 1993; Fedak *et al.*, 1994). Ces animaux passent le reste du temps en mer à s'alimenter, afin de renouveler les réserves d'énergie allouées lors de la reproduction et de la mue.

Reproduction

Le système de reproduction des éléphants de mer est basé sur la polygynie, c'est-à-dire qu'un mâle peut s'accoupler avec plusieurs femelles, regroupées en harem. Un harem est donc composé de plusieurs femelles et d'un mâle dominant qui se livre régulièrement à des combats pour empêcher les mâles périphériques de s'accoupler avec l'une de leurs femelles. Chez les femelles, la maturité sexuelle est atteinte vers 3-4 ans, tandis que chez les mâles, elle est atteinte une année plus tard vers 4-5 ans. Compte tenu du système de reproduction et de l'accessibilité à la reproduction, ces jeunes mâles ne s'accoupleront que vers l'âge de 9-10 ans, lorsqu'ils pourront prétendre défendre un harem.

Ces mâles en âge de se reproduire arrivent à la fin de l'hiver austral, en août, pour y rester huit semaines et établir leur territoire. Les femelles reviennent quant à elles un mois plus tard pour le début du printemps austral, en septembre. Dans les premiers jours qui suivent leur arrivée, les femelles mettent bas en général d'un unique petit pesant une quarantaine de kilogrammes. Elles l'allaitent durant 22 jours d'un lait riche en matière grasse, permettant au petit d'atteindre un poids moyen au sevrage de 107 kilogrammes (Guinet, 1991).

La saillie des femelles a lieu peu de temps avant le sevrage du petit, puis elles repartent en mer quelques semaines plus tard, en octobre, à la fin du printemps austral. L'implantation du blastocyte n'a lieu que trois mois plus tard, pour une gestation apparente de quasiment une année (Gibbney, 1953).

Mue

Trois à quatre mois après leur séjour en mer suivant la reproduction, les éléphants de mer reviennent une seconde fois à terre, mais cette fois-ci pour muer. Cette période peut s'étaler sur plusieurs mois selon le sexe et la classe d'âge des individus, entre novembre et avril (Bradshaw *et al.*, 2004). La mue des éléphants de mer et des phoques moines est particulière puisqu'elle consiste en la perte des poils et de l'épiderme, contrairement aux autres espèces de pinnipèdes (Worthy *et al.*, 1992). Cette particularité associée à une période de jeûne à terre représente un coût énergétique important pour ces animaux. En effet, les femelles peuvent investir jusqu'à la moitié de l'énergie qu'elle consacre à la croissance de leur petit et au renouvellement de leur fourrure (Boyd *et al.*, 1993).

Plongée

En dehors de la période de reproduction et de mue, l'éléphant de mer austral passe l'essentiel de son temps en mer, plongeant quasi continuellement. Ces animaux ne passent en effet que quelques minutes à la surface (McConnell *et al.*, 1992) avant de plonger à de grandes profondeurs. Ces plongées durent en moyenne 20 minutes pendant lesquelles ces phoques atteignent une profondeur moyenne de 600 mètres (2149 m maximum; McIntyre *et al.*, 2010). Du fait de la migration nycthémérale des myctophidés, les femelles éléphants de mer plongent plus profondément le jour que la nuit (en moyenne 800 m le jour et 400 m la nuit).

2.1.3 Distribution et Régime Alimentaire

Que ce soit en Géorgie du Sud, sur l'île Macquarie ou bien sur l'archipel des Kerguelen, les éléphants de mer austraux ont une distribution circumpolaire (Figure 2.2). Le trajet en mer qu'effectuent ces animaux est l'occasion de renouveler les réserves d'énergie qui ont été allouées durant leurs périodes de jeûne à terre pour la mue et la reproduction. Il est normal que la distribution géographique de leur trajet soit corrélée aux types de proies rencontrées et donc à leur régime alimentaire. En fonction de l'âge et du sexe de l'animal, plusieurs types d'environnement ont ainsi pu être identifiés. Les jeunes des deux sexes âgés de moins de cinq ans et les femelles adultes vont préférentiellement s'alimenter en milieu pélagique antarctique, dans la zone marginale des glaces, et subantarctique, dans la

zone interfrontale. (Bailleul *et al.*, 2007a; Ducatez *et al.*, 2008; Cherel *et al.*, 2008; Bailleul *et al.*, 2010a), de petits poissons-lanternes que l'on appelle les *myctophidés*. Cherel *et al.* (2008) ont montré à l'aide d'analyse isotopique que trois espèces de myctophidés étaient majoritairement présentes dans leur bol alimentaire : *Gymnoscopelus nicholsi*, *Electrona Antarctica* et *Electrona calsbergi*. Une fois adulte, le niveau trophique des mâles est plus élevé ce qui signifie qu'ils s'alimentent sur des échelons trophiques supérieurs comme des céphalopodes (*Psychroteuthis glacialis*, *Gonatus antarcticus* et *Kondakovia longimana*, Slip 1995; Daneri *et al.* 2000) ou de la légine australe (*Dissostichus eleginoides*, Slip 1995). Ils ont ainsi tendance à délaisser le milieu pélagique pour venir se nourrir principalement sur le plateau antarctique et le plateau de Kerguelen.

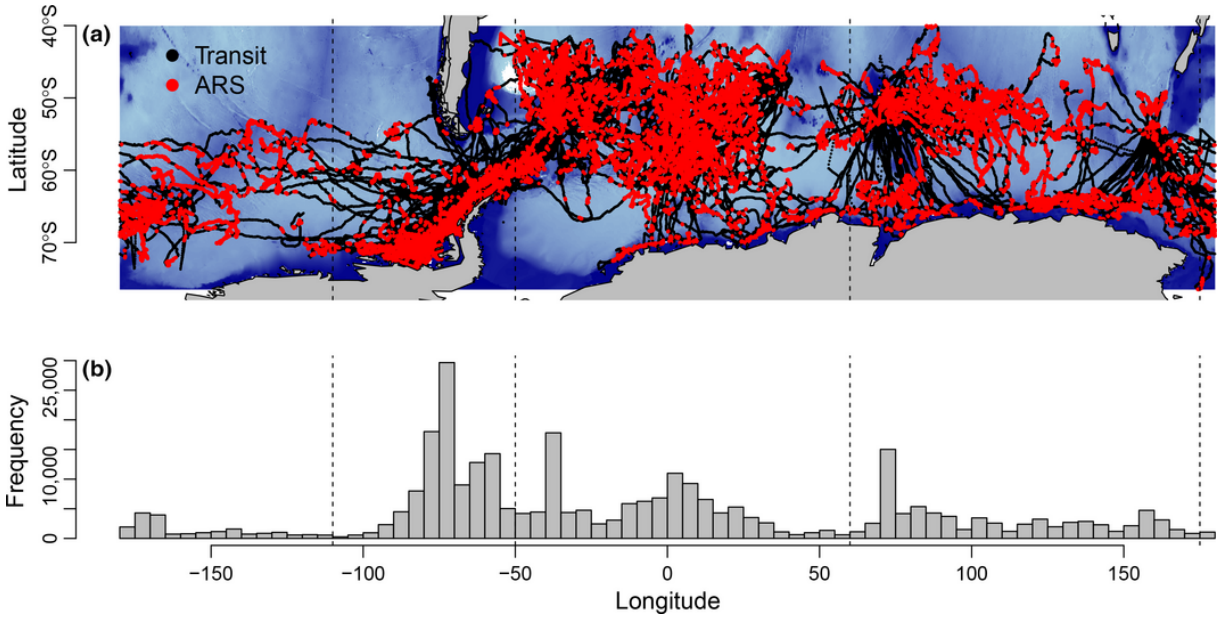

FIGURE 2.2 – Tirée de Hindell *et al.* (2016), cette figure représente (a) 568136 localisations d'éléphants de mer dans l'océan austral catégorisées en deux états comportementaux, transit ou zone de recherche restreinte (ARS). (b) La fréquence des localisations en ARS tous les 10 degrés de longitude

2.2 L'Océan Austral

2.2.1 Un Environnement sous Changements Permanents

L'océan Austral, ou océan Antarctique, est constitué d'un système dynamique composé de plusieurs structures océanographiques dont la position et l'intensité varient au cours du temps. Cet océan a pour particularité d'être annulaire, c'est-à-dire qu'il entoure le continent antarctique sans qu'aucun autre continent n'entrave son chemin. Cette particularité est associée à la présence du plus puissant courant océanique (Pickard & Emery, 1990), le courant circumpolaire (ACC, Deacon 1933), qui circule d'ouest en est sous l'effet

de la force de Coriolis et des vents d'ouest. L'océan Austral s'étend du 60 °S au niveau de la Nouvelle-Zélande, jusqu'au 48 °S au sud de l'océan Atlantique, sur plus de 24 000 kilomètres.

Au sein de cet océan, plusieurs structures ont été identifiées pour délimiter les différentes masses d'eaux qui le composent. Une masse d'eau est définie comme un compartiment océanique homogène, caractérisé par des propriétés physico-chimiques (température, salinité et pression) qui lui sont propres. Deux masses d'eau qui se touchent sont donc délimitées par un front, c'est-à-dire par une structure océanographique caractérisée par un gradient physico-chimique. Trois masses d'eaux sont ainsi généralement distinguées dans l'océan Austral : les eaux subtropicales, les eaux subantarctiques et les eaux antarctiques (Figure 2.3). On trouve respectivement au nord de chacune de ces zones : le front subtropical (STF), le front subantarctique (SAF) et le front polaire (PF).

L'évolution de ces structures dans le temps et l'espace n'est pas figée (Langlais *et al.*, 2011). En effet, sous l'effet des courants, des structures dites méso et subméso-échelle apparaissent sous la forme de tourbillons et de filaments. Ces structures peuvent persister durant quelques jours et s'étendre sur plusieurs centaines de kilomètres. Elles vont alors façonner la dynamique de l'océan Austral et ainsi conditionner la répartition spatio-temporelle des ressources (Strass *et al.*, 2002).

2.2.2 Productivité des Eaux de Kerguelen

Contrairement à la zone interfrontale[1] caractérisée par un fort apport en nutriments, mais une faible concentration en chlorophylle (*High Nutrient-Low Chlorophyll*, Pitchford, 1999), le plateau continental de Kerguelen présente un important bloom phytoplanctonique (Moore & Abbott, 2000; Mongin *et al.*, 2008) en raison de sa faible bathymétrie et des structures océanographiques qui y sont présentes. Associés aux vents d'ouest et au courant circumpolaire, les nutriments du plateau vont alors migrer à l'est pour former des zones à forte richesse biologique (Dragon *et al.*, 2011). Ce phénomène va structurer la répartition spatio-temporelle de l'ensemble des ressources en agissant principalement à la base du réseau trophique, sur la production primaire. La distribution de la biomasse phytoplanctonique apparaît donc comme contrainte par des facteurs environnementaux qui par nature, fluctuent tout au long de l'année.

La présence de structures océanographiques telles que les tourbillons ou les filaments va augmenter l'hétérogénéité spatiale en multipliant les conditions environnementales présentes au sein de cet océan. L'hypothèse de l'*hétérogénéité de l'habitat* développée par

[1] La zone inter-frontale correspond à la région située entre le front sub-tropical et le front polaire.

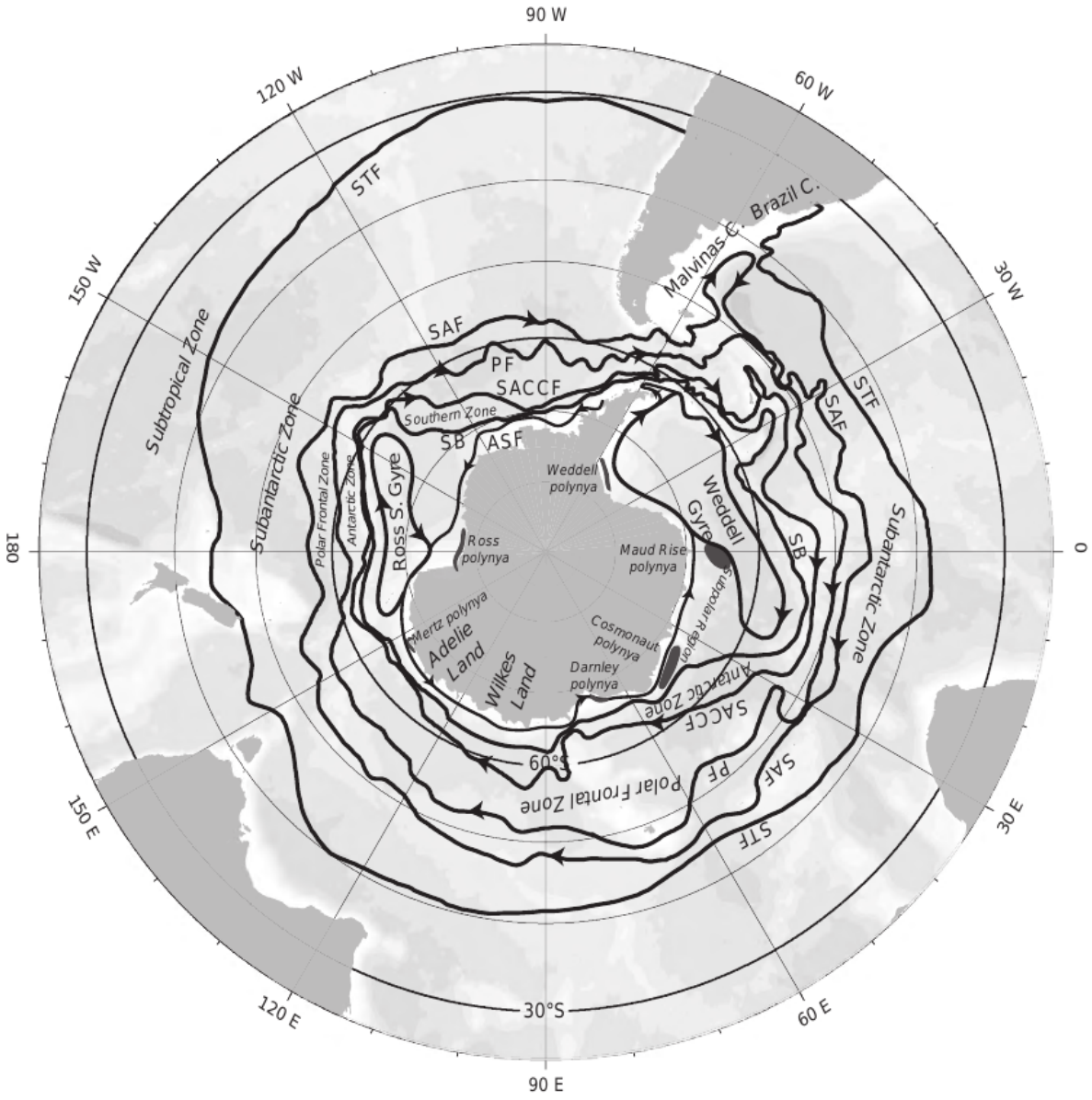

FIGURE 2.3 – Carte de l'océan Austral en vue orthographique centrée sur le continent antarctique (Talley *et al.*, 2011). La position des principaux fronts cités dans ce manuscrit y est représentée : le front subtropical (STF), le front subantarctique (SAF) et le front polaire (PF).

MacArthur & MacArthur (1961), suggère qu'une augmentation de la diversité des habitats peut favoriser une diversité spécifique plus importante. Confirmant cette hypothèse, les fronts océaniques présentent ainsi une production biologique importante (Bost *et al.*, 2009). La variabilité de l'abondance de certaines espèces de poissons-lanternes telles que les myctophidés est directement liée à la position du front polaire (Loots *et al.*, 2007) et aux structures océanographiques environnantes.

2.3 Déploiement et Traitement des Données

2.3.1 Description des Appareils Embarqués

SPOT

Les balises SPOT (Figure 2.4) sont des balises conçues par Wildlife Computers™ dédiées à la localisation des animaux via le système Argos. En plus de permettre le suivi du trajet des animaux en mer, ces balises sont dotées d'une importante autonomie nous permettant de localiser plus facilement un éléphant de mer lors de son retour à terre. Les données de localisation sont transmises lorsque la balise est immergée, *i.e.* à terre ou en surface. La qualité des localisations est variable, car elle dépend des conditions météorologiques, mais également du nombre de satellites utilisés pour calculer la position.

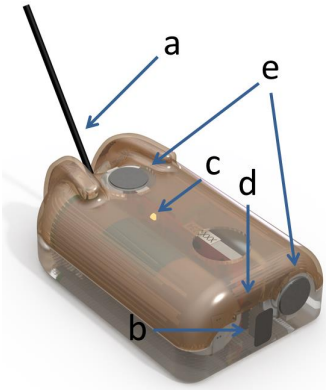

FIGURE 2.4 – Schéma d'une balise SPOT: (a) antenne Argos, (b) port de communications, (c) témoin lumineux, (d) déclencheur magnétique et (e) capteur sec/mouillé. Cette balise mesure $7,2 \times 5,4 \times 2,4$ cm, pour un poids de 119 g. Image téléchargée sur le site de Wildlife Computer™ http://wildlifecomputers.com/wp-content/uploads/manuals/SPOT6-User-Guide.pdf

CTD-SRDL

Les balises CTD-SRDL (Conductivity-Temperature-Depth Satellite-Relayed-Data-Logger, Figure 2.5) sont quant à elles fabriquées en Écosse, au Sea Mammal Research Unit Instrumentation. Conçues pour mesurer des variables océanographiques comme la température et la salinité de l'eau, ces balises ont été utilisées dans cette thèse pour leur mesure de la profondeur (elles mesurent en fait la pression de 0 à 2000 dBar, avec une précision de 2 dBar et une résolution de 0.05 dBar). Pour cela, elles ont été programmées pour enregistrer la pression toutes les deux secondes. De la même façon que pour les SPOTs, ces balises transmettent la localisation de l'animal en direct via le système Argos. En plus de ces données de localisations, elles transmettent également des profiles de plongées

résumés. Chaque plongée est résumée au sein de la balise à l'aide d'un algorithme en ligne brisée qui réduit la plongée à cinq segments (Fedak *et al.*, 2001). Ces données sont ensuite compressées et envoyées via Argos (Fedak *et al.*, 2002; Argos, 2011).

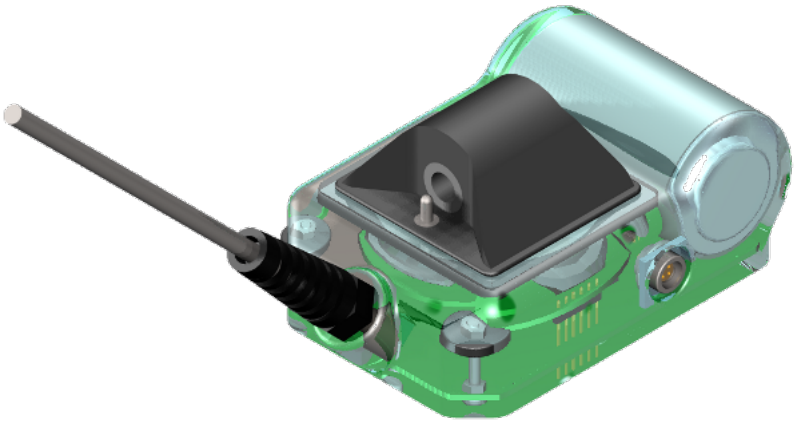

FIGURE 2.5 – Schéma d'une balise CTD-SRDL. Cette balise mesure $10,5 \times 7 \times 4$ cm, pour un poids de 545 g. Image téléchargée sur le site du SMRU http://www.smru.st-andrews.ac.uk/Instrumentation/images/CTD_trans_600x450.png

MK10-X

Les balises MK10-X (Figure 2.6) sont construites par Wildlife Computers™ et contrairement aux CTD-SRDLs et aux SPOTs, elles ne télétransmettent aucune données. Toutes les données enregistrées par cette balise sont donc stockées dans la mémoire interne de celle-ci, ce qui nécessite de retrouver l'éléphant de mer et de lui enlever la balise pour accéder aux informations enregistrées. Ces balises ont été utilisées pour échantillonner la profondeur (avec une précision correspondant à 1 % de la mesure et une résolution de 0,5 m), la température et la lumière à 1 Hz. Ces deux derniers paramètres n'ont pas été utilisés dans le cadre de cette thèse. Ces balises comprennent également un accéléromètre à trois axes configuré pour enregistrer à 16 Hz et dont la résolution est de 0,05 $m.s^{-2}$.

SPLASH10-F

Comme pour les SPOTs et les MK10-Xs, ces balises sont fabriquées par Wildlife Computers™. Elles comprennent les mêmes capteurs que les MK10-Xs, sans l'accéléromètre. En plus de cela, les SPLASH10-F (Figure 2.7) peuvent transmettre la localisation de l'animal via le système Argos. Elles sont également couplées à un récepteur GPS, permettant une fois la balise récupérée de recalculer les positions de l'animal au cours de son trajet en

FIGURE 2.6 – Schéma d'une balise MK10-X. Cette balise mesure $5,6 \times 3,8 \times 2$ cm, pour un poids de 58 g. Image téléchargée sur le site de Wildlife Computer™ http://wildlifecomputers.com/wp-content/uploads/product-images/TDR10-X-279A.png

mer. L'avantage du récepteur GPS sur le système Argos, est qu'il permet d'enregistrer à une fréquence plus rapide (de l'ordre de quelques minutes) et à une meilleure résolution (de l'ordre de quelques dizaines de m) la localisation de l'animal.

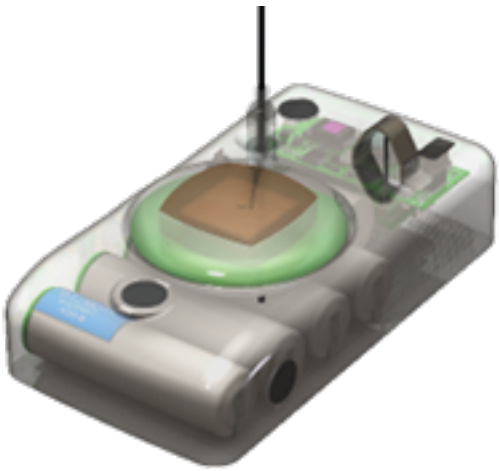

FIGURE 2.7 – Schéma d'une balise SPLASH10-F. Cette balise mesure $10,5 \times 5,6 \times 3$ cm, pour un poids de 217 g. Image téléchargée sur le site de Wildlife Computer™ http://wildlifecomputers.com/wp-content/uploads/product-images/SPLASH10-F-238A.png

Acousonde

Les Acousondes™ sont des balises construites par Acoustimetrics, une filiale de Greeneridge Sciences, Inc. Le modèle 3A (Figure 2.8) utilisé dans le cadre de cette thèse comprend un capteur de pression configuré à 1 Hz, pour mesurer la profondeur, ainsi qu'un accéléromètre et un magnétomètre trois axes configurés à 5 Hz. La particularité de cette balise est qu'elle comprend également un hydrophone, permettant d'enregistrer l'environnement sonore lorsque l'animal plonge. Cet hydrophone a été configuré pour enregistrer 3 h toutes les 12 ou 24 h (varie selon l'année de déploiement) à une fréquence de 6 ou 12 kHz (varie également selon l'année de déploiement).

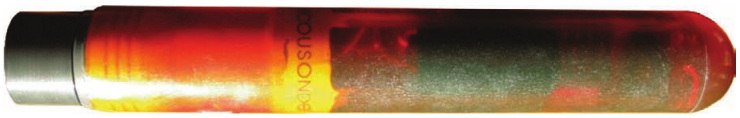

FIGURE 2.8 – Photographie d'une balise Acousonde™ modèle 3A. Cette balise mesure 22,1 cm, pour un poids de 262 g. Image téléchargée sur le site d'Acoustimetrics http://www.acoustimetrics.com/downloads/Acousonde3A_Brochure.pdf

2.3.2 Déploiement des Appareils Embarqués

Les données sur lesquelles s'appuie ce travail de thèse ont été récoltées sur des éléphants de mer équipés de différents assemblages de balise, lors de leurs retours à terre pour la mue et la reproduction entre 2004 et 2015, sur l'archipel des Kerguelen. J'ai pour ma part eu l'occasion de participer à une campagne de terrain de septembre 2014 à décembre 2014, pour la récupération des balises posées sur des individus post-mues en début d'année et le déploiement de nouvelles balises sur des individus post-reproducteurs au cours du mois d'octobre 2014.

Préalablement à la pose de ces appareils embarqués sur l'animal, les balises sont synchronisées sur le temps universel coordonné pour faciliter le traitement des données *a posteriori*. Une fois allumée et synchronisée, le dessous de chacune des balises est enduit d'une couche de pâte marine que l'on coupe lorsque l'on retire la balise de l'animal. La pose d'une balise sur un éléphant de mer se fait préférentiellement à l'écart du harem. Une fois l'animal prit dans une capuche, il est immobilisé à l'aide de deux personnes (voire plus, en fonction de la taille de l'animal), tandis qu'une troisième personne anesthésie l'animal en intra-veineux (McMahon *et al.*, 2000; Field *et al.*, 2002) à l'aide d'une solution 1:1 de tilétamine et de zolazépam, sur la base de 0,8 ml pour 100 kg. Après l'anesthésie de l'animal, sa fourrure est nettoyée avec de l'acétone avant d'être enduite avec de la colle à époxy, à l'endroit de la pose de balise. Un filet préalablement découpé de la forme de la balise est ensuite englué dans la colle. Ce filet contient un ou plusieurs collier colson, qui serviront à maintenir la balise. Une couche de colle époxy est ensuite ajoutée sous la couche de pâte marine en-dessous de la balise. La balise est ensuite positionnée sur le filet et les colliers colson sont serrés. Cette opération est bien évidemment effectuée avant le réveil de l'animal, qui survient dans les 20 à 40 minutes suivant l'anesthésie.

Pour récupérer les balises lorsque les éléphants de mer reviennent à terre, le même protocole est utilisé. Une fois l'animal anesthésié, il ne reste plus qu'à couper les colliers colson et la pâte marine pour libérer la balise. Le reste d'époxy présent sur la fourrure de l'animal tombe ensuite naturellement lors de la mue.

2.3.3 Traitement et Calcul des Principales Variables Utilisées

Délimitation des Différentes Phases d'une Plongée

Avant de traiter la donnée de profondeur pour identifier les plongées, il est nécessaire de corriger au préalable la dérive du capteur de pression au cours du temps. Initialement développée sous Matlab, cette étape a récemment été implémentée dans la fonction `correct_depth` du package `rbl` (Le Bras, 2016). Un seuil a ensuite été fixé à 15 m pour définir la zone de plongée et la zone de surface.

La définition de la phase de descente, de fond et de remontée est basée sur la vitesse verticale, c'est-à-dire sur le rapport entre la différence de profondeur entre deux points et la différence de temps entre ces deux points (Figure 2.9). À chaque point est donc associée une valeur de vitesse verticale. Puis pour chaque plongée, la série temporelle des vitesses verticales est modélisée à l'aide d'un polynôme de degrés 4. Le choix d'un tel polynôme autorise la présence d'une phase plateau lorsque l'animal est au fond de la plongée, ce qui n'est pas toujours le cas avec un polynôme de degrés inférieur. Après une étude de sensibilité réalisée par Yves Le Bras (données non publiées), un seuil fixé à 0,75 m.s^{-1} a ensuite été choisi pour identifier les trois phases qui constituent une plongée. Lorsque la vitesse verticale est inférieure à $-0,75$ m.s^{-1}, l'animal est considéré en descente, entre $-0,75$ et $0,75$ m.s^{-1} il est considéré au fond et au-delà de $0,75$ m.s^{-1} en remontée. Cette étape est l'objet de la fonction `dive_delim` du package `rbl` (Le Bras, 2016).

Tentative de Capture de Proies

L'identification des tentatives de captures est réalisée à l'aide d'un accéléromètre trois axes, indépendamment de sa position sur l'animal. Suivant la procédure décrite par Vacquié Garcia (2014) s'inspirant elle-même de la méthode de Viviant *et al.* (2010) développée chez les otaries, chaque axe de l'accéléromètre est filtré avec un filtre passe-haut dont la fréquence de coupure est fixée à 2,64 Hz de façon à s'affranchir de la composante liée aux mouvements de l'animal. Chaque axe ainsi filtré est ensuite réduit en calculant l'écart type pour chaque seconde. Le signal des trois axes est donc réduit à 1 Hz, où chaque valeur correspond à l'écart type d'une seconde du signal filtré. Une moyenne mobile sur une fenêtre de cinq secondes est ensuite appliquée sur chacun des axes. Enfin, un partitionnement à deux classes est réalisé sur chaque axe à l'aide de la méthode des k-moyennes[2], pour distinguer les valeurs importantes des plus faibles. Chaque valeur est ainsi catégorisée comme appartenant à une classe de valeurs importantes ou à une classe de valeurs plus faibles. L'identification d'une tentative de capture se fait lorsque sur les trois axes, les trois valeurs appartiennent à la classe de valeurs importantes. Une série continue de valeurs

[2]Plus connus sous le nom de *k-means* en anglais

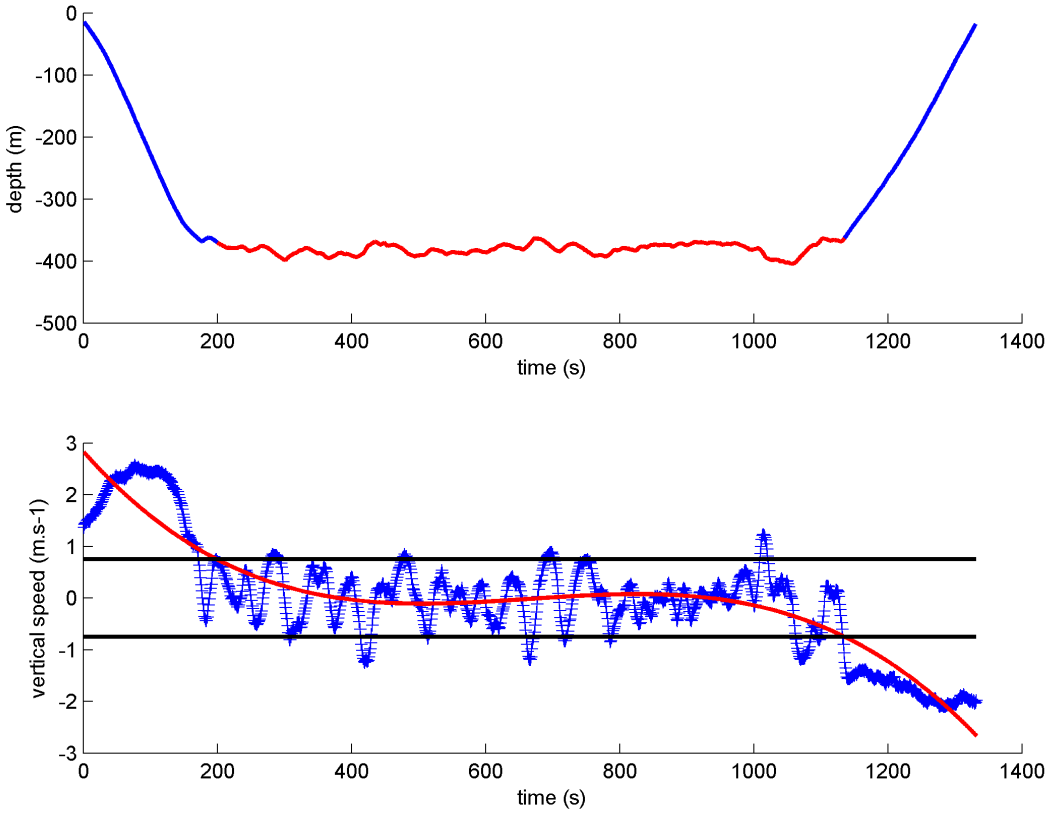

FIGURE 2.9 – Détermination de la phase de fond (en rouge sur le profil de plongée). Cette phase correspond au moment où la vitesse verticale (en bleus sur le graphique du bas), modélisée par un polynôme de degrés 4 (la courbe rouge sur le graphique du bas), se situe entre -0.75 et 0.75 $m.s^{-1}$.

identifiées comme appartenant à la classe de valeurs importantes sur les trois axes est considérée comme une seule et même capture. Autrement dit, deux tentatives de captures sont considérées distinctes lorsqu'elles sont séparées par au moins une seconde.

Effort de nage

L'effort de nage est calculé à partir de l'axe latéral, *i.e.* droite-gauche, dont la densité spectrale de puissance présente une bi-modalité marquée. Bien qu'il n'y ait pas eu de validation en bassin, nous avons présupposé que le pic identifié pour de hautes fréquences était lié aux mouvements de queue de l'animal. Compte tenu de cette hypothèse, isoler les fréquences liées à ce pic nous permet d'obtenir un signal reflétant les mouvements de queue de l'animal. Le signal d'accélérométrie est alors traité à l'aide d'un filtre passe bande, dont la résultante est utilisée pour calculer l'effort de nage. Pour cela nous avons sommé la valeur absolue des pics, censée représenter la somme des coups de nageoires de l'animal (Aoki *et al.*, 2011; Sato *et al.*, 2003). Selon la question posée, cette somme a ensuite pu être divisée par le temps de la période considérée, pour obtenir un effort de

nage par unité de temps.

Angle de plongée

Dans le cadre de cette thèse, l'angle de plongée est défini en fonction du plan horizontal. Lorsque l'animal descend, l'angle est négatif et lorsqu'il remonte, son angle de plongée est positif. L'angle de plongée est calculé en utilisant la composante statique du signal d'accélérométrie, c'est-à-dire celle liée à l'intensité de pesanteur. Cette composante est isolée à l'aide d'un filtre passe bas appliqué sur chacun des axes.

Vitesse de nage

Le calcul de la vitesse de nage n'a été possible que sur les animaux équipés d'Acousonde™, grâce aux enregistrements acoustiques. La méthode présentée ici a été implémentée sous Matlab (MATLAB 8.1; The MathWorks, Natick, MA, USA) par Alexandre Génin, lors d'un stage de césure. Fondamentalement, l'estimation de la vitesse de l'animal sous l'eau est basée sur la relation qu'il existe entre l'augmentation du bruit de fond et la vitesse verticale absolue (Fletcher *et al.*, 1996; Burgess *et al.*, 1998; Goldbogen *et al.*, 2006; Simon *et al.*, 2009). À l'échelle de l'individu, chaque enregistrement audio a été filtré à l'aide d'un filtre passe bas d'une fréquence de coupure de 110 Hz pour ne garder que le bruit de fond. Puis, seuls les enregistrements où l'animal plonge au-delà de 200 m avec un angle de descente compris en $-75°$ et $-90°$ et une accélération sur les trois axes inférieure à 1 m.s^{-2} ont été gardés. Dans cette situation, la vitesse verticale absolue (v_D, Équation 2.1) calculée à partir de l'angle de descente l'animal (β) et de sa vitesse verticale (v_z) approche sensiblement la vitesse de l'animal.

$$v_D = \frac{v_z}{sin(\beta)} \tag{2.1}$$

La relation qui lie la vitesse de descente absolue au bruit de fond est ensuite modélisée à l'aide d'une régression exponentielle (Simon *et al.*, 2009). C'est cette relation (Figure 2.10) qui est ensuite utilisée sur tout le jeu de données pour calculer la vitesse de nage pour chaque individu.

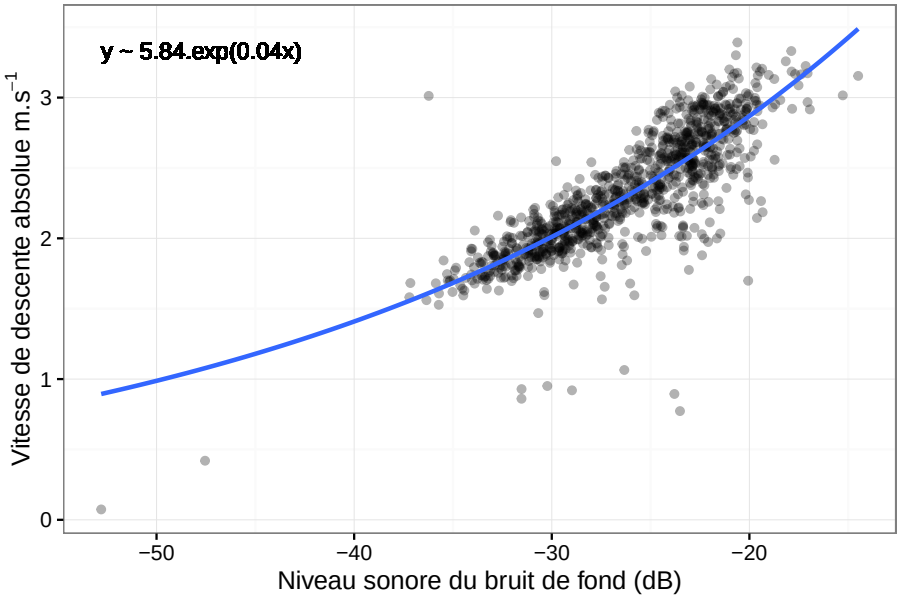

FIGURE 2.10 – Exemple de relation trouvée sur l'Acousonde A032 déployée en 2011, entre la vitesse de descente absolue et le niveau sonore du bruit de fond.

CHAPITRE 3

Three-Dimensional Assessment of Hunting Strategies in a Deep Diving Predator

Sommaire

3.1 Résumé

Introduction

Du fait des difficultés techniques à travailler sur des animaux sauvages, trop peu d'études s'attardent à étudier l'écologie comportementale des prédateurs supérieurs. C'est d'autant plus vrai lorsqu'il s'agit d'animaux évoluant en milieu marin, où la dimension verticale s'ajoute à la dimension horizontale déjà présente en milieu terrestre. Le développement de nouveaux enregistreurs de données permet aujourd'hui de reconstruire le mouvement et la trajectoire d'un animal en trois dimensions, indépendamment de l'observateur et du milieu exploré. En utilisant ces nouveaux outils et grâce à des techniques de navigation à l'estime et de classification non-supervisée, nous avons étudier les techniques de chasses des éléphants de mer, en examinant notamment la cinématique du mouvement de leur corps précédant une tentative de capture de proie.

Matériels & Méthodes

Six femelles post-reproductrices éléphants de mer ont été équipées à Kerguelen d'Acousonde™ comprenant un enregistreur temps-pression, un accéléromètre, un magnétomètre et un hydrophone. Le bruit de fond sur les enregistrements acoustiques a permis d'estimer la vitesse des animaux, pour une reconstitution de leurs plongées en trois-dimensions au plus juste, grâce aux méthodes de navigation à l'estime. L'utilisation du temps de premier passage dans une sphère sur la trajectoire reconstruite nous à permis de caractériser les zones de recherche restreinte, tandis que la donnée d'accélérométrie nous a permis d'identifier des événements de tentatives de capture. Enfin, la classification non-supervisée des données d'accélérométrie précédant une tentative de capture, nous a permis de mettre en évidence différentes approches comportementales liées à la tentative de capture d'une proie.

Résultats

Les zones de recherche restreinte ont été identifiées dans 46,4 ± 0,9 % des plongées reconstruites en trois-dimensions. L'échelle spatiale de ces zones est comprise dans une sphère de 36,6 m de rayon médian. Durant la phase de fond de ces plongées, ces zones qui représentent 36.9 ± 7.6 % du temps passé au fond, sont caractérisées par un taux de tentatives de capture de proies significativement plus élevé qu'en dehors (respectivement 1,2 ± 0,3 et 0,3 ± 0,2, Wilcoxon-Mann-Whitney *p-value* $< 0{,}01$). À l'intérieur de ces zones, trois modes d'approche d'une proie ont été identifiés :

1 Une approche à l'horizontale, très active, caractérisée par une importante sinuosité horizontale, un mouvement de roulement très important, ainsi qu'un effort de nage

élevé. Cette approche, associée à un fort taux de capture (5,7 ± 2,5 tentatives.min^{-1}), représente 56,6 % des tentatives de captures.

2 Une approche par le dessous, caractérisée par un effort de nage important et une faible sinuosité horizontale. Cette approche, associée à un plus faible taux de capture (3,6 ± 1,5 tentatives.min^{-1}), représente 10,6 % des tentatives de captures.

3 Une approche par le dessus, qui ressemble à une approche passive car l'effort de nage et la sinuosité horizontale associés sont faibles. Cette approche, associée à un faible taux de capture (3,6 ± 1,4 tentatives.min^{-1}), représente 32,8 % des tentatives de captures.

Discussion

Les zones de recherche restreinte apparaissent comme des zones où les éléphants de mer réduisent leur vitesse, mais augmentent leur sinuosité. Associé à cela, ces zones qui ne représentent qu'une petite partie du temps passé au fond, sont également associées à un taux de capture de proies plus important, ce qui suggère une agrégation de la ressource sous forme de patch, dont la densité locale de proies serait supérieure à la densité moyenne de l'environnement. L'étude à fine échelle de la cinématique du mouvement de ces animaux lors de la tentative de capture d'une proie, suggère trois modes de chasse différents, tant par le comportement de nage que par le taux de capture associé, laissant à penser que différentes proies sont chassées. Ces résultats révèlent un lien fort entre les mouvements à fine échelle des éléphants de mer et leur activité d'alimentation.

3.2 Article

3.2.1 Introduction

Movement ecology provides a conceptual framework aiming at better understanding how organisms of all kinds move, and how their movement patterns modulate essential features such as survival and reproduction of individuals, as well as the structure and dynamic of population (Nathan *et al.*, 2008). Therefore, movement can be considered as a crucial behavioral response to diverse processes such as feeding, finding mates, avoiding predators or harmful environmental conditions. Yet, the investigation of the mechanisms connecting animal movement to these key processes is limited by our ability to track animals in sufficiently high spatial and temporal resolution at which they sense and response to various environmental cues. The recent development of bio-logging technologies have significantly contributed to filling the gap in our knowledge, by relating animal movements to physiology (Butler & Jones, 1997; Génin *et al.*, 2015), physical environment (Heupel

& Simpfendorfer, 2008; Ortega *et al.*, 2009) and exploited resources (Guinet *et al.*, 2014; Kuhn *et al.*, 2015; Goldbogen *et al.*, 2015; Wilmers *et al.*, 2015; Adachi *et al.*, 2016). In this context, high-sampling frequency tracking systems and loggers deployed on wild animals made possible the recording of information that would have been impossible to get otherwise, without being restricted by visibility, observer bias, or geographic scale (Brown *et al.*, 2013).

Such studies on diving animals are important since little is known about their life history under the water compared to terrestrial animals. Indeed, while movements of terrestrial organisms are almost exclusively determined by a two-dimensional space, aquatic animals evolve in a domain that includes a vertical dimension, modifying the general approach to space use. The advances in bio-logging technologies have greatly improved the ability to monitor the behavior and movements of such animals, since it allows now to reconstruct their three-dimensional path at very fine scale using high-sampling frequency loggers (Mitani *et al.*, 2003; Laplanche *et al.*, 2015). Considering the animal's trajectory underwater in three dimensions allow to assess a level of detail that was not possible using a two-dimensional representation, *i.e.* time-depth representation (Harcourt *et al.*, 2000), in particular on the animal sinuosity (Bailleul *et al.*, 2010b). For instance, Hindell *et al.* (2002) revealed how the three-dimensional space use under ice of lactating Weddell seals (*Leptonychotes weddellii*) can influence its reproductive strategies over several consecutive breeding seasons. Narazaki *et al.* (2009) showed that loggerhead turtle (*Caretta caretta*) performed highly straight-line courses while diving, and large movement in heading at the surface that could be interpreted as direction-searching behavior. In blue whales (*Balaenoptera musculus*), Goldbogen *et al.* (2015) showed that several adaptive foraging strategies were used to maximize prey capture in different ecological contexts, depending on the required energy for manoeuvres. The use of three-dimensional tracking data associated with high-sampling frequency loggers, such as accelerometer, appears to be then relevant to investigate the foraging behavior of aquatic animals, since it allows to study the relationship between animal movement and its feeding behavior.

Therefore, tracking data analyses developed for two-dimensional data to investigate the spatial distribution of foraging effort have been adapted to three-dimensional data. Such is the case for the First Passage Time (FPT) method developed by Fauchald & Tveraa (2003) as a measure of search effort along a path. This method identifies the spatial scale and position of the area-restricted search (ARS, Kareiva & Odell, 1987), which is a fundamental aspect of movement patterns analyses. Studies that investigate the foraging ecology of a top marine predator, through both tracking and diving data, can use the FPT method by integrating the vertical dimension (Bailleul *et al.*, 2007b, 2010b; Hoskins & Arnould, 2013; Adachi *et al.*, 2016). This is the case for the approach

developed by Bailleul *et al.* (2010b) to investigate ARS in three-dimensional movements: the spherical first-passage time (SFPT). This method is similar to the FPT, except it considers both the vertical and the horizontal dimensions simultaneously, leading to the concept of time spent inside a sphere rather than a circle.

By recording a high level of detail through the biomechanics (Cooke *et al.*, 2004) and exercise science (Suzuki *et al.*, 2009), acceleration data also provide a powerful tool to investigate foraging ecology. First, accelerometers can provide an estimate of the energy expenditure based on the variation in acceleration (Halsey *et al.*, 2011 Mar-Apr). Additionally, the waveform of the signal informs on the body posture and the animal movements (Shepard *et al.*, 2008a). The movements identified using this technique can be used to construct ethograms and differentiate a range of discrete behaviors (Sakamoto *et al.*, 2009; Bom *et al.*, 2014; Berman *et al.*, 2014), by ensuring they are biologically meaningful. To date, three methods have been developed for assigning acceleration data to behavioral categories based on signal properties (Brown *et al.*, 2013). (1) The manual examination consists in detecting reference patterns and fixing thresholds (Collins *et al.*, 2015), *e.g.* mouth opening detection interpreted as prey catch attempts (Viviant *et al.*, 2010). (2) The supervised machine learning algorithms, based on algorithms which are trained on data generated from known behaviors (Nadimi *et al.*, 2008). And (3) the unsupervised machine learning algorithms (Sakamoto *et al.*, 2009; Chimienti *et al.*, 2016). This latter method presents the advantage to infer categories from the dataset itself by finding hidden structure, rather than from a labelled dataset. Considering acceleration data without prior knowledge gives the opportunity to detect in a more objective way new behaviors that no one has observed or described before (Chimienti *et al.*, 2016).

Southern elephant seals (SES) spent several months at sea after the breeding season on land. During this period at sea, several foraging habitats have been identified for the Kerguelen Islands population, depending on age and sex. Juveniles of both sexes, *i.e.* under five years old, and adult females mainly feed in the Antarctic pelagic zone (marginal sea-ice zone) and the Subantarctic zone (interfrontal zone, Bailleul *et al.*, 2007a; Ducatez *et al.*, 2008; Cherel *et al.*, 2008; Bailleul *et al.*, 2010a) on small bioluminescent fishes called myctophids (Cherel *et al.*, 2008). Once adult, isotope analyses suggest a higher trophic level for males, likely feeding on cephalopods (Slip, 1995; Daneri *et al.*, 2000).

The purpose of this study was to investigate the foraging behaviors of six post-breeding female SES by combining acceleration data analysis and three-dimensional trajectory analysis. Using the three-dimensional reconstruction of animal's path underwater, we therefore aimed at (1) determining the three-dimensional spatial scale of ARS, (2) comparing the foraging behaviors inside and outside ARS region within the dive bottom phase, and

(3) identifying hunting behaviors within an ARS, using an unsupervised classification approach.

3.2.2 Materials & Methods

Ethics Statements

The Ethics Committee of the French Polar Institute validated all scientific procedures applied on elephant seals. All animals in this study were handled and cared for in total accordance with its guidelines and recommendations.

Deployment of Devices and Data Collection

Six post-breeding female SES (mean mass = 277 ± 47 kg; mean length = 238 ± 11 cm, Table 3.1) were equipped on the Kerguelen Islands (49°20'S, 70°20'E) with an Argos-GPS satellite tag (Splash 10-F, Wildlife Computer, USA), and an autonomous acoustic/accelerometer/magnetometer and pressure logger named Acousonde™, model 3A (Acoustimetrics, Greeneridge Scences, Inc, USA). The six Splash 10-F tags were glued to the fur on the seals' heads, whereas the Acousondes™ were glued on the back of the animals on the longitudinal axis, 10 cm behind the scapula. Two animals were equipped in 2011 and the other four in 2012. Data loggers were set to collect and archive pressure every second, while tri-axial acceleration and magnetometer were sampled at 5 Hz. All sensors were calibrated by their respective manufacturers. Because sound recording requires high levels of energy consumption, Acousondes™ were programmed to record sound at a frequency of 6 kHz for three hours every 12 h in 2011 and at a frequency of 12.2 kHz for four hours every 24 h for the four individuals equipped in 2012.

Table 3.1 – Descriptive information about the six post-breeding female southern elephant seals (*Mirounga leonina*).

Seal	Body mass (kg)	Size (cm)	n days recorded	n dives	n dives with sound	Departure date	Acousonde ID
1	230	232	24	1945	227	2012-10-28	626019
2	362	235	12	409	60	2012-11-03	626020
3	282	248	4	288	46	2012-10-28	626022
4	292	225	29	1777	212	2012-11-01	626040
5	255	254	13	821	123	2011-10-26	A031
6	245	238	13	1081	211	2011-10-28	A032

The seals were captured with a canvas head-bag and anaesthetized using a 1:1 combination of Tiletamine and Zolazepam (Zoletil 100) injected intravenously (McMahon *et al.*, 2000; Field *et al.*, 2002). Data loggers were glued using a quick-setting epoxy glue (Araldite AW 2101), after the fur was cleaned with acetone. The loggers were then recovered when

female SES returned to shore to molt (*i.e.* January-February following deployments). Seals were located using their Argos locations.

Unless otherwise stated, most of our analyses were conducted using R (R Core Team, 2015). All scripts used here for data treatment and analyses are available upon request.

Diving Behavior Parameters

We consider the seal is diving when the depth exceed 15 meters. This threshold was chosen to avoid subsurface movements to be identified as dives. Each dive was then divided into three different phases: descent, bottom and ascent phases by using a vertical speed criterion chosen after a sensitivity analyses. Descent and ascent phases were characterized, as a period when the vertical speed from or towards the surface, fitted to a polynomial of degree 4, was higher than 0.75 m s^{-1} (Vacquié-Garcia, Guinet, Dragon, et al. 2015). The bottom phase refers to a period between the descent and ascent phase, where the fitted curve of the vertical speed was lower than 0.75 m s^{-1}, in absolute terms. Using a custom script, this analysis was performed with a commercial software package (MATLAB 8.1; The MathWorks, Natick, MA, USA).

Data from the accelerometers were used to calculate a swimming effort index based on stroke rate and amplitude, by using a band pass filter (lower cut-off frequency: 0.44 Hz; higher cut-off frequency: 1 Hz) on the lateral axis. The swimming effort (m s^{-2}) was then defined as the summed absolute values of the filtered lateral acceleration (Richard *et al.*, 2014; Jouma'a *et al.*, 2016). Acceleration data were also used to calculate a proxy of the energy expenditure called the vector of dynamic body acceleration, named hereafter VeDBA (Equation 3.1, Qasem *et al.* 2012). For that purpose, we used a high-pass filter with a cut-off frequency of 0.5 Hz to remove the static acceleration on each channel, and then calculated the square root of the sum of the squared of these filtered acceleration following the formula:

$$\text{VeDBA} = \sqrt{A_x^2 + A_y^2 + A_z^2} \tag{3.1}$$

Where A refers to the filtered acceleration.

Body orientation in three dimensions, *i.e.* the pitch, the roll and the heading were calculated using the `animalTrack` R package (Farrell & Fuiman, 2013) by using filtered acceleration and geomagnetism obtained with a 0.5 Hz low-pass filtering. Using the same filter for both acceleration and geomagnetism data allows us to limit the occurrence of artefacts in calculated headings (Shiomi *et al.*, 2010). Therefore, in a way to assess the animal movement in three dimensions, the circular average of the pitch as well as the circular

variance of the roll and the heading were calculated using respectively the `circ.mean` and `circ.disp` function from the `CircStats` R package (Agostinelli, 2012).

Three Dimensional Reconstruction and Speed Estimation

Knowing the depth and the orientation of the animal allows us to reconstruct the path of the animal under water (Figure 3.1a) by using the `dead_reckoning` function from the R package `animalTrack` (Farrell & Fuiman, 2013), and therefore to have a better representation of the animal's path than in two dimensions (Figure 3.1b). Such a reconstruction has to make assumptions of the animal's speed. Here, the speed of the animal has been calculated from the low frequency flow noise on the acoustic recorder (Fletcher *et al.*, 1996; Burgess *et al.*, 1998; Goldbogen *et al.*, 2006; Simon *et al.*, 2009). For each individual, the noise power was computed with a 110 Hz low-pass filter during periods under 200 m depth, with an animal's pitch between -90 ° and -75 ° and an acceleration on the three axes below 1 m s^{-2}. We used these descent periods for the speed–noise calibration because in this situation, the absolute descent speed of the seal can be easily estimated knowing the pitch and the vertical speed. We then fitted a single-term exponential curve between the flow noise (Simon *et al.*, 2009), and the absolute descent speed. This relation was used to estimate the swimming speed in any part of the dataset that includes sound recordings.

Spherical First Passage Time

SFPT has been developed in the case of three-dimensional movements to account for the vertical dimension in ARS scale identification and description (Bailleul *et al.*, 2010b). Based on FPT Fauchald & Tveraa (2003), the SFPT is defined as the time required to cross a sphere with a given radius. To determine the optimal radius of the sphere used for ARS detection, we tested different radii, range 10 - 300 m by 10 m, and visually chose the one providing the highest contrast in SFPT, *i.e.* a radius of 50 m in this study. Then we used `lavielle` function from R package `adehabitatLT` (Calenge, 2006) that performs a non-parametric segmentation on time series based on Lavielle's method (Lavielle, 2005), to finally identified ARS in SFPT time series (Figure 3.1c). To estimate the scale of an ARS, we considered the radius and the time spent inside a sphere centered on the centroid of the ARS that included 95 % of animal's position inside.

Detection of Prey Catch Attempts

Mouth opening events indicative of prey catch attempts can be detected from acceleration data (Viviant *et al.*, 2010; Naito *et al.*, 2010; Gallon *et al.*, 2013). Here we used a method derived from Viviant *et al.* (2010) and adapted by Vacquié-Garcia *et al.* (2015a) to identify rapid head movement, interpreted to be associated with prey encounter events, with a

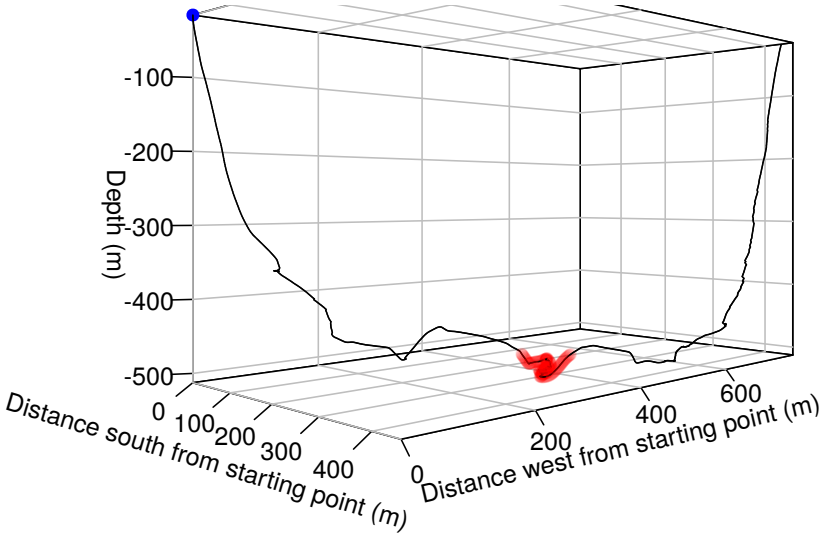

(a)

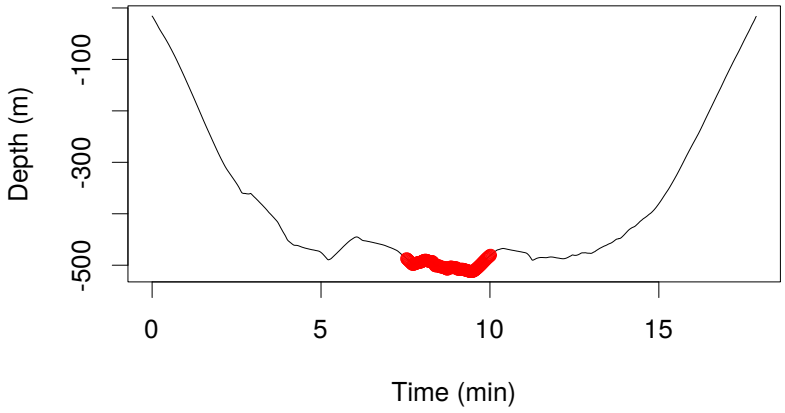

(b)

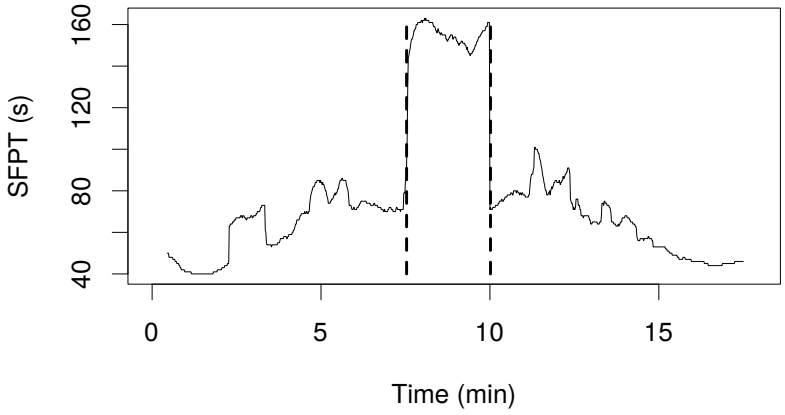

(c)

Figure 3.1 – (a) Three-dimensional trajectory of dive 994 from southern elephant seal 1, starting at the blue point (•), with an area-restricted search (ARS) identified in red. (b) The same dive in two-dimension, highlighting the necessity of using one more dimension to assess path sinuosity. (c) The spherical first passage time (SFPT) associated with this dive across time. Using the Lavielle's method, we then identified an ARS that took place, in a sphere of 37.9 m radius and where southern elephant seal 1 spent 142 s.

custom script performed with MATLAB. We first applied on the signal a high-pass filter of 2.64 Hz in order to remove noise corresponding to swimming movements. Then, a fixed window of one second was used to calculate the standard deviation every second on each channel. Signals reduced in this way were smoothed using a moving standard deviation with a five-second window size. Finally, a 2-mean clustering was performed on the final three signals. Prey catch attempt was defined as a continuous sequence of samples in which all of the three axes were classified in the high-variance cluster.

Behavioral Comparison of Foraging Effort Inside and Outside ARS during the Bottom Phase

For each SESs, in dives where ARS were detected, we calculated both proportion of prey catch attempts and the associated catch attempts rate occurring during the bottom phase, first inside and then outside ARS. We focused on the bottom phase to avoid the effect of directed movements associated with the ascent and the descent phase. Then focusing on hunting behavior, defined as the animal's behavior before prey catch attempts, the average speed, the sum of the swimming effort and the VeDBA, as well as the circular variance of the heading and the roll, and the circular mean of the pitch were calculated during the 20 s preceding the catch attempts. Using Wilcoxon-Mann-Whitney tests for paired data, we then compared averaged values for each SES of these variables inside *vs* outside ARS, since the normality assumption was not met.

Unsupervised Hunting Behavior Classification Inside ARS

To identify different hunting behaviors inside ARS, we based our classification on acceleration signal properties from the three channels by considering an arbitrary time window before prey catch attempts. We present the outputs for a 20 s time window, but a sensitivity analysis revealed a similar classification for a time window ranging from 10 to 60 s (Appendix G, Figure G.1).

The calculated signal properties were the mean, the maximum, the minimum, the skewness and the kurtosis (respectively `skewness` and `kurtosis` from moments R package Komsta & Novomestky, 2015), as well as the main frequency that composed the signal and the associated power spectral density (`pspectrum` from `psd` R package, Barbour & Parker, 2014) for each raw acceleration axis. The same parameters were calculated on acceleration data filtered with a 0.5 Hz low-pass and a 0.5 Hz high-pass filter, respectively, to retain the gravitational part of the signal, and the one due to animal's movements.

A PCA analysis was conducted to create a set of orthogonal variables. The optimal number of factors to extract from the PCA, was determined with the Kaiser's rule (Kaiser,

1960) through the `nScree` function from the R package `nFactors` (Raiche, 2010).

We finally performed an agglomerative hierarchical clustering on results from the factor analysis using `HCPC` function from `FactoMineR` R package (Husson *et al.*, 2015), by computing the Euclidian distance matrix and following the Ward's criterion. The suggested partition was the one with the higher relative loss of inertia.

Assuming each cluster is a specific hunting behavior, we described these behaviors in terms of average speed, swimming effort and VeDBA, circular average roll and pitch, circular variance of heading, and average prey capture rate during the time window of 20 s before prey catch attempts. We tested the independence of the proportion of prey catch attempts associated with each cluster, between the six southern elephant seals, using a Chi-squared test.

3.2.3 Results

Detection and Scale of ARS

The average percentage of dive with ARS (Table 3.2) was 46.4 ± 0.9 %, range: 34.1 (Seal 6) – 58.7 % (Seal 3). Overall, the scale of an ARS was similar for the six elephant seals with an average of 48.2 ± 25.7 m radius, and a median of 36.6 m (Figure 3.2a). This represents an average of 165.1 ± 109.4 s spent inside the ARS, with a median of 123 s (Figure 3.2b).

Table 3.2 – Descriptive information about area restricted search (ARS) for the six post-breeding female southern elephant seals (*Mirounga leonina*).

Seal	Time in ARS (s)	Radius ARS (m)	Proportion of dive with ARS (%)
1	131.5 ± 61.5	39.7 ± 19.9	55.5
2	138.6 ± 60.6	42.1 ± 21.8	43.3
3	176.1 ± 121.4	54.9 ± 37.9	58.7
4	182.2 ± 132.9	44.6 ± 30.9	39.6
5	230.3 ± 188.2	63.1 ± 15.9	47.2
6	131.5 ± 91.6	44.7 ± 28.0	34.1

Differences of Foraging Behaviors Inside and Outside ARS

When ARS were detected within a dive, they represented an average 36.9 ± 7.6 % of the bottom time, with an associated mean prey capture attempts rate of 1.2 ± 0.3 per minute (Table 3.3). Non-ARS represented 63.1 ± 7.6 % of bottom time for each animal, with a

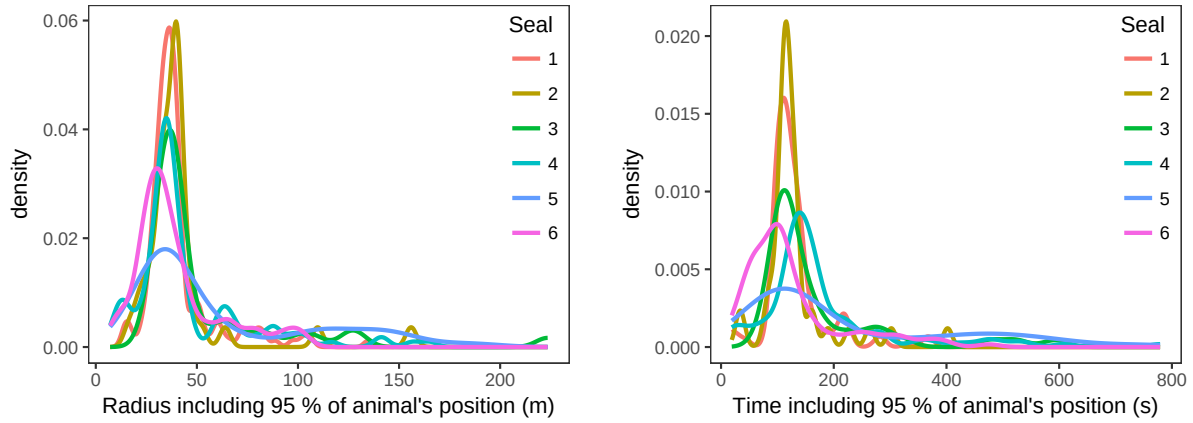

(a) The median is at 36.6 m

(b) The median is at 123 s

Figure 3.2 – Density distribution of the radius and the time for a sphere centred on the centroid of each ARS identified within the bottom phase of southern elephant seals' (*Mirounga leonina*) dive, including 95 % of their position.

significant lower mean capture attempts rate of 0.3 ± 0.2 per minute (Wilcoxon-Mann-Whitney p-value < 0.01).

Table 3.3 – Proportion of bottom time spent inside and outside area restricted search (ARS), with the associated prey catch attempts rate for the six southern elephant seals (*Mirounga leonina*).

Seal	ARS		non ARS	
	Proportion (%)	Prey catch attempts.min^{-1}	Proportion (%)	Prey catch attempts.min^{-1}
1	38.7	1.4	61.3	0.3
2	23.6	1.5	76.4	0.4
3	43.5	1.2	56.5	0.1
4	33.2	1.1	66.8	0.4
5	43.8	0.8	56.2	0.2
6	38.4	1.4	61.7	0.6

At the bottom phase of these dives, before a prey catch attempt, only the circular variance of the heading and the roll were significantly different outside and inside ARS (Figure 3.3, Wilcoxon-Mann-Whitney p-value < 0.01). Indeed, during the 20 s preceding the prey catch attempts, both parameters were higher in ARS than outside. The sum of the swimming effort and the circular mean of the pitch were not significantly different inside vs outside ARS (Figure 3.3, Wilcoxon-Mann-Whitney p-value > 0.05). We found the same result for the average speed and the sum of VeDBA, even if visual inspection tend to suggest lower values inside ARS.

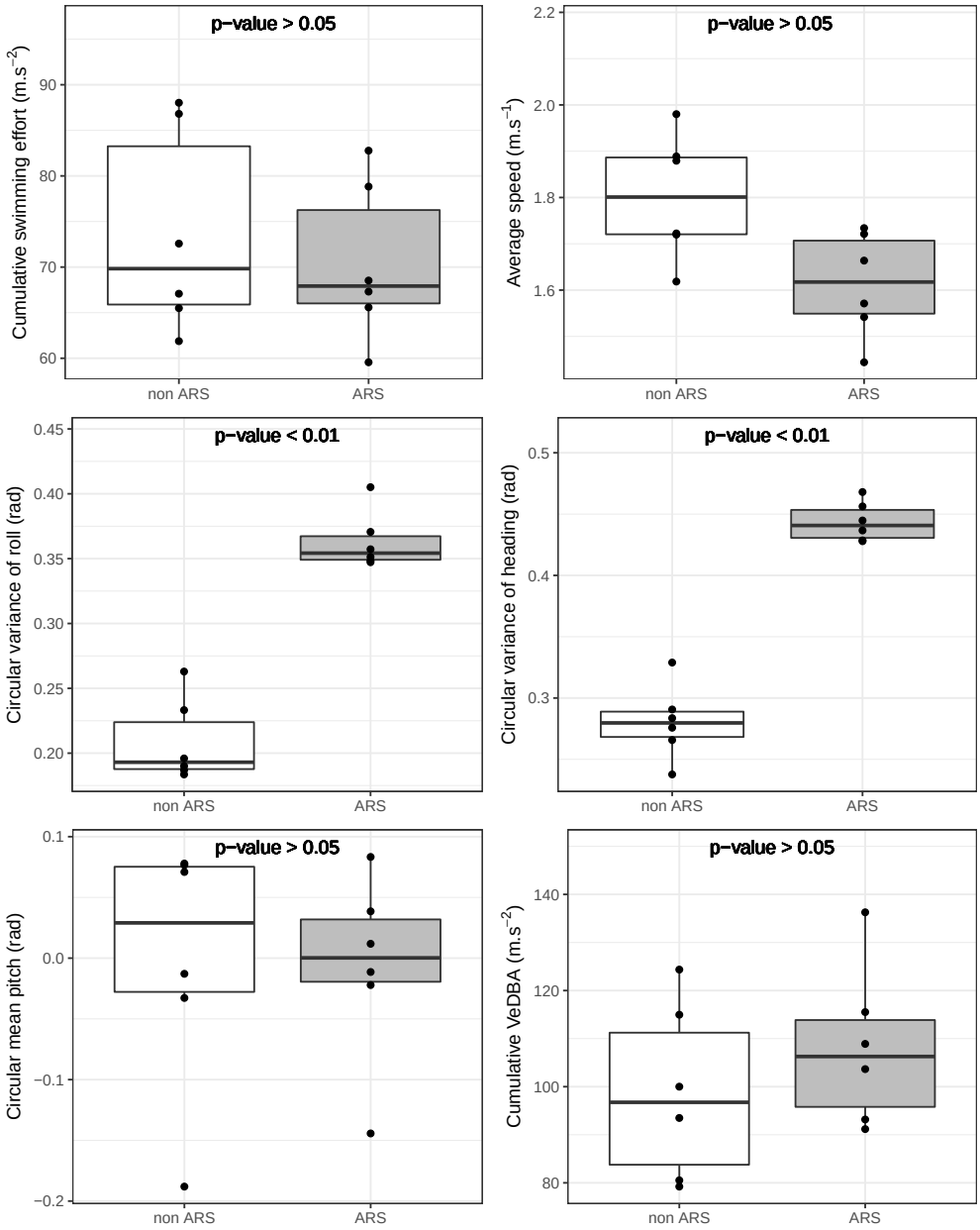

Figure 3.3 – Behavioural comparison of prey catch attempts occurring during both area restricted search (ARS) and non-ARS regions at the bottom of southern elephant seals' dive (*Mirounga leonina*; SES). The boxplots show the distribution of the average swimming effort, VeDBA, speed, pitch, the variance of heading and roll during the 20 s preceding prey catch attempts. Each point represents the average value for each SES. The p-value is the result of a median two-sample Wilcoxon test.

Characterization of Hunting Behaviors Inside ARS at the Bottom

Using the Kaiser's rule to reduce the number of variable as inputs for the classification, we only considered the first 16 component scores of the PCA (Appendix G, Figure G.2). The hierarchical clustering (Figure 3.4), through the higher loss of inertia by partitions, revealed the presence of three related clusters obtained from the factor map. High values of encounter rate associated with each cluster (Table 3.4) compared to values in Table 3.3,

result from the average of the number of catch attempts during the 20 s preceding prey catch attempts over a minute.

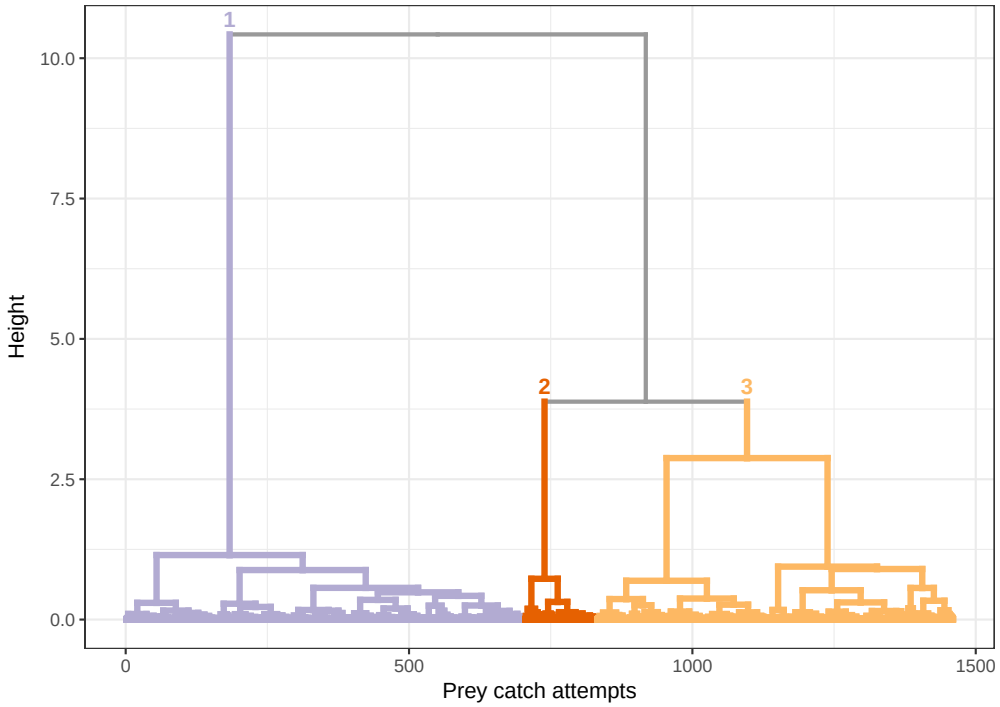

Figure 3.4 – Hierarchical clustering of prey catch attempts within area restricted search based on southern elephant seals' behavioural features during 20 s previous to captures at the bottom phase of dives. Using the higher relative loss of inertia, the partition suggested of prey catch attempts is in three groups: 1, 2 and 3.

The first cluster (n = 826, Table 4) was characterized by high values of circular variance for the heading (37.6 ± 1.2 °) and the roll (32.5 ± 1.1 °), and a circular mean for the pitch near zero degrees (-1.5 ± 2.0 °). It was also associated with a large catch attempts rate of 5.7 ± 2.5 prey catch attempts.min−1 and the highest values of VeDBA (138.2 ± 45.9 m s−2). Catch attempts contained in the second cluster (n = 155) were associated with lower but high values of VeDBA and high values of swimming effort (respectively 132.1 ± 38.8 m s^{-2} and 124.3±33.1 m s^{-2}), a circular mean for the pitch of 41.8 ± 1.9 ° and a low capture rate of 3.6 ± 1.5 prey catch attempts.min^{-1}. The last behavior associated with the third cluster (n = 479) included catch attempts with the lowest values of swimming effort (45.6 ± 27.8 m s^{-2}), a circular mean for the pitch of -12.0 ± 3.0 °, a capture rate of 3.6 ± 1.4 prey catch attempts.min^{-1} and the lowest values for VeDBA (54.8 ± 30.5 m s^{-2}).

The proportion of these three classes of hunting mode leading to prey catch attempts did not depend on individuals (Figure 3.5, Chi-squared test p-value > 0.05). The cluster 1 containing the largest proportion of catch attempts, followed by cluster 3 and cluster 2 (respectively 56.6 %, 32.8 % and 10.6 % of prey catch attempts).

Table 3.4 – Summary of the behaviour during the 20 s preceding prey catch attempts performed by six post-breeding female southern elephant seals (*Mirounga leonina*) within area restricted search, in each groups identified from the unsupervised classification (Figure 3.4). Mean values and circular mean values are respectively given ± standard deviation and circular variance.

Cluster	n	VeDBA ($m.s^{-2}$)	Swimming effort ($m.s^{-2}$)	Speed ($m.s^{-1}$)	Roll (°)	Pitch (°)	Heading (°)	Prey catch attempts.min^{-1}
1	826	138.15±45.94	80.44±26.03	1.6±0.26	32.49±1.14	-1.47±2.02	37.61±1.08	5.65±2.47
2	155	132.13±38.83	124.31±33.14	1.76±0.3	8.68±1.04	41.76±1.92	12.56±1.39	3.64±1.45
3	479	54.77±30.46	45.57±27.76	1.64±0.34	5.06±0.48	-12.04±2.97	9.65±1.03	3.61±1.43

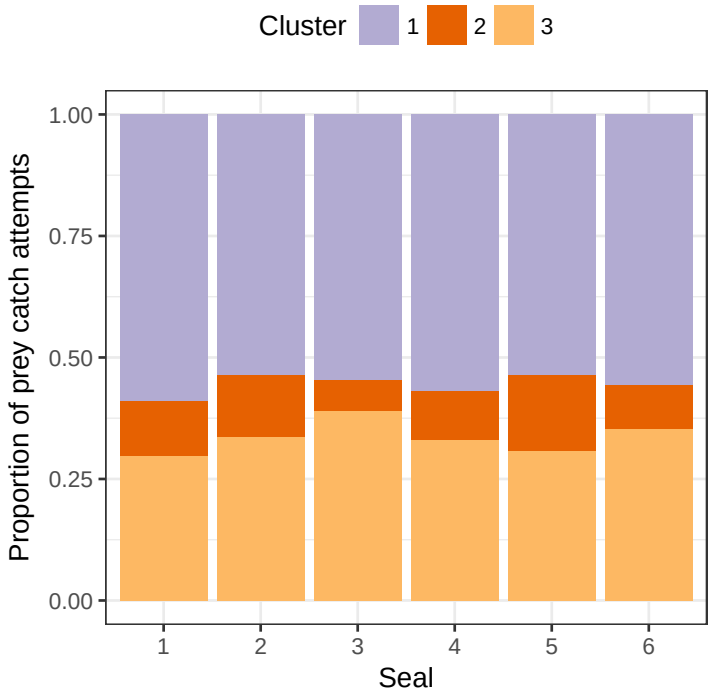

Figure 3.5 – Partitioning of prey catch attempts identified within area restricted search for six southern elephant seals, among the three groups identified through the hierarchical clustering on principle components (Figure 3.4).

3.2.4 Discussion

Path Reconstruction

Despite recent advances in the bio-logging field, still many biases have to be considered when using new tools to study marine animals' path. When predicting the position of an animal underwater, the term pseudo-track is preferred rather than track to reinforce the idea that absolute position is unknown (Hazen *et al.*, 2009). Such differentiation is crucial, as the reconstruction process relies on multiple assumptions. For instance, to simplify the reconstruction we assume that the animal frame is the same as the tag frame, which is not always the case (Laplanche *et al.*, 2015). To make a reliable estimation of the speed, we also assume that recording sound under a certain frequency is proportional to the

animal's speed due to the noise of the water flow. However, in some situations like if the seal was swimming in the current direction or moving into a position in which its head creates a depression, diminishing therefore the flow noise over the tag, this estimation can be misleading. As mentioned by Laplanche *et al.* (2015), the implementation of these approximation can have considerable impacts on the estimated track. Nonetheless, new methods based on Bayesian statistics (Laplanche *et al.*, 2015; Wensveen *et al.*, 2015) developed to compensate these approximations are time consuming and still inadequate to analyze very large sample size of dives. Therefore, dealing with a relatively large sample size of dives, we consider the method employed in our study as a likely acceptable trade-off between accuracy and processing time.

Areas of Increased Foraging Effort

A reliable estimation of the animal's track underwater is required to assess and understand the role of marine predators within their ecosystem. Because they perceive and react to the environmental heterogeneity, their reactions detected through changes in movements are usually interpreted as interaction and response to physical and/or biological changes (Gordon, 1991; Nathan *et al.*, 2008). In a foraging context, an inaccurate estimation of the scale at which animals are searching could lead to misinterpreting their response to environmental changes or disturbances. By using the SFPT (Bailleul *et al.*, 2010b) we accounted for the vertical dimension to improve movement analyses in three-dimensions. Based on tracking and diving data, this is the first study to implement this innovative method for looking at ARS in order to differentiate behavioral states, thanks to unsupervised classification. Our study revealed that SESs perform active search in an optimal sphere of 48.2 ± 25.7 m radius (Table 3.3). The smaller radii (9 and 18 m) found by Adachi *et al.* (2016) could be due to behavioral differences between both species (*Mirounga angustirostris* vs *Mirounga leonina*), or between prey targeted. In addition, the method used by Adachi *et al.* (2016) is different from ours, since they considered the radius of the sphere used to detect ARS as the actual radius of the ARS. In our study, we showed that using a sphere of 50 m radius for ARS detection allows us to detect ARS within a sphere of 36.6 m median radius (Figure 3.2a). Detected in half of the dives, our ARS represent just 36.9 % of bottom times, but due to higher prey capture rate, they represent 67.6 % of the whole prey catch attempts performed during the bottom phase of dives. Our results were consistent with those from Adachi *et al.* (2016) that most feeding events occurred in ARS zones (78 and 86 % for small and large ARS, respectively). SESs appears therefore to have higher encounter rates in small regions of the bottom phase, considered as the main foraging phase in southern elephant seals (Guinet *et al.*, 2014; Jouma'a *et al.*, 2016). These results would suggest prey aggregation, which seems to be consistent with the patchy distribution of their main prey, the myctophids (Auster *et al.*, 1992; Cherel *et al.*, 2008). However, since a substantial proportion of prey catch attempts occurred

outside ARS, *i.e.* 32.4 %, we would define a prey aggregation as an area where the local prey density is higher than the average overall prey density in the environment, and so the distribution of prey as a continuum, in which the prey density may vary locally.

Regarding swimming behaviors before prey catch attempts at the bottom level, the hunting behavior inside vs outside was different. ARS appeared to be zones with a higher swimming activity, where animals seems to reduce speed, with a significant increase of horizontal sinuosity, *i.e.* high values of circular variance for heading, and high values in the circular variance for the roll, meaning that animals tend to have a rotating movement when capturing prey (Figure 3.3). The increase of sinuosity within an ARS suggests that such behavior results from higher resource concentration as revealed in satellite tracking study in birds (Veit & Prince, 1997; Pinaud & Weimerskirch, 2005) and mammals (Haskell, 1997; Thums *et al.*, 2011). In this study, we showed that SESs increase their three-dimensional track sinuosity at the dive scale in relation to a higher prey encountered rate (Figure 3.3; Table 3.3). This is a finding consistent with the increase of both horizontal and vertical sinuosity detected in relation to the increasing number of prey catch attempts (Le Bras *et al.*, 2017).

We interpret the likely reduction of speed before prey catch attempts within an ARS as a way to improve precision by favoring specific hunting strategies over just fast swimming. During the bottom phase, the animal could capture prey on its way and alter its behavior, such as reducing speed, as a result of higher prey density. This tactic of switching from extensive to intensive search mode by regulating speed has also been found in plaice, *Pleuronectes platessa* (Hill *et al.*, 2002). Because the horizontal speed of an animal is linked to its swimming effort (Sato *et al.*, 2013), we would then expect higher swimming effort before a catch attempt outside ARS. Such a difference was not observed, and this could be due to our proxy of the speed which is known to be limited when animal's sinuosity increase, because of interference noises. Another explanation would be that SES, by reducing its speed, would reallocate energy saved in this case for rolling movements or quick direction changes, potentially responsible for the reduction in travelling speed compared to more linear tracks outside ARS. The fact that pursuing prey inside ARS seems to require more energy, *i.e.* high value of VeDBA, than chasing outside, by increasing sinuosity for instance, could be partly balanced by reducing speed. These hypotheses need, however, to be taken with caution since no significant differences in swimming speed and VeDBA were detected outside vs inside ARS (Figure 3.3). The other way SESs have to compensate for the extra energy required to chase inside ARS, would be to be more efficient inside these areas, by catching more prey.

Behavioral Classification

Techniques based on acceleration data for animal movement classification are beginning to emerge in the ecological literature (Shepard *et al.*, 2008b; Nathan *et al.*, 2012; Brown *et al.*, 2013; Collins *et al.*, 2015). An increasing number of studies have developed supervised algorithm classification, but only a few suggested using unsupervised method (Sakamoto *et al.*, 2009; Chimienti *et al.*, 2016). Here, like Sakamoto *et al.* (2009), the classification was based on k-means clustering, except that the number of clusters was estimated using hierarchical clustering on principle components. We believe that our method reduces the decision-biases associated with supervised method. This innovative method enabled to identify objectively three different clusters interpreting as hunting modes in ARS.

The first cluster is likely related to a substantial horizontal sinuosity as though SESs were chasing fishes all round them within the patch, while remaining at the same depth, *i.e.* low variability in the pitch (Table 3.4), suggesting a distribution of prey in thin vertical layer. This hunting mode agreed with findings of Le Bras *et al.* (2017) that female elephant seals were found to be more successful when foraging inside a prey patch distributed in narrow vertical layers. During this hunting mode, SESs appear to roll alternating almost from back to belly, which is not observed in any other cluster. These variations in the roll has been documented in northern fur seal (Battaile *et al.*, 2015) and sperm whales (Miller *et al.*, 2004a). In this latter case, this behavior was associated with active clicking, indicative of prey catch attempts. Here, these variations are in part responsible for the associated high-energy expenditure. Indeed, this hunting mode appeared to be the most costly in energy with the highest values of VeDBA. In addition to three-dimensional movements, this energy expenditure is also due to the swimming effort necessary to maintain these negatively buoyant animals at the same depth (Richard *et al.*, 2014). According to the associated high capture rate (almost twice higher than the others identified modes) we believed that SESs would compensate the energy required to catch these prey, which represents 56.6 % of capture attempts, by catching as much prey as possible and potentially by feeding on prey with high energy density. With their patchy distribution (Auster *et al.*, 1992) and their lethargic behavior (Barham, 1971), small myctophids, which are high energy density fishes (Lenky *et al.*, 2011) are the most plausible candidate prey.

We interpreted the second mode as an active chase, as SESs attack from below with a large swimming effort (Table 3.4). Here, the energy expenditure is almost exclusively due to the animal's stroke, as if the only purpose of the animal was to charge into prey. Depending on the depth and the prey, SES could in this case use the prey drop shadow to better target them. As the associated prey catch attempt rate was also found to be low, we hypothesized that SESs would compensate for the extra energy required to catch

fast moving prey while ascending, by favoring large prey, like squids for instance or larger myctophids species such as *Gymnoscopelus bolini*.

Finally, the last cluster reveals a passive hunting mode that would consist of catching prey from above, by gliding down on them at a relatively low angle (Table 3.4). All females were found to remain negatively buoyant during post-breeding foraging trips (Richard *et al.*, 2014), particularly during the first weeks following their departure from the colony, and therefore glide when moving down (Davis & Weihs, 2007). This attitude, while being interpreted as an energy-saving strategy, *i.e.* low values for VeDBA, could also be interpreted as opportunistic captures, by catching prey by stealth during the approach phase. In this case, the associated low sinuosity could be perceived as if SESs travelled in a straight direction, gliding down at a low angle and picking low density prey on their way.

While ARS are associated with a higher prey encounter rate, these three foraging strategies were also found to be the same outside these regions (Appendix G, Figure G.3), highlighting that hunting behavior is not dependent on the ARS mode. Presumably, areas of increasing foraging effort appear then to be contingent upon prey aggregation, revealing three-dimensional ARS regions as a way to assess the heterogeneity of resource distribution. Although we may associate different foraging strategies based on energy balance associated with each behavioral mode, it is also possible that elephant seals pursue a variety of prey and that their behavior is simply a result of pursuing different species.

Foraging Ecology

Marine ecosystems are difficult to access and to study. However, the combination of diving and tracking data from top predators can be extremely useful to improve our understanding of the role and the structure of marine resources. Following the conceptual framework of the optimal foraging theory (Charnov, 1976), predators should adjust their movements to prey encounters or environmental conditions. In a favorable environment, or when prey is encountered, predators are expected to increase their turning rate (Davis *et al.*, 1991) and decrease their speed (Patlak, 1953; Turchin, 1991), which was found in southern elephant seal (Figure 3.3; Table 3.3).

As no differences in the proportion of hunting modes were observed between individual, our results on hunting classification seem generalizable, but the small number of individuals, the short recording periods (Table 3.1) and the geographical bias (all animals went East) do not allow us to conclude at the population level. This also applies to the hunting strategies analysis, since only subsampled data from six elephant seals were used for the classification. Here, three different strategies emerge from the unsupervised

classification. One of them is associated with opportunistic attempts and represents 32.8 % of prey capture. It consists of catching prey at a lower rate, by adopting some kind of energy-saving strategy. The other two strategies are much more energy consuming, in part because of the swimming effort required for these animals to the ascent or to stay at the same depth. In addition to this effort, the energy expenditure was also found to be related to three-dimensional movement for the main hunting behaviors used in 56.6 % of the prey catch attempts. We believe the extra energy required by employing this hunting mode would be compensated with a greater number of captured prey; furthermore if these prey have higher energy density. As this strategy seems to be preferred over the others, we believe the associated energy balance (energy intake vs energy expenditure) is more favorable than the others.

These findings challenge the general assumption that elephant seals mainly adopt energy saving foraging behaviors. Based on previous studies (Richard *et al.*, 2014; Adachi *et al.*, 2014; Maresh *et al.*, 2015; Jouma'a *et al.*, 2016), we believe that SESs adopt an energy saving strategy when transiting between patches, through the minimal cost of transport (Miller *et al.*, 2012), but increase their swimming costs when actively pursuing prey. While this classification is indicative of different foraging strategies, one can consider that it may also be indicative of different prey species. Further investigations, such as these initiated by Vacquié-Garcia *et al.* (2015b) on the delineation of SESs' foraging environments defined by temperature, light level and depth or Bailleul *et al.* (2015) on the dissolved oxygen in water masses visited by SESs would be interesting to assess the distribution and the ecology of their prey.

CHAPITRE 4

Adjustment of diving behaviour with prey encounters and body condition in a deep diving predator: the Southern Elephant Seal

Sommaire

4.1 Résumé

Introduction

Les prédateurs plongeurs à respiration pulmonée sont souvent considérés comme des animaux à place centrale de part leur nécessité de remonter à la surface pour renouveler l'air de leurs poumons. Cette particularité a permis la construction de nombreux modèles comportementaux essentiellement basés sur la capacité aérobie de l'espèce étudiée. Dans ces modèles, la décision de quitter un banc de proies était donc uniquement basée sur les réserves en dioxygène de l'animal. Par simplification et en l'absence d'études caractérisant la relation entre le temps passé au fond d'une plongée et le succès de pêche, ces modèles faisaient alors bien souvent l'hypothèse que le nombre de proies rencontrées par le prédateur était proportionnelle au temps qu'il passait à en chercher. L'animal devait donc maximiser le temps passé au fond de la plongée pour maximiser son succès de pêche. Dans cette partie, nous explorons justement le lien qui existe entre le temps passé au fond d'une plongée, souvent considéré comme le temps efficace de pêche[1], et le nombre de proies qu'un éléphant de mer tente de capturer. En s'appuyant sur des modèles théoriques plus récents, nous testons différentes hypothèses quant à la décisions de quitter un banc de proies pour remonter à la surface, liées à la flottabilité de l'animal, ainsi qu'au nombre de proies qu'il a rencontrées.

Matériels & Méthodes

Pour cette étude, six femelles post-reproductrices éléphants de mer ont été équipées à Kerguelen d'enregistreurs temps-pression couplés à un accéléromètre. La donnée de profondeur nous a permis de calculer différentes variables caractérisant un cycle de plongée, comme le temps passé au fond ou le temps passé à la surface. Les données issues de l'accéléromètre nous ont quant à elles permis de calculer l'effort de nage et l'orientation de l'animal, mais également d'identifier les événements de tentative de capture. La combinaison des variables issues de ces deux enregistreurs de données, nous a aussi permis de calculer l'évolution de la densité corporelle de ces six individus au cours de leur trajet en mer. Nous avons ensuite réalisé un modèle pour expliquer les variations du temps passé au fond d'une plongée en fonction de toutes les variables liées au comportement de plongée. Ce modèle nous a ensuite servi de base pour tester notamment l'effet du nombre de proies rencontrées, de la profondeur et de la densité corporelle de l'animal sur le temps qu'un éléphant de mer passe au fond d'une plongée.

[1] Autrement dit le temps passé à rechercher de la nourriture.

Résultats

Sur l'ensemble du jeu de données, 72,6 % des tentatives de capture de proies ont eu lieu durant la phase de fond des plongées.

- À faible profondeur ($<$ 300 m), le temps passé au fond d'une plongée est plus important lorsque les éléphants de mer tentent de capturer une proie. Inversement, à de plus grandes profondeurs lorsqu'ils chassent, ces phoques ont tendance à diminuer le temps passé au fond, en lien avec une diminution de leur effort de nage. En ne considérant que les plongées où l'animal rencontre des proies, nous avons également trouvé une relation positive entre le temps passé au fond et le nombre de tentatives de capture.

- En l'absence de tentative de capture, une relation quadratique caractérisée par une augmentation suivie d'une diminution a été significativement identifiée entre la durée de la phase de fond et la profondeur. Pour les plongées présentant au moins une tentative de capture, seule une relation décroissante semble lier ces deux paramètres.

- La densité corporelle et donc la flottabilité des animaux joue positivement sur l'effort de nage ainsi que sur la durée de la phase de fond.

- Le temps passé à la surface a également pu être relié à l'effort de nage ainsi qu'à la durée de la plongée précédente.

Discussion

Cette étude suggère que pour rester dans leur limite aérobie, les éléphants de mer vont ajuster leur comportement de plongée en fonction d'un certain nombre de paramètres comme le succès de pêche ou leur flottabilité. Indépendamment de ces deux variables, la durée de la phase de fond, identifiée comme la phase d'alimentation, diminue avec la profondeur, c'est-a-dire avec le coût d'accès à la ressource. Plus l'éléphant de mer plonge profondément, plus il va s'épuiser à atteindre la ressource et moins de temps il pourra consacrer à la phase d'alimentation. Ce compromis entre phase de transit et phase de recherche alimentaire est illustré chez les plongées sans tentatives de capture. En effet, en l'absence de tentative de capture, une augmentation du temps passé au fond avec la profondeur, suivie d'une diminution est observée. La profondeur à partir de laquelle l'animal décide de réduire la durée consacrée à la phase d'alimentation, correspond à la profondeur pour laquelle le coût d'accès à la ressource devient supérieur aux coûts liés à la phase de fond. Il semble également que le temps passé au fond soit proportionnel au nombre de proies rencontrées, si et seulement si on ne considère que les plongées pour lesquelles au moins une tentative de capture ait eu lieu. Cette spécificité est importante puisque qu'en l'absence de tentative de capture, le temps passé au fond varie différemment avec la

profondeur. Autrement dit, cette étude montre que l'on ne peut pas utiliser uniquement la durée de la phase de fond pour estimer le succès de pêche d'un prédateur plongeur. En outre, cette étude révèle que la flottabilité de l'animal est un facteur important dans l'étude des variations du temps passé au fond, puisque l'on a démontré qu'elle jouait sur l'effort de nage de l'animal et donc sur le coût d'accès à la ressource.

4.2 Article

4.2.1 Introduction

Many animals are bound to a specific site which they have to return to, often for catching their prey or feeding their offspring, like seabirds returning to the colony to feed their chicks. They are thus limited to areas around this central place to find resources. This specificity leads to particular temporal and energetic constraints, due to energy expenditure to travel to and from this central place and/or a limited time available for feeding before returning to the central place (Pyke, 1984; Kacelnik *et al.*, 1986). In an aquatic environment, dives performed by air-breathing predators can be considered as a special case of the central place foraging theory (Houston & McNamara, 1985). Because they are physiologically constrained to come up to the surface to renew their oxygen supply, it induces complex decisions rule in order to optimise resource acquisition.

The number of encountered prey was generally assumed to be proportional to the time spent searching since there are few data on the quality of the patches encountered by animal. The first studies on optimal diving behaviours therefore examined strategies that maximise time spent at the foraging patch, and it was expected that the decision to end a dive was entirely based on oxygen reserves (Kramer, 1988; Houston & Carbone, 1992; Thompson *et al.*, 1993; Carbone & Houston, 1994). The main prediction of this assumption is that breath-holding divers should stay at depth as long as their oxygen store allows it. The duration of most dives was therefore expected to approach the aerobic dive limit (Thompson & Fedak, 2001), which is the dive duration at which all the usable oxygen stores have been used (Houston, 2011). However, models based on this theory were unrealistic because many species end most of their dives before reaching this limit (Costa *et al.*, 2001, 2004).

Although the diving performance of an air-breathing animal clearly depends on its physiological abilities, it was found that other factors play important roles in the decision to stay or leave a patch, such as predation risk (Heithaus & Frid, 2003), distribution, abundance, depth and energy content of the prey (Ydenberg & Clark, 1989; Thompson & Fedak, 2001; Cornick & Horning, 2003; Sparling *et al.*, 2007). Thompson & Fedak (2001)

model examined how breath-holding predators adjust their dive time budget in relation to depth and patch quality, whilst taking into account the oxygen balance. They showed that there is a net benefit to ending dives early, without fully depleting their oxygen stores, if no prey is encountered. This benefit is higher in lower density patches and reduced in the deepest dives. Thompson *et al.* (1993) showed that in deep dives, animals swim with the minimum cost of transport during the transit phase, suggesting that the costs associated with deepest dives can be minimized by behavioural mechanisms.

Animals can adjust their swimming effort finely through variations in stroke frequency and body (Sato *et al.*, 2003; Fossette *et al.*, 2010; Miller *et al.*, 2012) to reduce oxygen consumption and maximize time at depth. However, they are also affected by intrinsic parameters such as buoyancy, which is determined by body composition, and more specifically, by the percentage of adipose tissue (Crocker *et al.*, 1997; Beck *et al.*, 2000; Sato *et al.*, 2003). Several studies highlight the influence of buoyancy on different aspects of diving behaviour, such as rate of ascent and descent (Webb *et al.*, 1998; Beck *et al.*, 2000; Sato *et al.*, 2003; Adachi *et al.*, 2014). In a recent study on southern elephant seal, *Mirounga leonina* (SES hereafter), Richard *et al.* (2014) showed that, in negatively buoyant SES, 1 % variation in buoyancy resulted in a 20 % variation of swimming effort, during the ascent phase. Therefore, taking into account buoyancy appears to be essential for the prediction of the optimal diving behaviour.

This result reflects the recent development of bio-logging. Today, mouth-opening and head movement can be detected using Hall sensors (Wilson *et al.*, 2002) or accelerometers (Okuyama *et al.*, 2009; Suzuki *et al.*, 2009; Naito *et al.*, 2010; Viviant *et al.*, 2010; Naito *et al.*, 2013) to provide a set of new proxies for prey encounter rates. Furthermore, accelerometers can be also used to monitor swimming effort as well as animal posture such as pitch in water. Changes in Prey Catch Attempts (PCA hereafter) and swimming behaviour can then be monitored throughout the dive when pressure sensors are added. With these series of information (occurrence and number or history of PCA), we can indirectly assess the quality of the area visited by animals and investigate the fine-scale behavioural responses of diving predators in relation to the habitat quality.

As part of this study we investigated how a free-ranging marine predator, the southern elephant seal, adjusts its diving behaviour to recent prey encounters, distance to prey patches (depth) and its buoyancy. Knowing that time spent at the bottom of a dive corresponds to the main foraging time of SES (Guinet *et al.*, 2014) we make the following predictions:

1 Seals should first increase their foraging time with increasing distance, *i.e.* dive depth, to the foraging patch and then decrease it, whether they encounter prey or

not (Houston & Carbone, 1992);

2 In agreement with Thompson & Fedak's (2001) prediction for a given diving depth, seals should increase their bottom time when more PCA occur at the dive's bottom phase compared to when no PCA occur;

3 The amount of time the seal allocates to foraging at the bottom of their dive should be related to both its body density and to its swimming effort to catch prey as we expect that seals are more active when catching prey. Furthermore, individuals closer to neutral buoyancy should be able to allocate more time at the bottom of their dive because the round trip cost of transport is minimum at neutral buoyancy (Miller *et al.*, 2012; Adachi *et al.*, 2014), and as a consequence, the amount of energy spent by the individual and the amount of oxygen consumed are both reduced (Tucker, 1975);

4 Because oxygen is acquired at the surface with diminishing returns, *i.e.* is non-linear (Butler & Jones, 1997), recovery times increase with the duration of the preceding dive (Kooyman & Ponganis, 1998). Thus, shallow dives yield a higher net rate of oxygen acquisition and deeper dives result in a higher proportion of time spent recuperating at the surface (Kramer, 1988). To maximize the proportion of time spent in the food patch, we predict that surface time should increase with target depth (Houston & Carbone, 1992).

4.2.2 Materials & Methods

Ethics Statements

The Ethics Committee of the French Polar Institute (IPEV) validated all scientific procedures applied on elephant seals. All animals in this study were handled and cared for in total accordance with its guidelines and recommendations.

Deployment of Devices and Data Collection

We used data from six post-breeding females SES (mean mass = 309 ± 68 kg; mean length = 247 ± 17 cm, Table 4.1) equipped on the Kerguelen Islands (49°20'S, 70°20'E) with an Argos-GPS satellite tag (Splash 10-F, Wildlife Computer, USA) combined with a time depth recorder-accelerometer (TDR-MK10-X, Wildlife Computer, USA). The six Splash-10-F tags were glued to the fur on the seals' heads. In 2010, three time-depth recorder- accelerometers were also glued on the head of three different seals, with another time-depth recorder accelerometer (MK10-X, Wildlife Computer, USA) on the back of one of them. The following year, two MK10-X were deployed on the animals' backs and one on the head, again on three different seals. Pressure was sampled at 1 Hz by TDR, ±

1 % of reading. Data loggers were set to collect and archive pressure every second, while triaxial acceleration was sampled at 16 Hz.

The seals were captured with a canvas head-bag and anaesthetized using a 1:1 combination of Tiletamine and Zolazepam (Zoletil 100) injected intravenously (McMahon *et al.*, 2000; Field *et al.*, 2002). Data loggers were glued using a quick-setting epoxy glue (Araldite AW 2101), after the fur was cleaned with acetone. The loggers were then recovered when females SES returned to shore to moult (*i.e.* January-February following deployments). Seals ashore were located using their Argos locations.

All scripts used thereafter for data treatment and analysis are available upon request.

Table 4.1 – Descriptive information about the six post-breeding females SESs

Seal ID	Body mass (kg)	Size (cm)	Date departure	Days recorded	Number of dives	Number of drift dives
10A5015	377	266	11/21/2010	74	4515	90
10A5017	245	225	10/29/2011	54	3768	48
10A5019	249	240	10/31/2011	56	3707	123
10A5022	255	232	10/31/2011	58	3727	61
78524	331	266	10/28/2010	61	3361	125
78525	395	252	11/01/2010	81	4118	49

Dive Cycle Statistics

A dive cycle is defined as a dive (descent, bottom and ascent phases) followed by a period of time spent at the surface. Because there is drift over time in pressure transducers in TDR, due to different factors during a dive, a zero offset correction of depth was applied to our data set using a custom script performed with a commercial software package (Matlab 8.1, The MathWorks, Natick, MA, USA). Only dives deeper than 15 m were kept for analysis, otherwise seals were considered to be at the surface. This threshold was chosen to avoid subsurface movements to be identified as dives. Each dive was then divided into three different phases: descent, bottom and ascent phases by using a vertical speed criterion chosen after a sensitivity analyses. Descent and ascent phases were characterized as a period when the vertical speed from or towards the surface, fitted to a polynomial of degree 4, was greater than 0.75 $m.s^{-1}$. This is similar to the approach of Luque (2007) in its R package `diveMove`, but differs from most studies which determine the bottom time from the moment when a certain percentage of the maximum dive depth is achieved (Lesage *et al.*, 1999; Insley *et al.*, 2008). Here, the bottom phase refers to a period between the descent and ascent phase where the fitted curve of the vertical speed was lower than 0.75 $m.s^{-1}$, in absolute terms. Time spent at the surface is the time lapse between two

dives. This definition of the surface time results in a conservative definition of a dive, which avoids considering small subsurface excursions as dives. However it also introduces consistent overestimation of time spent loading oxygen at the surface, as it includes the periods of descent and ascent above 15m. Diving variables were calculated for each dive with Matlab, using custom dive-analysis scripts. The selected diving variables were maximum depth (m), dive duration (s), time spent during descent, bottom and ascent phases (s). Data from the accelerometers were used to estimate stroke rate (Sato *et al.*, 2003) and the intensity of the hind flipper movement, and subsequently used to calculate a swimming effort index (Equation 4.1), by using a 0.6 Hz wide band-pass centred on the second peak identified from the power spectral density.

$$\text{Swimming effort} = \frac{\sum |peaks|}{\Delta t} \tag{4.1}$$

The swimming effort ($m.s^{-3}$) was defined as the summed value of absolute acceleration peaks, $|peaks|$ ($m.s^{-2}$), over the relevant periods t (s) (Richard *et al.*, 2014). Hereafter, the total swimming effort is defined as the sum of the absolute lateral acceleration ($m.s^{-2}$) only, *i.e.* without considering effort duration. Dive angles, defined as angles from the horizontal plane, were then calculated according to Tuck (2007) by using static acceleration obtained with a low-pass filtering (cut-off frequency of 0.2 Hz) applied to the three axes (Equation 4.2).

$$\text{Pitch} = arctan\left(\frac{x}{\sqrt{x^2 + z^2}}\right) \tag{4.2}$$

Body Density

Body density variation over time was estimated according to methodology outlined by Richard *et al.* (2014). For each drift dive, a drift rate was determined by calculating the slope between depth and time using linear regression (Biuw *et al.*, 2003; Bailleul *et al.*, 2007a; Mitani *et al.*, 2010). If there were several drift dives, the drift rate was averaged by day. A model was then built to monitor these daily drift rate variations with changes in daily average swimming speed during the descent phase (Richard *et al.*, 2014). Using this relationship, variations in daily drift rate were then calculated for every daily average descent swimming speed calculated from others dives. Finally, based on the drift dives model developed by Biuw *et al.* (2003), we then used the change in drift rate to assess body density variations. This method provided us daily estimates of body density for each animal.

Patch Quality

The patch quality was assessed by considering the number of PCA per unit of time spent in the bottom phase of the dive (as detected by acceleration). PCA rate was considered to be a good proxy for prey encounter rate; we assume prey encounter rate is positively correlated with improved patch quality. Dynamic accelerations resulting from strokes and rapid head movements were extracted from the three axes with an order 3 high-pass digital Butterworth filter with a normalized cut-off frequency of 0.33 Hz (performed with `butter` function). For each axis, a fixed window of one second was used to calculate the standard deviation every second. Signals reduced in this way were smoothed using a moving standard deviation with a window size of 5 seconds. Finally, a 2-mean clustering was performed for each signal. 1 was associated with data from the higher cluster and 0 to the others. Possible PCAs occur when a 1 was found in the three axes. A continuous succession of 1 was identified as a single PCA.

Data Analysis

All statistical analyses were conducted using R (Team, 2014). Linear mixed-effects models were fit with the `nlme` package (Pinheiro *et al.*, 2013). Individuals were included as random factors and we accounted for the temporal correlation in our data using an autoregressive variance-covariance matrix (`corAR1`). Drift dives were identified using Dragon *et al.*'s (2012) method. These dives which are not thought to be foraging dives, but rather recovery dives (Crocker *et al.*, 1997), were excluded from our analyses.

A basic model including all diving variables was constructed to explain bottom time variations in order to test the effect of the number of PCA and the depth on bottom time. Basic models investigated the bottom time duration in relation to dive duration, dive angle, diving depth, and swimming effort. The animal's body density was also included to our models due to its important influence on diving behaviour. Following our preliminary analysis, three analyses were conducted: dives with PCA, dives without PCA, and all dives. For each analysis, multi-model inference was used to select the best basic model according to Akaike Information Criterion (AIC), using `dredge` from the `MuMIn` R package (Barbour & Parker, 2014).

To explore the relationship between bottom times and patch quality, the number of PCA was added to the basic model chosen. Similarly, a quadratic depth term was set as a co-variable, representing an increase, followed by a decrease of bottom time with depth, as predicted in the Houston & Carbone (1992) model. We assessed the significance of both parameters by comparing the basic model with the addition of one variable to the basic model, using an ANOVA test. To investigate the variations of bottom time with

the availability and the vertical accessibility of prey according to energy spent, a model based only on swimming effort during the bottom phase was built. This parameter was examined in relation to depth, bottom duration, body density and number of PCA.

To identify a possible change in the influence of PCA (occurrence and number of events) and body density on bottom duration and swimming behaviour according to diving depth, simple linear mixed effects models including the variable considered and the depth were fitted for every 50 m depth class, from 50 m to 1050 m. The effects of PCA and body density were assessed by the associated estimate and confidence interval (Appendix H, Table S4), which were represented on all figures by ribbon graphs.

Finally, we investigated post-dive intervals in relation to the effort expended by SESs in the previous dive, in terms of time, total swimming effort and patch quality explored. Post-dive surface intervals were found to be directly related to the number of breaths taken by SES (Génin *et al.*, 2015). All models were evaluated for surface intervals ranging between upper and lower fences (Q3 + 1.5 IQR and Q1 - 1.5 IQR) where Q1 is the lower 25 % quantile, Q3 is the upper 25 % quantile and IQR = Q3 - Q1, to remove outliers. Less than 3.4 % (n = 782) of the surface interval data (n = 23196) were excluded from the analyses at the dive scale. We focused on recovery periods likely to be related directly to the previous dive. Extended surface intervals may represent other surface behaviours, such as socializing or extended recovery periods at a multi-dive scale.

4.2.3 Results

Overall Diving Behaviour

A total of 23 196 dives were recorded from the six post-breeding females SESs: 2.1 % were drift dives; the other 97.9 % were processed to extract the number of PCA, dive angles and swimming effort. Mean dive duration was 20.7 ± 4.8 min and the maximum dive duration was 56.0 min (Table 4.2). The overall mean dive depth was 542 ± 226 m reaching up to 1318 m. PCA were detected in 89.0 % of non-drift dives. Within those dives, 14.8 % of PCA occurred during the descent phase, 12.6 % during the ascent and 72.6 % during the bottom phase (Table 4.2).

Basic Models

Although three different analyses were considered, *i.e.* situations considering all dives, dives with PCA and dives without, the global model, *i.e.* including all variables, was the most parsimonious in each situation (wAIC = 0.94, wAIC = 0.99 and wAIC = 0.62 respectively; see Appendix H, Table S1). We found a positive relationship between bottom

Table 4.2 – Main dive characteristics obtained for the six post-breeding females SESs, drift dives excluded. Mean values are given with ± s.d.

Seal ID	10A5015	10A5017	10A5019	10A5022	78524	78525
Number of dives	4425	3768	3707	3727	3361	4118
Mean dive duration (s)	1269.16±307.76	1070.61±198.45	1157.36±281.87	1190.12±212.46	1376.75±286.89	1350.54±271.27
Maximum dive duration (s)	3027	3004	2968	3114	2801	3362
Mean bottom duration (s)	758.35±243.52	458.75±216.37	571.55±239.39	502.10±270.14	573.78±346.98	792.19±329.49
Mean descent swimming effort ($m.s^{-3}$)	0.25±0.09	0.33±0.09	0.25±0.14	0.23±0.10	0.20±0.14	0.20±0.12
Mean bottom swimming effort ($m.s^{-3}$)	0.55±0.14	0.85±0.23	0.73±0.21	0.70±0.20	0.69±0.23	0.53±0.16
Mean ascent swimming effort ($m.s^{-3}$)	0.78±0.17	1.52±0.21	1.16±0.20	1.32±0.27	1.35±0.20	0.89±0.15
Mean descent angle (°)	-42.72±11.23	-51.78±11.39	-54.70±12.71	-43.92±10.50	-43.88±9.62	-34.39±9.51
Mean ascent angle (°)	52.62±14.64	71.54±7.08	69.01±9.06	63.37±11.20	46.52±14.58	53.40±13.93
Mean dive depth (m)	469±230	563±186	532±215	583±231	643±221	508±234
Maximum dive depth (m)	1318	1271	1183	1300	1188	1260
Mean number of PCA during descent phase	0.79±1.54	1.76±1.95	0.91±1.47	2.28±2.65	0.88±1.47	1.31±2.38
Mean number of PCA during bottom phase	8.88±7.33	5.66±4.65	6.62±5.22	8.10±7.98	4.43±5.12	4.53±6.05
Mean number of PCA during ascent phase	1.08±1.78	1.29±1.67	0.95±1.39	1.66±1.97	0.91±1.55	1.05±1.86
Mean surface time (s)	129.39±129.52	143.26±73.26	128.63±72.17	138.85±89.41	172.55±159.48	143.43±51.51

Table 4.3 – Relationships between bottom time and its predictors from best model chosen with parsimony (Appendix H, Table S1) in each situation and associated p-value. Covariables were dive duration (diveTime), maximum depth (mxDpth), ascent and descent angles (ascntAngl, dscntAngl), ascent and descent effort (ascntEffrt, dscntEffrt) and body density (bdDnsty)

		All dives (N=22700)		Dives with captures (N=18770)		Dives without captures (N=3930)	
Models	Parameters	Estimate	p-value	Estimate	p-value	Estimate	p-value
bttmTime ~	diveTime	266.83±0.91	<0.01	262.08±0.95	<0.01	278.34±2.14	<0.01
	mxDpth	-275.11±0.95	<0.01	-273.84±0.95	<0.01	-288.99±4.48	<0.01
	dscntAngl	-24.25±0.70	<0.01	-24.50±0.80	<0.01	-31.15±2.08	<0.01
	ascntAngl	25.48±0.74	<0.01	22.15±0.76	<0.01	49.14±2.93	<0.01
	dscntEffrt	-5.55±0.64	<0.01	-5.57±0.66	<0.01	-1.69±2.79	0.55
	ascntEffrt	15.81±0.81	<0.01	13.91±0.84	<0.01	23.95±2.73	<0.01
	bdDnsty	-3.52±1.10	<0.01	-3.15±1.06	<0.01	-1.42±4.67	0.76

time and dive duration, dive angles and swimming effort. Conversely, we found a negative relationship between bottom time and depth, swimming effort during descent phase and animal's body density (Table 4.3).

Bottom Time *vs.* Depth Related to Prey Availability & Body Density

The quadratic depth term emerged as a significant parameter in dives with and without PCA (p-value = 0.004 and p-value < 0.001 respectively; Table 4.4). However, even if the negative parameter tended to be in agreement with Houston & Carbone (1992) when considering all dives together, this variable was not significant (p-value = 0.302). In PCA dive, bottom time did not change with diving depth up to 550 m and decreased with greater diving depth. In non PCA, bottom time increased with diving depth up to 550 m and then decreased with increasing diving depth (Fig. 4.1). For both dives with and without PCA, we therefore observed a break in bottom time, followed by a decrease around 550 m depth (Fig. 4.1).

Bottom time was significantly shorter when PCA were present (Table 4.4) compared to dives without PCA in the model that considered all dives. However, when considering diving depth, SESs exhibited longer bottom durations in presence of PCA until 350 m (Fig. 4.1) Between 350 m and 750 m dives with PCA had a shorter bottom duration compared to dives without. Beyond this depth, the difference is more tenuous, *i.e.* PCA estimate closer to 0, but seals spent more time at the bottom in PCA dives (Fig. 4.1). When only dives with PCA were taken into account, bottom duration was found to be negatively correlated (p-value < 0.001) to PCA occurring in the transit phases but positively (p-value < 0.001) to those occurring at the bottom of the dive (Table 4.4). The latter pattern is significant for depths ranging between 250 and 950 m (Fig. 4.2). Outside this depth range, the number of PCA does not significantly influence the time spent at

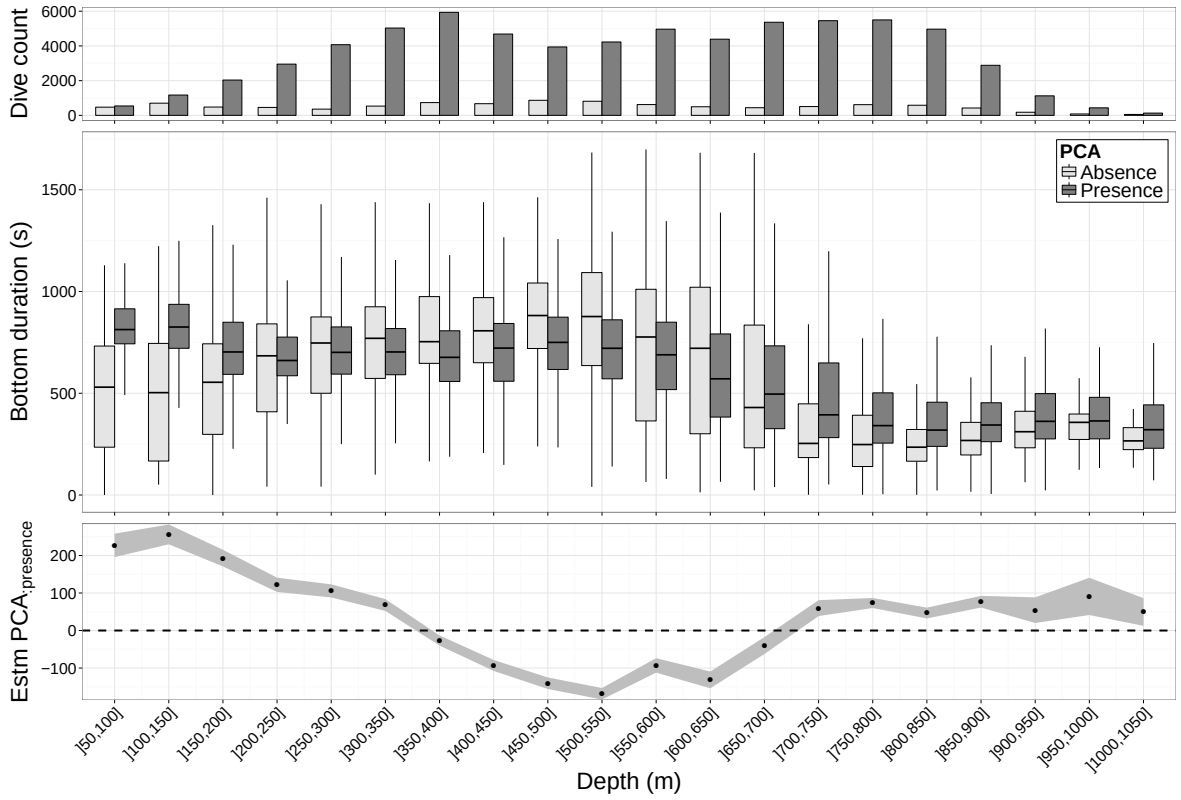

Figure 4.1 – Bottom duration related to depth and prey availability. The histogram represents the number of dives per boxplots. Between 350 and 700 m, bottom duration is less important when animals catch prey (estimate PCA:presence < 0, Appendix H, Table S4), whereas it is the opposite deeper (estimate PCA:presence > 0, Appendix H, Table S4).

Table 4.4 – Results from ANOVAs between basic models and basic models with a quadratic term of maximum depth (mxDpth2), the number of PCA (PCA count) or the presence of PCA (PCA:presence) added. For each models, the Akaike's information criterion (AIC) and the Bayesian information criterion (BIC) were calculated. For each co-variable added, the value and the standard deviation associated were calculated (Estimate) as well as the log-likelihood ratio (L.ratio) and associated p-value for each ANOVAs performed.

Models	Parameters	AIC	BIC	Estimate	L.ratio	p-value
bttmTime ∼ (All dives)	Basic model	258515.7	258603.8			
	Term added:					
	mxDpth2	258516.7	258612.7	-0.128±0.67	1.07	0.302
	PCA:presence	258489.2	258585.3	-11.55±2.31	28.49	<0.001
bttmTime ∼ (Dives with PCA)	Basic model	229518.5	229605.4			
	Term added:					
	mxDpth2	229512.1	29606.9	1.85±0.68	8.41	0.004
	Bottom PCA count	229486.5	229581.3	4.33±0.75	34.03	<0.001
	Transit PCA count	229503.7	229598.5	-2.79±0.71	16.77	<0.001
bttmTime ∼ (Dives without PCA)	Basic model	27693.1	27755.8			
	Term added:					
	mxDpth2	27683.9	27752.4	-7.46±2.75	11.17	<0.001

the bottom.

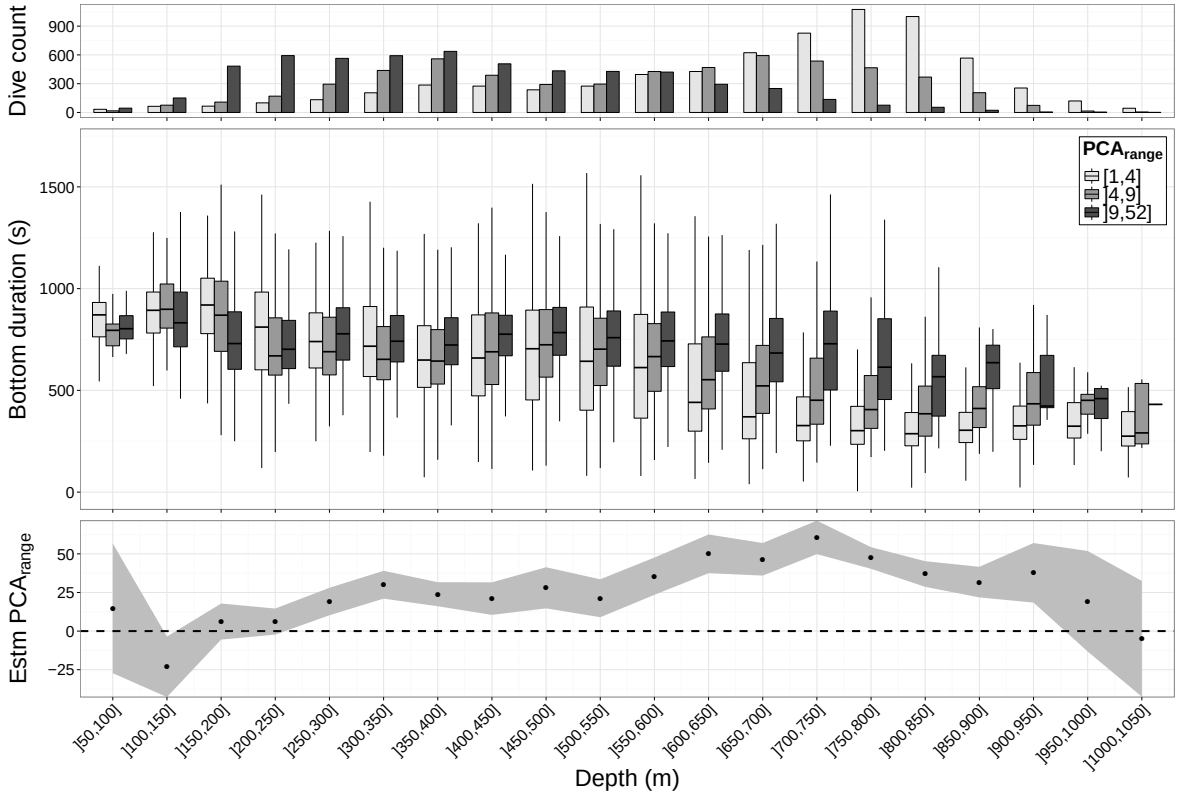

Figure 4.2 – Bottom duration related to depth and number of PCA at the bottom phase. The histogram represents the number of dives per boxplots. Below 250 m depth, bottom duration increases significantly with the number of PCA (estimate PCA:Range > 0, Appendix H, Table S4).

All seals remained negatively buoyant during the time of this study, with seal density ranging from 1036 to 1059 kg.m^{-3}. The negative relationship found in basic models between bottom duration and body density occurred at almost all depth ranges (Fig. 4.3). Apart from 50 - 250 m and between 550 - 600 m, the closer to neutral buoyancy the SES was, the longer the dive bottom duration was.

Swimming Effort *vs.* Body Density

The total swimming effort increased almost linearly with depth (Fig. 4.4). However, a shift was observed at 300 m according to seal density. At shallower depth, body density does not influence significantly the total swimming effort. At greater diving depth, seals closer to neutral buoyancy exhibit a smaller swimming effort compared to denser ones (Fig. 4.4).

The distribution of bottom swimming effort according to depth ranges showed clear

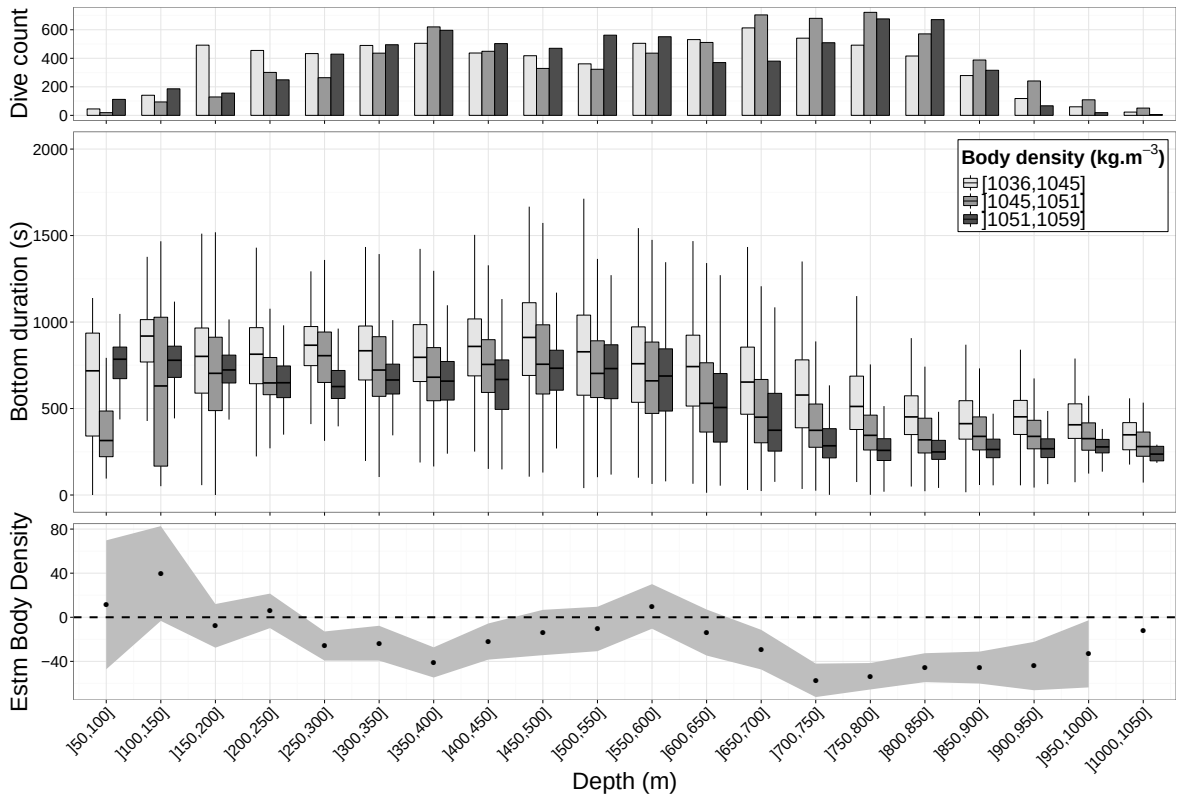

Figure 4.3 – Bottom duration related to depth and animal's body density. The histogram represents the number of dives per boxplots. Except until 250 m depth and between 450 and 650 m, the fatter a SES, the more it can spend time at the bottom (estimate Body Density < 0, Appendix H, Table S4).

differences between dives with and without PCA (Fig. 4.5; Table 4.5). Generally, swimming effort at the bottom of the dive increased when PCA were present. However, from 150 m in absence of PCA, seals clearly decreased their swimming effort at the bottom of their dive. We also found a positive relationship of the bottom swimming effort with maximum depth and body density, and a negative relationship with the bottom time (Table 4.5).

The model that considers only dives with PCA provides support for an increase of bottom swimming effort with the number of PCA, mediated by seal density (Table 4.5). In these dives, the seals swimming effort in the bottom phase was also found to increase with their body density.

A shift of the ratio of the total swimming effort at the bottom to the total swimming effort during transit phases, *i.e.* descent and ascent phases, is observed for diving depth close to 550 m (Appendix H, Figure S1). At this depth, the total bottom swimming effort becomes greater than the total transiting swimming effort. This ratio is also depending on the animal's body density (Table 4.6), which means the depth limit from which this

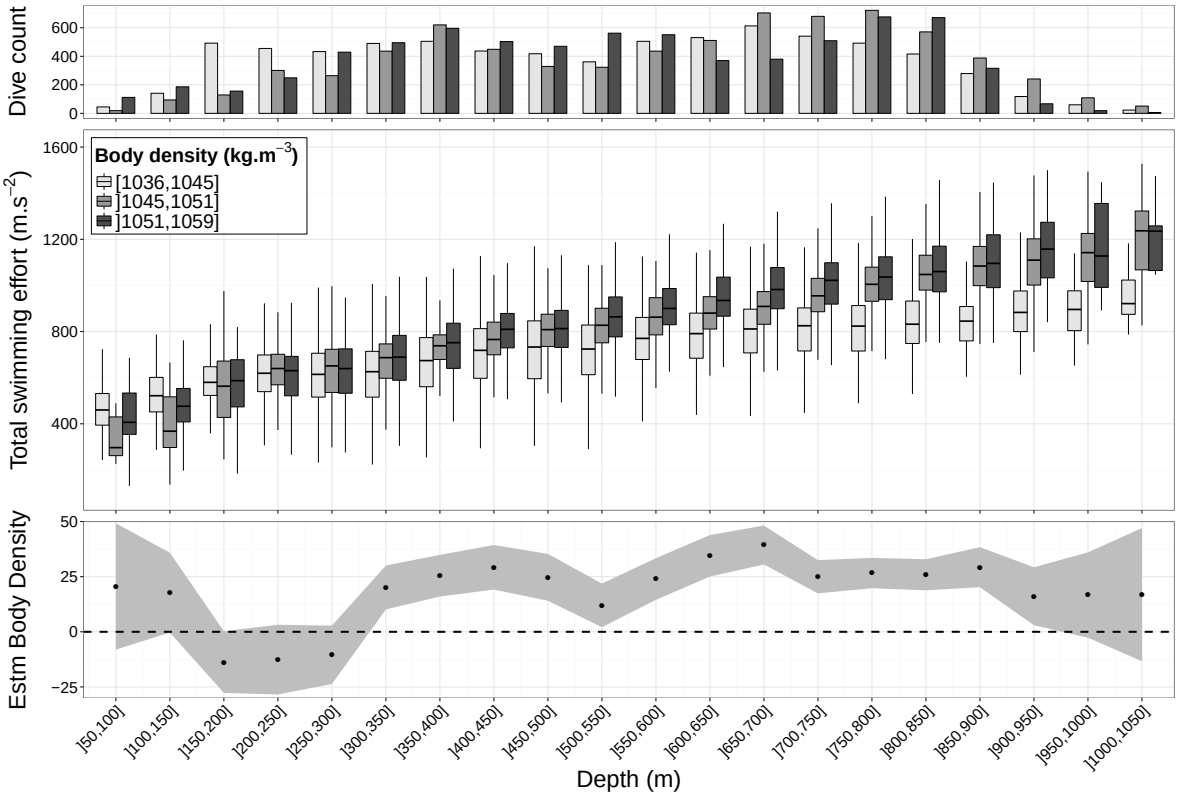

Figure 4.4 – Total swimming effort related to depth and animal's body density. The histogram represents the number of dives per boxplots. A shift is observed around 300 meters depth; denser animals must provide a higher effort below that depth (estimate Body Density > 0, Appendix H, Table S4).

Table 4.5 – Relationship for the top-ranked model of the bottom swimming effort (bttmEffrt) with bottom time (bttmTime), maximum depth (mxDpth), body density (bdDnsty), occurrence of PCA (PCA) or number of capture attempts (PCA count), depending on the situation (all dives or dives with PCA), and associated p-value

Models	Parameters	Estimate	P-value
bttmEffrt ∼ (All dives)	bttmTime	-0.11±0.001	<0.001
	mxDpth	0.05±0.001	<0.001
	bdDnsty	0.02±0.002	<0.001
	PCA:Presence	0.05±0.004	<0.001
bttmEffrt ∼ (Dives with PCA)	bttmTime	-0.12±0.001	<0.001
	mxDpth	0.02±0.001	<0.001
	bdDnsty	0.02±0.001	<0.001
	PCA count	0.05±0.001	<0.001

ratio drops below 1, *i.e.* total transiting swimming effort > total bottom swimming effort, is reached sooner for denser (550 m for a seal density ranging between 1036 and 1045 kg.m^{-3}, Appendix H, Figure S1) than lighter animals (600 m for a seal density ranging between 1051 and 1059 kg.m^{-3}, see Figure S1).

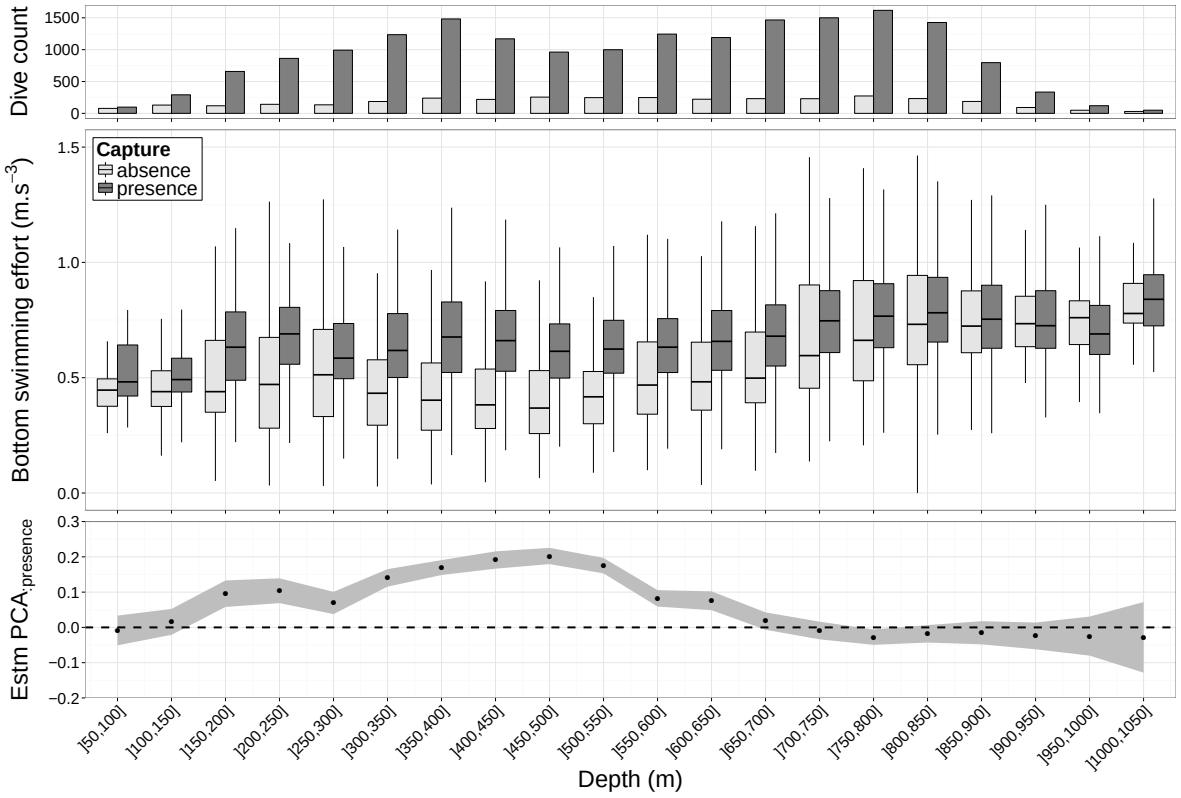

Figure 4.5 – Bottom swimming effort related to depth and prey availability. The histogram represents the number of dives per boxplots. Below 150 meters depth, bottom swimming effort is more important for dives with prey catch attempts (estimate PCA:presence > 0, Appendix H, Table S4). This difference disappears beyond 550 meters depth.

Table 4.6 – Relationship for the ratio of total bottom swimming effort to total transit swimming effort with depth (mxDpth) and body density (bdDnsty), and associated p-value

Model	Parameters	Estimate	P-value
$\frac{\text{TOTbottomEffort}}{\text{TOTtransmitEffort}} \sim$	mxDpth	-0.09 ±0.01	<0.001
	bdDnsty	-0.07±0.02	0.015

Surface Time *vs.* Effort Made

The selected model that surface intervals were best explained and positively related to the total swimming effort and dive duration (Table 4.7; wAIC = 0.73, Appendix H, Table S3). Adding PCA did not improve the model (wAIC = 0.27, Appendix H, Table S3).

Table 4.7 – Relationship for the top-ranked model of the surface time (surfTime) with total swimming effort (diveEffrt), dive time (diveTime) of the previous dive, and associated *p*-value.

Model	Parameters	Estimate	*P*-value
surfTime ~	diveEffrt	3.68±0.08	<0.001
	diveTime	2.90±0.13	<0.001

4.2.4 Discussion

Although neither the exact quantity of prey ingested, nor their quality can be assessed, the accelerometer provides a quantitative index of the number of PCA. It allows us to investigate the changes in foraging behaviour of SES females in relation to their dive patterns. This method provides an estimate of where, when and how often foraging events occurred within a dive in these free ranging marine predators. An increasing body of evidence suggests that diving predators remain within their aerobic dive limit while diving (Costa *et al.*, 2001, 2004) as the incurred costs of anaerobic dives are too high to forage efficiently (Kooyman *et al.*, 1980, 1983). Only aerobic metabolism allows frequent, repetitive dives as elephant seals do. The current study suggests that to remain within their aerobic limit, SESs optimise their diving behaviour and duration according to a number of parameters including foraging success and buoyancy.

Bottom Time & Depth

Regardless of the prey encounter events, bottom time was found to decrease linearly with depth. However, this relationship was not significant according to the quadratic polynomial relationship as predicted by Houston & Carbone's (1992), which assumes that the foraging time correspond to the bottom duration. When distinguishing dives with and without PCA, the bottom duration was found to vary according to a quadratic polynomial for non-PCA (unsuccessful) dives. Bottom time first increased then decreased with depth in non-PCA dives. In successful dives, model outcome suggests the opposite: a decrease then an increase (Table 4.4). This result must be taken with caution due the weakness of the quadratic depth term (estimate = 1.85 ± 0.68 m^2; p-value = 0.004). Bottom time remained fairly constant until the seals reached 550 m, whereupon bottom time was negatively related to increasing diving depth (Fig. 4.1). The patterns found for PCA dives were therefore consistent with studies examining behaviour of diving birds (Carbone & Houston, 1994; Cook *et al.*, 2008), where a nonlinear relationship of bottom time with depth are also found. At shallow depths, birds maintain low oxygen reserves in order to experience higher rates of oxygen intake. As dive depth increases, birds increase the size of their oxygen stores to allow more foraging time. When approaching the maximum dive duration, they decrease their foraging time at the bottom to compensate for increasing

travel time with increasing diving depth (Carbone & Houston, 1994). Our results are consistent with such a trade-off between foraging time and travel time. Beyond 550 m dive depth, depending on the seal's body density, the overall transiting swimming effort and therefore the cost to access the prey were found to exceed the swimming effort spent by the seal at the bottom of the dive (Fig. 6). This depth corresponds to the point at which bottom time starts decreasing with increasing dive depth (Fig. 4.1).

Bottom Time & PCA

Our results indicate that SES have shorter bottom times in dives when PCA occurred compared to non-PCA dives. This is true between 350 and 700 m, but not for shallower depths where bottom time was longer in the presence of PCA. For dives deeper than 700 m, there was almost no difference in bottom time between dives with and without PCA. Therefore, at shallow and greater depths our results were consistent with Thompson & Fedak's (2001) predictions. They suggest that there is a benefit to ending dives earlier when no PCA occur at shallow depths. Regardless of foraging success, seals should also maximize the bottom time for very deep dives to compensate for transit time between the surface and the dive bottom. Other empirical studies agree with other results, such as Sparling *et al.* (2007) on grey seals (*Halichoerus grypus*) and Mori *et al.* (2002) on Brünnich's guillemots, (*Uria lomvia*).

However, between 350 and 700 m our results differ from predictions. SESs were found to perform longer bottom durations when no PCA occurred. They did it by reducing their swimming effort during the bottom phase. It is unclear at this stage if the reduction in the swimming effort is either related to a searching strategy where the seal ceases to actively swim to investigate their environment using visual or auditory cues, or to a general slow descending behaviour (mainly gliding) as long as they do not encounter prey. Preliminary investigation suggests that negatively buoyant post breeding seals rely on their negative buoyancy to glide down at a low negative pitch while searching for their prey during the bottom phase of the dive. On average the end of the bottom phase was 61 $\pm$ 109 m deeper than the beginning of the bottom phase in non-PCA dives while no trends were found in PCA dives. The reduction in energy and oxygen consumption could then allow them to stay at the bottom for longer periods (Boyd, 1997; Cornick & Horning, 2003). It also provides support for the inclusion of the energetic approach to study optimal foraging in free-ranging animals. This point should be investigated further: if our interpretation is correct, we expect to observe the opposite trend in positively buoyant seals with a decreasing depth between the beginning and the end of the bottom phase in non-PCA dives.

When considering dives where at least one PCA occurred, the more PCA performed by

seals at any given bottom depth, the longer the bottom time was. This result is consistent with what Cornick & Horning (2003) found in captive Steller sea lion, *Eumetopias jubatus*. This finding provides further support for the assumption that bottom time is positively related to patch quality. When SESs perform at least one PCA during the bottom phase, bottom time increases significantly with PCA, which is also consistent with Thompson & Fedak's (2001) prediction. However, when only dive data are available, it is not possible to distinguish between non-PCA and PCA dives. Consequently, using the duration of the bottom foraging phase according to diving depth as a proxy of foraging success (Boyd *et al.*, 1995; Fedak *et al.*, 2001; Watwood *et al.*, 2006) can be seriously misleading in SES. Non-PCA dives will be detected as the most successful dives over a broad range of diving depth. While positive residuals at shallow depths (up to 350 m) are likely to be indicative of higher foraging success, higher bottom duration residuals than expected at depths ranging from 300 to 700 m are likely to be indicative of a poor foraging success. This latter pattern is consistent with what Thums *et al.* (2013) found on adult female southern elephant seals at Macquarie Island.

When PCA occurred in descent and ascent phases, SESs significantly reduced the time they spent at the bottom with increasing numbers of PCA during these transit phases. This suggests that energy expenditure increases when the seal is catching prey. This is expected to have direct consequences on the amount of time SESs are able to allocate to stay at the bottom of their dive (McConnell *et al.*, 1992).

Bottom Time & Body Density and Swimming Effort

The animal's body density, or buoyancy, was an important parameter in controlling the duration of the dive bottom phase. The three basic models (Table 4.4) provide support for a negative relationship between bottom time and body density, *i.e.* the more negatively buoyant the seals, the shorter the bottom duration. This finding is consistent with results found by Beck *et al.* (2000) that showed denser grey seals displayed shorter bottom duration compared to fatter seals. Our results are also in accordance with several other studies which show buoyancy as an important variable of diving behaviour (Webb *et al.*, 1998; Beck *et al.*, 2000; Miller *et al.*, 2004b; Richard *et al.*, 2014; Adachi *et al.*, 2014), and that the round trip cost of transport is lowest at neutral buoyancy (Miller *et al.*, 2012; Sato *et al.*, 2013). Negatively buoyant animals are assisted during descent phase by their higher density, but must swim harder during the ascent (Richard *et al.*, 2014). Williams *et al.* (2000) showed that several marine mammals used their buoyancy to adopt this energy-conserving strategy.

Seals are subjected to body compression during the whole dive, but particularly at the beginning which may explain inversions of slope for the first depth ranges (Fig. 4.4).

Complete lung collapse is supposed to occur at these depths (Kooyman & Sinnett, 1982; Falke *et al.*, 1985; McDonald & Ponganis, 2012). When their lungs are not completely collapsed, seals which are negatively buoyant but close to neutral buoyancy remain positively buoyant and should provide an overall greater total swimming effort to remain at those depths, compared to more negatively buoyant seals. The opposite relationship is found at greater diving depths, where buoyancy is almost exclusively related to body composition, *i.e.* lipid proportion: seals tending to provide higher total swimming effort when they are further from neutral buoyancy.

We found a positive relationship between the swimming effort at the bottom and the number of PCA occurring during the bottom of a dive. In other words, SESs are swimming more actively when catching prey. Seals closer to neutral buoyancy spend more time at the bottom of their dive compared to denser animals which were observed to make a greater swimming effort during the bottom phase to maintain themselves at their preferred foraging depth.

Surface Time & Diving Behaviours

Surface time is expected to vary with increasing dive duration and foraging effort in diving predators. Kramer (1988) claimed that post-dive interval should increase with depth due to the shape of the oxygen uptake function. We found that the time spent at surface replenishing the oxygen stores was positively related to dive duration and total swimming effort exerted during the previous dive. Le Boeuf *et al.* (2000) also found a strong effect of dive duration on surface time, but this was highly variable and depended on the seal studied. That variability observed could be due to the variation of the total swimming effort measured in the current study. Because dive duration and total swimming effort are both positively related to diving depth, the maximum depth reached was also found to positively influence the duration of the surface interval. Despite the fact that the swimming effort at the bottom of the dive was positively related to the number of PCA, the number of PCA itself was not found to be a significant parameter in this model. Similarly, the swimming effort is likely to be related to the seal's buoyancy, and was found to contribute significantly to the bottom duration in our study.

4.2.5 Conclusions

This study highlights the importance of using a correct metrics of foraging success to accurately reflect true foraging success. This is essential to investigate further the relationship between time spent at the bottom and prey acquisition, which is assumed by most of the optimal foraging models developed (Kramer, 1988; Houston & Carbone, 1992; Thompson *et al.*, 1993; Carbone & Houston, 1996). Finally, this study demonstrates the usefulness

of accelerometers to understand diving behaviour. Data from these highlight for the first time the combined effects of buoyancy, prey encounters and diving depth, on variations in swimming effort in a free ranging marine predator, and consequently, in the control at very fine-scale of the diving behaviours in a marine mammal.

CHAPITRE 5

Spatio-Temporal Variations in Field Metabolic Rate of Post-Moulting Southern Elephant Seals

Sommaire

5.1 Résumé

Introduction

À l'échelle d'un écosystème, connaître le bilan énergétique d'un organisme est un élément clé dans la compréhension des transferts d'énergie au sein de la chaîne trophique et entre les individus. À l'échelle individuelle, ce bilan peut être relié à des traits d'histoire de vie comme la croissance, la survie ou l'âge d'accès à la reproduction. Dans ce contexte, un individu va chercher à maximiser la différence entre l'énergie acquise par les ressources en proies et la dépense énergétique associée, afin de maximiser le gain net d'énergie allouée à la survie et à la reproduction. Déterminer ces besoins énergétiques chez les mammifères marins se révèle particulièrement compliqué de par leur comportement cryptique et leur grande aire de répartition. En se basant sur de précédents travaux reliant la dépense énergétique à un nombre de coups de nageoire, notre étude se propose d'examiner sur une période de 11 ans, les variations inter-sexe et spatio-temporelles de la dépense énergétique chez l'éléphant de mer austral en période post-mue.

Matériels & Méthodes

Huit femelles post-reproductrices éléphants de mer ont été équipées à Kerguelen d'enregistreurs temps-pression et d'accéléromètres trois axes. Grâce à la donnée d'accélération nous avons pu calculer le nombre de coups de nageoire par plongée. Nous avons ensuite construit un modèle prédictif pour expliquer le nombre de coups de nageoire par plongée en fonction de quatre paramètres : la durée de la plongée, la profondeur maximale atteinte, la durée de la surface suivant la plongée ainsi que le taux de dérive de l'animal, considéré ici comme un indice de sa condition corporelle.

Ce modèle a ensuite été utilisé pour prédire le nombre de coups de nageoire par plongées sur 107 individus post-mues (64 femelles et 43 mâles) équipés à Kerguelen entre 2004 et 2015 de balises SRDLs[1], transmettant des profils de plongées résumés (4 profondeurs par plongée). Nous avons ensuite partitionné le jeu de données en fonction de la destination des éléphants de mer (Antarctique ou autre) et des différentes phases de leur trajet en mer (aller, centrale et retour). Enfin, nous avons utilisé le nombre de coups de nageoire par plongée pour examiner les variations de la dépense énergétique moyenne, en fonction du sexe des individus, de leur destination, des différentes phases de leur séjour en mer et des années.

[1]Pour *Satellite-Relay Data Loggers*, un descriptif de ce type de balise est disponible ici 2.3.1

Résultats

Construit sur 29288 plongées d'individus post-reproducteurs, le modèle prédictif explique 60 % de la variation du nombre de coups de nageoires par plongées. 10 % de cette variation est expliquée par des changements dans la flottabilité des animaux, 20 % par la durée de la plongée, 2 % par la durée de l'intervalle de surface, 12 % pour la profondeur maximale et 16 % par de la variabilité individuelle. Appliqué sur 409531 plongées, ce modèle prédit chez les individus post-reproducteurs :

- Que les femelles ont une dépense énergétique moyenne inférieure à celle des mâles (80,9 ± 39,2 vs. 105,3 ± 13,7 kJ.kg^{-1}.d^{-1}, respectivement)
- Que la dépense énergétique moyenne de la phase aller (109,7 ± 63 kJ.kg^{-1}.d^{-1}) est plus importante de celle de la phase centrale (91,4 ± 62,1 kJ.kg^{-1}.d^{-1}), elle-même plus importante que la phase retour (82,8 ± 61,4 kJ.kg^{-1}.d^{-1}).
- Que les animaux se rendant en Antarctique ont une dépense énergétique moyenne supérieure à ceux restant sur le plateau de Kerguelen ou évoluant en milieu pélagique (108,6 ± 52,1 vs. 71,73 ± 13,7 kJ.kg^{-1}.d^{-1}, respectivement)

Ces prédictions révèlent également une variabilité inter-annuelle de la dépense énergétique, dés lors que l'on différencie la série temporelle des mâles, de celle des femelles.

Discussion

Cette étude est la première à suivre l'évolution de la dépense énergétique d'un prédateur marin sur une aussi longue période (11 ans). Elle révèle que les mâles éléphants de mer ont une dépense énergétique plus importante que les femelles, indépendamment de leur zone d'alimentation. Bien que ce résultat soit à prendre avec précaution en raison de l'absence de données sur les mâles dans la construction du modèle prédictif, les mâles semblent avoir une fréquence de coups de nageoire plus importante que les femelles. À vitesse équivalente, nos résultats suggèrent que les mâles, dont la masse peut être plusieurs fois supérieure à celle des femelles, doivent augmenter leur fréquence de coups de nageoire. Les animaux atteignant le plateau Antarctique ont également une dépense énergétique supérieure à ceux évoluant plus au Nord. Cette différence peut s'expliquer par des comportements moins coûteux en énergie pour les animaux restants au large, ou bien à une augmentation de la dépense énergétique en lien avec une augmentation de la quantité et/ou de la qualité des ressources en proies disponibles et proches de l'Antarctique. La diminution de la dépense énergétique au cours du trajet des éléphants de mer est expliquée par la diminution de la densité corporelle; les animaux se rapprochant de la flottabilité nulle à mesure qu'ils s'alimentent. Enfin, cette étude révèle que la dépense énergétique moyenne des

éléphants de mer varie avec les années en différenciant les sexes. Cette variabilité est très certainement liée au succès d'alimentation, qui lui-même est dépendant de l'accessibilité des ressources en proies.

5.2 Article

5.2.1 Introduction

To understand and to evaluate the metabolism of a species is one of the fundamental questions in ecology since it allows to link all the components of an ecosystem, from the individual to the population level (Brown *et al.*, 2004). An animal's metabolic rate determines its resource requirements, such as food (Nagy, 1987), but also life history traits as growth rate, lifespan or age at maturity (van Noordwijk & de Jong, 1986; Kozłowski & Wiegert, 1986). At the ecosystems scale, the field metabolic rate (FMR) or animal energy expenditure is a key input in the energy transfer within food webs and across individuals. Assessing these energy requirements provides a broader picture of how organisms are interlinked within an ecosystem, which is essential to evaluate their resilience to anthropogenic disturbance and rapid environmental changes.

Direct monitoring of energy requirements is quite challenging in free-ranging animals, especially for top predators which are often difficult to access. To cope with such difficulties, many studies have focused on indirect information, such as the spatiotemporal distribution of the foraging effort (Guinet *et al.*, 2001; Ainley *et al.*, 2003) or the prey distribution (Eide *et al.*, 2004; Thayer & Sydeman, 2007). The balance between energy expenditure and energy intake drives many aspects of the physiology, biology, and ecology of organisms, affecting therefore their reproduction and survival (Magni *et al.*, 2000; Stubbs & Tolkamp, 2006). While these information are challenging to get for terrestrial animals, it is even more complicated for marine animals since they widely disperse in a three-dimensions habitat.

Deep diving marine mammals require high energy demands in response to high hydrostatic pressure and cold temperatures (Seibel & Drazen, 2007). To keep the energy balance positive, the energy intake has therefore to exceed the foraging cost. This can be done by several behavioural adaptations like swimming at the minimum cost of transport speeds (Miller *et al.*, 2012), adopting a burst-and-glide strategy (Williams *et al.*, 2000), or targeting specific depths (Williams, 1989; Mori, 1998). By adjusting their diving behaviours in such a way, air breathing marine mammals should maximize the difference between the energy expenditure, and the energy intake. The foraging cost can thus be considered as one way to reflect the energy demands through the cost of transport, and

the cost of chasing and capturing prey (Elliott *et al.*, 1977; Shipman & Walker, 1989; Gorman *et al.*, 1998; Carbone *et al.*, 2007).

As a central place forager, the southern elephant seal, *Mirounga leonina* (SES hereafter), comes ashore twice a year, once for the reproduction and once for the moult. Right after this second period ashore, embryos are released from diapause and implantation occurs (Gibbney, 1953). During this period, a significant change in the energy balance could then have serious consequences on the survival of the embryo. Keeping a positive energy balance during the post-moulting period appears therefore to be a key component for the allocation of more energy to survival but also to reproduction, resulting in the enhancement of the population's fitness (Costa, 2012).

The use of even more efficient data loggers made it possible to get precious information on both the energy expenditure and the energy intake in wild animals (Charrassin *et al.*, 2001; Wilson *et al.*, 2002, 2006). In SES, the use of accelerometers has eased the acquisition of information on the swimming effort (Richard *et al.*, 2014; Jouma'a *et al.*, 2016), the foraging effort in term of prey catch attempts (Gallon *et al.*, 2013; Vacquié-Garcia *et al.*, 2015b) and the animal's body density (Aoki *et al.*, 2011; Richard *et al.*, 2014; Adachi *et al.*, 2014). Despite the large deployment of accelerometers over the past decade, the number of studies focusing on the energy expenditure over the post-moulting trip of this species is very limited. The only studies that tempted to monitor changes in the energy expenditure over the post-moulting period used the number of flipper stroke calculated from acceleration data as a proxy of the FMR in northern elephant seals, *Mirounga angustirostris*, (Maresh *et al.*, 2014, 2015). While the acceleration data recording duration are not mentioned in these studies, the estimation of the energy expenditure is usually restricted to the post-breeding period at sea (Carlini *et al.*, 2005; Richard *et al.*, 2014), as the high-resolution dataset required to estimate such parameter can usually not be recorded during the whole post-moulting season due to battery limitation. One way to estimate the energy expenditure for post-moulting dives without the acceleration data, is therefore to build a predictive model on post-breeding dives of the energy expenditure, derived from the acceleration data, and then uses it to predict on post-moulting dive.

In this context, we used high resolution datasets (time-depth and acceleration) from 8 post-breeding SESs to examine how to best predict variations in the number of flipper strokes, from low-resolution based dive metrics and buoyancy changes. Using this model, we first predicted the number of flipper strokes on the low-resolution dives of 107 post-moulting SESs over an 11 years' period (2004-2015). Then, using the Maresh *et al.* (2014) equation relating the number of flipper strokes to the energy expenditure, we tested if the energy expenditure in post-moulting SESs' dives varies in space, time and among sex.

5.2.2 Materials & Methods

Ethics Statements

The Ethics Committee of the French Polar Institute validated all scientific procedures applied on elephant seals. All animals in this study were handled and cared for in total accordance with its guidelines and recommendations.

Animal Tagging

The seals were captured with a canvas head-bag and anaesthetized using a 1:1 combination of Tiletamine and Zolazepam (Zoletil 100) injected intravenously (McMahon *et al.*, 2000; Field *et al.*, 2002). Data loggers were glued using a quick-setting epoxy glue (Araldite AW 2101), after the fur was cleaned with acetone. The loggers were then recovered when female SES returned to shore to moult (*i.e.* January-February following deployments). Seals ashore were located using their Argos locations.

Biological Data Collection

Post-breeding Dataset We used a first dataset composed of 8 post-breeding females equipped on the Kerguelen Islands (49°20'S, 70°20'E), in 2010 (n = 3), 2011 (n = 3) and 2014 (n = 2) with SPLASH-10 and TDR-MK10-X (Wildlife Computers). SPLASH-10 loggers archive sampled dive depth at every second, while locations are transmitted directly via the Argos system. TDR-MK10X includes a time-depth recorder sampling at 1 Hz, and a 3D accelerometer, sampling acceleration at 16 Hz. Both data were stored in the logger's memory meaning the tag needs to be recovered to retrieve them.

Post-moulting Dataset The second dataset was composed of 107 post-moulting SESs (64 females and 43 males) also equipped on the Kerguelen Islands of satellite-relay data loggers [SRDLs; Sea Mammal Research Unit (SMRU) Instrumentation, St Andrews, UK] as part of the MEMO Observatory (`http://www.insu.cnrs.fr/node/4125`) between 2004 and 2015. The SRLDs recorded high-resolution time-depth profiles at 2 s intervals before being resumed using a broken-stick algorithm on-board which reduced the data to four at-depth and two surface dive inflection points (Fedak *et al.*, 2001; Gordine *et al.*, 2015). The abstracted data were then compressed and relayed via the Argos satellite system (Fedak *et al.*, 2002; Argos, 2011).

Unless otherwise stated, most of our analyses were conducted using R (R Core Team, 2015). All scripts used below for data treatment and analyses are available upon request.

Parameters Calculation

General Approach As body density changes are important in the energy balance of elephant seals, we based our predictive model of the number of flipper strokes (from post-breeding dives), on dive metrics and buoyancy changes. Dive metrics were calculated from high resolution dataset for post-breeding dives, and directly transmitted for post-moulting dives from SRDLs tags. To calculate buoyancy changes in the same way for post-moulting and post-breeding dives, we degraded the high-resolution post-breeding dataset to be equivalent to the low-resolution post-moulting dataset (four depth records per dives). Using the same method, we then calculated a proxy of the daily body density changes in both low-resolution datasets (the post-moulting one and the degraded post-breeding one). We were therefore able to build a model on post-breeding dives that will be used to predict on post-moulting dives.

Diving Parameters Dive metrics of low resolution dataset were directly transmitted for post-moulting dives from SRDLs tag, *i.e.* post-dive surface interval, dive duration and the maximum depth (Fedak *et al.*, 2001). For high-resolution dataset of post-breeding dives, data were processed using the `rbl` R packages available on GitHub (`https://github.com/SESman/rbl`). Basically, we applied an offset correction of depth measurements to account for the drift that occurred over time, through the `offset-correction` function. Dives were then identified when deeper than 15 metres using `dive_delim` function. This threshold was used to avoid subsurface movement to be considered as dives.

Proxy of Buoyancy Changes To calculate buoyancy changes in the same way for post-moulting and post-breeding dives, we degraded the high-resolution post-breeding dives to be equivalent to the low-resolution post-moulting dives based on Heerah *et al.* (2015) through the `brokenstick` function in the `rbl` R package (Le Bras, 2016). Using the method developed by Gordine *et al.* (2015), we then calculated daily values for the drift rate considering only the segment 2, 3 and 4 of each dive. We then calculated the vertical speed associated with each of these segments. We removed any segments with a zero vertical speed, those with an absolute vertical speed higher than 0.6 $m.s^{-1}$, and those shorter than 40 % of the dive duration. To avoid keeping "U"-shaped dives, we calculated for each dive the ratio between the actual dive area (defined in the same way as Fedak *et al.*, 2001) and the rectangle defined by the maximum depth and the dive time. We preferred this metric to the time allocation at depth index (Fedak *et al.*, 2001) to avoid the arbitrary choice of the animal's speed. We finally kept segments for which this ratio was below 0.75. With the set of remaining segments, we took the daily median of their vertical speed as a proxy of daily changes in buoyancy. This proxy was then modelled using a constrained beta spline (Ng & Maechler, 2007) with the `cobs` function from the R package of the same name (Ng & Maechler, 2015). To reduce the effect of noise in the

data but also to get the trend over the whole trip at sea, the maximum number of knots was set to five. These knots were generated using the quantile method with a level fixed at 80 % (Gordine *et al.* (2015) fixed this level at 20 %, but their definition of the vertical speed was the opposite than ours, which finally results in the same level).

Count Flipper Strokes The number of flipper stroke was obtained from accelerometers deployed on post-breeding animals. For each animal, we randomly select 50 dives over their whole trip at sea. Then using a band-pass filter on the lateral axis, we only kept frequencies including the second peak observed on the power spectral density. To automatically detect the low and high cut-off frequency on the power spectral density (Appendix I, Figure I.1), we used the segmentation of Lavielle on time series (`lavielle` function in the `adehabitatLT` R package, Calenge 2006). The minimum number of observations in each segment was set to 1000 values, with a maximum number of segments of five, and a contrast function based on the variance. The third segment identified was the one related to the animal's stroke, since it overlapped the second peak. This segment was characterized by a minimum and a maximum frequency defined then as the low and high cut-off frequency of the band-pass filter used to isolate frequencies due to animal's flipper stroke. The remaining peaks on the filtered signal with an amplitude greater than a threshold were considered to be flipper strokes and so used in our analyses as a proxy of energy expenditure (Maresh *et al.*, 2014, 2015). Contrary to Maresh *et al.* (2014, 2015), this amplitude threshold was defined for each animal as the quantile 0.5 of the absolute amplitude associated with each flipper stroke.

We believed that counting flipper stroke based on a filter and a threshold calculating at the individual level allows us to partly take into account for small differences in accelerometer placement during attachment, and inherent differences between seals.

Predictive Model

To predict the number of strokes performed in each post-moulting dives, we built a predictive model on post-breeding dives of the count flipper stroke with the post-dive surface interval (srf_inter), the dive duration (dv_dur), the maximum depth (max_depth) and a proxy of the buoyancy (buoyancy_proxy) as explanatory variables. To get the overall variation of the body density during a complete trip at sea, we only selected post-breeding animals that remained at least one month (31 days) at sea. All the variables considered in our models were previously tested for collinearity (Zuur *et al.*, 2010), and revealed a variance inflation factor below 3. Because the script used to identify dives in post-breeding animals may have missed some of them, some estimated surface intervals were unusually long. Based on the histogram of the surface interval, only the dives associated with a surface interval below 350 s were therefore retained (Appendix I, Figure I.2). To reduce

the influence of autocorrelations in our data, we subsampled our dataset by taking one dive every 20 dives per individual.

We then used the `bam` function from the `mgcv` R package to perform a generalized additive model (Wood *et al.*, 2015), with the individual as a random intercept and a Gaussian distribution. As we wanted the best fit, we allowed for each smooth a degree of freedom up to 20. Models used further could be specified as:

Count flipper stroke $\sim$ alpha + s(dv_dur, k = 20) + s(srf_inter, k = 20) + s(max_depth, k = 20) + s(buoyancy_proxy, k = 20) + s(id, bs = "re")

where *s()* indicated a smooth function based on natural splines, *k* the number of degrees of freedom allowed and *bs* a way to specify a random intercept (Wood, 2016).

Analyses

Data Partioning To explore the variability in the average energy expenditure per dive, we separated animals that went to Antarctica, *i.e.* below -60 ° of latitude, from the others. For the same reason, each trip was segmented into three phases: the outward, the central and the return phase. The central phase was defined as any position located at a distance longer than 80 % of the maximum distance from the departure location. This threshold was chosen after visual inspection of the relation between the distance from the coast and the time spent at sea (Appendix I, Figure I.3). The outward phase was defined from the first location to the first one of the central phase, and the return phase from the last one of the central phase to the last one of each animal's track.

Average Energy Expenditure Variability The average energy expenditure per dive (in J kg^{-1} s^{-1}, noted FMR hereafter, Equation 5.1) was then calculated using the (Maresh *et al.*, 2014) equation for all post-moulting dives:

$$\text{FMR} = \frac{2.58.S_n}{\text{Dive duration}} \tag{5.1}$$

where S_n is the predicted value of the number of flipper strokes per dive, for post-moulting dives.

A linear mixed-effects model was fitted using the `nlme` package (Pinheiro *et al.*, 2013) to explore the variability of FMR in relation to four parameters: the destination (Antarctica or others), the trip phase (outward, central or return), the sex and the year. Individuals were included as random factors, and we accounted for the temporal correlation in our data by taking one dive every 20.

Table 5.1 – Overall information on animals post breeding animals used in the predictive model. Mean values are given with ± sd.

id	*n* days	*n* dives	Departure date	Dive duration (s)	Surface interval (s)	Dive depth (m)	Stroke count per dives
2010-18	60	2544	10/28/2010	1420.67 ± 259.96	159.49 ± 29.99	645.99 ± 199.17	715.71 ± 174.86
2010-19	69	3288	11/05/2010	1368.87 ± 253.64	139.71 ± 20.62	512.83 ± 227.18	959.62 ± 224.05
2010-21	72	3546	11/22/2010	1300.68 ± 281.31	120.56 ± 21.80	482.19 ± 207.33	879.00 ± 212.21
2011-21	53	3306	10/29/2011	1081.04 ± 194.89	137.67 ± 21.71	566.84 ± 179.61	659.60 ± 124.97
2011-26	58	3290	10/31/2011	1191.97 ± 208.16	133.28 ± 21.67	568.56 ± 226.85	806.83 ± 164.93
2011-28	55	3212	11/01/2011	1168.79 ± 276.95	121.04 ± 17.27	523.87 ± 204.98	827.92 ± 193.61
2014-22	79	5625	10/29/2014	963.91 ± 288.46	107.17 ± 19.91	359.78 ± 148.05	647.84 ± 191.07
2014-23	73	4477	10/29/2014	1054.5 ± 240.82	128.25 ± 14.77	477.12 ± 128.38	782.03 ± 162.81

To investigate further inter-annual variability of the FMR, we performed a Kruskall-Wallis test considering independently male and female. To account for the high variability in the FMR at the individual level, the median was chosen rather than the average of FMR per individual.

5.2.3 Results

Predictive Model

General Results Among the eight post-breeding female elephant seals used to build the predictive model, an average of (mean ± sd) 3661 ± 955 dives were recorded per individual, for a total 29288 dives. The females spent 65 ± 10 d at sea (Table 5.1), diving at an average maximum depth of 517 ± 84 m. They spend on average 130.9 ± 15.68 s at the surface between two consecutive dives, and dove during 1193.8 ± 159.97 s.

The predictive model was applied on 107 post-moulting SESs, representing a total of 409531 dives, with an average of 3828 ± 1790 dives recorded per individual (Appendix I, Table 1). These animals spent 204 ± 56 d at sea, and 128 ± 22 s at the surface between two dives. They dove during 1631 ± 340 s at an average maximum depth of 424 ± 110 m.

Power Predictive and Residual Diagnostic The predictive model accounted for 60 % of the deviance, with 16 % of the deviance explained by the individual random effect only (Table 5.2). Our proxy of the buoyancy changes explained 13 %, and the dive duration 20 %. The distribution of residuals is a bit shifted towards positive values, with a heavy tail for negative values, compared to a Gaussian distribution (Figure 5.1). An increase of the number of strokes per dive was found with an increase of the dive duration and the maximum depth, and a decrease with the post-dive surface interval and the body density (Figure 5.2).

Table 5.2 – Percent of deviance explained by each term of the predictive model: stroke count ∼ alpha + s(dv_dur, k = 20) + s(srf_inter, k = 20) + s(max_depth, k = 20) + s(buoyancy_proxy, k = 20) + s(id, bs = "re")

	Covariates	Percent of deviance explained (%)
Stroke count ∼	Dive time	20
	Surface interval	2
	Max depth	12
	Drift rate	10
	Random(individual)	16
Total		60

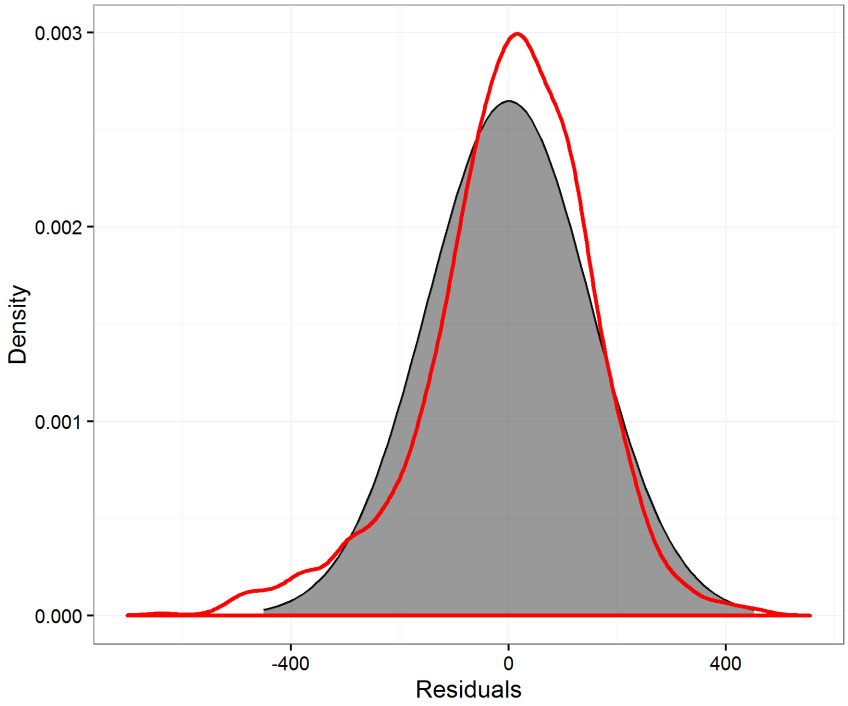

Figure 5.1 – Comparison between the distribution of the residuals from the predictive model (red curve) and a Gaussian distribution. The heavy tail for negative residual values means it overestimates the small numbers of strokes per dives.

Predictions Analysis

Energy Expenditure & Destination, Sex and Trip Phases Regardless of the destination, the trip phase or the year, the FMR was significantly higher for males than females (105.3 ± 13.7 vs. 80.9 ± 39.2 kJ kg^{-1} d^{-1} respectively; p-value < 0.01, Table 5.3). Similarly, but independently of the sex instead of the destination, animals reaching Antarctica had a significantly higher FMR (108.6 ± 52.1 vs. 71.73 ± 13.7 kJ kg^{-1} d^{-1} respectively; p-value < 0.01, Table 5.3). In the same way, the energy expenditure during the central phase (91.4 ± 62.1 kJ kg^{-1} d^{-1}) of the trip was significantly lower than during the outward phase (109.7 ± 63 kJ kg^{-1} d^{-1}), and significantly higher than the return phase (82.8

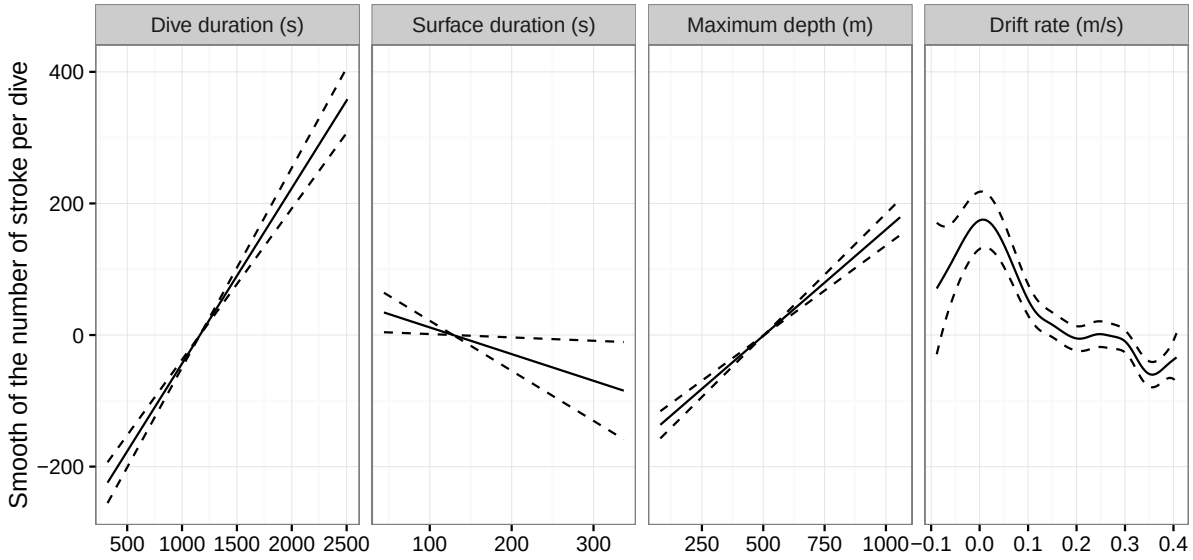

Figure 5.2 – Relationships from the predictive model between the number of flipper stroke per dives and the dive duration, the post-dive surface duration, the maximum depth and the drift rate.

$\pm$ 61.4 kJ kg^{-1} d^{-1}; both p-value < 0.01, Table 5.3).

Table 5.3 – Relationships between the energy expenditure (FMR) and the destination, the sex, the trip phase and the year, and the associated p-values from a linear mixed effect model with individual as a random intercept. For each qualitative covariate, the estimate represents how stroke count varies with the modality presented here, compared to the one which is not presented. The year covariate was set as a quantitative variable to avoid the multiplicity of the modalities.

	Covariate	Modality	Estimate	p-value
FMR $\sim$	Destination	Antarctica	0.31	<0.01
	Sex	Male	0.19	<0.01
	Phase of the trip at sea	Outward	0.11	<0.01
		Return	-0.10	<0.01
	Year	-	0.00	0.78

Inter-Annual Variability in Energy Expenditure Without any consideration on the sex, the destination or the trip phase, the covariate year has no effect on the FMR (p-value = 0.78, Table 5.3). However, when distinguishing sexes (Figure 5.3), at least one year differed from the others for males (Kruskal-Wallis chi-squared = 20.50, df = 10, p-value = 0.03) and females (Kruskal-Wallis chi-squared = 24.26, df = 10, p-value < 0.01).

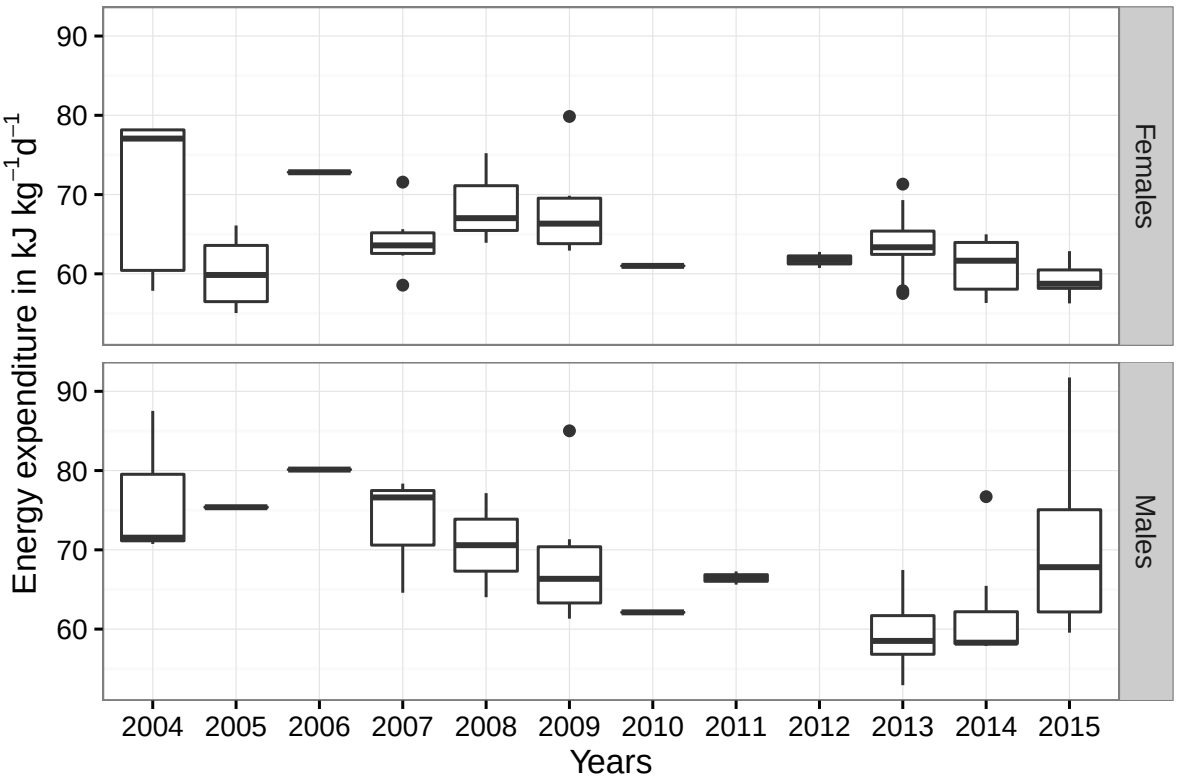

Figure 5.3 – Distribution of the energy expenditure (kJ.kg^{-1}.d^{-1}) in post-moulting southern elephant seals (*Mirounga leonina*) from 2004 to 2015 in males and females.

5.2.4 Discussion

This study illustrates the necessity to monitor individual parameters over long-term to get the overall picture of the relationships between biological and physical parameters within an ecosystem. Using a predictive model to estimate the energy expenditure over an 11-year period, our findings revealed spatial and temporal variability of the energy expenditure, which differs between sexes.

Using the Maresh *et al.* (2014) equation based on the number of strokes as a proxy of the energy expenditure stated several assumptions that need to be clarified. First, it assumes the number of strokes to be comparable between individuals of different ages. This assumption is based on Maresh *et al.* (2014) which found no significant relationships between size or age in the FMR of 12 female northern elephant seals. While differences between sexes were not tested, we made the assumption of similar relationship between stroke counts and FMR for both sexes. In the absence of information relating both information for male elephant seals, we acknowledge that is a strong assumption leading possibly to a miscalculation of the FMR. The second assumption states that the energy expenditure, defined in this way, represents the sum of all components costs (digestion, maintenance and locomotion) except for the energy lost in via faeces, urine and ther-

moregulation (Maresh *et al.*, 2015).

Given the above, the proportion of the deviance explained by our model to predict the number of flipper strokes was 60 %. Given the high deviance explained, we believe this model captures a sufficient part of the stroke counts variability to use it to predict on the post-moulting SESs. The shape of the residual distribution from this model suggests a tendency to overestimate small number of flipper stroke, resulting in an overestimation of low FMR values. In accordance with several studies, we found that the number of strokes per dive, and so the energy expenditure, was linked to diving parameters (Arnould *et al.*, 1996; Costa & Gales, 2000; Elliott *et al.*, 2013). Using method developed by Gordine *et al.* (2015), the calculated proxy of the animal's body density accounted for 13 % of the deviance explained, which reveals the buoyancy variation as a strong driver of the animal energy expenditure. This is consistent with the findings of Thums *et al.* (2008), which found that drift rate accounted for 77 % of the deviance explained in a model that investigated the relationship between body lipid content and several diving variables. These results are also in accordance with previous studies like Richard *et al.* (2014), which found that one percent variation in buoyancy resulted in a 20 % variation of swimming effort, and Jouma'a *et al.* (2016) demonstrating that the time spend at the bottom increases with the animal buoyancy.

Using this model to predict the number of flipper strokes associated with each post-moulting dive, we found that the variability in the energy expenditure during post-moulting trip could be related to several parameters (Table 5.3). We found that no matter the destination, the sex or the year, the central phase of SES trip at sea costs less energy than the outward phase, and more energy than the return phase. This is consistent with previous studies focusing on the buoyancy variations of elephant seals (Aoki *et al.*, 2011; Richard *et al.*, 2014; Adachi *et al.*, 2014). Once elephant seals leave the land after the moulting period, they have poor body condition with a negative buoyancy (Thums *et al.*, 2008) due to the high energy requirements over the moulting fast (Slip *et al.*, 1992). As they feed on more and more prey during their trip at sea, they make fat, improving therefore their body condition by increasing the percentage of their body lipid content (Thums *et al.*, 2008). By approaching the neutral buoyancy, they reduce the cost of transport (Sato *et al.*, 2013; Adachi *et al.*, 2014) and so the energy expenditure, which likely explain its decrease from the outward phase to the return phase.

In the same way, regardless of their sex, the year or the trip phase, SESs reaching Antarctica have higher energy expenditure than the others remaining on the Kerguelen shelf or pelagic compartments. While this relationship was expected for the central phase of their trip at sea, because SESs reaching those regions have to deal with sea ice when

approaching Antarctica (Bailleul *et al.*, 2007a; van den Hoff *et al.*, 2014; Labrousse *et al.*, 2015), it was not the case for the others part of their trip. As suggested by Bailleul *et al.* (2007a), we believe that sea ice locality presents particular environmental conditions explaining the presence of richer habitats. This means better prey quality or a wider range of prey sources that could justify higher energy costs during the outward and return phases. In this way, we assume the energy required for transit phases (outward and return phases) would be compensated by higher energy intake once near Antarctica. More than the energy expenditure associated with a foraging zone, it is the difference between energy expenditure and energy intake that should drive animal's decision. One can well imagine that higher energy expenditure would allow SESs to access better prey quality, resulting in a higher net energy gain. Indeed, it would be interesting to see if animals reaching Antarctica have higher reproductive success and survival rate.

The explanatory model also revealed that male SESs have higher energy expenditure than the females, and no matter where they are going, the year or the trip phase. As no sexual difference was found in the swimming speed of northern elephant seals (Hassrick *et al.*, 2007), we believe that differences in the energy expenditure was mainly due to a higher flipper stroke frequency required to move the male SESs' body. Since male SESs are several times heavier than females (McCann *et al.*, 1989), they probably need to increase their flipper stroke frequency to swim as fast as the females. This increase in the number of strokes per unit of time results in an increasing FMR. We should, however, take this result with caution since the model used to predict FMR male SESs, was fitted on female SESs, including then a possible bias in the estimation of energy expenditure of males. With all uncertainties around the measurement of our FMR, we also found that female SESs have similar energy expenditure than those found in northern elephant seals (80.9 $\pm$ 39.2 kJ kg^{-1} d^{-1} vs. 69.4 $\pm$ 3.0 kJ kg^{-1} d^{-1}, respectively, Maresh *et al.*, 2014).

These sexual differences in the variation of the energy expenditure enabled to highlight an inter-annual variability (Figure 5.3) that was not detected in our explanatory model (Table 5.3) because of confounding covariates. The lack of individuals for some years prevented from statistically identifying a specific year different from the others in both, male and female time series. This could be due to a small number of SESs equipped in some years, e.g. 2006 was only represented by one male and one female SESs. A greater number of SESs would have provided a better picture of the inter-annual variability at the population level. We however observed a trend toward reduction in energy expenditure in 2007, with a possible increase in 2011 for male SESs energy expenditure (Figure 5.3).

There might be numerous and complex reasons for this inter-annual variability. These variations in the energy expenditure are linked to their ecological niches, since adult male

and female SESs are known to forage in different habitats (Bailleul *et al.*, 2010a). Males mainly forage from the Antarctica coasts within the sea-ice pack, while females forage in more pelagically habitats. The accessibility and quality of resources therefore strongly differ among sexes, which could explain the differences observed in the energy expenditure. The accessibility to prey resources may be driven by climatic events through respectively the extent of sea-ice (Wolff *et al.*, 2006) and changes in mixed layer depth (Sallée *et al.*, 2010). Climatic variations such as El Niño Southern Oscillation (ENSO) or the Southern Annular Mode (SAM) are known to influence the productivity of the Southern Ocean and the abundance, quality and distribution of prey, where SESs forage (Wilson *et al.*, 2001; Atkinson *et al.*, 2004), which in fine could influence the variations in energy expenditure.

Since elephant seals are capital breeders, they depend on the energy collected and stored as lipids during their foraging migration for the costs of maintenance and the costs of reproduction. This is particularly true for females in which the survival in the first year of their pups is directly related to their ability to store and acquire resources (McMahon & Burton, 2005). It is also true for males which have to be in a good condition to fight for access to the breeding. In addition, SESs are known to be faithful to their foraging area (Bradshaw *et al.*, 2004), so any changes of the area quality due to large scale oceanographic events could have an important impact on the energy expenditure and potentially on the survival and the breeding success (Authier *et al.*, 2012).

CHAPITRE 6

Discussion Générale

Sommaire

6.1 Synthèse et Mise en Relation des Principaux Résultats

L'étude à fine échelle de la cinématique associée aux tentatives de capture de proies nous a permis de mettre en évidence un lien important entre les mouvements en trois dimensions d'un prédateur marin et leur activité d'alimentation à l'échelle d'une plongée (Chapitre 3). Cette étude a montré l'existence de zones en recherche restreinte présentes durant les plongées d'alimentation et caractérisées par une diminution de la vitesse de nage et une augmentation de la sinuosité. Ces zones sont associées à un changement de comportement de nage, mais également à un taux de rencontre de proies plus élevé. Identifiées dans une sphère d'un rayon médian de 37 m, ces zones laissent suggérer une distribution de la ressource sous forme de parcelles, en accord avec ce que l'on trouve dans la littérature sur la distribution des myctophidés, principales proies des femelles éléphants de mer (Auster *et al.*, 1992; Cherel *et al.*, 2008). La faible différence entre les taux de rencontre de proies à l'intérieur et à l'extérieur de ces zones suggère que ces parcelles sont caractérisées par des densités de proies plus importantes que la densité moyenne dans l'environnement. Cela suggérerait une structuration continue du champ de proies, avec des variations locales de densité, identifiées dans cette étude comme des parcelles. En plus de l'identification de ces zones où les éléphants de mer semblent augmenter leur effort d'alimentation, trois modes comportementaux précédant la rencontre d'une proie ont pu être identifiés. Ces modes d'approche des proies sont caractérisés par des comportements de nage et des taux de rencontre différents. Le premier mode est caractérisé par une approche horizontale, où l'animal semble tourner sur lui-même et capturer des proies tout autour de lui, marquée par une importante sinuosité horizontale. Le second est caractérisé par une approche plus verticale, par le dessous, qui semble nécessiter un effort de nage important. Enfin le troisième mode semble être caractéristique d'une attaque par le dessus, comme si l'éléphant de mer se laissait tomber sur sa proie. Les différences comportementales marquées entre ces trois modes d'approches nous laissent penser que différentes proies sont ciblées et donc que l'apport énergétique varie selon la quantité et la qualité des espèces capturées. Bien que l'on ne puisse pas avoir accès à la densité énergétique associée aux différents types de proies chassées, nous avons cependant accès aux taux de rencontre de proies associé à chacun des modes comportementaux identifiés. En se basant sur cette information, il semblerait que les éléphants de mer favorisent la capture de proies présentes en plus grand nombre. En effet, la principale stratégie de chasse identifiée est associée à un taux de rencontre de proies presque deux fois supérieur aux deux autres stratégies, et ce malgré une importante activité natatoire laissant supposer un coût élevé d'acquisition de la ressource. Pour maintenir un bilan énergétique positif lors de leur trajet en mer, les éléphants de mer ont donc le choix d'augmenter le nombre de proies capturées ou bien de

cibler des proies de meilleure qualité, même si cette dernière hypothèse n'a pas pu être vérifiée dans le cadre de cette thèse.

Outre le choix des proies pour maximiser leur rendement énergétique, les éléphants de mer peuvent également jouer sur le temps qu'ils sont capables de rester au fond d'une plongée pour augmenter leurs chances d'accéder aux ressources d'une parcelle et donc d'accumuler de l'énergie pour maintenir un bilan énergétique positif (Jouma'a *et al.*, 2016). L'étude du temps passé au fond d'une plongée (Chapitre 4) montre que la décision de quitter une parcelle de proies est liée à l'accessibilité verticale de celle-ci, mais également au nombre de proies rencontrées, ainsi qu'à la flottabilité (*i.e.* densité) de l'éléphant de mer, et par conséquent au coût du transport qui augmente quand l'animal s'éloigne de la flottabilité neutre. L'un des résultats majeurs est d'ailleurs que l'on ne peut pas considérer le temps passé au fond d'une plongée comme l'unique façon d'estimer le succès de pêche des éléphants de mer, comme c'est le cas dans de nombreuses études. En effet, selon la profondeur d'alimentation, l'animal ne passera pas le même temps au fond en présence ou en l'absence de proies. À faible profondeur, ils auront par exemple tendance à terminer leur plongée plus tôt s'ils ne rencontrent aucune proie, tandis que l'inverse est observé pour des profondeurs plus importantes. Cette étude montre également qu'en présence d'une parcelle présentant un important taux de rencontre de proies, les éléphants de mer ont tendance à augmenter leur temps de résidence indépendamment de la profondeur. La profondeur, et donc l'accessibilité verticale de la ressource, s'est également révélée être un facteur important dans le fait de rester plus ou moins longtemps dans une parcelle. À mesure que la profondeur augmente, l'éléphant de mer augmente son temps passé au fond jusqu'au moment où il atteint sa limite aérobie. Pour des profondeurs plus importantes, ces phoques vont donc diminuer le temps passé dans la parcelle pour compenser l'énergie requise pour accéder aux ressources. Cette diminution du temps passé au fond est observée avec la profondeur aux alentours de 550 m et correspond justement au moment où la dépense énergétique liée aux phases de transit devient supérieure à celle allouée au fond des plongées et donc nécessaire à la capture des proies. L'accessibilité verticale des proies va donc en partie conditionner le temps d'exploitation de la parcelle au travers de la dépense énergétique associée aux phases de transit. Cette accessibilité est également l'un des paramètres les plus soumis aux variations environnementales à grande échelle, susceptibles d'impacter la dépense énergétique moyenne d'un individu d'une année sur l'autre.

L'étude des variations de la dépense énergétique moyenne des éléphants de mer en période post-mue sur une durée de 11 ans (Chapitre 5), nous a permis de mettre en évidence des différences inter-sexes, ainsi qu'une structuration spatio-temporelle en fonction de la zone d'alimentation ciblée, des différentes phases du trajet en mer et de l'année.

Nous avons ainsi pu montrer que les individus atteignant l'Antarctique avaient une dépense énergétique supérieure à ceux évoluant au niveau du plateau de Kerguelen ou en milieu pélagique. Cette différence peut être liée à des comportements de plongée moins coûteux, comme des profondeurs et des durées de plongées moins importantes, pour les individus n'atteignant pas l'Antarctique. On peut également attribuer cette différence à la dépense d'énergie supplémentaire requise pour plonger en présence de glace de mer lorsque ces animaux se nourrissent en Antarctique. Le fait que cette différence soit retrouvée indépendamment de la phase du trajet considérée laisse suggérer que les éléphants de mer augmentent *volontairement* leur dépense énergétique lors des phases de transit, pour atteindre probablement plus rapidement leur zone d'alimentation. L'accès plus coûteux à la zone antarctique pourrait être compensé par un apport énergétique plus important qu'ailleurs. La présence de glace de mer est en effet connue pour favoriser la production primaire (Loeb *et al.*, 1997) et donc *in fine* celle des ressources disponibles pour les éléphants de mer. Les mâles éléphants de mer austraux sont connus pour s'alimenter essentiellement près des côtes antarctiques. Notre étude révèle qu'ils ont une dépense énergétique supérieure à celle des femelles et que cette différence n'est pas uniquement liée à leur zone d'alimentation. Ici, nous avons fait l'hypothèse que pour maintenir une vitesse de nage équivalente à celle des femelles, les mâles éléphants de mer, dont la masse est plusieurs fois supérieure à celle des femelles, doivent augmenter leur fréquence de coup de nageoire, résultant en une augmentation de la dépense énergétique moyenne. Cette étude montre également qu'indépendamment du sexe, la phase centrale de leur trajet en mer présente une dépense énergétique moyenne supérieure à la phase retour et inférieure à la phase aller. On explique cette différence par l'amélioration de la condition corporelle des animaux au cours de leur trajet en mer. À mesure que ces animaux s'alimentent, ils reconstituent leurs réserves énergétiques sous forme de lipides. Ces réserves influencent la flottabilité de l'animal et donc le coût du transport (Thums *et al.*, 2008). Plus ces animaux sont gras, et moins ils auront à dépenser d'énergie pour se déplacer. Cette série temporelle nous a également permis de mettre en évidence des variations inter-annuelles de la dépense énergétique moyenne. Bien que l'on ne puisse pas directement expliquer ces variations, nous faisons ici l'hypothèse qu'elles sont très fortement liées aux succès d'alimentation. L'accessibilité des ressources en proies est en effet un paramètre susceptible de varier d'une année sur l'autre, car elle est notamment conditionnée à plus grande échelle par des variations climatiques telles que l'oscillation antarctique ou le phénomène *El Niño Southern Oscillation* (ENSO). Ces deux variations climatiques sont connues pour structurer la productivité de l'océan austral, influençant notamment la profondeur de la couche de mélange ainsi que l'étendue de glace de mer et *in fine*, le succès d'alimentation des éléphants de mer.

6.2 Limites des Méthodes Employées

6.2.1 Impact des Balises sur le Comportement des Animaux

Bien que l'ensemble des expérimentations sur le terrain lié à ce travail de thèse ait été approuvé par le comité d'éthique de l'Institut polaire français Paul Émile Victor, peu d'études se sont intéressées à l'impact du déploiement d'enregistreurs de données et de la manipulation des éléphants de mer sur leur comportement, et à plus long terme sur leur survie. McMahon *et al.* (2008) n'ont trouvé aucune différence concernant la masse des éléphants de mer de retour à terre, indépendamment de la pose de balise. Ils ont également montré l'absence de différence sur la survie de ces animaux, équipés avec et sans balise, comme c'est le cas chez de nombreuses autres espèces (Walker *et al.*, 2012). Les conclusions de McMahon *et al.* (2008) semblent être indépendantes du sexe et de l'âge des individus, cependant ils n'abordent pas la question liée à l'augmentation de la force de traînée lorsque les balises sont fixées sur l'animal. Cette question a en partie été traitée en soufflerie chez les manchots (*Pygoscleis* sp.) et les tortues vertes (*Chelonia mydas*), permettant de mettre en évidence une réduction de la vitesse de nage et une augmentation de la dépense énergétique (Bannasch *et al.*, 1994; Watson & Granger, 1998; Todd Jones *et al.*, 2013). Chez l'éléphant de mer du nord, Maresh *et al.* (2015) ont pu montrer, lors du déploiement d'un dispositif expérimental de sonde acoustique d'un poids apparent de 1,3 kg et d'une aire de section de 2502 cm^2, une augmentation des coûts de locomotion de 14,5 %. Le poids apparent et la surface des balises déployées dans le cadre de ce travail de thèse étant bien inférieurs à ceux de Maresh *et al.* (2015), nous avons supposé négligeable l'effet des appareils embarqués sur le comportement de plongées des éléphants de mer austraux.

6.2.2 Détection des Événements de Tentative de Capture

Mesurer l'activité d'alimentation d'un prédateur plongeur tel que l'éléphant de mer se révèle être un défi de taille aux vues des conditions environnementales extrêmes rencontrées lors de ses trajets en mer. C'est d'autant plus vrai lorsque l'on souhaite obtenir une mesure assez fine à la fois spatialement et temporellement pour confronter empiriquement les prédictions de la théorie de l'approvisionnement optimal. Plusieurs méthodes déjà éprouvées sur d'autres espèces se sont révélées infructueuses chez l'éléphant de mer, comme les sondes œsophagiennes ou stomacales trop facilement régurgitées, ou bien l'utilisation de caméras rendue difficile en l'absence de lumière, à de fortes profondeurs et sur une longue période. Pour contourner ces limites logistiques, Gallon *et al.* (2013) et Vacquié Garcia (2014) ont développé une méthodologie basée sur l'utilisation d'accéléromètres pour quantifier ce que l'on a appelé les *événements de tentatives de capture*. Facile à mettre en place,

cette méthode nous renseigne sur l'activité d'alimentation via une estimation quantitative, mais non qualitative, des tentatives de prises alimentaires, nous permettant d'identifier qualitativement des zones plus favorables que d'autres à l'acquisition de ressource. La limite associée à cette méthode est que l'on estime une tentative et non un succès, autrement dit nous n'estimons pas le nombre de proies que l'animal a réellement ingérées, mais bien le nombre de fois qu'il a tenté d'en capturer une, avec pour conséquence une surestimation probable du nombre de prise alimentaire. Par ailleurs, nous n'avons aucune information sur la qualité (*i.e.* densité énergétique) des proies consommées. De récents travaux conduits par Guillemette Labadie lors d'un stage en césure ont permis de mettre en évidence que de nombreux événements de tentatives de captures détectés à l'aide des accéléromètres pouvaient également être identifiés à partir d'enregistrements audio issus des Acousondes™. Bien qu'une validation visuelle serait la solution parfaite pour valider cette méthode, ce genre d'études nous conforte dans l'utilisation du nombre de tentatives de capture comme mesure de l'activité d'alimentation chez l'éléphant de mer.

6.2.3 Mesure de la Dépense Énergétique & Accélérométrie

La dépense énergétique est une composante importante de l'écologie alimentaire qui est extrêmement difficile à mesurer *in situ*. L'émergence de techniques basées sur l'accélération pour rendre compte de cette mesure présuppose que les grandeurs calculées reflètent le taux de consommation en dioxygène.

La mesure de l'accélération dynamique totale (ODBA, pour la somme des accélérations dynamiques et VeDBA, pour la somme vectorielle des accélérations dynamiques) s'est révélée être un bon indicateur du taux de consommation en dioxygène chez de nombreuses espèces. Cette relation a en effet été mise en évidence chez le grand cormoran (*Phalacrocorax carbo*, Wilson *et al.*, 2006), mais également chez un grand nombre de mammifères et d'oiseaux, ainsi que chez l'humain (Halsey *et al.*, 2009), lors d'activités monospécifiques. Ce détail est important puisqu'une récente étude de Jeanniard-du Dot *et al.* (2016), montre chez l'otarie de Kerguelen et l'otarie à fourrure du Nord que l'utilisation de l'accélération dynamique ne prédit pas correctement la dépense énergétique sur la totalité de leurs trajets d'alimentation ($R^2 = 0.36$), mais qu'elle se révèle être un bon prédicteur dès lors que le trajet est partitionné en différentes activités (plongée, transit, surface et repos, $R^2 = 0.70$).

Comme précisé par Hanuise (2011), deux aspects sont à prendre en compte lors de l'utilisation de l'accélération dynamique comme un indice de la dépense énergétique. Le premier est d'ordre technique, il concerne la méthode employée pour séparer l'accélération dynamique de l'accélération statique. Deux méthodes sont couramment utilisées, celle de

la moyenne glissante (Wilson *et al.*, 2006) et celle du filtre fréquentiel passe-bas (Sato *et al.*, 2003). Shepard *et al.* (2008a) ont ainsi démontré que le choix des paramètres lié au filtre passe-bas, et à la moyenne glissante (respectivement, fréquence de coupure et taille de la fenêtre) avait des conséquences importantes sur l'estimation de l'accélération dynamique. Hanuise (2011) précise qu'il serait plus juste de dire qu'à l'aide de ces méthodes, on calcule des approximations de l'accélération de gravité et de l'accélération propre. Le second aspect concerne l'utilisation de l'accélération dynamique comme un indice de la dépense énergétique en plongée. Cette dépense énergétique peut être décomposée en quatre compartiments : (1) les coûts de maintenance ou métabolisme basal, (2) les coûts de digestion liés à l'ingestion de proies, (3) ceux liés à la thermorégulation et enfin (4) ceux liés à la locomotion. Lorsque l'on considère les variations de l'accélération dynamique comme un indice de la variation de la dépense énergétique, cela revient à n'étudier que les variations des coûts de locomotion et donc à supposer l'ensemble des autres coûts constants (Rosen & Trites, 1997; Green *et al.*, 2009). Costa (2007) montre que l'impact des autres facteurs est minimal si l'animal a des coûts de locomotion importants et qu'il évolue à des taux métaboliques proches de sa limite métabolique maximale, comme c'est le cas pour l'éléphant de mer.

Dans le cadre de ce travail de thèse, nous avons souhaité nous affranchir du biais lié au choix de la fréquence de coupure séparant l'accélération dynamique de l'accélération statique, et privilégier le choix de compter le nombre de coups de nageoire, comme un indice du coût de locomotion et donc de la dépense énergétique (Maresh *et al.*, 2014). Ce choix nous permet également de comparer plus facilement les valeurs obtenues entre individus puisqu'aucune différence significative de l'énergie associée aux coups de nageoire n'a été trouvée entre des individus d'âge et de taille différente chez l'éléphant de mer du nord (Maresh *et al.*, 2014). Cela permet donc de nous affranchir de la variabilité associée au calcul de l'accélération dynamique, mais pas de l'approximation de la dépense énergétique via les coûts de locomotion. L'une des voies explorées pour mesurer plus efficacement l'ensemble des coûts énergétiques associés à la plongée est d'estimer le métabolisme à l'aide de la fréquence cardiaque. En Annexe E, Day *et al.* (2017) ont par exemple montré qu'il était possible à partir des Acousondes™ de suivre le rythme cardiaque de l'animal à la surface. Cette étude a permis de mettre en évidence une augmentation du rythme cardiaque à la surface qui n'a pas pu être liée à la durée et à l'effort de nage de la plongée précédente. En revanche, la récupération entre deux plongées semble être reliée au nombre de battements cardiaques et donc au temps de surface.

6.3 Comparaison à d'Autres Prédateurs Marins

Les travaux présentés dans le cadre de cette thèse se sont intéressés aux différentes stratégies d'alimentation mises en place par l'éléphant de mer austral, mais retrouve-t-on ces résultats chez d'autres espèces de prédateurs marins ? Y a-t-il des tendances générales qui se dégagent ? Dans le premier article (CHAPITRE 3), nous avons identifié la présence de zones en recherche restreinte au cours des plongées, caractérisées par un taux de rencontre de proies plus important. On trouve dans la littérature de nombreuses études qui vont dans le sens d'une relation forte entre la trajectoire d'un individu et son comportement d'alimentation (Weimerskirch *et al.*, 2007; Hoskins *et al.*, 2015). Mais pour l'essentiel de ces études, il s'agit de trajectoires à deux dimensions d'échelle temporelle bien plus importante que la nôtre (plusieurs jours). À notre connaissance, seule l'étude de Adachi *et al.* (2016) s'est intéressée à cette question en utilisant la méthode du *temps de premier passage dans une sphère* (Bailleul *et al.*, 2010b). Les autres études intégrant la dimension verticale portent généralement sur de la modélisation d'habitat et donc sur une échelle temporelle supérieure (Tracey *et al.*, 2014; Simpfendorfer *et al.*, 2012). Adachi *et al.* (2016) trouvent une augmentation de la sinuosité en lien avec une augmentation du taux de rencontre de proie chez l'éléphant de mer du nord. Les échelles trouvées sont plus petites que les nôtres, mais suggèrent également une agrégation des proies chassées par les éléphants de mer sous forme de parcelles. L'identification de différentes stratégies de chasse basée sur la cinématique du mouvement avant une tentative de capture de proie nous permet de supposer que plusieurs types de proies sont donc ciblées. Cette variabilité comportementale selon le type de proie chassée a également été observée chez les phoques veaux marins (*Phoca vutlina*, Bowen *et al.*, 2002), le guillemot de Brünnich (*Uria lomvia*, Elliott *et al.*, 2008) ou encore chez le cormoran à aigrettes (*Phalacrocorax auritus*, Enstipp *et al.*, 2007). Chez cette dernière espèce, Halsey *et al.* (2007b) ont par exemple montré que les temps de plongée étaient moins importants lorsque des proies mobiles étaient chassées, vraisemblablement dus aux dépenses énergétiques engendrées par la poursuite et la capture de ces proies plus véloces.

En ce qui concerne l'ajustement du temps passé au fond (CHAPITRE 4), nous avons vu que le lion de mer de Steller se comportait de la même façon que l'éléphant de mer en augmentant le temps passé au fond lorsque de nombreuses proies sont rencontrées (Cornick & Horning, 2003). De la même façon, cette relation a été trouvée chez le manchot royal (*Aptenodytes patagonicus*, Hanuise *et al.*, 2013). Cette espèce montre aussi une augmentation du temps passé au fond avec l'augmentation de l'accessibilité verticale des proies comme c'est le cas pour les plongées jusqu'à 550 m de profondeur chez les éléphants de mer. La diminution du temps passé au fond que l'on observe au-delà de ces profondeurs n'est cependant pas observée chez le manchot royal. Cette diminution, très certainement

liée à la limite de plongée aérobie, est en revanche observée chez le cormoran de Crozet (*Phalacrocorax melanogenis*, Cook *et al.*, 2008). Les différences d'ajustements comportementaux observées entre espèces, en lien avec la profondeur, témoignent des contraintes physiologiques propres à chacune d'entre elles. L'effet de la condition corporelle sur le comportement de plongée a ainsi été mis en évidence chez les manchots (Sato *et al.*, 2002), mais contrairement aux éléphants de mer qui ont majoritairement une flottabilité négative, les manchots flottent. Cette particularité entraîne des ajustements comportementaux différents des éléphants de mer avec par exemple, un effort de nage plus important à la descente qu'à la remontée. Chez le manchot royal on retrouve également une diminution des temps de transit via l'augmentation des angles de plongées (Hanuise *et al.*, 2013). Tout comme chez les éléphants de mer (Jouma'a *et al.*, 2016), Viviant *et al.* (2016) ont montré chez l'otarie de Kerguelen que le temps passé au fond d'une plongée ne pouvait pas être considéré comme un bon indicateur de la qualité de la parcelle visitée, contrairement à ce qui a été fait dans de nombreuses publications (Boyd *et al.*, 1995; Mori & Boyd, 2004). En effet, cette relation n'est vraie que pour une certaine gamme de profondeur de plongées. Ces résultats soulignent l'importance de tester au préalable un indicateur comportemental qui a pu se révéler pertinent chez une espèce avant de l'appliquer chez une autre.

Dans le Chapitre 5, nous avons déjà vu que les valeurs de dépenses énergétiques journalières estimées à l'aide du modèle prédictif étaient similaires à ce que l'on trouve chez l'éléphant de mer du nord (Maresh *et al.*, 2014). Avec une moyenne de 91 $\pm$ 23 kJ.kg^{-1}.d^{-1} tout individu confondu, et compte tenu de l'erreur associée au calcul de cette valeur, les éléphants de mer australs ont une dépense énergétique moyenne du même ordre de grandeur que le plus petit mammifère marin, la loutre de mer (*Enhydra lutris*), dont la dépense énergétique journalière est comprise entre 50 et 220 kJ.kg^{-1}.d^{-1}, selon les activités (Yeates *et al.*, 2007). À titre de comparaison, un petit mammifère terrestre comme le koala *Phascolarctos cinereus* à une dépense énergétique journalière comprise entre 330 et 750 kJ.kg^{-1}.d^{-1} (Ellis *et al.*, 1995). Il n'existe, à notre connaissance, aucune étude s'intéressant aux variations spatio-temporelles de la dépenses énergétique chez un prédateur marin. Notre calcul de la dépense énergétique étant basé sur le nombre de coups de nageoire, qui est une variable elle-même modélisée à partir des paramètres de plongées, cela nous permet de relier les variations de la dépense énergétique à celles des comportements de plongées et donc *in fine* aux variations des comportements d'alimentation. Il a ainsi été montré chez une population de phoque gris en Nouvelle-Écosse que les mâles s'alimentent au niveau du plateau continental tandis que les femelles restent dans des zones intermédiaires sur le plateau (Breed *et al.*, 2006). Cette différence dans les zones d'alimentation prospectées semble également être dépendante de la période de l'année, avec une différenciation plus marquée en fin d'année et juste après la période de reproduction. On peut donc facilement imaginer que ces variations inter-sexes et spatio-temporelles des stratégies d'alimentation

puissent être reliées à des variations spatio-temporelles et à des différences inter-sexes de la dépense énergétique moyenne.

6.4 L'Éléphant de mer Austral, une Espèce Bio-indicatrice

À travers nos résultats, l'étude du comportement de plongée nous a permis d'obtenir des informations indirectes sur les proies des éléphants de mer. Nous avons ainsi mis en évidence des comportements en recherche restreinte, à l'échelle de la plongée, qui laisserait supposer une agrégation de la ressource sous la forme de zone ayant une densité locale de proies supérieures à celle de l'environnement proche. De récents travaux suggèrent un lien fort entre l'agrégation verticale des proies et le taux de rencontre de proie (Le Bras *et al.*, 2016, Annexe D). Dans la même lignée, des travaux en cours sur la forme en trois dimensions des phases de fond vont plus loin et suggèrent une agrégation des proies sous la forme de bancs discrets, structurés en couches, et dont la densité d'organismes serait contrôlée par des contraintes verticales (Le Bras *et al.*, 2017, Annexe F). L'étude à fine échelle des comportements de prédation nous a également permis de distinguer trois stratégies comportementales possiblement reliées à trois espèces différentes de proies. En utilisant les paramètres environnementaux (température, intensité lumineuse et profondeur) associés à ces tentatives, Vacquié-Garcia *et al.* (2015b) ont également pu identifier cinq habitats d'alimentation pouvant représenter autant de communautés de proies potentielles. Ces tentatives de capture, qui peuvent être associées à des événements de bioluminescence (Vacquié-Garcia *et al.*, 2012), sont identifiées plus profondément de jour que de nuit. Comme suggéré dans de nombreuses autres études (Naito *et al.*, 2013; Ducatez *et al.*, 2008; Authier, 2011), ces résultats tendent à prouver que l'éléphant de mer chasse des proies mésopélagiques effectuant des migrations nycthémérales, un comportement caractéristique des espèces de myctophidés (Auster *et al.*, 1992) qui constitue la ressource alimentaire principale des femelles éléphant de mer (Cherel *et al.*, 2008). En recoupant toutes ces informations, l'activité d'alimentation de l'éléphant de mer se révèle donc être un bio-indicateur pertinent de la distribution des myctophidés, dont la niche écologique reste encore mal connue.

Au-delà des aspects biologiques, les éléphants de mer sont utilisés depuis le début des années 2000 comme des plateformes océanographiques pour échantillonner de l'océan austral (Boehlert *et al.*, 2001). L'utilisation de balise CTD[1] permet d'échantillonner la température et la salinité de l'environnement visité par ces prédateurs plongeurs. La mise en commun de jeux de données issus des différentes populations de l'hémisphère sud permet la mise en place de bases de données à grande échelle (Roquet *et al.*, 2013,

[1]Pour *Conductivity-Temperature-Depth*, un descriptif de ce type de balise est disponible dans la sous-section 2.3.1

2014), comme le projet MEOP (Marine mammals Exploring the Oceans Pole to Pole, http://www.meop.net). Ces données viennent en appui de celles obtenues par d'autres systèmes d'observation de l'océan, comme le système Argo. De plus en plus utilisées, ces données montrent une contribution croissante dans la construction de modèles climatologiques à partir de bases de données océanographiques déjà existantes telles que la World Ocean Database (Levitus *et al.*, 2013). En plus d'échantillonner la température et la salinité *in situ*, une récente étude vient de montrer qu'il était également possible d'utiliser les éléphants de mer pour mesurer efficacement le dioxygène dissous et donc d'améliorer notre compréhension du fonctionnement des océans via le déploiement d'enregistreurs embarqués adaptés (Bailleul *et al.*, 2015). De la même façon, Cazau *et al.* (2016) (Annexe C) ont montré que l'on pouvait à partir des enregistrements acoustiques issus des Acousondes™ estimer de façon précise la vitesse du vent ($\pm$ 2 m.s^{-1}). Sans tomber dans le suréquipement, l'ensemble de ces études montre l'intérêt d'utiliser le bio-logging pour échantillonner des environnements difficiles d'accès pour l'homme. Dans le cas de l'océan austral, l'éléphant de mer semble être le modèle idéal de par ses performances de plongée et son importante aire de répartition en mer, pour mener à bien ce genre de mission.

6.5 Perspectives

6.5.1 Un Bilan Énergétique Complet

Comme nous l'avons vu, notre étude comporte de nombreuses approximations liées à la nature même de nos données, qui ne nous permettent pas de répondre en intégralité aux problématiques soulevées en introduction. Basées sur des limitations en dioxygène, l'essentiel des théories de la plongée optimale prédisent comment un animal plongeur doit ajuster son comportement selon des contraintes qui lui sont propres. Nous avons ainsi pu mettre en évidence une augmentation du temps passé au fond avec une augmentation du taux de rencontre de proies, mais qu'en est-il si différents types de proies sont chassées ? L'apport énergétique et le coût d'accès associés sont-ils les mêmes ? Et si le taux de rencontre de proies ne reflétait pas le nombre de proies ingérées ? Une meilleure compréhension des coûts et bénéfices mis en jeu apparaît donc nécessaire pour une compréhension plus fine des mécanismes mis en place à l'échelle de la plongée. Il serait donc intéressant dans un premier temps de pouvoir estimer la relation entre le taux de rencontre de proies et le nombre réel de proies consommées, comme a pu le faire Viviant *et al.* (2010) chez le lion de mer de Steller. Une validation en bassin paraît difficilement réalisable sur les éléphants de mer, mais avec la miniaturisation des balises, une validation visuelle à l'aide de caméra infrarouge permettrait sans doute de répondre à cette question. De la même façon, avoir accès à la densité énergétique des proies consommées serait fortement utile dans le bilan énergétique global de l'éléphant de mer. À défaut d'avoir une information aussi précise

des proies, une identification à l'échelle du genre (Naito *et al.*, 2013) pourrait déjà nous permettre d'apporter une réponse plus claire et plus précise aux variations de la densité corporelle, ainsi qu'aux différents habitats prospectés et comportements de chasse observés.

L'utilisation des enregistrements acoustiques s'est révélée être un outil intéressant pour le suivi des cycles respiratoires (Génin *et al.*, 2015, Annexe B), ainsi que du rythme cardiaque de l'animal à la surface (Day *et al.*, 2017, Annexe E). N'étant initialement pas programmées pour ça, l'utilisation des Acousonde™ , moyennant une révision du protocole d'enregistrement, couplée à l'utilisation accéléromètres sous-cutanés, pourrait se montrer pertinente dans le suivi des battements cardiaques de l'animal sous l'eau. Cela nous permettrait d'estimer le métabolisme de l'animal non plus à l'aide du nombre de coups de nageoire, mais bien à l'aide d'une variable connue pour être corrélée à la dépense énergétique : le rythme cardiaque. Tout récemment, une étude réalisée chez le phoque gris montre qu'il est aujourd'hui possible de mesurer des paramètres physiologiques directement sur l'animal en plongée, en échantillonnant son sang. Takei *et al.* (2016) ont en effet développé un nouveau type de balise permettant d'échantillonner du sang et d'en mesurer *in situ* la concentration en cortisone, cortisol et autres hormones cardiovasculaires. Cette étude montre que la régulation cardiovasculaire observée chez cette espèce n'est pas celle attendue pour des mammifères terrestres, suggérant une adaptation au cours de l'évolution à la vie semi-aquatique. Peut-être qu'un jour ce type de balises pourra nous permettre de suivre en dehors des bassins, l'évolution de la concentration en dioxygène dissous dans le sang de prédateurs plongeurs tels que l'éléphant de mer.

6.5.2 Vers une Meilleure Compréhension de l'Écosystème Austral

L'éléphant de mer, via son rôle de bio-échantillonneur, nous renseigne depuis maintenant de nombreuses années sur la structure physico-chimique de l'océan austral. En revanche, très peu d'information sont disponibles sur la structuration des communautés d'êtres vivants peuplant cet océan. Le déploiement d'appareils de mesure toujours plus précis nous permet aujourd'hui d'utiliser les éléphants de mer pour obtenir des informations indirectes sur les échelons trophiques inférieurs sur lesquels se nourrit. L'ANR Mycto3D-Map avait justement pour objectif de caractériser la distribution et les habitats en trois dimensions des poissons lanternes, en utilisant conjointement les données fournies par leurs prédateurs, l'écho-intégration et la modélisation. En poussant cette réflexion un peu plus loin, il serait intéressant d'utiliser l'éléphant de mer pour en apprendre un peu plus sur les communautés phytoplanctoniques, premier maillon de la chaîne trophique dans l'océan austral. Le déploiement de fluorimètres a déjà permis de mettre en évidence une relation entre l'atténuation de la lumière et la concentration en chlorophylle a (Jaud *et al.*, 2012),

mais il serait intéressant de pouvoir y associer l'identification de groupes phytoplanctoniques. Même si la mise en place d'un système embarqué permettant l'identification des différents taxons phytoplanctoniques semble utopique, de nouveaux outils permettent aujourd'hui l'identification automatique de groupes phytoplanctoniques à partir d'image obtenue par microscope (Schulze *et al.*, 2013). L'étude de la distribution spatio-temporelle de la production primaire en lien avec le succès d'alimentation d'un prédateur supérieur tel que l'éléphant de mer, permettrait une meilleure compréhension des conséquences écologiques de la variabilité en phytoplancton sur les échelons trophiques supérieures et *in fine* sur tout l'écosystème austral.

6.5.3 Succès d'Approvisionnement et Valeur Sélective, l'Effet des Changements Environnementaux

Prévoir l'impact des changements environnementaux sur le comportement d'alimentation et donc *in fine* sur la survie et la reproduction n'est pas chose aisée. L'utilisation de modèle individu centré permet d'apporter des premiers éléments de réponse, mais présuppose bien souvent de connaître toutes les relations mises en jeux pour modéliser au plus juste les variations comportementales en lien avec l'environnement, ainsi que son impact à plus grande échelle sur la population. L'utilisation de jeux de données à long terme est un autre moyen d'estimer les conséquences de ses changements environnementaux. Il s'agit de mettre en relation des variations environnementales avec celles du comportement de plongée, du succès d'alimentation, de la survie ou encore de la reproduction. Il serait donc tout particulièrement intéressant d'étudier dans ce cadre, le lien qu'il existe entre chacun de ces paramètres.

Sur l'archipel des Kerguelen, les femelles éléphants de mer sont par exemple connues pour fréquenter deux zones d'alimentation : l'une en zone inter-frontale et l'autre en Antarctique (Hindell *et al.*, 2003; Bailleul *et al.*, 2007a, 2010a). Des différences dans la composition du régime alimentaire (Bradshaw *et al.*, 2003), mais également dans la masse des petits au sevrage, sont retrouvées entre les femelles s'alimentant en milieu pélagique et en Antarctique (Authier *et al.*, 2012). Relier ces différentes stratégies d'alimentation aux variations du comportement de plongée, ainsi qu'aux variations des traits d'histoire de vie observées, permettrait une meilleure compréhension de l'impact des changements environnementaux sur les populations d'éléphants de mer. De la même façon, étudier quels sont les traits phénotypiques qui vont le plus influencer les comportements de plongée et donc l'accès aux ressources, me semble important. Comprendre quels sont les critères phénotypiques qui vont jouer le plus sur le succès d'alimentation, permettrait *in fine* de mieux comprendre les variations démographiques. Enfin, il serait également intéressant d'étudier les différences au niveau des stratégies d'alimentation mises en place au sein de

populations ayant une trajectoire démographique différente, comme c'est le cas pour la population d'éléphants de mer de Macquarie et celle de Kerguelen (McMahon & Burton, 2005). Ce type d'étude comparative nous permettrait de mieux comprendre quels sont les facteurs pouvant, par exemple, contribuer au déclin d'une population.

Liste des sigles et acronymes

- ACC = Antarctic Circumpolar Current
- ADL = Aerobic Dive Limit
- AIC = Akaike Information Criterion
- ANOVA = Analyse de variance
- ANR = Agence Nationale de la Recherce
- ARS = Area Restricted Search
- CEBC = Centre d'Études Biologiques de Chizé
- CNRS = Centre National de la Recherche Scientifique
- CTD = Conductivity Temperature Depth
- ENSO = El Niño Southern Oscillation
- ENSTA = École National Supérieure de Techniques Avancées
- FMR = Field Metabolic Rate
- FPT = First Passage Time
- GPS = Global Positioning System
- IPEV = Institut polaire français Paul Émile Victor
- IQR = Interquartile Range
- MEOP = Marine mammals Exploring the Oceans pole to Pole

- ODBA = Overall Dynamic Body Acceleration
- PCA analysis = Principal Component Analysis
- PCA = Prey Catch Attempt
- PF = Polar Front
- SAF = Subantartic Front
- SAM = Southern Annular Mode
- SES = Southern Elephant Seal
- SFPT = Spherical First Passagge Time
- SMRU = Sea Mammal Research Unit
- SOI = Southern Oscillation Index
- SRDL = Satellite Relay Data Logger
- STF = Subtropical Front
- TDR = Time Depth Recorder
- UMR = Unité Mixte de Recherche
- VeDBA = Vectorial Dynamic Body Acceleration
- wAIC = weighted AIC

Table des figures

Liste des tableaux

Bibliographie

Adachi, T., Costa, D.P., Robinson, P.W., Peterson, S.H., Yamamichi, M., Naito, Y. & Takahashi, A. (2016) Searching for prey in a three-dimensional environment: Hierarchical movements enhance foraging success in northern elephant seals. *Functional Ecology* . 36, 48, 98

Adachi, T., Maresh, J.L., Robinson, P.W., Peterson, S.H., Costa, D.P., Naito, Y., Watanabe, Y.Y. & Takahashi, A. (2014) The foraging benefits of being fat in a highly migratory marine mammal. *Proceedings of the Royal Society of London B: Biological Sciences* **281**, 20142120. 14, 52, 57, 58, 72, 79, 88

Agostinelli, C. (2012) CircStats: Circular Statistics, from "Topics in circular Statistics" (2001). *R package version 0.2-4* S-plus original by Ulric Lund and R port by Claudio Agostinelli. 40

Ainley, D.G., Ballard, G., Barton, K.J., Karl, B.J., Rau, G.H., Ribic, C.A. & Wilson, P.R. (2003) Spatial and temporal variation of diet within a presumed metapopulation of adélie penguins. *The Condor* **105**, 95–106. 78

Andersson, M. (1981) Central Place Foraging in the Whinchat, Saxicola Rubetra. *Ecology* **62**, 538–544. 9

Aoki, K., Watanabe, Y.Y., Crocker, D.E., Robinson, P.W., Biuw, M., Costa, D.P., Miyazaki, N., Fedak, M.A. & Miller, P.J.O. (2011) Northern elephant seals adjust gliding and stroking patterns with changes in buoyancy: Validation of at-sea metrics of body density. *The Journal of experimental biology* **214**, 2973–2987. 29, 79, 88

Argos (2011) Argos User's Manual. Worldwide Tracking and Environmental Monitoring by Satellite. *Toulouse, France: Collecte Localisation Satellites.* . 25, 80

Arnould, J.P.Y., Boyd, I.L. & Speakman, J.R. (1996) The relationship between foraging behaviour and energy expenditure in Antarctic fur seals. *Journal of Zoology* **239**, 769–782. 88

Arzel, O., Fichefet, T. & Goosse, H. (2006) Sea ice evolution over the 20th and 21st centuries as simulated by current AOGCMs. *Ocean Modelling* **12**, 401–415. 3

Atkinson, A., Siegel, V., Pakhomov, E. & Rothery, P. (2004) Long-term decline in krill stock and increase in salps within the Southern Ocean. *Nature* **432**, 100–103. 3, 90

Auster, P.J., Griswold, C.A., Youngbluth, M.J. & Bailey, T.G. (1992) Aggregations of myctophid fishes with other pelagic fauna. *Environmental Biology of Fishes* **35**, 133–139. 48, 50, 92, 100

Authier, M. (2011) *L'écologie En Mer Des Éléphants de Mer Australx Au Travers Des Isotopes Stables Du Carbone et de l'azote*. Ph.D. thesis, Poitiers. 100

Authier, M., Delord, K. & Guinet, C. (2011) Population trends of female Elephant Seals breeding on the Courbet Peninsula, îles Kerguelen. *Polar Biology* **34**, 319–328. 18

Authier, M., Dragon, A.C., Richard, P., Cherel, Y. & Guinet, C. (2012) O' mother where wert thou? Maternal strategies in the southern elephant seal: A stable isotope investigation. *Proceedings of the Royal Society of London B: Biological Sciences* **279**, 2681–2690. 90, 103

Bailleul, F., Authier, M., Ducatez, S., Roquet, F., Charrassin, J.B., Cherel, Y. & Guinet, C. (2010a) Looking at the unseen: Combining animal bio-logging and stable isotopes to reveal a shift in the ecological niche of a deep diving predator. *Ecography* **33**, 709–719. 21, 37, 90, 103

Bailleul, F., Charrassin, J.B., Ezraty, R., Girard-Ardhuin, F., McMahon, C.R., Field, I.C. & Guinet, C. (2007a) Southern elephant seals from Kerguelen Islands confronted by Antarctic Sea ice. Changes in movements and in diving behaviour. *Deep Sea Research Part II: Topical Studies in Oceanography* **54**, 343–355. 21, 37, 60, 89, 103

Bailleul, F., Charrassin, J.B., Monestiez, P., Roquet, F., Biuw, M. & Guinet, C. (2007b) Successful foraging zones of southern elephant seals from the Kerguelen Islands in relation to oceanographic conditions. *Philosophical transactions of the Royal Society of London. Series B, Biological sciences* **362**, 2169–2181. 36

Bailleul, F., Lesage, V. & Hammill, M.O. (2010b) Spherical First Passage Time: A tool to investigate area-restricted search in three-dimensional movements. *Ecological Modelling* **221**, 1665–1673. 36, 37, 40, 48, 98

Bailleul, F., Vacquie-Garcia, J. & Guinet, C. (2015) Dissolved Oxygen Sensor in Animal-Borne Instruments: An Innovation for Monitoring the Health of Oceans and Investigating the Functioning of Marine Ecosystems. *PLoS ONE* **10**, e0132681. 52, 101

Bannasch, R., Wilson, R.P. & Culik, B. (1994) Hydrodynamic Aspects of Design and Attachment of a Back-Mounted Device in Penguins. *Journal of Experimental Biology* **194**, 83–96. 95

Barbour, A.J. & Parker, R.L. (2014) Psd: Adaptive, sine multitaper power spectral density estimation for R. *Computers & Geosciences* **63**, 1–8. 42, 61

Barham, E.G. (1971) Deep-sea fishes: Lethargy and vertical orientation. *Proceedings of an International Symposium on Biological Sound Scattering in the Ocean*, pp. 100–116, G. B. Farquhar (ed.). U.S. Gov. Printing Office, Washington, DC. 50

Battaile, B.C., Sakamoto, K.Q., Nordstrom, C.A., Rosen, D.A.S. & Trites, A.W. (2015) Accelerometers Identify New Behaviors and Show Little Difference in the Activity Budgets of Lactating Northern Fur Seals (Callorhinus ursinus) between Breeding Islands and Foraging Habitats in the Eastern Bering Sea. *PLoS ONE* **10**, e0118761. 50

Beck, C.A., Bowen, W.D. & Iverson, S.J. (2000) Seasonal changes in buoyancy and diving behaviour of adult grey seals. *The Journal of experimental biology* **203**, 2323–2330. 14, 57, 72

Behrenfeld, M.J., O'Malley, R.T., Siegel, D.A., McClain, C.R., Sarmiento, J.L., Feldman, G.C., Milligan, A.J., Falkowski, P.G., Letelier, R.M. & Boss, E.S. (2006) Climate-driven trends in contemporary ocean productivity. *Nature* **444**, 752–755. 3

Berman, G.J., Choi, D.M., Bialek, W. & Shaevitz, J.W. (2014) Mapping the stereotyped behaviour of freely moving fruit flies. *Journal of The Royal Society Interface* **11**, 20140672. 37

Biuw, M., McConnell, B., Bradshaw, C.J.A., Burton, H. & Fedak, M. (2003) Blubber and buoyancy: Monitoring the body condition of free-ranging seals using simple dive characteristics. *Journal of Experimental Biology* **206**, 3405–3423. 60

Boehlert, G.W., Costa, D.P., Crocker, D.E., Green, P., O'Brien, T., Levitus, S. & Le Boeuf, B.J. (2001) Autonomous Pinniped Environmental Samplers: Using Instrumented Animals as Oceanographic Data Collectors. *Journal of Atmospheric and Oceanic Technology* **18**, 1882–1893. 100

Bom, R.A., Bouten, W., Piersma, T., Oosterbeek, K. & van Gils, J.A. (2014) Optimizing acceleration-based ethograms: The use of variable-time versus fixed-time segmentation. *Movement Ecology* **2**, 6. 37

Bost, C.A., Cotté, C., Bailleul, F., Cherel, Y., Charrassin, J.B., Guinet, C., Ainley, D.G. & Weimerskirch, H. (2009) The importance of oceanographic fronts to marine birds and mammals of the southern oceans. *Journal of Marine Systems* **78**, 363–376. 23

Bost, C.A., Cotté, C., Terray, P., Barbraud, C., Bon, C., Delord, K., Gimenez, O., Handrich, Y., Naito, Y., Guinet, C. & Weimerskirch, H. (2015) Large-scale climatic anomalies affect marine predator foraging behaviour and demography. *Nature Communications* **6**, 8220. 2

Bouskila, A. & Blumstein, D.T. (1992) Rules of Thumb for Predation Hazard Assessment: Predictions from a Dynamic Model. *The American Naturalist* **139**, 161–176. 7

Bowen, W., Tully, D., Boness, D., Bulheier, B. & Marshall, G. (2002) Prey-dependent foraging tactics and prey profitability in a marine mammal. *Marine Ecology Progress Series* **244**, 235–245. 9, 98

Boyd, I.L. (1997) The behavioural and physiological ecology of diving. *Trends in Ecology & Evolution* **12**, 213–217. 71

Boyd, I.L., Arnbom, T. & Fedak, M. (1993) Water Flux, Body Composition, and Metabolic Rate during Molt in Female Southern Elephant Seals (Mirounga leonina). *Physiological Zoology* **66**, 43–60. 19, 20

Boyd, I.L., Reid, K. & Bevan, R.M. (1995) Swimming speed and allocation of time during the dive cycle in Antarctic fur seals. *Animal Behaviour* **50**, 769–784. 13, 14, 72, 99

Bradshaw, C.J.A., Hindell, M.A., Best, N.J., Phillips, K.L., Wilson, G. & Nichols, P.D. (2003) You are what you eat: Describing the foraging ecology of southern elephant seals (Mirounga leonina) using blubber fatty acids. *Proceedings of the Royal Society of London B: Biological Sciences* **270**, 1283–1292. 103

Bradshaw, C.J.A., Hindell, M.A., Sumner, M.D. & Michael, K.J. (2004) Loyalty pays: Potential life history consequences of fidelity to marine foraging regions by southern elephant seals. *Animal Behaviour* **68**, 1349–1360. 20, 90

Breed, G.A., Bowen, W.D., McMillan, J.I. & Leonard, M.L. (2006) Sexual segregation of seasonal foraging habitats in a non-migratory marine mammal. *Proceedings of the Royal Society of London B: Biological Sciences* **273**, 2319–2326. 99

Brown, D.D., Kays, R., Wikelski, M., Wilson, R. & Klimley, A.P. (2013) Observing the unwatchable through acceleration logging of animal behavior. *Animal Biotelemetry* **1**, 1–16. 36, 37, 50

Brown, J.H., Gillooly, J.F., Allen, A.P., Savage, V.M. & West, G.B. (2004) Toward a Metabolic Theory of Ecology. *Ecology* **85**, 1771–1789. 78

Burgess, W.C., Tyack, P.L., Le Boeuf, B.J. & Costa, D.P. (1998) A programmable acoustic recording tag and first results from free-ranging northern elephant seals. *Deep Sea Research Part II: Topical Studies in Oceanography* **45**, 1327–1351. 30, 40

Butler, P.J. (2006) Aerobic dive limit. What is it and is it always used appropriately? *Comparative Biochemistry and Physiology. Part A, Molecular & Integrative Physiology* **145**, 1–6. 10

Butler, P.J. & Jones, D.R. (1997) Physiology of diving of birds and mammals. *Physiological Reviews* **77**, 837–899. 35, 58

Cai, W.J., Hu, X., Huang, W.J., Murrell, M.C., Lehrter, J.C., Lohrenz, S.E., Chou, W.C., Zhai, W., Hollibaugh, J.T., Wang, Y., Zhao, P., Guo, X., Gundersen, K., Dai, M. & Gong, G.C. (2011) Acidification of subsurface coastal waters enhanced by eutrophication. *Nature Geoscience* **4**, 766–770. 2

Calenge, C. (2006) The package "adehabitat" for the R software: A tool for the analysis of space and habitat use by animals. *Ecological Modelling* **197**, 516–519. 40, 82

Carbone, C. & Houston, A.I. (1994) Patterns in the diving behaviour of the pochard, Aythya ferina : A test of an optimality model. *Animal behaviour* **48**, 457–465. 12, 56, 70, 71

Carbone, C. & Houston, A.I. (1996) The optimal allocation of time over the dive cycle: An approach based on aerobic and anaerobic respiration. *Animal Behaviour* **51**, 1247–1255. 11, 12, 73

Carbone, C., Teacher, A. & Rowcliffe, J.M. (2007) The Costs of Carnivory. *PLOS Biol* **5**, e22. 79

Carlini, A.R., Daneri, G.A., Márquez, M.E.I., Bornemann, H., Panarello, H., Casaux, R., Ramdohr, S. & Plötz, J. (2005) Food consumption estimates of southern elephant seal females during their post-breeding aquatic phase at King George Island. *Polar Biology* **28**, 769–775. 79

Carrete, M. & Donázar, J.A. (2005) Application of central-place foraging theory shows the importance of Mediterranean dehesas for the conservation of the cinereous vulture, Aegypius monachus. *Biological Conservation* **126**, 582–590. 9

Cazau, D., Bonnel, J., Jouma'a, J., le Bras, Y. & Guinet, C. (2016) Measuring the Marine Soundscape of the Indian Ocean with Southern Elephant Seals Used as Acoustic Gliders of Opportunity. *Journal of Atmospheric and Oceanic Technology* **34**, 207–223. 101

Cezilly, F. & Benhamou, S. (1996) Les stratégies optimales d'approvisionnement. *Revue d'écologie* **51**, 43–86. 7

Charnov, E.L. (1976) Optimal foraging, the marginal value theorem. *Theoretical Population Biology* **9**, 129–136. 5, 6, 51, 107

Charrassin, J.B., Kato, A., Handrich, Y., Sato, K., Naito, Y., Ancel, A., Bost, C.A., Gauthier-Clerc, M., Ropert-Coudert, Y. & Le Maho, Y. (2001) Feeding behaviour of free-ranging penguins determined by oesophageal temperature. *Proceedings. Biological Sciences / The Royal Society* **268**, 151–157. 14, 79

Cherel, Y., Ducatez, S., Fontaine, C., Richard, P. & Guinet, C. (2008) Stable isotopes reveal the trophic position and mesopelagic fish diet of female southern elephant seals breeding on the Kerguelen Islands. *Marine Ecology Progress Series* **370**, 239–247. 21, 37, 48, 92, 100

Chimienti, M., Cornulier, T., Owen, E., Bolton, M., Davies, I.M., Travis, J.M. & Scott, B.E. (2016) The use of an unsupervised learning approach for characterizing latent behaviors in accelerometer data. *Ecology and Evolution* **6**, 727–741. 37, 50

Clarke, A., Murphy, E.J., Meredith, M.P., King, J.C., Peck, L.S., Barnes, D.K. & Smith, R.C. (2007) Climate change and the marine ecosystem of the western Antarctic Peninsula. *Philosophical Transactions of the Royal Society B: Biological Sciences* **362**, 149–166. 3

Collins, P.M., Green, J.A., Warwick-Evans, V., Dodd, S., Shaw, P.J.A., Arnould, J.P.Y. & Halsey, L.G. (2015) Interpreting behaviors from accelerometry: A method combining simplicity and objectivity. *Ecology and Evolution* **5**, 4642–4654. 37, 50

Conti, M.E. & Botrè, F. (2001) Honeybees and their products as potential bioindicators of heavy metals contamination. *Environmental Monitoring and Assessment* **69**, 267–282. 4

Cook, T.R., Kato, A., Tanaka, H., Ropert-Coudert, Y. & Bost, C.A. (2010) Buoyancy under control: Underwater locomotor performance in a deep diving seabird suggests respiratory strategies for reducing foraging effort. *PloS One* **5**, e9839. 14

Cook, T.R., Lescroël, A., Tremblay, Y. & Bost, C.A. (2008) To breathe or not to breathe? Optimal breathing, aerobic dive limit and oxygen stores in deep-diving blue-eyed shags. *Animal Behaviour* **76**, 565–576. 10, 12, 70, 99

Cooke, S.J., Hinch, S.G., Wikelski, M., Andrews, R.D., Kuchel, L.J., Wolcott, T.G. & Butler, P.J. (2004) Biotelemetry: A mechanistic approach to ecology. *Trends in Ecology & Evolution* **19**, 334–343. 37

Cornick, L.A. & Horning, M. (2003) A test of hypotheses based on optimal foraging considerations for a diving mammal using a novel experimental approach. *Canadian Journal of Zoology* **81**, 1799–1807. 13, 56, 71, 72, 98

Costa, D.P. (1991) Reproductive and Foraging Energetics of High Latitude Penguins, Albatrosses and Pinnipeds: Implications for Life History Patterns. *American Zoologist* **31**, 111–130. 9

Costa, D.P. (2007) A conceptual model of the variation in parental attendance in response to environmental fluctuation: Foraging energetics of lactating sea lions and fur seals. *Aquatic Conservation: Marine and Freshwater Ecosystems* **17**, S44–S52. 97

Costa, D.P. (2012) A bioenergetics approach to developing a population consequences of acoustic disturbance model. *Advances in Experimental Medicine and Biology* **730**, 423–426. 79

Costa, D.P. & Gales, N.J. (2000) Foraging energetics and diving behavior of lactating New Zealand sea lions, Phocarctos hookeri. *The Journal of Experimental Biology* **203**, 3655–3665. 88

Costa, D.P., Gales, N.J. & Goebel, M.E. (2001) Aerobic dive limit: How often does it occur in nature? *Comparative biochemistry and physiology. Part A, Molecular & integrative physiology* **129**, 771–783. 9, 56, 70

Costa, D.P., Kuhn, C., Weise, M., Shaffer, S. & Arnould, J. (2004) When does physiology limit the foraging behaviour of freely diving mammals? *International Congress Series* . 56, 70

Cowie, R.J. (1977) Optimal foraging in great tits (Parus major). *Nature* **268**, 137–139. 7

Crocker, D.E., Gales, N.J. & Costa, D.P. (2001) Swimming speed and foraging strategies of New Zealand sea lions (Phocarctos hookeri). *Journal of Zoology* **254**, 267–277. 13, 14

Crocker, D.E., Le Boeuf, B.J. & Costa, D.P. (1997) Drift diving in female northern elephant seals: Implications for food processing. *Canadian Journal of Zoology* **75**, 27–39. 57, 61

Croxall, J.P., Trathan, P.N. & Murphy, E.J. (2002) Environmental Change and Antarctic Seabird Populations. *Science* **297**, 1510–1514. 4

Cuthill, I.C. & Houston, A.I. (1997) Managing time and energy. *Behavioural Ecology. An Evolutionary Approach*, pp. 97–120, Blackwell, Oxford. 8

Daneri, G., Carlini, A. & Rodhouse, P. (2000) Cephalopod diet of the southern elephant seal, Mirounga leonina, at King George Island, South Shetland Islands. *Antarctic Science* **12**. 21, 37

Davis, C.S., Flierl, G.R., Wiebe, P.H. & Franks, P.J.S. (1991) Micropatchiness, turbulence and recruitment in plankton. *Journal of Marine Research* **49**, 109–151. 51

Davis, R.W. & Weihs, D. (2007) Locomotion in diving elephant seals: Physical and physiological constraints. *Philosophical Transactions of the Royal Society B: Biological Sciences* **362**, 2141–2150. 51

Day, L., Jouma'a, J., Bonnel, J. & Guinet, C. (2017) Acoustic measurements of post-dive cardiac responses in southern elephant seals (Mirounga leonina) during surfacing at sea. *Journal of Experimental Biology* **220**, 1626–1633. 97, 102

Deacon, G. (1933) *A General Account of the Hydrology of the South Atlantic Ocean,*. University Press, Cambridge, oCLC: 14073980. 21

Doniol-Valcroze, T., Lesage, V., Giard, J. & Michaud, R. (2011) Optimal foraging theory predicts diving and feeding strategies of the largest marine predator. *Behavioral Ecology* p. arr038. 12

Dragon, A.C., BarHen, A., Monestiez, P. & Guinet, C. (2012) Horizontal and vertical movements as predictors of foraging success in a marine predator. *Marine Ecology Progress Series* **447**, 243–257. 61

Dragon, A.C., Marchand, S., Authier, M., Cotté, C., Blain, S. & Christophe, G. (2011) Insights into the spatio-temporal productivity distribution in the Indian Sector of the Southern Ocean provided by satellite observations. *Cybium* . 22

Ducatez, S., Dalloyau, S., Richard, P., Guinet, C. & Cherel, Y. (2008) Stable isotopes document winter trophic ecology and maternal investment of adult female southern elephant seals (Mirounga leonina) breeding at the Kerguelen Islands. *Marine Biology* **155**, 413–420. 21, 37, 100

Eide, N.E., Jepsen, J.U. & Prestrud, P. (2004) Spatial organization of reproductive Arctic foxes Alopex lagopus: Responses to changes in spatial and temporal availability of prey. *Journal of Animal Ecology* **73**, 1056–1068. 78

Elliott, J.P., Cowan, I.M. & Holling, C.S. (1977) Prey capture by the African lion. *Canadian Journal of Zoology* **55**, 1811–1828. 79

Elliott, K.H., Davoren, G.K. & Gaston, A.J. (2008) Time allocation by a deep-diving bird reflects prey type and energy gain. *Animal Behaviour* **75**, 1301–1310. 98

Elliott, K.H., Hare, J.F., Le Vaillant, M., Gaston, A.J., Ropert-Coudert, Y. & Anderson, W.G. (2015) Ageing gracefully: Physiology but not behaviour declines with age in a diving seabird. *Functional Ecology* **29**, 219–228. 10

Elliott, K.H., Le Vaillant, M., Kato, A., Speakman, J.R. & Ropert-Coudert, Y. (2013) Accelerometry predicts daily energy expenditure in a bird with high activity levels. *Biology Letters* **9**, 20120919. 88

Ellis, W., Melzer, A., Green, B., Newgrain, K., Hindell, M. & Carrick, F. (1995) Seasonal-Variation in Water Flux, Field Metabolic-Rate and Food-Consumption of Free-Ranging Koalas (Phascolarctos-Cinereus). *Australian Journal of Zoology* **43**, 59–68. 99

Enstipp, M.R., Grmillet, D. & Jones, D.R. (2007) Investigating the functional link between prey abundance and seabird predatory performance. *Marine Ecology Progress Series* **331**, 267–279. 98

Fabry, V.J., Seibel, B.A., Feely, R.A. & Orr, J.C. (2008) Impacts of ocean acidification on marine fauna and ecosystem processes. *ICES Journal of Marine Science: Journal du Conseil* **65**, 414–432. 2

Falke, K.J., Hill, R.D., Qvist, J., Schneider, R.C., Guppy, M., Liggins, G.C., Hochachka, P.W., Elliott, R.E. & Zapol, W.M. (1985) Seal lungs collapse during free diving: Evidence from arterial nitrogen tensions. *Science (New York, N.Y.)* **229**, 556–558. 73

Farrell, E. & Fuiman, L. (2013) animalTrack: Animal track reconstruction for high frequency 2-dimensional (2D) or 3-dimensional (3D) movement data. *R package version 1.0.0* R package version 1.0.0. 39, 40

Fauchald, P. & Tveraa, T. (2003) Using First-Passage Time in the Analysis of Area-Restricted Search and Habitat Selection. *Ecology* **84**, 282–288. 36, 40

Fedak, M.A., Arnbom, T., McConnell, B.J., Chambers, C., Boyd, I.L., Harwood, J. & McCann, T.S. (1994) Expenditure, Investment, and Acquisition of Energy in Southern Elephant Seals. *Elephant Seals: Population Ecology, Behavior, and Physiology*, pp. 254 – 373, University of California Press. 19

Fedak, M.A., Lovell, P. & Grant, S.M. (2001) Two Approaches to Compressing and Interpreting Time-Depth Information as as Collected by Time-Depth Recorders and Satellite-Linked Data Recorders. *Marine Mammal Science* **17**, 94–110. 25, 72, 80, 81

Fedak, M.A., Lovell, P., McConnell, B. & Hunter, C. (2002) Overcoming the constraints of long range radio telemetry from animals: Getting more useful data from smaller packages. *Integrative and Comparative Biology* **42**, 3–10. 25, 80

Field, I.C., Bradshaw, C.J.A., McMahon, C.R., Harrington, J. & Burton, H.R. (2002) Effects of age, size and condition of elephant seals (Mirounga leonina) on their intravenous anaesthesia with tiletamine and zolazepam. *The Veterinary record* **151**, 235–240. 27, 38, 59, 80

Fletcher, S., Boeuf, B.J.L., Costa, D.P., Tyack, P.L. & Blackwell, S.B. (1996) Onboard acoustic recording from diving northern elephant seals. *The Journal of the Acoustical Society of America* **100**, 2531–2539. 30, 40

Fossette, S., Gaspar, P., Handrich, Y., Maho, Y.L. & Georges, J.Y. (2008) Dive and beak movement patterns in leatherback turtles Dermochelys coriacea during internesting intervals in French Guiana. *Journal of Animal Ecology* **77**, 236–246. 12, 14

Fossette, S., Gleiss, A.C., Myers, A.E., Garner, S., Liebsch, N., Whitney, N.M., Hays, G.C., Wilson, R.P. & Lutcavage, M.E. (2010) Behaviour and buoyancy regulation in the deepest-diving reptile: The leatherback turtle. *The Journal of Experimental Biology* **213**, 4074–4083. 14, 57

Furness, R.W. & Greenwood, J.J.D. (1993) *Birds as Monitors of Environmental Change*. Chapman & Hall, London; New York, oCLC: 28255680. 4

Fuster, J.F., Pagés, T. & Palacios, L. (1997) Effect of temperature on oxygen stores during aerobic diving in the freshwater turtle Mauremys caspica leprosa. *Physiological Zoology* **70**, 7–18. 10

Fyfe, J.C., Saenko, O.A., Zickfeld, K., Eby, M. & Weaver, A.J. (2007) The Role of Poleward-Intensifying Winds on Southern Ocean Warming. *Journal of Climate* **20**, 5391–5400. 3

Gallon, S., Bailleul, F., Charrassin, J.B., Guinet, C., Bost, C.A., Handrich, Y. & Hindell, M. (2013) Identifying foraging events in deep diving southern elephant seals, Mirounga leonina, using acceleration data loggers. *Deep Sea Research Part II: Topical Studies in Oceanography* **88–89**, 14–22. 14, 40, 79, 95

Génin, A., Richard, G., Jouma'a, J., Picard, B., El Ksabi, N., Vacquié Garcia, J. & Guinet, C. (2015) Characterization of postdive recovery using sound recordings and its relationship to dive duration, exertion and foraging effort of southern elephant seals (Mirounga leonina). *Marine Mammal Science* **31**, 1452–1470. 35, 62, 102

Gibbney, L. (1953) Delayed Implantation in the Elephant Seal. *Nature* **172**, 590–591. 20, 79

GIEC (2014) Changements climatiques 2014: Rapport de synthèse. *Contribution Des Groupes de Travail I, II et III Au Cinquième Rapport d'évaluation Du Groupe d'experts Intergouvernemental Sur l'évolution Du Climat*, (Sous la direction de l'équipe de rédaction principale, R.K. Pachauri et L.A. Meyer). GIEC, Genève, Suisse, 161 p. 2

Goldbogen, J.A., Calambokidis, J., Shadwick, R.E., Oleson, E.M., McDonald, M.A. & Hildebrand, J.A. (2006) Kinematics of foraging dives and lunge-feeding in fin whales. *Journal of Experimental Biology* **209**, 1231–1244. 30, 40

Goldbogen, J.A., Hazen, E.L., Friedlaender, A.S., Calambokidis, J., DeRuiter, S.L., Stimpert, A.K. & Southall, B.L. (2015) Prey density and distribution drive the three-dimensional foraging strategies of the largest filter feeder. *Functional Ecology* **29**, 951–961. 36

Gordine, S.A., Fedak, M. & Boehme, L. (2015) Fishing for drifts: Detecting buoyancy changes of a top marine predator using a step-wise filtering method. *The Journal of Experimental Biology* **218**, 3816–3824. 80, 81, 82, 88

Gordon, D.M. (1991) Variation and Change in Behavioral Ecology. *Ecology* **72**, 1196–1203. 48

Gorman, M.L., Mills, M.G., Raath, J.P. & Speakman, J.R. (1998) High hunting costs make African wild dogs vulnerable to kleptoparasitism by hyaenas. *Nature* **391**, 479–481. 79

Green, J.A., Halsey, L.G., Butler, P.J. & Holder, R.L. (2007) Estimating the rate of oxygen consumption during submersion from the heart rate of diving animals. *American Journal of Physiology. Regulatory, Integrative and Comparative Physiology* **292**, R2028–2038. 10

Green, J.A., Halsey, L.G., Wilson, R.P. & Frappell, P.B. (2009) Estimating energy expenditure of animals using the accelerometry technique: Activity, inactivity and comparison with the heart-rate technique. *Journal of Experimental Biology* **212**, 471–482. 97

Gregory, J.M., Dixon, K.W., Stouffer, R.J., Weaver, A.J., Driesschaert, E., Eby, M., Fichefet, T., Hasumi, H., Hu, A., Jungclaus, J.H., Kamenkovich, I.V., Levermann, A., Montoya, M., Murakami, S., Nawrath, S., Oka, A., Sokolov, A.P. & Thorpe, R.B. (2005) A model intercomparison of changes in the Atlantic thermohaline circulation in response to increasing atmospheric CO2 concentration. *Geophysical Research Letters* **32**, L12703. 3

Grémillet, D. & Wilson, R.P. (1999) A life in the fast lane: Energetics and foraging strategies of the great cormorant. *Behavioral Ecology* **10**, 516–524. 10

Guinet, C. (1991) Growth from Birth to Weaning in the Southern Elephant Seal (Mirounga leonina). *Journal of Mammalogy* **72**, 617–620. 19

Guinet, C., Dubroca, L., Lea, M.A., Goldsworthy, S., Cherel, Y., Duhamel, G., Bonadonna, F. & Donnay, J. (2001) Spatial distribution of foraging in female Antarctic fur seals Arctocephalus gazella in relation to oceanographic variables: A scale-dependent approach using geographic information systems. *Marine Ecology Progress Series* **219**, 251–264. 78

Guinet, C., Jouventin, P. & Weimerskirch, H. (1999) Recent population change of the southern elephant seal at Îles Crozet and Îles Kerguelen: The end of the decrease? *Antarctic Science* **11**. 18

Guinet, C., Vacquié-Garcia, J., Picard, B., Bessigneul, G., Lebras, Y., Dragon, A.C., Viviant, M., Arnould, J.P.Y. & Bailleul, F. (2014) Southern elephant seal foraging success in relation to temperature and light conditions: Insight into prey distribution. *Marine Ecology Progress Series* **499**, 285–301. 12, 36, 48, 57

Halsey, L.G., Bost, C.A. & Handrich, Y. (2007a) A thorough and quantified method for classifying seabird diving behaviour. *Polar Biology* **30**, 991–1004. 10

Halsey, L.G., Shepard, E.L.C., Quintana, F., Gomez Laich, A., Green, J.A. & Wilson, R.P. (2009) The relationship between oxygen consumption and body acceleration in a range of species. *Comparative Biochemistry and Physiology. Part A, Molecular & Integrative Physiology* **152**, 197–202. 96

Halsey, L.G., White, C.R., Enstipp, M.R., Jones, D.R., Martin, G.R. & Butler, P.J. (2007b) When cormorants go fishing: The differing costs of hunting for sedentary and motile prey. *Biology Letters* **3**, 574–576. 98

Halsey, L.G., White, C.R., Enstipp, M.R., Wilson, R.P., Butler, P.J., Martin, G.R., Grémillet, D. & Jones, D.R. (2011 Mar-Apr) Assessing the validity of the accelerometry technique for estimating the energy expenditure of diving double-crested cormorants Phalacrocorax auritus. *Physiological and biochemical zoology: PBZ* **84**, 230–237. 37

Halsey, L.G., Woakes, A. & Butler, P. (2003) Testing optimal foraging models for air-breathing divers. *Animal Behaviour* **65**, 641–653. 13

Hanuise, N. (2011) *Stratégies de Chasse Chez Le Manchot Royal : Prise Alimentaire et Optimisation Du Comportement de Plongée*. Ph.D. thesis, Strasbourg. 96, 97

Hanuise, N., Bost, C.A. & Handrich, Y. (2013) Optimization of transit strategies while diving in foraging king penguins: Optimization of transit in diving king penguins. *Journal of Zoology* **290**, 181–191. 98, 99

Harcourt, R.G., Hindell, M.A., Bell, D.G. & Waas, J.R. (2000) Three-dimensional dive profiles of free-ranging Weddell seals. *Polar Biology* **23**, 479–487. 36

Haskell, D.G. (1997) Experiments and a model examining learning in the area-restricted search behavior of ferrets (Mustela putorius furo). *Behavioral Ecology* **8**, 448–449. 49

Hassrick, J.L., Crocker, D.E., Zeno, R.L., Blackwell, S.B., Costa, D.P. & Le Boeuf, B.J. (2007) Swimming speed and foraging strategies of northern elephant seals. *Deep Sea Research Part II: Topical Studies in Oceanography* **54**, 369–383. 13, 14, 89

Hazen, E.L., Friedlaender, A.S., Thompson, M.A., Ware, C.R., Weinrich, M.T., Halpin, P.N. & Wiley, D.N. (2009) Fine-scale prey aggregations and foraging ecology of humpback whales Megaptera novaeangliae. *Marine Ecology Progress Series* **395**, 75–89. 47

Heaslip, S.G., Bowen, W.D. & Iverson, S.J. (2014) Testing predictions of optimal diving theory using animal-borne video from harbour seals (Phoca vitulina concolor). *Canadian Journal of Zoology* **92**, 309–318. 12

Heerah, K., Hindell, M., Guinet, C. & Charrassin, J.B. (2015) From high-resolution to low-resolution dive datasets: A new index to quantify the foraging effort of marine predators. *Animal Biotelemetry* **3**, 42. 81

Heithaus, M.R. & Frid, A. (2003) Optimal diving under the risk of predation. *Journal of Theoretical Biology* **223**, 79–92. 56

Heupel, M. & Simpfendorfer, C. (2008) Movement and distribution of young bull sharks Carcharhinus leucas in a variable estuarine environment. *Aquatic Biology* **1**, 277–289. 35

Hill, S., Burrows, M. & Hughes, R. (2002) Adaptive search in juvenile plaice foraging for aggregated and dispersed prey. *Journal of Fish Biology* **61**, 1255–1267. 49

Hindell, M., Harcourt, R., Waas, J. & Thompson, D. (2002) Fine-scale three-dimensional spatial use by diving, lactating female Weddell seals Leptonychotes weddellii. *Marine Ecology Progress Series* **242**, 275–284. 36

Hindell, M.A., Bradshaw, C.J.A., Sumner, M.D., Michael, K.J. & Burton, H.R. (2003) Dispersal of female southern elephant seals and their prey consumption during the austral summer: Relevance to management and oceanographic zones. *Journal of Applied Ecology* **40**, 703–715. 103

Hindell, M.A. & Lea, M.A. (1998) Heart Rate, Swimming Speed, and Estimated Oxygen Consumption of a Free-Ranging Southern Elephant Seal. *Physiological Zoology* **71**, 74–84. 13, 14

Hindell, M.A., McMahon, C.R., Bester, M.N., Boehme, L., Costa, D., Fedak, M.A., Guinet, C., Herraiz-Borreguero, L., Harcourt, R.G., Huckstadt, L., Kovacs, K.M., Lydersen, C., McIntyre, T., Muelbert, M., Patterson, T., Roquet, F., Williams, G. & Charrassin, J.B. (2016) Circumpolar habitat use in the southern elephant seal: Implications for foraging success and population trajectories. *Ecosphere* **7**, n/a–n/a. 21, 107

Hofmann, M. & Schellnhuber, H.J. (2009) Oceanic acidification affects marine carbon pump and triggers extended marine oxygen holes. *Proceedings of the National Academy of Sciences* **106**, 3017–3022. 2

Hoskins, A.J. & Arnould, J.P.Y. (2013) Temporal Allocation of Foraging Effort in Female Australian Fur Seals (Arctocephalus pusillus doriferus). *Plos One* **8**, e79484, wOS:000327143800082. 36

Hoskins, A.J., Costa, D.P. & Arnould, J.P.Y. (2015) Utilisation of Intensive Foraging Zones by Female Australian Fur Seals. *PLoS ONE* **10**, e0117997. 98

Houston, A.I. (1995) Energetic constraints and foraging efficiency. *Behavioral Ecology* **6**, 393–396. 8

Houston, A.I. (2011) Assessing models of optimal diving. *Trends in Ecology & Evolution* **26**, 292–297. 9, 56

Houston, A.I. & Carbone, C. (1992) The optimal allocation of time during the diving cycle. *Behavioral Ecology* **3**, 255–265. 8, 9, 10, 11, 12, 14, 56, 58, 61, 64, 70, 73

Houston, A.I. & McNamara, J.M. (1985) The variability of behaviour and constrained optimization. *Journal of Theoretical Biology* **112**, 265–273. 56

Husson, F., Josse, J., Le, S. & Mazet, J. (2015) FactoMineR: Multivariate Exploratory Data Analysis and Data Mining. *R package version 1.31.3* . 43

Inchausti, P., Guinet, C., Koudil, M., Durbec, J.P., Barbraud, C., Weimerskirch, H., Cherel, Y. & Jouventin, P. (2003) Inter-annual variability in the breeding performance of seabirds in relation to oceanographic anomalies that affect the Crozet and the Kerguelen sectors of the Southern Ocean. *Journal of Avian Biology* **34**, 170–176. 3

Insley, S., Robson, B., Yack, T., Ream, R. & Burgess, W. (2008) Acoustic determination of activity and flipper stroke rate in foraging northern fur seal females. *Endangered Species Research* **3**, 147–155. 59

Jacobs, S.S. & Comiso, J.C. (1997) Climate Variability in the Amundsen and Bellingshausen Seas. *Journal of Climate* **10**, 697–709. 2

Jaud, T., Dragon, A.C., Garcia, J.V. & Guinet, C. (2012) Relationship between Chlorophyll a Concentration, Light Attenuation and Diving Depth of the Southern Elephant Seal Mirounga leonina. *PLOS ONE* **7**, e47444. 102

Jeanniard-du Dot, T., Guinet, C., Arnould, J.P., Speakman, J.R. & Trites, A.W. (2016) Accelerometers can measure total and activity-specific energy expenditures in free-ranging marine mammals only if linked to time-activity budgets. *Functional Ecology* pp. n/a–n/a. 96

Jouma'a, J., Le Bras, Y., Richard, G., Vacquié-Garcia, J., Picard, B., El Ksabi, N. & Guinet, C. (2016) Adjustment of diving behaviour with prey encounters and body condition in a deep diving predator: The Southern Elephant Seal. *Functional Ecology* **30**, 636–648. 39, 48, 52, 79, 88, 93, 99

Kacelnik, A., Houston, A.I. & Schmid-Hempel, P. (1986) Central-place foraging in honey bees: The effect of travel time and nectar flow on crop filling. *Behavioral Ecology and Sociobiology* **19**, 19–24. 56

Kaiser, H.F. (1960) The application of electronic computers to factor analysis. *Educational and Psychological Measurement* **20**, 141–151. 42

Kareiva, P. & Odell, G. (1987) Swarms of Predators Exhibit "Preytaxis" if Individual Predators Use Area-Restricted Search. *The American Naturalist* **130**, 233–270. 36

Komsta, L. & Novomestky, F. (2015) Moments: Moments, cumulants, skewness, kurtosis and related tests. *R package version 0.14* . 42

Kooyman, G.L., Castellini, M.A., Davis, R.W. & Maue, R.A. (1983) Aerobic diving limits of immature Weddell seals. *Journal of comparative physiology* **151**, 171–174. 9, 70

Kooyman, G.L. & Ponganis, P.J. (1998) The physiological basis of diving to depth: Birds and mammals. *Annual review of physiology* **60**, 19–32. 58

Kooyman, G.L. & Sinnett, E.E. (1982) Pulmonary shunts in harbor seals and sea lions during simulated dives to depth. *Physiological Zoology* pp. 105–111. 73

Kooyman, G.L., Wahrenbrock, E.A., Castellini, M.A., Davis, R.W. & Sinnett, E.E. (1980) Aerobic and anaerobic metabolism during voluntary diving in Weddell seals: Evidence of preferred pathways from blood chemsitry and behavior. *Journal of comparative physiology* **138**, 335–346. 10, 70

Kozłowski, J. & Wiegert, R.G. (1986) Optimal allocation of energy to growth and reproduction. *Theoretical Population Biology* **29**, 16–37. 78

Kramer, D.L. (1988) The behavioral ecology of air breathing by aquatic animals. *Canadian Journal of Zoology* **66**, 89–94. 9, 10, 11, 56, 58, 73, 107

Kroeker, K.J., Kordas, R.L., Crim, R., Hendriks, I.E., Ramajo, L., Singh, G.S., Duarte, C.M. & Gattuso, J.P. (2013) Impacts of ocean acidification on marine organisms: Quantifying sensitivities and interaction with warming. *Global Change Biology* **19**, 1884–1896. 2

Kuhn, C.E., Sterling, J.T. & Zeppelin, T.K. (2015) Linking northern fur seal behavior with prey distributions: The impact of temporal mismatch between predator studies and prey surveys. *Animal Biotelemetry* **3**, 9. 36

Labrousse, S., Vacquié-Garcia, J., Heerah, K., Guinet, C., Sallée, J.B., Authier, M., Picard, B., Roquet, F., Bailleul, F., Hindell, M. & Charrassin, J.B. (2015) Winter use of sea ice and ocean water mass habitat by southern elephant seals: The length and breadth of the mystery. *Progress in Oceanography* **137**, 52–68. 3, 89

Langlais, C., Rintoul, S. & Schiller, A. (2011) Variability and mesoscale activity of the Southern Ocean fronts: Identification of a circumpolar coordinate system. *Ocean Modelling* **39**, 79–96. 22

Laplanche, C., Marques, T.A. & Thomas, L. (2015) Tracking marine mammals in 3D using electronic tag data. *Methods in Ecology and Evolution* **6**, 987–996. 36, 47, 48

Lavielle, M. (2005) Using penalized contrasts for the change-point problem. *Signal Processing* **85**, 1501–1510. 40

Le Boeuf, B.J., Crocker, D.E., Grayson, J., Gedamke, J., Webb, P.M., Blackwell, S.B. & Costa, D.P. (2000) Respiration and heart rate at the surface between dives in northern elephant seals. *Journal of Experimental Biology* **203**, 3265–3274. 73

Le Bras, Y. (2016) Rbl: Biologging tools for diving predators. *R package version 0.1.28* . 28, 81

Le Bras, Y., Jouma'a, J. & Guinet, C. (2017) Usage of the three-dimensional space at the bottom of the southern elephant seals' dives. *Movement Ecology* . 49, 50, 100

Le Bras, Y., Jouma'a, J., Picard, B. & Guinet, C. (2016) How Elephant Seals (Mirounga leonina) Adjust Their Fine Scale Horizontal Movement and Diving Behaviour in Relation to Prey Encounter Rate. *PLOS ONE* **11**, e0167226. 100

Lenky, C., Eisert, R., Oftedal, O.T. & Metcalf, V. (2011) Proximate composition and energy density of nototheniid and myctophid fish in McMurdo Sound and the Ross Sea, Antarctica. *Polar Biology* **35**, 717–724. 50

Lesage, V., Hammill, M.O. & Kovacs, K.M. (1999) Functional classification of harbor seal (Phoca vitulina) dives using depth profiles, swimming velocity, and an index of foraging success. *Canadian Journal of Zoology* **77**, 74–87. 59

Levitus, S., Antonov, J. & Boyer, T. (2005) Warming of the world ocean, 1955–2003. *Geophysical Research Letters* **32**, L02604. 2

Levitus, S., Antonov, J.I., Baranova, O.K., Boyer, T.P., Coleman, C.L., Garcia, H.E., Grodsky, A.I., Johnson, D.R., Locarnini, R.A., Mishonov, A.V., Reagan, J.R., Sazama, C.L., Seidov, D., Smolyar, I., Yarosh, E.S. & Zweng, M.M. (2013) The World Ocean Database. *Data Science Journal* **12**, WDS229–WDS234. 101

Loeb, V., Siegel, V., Holm-Hansen, O., Hewitt, R., Fraser, W., Trivelpiece, W. & Trivelpiece, S. (1997) Effects of sea-ice extent and krill or salp dominance on the Antarctic food web. *Nature* **387**, 897–900. 94

Loots, C., Koubbi, P. & Duhamel, G. (2007) Habitat modelling of Electrona antarctica (Myctophidae, Pisces) in Kerguelen by generalized additive models and geographic information systems. *Polar Biology* **30**, 951–959. 23

Luque, S.P. (2007) Diving Behaviour Analysis in R. *R News* **7**, 8–14, contributions from: John P.Y. Arnould, Laurent Dubroca, and Andy Liaw. 59

MacArthur, R.H. & MacArthur, J.W. (1961) On Bird Species Diversity. *Ecology* **42**, 594–598. 23

MacArthur, R.H. & Pianka, E.R. (1966) On Optimal Use of a Patchy Environment. *The American Naturalist* **100**, 603–609. 6

Magni, P., Motta, M. & Martini, L. (2000) Leptin: A possible link between food intake, energy expenditure, and reproductive function. *Regulatory Peptides* **92**, 51–56. 78

Maresh, J.L., Adachi, T., Takahashi, A., Naito, Y., Crocker, D., Horning, M., Williams, T. & Costa, D. (2015) Summing the strokes: Energy economy in northern elephant seals during large-scale foraging migrations. *Movement Ecology* **3**. 52, 79, 82, 88, 95

Maresh, J.L., Simmons, S.E., Crocker, D.E., McDonald, B.I., Williams, T.M. & Costa, D.P. (2014) Free-swimming northern elephant seals have low field metabolic rates that are sensitive to an increased cost of transport. *The Journal of Experimental Biology* **217**, 1485–1495. 79, 82, 83, 87, 89, 97, 99

Mayewski, P.A., Meredith, M.P., Summerhayes, C.P., Turner, J., Worby, A., Barrett, P.J., Casassa, G., Bertler, N.A.N., Bracegirdle, T., Naveira Garabato, A.C., Bromwich, D., Campbell, H., Hamilton, G.S., Lyons, W.B., Maasch, K.A., Aoki, S., Xiao, C. & van Ommen, T. (2009) State of the Antarctic and Southern Ocean climate system. *Reviews of Geophysics* **47**. 2

McCann, T.S., Fedak, M.A. & Harwood, J. (1989) Parental investment in southern elephant seals, Mirounga leonina. *Behavioral Ecology and Sociobiology* **25**, 81–87. 89

McConnell, B.J., Chambers, C. & Fedak, M.A. (1992) Foraging ecology of southern elephant seals in relation to the bathymetry and productivity of the Southern Ocean. *Antarctic Science* **4**, 393–398. 20, 72

McDonald, B.I. & Ponganis, P.J. (2012) Lung collapse in the diving sea lion: Hold the nitrogen and save the oxygen. *Biology letters* . 73

McIntyre, T., de Bruyn, P.J.N., Ansorge, I.J., Bester, M.N., Bornemann, H., Plötz, J. & Tosh, C.A. (2010) A lifetime at depth: Vertical distribution of southern elephant seals in the water column. *Polar Biology* **33**, 1037–1048. 20

McMahon, C.R., Bester, M.N., Burton, H.R., Hindell, M.A. & Bradshaw, C.J.A. (2005) Population status, trends and a re-examination of the hypotheses explaining the recent declines of the southern elephant seal Mirounga leonina. *Mammal Review* **35**, 82–100. 19

McMahon, C.R., Bester, M.N., Hindell, M.A., Brook, B.W. & Bradshaw, C.J.A. (2009) Shifting trends: Detecting environmentally mediated regulation in long-lived marine vertebrates using time-series data. *Oecologia* **159**, 69–82. 18, 19

McMahon, C.R., Burton, H., McLean, S., Slip, D. & Bester, M. (2000) Field immobilisation of southern elephant seals with intravenous tiletamine and zolazepam. *The Veterinary record* **146**, 251–254. 27, 38, 59, 80

McMahon, C.R. & Burton, H.R. (2005) Climate change and seal survival: Evidence for environmentally mediated changes in elephant seal, Mirounga leonina, pup survival. *Proceedings of the Royal Society B: Biological Sciences* **272**, 923–928. 90, 104

McMahon, C.R., Field, I.C., Bradshaw, C.J.A., White, G.C. & Hindell, M.A. (2008) Tracking and data–logging devices attached to elephant seals do not affect individual mass gain or survival. *Journal of Experimental Marine Biology and Ecology* **360**, 71–77. 95

Melillo, J.M., McGuire, A.D., Kicklighter, D.W., Moore, B., Vorosmarty, C.J. & Schloss, A.L. (1993) Global climate change and terrestrial net primary production. *Nature* **363**, 234–240. 2

Melzner, F., Thomsen, J., Koeve, W., Oschlies, A., Gutowska, M.A., Bange, H.W., Hansen, H.P. & Körtzinger, A. (2012) Future ocean acidification will be amplified by hypoxia in coastal habitats. *Marine Biology* **160**, 1875–1888. 2

Miller, P.J.O., Biuw, M., Watanabe, Y.Y., Thompson, D. & Fedak, M.A. (2012) Sink fast and swim harder! Round-trip cost-of-transport for buoyant divers. *Journal of Experimental Biology* **215**, 3622–3630. 13, 52, 57, 58, 72, 78

Miller, P.J.O., Johnson, M.P. & Tyack, P.L. (2004a) Sperm whale behaviour indicates the use of echolocation click buzzes 'creaks' in prey capture. *Proceedings of the Royal Society B: Biological Sciences* **271**, 2239–2247. 14, 50

Miller, P.J.O., Johnson, M.P., Tyack, P.L. & Terray, E.A. (2004b) Swimming gaits, passive drag and buoyancy of diving sperm whales Physeter macrocephalus. *The Journal of experimental biology* **207**, 1953–1967. 72

Miller, R.L., Schmidt, G.A. & Shindell, D.T. (2006) Forced annular variations in the 20th century Intergovernmental Panel on Climate Change Fourth Assessment Report models. *Journal of Geophysical Research: Atmospheres* **111**, D18101. 3

Mitani, Y., Andrews, R.D., Sato, K., Kato, A., Naito, Y. & Costa, D.P. (2010) Three-dimensional resting behaviour of northern elephant seals: Drifting like a falling leaf. *Biology letters* **6**, 163–166. 60

Mitani, Y., Sato, K., Ito, S., Cameron, M.F., Siniff, D.B. & Naito, Y. (2003) A method for reconstructing three-dimensional dive profiles of marine mammals using geomagnetic intensity data: Results from two lactating Weddell seals. *Polar Biology* **26**, 311–317. 36

Mongin, M., Molina, E. & Trull, T.W. (2008) Seasonality and scale of the Kerguelen plateau phytoplankton bloom: A remote sensing and modeling analysis of the influence of natural iron fertilization in the Southern Ocean. *Deep Sea Research Part II: Topical Studies in Oceanography* **55**, 880–892. 22

Moore, J.K. & Abbott, M.R. (2000) Phytoplankton chlorophyll distributions and primary production in the Southern Ocean. *Journal of Geophysical Research: Oceans* **105**, 28709–28722. 22

Mori, Y. (1998) The Optimal Patch Use in Divers: Optimal Time Budget and the Number of Dive Cycles During Bout. *Journal of Theoretical Biology* **190**, 187–199. 12, 78

Mori, Y. (1999) The optimal allocation of time and respiratory metabolism over the dive cycle. *Behavioral Ecology* **10**, 155–160. 11

Mori, Y. & Boyd, I.L. (2004) Segregation of foraging between two sympatric penguin species: Does rate maximisation make the difference? *Marine Ecology Progress Series* **275**, 241–249, wOS:000223426100023. 99

Mori, Y., Takahashi, A., Mehlum, F. & Watanuki, Y. (2002) An application of optimal diving models to diving behaviour of Brünnich's guillemots. *Animal Behaviour* **64**, 739–745. 71

Morris, D.W., Kotler, B.P., Brown, J.S., Sundararaj, V. & Ale, S.B. (2009) Behavioral indicators for conserving mammal diversity. *Annals of the New York Academy of Sciences* **1162**, 334–356. 5

Moss, R.H., Edmonds, J.A., Hibbard, K.A., Manning, M.R., Rose, S.K., van Vuuren, D.P., Carter, T.R., Emori, S., Kainuma, M., Kram, T., Meehl, G.A., Mitchell, J.F.B., Nakicenovic, N., Riahi, K., Smith, S.J., Stouffer, R.J., Thomson, A.M., Weyant, J.P. & Wilbanks, T.J. (2010) The next generation of scenarios for climate change research and assessment. *Nature* **463**, 747–756. 2

Nadimi, E.S., Søgaard, H.T. & Bak, T. (2008) ZigBee-based wireless sensor networks for classifying the behaviour of a herd of animals using classification trees. *Biosystems Engineering* **100**, 167–176. 37

Nagy, K.A. (1987) Field Metabolic Rate and Food Requirement Scaling in Mammals and Birds. *Ecological Monographs* **57**, 111–128. 78

Naito, Y., Bornemann, H., Takahashi, A., McIntyre, T. & Plötz, J. (2010) Fine-scale feeding behavior of Weddell seals revealed by a mandible accelerometer. *Polar Science* **4**, 309–316. 40, 57

Naito, Y., Costa, D.P., Adachi, T., Robinson, P.W., Fowler, M. & Takahashi, A. (2013) Unravelling the mysteries of a mesopelagic diet: A large apex predator specializes on small prey. *Functional Ecology* **27**, 710–717. 57, 100, 102

Narazaki, T., Sato, K., Abernathy, K.J., Marshall, G.J. & Miyazaki, N. (2009) Sea turtles compensate deflection of heading at the sea surface during directional travel. *Journal of Experimental Biology* **212**, 4019–4026. 36

Nathan, R., Getz, W.M., Revilla, E., Holyoak, M., Kadmon, R., Saltz, D. & Smouse, P.E. (2008) A movement ecology paradigm for unifying organismal movement research. *Proceedings of the National Academy of Sciences of the United States of America* **105**, 19052–19059. 35, 48

Nathan, R., Spiegel, O., Fortmann-Roe, S., Harel, R., Wikelski, M. & Getz, W.M. (2012) Using tri-axial acceleration data to identify behavioral modes of free-ranging animals: General concepts and tools illustrated for griffon vultures. *The Journal of Experimental Biology* **215**, 986–996. 50

Ng, P. & Maechler, M. (2007) A fast and efficient implementation of qualitatively constrained quantile smoothing splines. *Statistical Modelling* **7**, 315–328. 81

Ng, P. & Maechler, M. (2015) Constrained B-splines (Sparse matrix based). 81

Nonacs, P. (2001) State dependent behavior and the Marginal Value Theorem. *Behavioral Ecology* **12**, 71–83. 7

Okuyama, J., Kawabata, Y., Naito, Y., Arai, N. & Kobayashi, M. (2009) Monitoring beak movements with an acceleration datalogger: A useful technique for assessing the feeding and breathing behaviors of sea turtles. *Endangered Species Research* **10**, 39–45. 57

Orians, G. & Pearson, N. (1979) On the theory of central place foraging. *Analysis of Ecological System, Eds D.J. Horn, E.T. Stairs & R.D. Mitchell, Columbus*, pp. 155–177. 8

Ortega, L.A., Heupel, M.R., Beynen, P.V. & Motta, P.J. (2009) Movement patterns and water quality preferences of juvenile bull sharks (Carcharhinus leucas) in a Florida estuary. *Environmental Biology of Fishes* **84**, 361–373. 36

Ozgul, A., Childs, D.Z., Oli, M.K., Armitage, K.B., Blumstein, D.T., Olson, L.E., Tuljapurkar, S. & Coulson, T. (2010) Coupled dynamics of body mass and population growth in response to environmental change. *Nature* **466**, 482–485. 2

Patlak, C.S. (1953) Random walk with persistence and external bias. *The bulletin of mathematical biophysics* **15**, 311–338. 51

Pickard, G.L. & Emery, W.J. (1990) Chapter 7 - Circulation and Water Masses of the Oceans. *Descriptive Physical Oceanography, An Introduction*, pp. 154 – 275, Permagon Press. 21

Pielou, E.C. (1969) *An Introduction to Mathematical Ecology*. Wiley-Interscience. 7

Pinaud, D. & Weimerskirch, H. (2005) Scale-dependent habitat use in a long-ranging central place predator. *Journal of Animal Ecology* **74**, 852–863. 49

Pinheiro, J., Bates, D., DebRoy, S., Sarkar, D. & R Core team (2013) Nlme: Linear and Nonlinear Mixed Effects Models. 61, 83

Pitchford, J. (1999) Iron limitation, grazing pressure and oceanic high nutrient-low chlorophyll (HNLC) regions. *Journal of Plankton Research* **21**, 525–547. 22

Ponikvar, M., Šnajder, J. & Sedej, B. (2005) Honey as a bioindicator for environmental pollution with SO2. *Apidologie* **36**, 403–409. 4

Pyke, G.H. (1978) Are animals efficient harvesters? *Animal Behaviour* **26, Part 1**, 241–250. 7

Pyke, G.H. (1984) Optimal Foraging Theory: A Critical Review. *Annual Review of Ecology and Systematics* **15**, 523–575. 56

Qasem, L., Cardew, A., Wilson, A., Griffiths, I., Halsey, L.G., Shepard, E.L.C., Gleiss, A.C. & Wilson, R. (2012) Tri-Axial Dynamic Acceleration as a Proxy for Animal Energy Expenditure; Should We Be Summing Values or Calculating the Vector? *PLoS ONE* **7**, e31187. 39

R Core Team, t. (2015) R: A Language and Environment for Statistical Computing. *R Foundation for Statistical Computing* . 39, 80

Raiche, G. (2010) nFactors: An R package for parallel analysis and non graphical solutions to the Cattell scree test. *R package version 2.3.3.* R package version 2.3.3. 43

Reid, K. & Croxall, J.P. (2001) Environmental response of upper trophic-level predators reveals a system change in an Antarctic marine ecosystem. *Proceedings. Biological Sciences / The Royal Society* **268**, 377–384. 3

Richard, G., Vacquié-Garcia, J., Jouma'a, J., Picard, B., Génin, A., Arnould, J.P.Y., Bailleul, F. & Guinet, C. (2014) Variation in body condition during the post-moult foraging trip of southern elephant seals and its consequences on diving behaviour. *The Journal of Experimental Biology* **217**, 2609–2619. 14, 39, 50, 51, 52, 57, 60, 72, 79, 88

Ropert-Coudert, Y., Wilson, R.P., Daunt, F. & Kato, A. (2004) Patterns of energy acquisition by a central place forager: Benefits of alternating short and long foraging trips. *Behavioral Ecology* **15**, 824–830. 9

Roquet, F., Williams, G., Hindell, M.A., Harcourt, R., McMahon, C., Guinet, C., Charrassin, J.B., Reverdin, G., Boehme, L., Lovell, P. & Fedak, M. (2014) A Southern Indian Ocean database of hydrographic profiles obtained with instrumented elephant seals. *Scientific Data* **1**, 140028. 101

Roquet, F., Wunsch, C., Forget, G., Heimbach, P., Guinet, C., Reverdin, G., Charrassin, J.B., Bailleul, F., Costa, D.P., Huckstadt, L.A., Goetz, K.T., Kovacs, K.M., Lydersen, C., Biuw, M., Nøst, O.A., Bornemann, H., Ploetz, J., Bester, M.N., McIntyre, T., Muelbert, M.C., Hindell, M.A., McMahon, C.R., Williams, G., Harcourt, R., Field, I.C., Chafik, L., Nicholls, K.W., Boehme, L. & Fedak, M.A. (2013) Estimates of the Southern Ocean general circulation improved by animal-borne instruments. *Geophysical Research Letters* **40**, 6176–6180. 100

Rosen, D.A. & Trites, A.W. (1997) Heat increment of feeding in Steller sea lions, Eumetopias jubatus. *Comparative Biochemistry and Physiology. Part A, Physiology* **118**, 877–881. 97

Rosenzweig, C. & Parry, M.L. (1994) Potential impact of climate change on world food supply. *Nature* **367**, 133–138. 2

Sakamoto, K.Q., Sato, K., Ishizuka, M., Watanuki, Y., Takahashi, A., Daunt, F. & Wanless, S. (2009) Can ethograms be automatically generated using body acceleration data from free-ranging birds? *PloS One* **4**, e5379. 37, 50

Sallée, J.B., Speer, K.G. & Rintoul, S.R. (2010) Zonally asymmetric response of the Southern Ocean mixed-layer depth to the Southern Annular Mode. *Nature Geoscience* **3**, 273–279. 90

Sato, K., Aoki, K., Watanabe, Y.Y. & Miller, P.J.O. (2013) Neutral buoyancy is optimal to minimize the cost of transport in horizontally swimming seals. *Scientific Reports* **3**, 2205. 14, 49, 72, 88

Sato, K., Mitani, Y., Cameron, M.F., Siniff, D.B. & Naito, Y. (2003) Factors affecting stroking patterns and body angle in diving Weddell seals under natural conditions. *The Journal of experimental biology* **206**, 1461–1470. 29, 57, 60, 97

Sato, K., Naito, Y., Kato, A., Niizuma, Y., Watanuki, Y., Charrassin, J.B., Bost, C.A., Handrich, Y. & Maho, Y.L. (2002) Buoyancy and maximal diving depth in penguins. *Journal of Experimental Biology* **205**, 1189–1197. 99

Schoener, T.W. (1979) Generality of the Size-Distance Relation in Models of Optimal Feeding. *The American Naturalist* **114**, 902–914. 8

Schulze, K., Tillich, U.M., Dandekar, T. & Frohme, M. (2013) PlanktoVision - an automated analysis system for the identification of phytoplankton. *BMC Bioinformatics* **14**, 115. 103

Seibel, B.A. & Drazen, J.C. (2007) The rate of metabolism in marine animals: Environmental constraints, ecological demands and energetic opportunities. *Philosophical Transactions of the Royal Society B: Biological Sciences* **362**, 2061–2078. 78

Shepard, E., Wilson, R., Halsey, L., Quintana, F., Gómez Laich, A., Gleiss, A., Liebsch, N., Myers, A. & Norman, B. (2008a) Derivation of body motion via appropriate smoothing of acceleration data. *Aquatic Biology* **4**, 235–241. 37, 97

Shepard, E.L.C., Wilson, R.P., Quintana, F., Laich, A.G., Liebsch, N., Albareda, D.A., Halsey, L.G., Gleiss, A., Morgan, D.T., Myers, A.E., Newman, C. & Macdonald, D.W.

(2008b) Identification of animal movement patterns using tri-axial accelerometry. *Endangered Species Research* **10**, 47–60. 50

Shiomi, K., Narazaki, T., Sato, K., Shimatani, K., Arai, N., Ponganis, P. & Miyazaki, N. (2010) Data-processing artefacts in three-dimensional dive path reconstruction from geomagnetic and acceleration data. *Aquatic Biology* **8**, 289–294. 39

Shipman, P. & Walker, A. (1989) The costs of becoming a predator. *Journal of Human Evolution* **18**, 373–392. 79

Simon, M., Johnson, M., Tyack, P. & Madsen, P.T. (2009) Behaviour and kinematics of continuous ram filtration in bowhead whales (Balaena mysticetus). *Proceedings of the Royal Society of London B: Biological Sciences* **276**, 3819–3828. 30, 40

Simpfendorfer, C.A., Olsen, E.M., Heupel, M.R. & Moland, E. (2012) Three-dimensional kernel utilization distributions improve estimates of space use in aquatic animals. *Canadian Journal of Fisheries and Aquatic Sciences* **69**, 565–572. 98

Slip, D., Gales, N. & Burton, H. (1992) Body-Mass Loss, Utilization of Blubber and Fat, and Energetic Requirements of Male Southern Elephant Seals, Mirounga-Leonina, During the Molting Fast. *Australian Journal of Zoology* **40**, 235–243. 88

Slip, D.J. (1995) The diet of southern elephant seals (Mirounga leonina) from Heard Island. *Canadian Journal of Zoology* **73**, 1519–1528. 21, 37

Slip, D.J., Hindell, M.A. & Burton, H.R. (1994) Diving Behavior of Southern Elephant Seals from Macquarie Island: An Overview. *Elephant Seals: Population Ecology, Behavior, and Physiology*, pp. 253–270, University of California Press. 18

Sparling, C.E., Georges, J.Y., Gallon, S.L., Fedak, M. & Thompson, D. (2007) How long does a dive last? Foraging decisions by breath-hold divers in a patchy environment: A test of a simple model. *Animal Behaviour* **74**, 207–218, wOS:000249370000007. 56, 71

Staniland, I.J. & Boyd, I.L. (2003) Variation in the foraging location of antarctic fur seals (arctocephalus gazella) and the effects on diving behavior. *Marine Mammal Science* **19**, 331–343. 7

Staniland, I.J., Boyd, I.L. & Reid, K. (2007) An energy–distance trade-off in a central-place forager, the Antarctic fur seal (Arctocephalus gazella). *Marine Biology* **152**, 233–241. 9

Stephens, D.W. & Krebs, J.R. (1986) *Foraging Theory*. Princeton University Press. 5, 7

Strass, V.H., Naveira Garabato, A.C., Pollard, R.T., Fischer, H.I., Hense, I., Allen, J.T., Read, J.F., Leach, H. & Smetacek, V. (2002) Mesoscale frontal dynamics: Shaping the environment of primary production in the Antarctic Circumpolar Current. *Deep Sea Research Part II: Topical Studies in Oceanography* **49**, 3735–3769. 22

Stubbs, R.J. & Tolkamp, B.J. (2006) Control of energy balance in relation to energy intake and energy expenditure in animals and man: An ecological perspective. *British Journal of Nutrition* **95**, 657. 78

Suzuki, I., Naito, Y., Folkow, L.P., Miyazaki, N. & Blix, A.S. (2009) Validation of a device for accurate timing of feeding events in marine animals. *Polar Biology* **32**, 667–671. 37, 57

Takei, Y., Suzuki, I., Wong, M.K.S., Milne, R., Moss, S., Sato, K. & Hall, A. (2016) Development of an animal-borne blood collection device and its deployment for the determination of cardiovascular and stress hormones in submerged phocid seals. *American Journal of Physiology - Regulatory, Integrative and Comparative Physiology* p. ajpregu.00211.2016. 102

Talley, L.D., Pickard, G.L., Emery, W.J. & Swift, J.H. (2011) Chapter 13 - Southern Ocean. *Descriptive Physical Oceanography (Sixth Edition)*, pp. 437–471, Academic Press, Boston. 2, 23, 107

Team, R.D.C. (2014) R: A language and environment for statistical computing. R Foundation for Statistical Computing, Vienna, Austria. 61

Thayer, J.A. & Sydeman, W.J. (2007) Spatio-temporal variability in prey harvest and reproductive ecology of a piscivorous seabird, Cerorhinca monocerata, in an upwelling system. *Marine Ecology Progress Series* **329**, 253–265. 78

Thompson, D. & Fedak, M.A. (2001) How long should a dive last? A simple model of foraging decisions by breath-hold divers in a patchy environment. *Animal Behaviour* **61**, 287–296. 7, 11, 12, 13, 56, 58, 71, 72

Thompson, D., Hiby, A.R. & Fedak, M. (1993) How fast should I swim? Behavioural implications of diving physiology. *Marine Mammals: Advances in Behavioural and Population Biology: The Proceedings of a Symposium Held at the Zoological Society of London on 9th and 10th April 1992*, Symposia of the Zoological Society of London, pp. 349–368, I.L. Boyd, clarendon press edn. 13, 56, 57, 73

Thompson, D.W.J. & Solomon, S. (2002) Interpretation of Recent Southern Hemisphere Climate Change. *Science* **296**, 895–899. 3

Thums, M., Bradshaw, C. & Hindell, M. (2008) Tracking changes in relative body composition of southern elephant seals using swim speed data. *Marine Ecology Progress Series* **370**, 249–261. 88, 94

Thums, M., Bradshaw, C.J.A. & Hindell, M.A. (2011) In situ measures of foraging success and prey encounter reveal marine habitat-dependent search strategies. *Ecology* **92**, 1258–1270. 49

Thums, M., Bradshaw, C.J.A., Sumner, M.D., Horsburgh, J.M. & Hindell, M.A. (2013) Depletion of deep marine food patches forces divers to give up early. *Journal of Animal Ecology* **82**, 72–83. 72

Timmermann, A., Oberhuber, J., Bacher, A., Esch, M., Latif, M. & Roeckner, E. (1999) Increased El Niño frequency in a climate model forced by future greenhouse warming. *Nature* **398**, 694–697. 3

Todd Jones, T., Van Houtan, K.S., Bostrom, B.L., Ostafichuk, P., Mikkelsen, J., Tezcan, E., Carey, M., Imlach, B. & Seminoff, J.A. (2013) Calculating the ecological impacts of

animal-borne instruments on aquatic organisms. *Methods in Ecology and Evolution* **4**, 1178–1186. 95

Toggweiler, J.R. & Russell, J. (2008) Ocean circulation in a warming climate. *Nature* **451**, 286–288. 3

Tong, S.C., Morse, R.A., Bache, C.A. & Lisk, D.J. (1975) Elemental analysis of honey as an indicator of pollution. Forty-seven elements in honeys produced near highway, industrial, and mining areas. *Archives of Environmental Health* **30**, 329–332. 4

Tracey, J.A., Sheppard, J., Zhu, J., Wei, F., Swaisgood, R.R. & Fisher, R.N. (2014) Movement-based estimation and visualization of space use in 3D for wildlife ecology and conservation. *PloS One* **9**, e101205. 98

Tremblay, Y. & Cherel, Y. (2000) Benthic and pelagic dives: A new foraging behaviour in rockhopper penguins. *Marine Ecology Progress Series* **204**, 257–267. 12

Tuck, K. (2007) Tilt sensing using linear accelerometers. Freescale Semiconductor, AN3461 Rev. 2. 60

Tucker, V.A. (1975) The Energetic Cost of Moving About: Walking and running are extremely inefficient forms of locomotion. Much greater efficiency is achieved by birds, fish—and bicyclists. *American Scientist* pp. 413–419. 58

Turchin, P. (1991) Translating Foraging Movements in Heterogeneous Environments into the Spatial Distribution of Foragers. *Ecology* **72**, 1253–1266. 51

Vacquié Garcia, J. (2014) *Variation Spatio-Temporelle de l'activité d'alimentation Des Éléphants de Mer En Relation Avec Les Paramètres Physiques et Biologiques de l'environnement*. phd, Université de Toulouse, Université Toulouse III - Paul Sabatier. 28, 95

Vacquié-Garcia, J., Guinet, C., Dragon, A., Viviant, M., El Ksabi, N. & Bailleul, F. (2015a) Predicting prey capture rates of southern elephant seals from track and dive parameters. *Marine Ecology Progress Series* . 40

Vacquié-Garcia, J., Guinet, C., Laurent, C. & Bailleul, F. (2015b) Delineation of the southern elephant seal's main foraging environments defined by temperature and light conditions. *Deep Sea Research Part II: Topical Studies in Oceanography* **113**, 145–153. 52, 79, 100

Vacquié-Garcia, J., Royer, F., Dragon, A.C., Viviant, M., Bailleul, F. & Guinet, C. (2012) Foraging in the Darkness of the Southern Ocean: Influence of Bioluminescence on a Deep Diving Predator. *PLoS ONE* **7**, e43565. 100

van den Hoff, J., McMahon, C.R., Simpkins, G.R., Hindell, M.A., Alderman, R. & Burton, H.R. (2014) Bottom-up regulation of a pole-ward migratory predator population. *Proceedings of the Royal Society of London B: Biological Sciences* **281**, 20132842. 89

van Noordwijk, A.J. & de Jong, G. (1986) Acquisition and Allocation of Resources: Their Influence on Variation in Life History Tactics. *The American Naturalist* **128**, 137–142. 78

Veit, R. & Prince, P. (1997) Individual and population level dispersal of black-browed albatrosses Diomedea melanophris and grey-headed albatrosses D. chrysostoma in response to Antarctic krill. *Ardea* **85**, 129–134. 49

Viviant, M., Jeanniard-du Dot, T., Monestiez, P., Authier, M. & Guinet, C. (2016) Bottom time does not always predict prey encounter rate in Antarctic fur seals. *Functional Ecology* . 12, 99

Viviant, M., Trites, A.W., Rosen, D.A.S., Monestiez, P. & Guinet, C. (2010) Prey capture attempts can be detected in Steller sea lions and other marine predators using accelerometers. *Polar Biology* **33**, 713–719. 14, 28, 37, 40, 57, 101

Walker, K.A., Trites, A.W., Haulena, M. & Weary, D.M. (2012) A review of the effects of different marking and tagging techniques on marine mammals. *Wildlife Research* **39**, 15–30. 95

Wallace, R.B., Baumann, H., Grear, J.S., Aller, R.C. & Gobler, C.J. (2014) Coastal ocean acidification: The other eutrophication problem. *Estuarine, Coastal and Shelf Science* **148**, 1–13. 2

Walther, G.R., Post, E., Convey, P., Menzel, A., Parmesan, C., Beebee, T.J.C., Fromentin, J.M., Hoegh-Guldberg, O. & Bairlein, F. (2002) Ecological responses to recent climate change. *Nature* **416**, 389–395. 2

Watanabe, Y.Y., Mitani, Y., Sato, K., Cameron, M. & Naito, Y. (2003) Dive depths of Weddell seals in relation to vertical prey distribution as estimated by image data. *Marine Ecology Progress Series* **252**, 283–288. 14

Watson, K.P. & Granger, R.A. (1998) Hydrodynamic effect of a satellite transmitter on a juvenile green turtle (Chelonia mydas). *The Journal of Experimental Biology* **201 (Pt 17)**, 2497–2505. 95

Watwood, S.L., Miller, P.J.O., Johnson, M., Madsen, P.T. & Tyack, P.L. (2006) Deep-diving foraging behaviour of sperm whales (Physeter macrocephalus). *Journal of Animal Ecology* **75**, 814–825. 72

Webb, P.M., Crocker, D.E., Blackwell, S.B., Costa, D.P. & Boeuf, B.J. (1998) Effects of buoyancy on the diving behavior of northern elephant seals. *The Journal of Experimental Biology* **201**, 2349–2358. 14, 57, 72

Weimerskirch, H., Inchausti, P., Guinet, C. & Barbraud, C. (2003) Trends in bird and seal populations as indicators of a system shift in the Southern Ocean. *Antarctic Science* **15**, 249–256. 2, 3

Weimerskirch, H., Pinaud, D., Pawlowski, F., Bost, C.A., Clarke, A.E.A. & Geber, E.M.A. (2007) Does Prey Capture Induce Area-Restricted Search? A Fine-Scale Study Using GPS in a Marine Predator, the Wandering Albatross. *The American Naturalist* **170**, 734–743. 98

Wensveen, P.J., Thomas, L. & Miller, P.J.O. (2015) A path reconstruction method integrating dead-reckoning and position fixes applied to humpback whales. *Movement Ecology* **3**, 1–16. 48

Williams, T.M. (1989) Swimming by sea otters: Adaptations for low energetic cost locomotion. *Journal of Comparative Physiology. A, Sensory, Neural, and Behavioral Physiology* **164**, 815–824. 78

Williams, T.M., Davis, R.W., Fuiman, L.A., Francis, J., Le, B.J., Boeuf, Horning, M., Calambokidis, J. & Croll, D.A. (2000) Sink or Swim: Strategies for Cost-Efficient Diving by Marine Mammals. *Science* **288**, 133–136. 10, 72, 78

Wilmers, C.C., Nickel, B., Bryce, C.M., Smith, J.A., Wheat, R.E. & Yovovich, V. (2015) The golden age of bio-logging: How animal-borne sensors are advancing the frontiers of ecology. *Ecology* **96**, 1741–1753. 36

Wilson, P.R., Ainley, D.G., Nur, N., Jacobs, S.S., Barton, K.J., Ballard, G. & Comiso, J.C. (2001) Adélie penguin population change in the pacific sector of Antarctica: Relation to sea-ice extent and the Antarctic Circumpolar Current. *Marine Ecology Progress Series* **213**, 301–309. 90

Wilson, R.P., Steinfurth, A., Ropert-Coudert, Y., Kato, A. & Kurita, M. (2002) Lip-reading in remote subjects: An attempt to quantify and separate ingestion, breathing and vocalisation in free-living animals using penguins as a model. *Marine Biology* **140**, 17–27. 14, 57, 79

Wilson, R.P., White, C.R., Quintana, F., Halsey, L.G., Liebsch, N., Martin, G.R. & Butler, P.J. (2006) Moving towards acceleration for estimates of activity-specific metabolic rate in free-living animals: The case of the cormorant. *The Journal of Animal Ecology* **75**, 1081–1090. 79, 96, 97

Wolff, E.W., Fischer, H., Fundel, F., Ruth, U., Twarloh, B., Littot, G.C., Mulvaney, R., Röthlisberger, R., de Angelis, M., Boutron, C.F., Hansson, M., Jonsell, U., Hutterli, M.A., Lambert, F., Kaufmann, P., Stauffer, B., Stocker, T.F., Steffensen, J.P., Bigler, M., Siggaard-Andersen, M.L., Udisti, R., Becagli, S., Castellano, E., Severi, M., Wagenbach, D., Barbante, C., Gabrielli, P. & Gaspari, V. (2006) Southern Ocean sea-ice extent, productivity and iron flux over the past eight glacial cycles. *Nature* **440**, 491–496. 90

Wood, S. (2016) *Generalized Additive Models: An Introduction with R, Second Edition*. Chapman and Hall/CRC, Place of publication not identified, 2 edition edn. 83

Wood, S.N., Goude, Y. & Shaw, S. (2015) Generalized additive models for large data sets. *Journal of the Royal Statistical Society: Series C (Applied Statistics)* **64**, 139–155. 83

Worthy, G.a.J., Morris, P.A., Costa, D.P. & Boeuf, B.J.L. (1992) Moult energetics of the northern elephant seal (Mirounga angustirostris). *Journal of Zoology* **227**, 257–265. 20

Ydenberg, R.C. & Clark, C.W. (1989) Aerobiosis and anaerobiosis during diving by western grebes: An optimal foraging approach. *Journal of Theoretical Biology* **139**, 437–447. 56

Yeates, L.C., Williams, T.M. & Fink, T.L. (2007) Diving and foraging energetics of the smallest marine mammal, the sea otter (Enhydra lutris). *Journal of Experimental Biology* **210**, 1960–1970. 99

Zuur, A.F., Ieno, E.N. & Elphick, C.S. (2010) A protocol for data exploration to avoid common statistical problems. *Methods in Ecology and Evolution* **1**, 3–14. 82

Annexes

ANNEXE A

Variation in body condition during the post-moult foraging trip of southern elephant seals and its consequences on diving behaviour

Richard, Gaëtan, Vacquié-Garcia, Jade, Jouma'a, Joffrey, Picard, Baptiste, Génin, Alexandre, Arnould, John, Bailleul, Frédéric & Guinet, Christophe, (2014) Variation in body condition during the post-moult foraging trip of southern elephant seals and its consequences on diving behaviour. *Journal of Experimental Biology*

© 2014. Published by The Company of Biologists Ltd | The Journal of Experimental Biology (2014) 217, 2609-2619 doi:10.1242/jeb.088542

RESEARCH ARTICLE

Variation in body condition during the post-moult foraging trip of southern elephant seals and its consequences on diving behaviour

Gaëtan Richard[1], Jade Vacquié-Garcia[1], Joffrey Jouma'a[1], Baptiste Picard[1], Alexandre Génin[1], John P. Y. Arnould[2], Frédéric Bailleul[1] and Christophe Guinet[1,*]

ABSTRACT

Mature female southern elephant seals (*Mirounga leonina*) come ashore only in October to breed and in January to moult, spending the rest of the year foraging at sea. Mature females may lose as much as 50% of their body mass, mostly in lipid stores, during the breeding season due to fasting and lactation. When departing to sea, post-breeding females are negatively buoyant, and the relative change in body condition (i.e. density) during the foraging trip has previously been assessed by monitoring the descent rate during drift dives. However, relatively few drift dives are performed, resulting in low resolution of the temporal reconstruction of body condition change. In this study, six post-breeding females were equipped with time–depth recorders and accelerometers to investigate whether changes in active swimming effort and speed could be used as an alternative method of monitoring density variations throughout the foraging trip. In addition, we assessed the consequences of density change on the swimming efforts of individuals while diving and investigated the effects on dive duration. Both descent swimming speed and ascent swimming effort were found to be strongly correlated to descent rate during drift dives, enabling the fine-scale monitoring of seal density change over the whole trip. Negatively buoyant seals minimized swimming effort during descents, gliding down at slower speeds, and reduced their ascent swimming effort to maintain a nearly constant swimming speed as their buoyancy increased. One per cent of seal density variation over time was found to induce a 20% variation in swimming effort during dives with direct consequences on dive duration.

KEY WORDS: Body condition, Buoyancy, Speed, Swimming effort, *Mirounga leonina*

INTRODUCTION

The investigation of the temporal change in foraging success of top predators provides essential information on their ecology, as well as on the distribution of their prey. Such information is inherently difficult to obtain in marine ecosystems because of logistical constraints. However, since the development of the first time–depth recorders (TDRs) (Kooyman, 1965), a broad range of bio-logging tools has become available to researchers. These instruments have enabled our understanding of foraging behaviour and its relationships to environmental and physiological variables to be refined in an increasing number of seabird and marine mammal species (Kooyman, 1965; Wilson, 1992; Pütz and Bost, 1994; Handrich et al., 1997; Pütz et al., 1998).

Recently, head-mounted accelerometers have been shown to provide reliable information on the occurrence of prey capture events in seals during extended foraging trips (Naito et al., 2010; Suzuki et al., 2009; Viviant et al., 2010, Gallon et al., 2013). This approach, however, does not provide information on the size and energy content (i.e. quality) of either the prey or the associated foraging costs, such that the energy gain by the individual cannot be assessed. In addition to the number of prey-catch events, data on energy expenditure, as well as the related change in body condition, are required to assess the type and quality of prey consumed. Indeed, the change in body condition reflects the ability of the animal to allocate excess assimilated food resources towards lipid stores when maintenance and foraging costs have been covered. Therefore, to assess prey quality, there is a need to estimate fine temporal changes in the condition of the seal, as well as the foraging costs.

In deep-diving phocid seals, such as the elephant seals (*Mirounga* spp.), the buoyancy of an individual is determined primarily by its body composition, in particular, by the ratio of lipid to lean tissue (Crocker et al., 1997; Webb et al., 1998). Lean tissue is denser than seawater, whereas adipose tissue is less dense and, therefore, animals with a large proportion of lipid will be more buoyant (Beck et al., 2000; Lovvorn and Jones, 1991a; Lovvorn and Jones, 1991b; Nowacek et al., 2001; Webb et al., 1998). Elephant seals regularly perform dives during which they spend a large proportion of time descending passively through the water column ('drift dives'). Monitoring of the descent rate during these dives has already been used to track density (i.e. lipid content) changes in elephant seals during their foraging trips (Crocker et al., 1997; Biuw et al., 2003). The vertical speed of elephant seals when descending passively is directly related to buoyancy, with more buoyant seals (i.e. with a higher lipid proportion) sinking at a slower rate, or even becoming positively buoyant, compared with leaner ones (Crocker et al., 1997; Biuw et al., 2003; Miller et al., 2012). However, such 'drift rate' data obtained from TDRs can only provide a general temporal trend in body composition change as few drift dives are detected daily (Dragon et al., 2012).

As the buoyancy of a seal is directly related to its density (ρ_{animal}), variations in speed and effort during active swimming must be related to variation in its lipid and muscle proportions (Miller et al., 2012). Miller et al. (Miller et al., 2004) and Watanabe et al. (Watanabe et al., 2006) working on sperm whales (*Physeter macrocephalus*) and Baikal seals (*Phoca sibirica*), respectively,

[1]CEBC, UMR 7273 ULR-CNRS, 79360 Villiers en Bois, France. [2]School of Life and Environmental Sciences, Deakin University, 221 Burwood Highway, Burwood, VIC 3125, Australia.

*Author for correspondence (guinet@cebc.cnrs.fr)

Received 21 March 2013; Accepted 15 April 2014

The Journal of Experimental Biology (2014) doi:10.1242/jeb.088542

List of symbols and abbreviations

a	acceleration
A	frontal or surface area
C_D	drag coefficient
COT	cost of transport
$Effort_{ascent}$	ascent swimming effort
F_B	buoyancy force
F_D	drag force
$\boldsymbol{g}$	gravitational gravity (9.8 m s^{-1})
G	girth
L	length or size
P_b	proportion of total amount of the bones to body mass
P_{bw}	proportion of total amount of the body water to body mass
P_l	proportion of total amount of the lipid to body mass
P_p	proportion of total amount of the protein to body mass
R	radius
S	surface area
SES(s)	southern elephant seal(s)
TDR	time depth recorder
U	speed
U_{phase}	speed during the phase
U_{abs}	absolute speed
U_{hor}	horizontal speed
U_{vert}	vertical speed
V	volume
θ	pitch
ρ_{animal}	density of the animal
ρ_b	density of the bone
ρ_{bw}	density of the body water
ρ_{drift}	density of the seal calculated by drift rates
ρ_l	density of the lipid
ρ_p	density of the protein
ρ_{seal}	density of the seal
ρ_{sw}	density of the sea water

showed that the variation of deceleration during glides and terminal speed during prolonged glides was a consequence of the variation in body condition as the buoyancy of animals changes with their density. Correspondingly, Watanabe et al. (Watanabe et al., 2006) demonstrated that body density can be estimated by speed and pitch during prolonged glides. Subsequently, in controlled experiments on northern elephant seals (*Mirounga angustirostris*), Aoki et al. (Aoki et al., 2011) have documented that individuals adjust their stroke patterns in relation to buoyancy, increasing their stroke rate during descents and decreasing it during ascents as they become more buoyant. This suggests that seals adjust propulsive force in relation to their density to maintain swim speed by increasing or decreasing their stroke cycle frequency and stroke intensity (lateral acceleration amplitude). Furthermore, Miller et al. (Miller et al., 2012) predict that cost of transport (i.e. the amount of energy consumed per unit of mass and distance covered) should increase when deviating from neutral buoyancy, they also predict that cost of transport should increase in animals which have been artificially manipulated; negatively buoyant northern elephant seals were found to glide down during the descent phase and to stroke actively during the ascent, whereas the opposite results were obtained for positively buoyant seals. These observations suggest that keeping track of the hydrodynamic gliding performance of freely diving animals should provide a powerful approach to track changes in body condition. Therefore, the monitoring of these parameters while animals are at sea can provide new tools to investigate at a fine temporal scale their change in body condition in relation to environmental parameters (Miller et al., 2012). This might be particularly useful for the vast majority of seal species that do not perform ‘drift dives’.

Capital breeding phocid seals lose a large proportion of their body mass while fasting during the lactation period (Arnbom et al., 1997). For example, southern elephant seal (SES) (*Mirounga leonina*, Linnaeus 1758) females lose 25–50% of their initial weight over the breeding season, mostly in lipid stores that are mobilised for milk production and maintenance of metabolism (McCann et al., 1989). Hence, when leaving the colony after the breeding season, female SESs have depleted a large proportion of their lipid stores, resulting in a higher body density and, therefore, more negative buoyancy. During the post-breeding foraging trip, female seals start replenishing their energy stores, resulting in an increase in buoyancy. Consequently, these animals provide an opportunity to test, in free-ranging individuals, the predictions by Watanabe et al. (Watanabe et al., 2006) and Aoki et al. (Aoki et al., 2011) that changes in swimming speed during the gliding phase, and stroking pattern during the descent or ascent of a dive, should be tightly related to changes in seal density.

The aims of this study, therefore, were to use such changes in swimming behaviour to monitor at a fine temporal scale the recovery in body condition in post-breeding SESs over the complete foraging trip. Furthermore, Miller et al. (Miller et al., 2012) predict that change in buoyancy should have direct consequences on swimming effort, and we wanted to assess whether changes in the mean dive duration observed through the whole foraging trip were related to changes in seal buoyancy.

RESULTS

Data

The accelerometers recorded data for between 54 and 81 days for a mean (±s.d.) number of dives of 3866±400 dives recorded per seals. The number of drifts selected varied from 50 to 125 (i.e. 2.1±1.1% of the dives), and we selected 48±15% of the descents and 55±10% of the ascents (see Materials and methods and Table 1).

Drift dive model

Drift dives allowed us to estimate the body density of seals (see Eqn 8) for each drift dive identified. When several drift dives occurred on the same day, the corresponding mean density (±s.d.) was calculated (Fig. 1). On average, the six seals performed 1.3±0.6 drift dives per day and 82.8±35.2 drift dives over the recording period (Table 1). Interestingly, all drift dives detected from TDR-only data were confirmed to be truly drifting dives when adding the accelerometer information. Indeed, no differences could be detected in the daily drift rate calculated from TDR-only data versus TDR–accelerometer data (paired Wilcoxon test, P=0.94), indicating that drift rates were precisely estimated from TDR-only data. However, the variance in drift rates calculated for a given day estimated from TDR-only data was marginally greater compared with that of TDR–accelerometers (paired Wilcoxon test, P=0.08).

Table 1. Comparison of duration of the trip and numbers of dives used and selected for the study

Individual	Total dives	Drift dive	Descents selected	Ascents selected
1	4515	90	1481	1880
2	3361	125	2190	2256
3	4123	50	1091	1866
4	3768	48	2246	2455
5	3707	123	1670	1857
6	3727	61	2094	2256

See also Materials and methods.

The Journal of Experimental Biology

The Journal of Experimental Biology (2014) doi:10.1242/jeb.088542

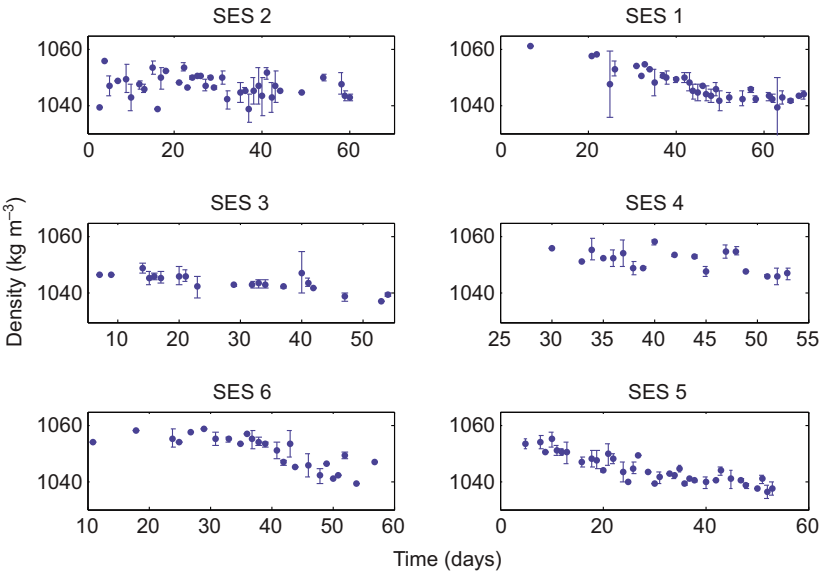

Fig. 1. Density of the six elephant seals, calculated by the mean drift rates per day. The charts in the left column represent seals that had the accelerometer fixed onto the head, those in the right column represent seals that had accelerometers on the back. Means ± s.d. are shown.

The six seals exhibited the same general trend: a decreasing density over the foraging trip, corresponding to decreasing drift rates (i.e. an increase in the proportion of lipids). Interestingly, very few drift dives were observed during the initial part of the foraging trip. After approximately 10 to 15 days, few drift dives were detected daily, and when several drift dives did occur on the same day, it is worth noting the large standard error (s.d.) associated with the mean value.

Speed versus swimming effort during ascent and descent

For each seal, both absolute speed and swimming effort during ascents and descents were calculated (see Materials and methods). All seals exhibited the same general swimming behaviour while diving.

For the descent phase, despite some day-to-day variation, no trends in swimming effort could be detected over the length of the recording period (Fig. 2A). Descent swimming effort values were very low (approximately 0.2 m s^{-3}). However, absolute descent speed showed a decreasing trend, with the noticeable exception of the first 10 to 15 days at sea, when absolute speed remained unchanged, or even increased (Fig. 2B).

For the ascent phase, after approximately the first 10–20 days where swimming effort increased, seals progressively decreased their swimming effort while heading to the surface (Fig. 2C). This allowed them to maintain nearly constant vertical and absolute ascent swimming speeds over the whole foraging trip (Fig. 2D). Indeed, for all individuals combined, we obtained a mean vertical speed (±s.d.) of 1.31±0.06 m s^{-1} (Fig. 3), a mean absolute ascent swimming speed of 1.55 m s^{-1} and a standard deviation of 0.08 m s^{-1} for a mean ascent pitch of 56.7±14.2 deg.

Estimation of density using the two models

Changes in seal density estimated from the drift rate, ρ_{drift} (kg m^{-3}), were related to the changes in absolute descent speed or ascent swimming effort through linear regressions. The first model related the mean seal density estimated from drift dives, ρ_{drift}, to the

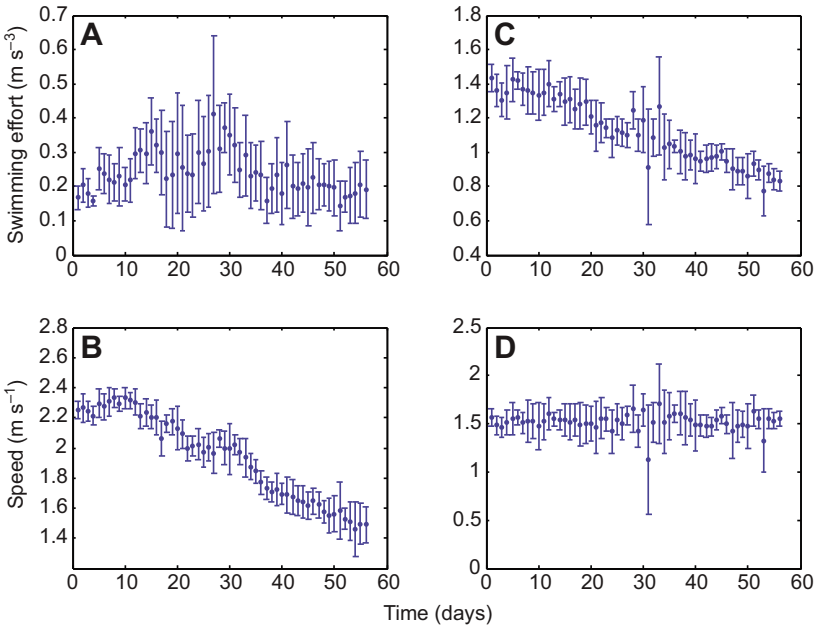

Fig. 2. Comparison of swimming effort and absolute speed between ascent and descent. Example of swimming effort during descent (A) and ascent (C), and absolute speeds during descent (B) and ascent (D) of seal 5 during the trip. Mean ± s.d. is shown.

The Journal of Experimental Biology (2014) doi:10.1242/jeb.088542

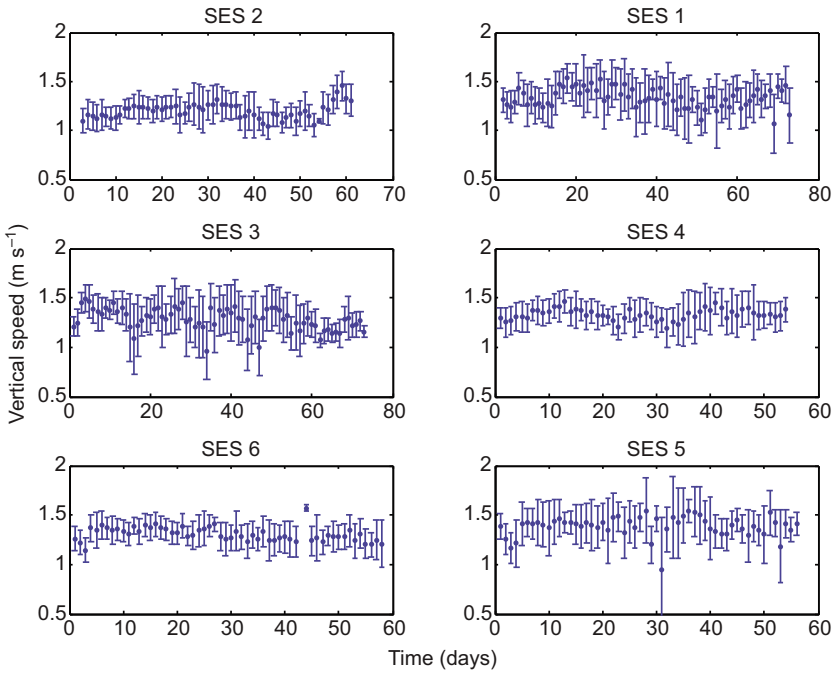

Fig. 3. Mean vertical speed per day over the trip for the six seals. Conventions are as Fig. 1. Means ± s.d. are shown.

corresponding mean absolute descent speed, $U_{descent}$ (m s^{-1}), for a given day (Eqn 1). The second model related ρ_{drift} to the mean ascent swimming effort, $Effort_{ascent}$ (m s^{-3}), for a given day (Eqn 2). The correlation coefficients for both models are shown in Table 2:

$$\rho_{drift} = a \times U_{descent} + b, \quad (1)$$

$$\rho_{drift} = a \times Effort_{ascent} + b. \quad (2)$$

For the linear regressions, we used values of mean absolute speed and mean swimming effort from days that values of drift rate were available.

Descent speed was positively correlated to ascent swimming effort for all seals (Table 3).

High to very high correlations were found between variations in density that were estimated from drift rates and descent speeds, and to a lesser extent, with ascent swimming effort (cf. r^2; Table 2). Higher correlations tended to be found for seals 1, 4 and 5 (back-mounted loggers) compared with seals 2, 3 and 6 (head-mounted loggers). However, among the seals with head-mounted accelerometers, very little variation in density was detected from the drift dives for seals 2 and 3. This indicates that they did poorly while foraging at sea. Indeed, correlation coefficients were significantly related to the absolute variation of the ρ_{drift} over the recording period (P<0.01). Therefore, the lower correlations found in some individuals might also be explained by their small density variations.

Using the relationships found, variation in seal density over the whole foraging trip was reconstructed from the descent absolute speed (Fig. 4).

Changes in diving behaviour and swimming effort in relation to seal density

Using linear mixed-effect models, we assessed how dive duration varied over time (measured in days after departure from Kerguelen Island), the corresponding estimated seal density, as well as the mean bottom depth of the dive. Time, density and mean bottom depth were fixed factors, and individuals were the random factor. Dive duration varied negatively with seal density (t=−3.77, P<0.01) and positively with the mean bottom depth of the dive (t=33.91, P<001), whereas time tended to have a positive but not significant effect (t=1.67, P=0.096).

The next step was to assess, when controlling for the mean bottom depth of the dive, which part of the dive (descent, bottom or ascent durations) varied most with increasing dive duration. For a given bottom depth of the dive, descent and bottom durations decreased, whereas ascent durations increased with increasing seal density with bottom duration variations explaining most of the variation in the complete dive duration (Table 4).

The variation of ascent swimming effort expressed as a percentage was found to be significantly related to the variation in seal density (t=1.9, P=0.05) but unrelated to the initial seal density (P=0.85).

Table 2. Results of the linear regression between density (obtained by drift rates) and absolute speed of descents (Eqn 1) and swimming effort of ascents (Eqn 2)

Individual and location of accelerometers	$\rho_{drift}=a\times U_{descent}+b$	r^2	$\rho_{drift}=a\times Effort_{ascent}+b$	r^2
1 back	$\rho_{drift}=24.62U_{descent}+991.8$	0.85	$\rho_{drift}=61.02Effort_{ascent}+1011$	0.64
2 head	$\rho_{drift}=8.65U_{descent}+1029$	0.13	$\rho_{drift}=13.13Effort_{ascent}+1031$	0.11
3 head	$\rho_{drift}=9.02U_{descent}+1021$	0.4	$\rho_{drift}=19.62Effort_{ascent}+1027$	0.66
4 back	$\rho_{drift}=22.13U_{descent}+1005$	0.85	$\rho_{drift}=22.04Effort_{ascent}+1022$	0.24
5 back	$\rho_{drift}=17.17U_{descent}+1011$	0.73	$\rho_{drift}=25.64Effort_{ascent}+1016$	0.96
6 head	$\rho_{drift}=23.39U_{descent}+1002$	0.45	$\rho_{drift}=43.21Effort_{ascent}+1006$	0.44

The Journal of Experimental Biology (2014) doi:10.1242/jeb.088542

Table 3. Results of the linear regression between mean absolute descent speed and mean ascent swimming effort per day for each seal with the linear regression equation and the correlation coefficient

Individual and location of accelerometers	$Effort_{ascent}=a\times U_{descent}+b$	r^2
1 back	$Effort_{ascent}=0.54U_{descent}-0.40$	0.88
2 head	$Effort_{ascent}=0.30U_{descent}+0.62$	0.94
3 head	$Effort_{ascent}=0.38U_{descent}-0.09$	0.63
4 back	$Effort_{ascent}=1.02U_{descent}-0.82$	0.87
5 back	$Effort_{ascent}=0.64U_{descent}-0.12$	0.97
6 head	$Effort_{ascent}=0.41U_{descent}+0.24$	0.93

Table 4. Results of the linear mixed-effect models explaining dive duration in relation to other dive factors with individuals as the random factor

Fixed factors	Value	*t*-value	*P*-value
Descent duration	166.7	281.2	<0.01
Bottom duration	295.3	873.9	<0.01
Ascent duration	125.7	245.6	<0.01
Mean bottom depth	21.9	29.7	<0.01

DISCUSSION

The results of the present study clearly demonstrate that monitoring descent swimming speed and ascent swimming effort using accelerometers combined with TDRs can provide information on changes in body density (i.e. body condition) in female SESs during their post-breeding foraging trip. Furthermore, as predicted by Miller et al. (Miller et al., 2012), this study reveals that limited changes in body density may have major consequences on an individual's swimming effort.

Drift dive model

The drift dive model was found to provide a good estimation of seal density in juvenile elephant seals (see Aoki et al., 2011). In our study, and despite inter-individual variation, the six seals exhibited a decrease of density over the foraging trip, indicating that the SES females increased their lipid proportion (i.e. body reserve).

All TDR-detected drift dives were retained from data analyses after checking the corresponding accelerometer data. This indicates that drift dives can be isolated with high accuracy from TDR data only. Furthermore, no differences in drift rates estimated from TDR-only data versus TDR–accelerometer data were found, but the variance of drift rate values for a given day was marginally larger in TDR-only data compared with that of TDR–accelerometers. The main limitation of using drift dives for the monitoring of body condition is the fact that they occur so rarely at certain times. This is particularly true for the initial part of the foraging trip (up to the first 20 days). Another limitation of this approach is the relatively large standard error associated with the mean daily drift rate, questioning the finer temporal scale accuracy. Furthermore, this approach can only be used for the few species that are known to perform drift dives.

Drift rate bias

Drift rate is a consequence of seal buoyancy directly related to body density, which is a function of body composition (proportion of total body fat). At greater deviation from neutral buoyancy, drag has a non-linear increasing effect to slow the absolute increase in drift rate (Miller et al., 2012).

In terms of a seal drifting passively through water, the terminal velocity will be influenced by external characteristics. These include the density of the seawater itself, which varies with salinity. Therefore, when seals cross water masses with contrasting densities, the estimation of seal density will also be affected. As the Splash10 tags have no salinity sensor, we were unable to assess sea water density and, therefore, account for these variations. However, this could be addressed in future work. Furthermore, according to previous work conducted on Kerguelen SESs equipped with tags measuring temperature and salinity, seawater densities that are likely to be encountered in these waters range from 1.027 to 1.030 g cm^{-3} (Charrassin et al., 2008; Bailleul et al., 2010). According to Biuw et

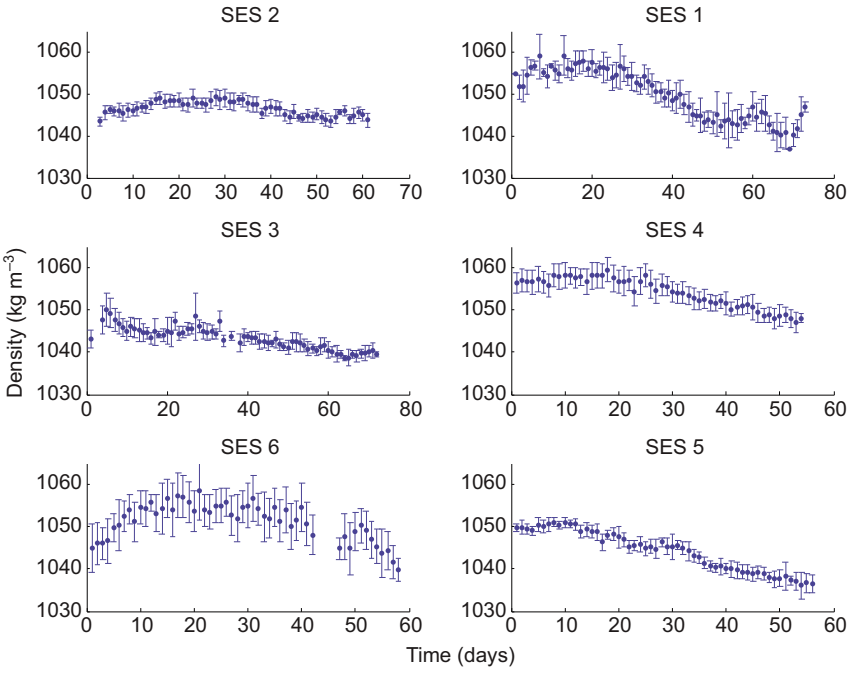

Fig. 4. Estimation of density using the linear regression equation 1. Means ± s.d. for the six seals are shown (see Table 2).

The Journal of Experimental Biology (2014) doi:10.1242/jeb.088542

al. (Biuw et al., 2003), such seawater density variations could explain approximately 2.5% of the variation seal density estimation. Therefore, the effect of sea water density on the estimation of seal density was considered marginal within the scope of this study.

Drift rate can also be influenced by physiological and behavioural changes, such as residual air in the lungs and the orientation of the seal's body in the water. In this study, calculations were only performed for dives deeper than 200 m. During diving, the increase in pressure from the surrounding water causes the lungs to collapse in seals, and complete lung collapse is supposed to occur between 150 and 200 m (Kooyman and Sinnett, 1982; Falke et al., 1985; McDonald and Ponganis, 2012). Interestingly, nearly identical results were obtained when performing the analyses and calculating descent speed and ascent swimming effort from, and up to, the surface, suggesting that the lung compression effect had a limited effect in the calculation of these parameters (supplementary material Fig. S1).

Speed versus swimming effort during ascent and descent

Both descent swimming speed and ascent swimming effort exhibited significant and concomitant changes over the foraging trips. According to the findings of Aoki et al. (Aoki et al., 2011), in a controlled experiment, such changes were most probably directly related to the variation of seal density. It is worth noting that negatively buoyant seals performed prolonged descent glides, regardless of their initial density. Inversely, all seals maintained a nearly constant swimming speed while ascending but, to do so, their density varied and modifications of swimming effort would be required. Our results suggest that seals try to reach the bottom part of their dive by passively gliding as long as they are denser than the surrounding sea water, which is likely to reduce their cost of transport. However, the descent gliding speed is highly sensitive to the buoyancy of the seal as it decreases with increasing buoyancy. During the ascent phase, the nearly constant swimming speed with very low intra-individual variance is likely to be related to the dive eco-physiological process in order to reduce the risk of decompression sickness, an acute phenomenon associated with gas uptake at pressure (for a review, see Hooker et al., 2012). Furthermore, lowering the swimming effort saves up their energy as buoyancy improves.

Both absolute descent speed and ascent swimming effort were correlated to seal density, indicating that a change in seal density has direct consequences on diving behaviour. We observed that SESs performed extended glides to descend. However, as their density decreased, so did their absolute descent speed, resulting in longer descent duration to reach a given depth for a given swimming angle. By contrast, as predicted by Miller et al. (Miller et al., 2012), as body condition improves, seals were able to decrease their swimming effort to maintain an identical absolute ascent speed, resulting in an overall decrease of swimming effort as their density decreased progressively over time. In recent studies, Miller et al. (Miller et al., 2012) and Sato et al. (Sato et al., 2013) have demonstrated theoretically and experimentally that the cost of transport in diving seals is reaching minimum value at neutral buoyancy. Through their post-breeding foraging trip, female density decreases toward neutral buoyancy and, as a consequence, the cost of transport should diminish.

Estimation of density using the two models

Absolute descent speed and ascent swimming effort were correlated to drift dive estimated seal density. According to this result, we suggest that the simultaneous monitoring of drift rate and the relative change of descent swimming speed or ascent swimming effort for negatively buoyant seals allows a high-temporal resolution indirect monitoring of seal density over the foraging trip. Indeed, the monitoring of drift rate provides an easy way to calculate the absolute value of seal density, whereas the monitoring of descent speed and ascent swimming effort variations provides a good relative variation at a fine temporal scale.

Nearly all seals exhibited an increase of their density during the first part (10 to 20 days) of their trip. This may be because, after one month fasting and lactating, post-breeding females may allocate most of their food resources to protein stores (muscle), resulting in an increase in body density. Alternatively, decreased density may indicate that female SESs are not foraging very successfully when leaving the colony, or may be focused on travelling to the detriment of foraging. Recent works on the monitoring of prey-catch events using head-mounted accelerometers on SESs (Gallon et al., 2013; Guinet et al., 2014) reveal that, in general, SESs exhibit a lower prey-catch rate per unit of time and travel greater distances when leaving and coming back to the colony. This suggests that they may, indeed, favour travelling over foraging (C.G., unpublished data).

Thereafter, all seals exhibited, to a different extent, a decrease in body density, indicative of a progressive increase of their lipid proportion, concomitant with an increasing mass. Indeed, on average, SES females were found to gain ~0.9 kg per day spent at sea (Guinet et al., 2014). Generally, the decrease in body density slowed towards the end of the foraging trip when the seals start to head back to the colony, again, when they are likely to favour travelling over foraging.

Back- or head-mounted accelerometers

Lower regression coefficients were found with head-mounted accelerometers compared with those that were back-mounted. This suggests that back-mounted accelerometers allow for a more precise assessment of swimming effort and may, therefore, return more accurate results. The main purpose of head-mounted accelerometers was to detect prey-catch events, whereas those that were back-mounted were deployed mostly to assess swimming effort. However, results suggest that this could be an artefact caused by confounding factors. Indeed, for two out of the three seals with head-mounted accelerometers, limited changes in body density over time was observed, preventing the detection of strong relationships with descent absolute speed and ascent swimming effort. Interestingly, accelerometers deployed simultaneously on the head and on the back (number 1) provided nearly identical results. Therefore, the exact influence of head- versus back-mounted accelerometers to monitor changes in seal density should be investigated in greater detail in the future.

Swimming effort

As body condition improves, absolute descent speed decreases and, as discussed earlier, as long as the seal remains negatively buoyant, the descent duration to reach a given depth will increase. Although large dive-to-dive variation in descent angle was observed, no trends in diving angle could be detected for the duration of the foraging trip. Seals do not appear to compensate their lower absolute descent speed by performing steeper dives. Changes in descent diving angle are more likely to be related to local variations of foraging success and are more likely to occur when seals are favouring horizontal displacements. Many diving predators, including SESs, king penguins and fur seals, dive at a steeper angle after a successful foraging event (Hanuise et al., 2013; Viviant et al., 2014). This

The Journal of Experimental Biology (2014) doi:10.1242/jeb.088542

resulted in a significant increase of transit time to reach a given depth as body condition improves and body density decreases, but no direct increase of the swimming effort is detected for the descent phase (but the overall expenditure related to the basal metabolic rate will increase with increasing descent duration). As predicted by Miller et al. (Miller et al., 2012), negatively buoyant SESs were found to minimize their swimming effort and, consequently, are likely to minimize their energy expenditure by performing extended glides for most of the descent, rather than minimizing their descent transit time.

During the ascent, seals are able to decrease their swimming effort as density decreased to maintain a nearly constant absolute ascent swimming speed. As a result and as long as the seal remains negatively buoyant, the overall swimming effort during the descent and ascent transit phases decreases with decreasing body density. One important finding of our study was that, regardless of the initial body density, a 1% variation in seal density (i.e. approximately 10.5 kg m^{-3}) resulted in a 15% variation in ascent swimming effort (Fig. 5), indicating that leaner seals exhibit a greater swimming effort than fatter ones, which are closer to neutral buoyancy, concurring with the prediction of Miller et al. (Miller et al., 2012). As seal density over the post-breeding foraging trip may vary by as much as 20 kg m^{-3}, this may represent a nearly 40% decrease in ascent swimming effort between the highest and lowest seal densities. This should result in a significant decrease in energy expenditure, which remains to be estimated. During the bottom phase of the dive, with the exception of few very active swimming chase phases, seals tend to, most of the time, alternate between active ascent phases and gliding descent phases (C.G., unpublished data). Variation in ascent swimming effort is, therefore, likely to be extrapolated over most of the dive. This important result is consistent with the findings of Beck et al. (Beck et al., 2000) on grey seals and of Thums et al. (Thums et al., 2013), who found that lipid content strongly influences the dive behaviour of seals, with fatter individuals having longer dive durations than leaner ones. This suggests that lipid content is likely to influence seal diving behaviour. However, as no accelerometers were deployed, those authors were not in a position to relate their findings to the variation of swimming effort with lipid content.

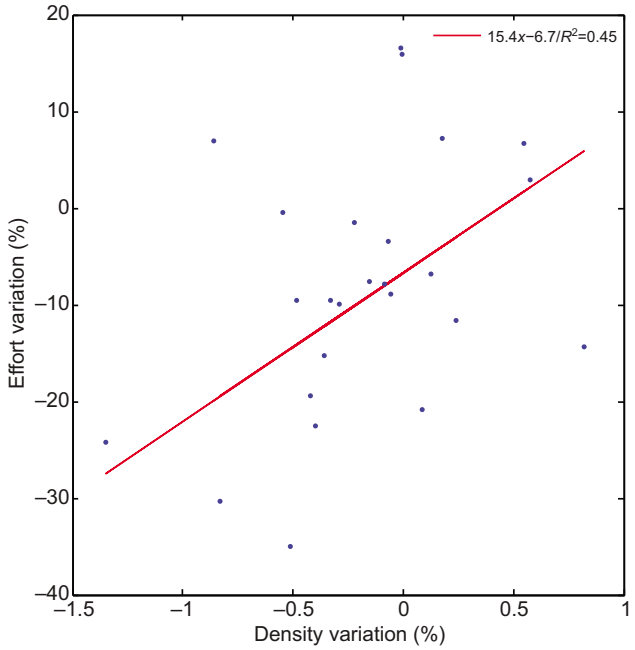

Fig. 5. Regression between percentages of ascent swimming effort variation and percentages of density variation for the six seals.

Furthermore, our results suggest that increased dive duration over the foraging trip could be explained by the number of days that had elapsed since departure. This suggests that the eco-physiological training, resulting in greater diving skills, of the seal improves, as has been suggested for northern elephant seals (Hassrick et al., 2010). Interestingly, however, the variation in dive duration when controlling for diving depth was, in fact, found to vary mostly with seal density. This result suggests that in negatively buoyant seals, swimming effort decreases with decreasing seal density, allowing the seal to perform longer dives. Therefore, according to Miller et al., 2012, we should expect that the cost of transport, and consequently the amount of energy a seal should produce to cover a given distance (i.e. the swimming effort), is minimal when seals are reaching neutral buoyancy and that the cost increases when they depart from it.

When controlling for the mean bottom depth, increased overall dive duration with decreasing density, in these negatively buoyant seals, was partly explained by a longer descent phase to reach a given depth and a longer ascent duration to swim back to the surface. However, the increase of bottom dive duration had the largest contribution to explaining the overall increase of dive duration. This result has strong ecological implications as it indicates that by improving their body condition (i.e. decrease their density towards neutral buoyancy), seals are able to decrease their swimming effort (locomotion costs) and, therefore, reduce the amount of oxygen that is allocated to swimming. As a consequence, they are able to spend more time underwater and, in particular, they can spend more time actively foraging at depth. As SES females forage mainly at the bottom of their dive [75% of prey-catch events take place at bottom phases (Guinet et al., 2014)], this result has strong implications on their foraging efficiency (i.e. seals reaching neutral buoyancy are more efficient than leaner seals). Indeed, variation of the swimming effort per unit of time spent diving both at the dive and at the multi-dive level were found to be related to seal density and to decrease with decreasing density.

We acknowledge that swimming effort provides only an indirect indication of energy expenditure during locomotion. However, numerous studies have highlighted strong and linear relationships between locomotion effort and oxygen consumption for a broad range of taxa (see Schmidt-Nielsen, 1972; Mayhew, 1977; Booth 2009). Furthermore, in a recent study on post-breeding SES females, Genin et al. (A.G., G.R., J.J., B.P., N. El Skabi, J.V.-G. and C.G., unpublished) found that surface interval duration, related to the number of breaths taken, was highly correlated to the dive duration and the overall swimming effort of the previous dive. According to the findings of Miller et al. (Miller et al., 2012), we predict that positively buoyant seals at the end of their long (i.e. 8 month) foraging trips should exhibit a decrease in their dive duration and an increase in body condition and, therefore, their foraging efficiency should decrease.

Perspectives

Accelerometers provide detailed insights into the change in seal density, as well as swimming strategy according to density. Our study suggests that in poor years, the foraging efficiency of elephant seals decreases owing to a lower prey-catch rate per unit of time, as well as an increase in foraging costs from decreasing body condition. This effect would ordinarily not be accounted for.

In the current study, accelerometers were used to assess the pitch of the seals and their swimming effort. Other studies (Viviant et al., 2010; Gallon et al., 2013; Guinet et al., 2014) underline the use of accelerometers for assessing prey-catch events during dives throughout the entire foraging trips of pinnipeds. As a result, future work should assess whether the variation in seal density along the foraging track can be related to the foraging success on one hand and swimming effort on the other hand. Furthermore, investigation of the variation of dive duration in relation to swimming effort should provide a new way to assess the respective contributions of basal metabolic rate and locomotion cost in the overall metabolic rate of free-ranging seals.

MATERIALS AND METHODS

Field site and study animals

Six post-breeding female SESs (mean mass=309±68 kg; mean length=247±17 cm; ±s.d.; Table 5) from Kerguelen Island (49°20′S, 70°20′E) were anaesthetized using a 1:1 combination of tiletamine and zolazepam (Zoletil 100), which was injected intravenously (McMahon et al., 2000), and equipped with an Argos-GPS satellite tag (Splash10-F, Wildlife Computer, USA) combined with a TDR-accelerometer (TDR-MK10-X, Wildlife Computer, USA). Splash10-F devices were set to transmit Argos locations daily and collect GPS location data. Sampling intervals of GPS locations was set to a minimum of 20 minutes, i.e. slightly shorter than the mean dive duration of the species (Hindell et al., 1991), pressure and temperature were sampled at 1 Hz. MK10-X was also set to collect and archive pressure and temperature levels every second. Three-axis accelerations (sway, surge and heave) that measure both dynamic acceleration (such as propulsive activities) and static acceleration (such as gravity or pitch) were sampled at 16 Hz. The six Splash10-F tags were glued onto the heads of seals. In 2010, three of the accelerometers were glued onto the back of the head, and one seal (number 1) was simultaneously equipped with an accelerometer glued onto its back (MK10-D, Wildlife Computer). In 2011, two accelerometers were deployed on the back of the seals and one was deployed on the head (Table 5).

Data loggers were glued onto the heads and the backs of the seals using quick-setting epoxy (Araldite AW 2101) after cleaning the fur with acetone. The loggers were recovered when SES females returned to shore to moult (i.e. January–February following deployments). Once ashore, seals were located using their Argos locations.

Data analysis

Data processing and analyses were conducted using MATLAB (The MathWorks, Natick, MA, USA). First, pressure data were used to identify surface intervals and dives. Dives were split into three phases: descent, bottom and ascent, and then classified into four categories based on diving behaviour, namely: drift dives, exploratory dives, shallow active dives and deep active dives (Dragon et al., 2012). The mean bottom depth corresponded to the mean value of the depth readings during the bottom phase of a dive. The passive drift phase of the drift dive was isolated to estimate the density of a seal according to Biuw et al. (Biuw et al., 2003).

Seal density was estimated from the drift dive model, which provides a simplified situation to estimate body density because balance of force is simpler when the animal is only sinking passively (Crocker et al., 1997; Biuw et al., 2003). However, because so few passive drift dives are performed daily (Dragon et al., 2012), body condition variation becomes difficult to assess at a fine temporal scale. In contrast, speed and swimming effort, calculated during the descent and ascent of each dive, provide a high-frequency time series with SESs performing ~60 to 70 dives daily (Boyd and Arnbom, 1991; Dragon et al., 2012). Although seal density can be estimated from descent or ascent glides (Watanabe et al., 2006), the correct calculation of seal density to take into account all forces is more complex. Therefore, our approach was to calculate seal density only from the drift dives, which is simpler. Swimming speed and swimming effort were used to obtain a high-resolution time series. When both pieces of information were available, we investigated the relationship between drift dive estimated seal density and the corresponding swimming speed and effort data on a daily basis.

Descent swimming speed

Information on the body angle (from the acceleration sensor) and vertical speed (as determined from the depth recorder) provided us with an estimate of the actual swimming speed during the long ascent and descent phase (Sato et al., 2003). However, this method is only reliable for steeper body angles.

Acceleration data were processed according to Sato et al. (Sato et al., 2003), Watanabe et al. (Watanabe et al., 2006) and Aoki et al. (Aoki et al., 2011). Different filters applied on the three axes were used to characterize the different components of seal movement. The gravity component of the movement was obtained by applying a low-pass filter at 0.2 Hz on the three axes. We used the lower-frequency gravity-based accelerations of the three axes to calculate the pitch, θ (Eqn 3), of the seal using the three axis acceleration data (Tuck, 2007) that was sampled at 16 Hz using:

$$\theta = \arctan\left(\frac{x}{\sqrt{y^2 + z^2}}\right), \quad (3)$$

where x, y and z are the filtered acceleration values for the longitudinal, lateral and vertical axis (Sato et al., 2003; Watanabe et al., 2006; Aoki et al., 2011). The comparison of the data obtained simultaneously from the head and back accelerometer (seal 1) revealed a difference between the mean pitches obtained by both of the accelerometers. Furthermore, the mean pitch calculated by both accelerometers when the seal was breathing at the surface between two dives revealed that the pitch obtained by the head accelerometer exhibited an offset compared with the back accelerometer. Consequently, we calculated a mean pitch difference between the three head and back accelerometers of 13.9 deg, and we used this mean value to inter-calibrate the accelerometers between seals. So head accelerometers were corrected accordingly to provide comparable data with those deployed on the back.

Swaying accelerations often contained low frequency variations that were assumed to be the result of various turning and rolling movements by the seals. These were separated using a high-pass filter in order to extract the information on flipper stroking activity. To select an appropriate filter band, the power spectral density of each swaying acceleration record was calculated using a fast Fourier Transformation. Lateral axis was processed with a 0.6 Hz-wide band-pass filter to assess the result of the swimming movement. The remaining peaks and troughs with absolute intensities greater than a set threshold of 0.2 m s^{-2} were considered to represent individual strokes (Sato et al., 2003). Stroking rate and the intensity of the hind-flipper movement allowed the calculation of a swimming effort index (Eqn 4):

$$\text{Swimming effort} = \frac{\sum|\text{peaks}|}{\Delta t}. \quad (4)$$

Table 5. Loggers deployed on the six elephant seals

Individual	Mass (kg)	Size (cm)	Accelerometer	Position	Date of departure	Days recorded
1	377	266	MK10-D/ MK10-X	Back and head	11/21/2010	74
2	331	266	MK10-X	Head	10/28/2010	61
3	395	252	MK10-X	Head	11/01/2010	81
4	245	225	MK10-X	Back	10/29/2011	54
5	249	240	MK10-X	Back	10/31/2011	56
6	255	232	MK10-X	Head	10/31/2011	58

The Journal of Experimental Biology

Similar to Aoki et al. (Aoki et al., 2011), swimming effort (m s^{-3}) was the sum of the absolute value of lateral acceleration peaks, Σ|peaks| (m s^{-2}), during the duration of the phase studied, Δt (s). The peaks correspond to the intensity of hind-flipper movements, and so the index reflects the intensity per second. It should be pointed out that the swimming effort calculated by us was strongly related to overall dynamic body acceleration (ODBA) (Wilson et al., 2006) with a mean correlation coefficient (±s.d.) of 0.77±0.15 between the two methods at the dive scale. Moreover, we compared swimming efforts calculated using the lateral axis and those calculated using the three axes during descents, bottoms and ascents over time for seal 1. We observed a good correlation between lateral axis and the three axes with mean coefficients of correlation of 0.95 for descents, 0.89 for bottoms and 0.83 for ascents (supplementary material Fig. S2). As a result, using the three axes to calculate the swimming effort index provides no additional information and adds noise as we worked on relative variation and not on absolute values (supplementary material Fig. S3). Furthermore, recent studies on fur seal have found that flipper stroke is a better predictor of energy expenditure, whereas no relationships are found with ODBA (J. du Dot, unpublished data). Therefore, this index of swimming effort was preferred to ODBA as it focused on lateral acceleration, which is a direct measurement of the propulsive activities, whereas ODBA provides an integrated index of all acceleration sources, some of them being unrelated to the propulsive effort. Only the lateral axis accelerations were used because phocid seals mostly use lateral movements of the hind-flippers for propulsion. In addition, the power spectral density of the longitudinal and the vertical axes obtained by a fast Fourier Transformation did not show high frequencies that corresponded to any swimming hind-flipper movement.

Forces and body composition

When swimming, seals are subjected to external forces. The balance of these forces affects the energetic cost of movement (Tucker, 1975). In marine mammals, the primary forces are hydrodynamic drag and buoyancy (Schmidt-Nielsen, 1972). The drag of the seal during drifts and glides depends on their speed (Watanabe et al., 2006; Aoki et al., 2011):

$$F_D = 0.5 C_D \rho_{sw} A U^2 , \quad (5)$$

where F_D is drag force (N), C_D is the drag coefficient, ρ_{sw} (kg m^{-3}) is the density of the seawater, A is the frontal or surface area of the seal (m^2) and U is swim speed (m s^{-1}). Drag force always opposes the direction of movement and increases with speed. Buoyancy is defined as the sum of the weight force and the Archimedes's force (Lovvorn et al., 1991; Beck et al., 2000):

$$F_B = (\rho_{sw} - \rho_{animal}) V \boldsymbol{g} , \quad (6)$$

where F_B is buoyant force (N), ρ_{animal} is the density of the animal (kg m^{-3}), V is the volume of the animal (m^3) and $\boldsymbol{g}$ is the acceleration of the gravity (=9.81 m s^{-2}). If ρ_{animal} is higher than ρ_{sw}, buoyancy will be negative and the animal will sink passively. Conversely, extra energy will have to be expended when the animal returns to the surface. In marine mammals, ρ_{animal} is mainly determined by the relative amount of lipid and lean tissue:

$$\rho_{animal} = \rho_l \times P_l = \rho_p \times P_p + \rho_b \times P_b + \rho_{bw} \times P_{bw} , \quad (7)$$

where ρ is the density of the component, P is the proportion of the component, and subscripts l, p, b and bw refer to lipid, protein, bone mineral (ash) and body water (Biuw et al., 2003; Aoki et al., 2011). To gain an idea of the density values, we can refer to human values: ρ_l=900.7, ρ_p=1340, ρ_a=2300 and ρ_{bw}=994 kg m^{-3} (Moore et al., 1963). We assume in the following models that female SESs on their post-breeding trip have a high proportion of lean tissue and that they will increase their proportion of lipid during their foraging trip. Consequently, the variation in density would mainly be due to the variation of lipid proportion. Bone and ash contribution to variation of density are assumed to be negligible.

We used a median (±s.d.) seawater density for the Southern Ocean of 1027.5±2 kg m^{-3}.

Drift dives model

Drift dive identification (Fig. 6) was processed in two steps: we used first the complete TDR allowing us to (i) identify drift dives and (ii) isolate the passive drift phase during those dives (see Dragon et al., 2012). For each drift dive, a drift rate was determined as the slope coefficient of a linear regression between depth and time (Biuw et al., 2003; Bailleul et al., 2007; Mitani et al., 2010). In a second step, we used accelerometer data to exclude phases of active swimming during drift phases assessed by the TDR-only data. Active swimming was considered to take place when lateral acceleration exceeded the –0.2 to 0.2 m s^{-2} range. Subsequently, we only analysed truly passive drift phases to estimate seal density.

During passive drift phases, SESs are only subject to drag force and buoyancy. Thus, during ascending drift phases F_B=F_D, and during descending drift phases F_B=–F_D (Biuw et al., 2003; Aoki et al., 2011). Given

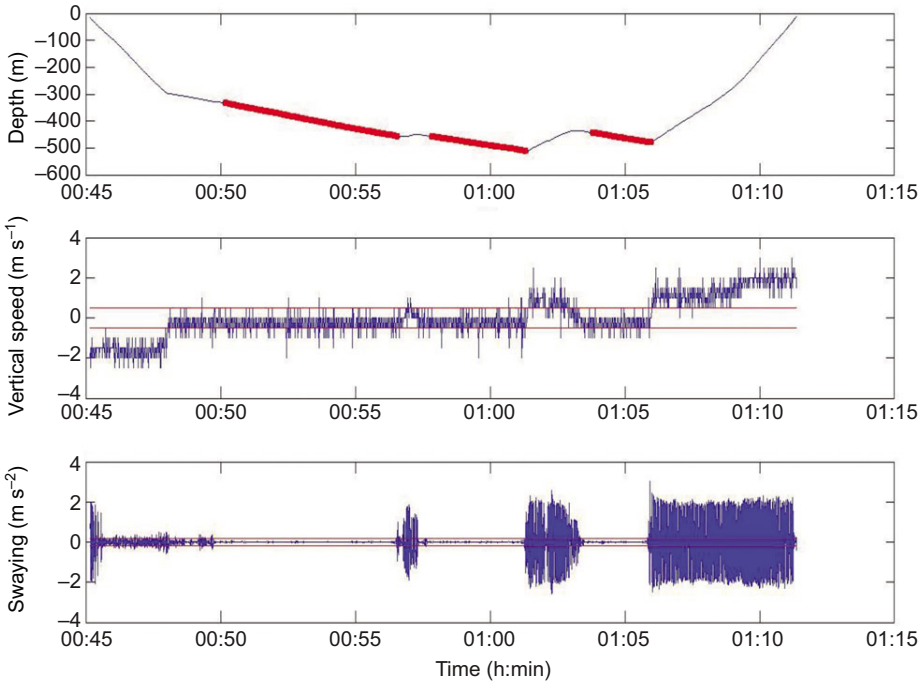

Fig. 6. Drift dive identification. Example of a drift dive depth profile (A) with the associated vertical speed profile (B) and the lateral axis of accelerometers representing the movement profile of the hind flipper (C). We consider the passive drifts during bottom (red on the depth profile) when vertical speed is bounded between –0.4 and 0.4 m s^{-1} and the lateral acceleration between –0.2 and 0.2 m s^{-2}.

Eqns 5 and 6, we obtain the mean seal density for descending drift phases (Eqn 8).

$$\rho_{seal} = \rho_{sw} + \frac{U_{drift}^2 \cdot C_D \cdot \rho_{sw} \cdot S_{seal}}{2\boldsymbol{g} \cdot V_{seal}}, \quad (8)$$

where U_{drift} is the speed (m s^{-1}) of the seal during the passive drift phase, i.e. the drift rate. C_D is the drag coefficient based on the total surface area (S_{seal}) and fixed to 0.69 (Biuw et al., 2003; Aoki et al., 2011). Animal volume is considered to be equivalent to two opposing cones with a common base that corresponds to total girth (Bell et al., 1997; Biuw et al., 2003; Aoki et al., 2011):

$$S_{seal} / V_{seal} = \frac{\sqrt{1+\frac{L^2}{3R^2}} + \sqrt{1+\frac{2L^2}{3R^2}}}{L}. \quad (9)$$

L is the mean size of the seal between the sizes measured at the beginning and the end of the trip at sea, and R is the radius of the cones common base (unmeasured in the field). To obtain R, we used the empirical relationship described by Castellini and Calkins (Castellini and Calkins, 1993) between m the mass (kg), L the size (m) and G the girth (m^2): m=45.7LG. As G=2ΠR, we obtain:

$$R^2 = \frac{m}{4\Pi^2 \times 45.7L}, \quad (10)$$

where m is the mean mass of the seal between the masses measured at the beginning and the end of the pelagic trip.

Speed versus swimming effort during ascent and descent

Previous experimental studies on seals have shown that stroking effort is tightly related to seal density (Aoki et al., 2011; Miller et al., 2012). However, the precise calculation of body density when the seal is actively swimming is complicated owing to the complex balance of forces. For this reason, we investigated the direct relationship between the body density estimated from drift dives and the swimming speed stroking effort during descent and ascent phases of the dive. Indeed, positively buoyant seals stroke actively during the descent phase of the dive. Negatively buoyant seals, however, stroke actively during their ascent (Watanabe et al., 2006; Aoki et al., 2011; Miller et al., 2012). Therefore, change in swimming effort and speed during the ascent and the descent phase of the dive were monitored through the whole foraging trip, assuming that a change in seal density should influence either one of these two parameters. During the ascent and descent, the swimming speed can be calculated by combining information on the vertical speed and the seal pitch (Fig. 7) using the following relationship:

$$U_{abs} = \frac{U_{vert}}{\sin\theta}. \quad (11)$$

Swimming speed calculated by Eqn 11 (see Miller et al., 2004) was considered reliable when the absolute body pitch was over 30 deg. As a result, we use this proxy for deep descents and ascents, i.e. ending and starting below 400 m deep, respectively, and with an absolute pitch over 30 deg (Watanabe et al., 2006).

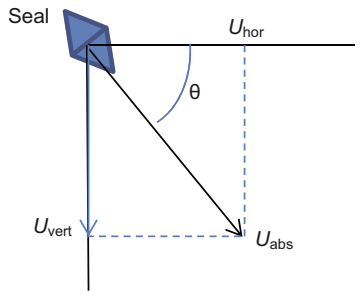

Fig. 7. Geometry of movement of a descending elephant seal. The absolute speed vector (U_{abs}) is the sum of the horizontal speed vector (U_{hor}) and the vertical speed vector (U_{vert}). The vertical speed is the depth covered by the seal per second.

Seals were considered as fully compressed for depths greater than 200 m [to exclude variation of density, which might be caused by lung collapse under pressure (see Biuw et al., 2003)].

During descents and ascents, seals are always subject to buoyancy and drag force but, as they are gliding, the balance of forces incorporates the acceleration of the seal. However, the derivation of speed incorporates error as the speed is already an estimate. Therefore, we used the variation of speed and the variation of stroking effort during ascents and descents over the trip to describe the variation of body condition over time.

Change in dive parameters – descent, ascent, dive and bottom time durations – along the foraging trip were assessed using a generalized linear model using diving depth, as well as pitch angle for the descent and ascent and body density as covariables. The individual was included as a random effect.

Change in swimming effort in relation to seal density

During their foraging trip, seals exhibited periods during which they increased or decreased their density. The minimum and maximum densities at the beginning and the end of each of these periods were assessed and density variation, expressed as a proportion (%) of the initial density for each of these periods, was calculated. For the corresponding periods, the variations in seal swimming effort were also calculated. As post-breeding females always remain negatively buoyant, most of their descents are characterized by prolonged glides, and therefore most of the swimming effort takes place during the ascent phase of the dive. The variations of ascent swimming effort were expressed as a percentage (%) of the initial swimming effort at the beginning of each of the corresponding density variation periods. Because accelerometers had not been inter-calibrated before deployment, we used the variation in percentage, rather than the absolute swimming effort. A calculation of absolute swimming effort, comparable between seals, would have required such absolute calibration, whereas the calculation of a relative variation did not.

Linear mixed-effect model

We used a linear mixed-effect model in the statistical platform R (R Development Core Team, 2012) to explain the variation of a dive factor by other dive explanatory variables (i.e. fixed factors) with individuals as the random factor. In order to compare the effects of the fixed factors, the fixed factors were standardized. The value of each coefficient is therefore indicative of its relative contribution to the explained factor. Several explanatory variables were found to be inter-correlated, and therefore multicollinearity could occur. As a consequence, only variables exhibiting a correlation coefficient lower than 0.75 were kept in the model. When higher correlation coefficients were found, the models were run with only one of the two inter-correlated variables.

Acknowledgements

The authors thank all the Kerguelen fieldworkers for field work that helped to collect data. This study is part of a national research program (no. 109, H. Weimerskirch and the observatory Mammifères Explorateurs du Milieu Océanique, MEMO SOERE CTD 02) supported by the French Polar Institute (Institut Paul Emile Victor; IPEV). This work was carried out in the framework of the ANR Blanc MYCTO-3D-MAP and ANR VMC 07: IPSOS-SEAL programs and CNES-TOSCA program ('Élephants de mer océanographes'). All animals in this study were cared for in accordance with its guidelines. We wish to thank all the people who contributed to the field work and data processing with special thought to: M. Authier, A. Chaigne, Q. Delorme, N. El Skaby, J. C. Vaillant and F. Vivier. We wish to thank two anonymous referees for their comments and suggestions; P. Miller for his very useful comments on an earlier version; and Laureen Biermann for correcting the English of this paper.

Competing interests

The authors declare no competing financial interests.

Author contributions

G.R. designed the global model with the participation of C.G. G.R., J.V.G., J.J., B.P. and A.G. performed the data and statistical analyses. All authors participated in the discussion and interpretation of results. The manuscript was primarily edited by G.R., J.A., F.B. and C.G.

Funding
The authors thank the Total Foundation for financial support. Deposited in PMC for immediate release.

Supplementary material
Supplementary material available online at
http://jeb.biologists.org/lookup/suppl/doi:10.1242/jeb.088542/-/DC1

References

Aoki, K., Watanabe, Y. Y., Crocker, D. E., Robinson, P. W., Biuw, M., Costa, D. P., Miyazaki, N., Fedak, M. A. and Miller, P. J. O. (2011). Northern elephant seals adjust gliding and stroking patterns with changes in buoyancy: validation of at-sea metrics of body density. *J. Exp. Biol.* **214**, 2973-2987.
Arnbom, T., Fedak, M. A. and Boyd, I. L. (1997). Factors affecting maternal expenditure in southern elephant seals during lactation. *Ecology* **78**, 471-483.
Bailleul, F., Charrassin, J. B., Monestiez, P., Roquet, F., Biuw, M. and Guinet, C. (2007). Successful foraging zones of southern elephant seals from the Kerguelen Islands in relation to oceanographic conditions. *Philos. Trans. R. Soc. B* **362**, 2169-2181.
Bailleul, F., Authier, M., Ducatez, S., Roquet, F., Charrassin, J. B., Cherel, Y. and Guinet, C. (2010). Looking at the unseen: combining animal bio-logging and stable isotope to reveal a shift in the ecological niche of a deep diving predator. *Ecography* **33**, 709-719.
Beck, C. A., Bowen, W. D. and Iverson, S. J. (2000). Seasonal changes in buoyancy and diving behaviour of adult grey seals. *J. Exp. Biol.* **203**, 2323-2330.
Bell, C. M., Hindell, M. A. and Burton, H. R. (1997). Estimation of body mass in the southern elephant seal, *Mirounga leonina*, by photogrammetry and morphometrics. *Mar. Mamm. Sci.* **13**, 669-682.
Biuw, M., McConnell, B., Bradshaw, C. J. A., Burton, H. and Fedak, M. (2003). Blubber and buoyancy: monitoring the body condition of free-ranging seals using simple dive characteristics. *J. Exp. Biol.* **206**, 3405-3423.
Booth, D. T. (2009). Swimming for your life: locomotor effort and oxygen consumption during the green turtle (*Chelonia mydas*) hatchling frenzy. *J. Exp. Biol.* **212**, 50-55.
Boyd, I. L. and Arnbom, T. (1991). Diving behaviour in relation to water temperature in the southern elephant seal – foraging implications. *Polar Biol.* **11**, 259-266.
Castellini, M. A. and Calkins, D. G. (1993). Mass estimates using body morphology in steller sea lions. *Mar. Mammal Sci.* **9**, 48-54.
Charrassin, J. B., Hindell, M., Rintoul, S. R., Roquet, F., Sokolov, S., Biuw, M., Costa, D., Boehme, L., Lovell, P., Coleman, R. et al. (2008). Southern Ocean frontal structure and sea-ice formation rates revealed by elephant seals. *Proc. Natl. Acad. Sci. USA* **105**, 11634-11639.
Crocker, D. E., le Boeuf, B. J. and Costa, D. P. (1997). Drift diving in female northern elephant seals: implications for food processing. *Can. J. Zool.* **75**, 27-39.
Dragon, A.-C., Bar-Hen, A., Monestiez, P. and Guinet, C. (2012). Horizontal and vertical movements as predictors of foraging success in a marine predator. *Mar. Ecol. Prog. Ser.* **447**, 243-257.
Falke, K. J., Hill, R. D., Qvist, J., Schneider, R. C., Guppy, M., Liggins, G. C., Hochachka, P. W., Elliott, R. E. and Zapol, W. M. (1985). Seal lungs collapse during free diving: evidence from arterial nitrogen tensions. *Science* **229**, 556-558.
Gallon, S., Bailleul, F., Charrassin, J. B., Guinet, C., Bost, C.-A., Handrich, Y. and Hindell, M. (2013). Identifying foraging events in deep diving southern elephant seals, *Mirounga leonina*, using acceleration data loggers. *Deep Sea Research Part II: Topical Studies in Oceanography* **88-89**, 14-22.
Guinet, C., Vacquié-Garcia, J., Picard, B., Bessigneul, G., Lebras, Y., Dragon, A. C., Viviant, M., Arnould, J. P. Y. and Bailleul, F. (2014). Foraging behaviour of southern elephant seals provides Insight into the distribution from their prey. *Mar. Ecol. Prog. Ser.* **499**, 285-301.
Handrich, Y., Bevan, R. M., Charrassin, J. B., Butler, P. J., Pütz, K., Woakes, A. J., Lage, J. and Le Maho, Y. (1997). Hypothermia in foraging king penguins. *Nature* **388**, 64-67.
Hanuise, N., Bost, C.-A. and Handrich, Y. (2013). Optimization of transit strategies while diving in foraging king penguins. *J. Zool. (Lond.)* **290**, 181-191.
Hassrick, J. L., Crocker, D. E., Teutschel, N. M., McDonald, B. I., Robinson, P. W., Simmons, S. E. and Costa, D. P. (2010). Condition and mass impact oxygen stores and dive duration in adult female northern elephant seals. *J. Exp. Biol.* **213**, 585-592.
Hindell, M., Slip, D. and Burton, H. (1991). The diving behaviour of adult male and female southern elephant seals, *Mirounga leonina* (Pinnipedia: Phocidae). *Aust. J. Zool.* **39**, 595-619.
Hooker, S. K., Fahlman, A., Moore, M. J., de Soto, N. A., de Quirós, Y. B., Brubakk, A. O., Costa, D. P., Costidis, A. M., Dennison, S., Falke, K. J. et al. (2012). Deadly diving? Physiological and behavioural management of decompression stress in diving mammals. *Proc. Biol. Sci.* **279**, 1041-1050.
Kooyman, G. L. (1965). Techniques used in measuring diving capacities of Weddell seals. *Polar Rec. (Gr. Brit.)* **12**, 391-394.
Kooyman, G. L. and Sinnett, E. E. (1982). Pulmonary shunts in harbor seals and sea lions during simulated dives to depth. *Physiol. Zool.* **55**, 105-111. 10.2307/30158447
Lovvorn, J. R. and Jones, D. R. (1991a). Effects of body size, body fat, and change in pressure with depth on buoyancy and costs of diving in ducks (*Aythya* spp.). *Can. J. Zool.* **69**, 2879-2887.
Lovvorn, J. R. and Jones, D. R. (1991b). Body mass, volume, and buoyancy of some aquatic birds, and their relation to locomotor strategies. *Can. J. Zool.* **69**, 2888-2892.
Lovvorn, J. R., Jones, D. R. and Blake, R. W. (1991). Mechanics of underwater locomotion in diving ducks: drag, buoyancy and acceleration in a size gradient of species. *J. Exp. Biol.* **159**, 89-108.
Mayhew, J. L. (1977). Oxygen cost and energy expenditure of running in trained runners. *Br. J. Sports Med.* **11**, 116-121.
McCann, T. S., Fedak, M. A. and Harwood, J. (1989). Parental investment in southern elephant seals, *Mirounga leanina*. *Behav. Ecol. Sociobiol.* **25**, 81-87.
McDonald, B. I. and Ponganis, P. J. (2012). Lung collapse in the diving sea lion: hold the nitrogen and save the oxygen. *Biol. Lett.* **8**, 1047-1049.
McMahon, C. R., Burton, H., McLean, S., Slip, D. and Bester, M. (2000). Field immobilisation of southern elephant seals with intravenous tiletamine and zolazepam. *Vet. Rec.* **146**, 251-254.
Miller, P. J. O., Johnson, M. P., Tyack, P. L. and Terray, E. A. (2004). Swimming gaits, passive drag and buoyancy of diving sperm whales *Physeter macrocephalus*. *J. Exp. Biol.* **207**, 1953-1967.
Miller, P. J. O., Biuw, M., Watanabe, Y. Y., Thompson, D. and Fedak, M. A. (2012). Sink fast and swim harder! Round-trip cost-of-transport for buoyant divers. *J. Exp. Biol.* **215**, 3622-3630.
Mitani, Y., Andrews, R. D., Sato, K., Kato, A., Naito, Y. and Costa, D. P. (2010). Three-dimensional resting behaviour of northern elephant seals: drifting like a falling leaf. *Biol. Lett.* **6**, 163-166.
Moore, F. D., Olsen, K. H., McMurray, J. D., Parker, H. V., Ball, M. R. and Boyden, C. M. (1963). *The Body Cell Mass and its Supporting Environment: Body Composition in Health and Disease*. Philadelphia, PA: W. B. Saunders.
Naito, Y., Bornemann, H., Takahashi, A., McIntyre, T. and Ploetz, J. (2010). Fine-scale feeding behaviour of Weddell seals revealed by a mandible accelerometer. *Polar Sci.* **4**, 309-316.
Nowacek, D. P., Johnson, M. P., Tyack, P. L., Shorter, K. A., McLellan, W. A. and Pabst, D. A. (2001). Buoyant balaenids: the ups and downs of buoyancy in right whales. *Proc. Biol. Sci.* **268**, 1811-1816.
Pütz, K. and Bost, C. A. (1994). Feeding-behaviour of free-ranging king penguins (*Aptenodytes patagonicus*). *Ecology* **75**, 489-497.
Pütz, K., Wilson, R. P., Charrassin, J. B., Raclot, T., Lage, J., le Maho, Y., Kierspel, M. A. M., Culik, B. M. and Adelung, D. (1998). Foraging strategy of king penguins (*Aptenodytes patagonicus*) during summer at the Crozet Islands. *Ecology* **79**, 1905-1921.
R Development Core Team (2012). *R: A Language And Environment For Statistical Computing*. R Foundation for Statistical Computing, Vienna, Austria. Available at: http://www.R-project.org/
Sato, K., Mitani, Y., Cameron, M. F., Siniff, D. B. and Naito, Y. (2003). Factors affecting stroking patterns and body angle in diving Weddell seals under natural conditions. *J. Exp. Biol.* **206**, 1461-1470.
Sato, K., Aoki, K., Watanabe, Y. Y. and Miller, P. J. O. (2013). Neutral buoyancy is optimal to minimize the cost of transport in horizontally swimming seals. *Sci. Rep.* **3**, 2205.
Schmidt-Nielsen, K. (1972). *Animal Physiology: Adaptation and Environment.* Cambridge: Cambridge University Press.
Suzuki, I., Naito, Y., Folkow, L. P., Miyazaki, N. and Blix, A. S. (2009). Validation of a device for accurate timing of feeding events in marine animals. *Polar Biol.* **32**, 667-671.
Thums, M., Bradshaw, C. J. A., Sumner, M. D., Horsburgh, J. M. and Hindell, M. A. (2013). Depletion of deep marine food patches forces divers to give up early. *J. Anim. Ecol.* **82**, 72-83.
Tuck, K. (2007). *Tilt Sensing Using Linear Accelerometers,* application note AN3461. Freescale Semiconductors Inc.
Tucker, V. A. (1975). The energetic cost of moving about. *Am. Sci.* **63**, 413-419.
Viviant, M., Trites, A., Rosen, D., Monestiez, P. and Guinet, C. (2010). Prey capture attempts can be detected in Steller sea lions and other marine predators using accelerometers. *Polar Biol.* **33**, 713-719.
Viviant, M., Monestiez, P. and Guinet, C. (2014). Can we predict foraging success in a marine predator from dive patterns only? Validation with prey capture attempt data. *PLoS ONE* **9**, e88503.
Watanabe, Y., Baranov, E. A., Sato, K., Naito, Y. and Miyazaki, N. (2006). Body density affects stroke patterns in Baikal seals. *J. Exp. Biol.* **209**, 3269-3280.
Webb, P. M., Crocker, D. E., Blackwell, S. B., Costa, D. P. and Boeuf, B. J. (1998). Effects of buoyancy on the diving behavior of northern elephant seals. *J. Exp. Biol.* **201**, 2349-2358.
Wilson, R. P. (1992). Environmental monitoring with seabirds – do we need additional technology. *South African Journal of Marine Science* **12**, 919-926.
Wilson, R. P., White, C. R., Quintana, F., Halsey, L. G., Liebsch, N., Martin, G. R. and Butler, P. J. (2006). Moving towards acceleration for estimates of activity-specific metabolic rate in free-living animals: the case of the cormorant. *J. Anim. Ecol.* **75**, 1081-1090.

ANNEXE B

Characterization of postdive recovery using sound recordings and its relationship to dive duration, exertion and foraging effort of southern elephant seals (*Mirounga leonina*)

Génin, Alexandre, Richard, Gaëtan, Jouma'a, Joffrey, Picard, Baptiste, El Ksabi, Nory, Vacquié-Garcia, Jade & Guinet Christophe, (2015) Characterization of postdive recovery using sound recordings and its relationship to dive duration, exertion and foraging effort of southern elephant seals (*Mirounga leonina*). *Marine Mammal Science*

Marine Mammal Science

MARINE MAMMAL SCIENCE, 31(4): 1452–1470 (October 2015)

DOI: 10.1111/mms.12235

Characterization of postdive recovery using sound recordings and its relationship to dive duration, exertion, and foraging effort of southern elephant seals (*Mirounga leonina*)

Alexandre Génin, Centre d'Études Biologiques de Chizé-Centre National de la Recherche Scientifique (CEBC-CNRS), 79360 Villiers-en-bois, France and Département de Biologie, École Normale Supérieure de Lyon, 46 allée d'Italie, 69007 Lyon, France; **Gaëtan Richard**, **Joffrey Jouma'a**, **Baptiste Picard**, **Nory El Ksabi**, **Jade Vacquié Garcia**, **Christophe Guinet**,[1] Centre d'Études Biologiques de Chizé-Centre National de la Recherche Scientifique (CEBC-CNRS), 79360 Villiers-en-bois, France.

Abstract

It is notoriously difficult to measure physiological parameters in cryptic free-ranging marine mammals. However, it is critical to understand how marine mammals manage their energy expenditure and their diving behavior in environments where the predation risks are low and where survival is mainly linked to capacities to maintain physiological homeostasis and energy budget balance. Elephant seals are top marine predators that dive deeply and continuously when at sea. Using acoustic recorders deployed on two postbreeding southern elephant seals (SES) females, we developed methods to automatically estimate breathing frequency at the surface. Using this method, we found that seals took successive identical breaths at high frequency (0.29 Hz) when recovering at the surface and that breath count was strongly related to postdive surfacing time. In addition, dive depth was the main factor explaining surfacing time through the effects of dive duration and total underwater swimming effort exerted. Finally, we found that recovery does not only occur over one dive timescale, but over a multidive time scale for one individual. The way these predators manage their recovery will determine how they respond to the change in oceanic water column structure in the future.

Key words: southern elephant seal, *Mirounga leonina*, bio-logging, acoustics, ecophysiology, diving behavior, dive recovery.

Foraging strategies of diving marine predators are heavily constrained by the management of their oxygen stores. Postdive recovery only occurs during surfacing times when breathing is possible. The management of oxygen stores is consequently crucial to foraging success and yet, remains poorly investigated in free-ranging animals. It has been investigated in ice seals, such as the Weddell seal (*Leptonychotes weddellii*) (Williams *et al.* 2004, Falke *et al.* 2008) and the emperor penguin (*Aptenodytes forsteri*) (Kooyman and Wahrenbrock 1980, Kooyman *et al.* 1983, Ponganis *et al.* 1997) that maintain specific breathing holes in the ice pack. In this case, it is possible to perform

[1]Corresponding author (e-mail: christophe.guinet@cebc.cnrs.fr).

direct measurement of breathing frequency, gas exchange, and metabolic rate for these animals.

These experiments provided insightful data on postdive or postforaging recovery of marine divers (Kooyman *et al.* 1983, Falke *et al.* 2008), but they have only been linked to energy expenditure recently. Williams *et al.* (2004) showed that the postdive oxygen intake of Weddell seals was linearly related to the swimming effort (in number of flipper strokes) and the duration of the dive. Similarly, trained Steller sea lions (*Eumetopias jubatus*) in semicaptive conditions were asked to dive at specific depths and recover by breathing in a metabolic chamber at the surface (Fahlman *et al.* 2008, Hindle *et al.* 2010). These studies showed that animals can voluntarily accumulate an oxygen debt that is paid for only a few dives later. However, data from free-ranging animals in the open sea remain scarce, but Maresh *et al.* (2014) recently estimated the absolute cost of locomotion for 12 translocated northern elephant seals (*Mirounga angustirostris*). They showed that seals spent more time recovering at the surface when cost of transportation was artificially increased.

The aim of this paper is to study the dive-recovery metabolism in seals with free-ranging individuals, using the southern elephant seal (*Mirounga leonina*, SES hereafter) as a case study. Elephant seals are known to be excellent pelagic divers. At the end of the reproduction season, SES disperse at sea in the Southern Ocean (between 45°S and 70°S), and continuously dive for 3 mo until they come back to land to molt. Elephant seals are among the most efficient divers in pinnipeds. They routinely dive for 20 min and at 450 m, but they can dive to over 1,400 m and stay submerged for up to 2 h (Slip *et al.* 1994). Their swimming effort has been shown to vary depending on their foraging success, as they are more likely to accelerate when catching prey (Thums *et al.* 2011). However, foraging does not necessarily imply active swimming. Elephant seals can glide passively during the ascent or descent phases of their dives (Davis and Weihs 2007) depending on their buoyancy. Cost of Transport (COT) is minimal at neutral buoyancy (Miller *et al.* 2012) but buoyancy can change over several days as body fat fluctuates. Furthermore, elephant seals drift passively during drift or recovery dives to rest and/or process food (Crocker *et al.* 1997, Biuw *et al.* 2003). Therefore, we expect the total energy spent during a dive to vary depending on the underwater behavior and swimming effort and to be correlated to breathing patterns when the seal surfaces. Oxygen consumption rates reflect energy expenditure (*e.g.*, Williams *et al.* 2004). Breathing behavior, breath count or breathing frequency during postdive intervals may thus provide insights on the energy expenditure while diving.

Fletcher *et al.* (2006) recorded respiratory frequency and heart rate of six translocated northern elephant seals (*Mirounga angustirostris*) using a tape recorder for about 4 h. Later, Le Boeuf *et al.* (2000) used sound recordings to determine the breathing rate of three adults and six juveniles Northern elephant seals during 8–29 postdive surface intervals. However, they only recorded the maximum dive depth and had no access to any other dive behavior or parameter. Dive depth was found to be a significant predictor of the surface interval duration, but with an estimated coefficient that varied widely (typically tenfold). Current technology allows collecting a more extensive set of data and provides a more complete understanding of diving behaviors. Using the latest acoustic tags, our goal is to quantitatively estimate how dive parameters affect the seal's postdive recovery. More specifically, this work aims at answering three questions. (1) Can we reliably and automatically estimate the number of breaths southern elephant seals take while at the surface from acoustic signals? (2) Is number of breaths related to dive parameters such as dive duration, foraging success and

swimming effort? (3) Do elephant seals recover from diving at a single-dive or multi-dive timescale?

Material and Methods

Logger Deployment

In October 2011 two postbreeding females of similar body conditions (see Table 1) were captured and equipped with data loggers on Kerguelen Island (49°20′S, 70°20′E). The two females (ind. 1 and ind. 2) were sedated using tiletamin and zolazepam (Zoletil 100) (McMahon *et al.* 2000) before gluing three tags on their fur using quick-setting epoxy (Araldite AW 2101, Ciba). First, an Argos-GPS satellite tag (SPLASH10 FastLoc GPS, Wildlife Computers, Redmond, WA) was attached to the head of the seals. It provided real-time position of the seals through the Argos system and collected GPS location data. Second, a TDR-accelerometer data logger (MK10-X, Wildlife Computers) was glued in front of the SPLASH10 tag. It samples tri-axial acceleration at 16 Hz and pressure (*i.e.*, dive depth) every second. Third, an Acousonde device (Greenridge Sciences) (Burgess and Tyack 1998, Burgess 2000) was glued on the back of the seal on the longitudinal axis, 10 cm behind the scapula. The Acousondes recorded sound at a frequency of 6,278 Hz by its built-in, low-frequency hydrophone. To save battery lifetime, the instrument only sampled for 3 h every 12 h. It also recorded depth and tri-axial acceleration at a 5 Hz frequency continuously. The tags stopped recording after 10–12 d of operation (Table 1) due to battery exhaustion, providing approximately 60–72 h of recording per animal.

Signal Processing

Estimating swimming effort—Dives were defined and separated into descent, bottom and ascent phases, and postdive surface intervals were quantified from data recorded by the Acousondes and using custom-made MATLAB scripts (available upon request) described in Vacquié-Garcia *et al.* (2012). We considered that animals were at the surface when depth was above 15 m. We chose this value to account for subsurface movements of seals between dives and to be able to separate dives with accuracy: a lower depth threshold produces short, bogus dives due to the seals' subsurface movements or wave effects on the pressure transducer. However, it introduces an underestimation of breathing rates (see Discussion). All acceleration signals were corrected for body orientation before analysis, using the mean surface orientation of ind. 1 as the frame of reference and assuming that the animals had the same mean position when at surface.

The frequency spectrum of the complete lateral acceleration data showed a clear bimodality (Fig. 1). The high-frequency peak corresponds to the dynamic acceleration due to tail movements (Watanabe *et al.* 2006). Using high-pass filters bounded at 0.63 Hz for ind. 1 and 0.72 Hz for ind. 2, we isolated this part of the signal and extracted peak number and values using the built-in *findpeaks* MATLAB function. We calculated swimming effort by summing the maximum value of these peaks over a time-series window that integrates the number of tail swings and their intensity. However, since our result does not have a straightforward SI unit (number of tail swings $\times$ m/s^2), we did not include it in the results.

Descent phases are mostly passive (gliding) for negatively buoyant elephant seals. It is also the case when animals alternate gliding descents and active ascents during

Table 1. Individual characteristics and dive habits of two equipped southern elephant seals (mean ± SD). Body characteristics are given at deployment time.

	Body characteristics			Deployment characteristics		Mean dive parameters						
	Length (cm)	Weight (kg)	Estimated density (kg/m^3)	Number of dives	Length of deployment (d)	Dive duration (min)	Maximum depth (m)	Number of capture attempts per dive	Swimming effort (total)	Swimming effort (bottom phase)	Swimming effort (ascent phase)	Time spent at surface (min)
Ind. 1	254	255	1,038.7 ± 3.4	590	10.3	19.8 ± 4.1	512.3 ± 186.1	5.3 ± 4.5	209.9 ± 39.4	71.7 ± 41.0	104.5 ± 48.2	2.5 ± 0.5
Ind. 2	238	245	1,033.1 ± 5.8	1021	12.1	14.8 ± 3.0	413.4 ± 156.3	6.6 ± 5.7	272.7 ± 50.9	106.0 ± 49.7	145.6 ± 49.8	2.3 ± 3.5

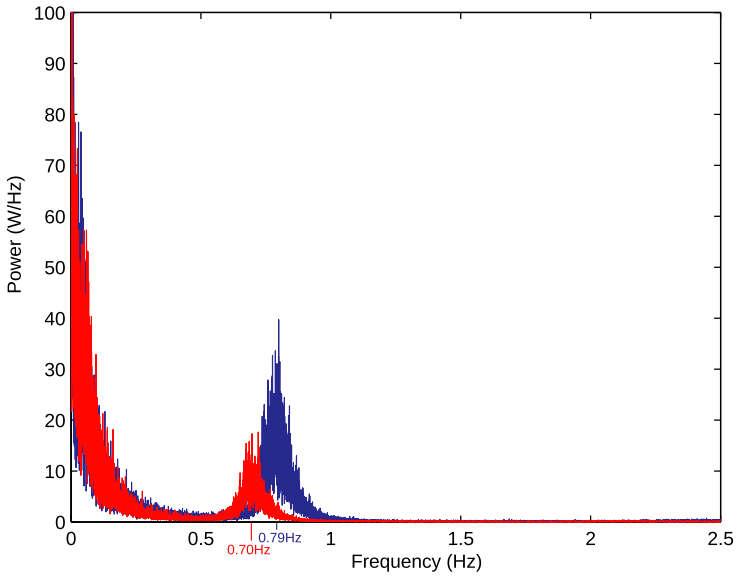

Figure 1. Power spectral density of the lateral acceleration for ind. 1 (red) and ind. 2 (blue). Note the peak in power for both individuals corresponding to the tail swing frequency. Colored ticks indicate value for maximum frequency.

the bottom phase of the dive. Consequently, negatively buoyant elephant seals only swim actively and continuously when ascending (Sala *et al.* 2011, Aoki *et al.* 2011, Miller *et al.* 2012, Richard *et al.* 2014) or during short feeding events. Therefore, we only calculated the total swimming effort during the ascent and the bottom phases, respectively referred to as SE_a and SE_b. We found differences in absolute values between our two individuals: a much lower swimming effort was found for ind. 1 for dives at identical depth (Table 1). We assessed whether methodological biases could explain this difference. We first verified that it was not due to differences in logger position using in-field photographs. Second, proper in-factory calibration of the accelerometers was also verified by comparing the recordings of the two loggers in several identical static positions and exposed to identical accelerations. We also tested the difference in density between the 2 individuals as seal buoyancy has a strong effect on seal swimming effort—seals closer to neutral buoyancy have a lower Cost of Transport (Miller *et al.* 2012)—following a methodology from Biuw *et al.* (2003) and Richard *et al.* (2014).

Estimating seal density—We estimated seal density using Richard *et al.*'s (2014) methodology. We isolated drifting phases by first selecting data (1) from the descent or bottom phase, (2) for which instantaneous swimming effort (as described previously) had values in the –0.2–0.2 m/s^2 range, and (3) for which vertical speed was below 0.4 m/s. We then only kept data sequences longer than 20 s and used the mean vertical speed of each sequence to obtain the seal density $\rho(seal)$ using the following equation:

$$\rho(seal) = \rho(sw) + \frac{U(drift)^2 \bullet Cd \bullet \rho(sw)}{2g} \times \frac{S(seal)}{V(seal)}$$

where $U(drift)$ is the mean vertical speed, Cd the drag coefficient of 0.69 (Aoki *et al.* 2011, Biuw *et al.* 2003), $\rho(sw)$ the average density of sea water (1,027 g/L), $V(seal)$,

and $S(seal)$ the volume and total area of the seal respectively, and g the gravity acceleration (9.8 m/s^2). Volume and total area were calculated by considering the shape of the seal as two opposing cones with a common base as followed:

$$\frac{S(seal)}{V(seal)} = \frac{\sqrt{1+\frac{L^2}{3R^2}} + \sqrt{1+\frac{2L^2}{3R^2}}}{L}$$

where L is the measured length of the seal at tag deployment and R is the radius of the cones' common base. R was not measured in the field and was obtained using empirical relationships between m the mass (kg), L the size (m), and G the girth (m) measured at tag deployment: (Castellini and Calkins 1993). The mass was estimated using a scale with a precision of ± 1.0 kg. Combining the previous equation and using R as follows:

$$R^2 = \frac{m}{45.7L \bullet 4\pi^2}$$

Prey capture attempts—Jaw opening motions indicative of prey capture attempts can be detected from head mounted accelerometers (Gallon *et al.* 2012, Naito *et al.* 2010, Viviant *et al.* 2010). We identified prey capture attempts from the acceleration data using custom-written MATLAB scripts applied on the signal obtained by the head-mounted SPLASH10 tag using a method derived from Viviant *et al.* (2010). First, we calculated the standard deviation over 1 s static windows of the three channels individually. Then, we calculated a standard deviation over a 5 s moving window on these signals. Finally, we applied a k-means clustering method using two output centroids on the final three signals. This categorized each sample of the acceleration signal into high- and low-variance clusters. A capture attempt was then defined as a continuous sequence of samples in which all of the three axes were classified in the high-variance cluster.

Breath count—We isolated and extracted sound samples when the seal was at the surface of the water only. Acoustic and visual inspections indicated that when the seal is surfacing, most of the sound recorded is due to breathing excepted when water splashes produced high-amplitude noise (possibly due to rough weather conditions) which masked the breathing sound. Spectrograms showed that each seal exhibited a stereotypical breathing behavior with constant breathing intensity (magnitude of one breath) and duration within and between breathing sequences (Fig. 2).

The sound signal amplitude reached a maximum in the middle of a breath when the seal stops inhaling and begins breathing out. Consequently, we estimated breathing frequency by identifying and counting these peaks using the following method: we first standardized the sound samples by dividing the signal by its standard deviation (computed on the whole data set) to remove any possible differences due to individual microphone sensitivity. We then applied a band-pass filter to select frequencies within the 200–240 Hz range. This attenuated the part of the signal that was not related to breathing. Filtered sound samples with amplitude above 0.3σ were considered water noise and their values were zeroed to limit their influence in subsequent processing. We then filtered the remaining signal using a moving average with 1, 1.2, and 5 s windows to obtain curves (a), (b), and (c) of Figure 3. Peaks

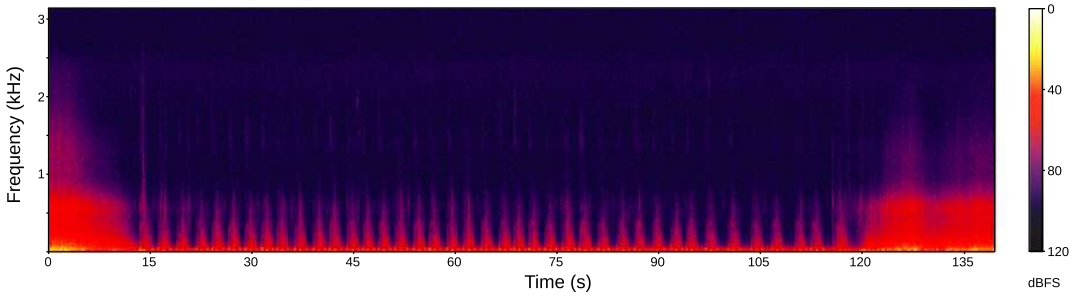

Figure 2. Spectrogram of recorded sound during a post dive surface interval performed by ind. 1 showing the stereotyped and continuous breathing behavior of the seal when surfacing. Seal surfaces at timestamp 15 s and dives at 120 s.

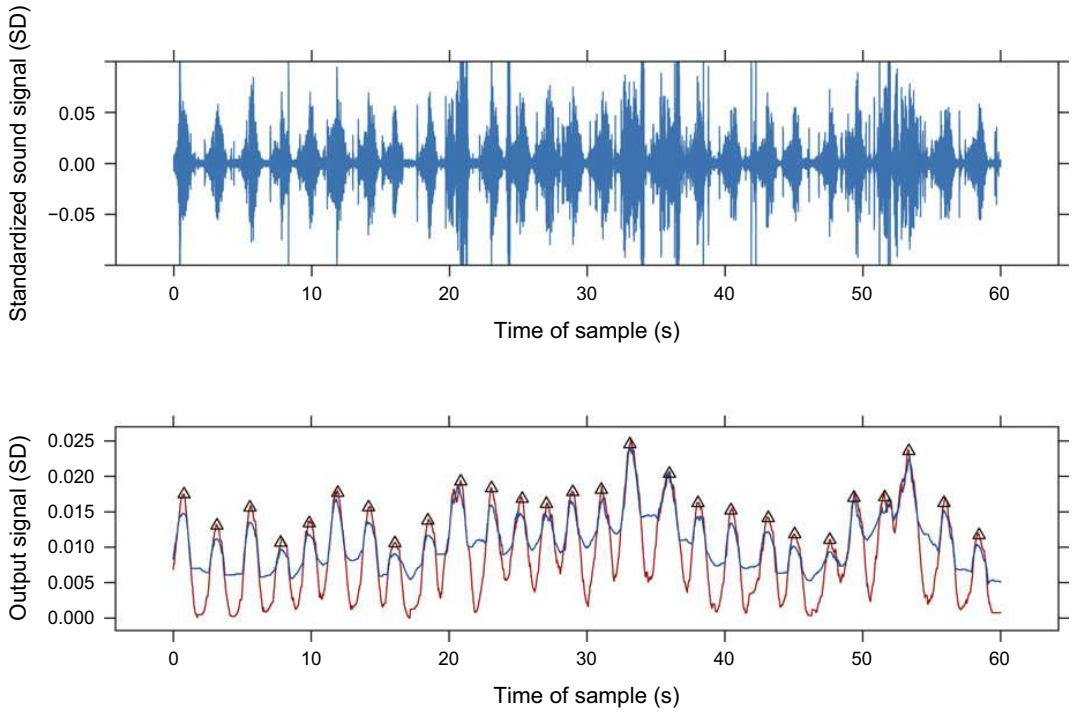

Figure 3. Extract of a sound recording processed for breath count. Upper panel: filtered input signal in which breaths are distinguishable. Lower panel: output smoothed amplitude in dark red (curve [a] in text), and lower bound for peak detection in blue (maximum of curves [b] and [c] in text). Triangles correspond to output detected peaks. *Y*-axis units have no absolute meaning.

corresponding to breathing were then detected in curve (a) using the MATLAB built-in function *findpeaks*. Only peaks separated by at least 1.2 s and with values above signal (b) and (c) were retained.

Water splash noise was the main source of peak miscount. We thus used the proportion of the signal during which splash noise did not occur as an accuracy index for this method. We only kept breathing events with an accuracy index over 0.994, which gave us 248 breathing sequences across the two individuals (86 sequences were omitted). We evaluated the accuracy of this method by comparing the result obtained from the automated algorithm mentioned above to a visual count on spectrograms of

eight randomly chosen surface intervals for each individual. The mean breath duration and interbreath durations were also visually evaluated using the same samples.

Statistical Analyses

Number of breaths taken during the surface interval

We looked at the relationship between the number of breaths and the duration of the surface interval using linear mixed-effects models. We set individuals as random factor to estimate the significance of variations in breathing rate across individuals. We used a stepwise model selection based on AIC to select the most adequate model between a model with random intercept and slope across individuals, random intercept only or without random effect. We followed the procedure suggested by Nakagawa and Schielzeth (2013) to obtain the R^2 for the relationship.

Energy spent and recovery time—We first used a linear-mixed effects model in R (R Development Core Team 2012) to explore the effects of dive parameters on postdive surface interval and the variation between individuals. We then used standard linear modeling to compare the effects of the fixed factors within individuals. To do so, we standardized the within-individuals fixed factors (by subtracting the mean and dividing them by the standard deviation) so that the value of each coefficient is indicative of its relative contribution to the explained factor. All models were evaluated for surface intervals between 0 and 450 s. Values exceeding the ± 1.5 interquartile range were considered outliers and removed from the analysis which represent 11 data points (less than 0.7 % of the whole surface interval data set of $n = 1{,}683$, 2 for ind. 1 and 9 for ind. 2). We focused on recovery periods likely to be related directly to the previous dive as extended surface intervals may be related to other surface behaviors, such as socializing or extended recovery periods linked to food processing (Sparling *et al.* 2007).

Time scale of recovery—Recovery can happen over a single dive time-scale during which the animal pays back its oxygen debt from its previous dive completely before the next dive. It can be also occur over a time-scale of a few dives depending on the effort made during the preceding sequence of dives. This could be the source of outliers mentioned earlier and removed from the linear model analysis. We summed dive durations, total swimming effort, and corresponding recovery times over an increasing number of dives to evaluate the time-scale used. We used Spearman's correlation coefficients to evaluate time-scale of recovery: if the seal recovered its oxygen debt over several dives, we expected a higher coefficient. This was done using the entire data set for each individual, including the extended surface intervals.

RESULTS

Ind. 1 performed significantly deeper and longer dives compared to ind. 2 ($t = 27.3$, $P \leq 0.001$; see Table 1).

Breath Characteristics

Both elephant seals in this study showed a stereotypical behavior during their surfacing intervals. They repeatedly took a series of regular, high-frequency breaths when surfacing, separated with short duration interbreath intervals. Using hand-counted samples, breath duration was found to be significantly different across

individuals, although the difference was minimal (mean ± standard deviation): 1.56 ± 0.22 s (ind. 1) and 1.52 ± 0.22s (ind. 2) ($t = 2.56$, $n = 16$, $P = 0.01$). A relative error of 7% ± 4% on automated breath counts was found compared to visual count. Ind. 1 took significantly more breaths during surface intervals (ind. 1: 56.6 ± 5.6, $n = 28$; ind. 2: 40.5 ± 6.1, $n = 135$, $t = 13.7$, $P \leq 0.001$) and made longer surface intervals than ind. 2 (152 ± 29 s *vs.* 128 ± 36 s, $n = 248$, $t = 15.31$, $P \leq 0.001$).

There is a strong linear relationship between number of breaths and time at the surface across both individuals (Fig. 4). The model selection process favored a mixed-model with random intercept only, thus supporting the assumption that both individuals had the same average breathing rate as measured by our automatic process: 0.30 ± 0.01 breaths/s (estimate ± SE). This model had a marginal R^2 (proportion of variance explained by fixed factors) of 0.81 and a conditional R^2 of 0.84 (proportion of variance explained by both fixed and random factors). Given these high R^2 values, we neglected the residual error in this relationship, and used the time spent at the surface as a direct proxy for the number of breaths taken. This procedure allowed us to have more robust estimates by using the whole data set and not only the short durations.

Swimming Effort

Ind. 1 showed a significantly lower total swimming effort compared to ind. 2 at the dive scale: ind. 1 = 0.177 ± 0.039, $n = 590$; ind. 2 = 0.313 ± 0.052,

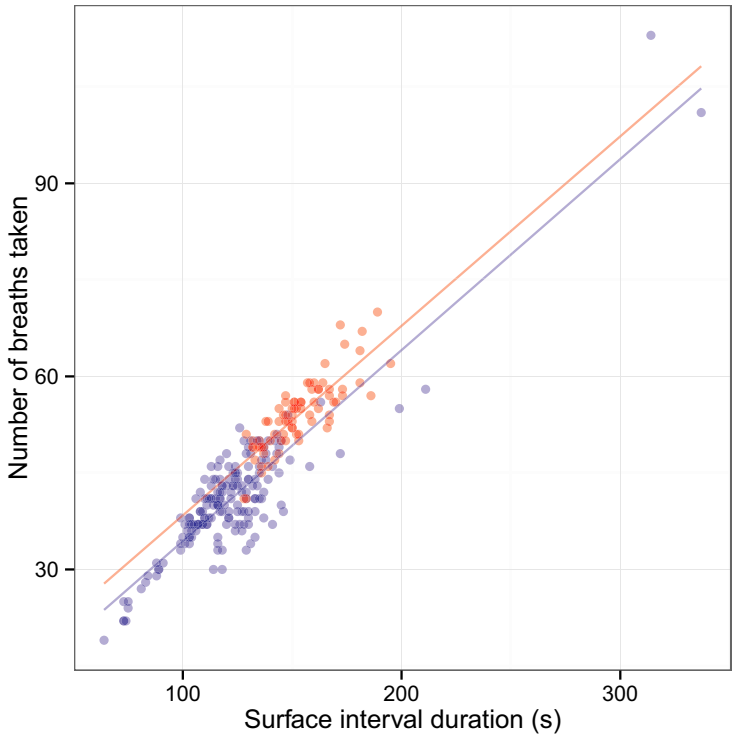

Figure 4. Linear relationship between surface duration (S_d) and number of breath (B_n) taken by the two seals (ind. 1 is in red, ind. 2 in blue). Only counts with a confidence index over 0.994 were used in this representation. Two linear fits are shown for both seals: ind. 1 $B_n = 8.95 + 0.29S_d$ and ind. 2 $B_n = 6.11 + 0.29S_d$. Model selection through AIC supports the similarity of the slopes which represent the breath rates (see Results).

$n = 1019$; $t = -59.6$, $P \leq 0.001$; bottom of the dive: ind. 1 = 0.211 ± 0.141; ind. 2 = 0.232 ± 0.146; $t = -2.79$, $P \leq 0.005$ or during ascent: ind.1 = 0.474 ± 0.190; ind. 2 = 0.737 ± 0.812; $t = -9.87$, $P \leq 0.001$). Similarly, ind. 2 swimming effort was on average 1.73 times greater than ind. 1 when departing from the same maximum depth (Fig. 5). No differences in Acousonde calibrations were detected, and visual inspection of logger position on the seal's back showed no conclusive difference. However, seal densities were found to differ significantly (ind. 1: 1,038.7 ± 3.4 kg/m^3, $n = 97$; ind. 2: 1,033.1 ± 5.8 kg/m^3, $n = 32$, $t = 5.13$, $P \leq 0.001$).

Postdive Recovery

The two individuals were found to adjust the duration of their surface interval according to dive duration (T), maximum diving depth (D_d), swimming effort during ascent (SE_a), swimming effort during bottom (SE_b), and the number of prey capture attempts (PCA). Correlations between pairs of variables were tested using the Pearson's correlation coefficient. When two variables had a correlation coefficient above 0.7, we kept the variable that was directly related to energy expenditure. Maximum diving depth was found to be highly correlated to SE_a. We kept SE_a as an explanatory variable to compare the respective contribution of SE_a and SE_b on surface recovery. The number of prey capture attempts was also found to be positively related to SE_b but the correlation coefficient (ind. 1, $R^2 = 0.33$, $n = 590$, $P \leq 0.001$; ind. 2 $R^2 = 0.42$, $n = 1{,}020$, $P \leq 0.001$) was lower than the threshold value so both variables were kept for the analyses. The relationship of post dive duration recovery was

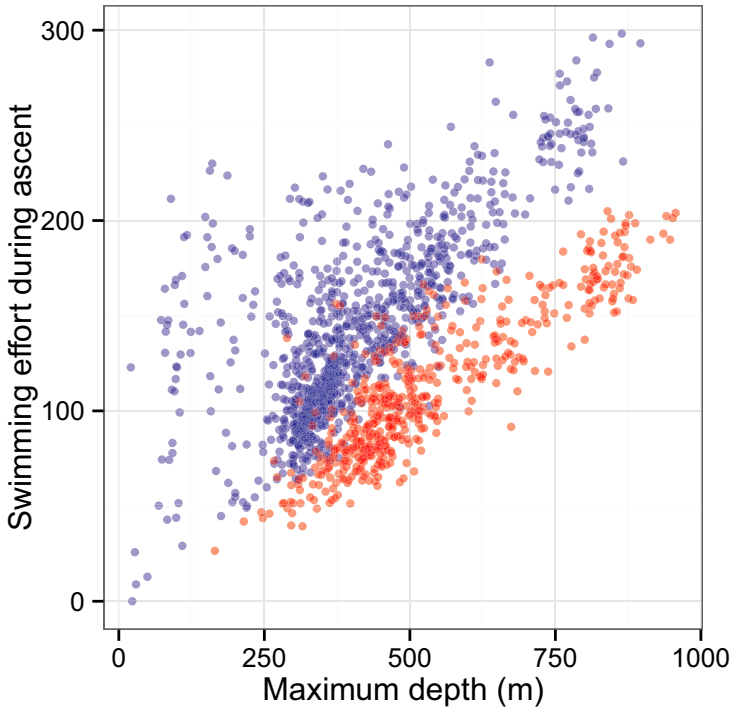

Figure 5. Swimming effort performed during the ascent phase compared to the maximum depth of the dive. Ind. 2 (blue) has a 1.7× greater swimming effort to return to the surface from the same depth than ind. 1 (red).

thus investigated in relation to dive duration, number of prey capture attempts, swimming effort at bottom (SE_b) and during ascent (SE_a) of the previous dive.

Linear mixed models showed that the relationships varied significantly depending on the individual: ind. 2 exhibited a greater SE_a for a given dive depth than ind. 1. Significant differences were found in the slope (ind. 1: 0.202 ± 0.005; ind. 2: 0.233 ± 0.007, $t = 36.5$, $P \leq 0.001$) and intercepts (ind. 1: 5.08 ± 2.66; ind. 2: 49.20 ± 2.99, $t = 48.17$, $P \leq 0.001$) of the two linear models (Fig. 6). A linear model was fitted for each individual to explore the relative importance of each explanatory variable. SE_a had the largest contribution for both seals, followed by dive duration and SE_b. Number of prey capture attempts did not influence the duration of the post dive surface interval for any of the individuals (see Table 2 and Fig. 5). However, ind. 2 spent a longer time at the surface than ind. 1 for a given dive duration, SE_a and SE_b as all parameter estimates were higher for ind. 2 (Table 2). Indeed, ind.

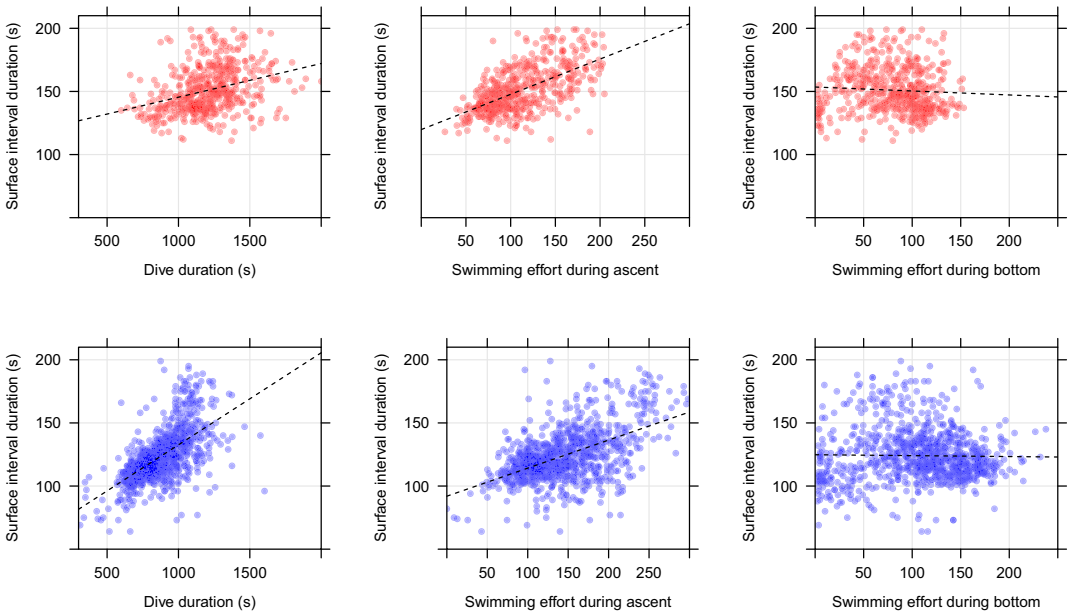

Figure 6. Relationship between the duration of the surface interval and dive duration (A–B), dive swimming effort (C–D), and swimming effort at the bottom of the dive (E–F). Ind. 1 is shown in red and ind. 2 in blue.

Table 2. Results of linear models looking at the surface interval durations in relation to dive parameters.

Explanatory variable	Individual 1 (red) Coefficient estimate (mean ± sd)	Individual 2 (blue) Coefficient estimate (mean ± SD)
Dive duration	4.14 ± 00.90***	9.00 ± 1.64***
Nb PCA	ns	ns
Swimming effort (bottom)	2.48 ± 1.14*	4.42 ± 1.41**
Swimming effort (ascent)	11.09 ± 0.91***	11.98 ± 1.53***

Note: Asterisks indicate levels of significance, either *** for $P < 0.001$, ** for $P < 0.01$, or * for $P < 0.05$. Color names in columns headers refer to colors in the graphs of this paper.

1 spent significantly less time at the surface per minute spent diving compared to ind. 2 (ind. 1: 8.16 ± 1.68, n = 590; ind. 2: 8.53 ± 3.78, n = 1,019, t = -3.25 P = 0.001).

Time-scale of Recovery

Previous studies have shown that some diving mammals can recover their oxygen debt over a few dives rather than over a single dive time-scale. The maximum correlation coefficient was found when dive duration and total swimming effort were summed over a window of about 20 dives for ind. 1 (Fig. 7). Adjustment capabilities then plateaued past this threshold. Ind. 2 exhibited no such trend.

Discussion

Describing the Respiration of Elephant Seals Through Sound Recordings

This study shows that southern elephant seals are breathing at very high frequency while at the surface. The relationship between number of breaths and surface duration suggest a mean breathing frequency of 0.3 Hz, which is within the range of breathing frequencies reported for juvenile and male northern elephant seals (Le Boeuf *et al.* 2000). Despite very short surfacing intervals, elephant seals recovered primarily by adjusting the duration of surface intervals—and therefore number of breaths—rather than breathing rate (R^2 = 0.84, Fig.4).

The low error in automatic detection shows that it is possible to reliably estimate the number of breaths taken by elephant seals when at the surface. This study acts as a proof-of-concept and highlights that automatic quantitative analyses of sound recordings provide a useful piece of information to explore multiple aspects of the recovery of these animals. However, acoustic recordings are a very information-rich support and much work remains to be done to fully extract the available information.

In this study we extracted the number of breaths from a sample based on the sole amplitude of the sound signal after filtering. However, a more robust spectrum analysis could certainly identify more precise breath patterns. This powerful technique is routinely used in the audio world where algorithms identify and match audio

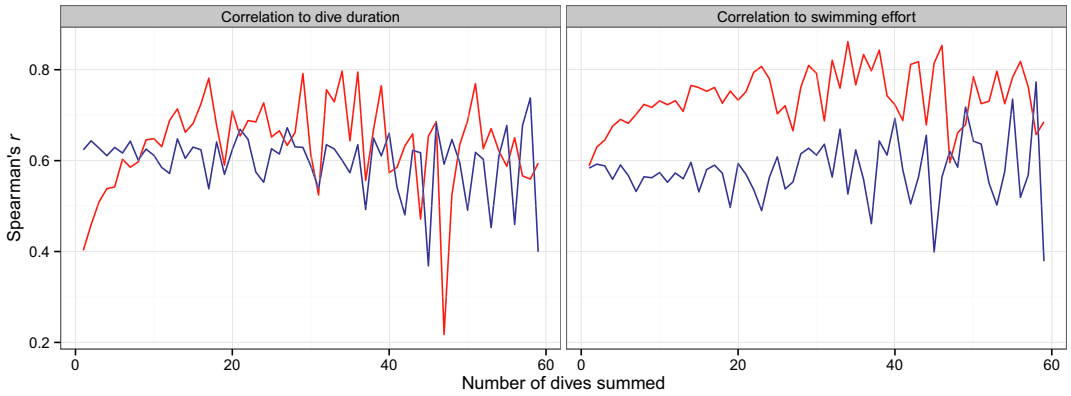

Figure 7. Correlation coefficient for different sizes of window used to sum the dive characteristics. For ind. 1 (red) both correlations plateaued after 20 dives summed. This suggests that ind. 1 is managing its effort over multiple dives. There is no comparable trend for ind. 2 (blue).

patterns against a database using the full dimensionality of the sound signal (Cano *et al.* 2005). This approach would likely be very efficient given the stereotyped nature of the elephant seal recordings presented here. It would also likely efficiently detect events such as hauling out for example during which the sound spectrum changes drastically (Fig. 2). In addition, robust estimates with biologically meaningful errors should be preferred instead of a confidence index quantifying noise. In other words, detecting a breath in a sound sample is likely to be straightforward given modern sound processing. However, extracting breath characteristics (*e.g.*, duration, intensity, volume of air inspired with errors) might remain challenging.

Recording sound for several months in cold water is expensive. It requires a sampling frequency that is several orders of magnitude higher than for other dive parameters. The two loggers deployed here were heavily duty-cycled and provided only 2 wk of data in a 2–3-mo-long postreproductive trip. However, this work suggests that breaths have a very low-frequency signature in the sound signal. This characteristic allowed us to detect and count them after submitting the raw signal to multiple smoothing low-pass filters. A much lower sampling frequency should thus still capture breathing frequency as the automatically extracted breathing rate of 0.30 Hz (Fig. 4) gives a theoretical minimum frequency of 0.60 Hz (Nyquist frequency). Of course, a proper threshold should be empirically determined by subsampling an existing signal for example. However, this shows that the sampling effort—and thus the battery drain—could be considerably reduced and yet similar results could still be obtained.

As far as breathing rate is concerned, a critical parameter to set is the maximum depth that defines surface intervals. In this work, we set it to 15 m to be able to rely on previous work (Vacquié-Garcia *et al.* 2012), and knowing that lower depth thresholds are known not to discriminate dive phases well enough for subsequent analyses. Lower thresholds result in short and very shallow, false positive dives. Indeed, closer inspection of simultaneous depth and acoustic recordings show that pressure variations are present even though the seal is breathing at the surface, possibly due to wave splash effects on the logger. However, the 15 m depth threshold we chose led to an overestimation of the surface interval of about 6%–8% and therefore an underestimation of breathing rates of 7%–10%: any time spent in shallow water (above 15 m) is considered as breathing time, although seals can obviously not breathe everywhere in the whole 0–15 m depth interval. Further processing of sound recordings could provide an elegant way to circumvent this, similar to the way swimming effort is computed. As elephant seals breathe in a very regular fashion at the surface, the spectrum of the corresponding sound recording should show a spike in the frequency that corresponds to the breathing patterns. This frequency is the breathing rate. The threshold of 15 m discussed above would thus only be used to roughly select the surface interval where the breathing behavior dominates the signal, and would not affect the actual breathing rate value.

We could also extract other interesting variables linked with effort and recovery from the sound signal. However, it would necessitate a refined process for automatic detection. For example, Le Boeuf *et al.* (2000) showed significant correlations between dive parameters and heart rate at the surface. These are visually and acoustically detectable in the sound signals recorded here but our automatic process does not yet provide enough resolution to extract heart rate. Beyond technical caveats linked to the automatic processing of these recordings, our results highlight that sound provides a useful tool to unravel how elephant seals manage their postdive recovery when associated with other loggers.

Recovery and Swimming Effort

Duration of the previous dive and the total swimming effort significantly predicted surface interval duration in southern elephant seals as also reported for their northern counterparts (Le Boeuf *et al.* 2000). Despite interindividual differences, both individuals exhibited the same general patterns of postdive recovery. Time at the surface was directly related to the dive duration and the swimming effort, and in particular to the ascent swimming effort. This is in accordance with previous results obtained on Weddell seals (Williams *et al.* 2004). Postbreeding females remain negatively buoyant during most if not the entire duration of their postbreeding trip. Therefore, they mostly passively glide down to the dive bottom but actively swim back to the surface. This is supported by our results that show that SE_a and dive duration have the largest contribution explaining the post dive recovery. Although it is commonly hypothesized that the main foraging costs for deep diving predators such as elephant seals are from getting to the resource location in the water column, our work provides direct evidence that in negatively buoyant recovery time is heavily influenced by the effort exerted to return to the surface from the foraging depth (SE_a). This is probably why Le Boeuf *et al.* (2000) found that dive duration had an unclear effect on recovery time. Another important result of our study is that individuals can manage their recovery either at a dive or at a multi-dives time scale.

Energy Management and Individual Characteristics

Both seals had similar body size (Table 1) but different body conditions: ind. 1 was in poorer condition (*i.e.,* denser) than ind. 2. We thus expected that ind.1 would exert a higher SE_a because of its higher density. However, ind. 1 was found to exert a lower SE_a suggesting the existence of interindividual differences in diving behaviors. Ind. 2 swam more actively than ind. 1 and exerted a significantly greater swimming effort per unit of time spent diving. When controlling for dive duration, ind. 2 was found to spend more time at the surface per unit of time spent diving, possibly due to its greater swimming effort per unit of time. In comparison, ind. 1 dove deeper, favored a less active diving strategy, and exerted a lower swimming effort per unit of time spent diving.

One possible explanation to these differences is that our measure of swimming effort was biased across individuals. Swimming effort is only an indirect proxy of energy expenditure and the direct proportionality between our estimated swimming effort and actual energetic costs remains to be validated (see *Perspectives*). While this may contribute to the interindividuals differences, it unlikely explains it all. Indeed, both accelerometers were calibrated and attached on an identical location for both seals. Another possible explanation is intrinsic differences in foraging/diving/swimming behavior between individuals. Ind. 1 showed a lower swimming effort per ascended meter (Fig. 5) and thus a lower locomotion cost compared to ind. 2, even though we expected the opposite due to its higher density. This suggests that ind. 1 was swimming differently than ind.2 as reflected also in a significantly steeper ascent angle for Ind. 1 ($50° \pm 17°$ *vs.* $48° \pm 13°$, $t = 2.2$, $P = 0.03$). This difference might be due to extrinsic factors such as the number of prey encounters (Gallon *et al.* 2012) or environmental cues (McIntyre *et al.* 2011, Guinet *et al.* 2014) known to affect swimming angle. However, intrinsic factors affecting physiology such as hypoxia conditioning (Hassrick *et al.* 2010) or differences in metabolic capacities (Tift *et al.* 2013) cannot be ruled out. Monitoring a broader number of individuals and over a

longer time period would help in better understanding the effect of these factors on swimming behaviors.

The recovery behavior of the two females also suggests interindividual differences. Ind. 2 performed shallower and shorter dives and was mainly recovering at the single-dive scale, while ind. 1 performed longer, deeper dives and with a lower swimming effort per unit of time recovered. This suggests that ind. 1 could manage its energy balance over several dives and thus accumulate an oxygen debt paid off only a few dives later. The body of literature suggests that elephant seals mostly dive aerobically to maximize time underwater (Meir *et al.* 2009, Hassrick *et al.* 2010, Meir *et al.* 2013). However, elephant seals sometimes do exceed their apparent aerobic dive limit (ADL) as observed by Hassrick *et al.* (2010). We thus cannot yet rule out that seals pay off their oxygen debt through sustained breathing during extended surface intervals. We did not see such intervals in our audio recordings probably because of our sampling constraints. The increase in sampling effort in future work could help answering this question. Seals could also defer digestion costs to periods of rest at the surface (Crocker *et al.* 1997). This could also explain the difference observed between our two seals.

Despite differences in their recovery strategy, similar general relationships were found for both individuals. Ascent swimming effort was the most influent factor on surface recovery time (or likely descent swimming effort in positively buoyant seal), then dive duration and to a lesser extent swimming effort at the bottom of the dive. This latter variable is probably positively correlated to the foraging success of these seals as the higher the swimming activity during the bottom phase, the higher the number of possibly successful prey capture attempts.

Measuring Swimming Effort

Tri-axial overall dynamic body acceleration (ODBA) has been shown to reflect swimming effort in numerous taxa (Wilson *et al.* 2006). In this study, we used a more selective measure of swimming effort because it favored the count and amplitude of tail swings, thus taking into account the propelling-related motions rather than the sum of the overall acceleration. While ODBA was found to provide a good proxy of energy expenditures in some species (Fahlman *et al.* 2008; Halsey *et al.* 2008, 2009), in other cases the relationship was weak.[2] It is possible to take partly into account the position of the logger on the animal by using a peak count and correcting for orientation. This is critical as further work based upon this study will be based on data collected by accelerometers attached on the head of the animal.

From Breath Counts to Oxygen Acquisition

We provided a method to count the number of breaths taken by seals when surfacing with reasonable accuracy using an automated counting process. This process depends on numerous parameters, especially the peak detection. We also showed that breath count could predict energy expenditure (dive duration and swimming effort). However, we need to determine the amount of oxygen inhaled in a breath to translate breath count into oxygen intake, the energetics currency. Refining the process using

[2]Personal communication from Tiphaine Jeanniard-du-Dot, Marine Mammal Research Unit, AERL Building, 2202 Main Mall, University of British Columbia, Vancouver, British Columbia V6T 1Z4, Canada, 4 November 2014.

mechanical data derived from sibling species such as the Weddell seal (Castellini *et al.* 1992, Falke *et al.* 2008) or by calibrating Acousondes on captive seals for example could provide better *Information on Breath Types and Inhaled Volumes*

Perspectives: Understanding the energy strategy of free-ranging marine mammals using indirect evidence—The relationships found between indirect measurements of energy gains (recovery time) and losses (underwater exertion and dive duration) suggest that estimating the energetic balance through indirect, noninvasive bio-logging data can be a valid strategy for free-ranging animals.

Energy costs are often split into several oxygen-consuming additive components: resting metabolism costs, locomotor costs, digestion costs, and thermoregulatory costs (Williams *et al.* 2004, Maresh *et al.* 2014). The multilinear relationship we found supports the additive effect of dive duration and swimming effort on oxygen consumption. However, these behavioral characteristics are not related to the above components in a simple way. The total number of strokes underwater has been shown to be strongly proportional to the *locomotor costs* (Williams *et al.* 2004), which corresponds here to our measure of swimming effort. Dive duration is likely to be most correlated to costs proportional to the time spent underwater such as resting metabolism and thermoregulation. However, our method does not provide insights on digestion costs. This is still hard to quantify as digestion is a complex process involving variables beyond oxygen consumption, such as prey quality or metabolism time lags. For example, some seals are known to defer their digestion costs to extended surface intervals (Rosen *et al.* 2007, Sparling *et al.* 2007) or drift dives (Crocker *et al.* 1997). In any case, the new variables presented here likely summarize accurately the short time-scale components of energy costs (basal metabolism, locomotion costs, and thermoregulatory costs).

However, since seals tend to end their dive at a given level of oxygen store (Meir *et al.* 2013), our results suggest that variations in surface intervals provide insights into energetic costs linked to digestion and/or thermoregulation after taking into account dive duration and swimming effort. Thermoregulatory costs, although probably very small in near −0°C water conditions (Noren 2002), could vary to some extent as elephant seals forage in water temperatures ranging from −1°C to 13°C (Guinet *et al.* 2014). Consequently, digestion costs are probably the main driver of the total oxygen expenditure during a dive after correcting for the above variables (Rosen *et al.* 2007).

Other parameters and longer time-scaled processes need to be better understood to get a fuller picture of the energy balance. In particular the relationship between energy balance and absolute costs should be better investigated for predictive analyses (*e.g.*, the work conducted by Maresh *et al.* (2014) on pricing the strokes of northern elephant seals). This is beyond the scope of this work but our results suggest that it is possible to estimate energy balance of free-ranging marine mammals through indirect, noninvasive logging. Understanding foraging cost benefit ratio of foraging and its energy efficiency is critical to better understand environmental changes will impact top predators.

Acknowledgments

The authors would like to thank all the Kerguelen field workers involved in the data acquisition and the students at CEBC for their insightful feedbacks. We also wish to thank Tiphaine Jeanniard du Dot, Malcolm O'Toole, and Grégoire Autin for editing the English of previous versions of this paper. In addition, we thank the three reviewers for their extensive

comments on this paper. This work is part of a national research program supported by the French Polar Institute (Institut Paul Emile Victor, IPEV), no. 109 (PI: Henri Weimerskirch). This work was done within the ANR Blanc MYCTO-3D-MAP framework. The authors also warmly thank the Fondation Total for financial support. All animal handling in this study was performed in accordance with its guidelines.

Literature Cited

Aoki, K., Y. Watanabe, D. E. Crocker, *et al.* 2011. Northern elephant seals adjust gliding and stroking patterns with changes in buoyancy: Validation of at-sea metrics of body density. Journal of Experimental Biology 214:2973–2987.

Biuw, M., B. McConnell, C. J. A. Bradshaw, B. Harry and M. Fedak. 2003. Blubber and buoyancy: Monitoring the body condition of free-ranging seals using simple dive characteristics. Journal of Experimental Biology 206:3405–3423.

Burgess, W. C., and P. L. Tyack. 1998. A programmable acoustic recording tag and first results from free-ranging northern elephant seals. Deep-Sea Research Part II 45:1327–1351.

Burgess, W. C. 2000. The bioacoustic probe: A general-purpose acoustic recording tag. The Journal of the Acoustical Society of America 108:2583.

Cano, P., E. Batlle, T. Kalker and J. Haitsma. 2005. A review of audio fingerprinting. The Journal of VLSI Signal Processing-Systems for Signal, Image, and Video Technology 41:271–284.

Castellini, M. A., and D. G. Calkins. 1993. Mass estimates using body morphology in Steller sea lions. Marine Mammal Science 9:48–54.

Castellini, M. A., G. L. Kooyman and P. J. Ponganis. 1992. Metabolic rates of freely diving Weddell seals: Correlations with oxygen stores, swim velocity and diving duration. Journal of Experimental Biology 165:181–194.

Crocker, D. E., B. J. Le Boeuf and D. P. Costa. 1997. Drift diving in female northern elephant seals: Implications for food processing. Canadian Journal of Zoology 75:27–39.

Davis, R. W., and D. Weihs. 2007. Locomotion in diving elephant seals: Physical and physiological constraints. Philosophical Transactions of the Royal Society B 362:2141–2150.

Fahlman, A., C. Svard, D. A. S. Rosen, D. R. Jones and A. W. Trites. 2008. Metabolic costs of foraging and the management of O_2 and CO_2 stores in Steller sea lions. Journal of Experimental Biology 211:3573–3580.

Falke, K. J., T. Busch, O. Hoffmann, *et al.* 2008. Breathing pattern, CO2 elimination and the absence of exhaled NO in freely diving Weddell seals. Respiratory Physiology and Neurobiology 162:85–92.

Fletcher, S., B. Le Boeuf, D. P. Costa, P. L. Tyack and S. B. Blackwell. 1996. Onboard acoustic recording from diving Northern elephant seals. Journal of the Acoustical Society of America 100:2531–2539.

Gallon, S., F. Bailleul, J.-B. Charrassin, C. Guinet, C.-A. Bost, Y. Handrich and M. Hindell. 2012. Identifying foraging events in deep diving Southern elephant seals, *Mirounga leonina*, using acceleration data loggers. Deep Sea Research Part II: Topical Studies in Oceanography 88–89:14–22.

Guinet, C., J. Vacquié-Garcia, B. Picard, *et al.* 2014. Southern elephant seal foraging success in relation to temperature and light conditions: Insight on their prey distribution. Marine Ecology Progress Series 499:285–301.

Halsey, L. G., E. L. C. Shepard, C. J. Hulston, M. C. Venables, C. R. White, A. E. Jeukendrup and R. P. Wilson. 2008. Acceleration versus heart rate for estimating energy expenditure and speed during locomotion in animals: Tests with an easy model species, *Homo sapiens*. Zoology 111:231–241.

Halsey, L. G., E. L. C. Shepard, F. Quintana, A. Gomez Laich, J. A. Green and R. P. Wilson. 2009. The relationship between oxygen consumption and body acceleration in a range of

species. Comparative Biochemistry and Physiology A, Comparative Physiology 152:197–202.
Hassrick, J. L., D. E. Crocker, N. M. Teutschel, *et al.* 2010. Condition and mass impact oxygen stores and dive duration in adult female northern elephant seals. The Journal of Experimental Biology 213:585–592.
Hindle, A. G., L. B. Young, D. A. S. Rosen, M. Haulena and A. W. Trites. 2010. Dive response differs between shallow- and deep-diving Steller sea lions (*Eumetopias Jubatus*). Journal of Experimental Marine Biology and Ecology 394:141–148.
Kooyman, G. L., and E. A. Wahrenbrock. 1980. Aerobic and anaerobic metabolism during voluntary diving in Weddell seals: Evidence of preferred pathways from blood chemistry and behavior. Journal of Comparative Physiology 138:335–346.
Kooyman, G. L., M. A. Castellini, R. W. Davis and R. A. Maue. 1983. Aerobic diving limits of immature Weddell seals. Journal of Comparative Physiology 151:171–174.
Le Boeuf, B. J., D. E. Crocker, J. Grayson, J. Gedamke, P. M. Webb, S. B. Blackwell and D. P. Costa. 2000. Respiration and heart rate at the surface between dives in northern elephant seals. Journal of Experimental Biology 203:3265–3274.
Maresh, J. L., S. E. Simmons, D. E. Crocker, B. I. McDonald, T. M. Williams and D. P. Costa. 2014. Free-swimming northern elephant seals have low field metabolic rates that are sensitive to an increased cost of transport. The Journal of Experimental Biology 217:1485–1495.
McMahon, C. R., H. Burton and D. Slip. 2000. Field immobilization of southern elephant seals with intravenous Tiletamine and Zolazepam. The Veterinary Record 146:251–254.
McIntyre, T., I. J. Ansorge, H. Bornemann, J. Plötz, C. A. Tosh and M. N. Bester. 2011. Elephant seal dive behaviour is influenced by ocean temperature: Implications for climate change impacts on an ocean predator. Marine Ecology Progress Series 441:257–272.
Meir, J., C. D. Champagne, D. P. Costa, C. L. Williams and P. J. Ponganis. 2009. Extreme hypoxemic tolerance and blood oxygen depletion in diving elephant seals. American Journal of Physiology. Regulatory, Integrative and Comparative Physiology. 297:927–939.
Meir, J. U., P. W. Robinson, L. Ignacio Vilchis, G. L. Kooyman, D. P. Costa and P. J. Ponganis. 2013. Blood oxygen depletion is independent of dive function in a deep diving vertebrate, the northern elephant seal. PLOS ONE 8:8–13.
Miller, P. J. O., M. Biuw, Y. Y. Watanabe, D. Thompson and M. A. Fedak. 2012. Sink fast and swim harder! round-trip cost-of-transport for buoyant divers. Journal of Experimental Biology 215:3622–3630.
Naito, Y., H. Bornemann, A. Takahashi, T. McIntyre and J. Plötz. 2010. Fine-scale feeding behavior of Weddell seals revealed by a mandible accelerometer. Polar Science 4:309–316.
Nakagawa, S., and H. Schielzeth. 2013. A general and simple method for obtaining R^2 from generalized linear mixed-effects models. Methods in Ecology and Evolution 4:133–142.
Noren, D. 2002. Thermoregulation of weaned northern elephant seal (*Mirounga angustirostris*) pups in air and water. Physiological and Biochemical Zoology 75:513–523.
Ponganis, P. J., G. L. Kooyman, L. N. Starke, R. A. Kooyman and T. G. Kooyman. 1997. Postdive blood lactate concentrations in emperor penguins, *Aptenodytes forsteri*. Journal of Experimental Biology 200:1623–1626.
R Development Core Team. 2012. R: A language and environment for statistical computing. R Foundation for Statistical Computing, Vienna, Austria.
Richard, G., J. Vacquié-Garcia and J. Jouma'a, *et al.* 2014. Variation in body condition during the post-moult foraging trip of southern elephant seals and its consequences on diving behaviour. Journal of Experimental Biology 217:2609–2619.
Rosen, D. A. S., A. J. Winship and L. A. Hoopes. 2007. Thermal and digestive constraints to foraging behaviour in marine mammals. Philosophical Transactions of the Royal Society of London B 362:2151–2168.

Sala, J. E., F. Quintana, R. P. Wilson, J. Dignani, M. N. Lewis and C. Campagna. 2011. Pitching a new angle on elephant seal dive patterns. Polar Biology 34:1197–1209.

Slip, D. J., M. A. Hindell and H. R. Burton. 1994. Diving behavior of Southern elephant seals from Macquarie Island: An overview. Pages 253–270 in B. J. Le Boeuf and R. M. Laws, eds. Elephant seals: Population ecology, behavior and physiology. University of California Press, Oakland, CA.

Sparling, C. E., M. A. Fedak and D. Thompson. 2007. Eat now, pay later? Evidence of deferred food-processing costs in diving seals. Biology Letters 3:95–99.

Tift, M. S., E. C. Ranalli, D. S. Houser, R. M. Ortiz and D. E. Crocker. 2013. Development enhances hypometabolism in northern elephant seal pups (*Mirounga angustirostris*). Functional Ecology 27:1155–1165.

Thums, M., C. J. A. Bradshaw and M. A. Hindell. 2011. In-situ measures of foraging success and prey encounter reveal marine habitat dependent search strategies. Ecology 92:1258–1270.

Vacquié-Garcia, J., F. Royer, A.-C. Dragon, M. Viviant, F. Bailleul and C. Guinet. 2012. Foraging in the darkness of the Southern Ocean: Influence of bioluminescence on a deep diving predator. PLOS ONE:e43565.

Viviant, M., A. , W. Trites, D. A. Rosen, P. Monestiez and C. Guinet. 2010. Prey capture attempts can be detected in Steller sea lions and other marine predators using accelerometers. Polar Biology 33:713–719.

Watanabe, Y., E. A. Baranov, K. Sato, Y. Naito and N. Miyazaki. 2006. Body density affects stroke patterns in Baikal seals. Journal of Experimental Biology 209:3269–3280.

Williams, T. M., L. A. Fuiman, M. Horning and R. W. Davis. 2004. The cost of foraging by a marine predator, the Weddell seal *Leptonychotes weddellii*: Pricing by the stroke. Journal of Experimental Biology 207:973–982.

Wilson, R. P., C. R. White, F. Quintana, L. G. Halsey, N. Liebsch, G. R. Martin and P. J. Butler. 2006. Moving towards acceleration for estimates of activity-specific metabolic rate in free-living animals: The case of the cormorant. Journal of Animal Ecology 75:1081–1090.

Received: 14 July 2014
Accepted: 17 March 2015

ANNEXE C

Measuring the marine soundscape of the Indian Ocean with Southern Elephant Seals used as acoustic gliders of opportunity

Cazau, Dorian, Bonnel, Julien, Joffrey, Jouma'a, Yves, Le Bras & Guinet Christophe, (2016) Measuring the marine soundscape of the Indian Ocean with Southern Elephant Seals used as acoustic gliders of opportunity. *Journal of Atmospheric and Oceanic Technology*

Measuring the Marine Soundscape of the Indian Ocean with Southern Elephant Seals Used as Acoustic Gliders of Opportunity

DORIAN CAZAU AND JULIEN BONNEL

ENSTA Bretagne, Lab-STICC (UMR CNRS 6285), Brest, France

JOFFREY JOUMA'A, YVES LE BRAS, AND CHRISTOPHE GUINET

Centre d'Etudes Biologiques de Chizé, UMR 7372 Université de La Rochelle-CNRS, Villiers-en-Bois, France

(Manuscript received 17 June 2016, in final form 1 September 2016)

ABSTRACT

The underwater ambient sound field contains quantifiable information about the physical and biological marine environment. The development of operational systems for monitoring in an autonomous way the underwater acoustic signal is necessary for many applications, such as meteorology and biodiversity protection. This paper develops a proof-of-concept study on performing marine soundscape analysis from acoustic passive recordings of free-ranging biologged southern elephant seals (SES). A multivariate multiple linear regression (MMLR) framework is used to predict the measured ambient noise, modeled as a multivariate acoustic response, from SES (depth, speed, and acceleration) and environmental (wind) variables. Results show that the acoustic contributions of SES variables affect mainly low-frequency sound pressure levels (SPLs), while frequency bands above 3 kHz are less corrupted by SES displacement and allow a good measure of the Indian Ocean soundscape. Also, preliminary results toward the development of a mobile embedded weather sensor are presented. In particular, wind speed estimation can be performed from the passive acoustic recordings with an accuracy of 2 m s^{-1}, using a rather simple multiple linear model.

1. Introduction

1In the frequency band from a few tens of a hertz up to 50 kHz, the dominant sources of ambient noise in the ocean can be broadly divided into sounds resulting from geophony (i.e., sounds from natural physical processes, e.g., wind-driven waves, rainfall, seismicity, breaking waves, current), biophony (i.e., sounds from biological activities, e.g., whale vocalizations, snapping shrimp beds), and anthropophony (i.e., man-made sounds, e.g., commercial shipping, sonar, seismic prospecting, oil and gas surveys) (Knudsen et al. 1948; Wenz 1962). All these sources contribute conjointly to the noise spectrum characteristics (e.g., pressure level, spectral slope) in varying degrees, depending on their strength and conditions prevailing at the measurement location. Thus, the underwater ambient sound field contains quantifiable information about the physical and biological marine environment. To extract this information, passive acoustic systems have been used for monitoring, recording, and interpreting in a continuous and autonomous way the underwater acoustic signal, facilitating an all-weather and all-season ocean monitoring.

The study of ocean ambient noise plays a growing role in many different research fields. In biodiversity, it helps in preserving marine animal ecosystems by better understanding the impacts of human activities on their ecology (Sirovic et al. 2013). In meteorology, global climate models and local weather forecasts rely on field information about weather across oceans. Observations of rain and wind phenomena from underwater noise allow for better study of air–sea interactions, and increase greatly the spatio-temporal resolution provided by satellite (Vagle et al. 1990; Nystuen and Selsor 1997; Ma and Nystuen 2005; Pensieri et al. 2015). In cryogenics, the noise generated by glaciers allows for quantification of melting processes in the Arctic and is a good indicator of rapid climate processes (Urick 1971; Glowacki et al. 2015). In oceanography, measurement and characterization of ambient noise

Corresponding author address: Dorian Cazau, ENSTA Bretagne, Lab-STICC (UMR CNRS 6285), 2 rue François Verny, 29806 Brest CEDEX 09, France.
E-mail: dorian.cazau@ensta-bretagne.fr

DOI: 10.1175/JTECH-D-16-0124.1

are essential to enhance the signal-to-noise ratio of acoustic-based underwater instruments (Rahmati et al. 2014). The need for better assessment of global change and its consequences have drawn attention and highlighted the need for an intense monitoring of underwater noise level and, consequently, for the development of innovative sensors and networks (Duennebier et al. 2002; Johnson and Tyack 2003; Aguzzi et al. 2011; Favali 2013) able to collect and analyze long-term underwater sound data.

Ambient noise studies mostly take place in the northeastern Pacific (Chapman and Price 2011) and Atlantic Oceans (Nieukirk et al. 2004). Previous studies in the Indian Ocean have focused on the northwestern (Wagstaff 2005) and the tropical regions of the Indian Ocean (Miksis-Olds et al. 2013; Hawkins et al. 2014; Tsang-Hin-Sun et al. 2015). Tournadre (2014) showed that the ship traffic has had a global increase in the Indian Ocean in the last two decades. In the Southern Ocean, a recent study highlighted the predominant role of icebergs in the Southern Hemisphere soundscape (Matsumoto et al. 2014). Miksis-Olds et al. (2013) reported that the observed sound floor increases are consistent with concurrent increases in shipping, wind speed, wave height, and blue whale abundance in the Indian Ocean. Nair et al. (2015) developed a semiempirical model to predict surface ambient sound spectra in 1–50 kHz for rainfall rates in 2–200 mm h^{-1} and wind speeds within 2–14 m s^{-1}.

Most often, hydrophones used for marine soundscape studies are bottom mounted, shore terminated, and fixed at a certain depth. Other studies have also used mobile hydrophones, either dragged behind a drifting buoy or boat (Nystuen and Selsor 1997), or attached to vertical profiler float (Ward et al. 2011; Küsel et al. 2011; Barclay and Buckingham 2013). More recently, with the development of miniaturized electronic devices, hydrophones have been embedded in underwater gliders (Baumgartner et al. 2008; Matsumoto et al. 2011; Klinck et al. 2012). These gliders can survey a large area by autonomously navigating the defined area (Rogers et al. 2004; Rudnick et al. 2004), and they have shown great promise in monitoring marine mammals (Baumgartner et al. 2008; Klinck et al. 2012), oceanographic phenomena (Matsumoto et al. 2011), and meteorological surface conditions (Cauchy et al. 2015).

In the same line of technological innovation, the use of animalborne autonomous recording tags, called biologging, is becoming widespread (Ropert-Coudert and Wilson 2005), and allows for the acquisition of huge quantitative datasets for inferences on movement, ecology, physiology, and behavior of animals moving freely in their natural environment. Multichannel dataloggers are used, and data are sampled at high resolution over large temporal and spatial ranges, including geographical areas uncovered by satellite data. In addition to providing parameters related to the animal biological processes, environmental parameters (e.g., temperature, salinity, light, fluorescence) can also be continuously recorded.

In this project, southern elephant seals (SES) of the Kerguelen Islands are used as acoustic gliders of opportunity. SES are wide-ranging animals during their postbreeding and postmoulting migrations. Adult females (*Mirounga leonina*) from the Kerguelen Islands (49°200′S, 70°200′E) forage mainly in oceanic waters of the Antarctic and polar frontal zones (below 60°S) from October to February (Bailleul et al. 2010). Among top marine predators, air-breathing diving species such as SES are particularly well suited for biologging because their large size allows them to carry electronic devices with minimal disturbance. These devices are stuck on SES while they are on land in their breeding colonies. The strong east–west current speeds and the thick ice surface layers in this part of the austral ocean make the use of regular gliders very complicated, while these harsh environmental conditions are not a problem for SES.

So far, these biologged SES have been used to collect measurements of physical (Charrassin et al. 2008; Costa et al. 2008; Roquet et al. 2009) and biological (Guinet et al. 2013) oceanographic parameters, in often inaccessible regions. The SES and their closed-loop migratory route also provide the opportunity for using Acousondes[1] (Acoustimetrics, Greeneridge Sciences, Inc., Felton, California) that can be retrieved at the end of their migration. Acoustic data have already been recorded and used to investigate behavioral and ecophysiological (breathing rate) parameters (Genin et al. 2015). While at sea, SES dive repeatedly to mesopelagic depths (300–500 m up to 2000 m) and tend to follow the diel vertical migration of their mesopelagic prey, diving generally deeper during the day (Guinet et al. 2014). SES regularly perform dives during which they spend a large proportion of time descending passively through the water column (Richard et al. 2014). In the following, this type of dive will be referred to as drift dives.

The main objective of this current study is to demonstrate that marine soundscape can be measured with biologged SES used as acoustic gliders of opportunity. However, the SES movements (e.g., depth/speed variations) impact the measured sound spectra. It is thus first required to identify, characterize, and if possible remove the acoustic noise produced by SES movements that corrupts the measured soundscape. Under the

[1] Acousondes are miniature, self-contained, autonomous acoustic recorder designed for underwater applications.

assumption that different sound sources have unique acoustic signatures, passive acoustics can be used to make a classification of the ambient sound field. In this paper, a multivariate acoustic response in a multivariate multiple linear regression (MMLR) framework is used to decompose the measured ambient noise into different acoustic sources (acting as predictors) related either to the environment or to the SES. The ambient noise is modeled as a multivariate response of spectral parameters, namely, sound pressure levels (SPLs) and spectral slopes (SS), in various frequency bands. These acoustic features have been widely used in studies on marine soundscape and acoustical meteorology (Nystuen and Selsor 1997; Ma and Nystuen 2005; Pensieri et al. 2015). Ancillary datasets on wind speed and on SES diving behavior are used to define the predictors. Once we have fully characterized the acoustic noise induced by the SES displacements, we present results on the measured soundscape, and we focus on the effect of wind speed on the ambient noise level. These measures are compared with those made in other ocean environments at comparable depths, and also with theoretical models.

This paper is organized as follows. Section 1 provides details on acoustic measurements and on the different variables used in the regression framework. Section 2 presents exploratory and qualitative results, with an emphasis on the differences between spectra measured during the drift and active swimming phases of the SES. Then, more quantitative results are presented, in particular to evaluate the accuracy of estimating wind speed from our passive acoustic recordings. Section 3 proposes two general discussions on the relations between the external influence variables and the measured spectra, and on the marine soundscape resulting from our acoustic glider of opportunity.

2. Methods

a. Materials

In the austral winter of 2012, five different postbreeding female SES of similar body conditions were captured and equipped with dataloggers on the Kerguelen Islands. These loggers included an Acousonde 3A device (already used in similar research studies; e.g., Burgess et al. 1998; Burgess 2000) glued on the back of the seal on the longitudinal axis, 10 cm behind the scapula. The Acousonde 3A recorded sound at a sampling frequency F_s of 12.2 kHz with an acoustic sampling resolution of 16 bits, using a built-in low-frequency hydrophone. It also has a high-pass filter at 22 Hz (to remove powerful low-frequency flow noise) and an antialias (low pass) filter at 4640 Hz. The hydrophone response is flat in this band so that overall the useable bandwidth is 22–4640 Hz (more details can be found at http://acousonde.com/faqtechnical.html). Total storage capacity is 64 GB. The unamplified raw sensitivity of the hydrophone is −201 dB (low-power-channel hydrophone) ref 1 V $(\mu\text{Pa})^{-1}$, that is, 0.089 mV Pa^{-1}. There is no onboard signal processing embedded into the Acousonde. The Acousonde's raw data have been converted to pressure data using a MATLAB (MathWorks, Natick, Massachusetts) program provided by Greeneridge Sciences, Inc. (the Acousonde manufacturer). The Acousonde also continuously recorded depth (pressure) and triaxial acceleration with a sampling frequency of 5 Hz.

TABLE 1. Global overview of the passive acoustic recording database, with C as the cumulated duration. Each recording lasts approximately 4 h.

Acousonde	No. of recordings	Period	C (h)
A626019	20	30 Oct–18 Nov 2012	76.4
A626020	13	22 Sep–10 Nov 2012	51.2
A626021	4	30 Oct–2 Nov 2012	16
A626022	5	30 Oct–3 Nov 2012	18.6
A626040	24	31 Oct–23 Nov 2012	95.4

b. Acoustic database

Table 1 provides a global overview of the sound database. The five Acousondes deployed were activated on the field almost at the same time, making their recordings overlap in time. The smaller number of recordings in Acousondes A626021 and A626022 was caused by technological deficiency. To save onboard storage space, a duty cycle was set up in each Acousonde that automatically turned it on for 4 h every 24 h. Each 4-h recording was segmented into 10-s time windows (except for the long-term averaged spectrogram, where we used 30-s time windows), using non-overlapping Hamming windows. We removed all the sound files for which the SES depth was less than 10 m, which includes phases when the SES is on land and phases when the SES is at the surface at sea. All data processing and analysis were conducted using MATLAB. A total of 184.2 h of audio recordings have eventually been used, providing 66 296 observations of 10 s long.

Figure 1 represents the migratory routes followed by the SES during which the Acousondes were active. The spatiotemporal coverage provided by SES routes ranges from 71° to 87° in longitude and from −46° to −52° in latitude.

c. Identification of drift phases

As already done in Dragon et al. (2012), pressure data were used to split the ascent and descent dive phases into two different categories based on diving behavior,

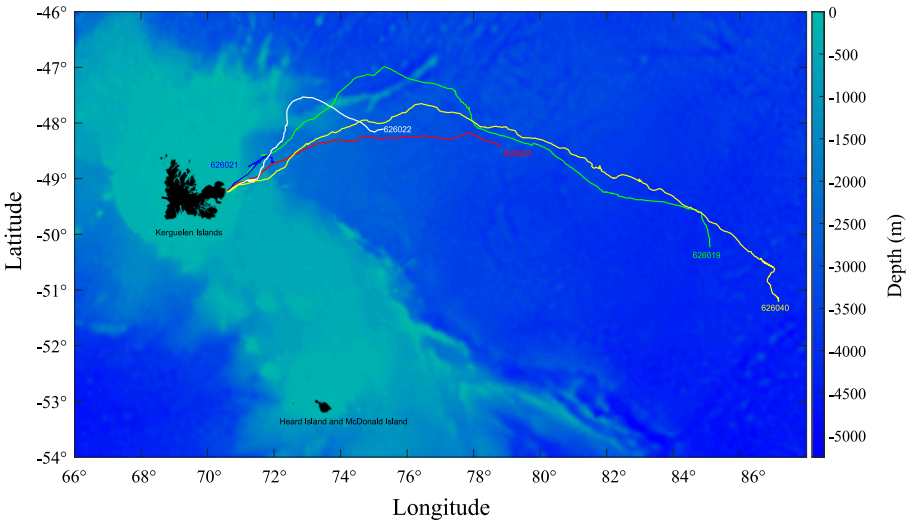

FIG. 1. Migratory routes of five different SES plotted on a map zoomed in on the Kerguelen Islands (49°200′S, 70°200′E), in the Indian Ocean. Details of individual SES are given in Table 1. These trajectories are based on GPS data from an *Argos* GPS satellite tag fixed on each SES. Only the segments of routes during which the Acousondes were active are drawn.

namely, drift dives and active swimming dives. In our study, drift dives are important, as they are expected to offer the cleanest acoustic measures. Drift dive identification was processed in two steps. First, we used first the complete time–depth recorder (TDR), which allowed us to (i) identify drift dives and (ii) isolate the passive drift phases during those dives (Dragon et al. 2012). For each drift dive, a drift rate was determined as the slope coefficient of a linear regression between depth and time (Bailleul et al. 2010; Mitani et al. 2010). In the second step, we used accelerometer data to exclude phases of active swimming during drift phases assessed by the TDR-only data. Active swimming was considered to take place when lateral acceleration exceeded the -0.2 to $0.2\,\mathrm{m\,s^{-2}}$ range. It is noteworthy that a more detailed taxonomy could have been used [e.g., Richard et al. (2014) subdivided the active swimming dives into exploratory dives, shallow active dives, and deep active dives], but in this paper diving characteristics of the SES will be limited to this two-class behavior, for the sake of clarity and conciseness with our acoustical meteorology application.

Table 2 provides statistical information on three different dive phases of SES, namely, surface, drifting, and active swimming phases. The R package Biologging tools[2] were used to estimate automatically the drift phases of SES. Drift phases have an average duration of 2 min. Overall, they cover only 6% of the total recording period, with a higher presence of more active swimming dives (83%). These estimated drift phases have already been used in previous biological studies (Vacquié-Garcia et al. 2012; Guinet et al. 2014; Richard et al. 2014; Genin et al. 2015).

d. Regression variables

Table 3 presents details on the different variables used in the regression analysis. They are detailed in the following.

1) ACOUSTIC VARIABLES

Each 10-s time series has been fast Fourier transformed (FFT) to obtain a 512-point power spectrum. Each spectrum is integrated on one-third octave frequency bands. The SPLs averaged over the one-third octave subband centered around f_c kHz, and the SS between the frequencies f_1 and f_2, have been extracted from the measured spectra; they are labeled SPL(f_c) and SS(f_1-f_2), respectively. SPL measures are computed as

$$\mathrm{SPL}(f_c)^{(m)} = 10\log_{10}\left[\frac{1}{p_{\mathrm{ref}}^2}\sum_{f=f_{\mathrm{lower}}}^{f=f_{\mathrm{upper}}}\frac{P^{(m)}(f)}{B}\right], \qquad (1)$$

TABLE 2. Statistics on dive phases, with D as the mean phase duration, C as the cumulated duration, and P_{tot} as the percentage over total acoustic recordings.

Dive phases	D (min)	C (h)	P_{tot} (%)
Surface	2.5	42.5	11
Drift phases	2	22.9	6
Active phases	3	311.8	83

[2] Developed by Yves le Bras (CEBC-CNRS-UMR 7372 Université de La Rochelle, Chizé, France) and available at https://github.com/SESman/rbl.

TABLE 3. Details of variables used in the regression analysis, classified into four categories: acoustics, SES displacements, SES status dive, and environment. All center frequencies f_c in the SPL descriptors have been rounded to a multiple of 10 for clarity in the notation.

Variable categories	Variable description	Variable labels	Units
Acoustics	Sound pressure levels	SPL(0.05), SPL(0.2), SPL(0.5), SPL(1), SPL(1.6), SPL(2.5), SPL(3.2), SPL(4)	dB
	Spectral slope	SS(1–2.5), SS(2.5–4)	dB f^{-1}
SES displacements	Speed	V	m s^{-1}
	Triaxial acceleration	a_x, a_y, a_z	m s^{-2}
	Depth	d	m
Environment	Wind speed	W	m s^{-1}

where $f_{\text{lower}} = f_c 10^{1/20}$ and $f_{\text{upper}} = f_c 10^{(-1)/20}$, $p_{\text{ref}} = 1\,\mu$Pa, and B is the noise power bandwidth of the window function ($B = 1.36$ for a Hamming window). The power spectrum $P^{(m)}(f)$ is defined as

$$P^{(m)}(f) = 2\left|\frac{X^{(m)}(f)}{N}\right|^2, \tag{2}$$

where $X^{(m)}(f)$ is the FFT of the mth segment, given by

$$X^{(m)}(f) = \sum_{n=0}^{N-1} x_{\text{win}}^{(m)}[n] e^{(-i2\pi fn)/N}, \tag{3}$$

where x_{win} is a windowed segment of a time series. SS are calculated using a least squares fit to the SPLs over the specified frequency band. After correlation analysis, it appeared that strong correlations exist between different pairs of acoustic features, implying that knowledge of one necessarily implies knowledge of the other. Then, to reduce the dimension of the acoustic feature vector, we kept only the SPL(f_c) measures per octave and the two slopes that maximize the Pearson correlation coefficient with the regression variables SES and Environment presented in sections 2d(2) and 2d(3), respectively. The acoustic descriptors resulting from this process, listed in Table 3, form a ten-dimensional feature vector over all the observations consisting of the following descriptors: {SPL(0.05), SPL(0.2), SPL(0.5), SPL(1), SPL(1.6), SPL(2.5), SPL(3.2), SPL(4), SS(1–2.5), SS(2.5–5)}. In the following, all f_c values have been rounded to a multiple of 10 for clarity in the notation, and all sound pressure levels are given in dB ref μPa^2.

2) SES DISPLACEMENTS

The raw triaxial acceleration data from the accelerometer of the Acousonde 3A were used and labeled a_x, a_y, and a_z (longitudinal, lateral, and vertical axes, respectively). To estimate swimming speed V, we first need to compute the pitch θ of the seal, defined as the angle θ between the SES body direction and the horizontal, that is,

$$\theta = \arctan\left(\frac{a_x}{\sqrt{a_y^2 + a_z^2}}\right). \tag{4}$$

As explained in Sato et al. (2003) and Aoki et al. (2011), the acceleration data used to compute the pitch using Eq. (4) have been filtered with a low-pass filter at 0.2 Hz in order to isolate the gravity component of the movement. Then V was computed by combining information on the vertical speed and the seal pitch as follows:

$$V = \frac{U_{\text{vert}}}{\sin(\theta)}, \tag{5}$$

where U_{vert} corresponds to the vertical speed (as determined from the depth recorder) of the SES, and V corresponds to the vertical speed corrected by the orientation of the SES given by its pitch. As already reported in past studies (Miller et al. 2004; Richard et al. 2014; Genin et al. 2015), this method is reliable only for steeper body angles (with an absolute body pitch over 30°). As a result, we use this proxy for deep descents and ascents, that is, ending and starting below 400 m deep, respectively, and with an absolute pitch over 30°. Eventually, the variable depth d is directly read from the TDR, with negative values below the ocean surface. Figures 2a–c represent the histograms of speed, acceleration, and depth data, respectively, matched with the analyzed passive acoustic recordings. As expected, higher extrema values of speed and rms acceleration (labeled rms $- a$) are obtained for active swimming periods (going from a range of [0.15–2] m s^{-1} and [0–6] m s^{-2} to [0.7–3] m s^{-1} and [0–10] m s^{-2}, respectively, for the drift and active swimming phases, respectively), while depth and wind speed are reasonably well balanced between the two categories.

3) ENVIRONMENT

The dataset on wind speed was extracted from the Advanced Scatterometer (ASCAT) retrievals[3] and

[3] Available at ftp://ftp.ifremer.fr/ifremer/cersat/products/gridded/MWF/L3/ASCAT/Daily/Netcdf/.

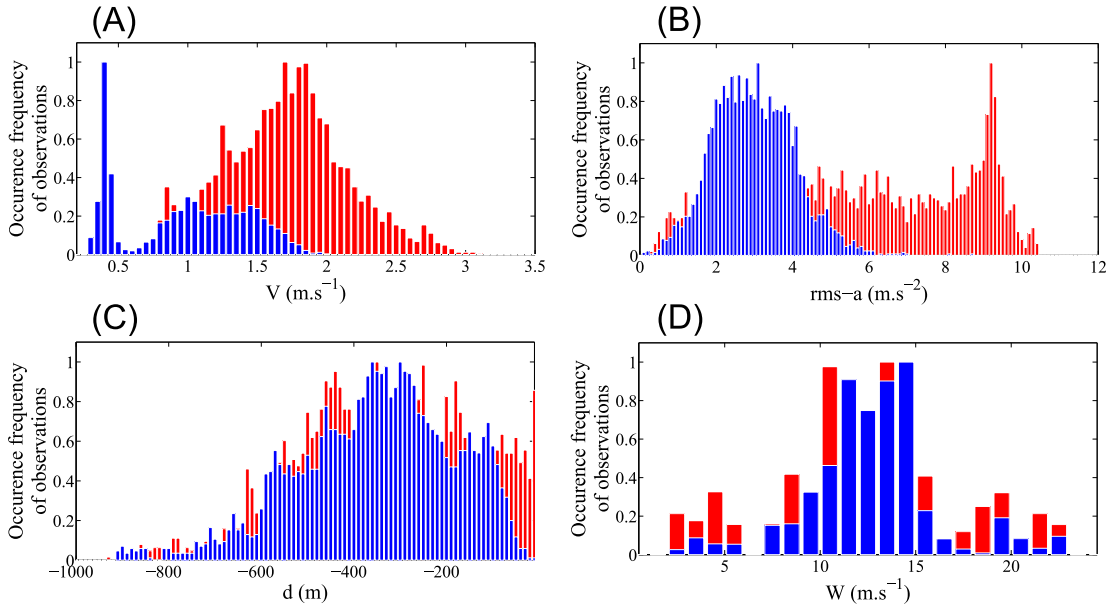

FIG. 2. Histograms of (a) SES swimming speed, (b) acceleration, (c) depth, and (d) wind speed data matched with the analyzed passive acoustic recordings. Each histogram has been individually unitary normalized. Each observation is labeled either as a drift phase (blue) or an active swimming phase (red).

provided gridded daily-averaged wind and wind stress fields over global oceans (Bentamy and Croize-Fillon 2012). The calculation of daily estimates uses ascending and descending available and valid retrievals. The objective method aims to provide daily-averaged gridded wind speed, zonal component, meridional component, wind stress, and the corresponding components at global scale. The error associated with each parameter, related to the sampling impact and wind space and time variability, is provided too. When compared with buoy measurements, this error for wind speed is below 2 m s^{-1} (Bentamy and Fillon 2015). More details about data, the objective method, and computation algorithm can be found in Bentamy and Croize-Fillon (2012). The European Centre for Medium-Range Weather Forecasts (ECMWF) analyses have been used as a temporal interpolation basis of ASCAT retrievals. The resulting fields are 10 m high above the ocean surface, and have spatial resolutions of 0.25° in longitude and latitude, and a 3-h temporal resolution.

An acoustic measurement is a spatially integrated measure, with an area of measurement at the ocean surface (also called the listening area in literature) that depends on the hydrophone depth and on the beam pattern of the ambient noise field. The listening area of a 500-m-depth hydrophone is around 8 km^2 (Nystuen et al. 2015), which is well included in the satellite pixel resolution (around 30 km^2 at the SES latitudes).

Figure 2d represents the histogram of wind speed data matched with the analyzed passive acoustic recordings. From operational point of view, it is more significant to provide the correct classification of wind speed class than wind speed estimates. We thus identified from these data four different classes of wind speeds, labeled W_1 (below 7.5 m s^{-1}), W_2 (between 7.5 and 12.5 m s^{-1}), W_3 (between 12.5 and 17.5 m s^{-1}), and W_4 (higher than 17.5 m s^{-1}). Each class corresponds to an average increase of 5 m s^{-1} in wind speed, except for classes W_2 and W_3. These classes correspond roughly to the sea states of the Beaufort scale from 2 to 5 (light wind) for W_1, from 6 to 7 (high wind) for W_2 and W_3, and from 8 to 9 (gale wind) for W_4 (Knudsen et al. 1948). Sea state 1 has not been used, as noise produced by weak wind speed is too low to be detected (Pensieri et al. 2013).

e. *Multivariate multiple linear regression*

1) MODEL FORMULATION

MMLR is a common statistical tool that informs about the linear relationship between dependent variables (i.e., the response) and independent variables (i.e., the predictors). With multiple response variables available, as in our case, the standard approach to modeling them is to regress each response variable separately on the same set of explanatory variables. However, although it is simple and popular, this univariate response approach may not be optimal, since they do not utilize the joint information among response variables. To solve this multiresponse regression problem, Breiman and Friedman (1997) proposed a method, called the curd

and whey, that uses the relationship among response variables to improve predictive accuracy. They showed that their method can outperform separate univariate regression approaches when there are correlations among the response variables. The multivariate general linear model is

$$\underbrace{\mathbf{Y}}_{(n,r)} = \underbrace{\mathbf{X}}_{(n,p+1)} \underbrace{\boldsymbol{\beta}}_{(p+1,r)} + \underbrace{\mathbf{E}}_{(n,r)}, \tag{6}$$

where $\mathbf{Y}$ is a matrix of n observations on r response variables. The $\mathbf{X}$ is a model matrix with columns for p regressors, including an initial column of ones for the regression constant, also called intercept. The $\boldsymbol{\beta}$ is a matrix of regression coefficients, one column for each response variable. The $\mathbf{E}$ is a matrix of errors that follows a Gaussian law $N(0, \sigma^2)$. Each response (dependent variable) gets its own linear equation of the form $\mathbf{Y}_r \sim \beta_{0p} + \sum_{p=1}^{P} \beta_{rp} \mathbf{X}_p + E_{n,r}$, conjointly estimated along with the other responses, and depending only on the predictors (independent variables), whose contributions are weighted by the regression coefficients β_{rp} (Breiman and Friedman 1997).

Parametric nonlinear models also exist, and represent the relationship between a continuous response variable and one or more continuous predictor variables in the form $\mathbf{Y} = f(\mathbf{X}, \beta) + \mathbf{E}$, where f is any function of $\mathbf{X}$ and $\boldsymbol{\beta}$ that evaluates each row of $\mathbf{X}$ along with the vector $\boldsymbol{\beta}$ to compute the prediction for the corresponding row of $\mathbf{Y}$.

In regression analysis terms, two noncorrelated predictors used in combination would predict unique variance in a response, while two more correlated predictors tend to predict shared variance, and so are less efficient. Prior to MMLR, a principal components analysis (PCA) can then be used to decorrelate predictors. PCA is a dimension reduction method that constructs independent new variables that are linear combinations of the original variables, by reducing redundancy (i.e., increasing standard deviation) between all variable dimensions. PCA was performed to see how our different SES and environmental variables were structured within the dataset, and whether the acoustic variables were responding to this structure. PCA also avoids multicollinearity problems in regression analysis (Zhang et al. 2006). Such problems make regression coefficients become unstable when highly correlated predictors are present. This further justifies the use of PCA in our study.

In this project, two different setups of the MMLR method were used. We first studied the contributions of SES and environment variables (i.e., the predictors $\mathbf{X}$, with $p = 6$) in the multivariate acoustic response characterizing the measured spectra (i.e., the responses $\mathbf{Y}$, with $r = 10$) over all 10-s observations ($n = 66\,296$). Here, predictors are the different physical processes contributing independently to the distribution of acoustic energy in the measured spectra. In the second application, we evaluated the classification accuracy of an MMLR on PCA-processed acoustic measures ($p = 10$) in predicting wind speed ($r = 1$).

Also, all variables were standardized (i.e., zero mean and unitary variance), which allows a better comparison of regression weights between each predictor (especially with variables having different range values, as for depth and wind speed in our study), as the unstandardized weights are a function of the variance of the predictor variables. Standardization removes most of the correlation between linear and higher-order terms, which reduces the chance of adding these terms unnecessarily.

2) EVALUATION METRICS

To assess quantitatively the quality of our regression analysis and estimation, we provided as evaluation metrics the p value and the multiple correlation coefficient squared [ordinary R^2 (%)], also called the coefficient of determination. To further evaluate the impacts of each predictor in the MMLR model, we performed a sequential significance testing of each dependent variable through the metric ΔR_a^2, defined as

$$\Delta R_a^2 = \frac{|R_a^2 - R_a^2(-p)|}{R_a^2}, \tag{7}$$

where R_a^2 refers to the adjusted R^2 metric, and $R_a^2(-p)$ refers to the adjusted R^2 metric obtained with an MMLR performed without the predictor p. This amount of change in R^2 is a measure of the increase in predictive power of a particular dependent variable, given the dependent variable or variables already in the model. In other words, this metric allows for performing significance testing to determine whether the addition of another dependent variable to the regression model significantly increases the value of R^2. Also, the ordinary R^2 value systematically increases with the addition of terms to the regression model; consequently, in order to compare models with different numbers of predictors, we use the adjusted R^2 metric.

3. Results

a. *Exploratory data analysis*

Figure 3 shows a typical long-term spectral average computed over four acoustic recordings (i.e., a total of 16 h of recordings from four different days) from the SES individual A626019. SES variables and wind speed values are superimposed onto this spectrogram. It can

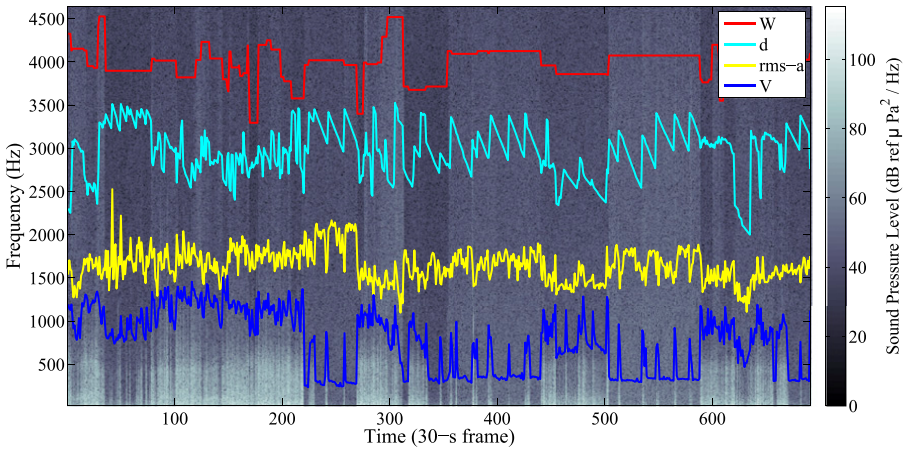

FIG. 3. Long-term spectrogram averaged over four acoustic recordings (i.e., a total of 16 h of recordings from four different days) from SES A626019. It was generated using 2048-point FFTs, Hamming windows, and no overlap, and averaged every 30 s. The four variables V, rms $-$ a, d, and W are superimposed onto the spectrogram with relative linear scales ranging from 0.3 to 2.7 m s^{-1}, 0.2 to 10 m s^{-2}, -150 to 600 m, and 4 to 18 m s^{-1}, respectively.

be seen that the drift and active swimming phases are clearly identified through the acoustic energy in low-frequency bands that correlate well with the SES speed. Also, acoustic energy in higher-frequency bands appear to be reinforced with higher wind speed, independently from other SES-related variables. In other words, two frequency regions of the spectra are mainly impacted, showing first strong evidence of correlations: a first region in frequency subbands below 2.5 kHz, modulated accordingly to SES speed, and a second region above this frequency that is more dominated by wind speed.

To provide more details on the shape of spectra measured during drift phases, Fig. 4 represents an averaged spectrum computed during temporal phases with values of SES speed and acceleration belonging to their 5th percentiles. In the following, these phases will be referred to as extreme drift phases. Also, this averaged spectrum will be associated with our measured soundscape. Regarding median levels across this acoustic dataset, they ranged between 47 and 70 dB ref 1 μPa^2 Hz^{-1}. The spectrum slope falls off quickly from its highest level at 50 Hz at a rate of about -5 dB per octave up to

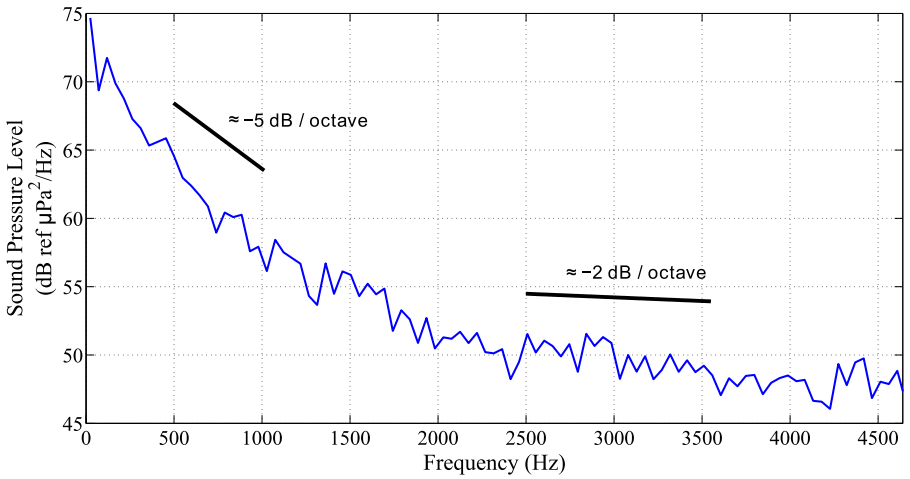

FIG. 4. Averaged spectrum computed during extreme drift phases, i.e., with values of SES speed and acceleration belonging to their 5th percentile. Two representative theoretical SS (dB per octave) are superimposed onto the spectrum. The approximate signs mean that these slopes are only locally correct in frequency (i.e., the first slope is a decrease of -5 dB within the octave 500–1000 Hz, and the second slope is a decrease of -2 dB within the octave 2500–5000 Hz).

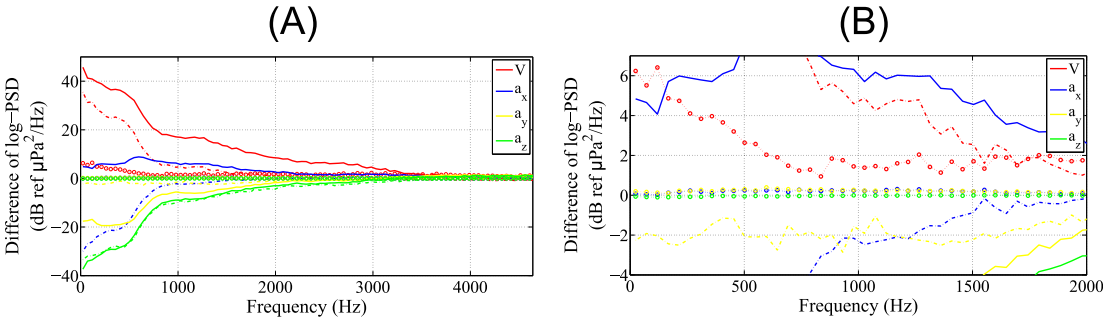

FIG. 5. Differences between averaged logarithmic PSD with values of SES speed and acceleration belonging to their 20th, 60th, and 95th percentiles (dot-plus-circle, dashed–dotted, and solid lines, respectively), and their 5th percentile. (a) The full spectrum, (b) a zoomed-in view of the frequency range [10; 2000] Hz and level range [−8; 8] dB.

2 kHz, where it becomes flatter up to 5000 Hz, assuming a slope of −5 dB per octave.

We then quantified the averaged deformation of spectra due to SES displacements relative to this extreme drifting behavior. In Fig. 5, we computed the differences between averaged logarithmic power spectral density (PSD) with values of SES speed and acceleration belonging to their 20th, 60th, 95th percentiles (dot-plus-circle, dashed–dotted, and solid lines, respectively), and their 5th percentile. From Fig. 5a, we can observe that SES speed strongly impacts the acoustic data for frequencies lower than 2000 Hz, with variations that can reach 40 dB. The three acceleration components contribute to an increase in the measured noise below 800 Hz, with gains from −30 to −10 dB. From Fig. 5b, it can be observed from the dashed–dotted curves that the acoustic distortions from our marine soundscape spectrum above (see Fig. 4) are quite minimal, that is, in the order of magnitude of 5 dB with the SES speed and less than 1 dB with the acceleration variables. Also, we did not find any significant influences of depth on the acoustic features (see Fig. A1).

b. *Correlation analysis*

To provide a more global insight into the correlation structure of our variables, we performed a PCA on the complete variable dataset. Figure 6 shows both the orthonormal principal component coefficients of each variable on the first two principal axes and the principal component scores for each observation (i.e., the coordinates of the original data in the new coordinate system defined by the principal components). In the space of the principal components of the acoustic/SES/environmental variables, the first two principal components distinctly separate the different acoustic features. Indeed, these features move from the first to the second principal axis as their center frequencies increase. In other words, low-frequency SPL observations remain in the bottom-right half-space, while the higher-frequency SPL observations are in the top-right half-space. We can now see how SES and wind speed variables distribute on the fan of SPL values. SES speed V is among low-frequency SPLs with a high score on the first PCA axis and a negative score on the second axis ($PCA_1 = 0.3$; $PCA_2 = -0.1$), while wind speed W contributes much more to the second PCA axis ($PCA_1 = -0.02$; $PCA_2 = 0.48$). The discriminative power over wind speeds with this PCA analysis is revealed by color mapping different classes of wind speed, W_1 to W_4 (defined in section 3) in Fig. 6. This plot illustrates the

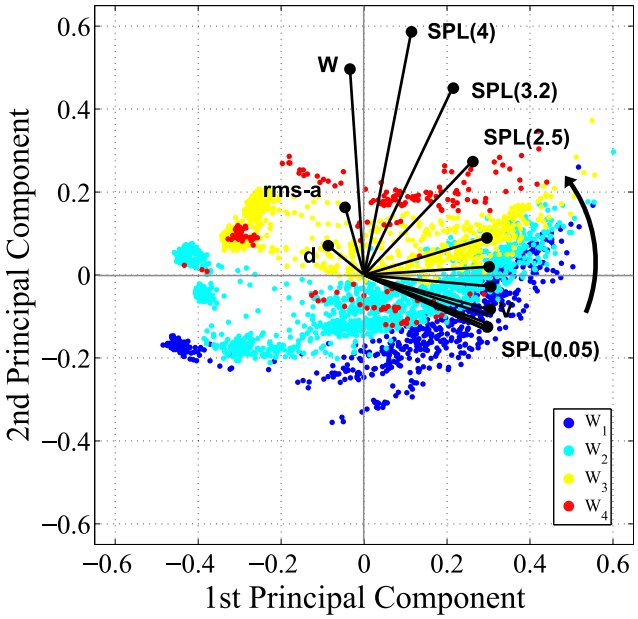

FIG. 6. Orthonormal PCA for each variable (blue lines), and the principal component scores for each observation resulting from the PCA in the first two PCA axes. For the sake of clarity, all the SPL acoustic features are located at their respective black bullet in increasing order, as illustrated by the black arrow. Also, observations are classified into four different classes of wind speeds, W_1–W_4, with different colors.

TABLE 4. Results of the MMLR model for the multivariate acoustic response. SES and environmental variables are taken as predictors. Results are reported in terms of regression coefficients, p values, ordinary R^2, and ΔR_a^2, as described in section 2. All numerical values have been rounded to the closest hundredth. Most significant regression results are in bold, and their P values are labeled with superscript letters.

	Regression coefficients							Ordinary R^2 (%)	ΔR_a^2					
	β_0	V	a_x	a_y	a_z	d	W	All	V	a_x	a_y	a_z	d	W
SPL(0.05)	0.1	**0.33**[a]	0.09	0.11	0.07	−0.02	−0.01	88	**0.76**[b]	0.12	0.1	0.11	<0.01	<0.01
SPL(0.2)	0.13	**0.35**[a]	0.1	0.13	0.08	0.04	0.03	83	**0.74**[b]	0.06	0.03	0.08	<0.01	<0.01
SPL(0.5)	0.04	**0.37**[a]	0.09	0.05	0.04	0.03	0.04	76	**0.88**[b]	0.04	0.02	0.06	<0.01	<0.01
SPL(1)	0.21	**0.24**[c]	−0.03	0.07	0.04	0.07	0.05	54	**0.66**[b]	0.04	0	0.05	0.01	0.1
SPL(1.6)	0.36	**0.17**[c]	0.02	0.03	0.05	0.04	0.07	51	**0.54**[b]	0.01	<0.01	0.02	0.08	0.26
SPL(2.5)	0.3	0.05	0.03	0.01	0.01	−0.01	0.08	45	0.37	0.09	<0.01	<0.01	0.1	**0.41**[b]
SPL(3.2)	0.74	0.04	0.04	0.04	0.02	0.02	**0.15**[c]	37	0.23	0.04	<0.01	<0.01	<0.01	**0.78**[b]
SPL(4)	0.8	0.03	0.01	0.02	0.01	−0.01	**0.16**[a]	41	0.19	0.1	<0.01	<0.01	0.02	**0.84**[b]
SS(1–2.5)	0.42	0.06	0.01	0.05	0.04	0.07	0.08	63	0.34	0.11	0.07	0.05	0.07	0.54
SS(2.5–4)	0.21	0.05	0.02	0.04	0.01	0.04	**0.11**[c]	45	0.26	<0.01	0.04	0.03	0.01	0.72

[a] $P < 0.01$.
[b] $P > 0.05$.
[c] $P < 0.05$.

positive correlation of wind speed over the second PCA axis. These first two principal components explained 80% (first component, 60%; second component, 20%) of the total variable variance.

These correlation tendencies were already highlighted through individual pairwise correlations between the acoustic, SES, and environmental features (see appendix B). To further compare the contributions of SES and environmental variables to the measured spectra, a multivariate regression analysis was eventually conducted. Previous correlation analysis (section 1) showed that our acoustic responses are at least moderately correlated, which is necessary for the multivariate regression analysis to make sense. Also, our acoustic database is assumed to be large enough so this analysis is reliable. We then modeled the multivariate ten-dimensional acoustic response with an MMLR model, and used SES and environment parameters as independent predictors. Table 4 shows the details of this analysis, with the regression coefficients β set up in the multivariate regression equations of the model displayed in the first column, and the evaluation metrics ordinary R^2 and ΔR_a^2 in the other two columns. The same results as in the previous analysis are reached, with this clear duality between the variables SES and wind speeds in explaining acoustic feature variations, largely dominating the other variables of SES depth and acceleration.

SES speed has coefficients at least around 10 times as superior as the other predictors in the response from SPL(0.05) to SPL(0.2). Wind speed becomes prevalent in the higher-frequency SPL responses, which is consistent with the correlation analysis results above. Above SPL(3.2), the coefficients of wind speed are at least around 4 times as superior as the other variables, and as high as 10 times for SPL(4). The acoustic response SPL(4) is predicted by the equation $\mathrm{SPL}(4) = 0.8 + 0.03 \times V + 0.01a_x + 0.02a_y + 0.01a_z - 0.01 \times d + 0.16 \times W$. Also, 41% of the variance in the measure of SPL(4) can be explained by measures of all predictors, with a relative contribution of the wind speed equal to 0.84. Observing the R^2 values, it can be stated that the model better fits the low-frequency data through the SES speed. Regarding depth and acceleration, their contributions remain quite constant in the different acoustic responses and are largely dominated by either the SES speed or the wind speed.

c. *Wind dependence of ambient noise*

1) QUALITATIVE OBSERVATIONS

In Fig. 7, passive acoustic recording spectra have been median averaged on the basis of our four wind speed classes, W_1–W_4, for the drift (Fig. 7a) and active swimming (Fig. 7b) phases. We superimposed onto these spectra the Wenz curves (Wenz 1962), expressed by

$$\mathrm{SPL}(f, U) = \alpha - 5\log_2(f) + 5\log_2(U), \qquad (8)$$

where we used the median of each wind speed class for the value of U, and arbitrarily set α so the first curve fits the first class W_1. Note that because of α, Eq. (8) does not depict exactly Wenz curves. Adding an offset is necessary, probably because the global ambient noise level is site specific. The Wenz curves state that doubling frequency reduces the noise level by 5 dB, and that doubling wind speed (in kt; $1\,\mathrm{kt} = 0.51\,\mathrm{m\,s^{-1}}$) increases the noise level by 5 dB. In Fig. 7, we can see that the averaged measured spectra follow the Wenz predictions. This is particularly true for frequencies above 2.5 kHz, both in terms of noise level (i.e., SPL increases of +5, 3, and

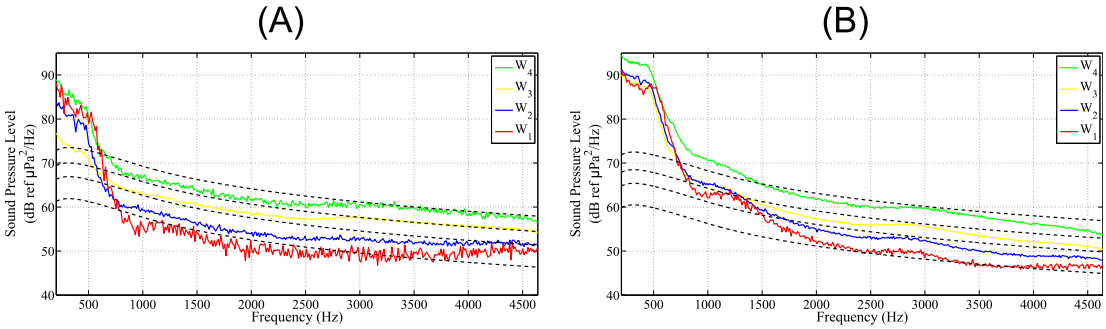

FIG. 7. Representation of four averaged ambient noise spectra corresponding to the different wind speed classes, W_1–W_4, for the (a) drift and (b) active swimming phases. The superimposed black dotted curves correspond to the Wenz curves, computed with the center wind speed value of each interval.

2.5 dB between our four classes at a given frequency) and in terms of spectral slope (for a given wind speed). Differences can also be observed between the measured spectra of the drift and active swimming phases, with a better fit to the Wenz curves for the drift phases. But still a strong discrimination is noticeable between the spectra of the different wind speed classes for both active swimming and drifting behavior.

2) QUANTITATIVE VALIDATION

In a further experiment, a sample fitting verification was performed to testify the effectiveness of different regression classifiers to predict wind speed. These classifiers were tested on a drift-only dataset and on the complete dataset. A fivefold cross validation with a stratified procedure has been applied to each dataset, meaning that each fold contains roughly the same proportions of observations from the different wind speed classes.

As listed in the first column of Table 5, we first tested a simple linear regression model, using the SPL(4) as the single predictor. This descriptor was the most correlated acoustic feature with wind speed ($r = 0.67$, $P < 0.001$, from Fig. B1). We also tested a multiple linear model and a nonlinear regression model, using as predictors the first three principal axes of a PCA performed on the ten-dimensional acoustic vector, labeled PCA_1, PCA_2, and PCA_3, respectively.

As an evaluation metric, we use the rms difference ε_{ws} between the ground truth and the estimated wind speed. The average error $\overline{\varepsilon_{ws}}$ was then computed on the resulting errors in each fold. We also report the median absolute deviation on these tests to assess the statistical significance of our experiments.

An example of wind speed prediction is represented in Fig. 8a using the multiple linear regression model superimposed onto the ground truth. Figure 8b represents the fitting plot of the adjusted model, showing that the model as a whole is significant (i.e., a horizontal line does not fit between the confidence bounds). The slope of this line is the slope of a fit to the predictors projected onto their best-fitting direction—in other words, the norm of the coefficient vector. Wind speed values are displayed in unstandardized (natural) units.

Table 5 displays for each regression model the average error $\overline{\varepsilon_{ws}}$ and coefficient R^2, differentiating the drift and active swimming phases. The regression equations (with their standard deviation over the folds) set during training and used for prediction are $4.74(\pm0.02) + 0.6(\pm0.03)\dot{S}PL(5)$ and $9.6(\pm0.002) + 0.01(\pm0.002)PCA_1 + 0.51(\pm0.006)PCA_2 - 0.42(\pm0.001)PCA_3$ for the simple linear model and the PCA-based multiple linear regression model, respectively. Globally, the classification performance with our models was very satisfactory, with ε_{ws} ranging from 1.9 to 3.4 m s^{-1}. The best-performing model for the drift phases was the PCA-based multiple linear regression model, although no major improvement was brought by any of our classifiers regarding the simple linear regression model. Indeed, taking the complete ten-dimensional

TABLE 5. Performance of different regression classifiers to estimate wind speed. Performance is reported in terms of the wind speed estimation error $\overline{\varepsilon_{ws}}$ (m s^{-1}), with its standard deviation.

Classifiers	Drift phases		Active swimming phases	
	$\overline{\varepsilon_{ws}}$ ($\pm$std dev) (m s^{-1})	Ordinary R^2	$\overline{\varepsilon_{ws}}$ ($\pm$std dev) (m s^{-1})	Ordinary R^2
Simple linear regression	2.2 ± 0.6	54	3.4 ± 0.8	74
PCA-based multiple linear regression	1.9 ± 0.3	63	2.7 ± 0.3	81
PCA-based nonlinear regression	2.1 ± 0.4	58	2.6 ± 0.5	65

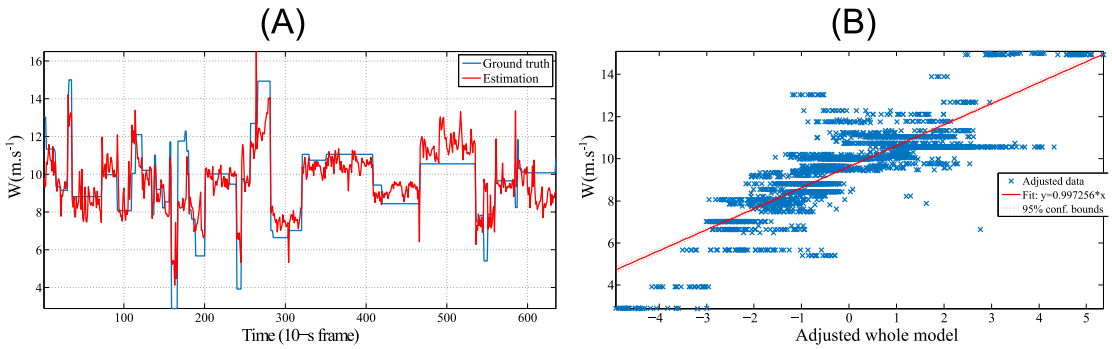

FIG. 8. Predictions of wind speeds obtained with an MMLR model, taking acoustic features as predictors. (a) The ground truth (blue) and the rms error of the model (orange) are superimposed. (b) The fitting plot of the adjusted model is represented.

acoustic feature vector instead of one single SPL feature only reduces ε_{ws} from 2.2 to $1.9^{-1}\,m\,s^{-1}$. Similarly, the increase in model complexity with the nonlinear model did not induce noticeable performance improvement, reducing ε_{ws} from 2.2 to $2.1^{-1}\,m\,s^{-1}$. For the active swimming phases, the use of more complex models brought more significant improvement, reducing the average error ε_{ws} from 3.4 to $2.7^{-1}\,m\,s^{-1}$ and 3.4 to $2.6^{-1}\,m\,s^{-1}$ for the multiple linear and nonlinear regression models, respectively, in reference to the simple linear regression model. For these phases, the multiple linear model includes a more complete modeling of the full spectrum that is beneficial to wind speed estimation. Also, we can note that the PCA-processed acoustic features stabilize wind speed predictions between the different folds.

4. Discussion

Our correlation and regression analysis allowed us to detail the acoustic contributions of different explanatory variables in the overall measured spectra. These variables depend on either the SES (displacements and dive types) or the environment. Our results show that the variables of SES swimming speed and acceleration impacted mostly low-frequency SPLs, with regression coefficients decreasing with the increase of SPL center frequencies (see Table 3). These high low-frequency SPL values most likely result from the turbulent flow noise generated by the SES body when moving in the fluid. Indeed, the turbulence of a flow is characterized by its Reynolds number, which mainly depends on a representative dimension of solid-fluid contact, and the speed of the solid. For the SES, the solid dimension D_h is taken as the dimension of the head, that is, 0.2 m, and with V between 1 and $3\,m\,s^{-1}$. The Reynolds number can then be computed as

$$R = \frac{\rho V D_h}{\mu} \approx 4 \times 10^5 \qquad (9)$$

with $\rho = 1000\,kg\,m^{-3}$ as the water density (rough approximation of the depth-dependent density of ocean water that is denser) and $\mu = 1$ cP is the water viscosity. For Reynolds numbers higher than 16 000, a fully developed turbulent flow field is generated around the hydrophone, since the pressure fluctuations in the surrounding fluid are in direct contact with the active area of the hydrophone. As shown in specialized literature (Tennekes and Lumley 1972; Van Dyke 1982), for frequencies in the inertial subrange, the energy spectrum of turbulence is expected to scale with frequency as $f^{-5/3}$, which is equivalent to a spectral slope of −17 dB decade^{-1}. To fully validate the hypothesis of a turbulent flow-generated noise, a comparison of the averaged spectra slope during active swimming phases and the theoretical slope of a chaotic flow noise, following a frequency decrease in $f^{-5/3}$, was performed over the band frequency ranging from 10 to 1000 Hz. A Pearson correlation of $r = 0.86$ ($P < 0.0001$) was found and then showed good agreement with turbulent self-noise. The effect of flow turbulence on the acoustic recordings has already been studied in previous studies. Barclay and Buckingham (2013) proposed a postprocessing method to remove from the computation of spatial coherence the contributions of pseudosound, while Burgess et al. (1998) showed that flow noise could be used as a proxy for the hydrophone carrier speed.

As SES speed and acceleration are highly reduced during drift phases (a strong negative correlation coefficient between drift phases and V, $r = -0.95$, $P < 0.0001$), the self-noise due to pressure fluctuations around the hydrophone is also reduced (Burgess et al. 1998). This tendency has already been documented in different moving hydrophone situations, like with vertical profilers (Barclay and Buckingham 2013). These drift phases then provide clean experimental conditions for acoustic analysis, with a domination of environment-related acoustic events over SES variables.

The SES depth d was seen to have much minor effects on the measured spectra, with regression coefficients inferior to 0.4 ($P < 0.0001$) over the different acoustic descriptors. This result can be explained easily. Indeed, the SES explanatory variables impacting the spectra are directly linked to the SES, and so independent from its depth. Also, our main explanatory variable for the environment, the wind speed, is assumed to be a uniformly distributed surface sound source, with an underwater propagation that is at near-vertical angle, as for most geophysical sound sources (wind/rain/drizzle). Refraction by the sound speed profile of the associated acoustic energy is then negligible, and is consequently independent of depth if absorption is neglected. In our data, absorption effects were not significant in comparison to the other explanatory variables of SES speed and wind speed. This property of depth independence has also been studied by Barclay and Buckingham (2013), validating experimentally Cron and Sherman's (1962) theory that predicts a constant (vertical) directional density function for wind-driven sources.

Our results from the marine soundscape part will be the focus now. To capture a marine soundscape, a full noncorrupted measured spectrum (typically from 10 to 10000 Hz) is needed. According to our correlation analysis, the most corrupted frequency bands are below 1 kHz, with major contributions from V. This ensures us that for low V values, corruption from nonenvironmental sources should be canceled out for these SPL responses. Following this idea, we performed a measure of our marine soundscape using only on the 5th percentile values of the SES speed and acceleration (see Fig. 4), referring to these dives as extreme drifts, when the SES is very slow. These V values range from 0.2 to 0.6 m s^{-1} and induce variations strictly inferior to 5 dB in the SPL(0.05) (from Fig. 5), which are negligible regarding SPL variations in the same frequency band from classical acoustic sources present in a marine soundscape [e.g., Tsang-Hin-Sun et al. (2015) reported, for the same geographical area, daily variations in the sound pressure level in the order of 20 dB at 10 Hz and 15 dB at 50 Hz, which are associated with tectonic and shipping noise, respectively]. The spectrum shape obtained during these drift phases is quite similar from standard deep-ocean ambient noise spectra. The deep-water Atlantic curve falls off rapidly from its highest level at 50 Hz at a rate of about −8 dB per octave. It is flat from 200 to 400 Hz and then assumes a slope of −4 dB to 1000 Hz (Perrone 1969; Marshall 2005). Our spectrum shape can also be well approximated by the standard Knudsen–Alford–Emling curves, which are straight lines of constant negative slope of 5 dB per octave over the full frequency range (Knudsen et al. 1948). Considering the median levels of our averaged spectrum, in the Kerguelen Islands region, they were the same order of magnitude as those recently reported in the Indian Ocean by Tsang-Hin-Sun et al. (2015). For example, our SPLs ranged generally from 65 to 75 dB ref 1 μPa^2 Hz^{-1} in the frequency band [50–100] Hz, whereas levels across the sites studied in Tsang-Hin-Sun et al. (2015) have been reported to be 75–85 dB ref and 65–70 dB ref 1 μPa^2 Hz^{-1} (with the hydrophone WKER1, moored at 500 m below the sea surface) at 50 and 100 Hz, respectively. These levels are quite coherent with a measure done above the sound fixing and ranging (SOFAR) channel.

Regarding the measurement of wind speed, studies in acoustical meteorology (Vagle et al. 1990; Nystuen and Selsor 1997; Ma and Nystuen 2005; Pensieri et al. 2015) have shown that surface wind speed impacts the linearly ocean ambient noise level in such a way that relatively simple computational approaches (typically a constant threshold set to a one-third octave subband-averaged SPL) are sufficient to predict wind speed from underwater acoustics. Selecting the proper frequency bands is often the critical issue in such studies. It is known that SPL spectra associated with wind result from resonant acoustic radiation from bubbles generated by breaking waves (Medwin and Beaky 1989). The population size distribution of the bubbles defines the shape of the SPL spectra, and this shape of distribution is invariant with wind speed. However, as wind speed increases, the total bubble concentration increases because the fractional area coverage of breaking waves increases. The increase in bubble concentration leads to a concomitant increase in the SPL across all frequencies. This uniform increase as a function of frequency allows the SPL at a single frequency to be used to estimate wind speed. For example, the wind speed algorithm Wind Observations Through Ambient Noise (WOTAN) from Vagle et al. (1990) is based on the SPL at 8 kHz. More recently, Cauchy et al. (2015) applied the WOTAN algorithm to acoustic passive recordings from an underwater glider, with an error of 2 m s^{-1} in wind speed estimates. In this paper, we first observed a uniform increase of sound levels with an increasing wind speed over a range of approximately 15 dB (from Fig. 7) that was observed in other studies for similar wind speed values (e.g., Pensieri et al. 2015). We also tested the use of different regression models to predict the wind speed from the acoustic descriptors detailed in Table 4. Our simplest model consists of a linear regression using the acoustic feature SPL(4) as predictor, in a very similar way as the WOTAN algorithm. The classification performance of this simple model was satisfactory, with an accuracy of 2.1 m s^{-1} that validates the possibility of predicting wind speed from our spectra using similar methods as those found in literature (although the 8-kHz sample frequency could not be used in our study due to

technological limitations). Our numerical experiments also tested more complex models, such as a multiple linear regression model, using PCA-based acoustic features as predictors and a multiple nonlinear regression model. Using a higher number of acoustic predictors and nonlinear fitting models did not induce significant performance enhancement, leading to the conclusion that the SES passive acoustic recordings do not increase the processing complexity in the task of extracting wind speed information from a measured spectra.

Another interesting finding of our study is that wind speed estimation can be performed quite independently of SES diving behavior. Indeed, the error estimations between the drift and active swimming phases do not show discrepancies statistically significant, with average errors of $\varepsilon_{ws} = 1.9 \pm 0.2\,\mathrm{m\,s^{-1}}$ and $\varepsilon_{ws} = 2.7 \pm 0.3\,\mathrm{m\,s^{-1}}$ for the multilinear regression model. This result can be explained as follows. Noise spectra for hydrophones in the deep ocean show little dependence on wind at frequencies below 400 Hz (Piggott 1964). Most "meteo bands" used in studies are between 2 and 10 kHz, which fit well with the frequency subbands identified in our study to extract wind speeds. This result shows great promise in using SES as an acoustic glider for wind speed estimation. Because so few passive drift dives are performed daily (Dragon et al. 2012), wind speed measures would become difficult to assess at a fine temporal scale using only these dives. In contrast, our ability to measure wind speed accurately over all dive phases provides a high-frequency time series, with SES performing approximately 60–70 dives daily (Dragon et al. 2012).

5. Conclusions

Measuring and interpreting marine soundscape require passive acoustic recordings that are free from nonenvironmental noise. This current study explored the possibility of measuring soundscape with recordings from biologged southern elephant seals (SES). This technological approach offers valuable advantages, such as a high temporal resolution in acoustic measurements (in comparison to satellite-based measures). Also, SES allow the exploration of regions that are inaccessible to other technologies (e.g., underwater gliders). Indeed, the strong east–west current speeds and the rough sea state in the Southern Ocean make the use of regular gliders very complicated, while these harsh environmental conditions are not a problem for SES.

In this study, a multivariate multiple linear regression framework was essentially used to discriminate the acoustic contributions between the processes related to SES and the ocean environment. Our results showed that with passive acoustic recordings from a tagged free-ranging SES, minimal sound corruption from the SES could be obtained during extreme drift phases, allowing for the analysis of marine soundscape. Also, in frequency bands higher than 2.5 kHz, wind speed could be estimated using simple classification approaches (such as linear regression models), independently from the SES biological processes.

Future studies should use a more complete recording dataset, including additional environmental (e.g., rain, current, aquatic seisms), anthropological (e.g., ship traffic), and biological (e.g., whale vocalizations) variables that were not significantly present in our current dataset. This will be needed to fully validate our system as an operational measuring system to measure marine soundscape and to explain its characteristics with a full set of acoustic sources. Also, the ability to associate mobile acoustic data with estimates of surface weather conditions allows for a novel approach to studying air–sea interactions, which will need to be tested at a larger scale, that is, using different types of mobile platforms (e.g., gliders, profiling floats), in different ocean environments.

Acknowledgments. The authors are indebted to several researchers of the CEBC (Chizé, France), in particular Gaetan Richard, for assistance in sample preparation, data collection, processing algorithms, as well as numerous exchanges on SES biology. This study was conducted as part of the Institut Polaire program 109 (ecology of seabirds and marine mammals, P. I. H. Weimerskirch). The authors also would like to thank the Direction Générale de l'Armement (DGA, France) for supporting this work, the Fondation Total for funding the Acousonde as part of the Sea Bio-Sound project, the CNES-TOSCA, and the French Polar Institute for logistical and financial support, as well as all the Kerguelen fieldworkers for collecting data.

APPENDIX A

Influence of Depth on the Acoustic Features

Figure A1 shows the effect of depth on the SPL descriptors. We computed the differences between the SPLs above 100 m and at successive depths down to 800 m, averaged over 200 descending dives of the SES. We made the assumption that during the duration of these dives, the ocean ambient noise does not vary significantly. We can observe that the two lowest-frequency SPLs, SPL(0.05) and SPL(0.5), vary accordingly with the SES swimming speed V (represented by the black dashed curve) rather

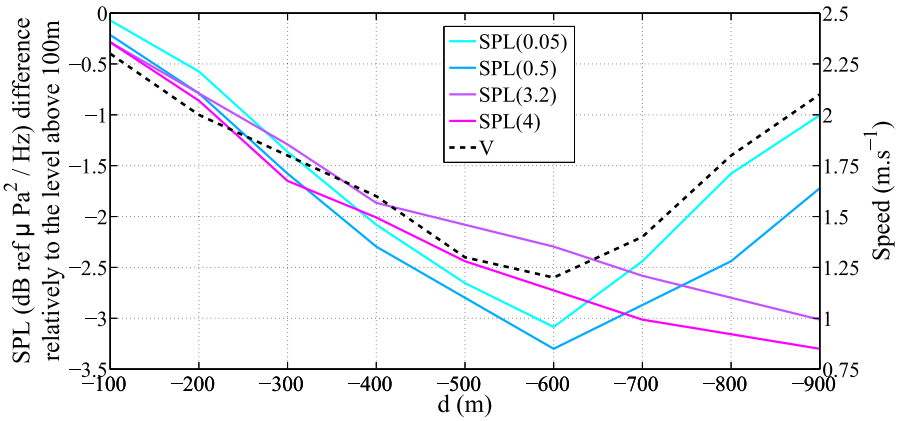

FIG. A1. Effects of depth on the SPL descriptors. The SES speed has also been superimposed onto these curves. Median values have been computed every 100 m in depth d.

than with depth, and remain nearly parallel from one depth measure point to another. On the contrary, the two highest-frequency SPLs, SPL(3.2) and SPL(4), have a lower decreasing rate that seems to be more decorrelated to V and could traduce some attenuation effects due to absorption or geometrical dispersion. Overall, depth induces some minor acoustic modifications that remain globally inferior to 2 dB above 500 m.

APPENDIX B

Pairwise Correlation and Scattering Plot of Variables

The pairwise correlation between the acoustic, SES, and environmental features was performed using standardized values. Resulting correlation coefficients are provided in Fig. B1 along with scattering plots. Strong

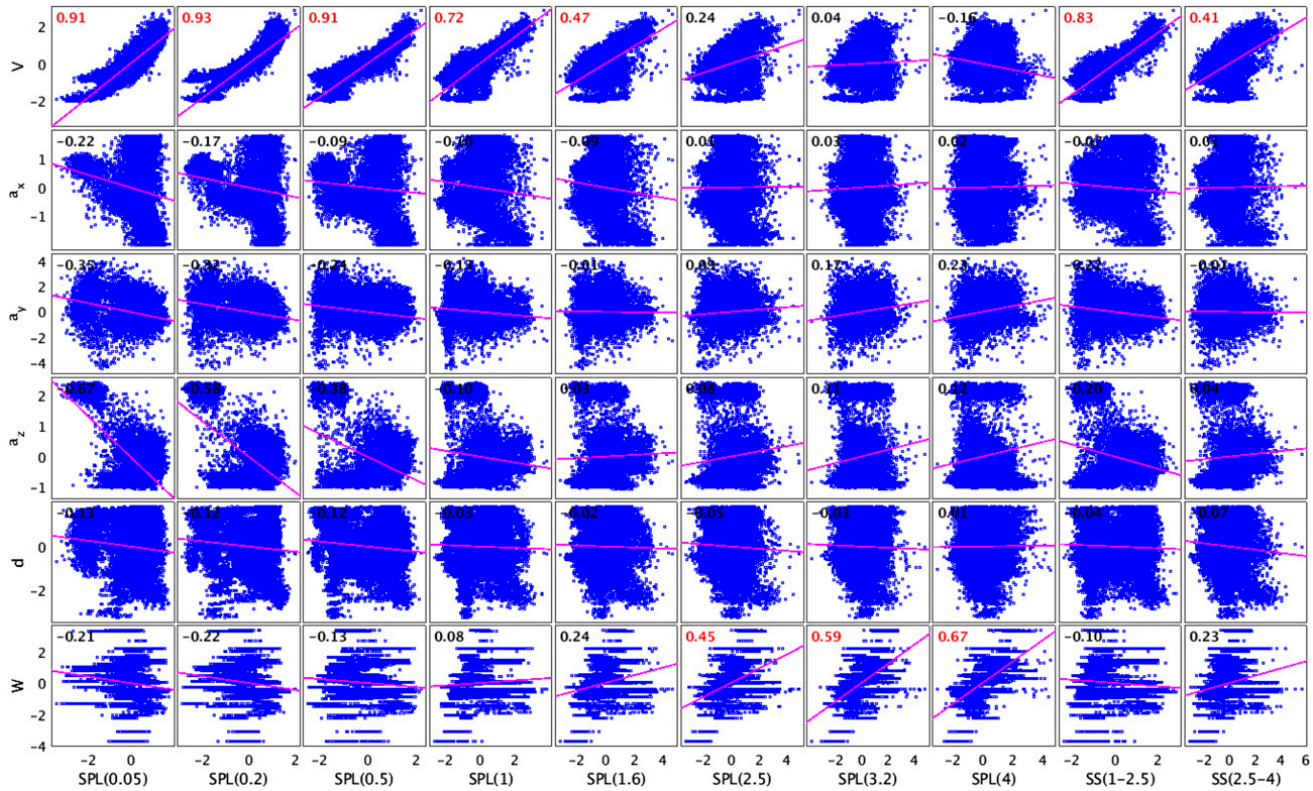

FIG. B1. Scattering plots and pairwise correlations between acoustic variables and SES and environment variables, using standardized values. Pearson correlation coefficients higher than 0.4, and with a P value below 0.001 (red).

correlation relations appear between specific parameters, such as SES speed with SPL(0.05), SPL(0.2), and SPL(0.5) ($r > 0.9$, $P < 0.001$), and wind speed with SPL(3.7) and SPL(4) (r of 0.59 and 0.67 with $P < 0.001$, respectively). Other variables, such as SES depth and acceleration, did not show significant correlation with any acoustic features, with coefficients remaining below 0.2 ($P < 0.001$). An analysis of pairwise correlations between SES and environment variables also informed us that they were relatively low ($r < 0.2$, with an average P value < 0.001). Also, we can observe that globally SPL descriptors explain better data variability than SS descriptors.

REFERENCES

Aguzzi, J., and Coauthors, 2011: The new seafloor observatory (OBSEA) for remote and long-term coastal ecosystem monitoring. *Sensors*, **11**, 5850–5872, doi:10.3390/s110605850.

Aoki, K., and Coauthors, 2011: Northern elephant seals adjust gliding and stroking patterns with changes in buoyancy: Validation of at-sea metrics of body density. *J. Exp. Biol.*, **214**, 2973–2987, doi:10.1242/jeb.055137.

Bailleul, F., M. Authier, S. Ducatez, F. Roquet, J. B. Charrassin, Y. Cherel, and C. Guinet, 2010: Looking at the unseen: Combining animal bio-logging and stable isotopes to reveal a shift in the ecological niche of a deep-diving predator. *Ecography*, **33**, 709–719, doi:10.1111/j.1600-0587.2009.06034.x.

Barclay, D. R., and M. J. Buckingham, 2013: Depth dependence of wind-driven, broadband ambient noise in the Philippine Sea. *J. Acoust. Soc. Amer.*, **133**, 62–71, doi:10.1121/1.4768885.

Baumgartner, M. F., S. M. Van Parijs, F. W. Wenzel, C. J. Tremblay, H. C. Esch, and A. M. Warde, 2008: Low frequency vocalizations attributed to sei whales (*Balaenoptera borealis*). *J. Acoust. Soc. Amer.*, **124**, 1339–1349, doi:10.1121/1.2945155.

Bentamy, A., and D. Croize-Fillon, 2012: Gridded surface wind fields from Metop/ASCAT measurements. *Int. J. Remote Sens.*, **33**, 1729–1754, doi:10.1080/01431161.2011.600348.

——, and ——, 2015: Daily ASCAT surface wind fields. IFREMER Tech. Rep., 15 pp.

Breiman, L., and J. H. Friedman, 1997: Predicting multivariate responses in multiple linear regression. *J. Roy. Stat. Soc.*, **59B**, 3–54, doi:10.1111/1467-9868.00054.

Burgess, W. C., 2000: The bioacoustic probe: A general-purpose acoustic recording tag. *J. Acoust. Soc. Amer.*, **108**, 2583–2583, doi:10.1121/1.4743598.

——, P. Tyack, B. Le Boeuf, and D. P. Costa, 1998: A programmable acoustic recording tag and first results from free-ranging northern elephant seals. *Deep-Sea Res. II*, **45**, 1327–1351, doi:10.1016/S0967-0645(98)00032-0.

Cauchy, P., T. Pierre, L. Mortier, and B. Marie-Noelle, 2015: Passive acoustics embedded on gliders—Weather observation through ambient noise. *Proc. Third Underwater Acoustics Conf. and Exhibition (UACE2015)*, Platanias, Crete, Greece, European Acoustics Association, 565–570.

Chapman, N. R., and A. Price, 2011: Low frequency deep ocean ambient noise trend in the Northeast Pacific Ocean. *J. Acoust. Soc. Amer.*, **129**, EL161, doi:10.1121/1.3567084.

Charrassin, J. B., and Coauthors, 2008: Southern Ocean frontal structure and sea-ice formation rates revealed by elephant seals. *Proc. Natl. Acad. Sci. USA*, **105**, 11 634–11 639, doi:10.1073/pnas.0800790105.

Costa, D. P., J. M. Klinck, E. E. Hofmann, M. S. Dinniman, and J. M. Burns, 2008: Upper ocean variability in west Antarctic Peninsula continental shelf waters as measured using instrumented seals. *Deep-Sea Res. II*, **55**, 323–337, doi:10.1016/j.dsr2.2007.11.003.

Cron, B. F., and C. H. Sherman, 1962: Spatial-correlation functions for various noise models. *J. Acoust. Soc. Amer.*, **34**, 1732–1736, doi:10.1121/1.1909110.

Dragon, A.-C., A. Bar-Hen, P. Monestiez, and C. Guinet, 2012: Horizontal and vertical movements as predictors of foraging success in a marine predator. *Mar. Ecol. Prog. Ser.*, **447**, 243–257, doi:10.3354/meps09498.

Duennebier, F. K., and Coauthors, 2002: HUGO: The Hawaii Undersea Geo-Observatory. *IEEE J. Oceanic Eng.*, **27**, 218–227, doi:10.1109/JOE.2002.1002476.

Favali, P., 2013: NEMO-SN1 abyssal cabled observatory in the Western Ionian Sea. *IEEE J. Oceanic Eng.*, **38**, 358–374, doi:10.1109/JOE.2012.2224536.

Genin, A., G. Richard, J. Jouma'a, B. Picard, N. El Ksabi, J. Vacquié-Garcia, and C. Guinet, 2015: Characterization of postdive recovery using sound recordings and its relationship to dive duration, exertion and foraging effort of southern elephant seals (*Mirounga leonina*). *Mar. Mammal Sci.*, **31**, 1452–1470, doi:10.1111/mms.12235.

Glowacki, O., G. B. Deane, M. Moskalik, Ph. Blondel, J. Tegowski, and M. Blaszczyk, 2015: Underwater acoustic signatures of glacier calving. *Geophys. Res. Lett.*, **42**, 804–812, doi:10.1002/2014GL062859.

Guinet, C., and Coauthors, 2013: Calibration procedures and first dataset of Southern Ocean chlorophyll *a* profiles collected by elephant seals equipped with a newly developed CTD-fluorescence tags. *Earth Syst. Sci. Data*, **5**, 15–29, doi:10.5194/essd-5-15-2013.

——, and Coauthors, 2014: Southern elephant seal foraging success in relation to temperature and light conditions: Insight into prey distribution. *Mar. Ecol. Prog. Ser.*, **499**, 285–301, doi:10.3354/meps10660.

Hawkins, R., J. Miksis-Olds, D. L. Bradley, and C. Smith, 2014: Periodicity in ambient noise and variation based on different temporal units of analysis. *Proc. Meet. Acoust.*, **17**, 070035, doi:10.1121/1.4772729.

Johnson, M., and P. Tyack, 2003: A digital acoustic recording tag for measuring the response of wild marine mammals to sound. *IEEE J. Oceanic Eng.*, **28**, 3–12, doi:10.1109/JOE.2002.808212.

Klinck, H., and Coauthors, 2012: Correction: Near-real-time acoustic monitoring of beaked whales and other cetaceans using a Seaglider. *PLoS One*, **7**, 1–8, doi:10.1371/annotation/57ad0b82-87c4-472d-b90b-b9c6f84947f8.

Knudsen, V., R. Alford, and J. Emling, 1948: Underwater ambient noise. *J. Mar. Res.*, **7**, 410–429.

Küsel, E. T., D. K. Mellinger, L. Thomas, T. A. Marques, D. Moretti, and J. Ward, 2011: Cetacean population density estimation from single fixed sensors using passive acoustics. *J. Acoust. Soc. Amer.*, **129**, 3610–3622, doi:10.1121/1.3583504.

Ma, B. B., and J. A. Nystuen, 2005: Passive acoustic detection and measurement of rainfall at sea. *J. Atmos. Oceanic Technol.*, **22**, 1225–1248, doi:10.1175/JTECH1773.1.

Marshall, S., 2005: Depth dependence of ambient noise. *IEEE J. Oceanic Eng.*, **30**, 275–281, doi:10.1109/JOE.2005.850876.

Matsumoto, H., J. H. Haxel, R. P. Dziak, D. Bohnenstiehl, and R. W. Embley, 2011: Mapping the sound field of an erupting

submarine volcano using an acoustic glider. *J. Acoust. Soc. Amer.*, **129**, EL94, doi:10.1121/1.3547720.

——, D. R. Bohnenstiehl, J. Tournadre, R. P. Dziak, J. H. Haxel, T.-K. A. Lau, M. J. Fowler, and S. A. Salo, 2014: Antarctic icebergs: A significant natural ocean sound source in the Southern Hemisphere. *Geochem. Geophys. Geosyst.*, **15**, 3448–3458, doi:10.1002/2014GC005454.

Medwin, H., and M. M. Beaky, 1989: Bubble sources of the Knudsen sea noise spectra. *J. Acoust. Soc. Amer.*, **86**, 1124–1130, doi:10.1121/1.398104.

Miksis-Olds, J. L., D. L. Bradley, and X. M. Niu, 2013: Decadal trends in Indian Ocean ambient sound. *J. Acoust. Soc. Amer.*, **134**, 3464–3475, doi:10.1121/1.4821537.

Miller, P. J. O., M. P. Johnson, P. L. Tyack, and E. A. Terray, 2004: Swimming gaits, passive drag and buoyancy of diving sperm whales *Physeter macrocephalus*. *J. Exp. Biol.*, **207**, 1953–1967, doi:10.1242/jeb.00993.

Mitani, Y., R. D. Andrews, K. Sato, A. Kato, Y. Naito, and D. P. Costa, 2010: Three-dimensional resting behaviour of northern elephant seals: Drifting like a falling leaf. *Biol. Lett.*, **6**, 163–166, doi:10.1098/rsbl.2009.0719.

Nair, N. R., N. Elizabeth Shani, R. Raju, and S. Satheeshkumar, 2015: Underwater ambient noise variability from satellite data—An Indian Ocean perspective. *2015 IEEE Underwater Technology (UT)*, 4 pp., doi:10.1109/UT.2015.7108285.

Nieukirk, S. L., K. M. Stafford, D. K. Mellinger, R. P. Dziak, and C. G. Fox, 2004: Low-frequency whale and seismic airgun sounds recorded in the mid-Atlantic Ocean. *J. Acoust. Soc. Amer.*, **115**, 1832–1843, doi:10.1121/1.1675816.

Nystuen, J. A., and H. D. Selsor, 1997: Weather classification using passive acoustic drifters. *J. Atmos. Oceanic Technol.*, **14**, 656–666, doi:10.1175/1520-0426(1997)014<0656:WCUPAD>2.0.CO;2.

——, M. A. Anagnostou, E. M. Anagnostou, and A. Papadopoulos, 2015: Monitoring Greek seas using passive underwater acoustics. *J. Atmos. Oceanic Technol.*, **32**, 334–349, doi:10.1175/JTECH-D-13-00264.1.

Pensieri, S., R. Bozzano, M. Anagnostou, E. Anagnostou, R. Bechini, and J. Nystuen, 2013: Monitoring the oceanic environment through passive underwater acoustics. *2013 MTS/IEEE OCEANS—Bergen*, 10 pp., doi:10.1109/OCEANS-Bergen.2013.6607995.

——, ——, J. A. Nystuen, E. N. Anagnostou, M. N. Anagnostou, and R. Bechini, 2015: Underwater acoustic measurements to estimate wind and rainfall in the Mediterranean Sea. *Adv. Meteor.*, **2015**, 612512, doi:10.1155/2015/612512.

Perrone, A. J., 1969: Deep-ocean ambient-noise spectra in the northwest Atlantic. *J. Acoust. Soc. Amer.*, **46**, 762, doi:10.1121/1.1911759.

Piggott, C. L., 1964: Ambient sea noise at low frequencies in shallow water of the Scotian Shelf. *J. Acoust. Soc. Amer.*, **36**, 2152, doi:10.1121/1.1919337.

Rahmati, M., P. Pandey, and D. Pompili, 2014: Separation and classification of underwater acoustic sources. *2014 Underwater Communications and Networking*, Sestri Levante, Italy, CMRE, doi:10.1109/UComms.2014.7017145.

Richard, G., J. Vacquié-Garcia, J. Jouma'a, B. Picard, A. Génin, J. P. Y. Arnould, F. Bailleul, and C. Guinet, 2014: Variation in body condition during the post-moult foraging trip of southern elephant seals and its consequences on diving behaviour. *J. Exp. Biol.*, **217**, 2609–2619, doi:10.1242/jeb.088542.

Rogers, E. O., J. G. Genderson, W. S. Smith, G. F. Denny, and P. J. Farely, 2004: Underwater acoustic glider. *2004 IEEE International Geoscience and Remote Sensing Symposium Proceedings*, Vol. 3, IEEE, 2241–2244, doi:10.1109/IGARSS.2004.1370808.

Ropert-Coudert, Y., and R. P. Wilson, 2005: Trends and perspectives in animal-attached remote sensing. *Front. Ecol. Environ.*, **3**, 437–444, doi:10.1890/1540-9295(2005)003[0437:TAPIAR]2.0.CO;2.

Roquet, F., Y.-H. Park, C. Guinet, F. Bailleul, and J.-B. Charrassin, 2009: Observations of the Fawn Trough Current over the Kerguelen Plateau from instrumented elephant seals. *J. Mar. Syst.*, **78**, 377–393, doi:10.1016/j.jmarsys.2008.11.017.

Rudnick, D. L., R. E. Davis, C. C. Eriksen, D. M. Fratantoni, and M. J. Perry, 2004: Underwater gliders for ocean research. *Mar. Technol. Soc. J.*, **34**, 73–84, doi:10.4031/002533204787522703.

Sato, K., Y. Mitani, M. F. Cameron, D. B. Siniff, and Y. Naito, 2003: Factors affecting stroking patterns and body angle in diving Weddell seals under natural conditions. *J. Exp. Biol.*, **206**, 1461–1470, doi:10.1242/jeb.00265.

Sirovic, A., S. M. Wiggins, and E. M. Oleson, 2013: Ocean noise in the tropical and subtropical Pacific Ocean. *J. Acoust. Soc. Amer.*, **134**, 2681–2689, doi:10.1121/1.4820884.

Tennekes, H., and J. L. Lumley, 1972: *A First Course in Turbulence*. MIT Press, 300 pp.

Tournadre, J., 2014: Anthropogenic pressure on the open ocean: The growth of ship traffic revealed by altimeter data analysis. *Geophys. Res. Lett.*, **41**, 7924–7932, doi:10.1002/2014GL061786.

Tsang-Hin-Sun, E., J.-Y. Royer, and E. C. Leroy, 2015: Low-frequency sound level in the southern Indian Ocean. *J. Acoust. Soc. Amer.*, **138**, 3439–3446, doi:10.1121/1.4936855.

Urick, R., 1971: Noise of melting icebergs. *J. Acoust. Soc. Amer.*, **50**, 337–341, doi:10.1121/1.1912637.

Vacquié-Garcia, J., F. Royer, A.-C. Dragon, M. Viviant, F. Bailleul, and C. Guinet, 2012: Foraging in the darkness of the Southern Ocean: Influence of bioluminescence on a deep diving predator. *PLoS One*, **8**, e43565, doi:10.1371/journal.pone.0043565.

Vagle, S., W. G. Large, and D. M. Farmer, 1990: An evaluation of the WOTAN technique for inferring oceanic wind from underwater sound. *J. Atmos. Oceanic Technol.*, **7**, 576–595, doi:10.1175/1520-0426(1990)007<0576:AEOTWT>2.0.CO;2.

Van Dyke, M., 1982: *An Album of Fluid Motion*. 14th ed. Parabolic Press, 176 pp.

Wagstaff, R., 2005: An ambient noise model for the northeast Pacific Ocean basin. *IEEE J. Oceanic Eng.*, **30**, 286–294, doi:10.1109/JOE.2004.836993.

Ward, J., and Coauthors, 2011: Beaked whale (*Mesoplodaon densirostris*) passive acoustic detection in increasing ambient noise. *J. Acoust. Soc. Amer.*, **129**, 662–669, doi:10.1121/1.3531844.

Wenz, G. M., 1962: Acoustic ambient noise in the ocean: Spectra and sources. *J. Acoust. Soc. Amer.*, **34**, 1936–1956, doi:10.1121/1.1909155.

Zhang, Z., J. Neubauer, and D. A. Berry, 2006: Aerodynamically and acoustically driven modes of vibration in a physical model of the vocal folds. *J. Acoust. Soc. Amer.*, **120**, 2841–2849, doi:10.1121/1.2354025.

ANNEXE D

How elephant seals (*Mirounga leonina*) adjust their fine scale horizontal movement and diving behaviour in relation to local prey encounter rate

Yves, Le Bras, Jouma'a, Joffrey, Picard, Baptiste & Guinet Christophe, How elephant seals (*Mirounga leonina*) adjust their fine scale horizontal movement and diving behaviour in relation to local prey encounter rate. *PLoS One* (in review)

PLOS ONE

RESEARCH ARTICLE

How Elephant Seals (*Mirounga leonina*) Adjust Their Fine Scale Horizontal Movement and Diving Behaviour in Relation to Prey Encounter Rate

Yves Le Bras*, Joffrey Jouma'a, Baptiste Picard, Christophe Guinet

Centre d'Etude Biologiques de Chizé, UMR, CNRS-ULR, France

* yves.lebras@cebc.cnrs.fr

OPEN ACCESS

Citation: Le Bras Y, Jouma'a J, Picard B, Guinet C (2016) How Elephant Seals (*Mirounga leonina*) Adjust Their Fine Scale Horizontal Movement and Diving Behaviour in Relation to Prey Encounter Rate. PLoS ONE 11(12): e0167226. doi:10.1371/journal.pone.0167226

Editor: Jan M Hemmi, University of Western Australia, AUSTRALIA

Received: May 12, 2016

Accepted: November 10, 2016

Published: December 14, 2016

Data Availability Statement: Data has been deposited on a Figshare repository entitled "Southern Elephant Seal: dive statistics" (doi: 10.6084/m9.figshare.4233458).

Funding: This work was supported by: http://www.poitou-charentes.fr/accueil.html; http://www.deux-sevres.com/deux-sevres/default.aspx; http://www.agence-nationale-recherche.fr/?Project=ANR-11-BSV7-0022; http://www.agence-nationale-recherche.fr/?Projet=ANR-07-VULN-0005; http://www.fondation.total.com/; https://cnes.fr/fr.

Abstract

Understanding the diving behaviour of diving predators in relation to concomitant prey distribution could have major practical applications in conservation biology by allowing the assessment of how changes in fine scale prey distribution impact foraging efficiency and ultimately population dynamics. The southern elephant seal (*Mirounga leonina*, hereafter SES), the largest phocid, is a major predator of the southern ocean feeding on myctophids and cephalopods. Because of its large size it can carry bio-loggers with minimal disturbance. Moreover, it has great diving abilities and a wide foraging habitat. Thus, the SES is a well suited model species to study predator diving behaviour and the distribution of ecologically important prey species in the Southern Ocean. In this study, we examined how SESs adjust their diving behaviour and horizontal movements in response to fine scale prey encounter densities using high resolution accelerometers, magnetometers, pressure sensors and GPS loggers. When high prey encounter rates were encountered, animals responded by (1) diving and returning to the surface with steeper angles, reducing the duration of transit dive phases (thus improving dive efficiency), and (2) exhibiting more horizontally and vertically sinuous bottom phases. In these cases, the distance travelled horizontally at the surface was reduced. This behaviour is likely to counteract horizontal displacement from water currents, as they try to remain within favourable prey patches. The prey encounter rate at the bottom of dives decreased with increasing diving depth, suggesting a combined effect of decreased accessibility and prey density with increasing depth. Prey encounter rate also decreased when the bottom phases of dives were spread across larger vertical extents of the water column. This result suggests that the vertical aggregation of prey can regulate prey density, and as a consequence impact the foraging success of SESs. To our knowledge, this is one of only a handful of studies showing how the vertical distributions and structure of prey fields influence the prey encounter rates of a diving predator.

Competing Interests: The authors have declared that no competing interests exist.

Introduction

Foraging behaviour and more specifically, foraging success, is critical to the growth, reproduction and survival of animals and is therefore subject to natural selection [1]. As a result, foraging behaviour is expected to be optimized so that net energy gains are maximized for a given level of time and energy spent foraging [2–4]. While foraging at sea, diving predators are central place foragers from the ocean's surface, where they need to come back to breathe between dives required to reach their prey at depth [5,6]. Under such constraints, the efficient diving behaviour of a predator is presumably the key to the optimization of their energy balance.

As the movements of free-ranging animals reflect how they interact with their physical and biological environment, spatial patterns in their trajectories provide a basis from which to understand foraging behaviour as well as gain insights on prey distribution and accessibility [6,7]. Recent technological advances in miniaturised electronic devices have enabled the detection of foraging events and the description of diving behaviour over very fine scales. Indeed, tri-axial jaw-mounted [8–10] or head-mounted [11,12] accelerometers has been successfully used to detect Prey Encounter Events (PEE hereafter) in several diving species of pinniped. Pitch angle, derived from three-dimensional acceleration data, provides spatial information on the vertical movements which cannot be obtained from time-depth dive profiles. As such, pitch angle can be helpful in addition to dive profiles for interpreting the diving behaviour of diving predators [13,14]. Three-dimensional magnetometry allows the computation of heading angle which, similarly to pitch angle according to vertical movement, complements time-depth data with information on horizontal movements. In this study, the spatial information obtained from pressure, accelerometer and magnetometer data are used to quantitatively assess how changes in vertical and horizontal diving behaviours relate to prey encounter rate.

Without acceleration data, accurate feeding indices are often difficult to obtain. A large number of studies use changes in surface GPS track patterns [15–18] or diving behaviour [19–22] as foraging indices. In various predator species, resource acquisition has been linked to a type of behaviour called area-restricted search (ARS) [23]. In a patchy environment, such as the open ocean, an animal will intensify its foraging in response to an increase in prey density [17]. Therefore, ARS is characterized by a decrease in displacement speed and an increase in track sinuosity in areas of putative prey aggregation [23,24].

Similarly, according to the vertical dimension, diving seabirds, marine mammals and leatherback turtles are expected to adjust their diving behaviour according to the quality and depth of the targeted prey patch [25–27]. A number of species, such as penguins and pinnipeds, perform behavioural adjustments in relation to prey density, such that they modulate the duration of the bottom phase of a dive [28–31]. The bottom phase of a dive has been validated as the time when most feeding occurs in several species including Antarctic fur seals (*Arctocephalus gazella*) [32,33], northern elephant seals (*Mirounga angustirostris*) [34], grey seals (*Halichoerus grypus*) [35], Magellanic penguins (*Spheniscus magellanicus*) [36], Weddell seals (*Leptonychotes weddellii*) [37] and leatherback turtles (*Dermochelys coriacea*) [38]. King penguins and macaroni penguins perform behavioural adjustments during the descent and ascent phases of their dives in relation to prey encounter rates during the previous dive [39,40], as predicted by Thompson and Fedak ([25]). Similarly, elephant seals increase their dive angles on putative foraging dives [14,41]. These adjustments take place mainly through changes in body angle, rather than through a change in swimming speed [40,42,43]. However, there is a lack of studies investigating quantitatively the mechanisms explaining how changes in diving behaviour (such as pitch angle adjustments during descent and ascent phases or pitch and heading variability during bottom phase) in response to prey encounter rate may impact the horizontal speed of the animal track at surface. Indeed, in most studies relating dive behaviour to

horizontal speed measured from surface locations, no acceleration data were available and analyses were conducted on pressure-only dive metrics.

Living in the Southern Ocean, female Southern Elephants Seals (SES hereafter) with their large size and their great diving abilities are well suited for studying foraging behaviour, as using bio-logging tools causes minimal disturbance. SES spend 10 months a year at sea, covering thousands of kilometres during foraging trips and 90% of which is spend diving [44]. An average dive lasts between 20 and 30 minutes, at a depth ranging generally between 300–500 m, punctuated by surface periods of 2–3 minutes [45]. As for many diving predators, SES forage mostly at the bottom of their dives [6,11,46].

Female SES feed mainly on myctophids and cephalopods [47], both ecologically important groups of species within the Southern Ocean [48–51]. Because of its overall abundance and individual body mass, the SES is a major consumer of Southern Ocean marine resources [52,53]. As such, understanding better the foraging behaviour of data rich species such as SES [54] could provide valuable insight toward the biology and distribution of these important groups of species which are otherwise difficult to sample [55]. Prey abundance and density within the water column are likely to be key factors in the foraging success of these predators. As such, understanding the diving behaviour of SES in response to prey density could help to predict how changes in prey distribution may impact predator populations.

In this study, we examine (1) how diving behavior relates to prey encounter rates during the bottom phase of a dive, (2) the repercussions of these relationships on the travel transit rate of SESs and (3) their diving efficiency.

- To achieve (1), we used two metrics of diving behaviour describing (i) the vertical location of foraging activity through the water column (such as the depth of the bottom phase and its vertical extent through the water column) and (ii) fine-scale indicators of active foraging search (such as directional changes in pitch and heading angles). Then, we addressed a series of two sub-objectives. First, quantitatively measure the behavioural response of SES to changes in a proxy of prey density (prey encounter rate). Second, assess how this proxy relates to the vertical foraging location in the water column for a given level of active foraging search as it could help to predict how prey distribution may impact SES population in the future.
- Horizontal speed, measured using GPS locations at the surface, with the track sinuosity, is one of the main metrics used in state-space models to infer intensive foraging behaviour. Therefore objective (2) of the study is to understand, using fine scale information, how the vertical and horizontal diving behaviours related to prey encounter rate mechanistically translate into a change of horizontal speed.
- Our final objective (3) is to better understand the response of SES to the prey encounter rate in terms of foraging strategy, by investigating how adjustments in diving behaviour, and particularly diving angle, benefit diving efficiency, as indicated by the proportion of a dive's total duration dedicated to the bottom phase.

Materials and Methods

Ethic statement

All fieldwork involving SES was approved and authorized by the ethics committee of the French Polar Institute (Institut Paul Emile Victor—IPEV) in May 2008. This Institute does not provide any permit number or approval ID, however animals were handled and cared for in total accordance with the guidelines and recommendations of this committee (dirpol@ipev.fr).

Animal handling and electronic devices

During the breeding seasons (October and November) of 2010 through to 2014, a total of 9 female SESs of the Kerguelen Islands (49° 20' S, 70° 20' E) were equipped with (1) a Daily Diary tag (TDR10-DD, Wildlife Computers™, USA) and (2) a location collector device. The location detector device was either a Conductivity-Temperature-Depth satellite-relay data logger (CTD-SRDL, Sea Mammal Research Unit—University of St Andrew), a Time-Temperature-Depth Fastloc GPS data logger (SPLASH10-F, Wildlife Computers™, USA) or a Smart Position or Temperature Transmitting tag (SPOT, Wildlife Computers™, USA). Animals were captured with a canvas head-bag and anesthetized using a 1:1 combination of Tiletamine and Zolazepam (Zoletil 100) injected intravenously [56]. A TDR10-DD was then glued on each seal's back and the location collector devices to the head using quick-setting Araldite (Araldite AW 2101). One individual was equipped with an additional accelerometer on its head. Details about the length and weight of each individual, logger-type deployment details are provided in the Table A in S1 Appendix.

The TDR10-DD logs depth (range = 0 to 2000 m, resolution = 0.5 m, accuracy = 1% of reading value, sampling frequency = 1Hz), temperature (range = -40˚C to +60˚C resolution = 0.05˚C, accuracy = 0.1˚C, sampling frequency = 1 Hz), and light (range = 5.10^{-10} $W.cm^{-2}$ to 5.10^{-2} $W.cm^{-2}$ (8 decades), resolution = 20 units per decade, accuracy = 0.1˚C, sampling frequency = 1 Hz) as well as tri-axial acceleration (range = –2 g to +2 g, resolution = 0.05 $m.s^{-2}$, sampling frequency = 16 Hz), tri-axial magnetometry (direction and strength of local magnetic field vector, range = -100 nTesla to +100 nTesla, resolution = 0.2 nTesla, sampling frequency = 16 Hz), and velocity (as the relative speed of the logger in surrounding water). The velocity sensor did not function correctly because of a build-up of dirt shortly after deployments which obstructed the propeller. Acceleration and magnetometry were measured along the same axes of the logger which were: (1) longitudinal (positive forward), (2) lateral (positive rightward) and (3) vertical (positive downward). TDR10-DD's were positioned so that the logger's X and Y axes approximately match longitudinal and lateral midlines of the SES.

The SPLASH10-F was the other type of data logger used in this study. They provided GPS locations 60% of the times the SES were back at surface to breathe. SPLASH10-F also measures depth, temperature and light (as described for the TDR10-DD) but these data were only used to synchronize with datasets from other loggers when it was necessary (when comparing head and back mounted accelerometers on a same individual, Figure A in Appendix S2). The CTD-SRDL and SPOT tags provided Argos locations (along with salinity and temperature in the case of CTD-SRDLs) that were used to locate the seals and retrieve the tags when they were back on land (but oceanographic data were not in this study).

Acceleration and magnetometry data processing

All data processing was performed using R version 3.1.1 [57]. The majority of acceleration and magnetometry data analyses used in this study were done using the R package "rbl" (unless otherwise stated), available online at [58].

Prey Encounter Events

The detection of Prey Encounter Events (PEE) was performed following Guinet *et al.* ([6]) and Vacquié-Garcia *et al.* ([59]). Dynamic accelerations, resulting from rapid head movements, were extracted from the longitudinal, lateral and vertical axes of the logger using an order 3 high-pass digital Butterworth filter with a normalized cut-off frequency of 2.64 Hz (performed with the signal package [60]). For each axis, a one-second fixed window was used to calculate

the standard deviation. Signals were then processed using a moving standard deviation across a window of five seconds. Finally, a two-mean clustering was performed for each signal to distinguish "high state" from "low state". A PEE occurred when the three axes were simultaneously in "high state" (see [59] for graphical illustration of the method). A continuous succession of "high state" was considered as a single PEE. One individual had both head-mounted and back-mounted accelerometers, so we used these data to check that these two acceleration data resulted in similar results (Pearson's product moment correlation coefficient = 93%, see Figure B in S2 Appendix).

Body posture angles

Pitch and roll describe the body posture of a SES with respect to the direction of the earth gravity vector whilst heading angle is in reference to the earth magnetic vector. Static acceleration is caused by the position of the gravity center of an animal compared with the gravity vector, which is always vertically orientated and can be used to infer pitch and roll angles. Static acceleration was obtained with an order 3 low-pass digital Butterworth filter with a normalized cut-off frequency of 0.20 Hz applied to the three axes as described in Richard *et al.* ([61]). The filtered output was then scaled to a unitary norm (function static_acceleration from the rbl package) so that pitch and roll angles could be computed directly from trigonometry formulas. Pitch and Roll angles were then calculated from this static acceleration, expressed in the North-East-Down (NED) frame of reference, using the pitch and roll functions from the animalTrack package [62]. The low-pass filter used to obtain static acceleration was applied to the magnetic data as well. Heading angle was then calculated (using the tilt_compensate function from the animalTrack package) from the pitch and roll angles alongside the filtered magnetic data expressed in the NED frame of reference.

Swimming effort

The frequency spectrum of the lateral acceleration displayed a clear bimodality (see [63]). The high-frequency peak corresponds to the dynamic acceleration due to tail movements [64,65] which was extracted using an order 3 band-pass (from 0.44 Hz to 1.02 Hz) digital Butterworth filter [61,64–66]. To measure the frequency and magnitude of these tail movements, the absolute value of the resulting signal is then averaged to 1 Hz. We called the latter "swimming effort" and used it as a proxy of the cost of locomotion. This method is implemented in the swimming_effort function of the "rbl" package.

Dive analyses

Dives. We defined dives as periods where animals were continuously deeper than 15 m under the surface. Because there is drift in the pressure readings of the tags over time, a zero offset correction of the depth time sequence was applied prior to the delimitation of dives (function offset_correction from the rbl package). SESs occasionally perform subsurface incursions, which results in a short number of atypical short and shallow dives. Moreover, unpredictable gaps in the time-depth sequence (due to a malfunction of the depth sensor) can sometimes cause different dives to be merged as a single very long one. According to the quantiles of all dive durations, dives lasting less than 8.33 min (500 s, Q1% = 511 s) or more than 32.50 min (1950 s, Q99% = 1947 s) were excluded in order to get rid of these irregular cases.

Dives phases. Each dive was divided into three phases: descent, bottom and ascent phases following Halsey *et al.* ([67]). This method defines the bottom of a dive as the period between the first and the last wiggle or step being deeper than a given depth threshold which is expressed as a percentage of the maximum depth in the dive. Steps and wiggles are time-depth

patterns observed in the bottom of dives. Steps are defined as periods where the vertical velocity slows down but stays above 0 m/s while wiggles as periods where depth increases and then decreases, drawing a concave shape in the dive profile [67]. The upper limits of vertical velocity threshold applied to identify the steps in the time-depth dive profiles was kept to its value for king penguins (0.35 m/s, [67]) as it is close from observed values of non-swimming SES (see histogram of drift rates in [68]). In our datasets the large majority of PEE occurred deeper than 75% of the maximum dive depth (77.24% of all PEE) so this ledge threshold value from Halsey *et al.* ([67]) was kept. This method is implemented in the bottom_delim function of the "rbl" package. We choose this method to delimitate bottom phases of dives instead of the method we previously used in [28] to make sure that bottom phase limits could not fall within a step or a wiggle which would introduce mistakes when counting them. Indeed, by definition, the method developed by Halsey *et al.* ([67]) defines the limits of the bottom at the start and the end of such events.

Dive statistics

A proxy of prey encounter density, PEE rate, was calculated as the total PEE of a bottom phase divided by its total duration in minutes. Our estimate of prey density is thus dependent on SES behavior. The diving behaviours to be used as explanatory variables were divided into two categories: variables related to the area of the water column targeted during the bottom phase and variables related to SES foraging activity, as described below.

Water column area targeted by elephant seals. The median depth at the bottom of dives is a standard variable to describe diving behaviour. During the bottom phase, a SES's focus is expected to be on foraging whilst descent and ascent phases are primarily used for transit to this foraging ground. The median depth of the bottom phase reflects the vertical location of the resources on which the predator decided to forage on. As such, the bottom phase depth is positively related to the amount of time and energy that a SES spends to access their prey at depth. As the objectives of SESs are different in transit and in bottom phase, we focused on the bottom and selected the PEE rate at bottom as an index of the prey encounter density which is independent from the duration of the transit phases. In this study the bottom median depth is used to test whether or not the prey encounter density varies according to depth.

To describe in more detail the vertical location of the bottom phase, "bottom vertical extent" was defined as the depth range between the 10% and 90% depth quantile. Using the quantiles rather than extremes of depth yields a more robust measure of the vertical extent of the water column layer targeted by SES, excluding extreme values from unrealistic bottom phase delineation or atypical diving behaviour (where SES perform a high amplitude wiggle thus exploring a wide depth range but only for very short time).

Foraging activity. The number of wiggles has been used as a proxy of the foraging success for various diving predators (e.g. Northern Elephant Seals and King penguins [20,69]) and are also encountered in the bottom of SES dives. While wiggles are correlated to the number of PEE, the steps rather resemble a gliding pattern (slow ascending or descending vertical speed) and it is not clear yet if this diving pattern is associated with foraging or not. Percentage of the bottom duration during which SES were performing steps and wiggles were included in the analyses as they stand for two distinct diving behaviors describing the foraging activity during the bottom phase.

The mean descent and ascent pitch angle (circular mean, CircStats package [70]), as well as the average descent and ascent swimming effort were computed to account for the transit time adjustments made by the SES in response to the foraging success and to the targeted bottom depth. In a way to assess the amount of directional changes performed by SESs during the

bottom phase of their dives, the circular variance ([69]) of the pitch and heading angles were calculated. The circular variance of the pitch and heading angles provide comparable indices of the sinuosity according to of the vertical (pitch angle) and horizontal (heading angle) dimensions. While pitch variance could be considered redundant with the percentage of time doing wiggles at bottom, it is actually complementary. Indeed for a given quantity of wiggles the greater the pitch variance the steeper they are. Another advantage of this measure over the wiggles is that it is a simple summary statistic of a quantitative variable and does not depend on an algorithm to detect specific events. Hence, it varies continuously, which results in a subtle description of the diving behaviour, and has no detection error issue.

Because our focus is on dives associated with foraging, drift dives, during which SES are resting and/or digesting [71], were removed from the dataset prior to the statistical analysis.

Statistical analysis

We implemented five models (numbered 1a, 1b, 2, 3 and 4) relating to the objectives articulated in the introduction (numbered 1, 2 and 3).

The first objective is to describe the relationships between the PEE rate at the bottom (the response variable) and the diving behaviours during daytime (model 1a) and night-time (model 1b). This allows testing whenever the PEE rate varies according to depth independently of the effect of daily vertical migrations of the SES prey. Namely, the diving behaviours used as explanatory variables in these models are: the median depth at the bottom of dives, the bottom phase vertical extent, the proportion of bottom time spent doing wiggles or steps during the bottom phase, the mean pitch angle in the descent and ascent phases and the variances of pitch and heading angles. We used the number of PEE at the bottom as the response variable of a count model (log link) but actually modelled PEE rate as response by providing the log-transformed bottom duration as an offset variable (the effect of an offset variable is not estimated but forced to one). Poisson family GLMs indicated over-dispersion. We used the Negative Binomial family GLM (MASS package [72]) to address over-dispersion. The inter-individual differences in PEE rate were modelled by specifying the SES identities as fixed effects intercepts.

The second objective is to examine how the horizontal speed at surface during dives–measured from the distance and duration between SES locations taken as they surface before and after dives—relates to the diving behaviours (model 2). To have a reliable estimate of this surface horizontal speed, we used only dives where observed GPS locations preceding and following the dive (39% of dives). This subset introduces a bias toward the selection of dives with longer recovery time that we could not account for (surface periods lasting 127 s for located surfaces but 120 s otherwise, see Table A and Figure B in S3 Appendix for details). We used a Linear Mixed Model (LMM, nlme package [73]) with the horizontal speed at surface as the response variable, and the same diving behaviours used in models 1a and 1b as explanatory variables and an individual as a random intercept.

The third objective is to investigate the effects of diving behaviours on dive efficiency (model 3). Diving efficiency is defined as the bottom phase duration divided by the full dive duration. The proportions typically display more variability around their mean so we used a variable dispersion beta regression model (betareg package [74]) to handle the heteroskedastic nature of this response variable. The diving behaviours used as explanatory variables are the same as in previous models (models 1a, 1b and 2) and the SES identities were specified as fixed effects intercepts.

The last model implemented in this study (model 4) is related to the third objective and aims at clarifying how the transit between surface and the bottom phase location may be

regulated by diving behaviour adjustment. As for model 2, we implemented a LMM. In this model, the response variable is the duration of the phase, and the explanatory variables are the type of phase (ascent or descent), the maximum depth reached during the phase and the average swimming effort during the phase. A random intercepts of SES individual was included. A single model was used for both types of transit phase (ascent or descent). We tested for interactions between the type of phase and other explanatory variables to enable the estimation of distinct relationships during ascent and descent phases.

The model selection procedure was performed in two stages. The first stage consisted in a stepwise AIC starting from the full model with all explanatory variables and dropping variables step by step until the AIC reached a minimum. In order to allow potentially non-linear relationships in the five models that we implemented, linear combinations of the powers of covariates (polynomials) were tested. These polynomials allow fitting a relationship of any shape but the more complex is the shape the more parameters it requires and the stronger it is penalized by AIC. Thus, the second stage of the model selection procedure was to test for non-linear relationships by computing the AIC with polynomials of the previously selected explanatory variables of increasing degree until the model AIC reached a new minimum. During the model selection, models were fitted with Maximum-Likelihood algorithm. Final models were re-fitted with Restricted Maximum Likelihood algorithm. For each of the five models the final set of explanatory variables selected is displayed on the corresponding figure. The specification of correlation structures (such as AR, ARMA or ARIMA) induces very large computation time and is not implemented for all types of model that we used. We addressed the temporal autocorrelation issue by selecting one dive every ten. The existence of an autocorrelation structure in the models' residuals was assessed by plotting their auto-covariance function for each individual (performed with the acf function). Colinearity issues between covariates was checked prior to model selection using Variance Inflation Factor (VIF < 5, usdm package [75]).

Various pseudo-R^2 were used to assess the amount of variation explained by the top models. For LMMs (models 2 and 4) we used an equivalent of the Ordinary Least-Squares (OLS) R^2 which has been developed by Nakagawa and Schielzeth ([76], implemented in the MuMIn R package [77]). It has a "marginal" (R^2m) and a "conditional" (R^2c) component which can be interpreted as the variance explained by fixed effects only (R^2m) and by the entire model (R^2c). For GLMs (models 1a and 1b) we calculated the percentage of the null model deviance explained (D^2, Table 1) by the top models as a substitute to OLS R^2 [78]. Moreover, for these models, we calculated the null model deviance explained (hereafter abbreviated NDE) by each explanatory variable. Finally, to evaluate goodness-of-fit of the beta regression (model 3) and to compare it to the other models, we calculated a pseudo R^2 metric defined as the squared Pearson's correlation coefficient between observed values (transformed with the link function) and fitted values of linear predictor. This pseudo R^2 metric (noted Pearson^2 in Table 1) ranges from 0 to 1 and provides an indication of correlation between predicted values and actual values (where the closer to 1 the better).

Table 1. Goodness-of-fit of the top models as indicated by pseudo-R^2. See the "Statistical analysis" section for details about these metrics.

Model	D^2	Nakagawa *et al.* R^2	Pearson^2
1a (Neg. Bin. GLM)	58%		56%
1b (Neg. Bin. GLM)	63%		60%
2 (LMM)		$R^2m = 41\%$, $R^2c = 48\%$	47%
3 (Beta regression)			87%
4 (LMM)		$R^2m = 93\%$, $R^2c = 94\%$	85%

doi:10.1371/journal.pone.0167226.t001

Results

Overall diving behaviour

A total of 20189 dives were recorded from the 9 post-breeding female SESs. Of these 8.4% were classified as drift dives. Mean dive duration was 18.38 min (1103 s) ± SD 5.13 min (308 s) and mean bottom duration was 7.95 min (477 s) ± SD 4.12 min (247 s). The overall average of mean depth at bottom was 409 m ± SD 192 m with a maximum of 1307 m. PEEs were detected in 91.1% of non-drift dives. 10.48% of PEE occurred in descents, 78.03% in bottom phases and 11.49% in ascent. Additional descriptive statistics of diving behaviours are available in the Table C in S1 Appendix.

Relationships between prey encounter rate and diving behaviours

The models 1a and 1b selected by the model selection process included ascent pitch diving angle, angular variances of pitch and heading during bottom phase, the median depth and vertical extent of bottom phase and, for model 1a only, the percentage of bottom time spent doing wiggle. The PEE rate at the bottom during day and night is positively related to ascent pitch diving angle (3% NDE for daytime and 11% NDE at night) and to the angular variances of pitch (5% NDE for daytime and 20% NDE at night) and heading (31% NDE for daytime and 6% NDE at night) angles at bottom (Figs 1 & 2). Negative relationships were found between PEE rate and the bottom median depth (10% NDE for daytime and 15% NDE at night) and to the bottom vertical extent (3% NDE for daytime and 1% NDE at night) (Figs 1–3). PEE rate at bottom responded to bottom time doing wiggles during day only (1% NDE).

According to the regression slopes, the strongest effects on prey encounter rate during the day are heading and pitch angle variances at the bottom (particularly for low values), the bottom vertical extent (again for low values) and the bottom median depth (Fig 1). Below 20% of bottom phase duration, the time at bottom spent doing wiggles has a large and positive effect on the PEE rate at bottom, but beyond this point the effect is weak (Fig 1). Similarly, the negative effect of the vertical extent of the bottom phase decreases from 60 m toward higher values (Fig 1).

Regression slopes for the night model (model 1b, Fig 2) display similar patterns to those of the day model. As in model 1a, the negative effect of the bottom vertical extent on the PEE rate at bottom decreases from low to high values going from a strong negative below 20 m, to an approximately flat relationship beyond this threshold (Fig 2). The regression line estimated for the bottom median depth differs from model 1a by displaying a non-linear shape and a steeper negative slope overall (Fig 2).

Relationships between horizontal speed at surface and diving behaviours

The model 2 with average pitch diving angle in descent and ascent phases, angular variance of pitch and heading, and percentage of time spent doing steps was selected by the model selection process. Descent and ascent diving angles and variances of heading angle at bottom have a linear negative effect on the horizontal speed measured at surface with GPS locations (Fig 4). We found a negatively orientated non-linear effect of the pitch angle variance at bottom on the surface speed (Fig 4). Finally, the amount of time doing steps in the bottom has a low positive effect in the range of low values (< 25%, Fig 4) but a negative effect beyond 25% (Fig 4). The strongest slopes are observable for ascent pitch angle and heading variance at bottom (Fig 4).

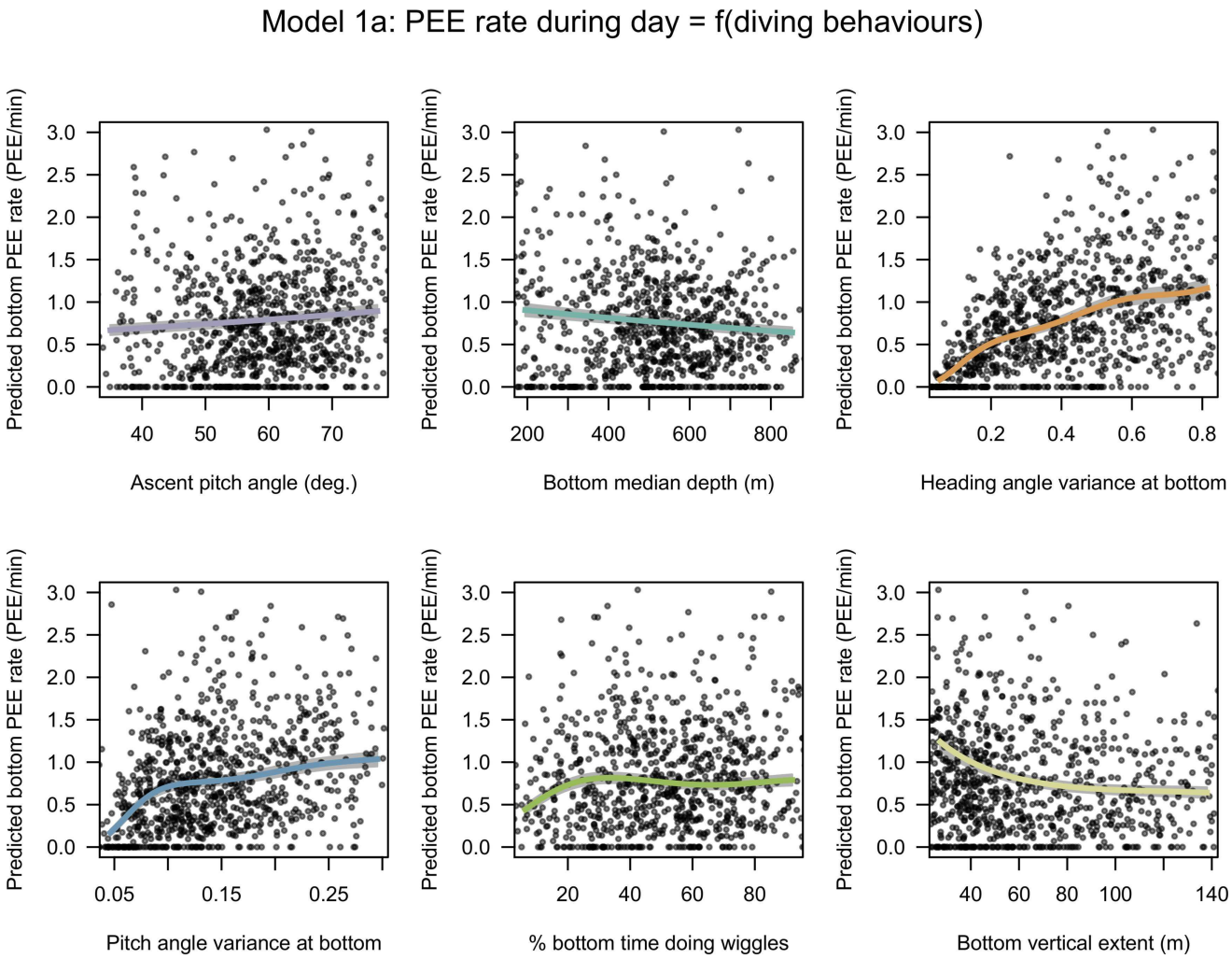

Fig 1. Estimated effects of covariates selected in model 1a. Expected response predicted with a covariate varying from the 5% to the 95% quantile of its observed values with other covariates at their mean. The x axes have been scaled to range from -2 to 2 normalized so that regression slopes are comparable but are annotated with raw units so that units are comprehensible. The grey shades around the regression lines indicate the standard error of the mean prediction estimates.

doi:10.1371/journal.pone.0167226.g001

Relationships between diving efficiency and diving behaviours

The model 3 with average pitch diving angle in descent and ascent phases, angular variance of pitch and heading, percentage of time spent doing wiggles and median depth in bottom phase was selected by the model selection process. The diving efficiency (proportion of dive time spent in the bottom phase) is positively related to descent and ascent pitch angle, and negatively related to the bottom median depth and the variance of heading angle at the bottom (Fig 5). In comparison to these diving behaviours, the bottom time spent doing wiggles, the bottom vertical extent and the variance of pitch angle at the bottom have weak effects (Fig 5).

The model 4 with average pitch diving angle, average swimming effort and maximum depth of the phases was selected by the model selection process. Descent and ascent durations are both negatively related to the steepness of pitch angles and positively related to the depth

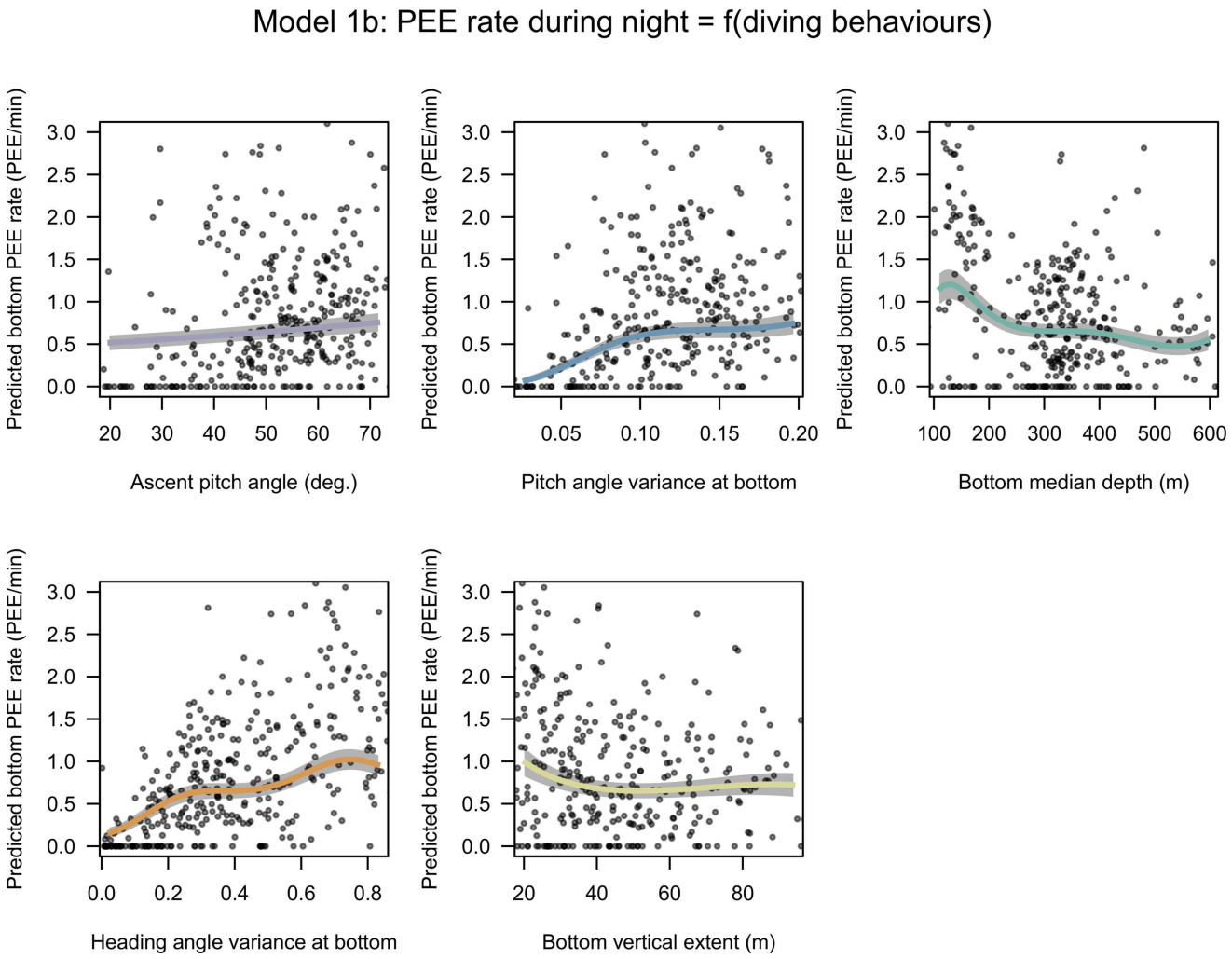

Fig 2. Estimated effects of covariates selected in model 1b. The predictions for each covariate varying from the 5% to the 95% quantile of observed values with other covariates at their mean. The x axes have been scaled to range from -2 to 2 normalized so that regression slopes are comparable but are annotated with raw units so that units are comprehensible. The grey shades around the regression lines indicate the standard error of the mean prediction estimates.

doi:10.1371/journal.pone.0167226.g002

(Fig 6). The swimming effort is another significant driver of the ascent duration but not of the descent duration (Fig 6). While increasing the ascent vertical speed implies greater swimming effort per unit of time it is associated to smaller duration and consequently to a smaller amount of swimming effort cumulated over the complete ascent phase (Fig C & Table E in S4 Appendix).

Models results

The datasets contained 950 complete observations for model 1a (30.64 observations per parameter) and 364 for model 1b (12.55 observations per parameter), 212 for model 2 (17.67 observations per parameter) and 1,823 for model 3 (41.43 observations per parameter). The pseudo-R^2 used to assess the response variation explained by the top models (Nakagawa and Schielzeth's R^2 for LMMs, D^2 for GLMs) or their goodness-of-fit (Pearson^2 for beta regression) are provided in Table 1.

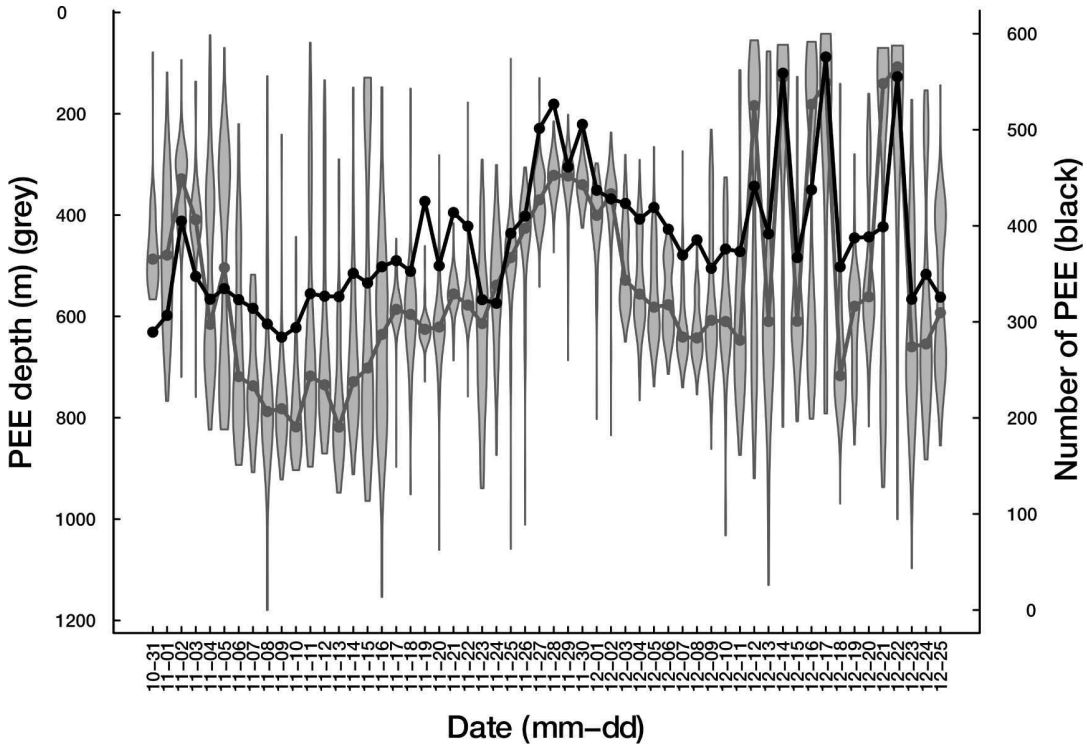

Fig 3. Time series of the vertical distribution of PEE in the bottom of dives and of the number of PEE rate (individual 2011–28). The black lines stand for the PEE rate (number of bottom PEE per day, daytime only), the grey violins for the vertical distribution of daytime bottom PEE (with median depth of daily PEE indicated by the grey dots).

doi:10.1371/journal.pone.0167226.g003

Discussion

These results reveal that the prey encounter rate of SESs is driven by two main factors: (1) the depth (i.e. the vertical accessibility) of a prey patch from the surface, where the closer to the surface the better, and (2) the bottom vertical extent, where lower values were associated with higher PEE rate. This suggests that the prey catch rate of female SESs increased when well defined, narrow layers of high density prey were encountered. As such, the fine scale density within the water column, possibly rather than the overall prey density over the whole water column visited by the SES, appears to be one of the main drivers of SES prey catch rate. When high prey encounter rate is met, elephant seals adjust their diving behaviour by increasing both their descent and ascent angle (Figs 1 and 2), likely to minimize their transit time (Figs 5 and 6), and increase both their horizontal and vertical sinuosity during the bottom phase of their dive zigzagging within the prey patch layer (Figs 1 and 2). The negative relationship between the horizontal transit rate and putative feeding activity has been observed for numerous marine predators (SES [19] see also Figure A in S3 Appendix, northern elephant seals (*Mirounga angustirostris*) [79], wandering albatross (*Diomedea exulan*), antarctic fur seals (*Arctocephalus gazella*) [80]). A number of these variables that impacted on the PEE rate at bottom (models 1a and 1b) affected oppositely the horizontal speed measured at surface with GPS location (model 2). Namely, these variables were the diving angle in ascent phase and the variances pitch and heading angle during bottom phases (Figs 1, 2 and 4). As a consequence, the horizontal speed measured at surface decreases when encountering more prey.

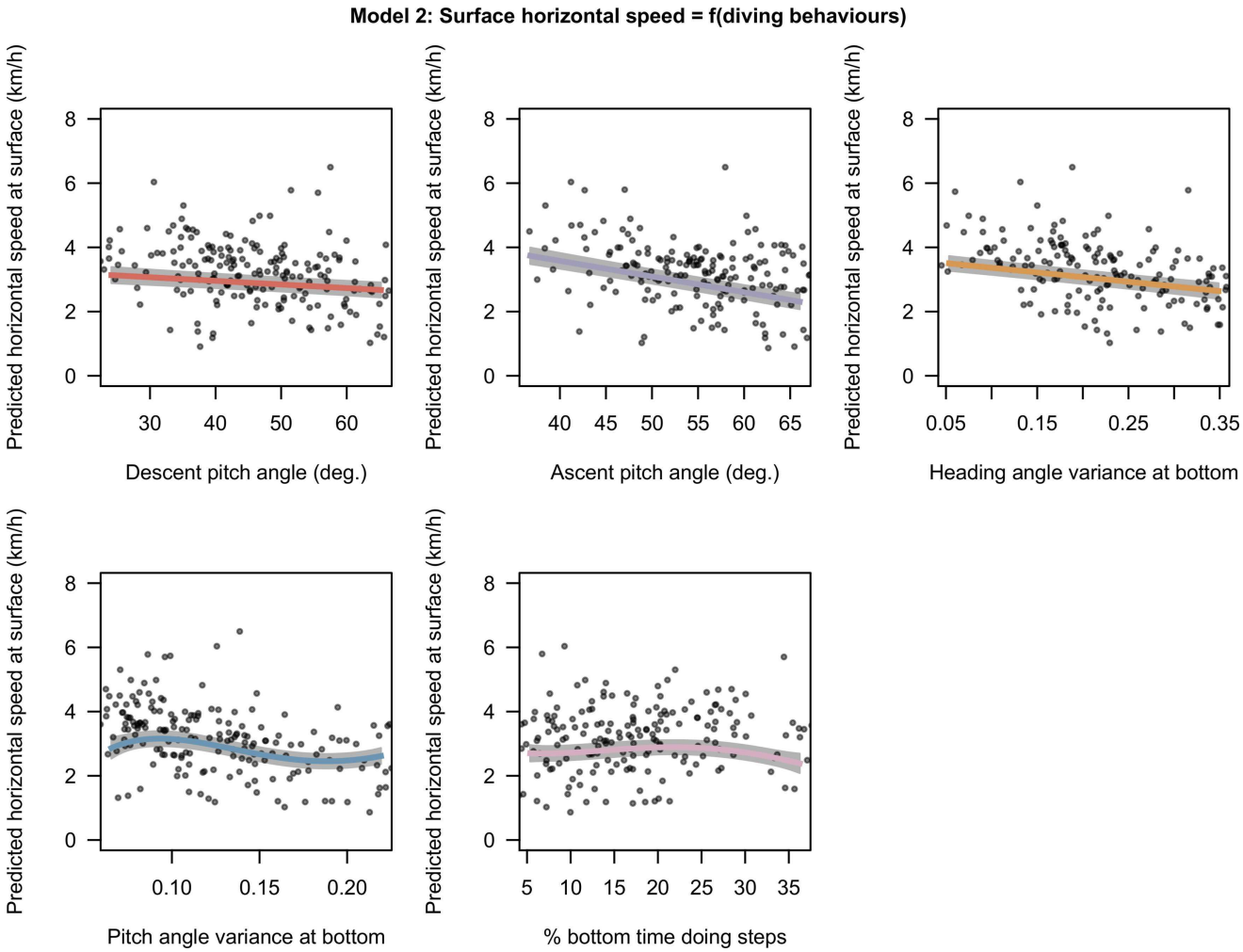

Fig 4. Estimated effects of covariates selected in model 2. The predictions for each covariate varying from the 5% to the 95% quantile of observed values with other covariates at their mean. The x axes have been scaled to range from -2 to 2 normalized so that regression slopes are comparable but are annotated with raw units so that units are comprehensible. The grey shades around the regression lines indicate the standard error of the mean prediction estimates.

doi:10.1371/journal.pone.0167226.g004

Behavioural adjustments to prey encounter rate

To reduce transit time and increase diving efficiency, SESs increase their vertical transit speed with steeper pitch angles mainly but also, in ascent, by increasing their swimming effort (Fig 6). We found that swimming effort had a greater importance on vertical speed in the ascent phase compared to the descent phase of the dives (Fig 6). This lower contribution of the swimming effort to the vertical speed during the descent is likely to be related to the negative buoyancy of post-breeding SES females, which tend to glide down to the bottom of their dive [61,66]. Indeed, the SES leaving Kerguelen after breeding are in poor condition and the post-breeding foraging trips do not last long enough to fully restore their lipid provisions. During the ascent phase, negatively buoyant female SES both increase their ascent angle and their swimming effort, with both factors having an equivalent contribution to explain the increased vertical transit speed (Fig 6). However, the overall swimming effort in response to an increased

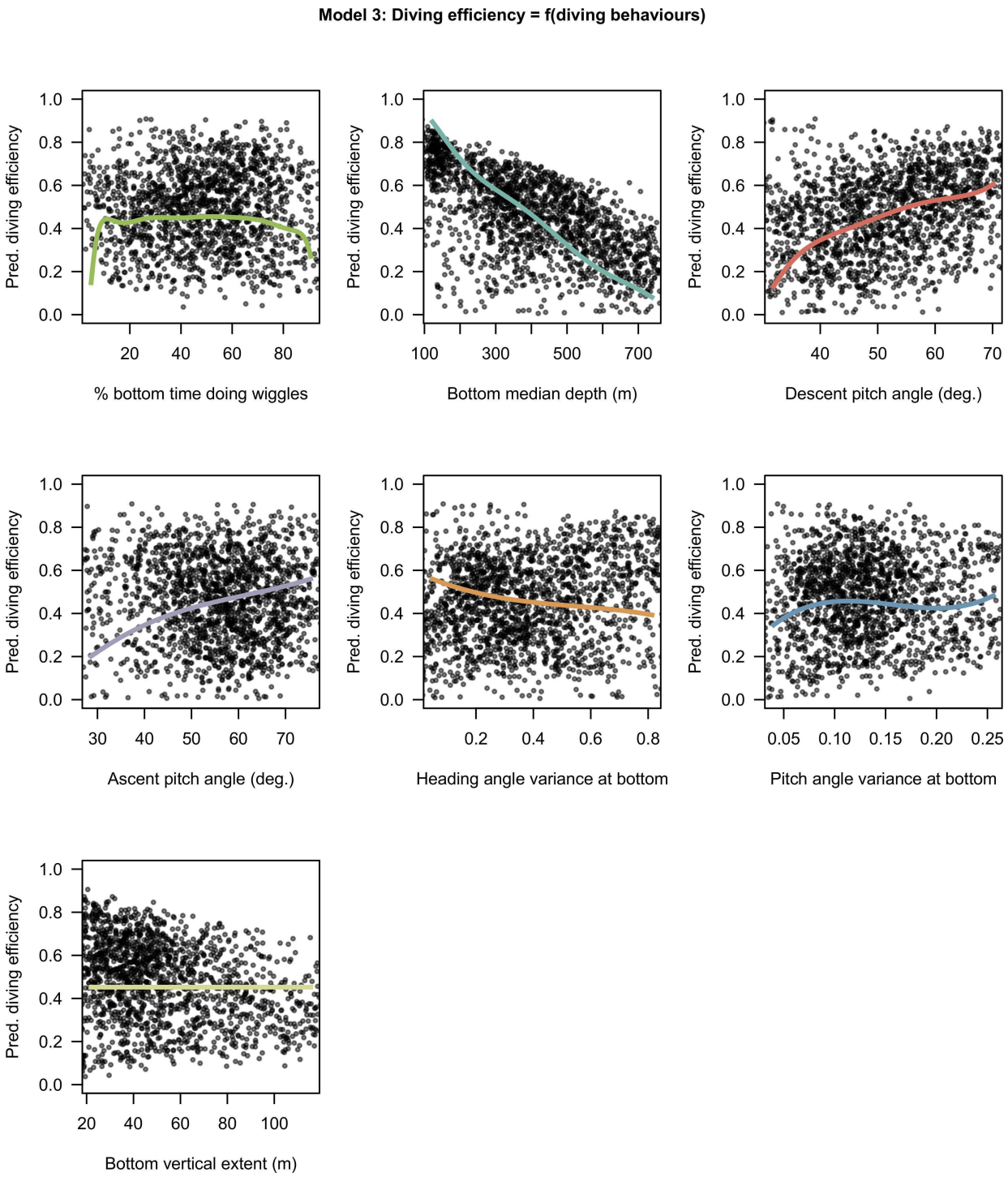

Fig 5. Estimated effects of covariates selected in model 3. The predictions for each covariate varying from the 5% to the 95% quantile of observed values with other covariates at their mean. The x axes have been scaled to range from -2 to 2 normalized so that regression slopes are comparable but are annotated with raw units so that units are comprehensible.

doi:10.1371/journal.pone.0167226.g005

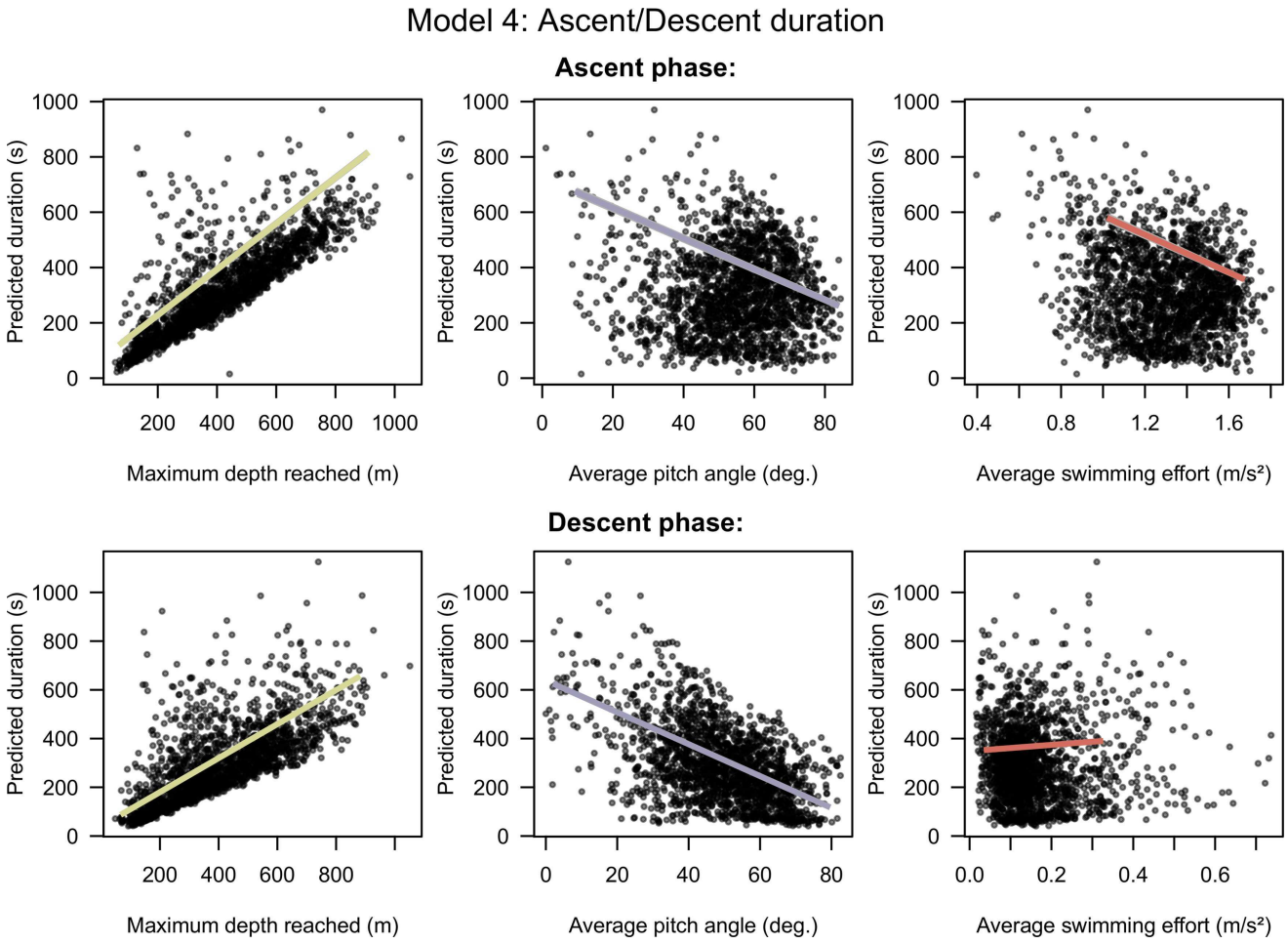

Fig 6. Estimated effects of covariates selected in model 4. The predictions for each covariate varying from the 1% to the 99% quantile of observed values with other covariates at their mean. The x axes have been scaled to range from -3 to 3 normalized so that regression slopes are comparable but are annotated with raw units so that units are comprehensible. The grey shades around the regression lines indicate the standard error of the mean prediction estimates.

doi:10.1371/journal.pone.0167226.g006

vertical speed is negative, with a greater swimming effort per unit of time being compensated by shorter transit duration (Figure C in S4 Appendix).

Steeper pitch angles in descent and ascent phases were found to slow down significantly the horizontal component of SES movement (model 2, Fig 4) and to increase the proportion of time the SES spent in bottom phase during their dives (model 3, Fig 5). Adjustments in diving angles lead to a trade-off between the amount of time the animal can spend to forage at depth and the horizontal speed. In an environment with a high prey density, steep diving angles allow individuals to spend longer time at depth in contact with prey and to remain in the same area for their next dives. However, in low prey density area, flat diving angles speed up horizontal transit rate and shorten search time to find a new prey patch. The positive relationship between the steepness of ascent angle and the PEE rate at bottom (model 1, Figs 1 & 2) could be interpreted according to the optimal foraging theory as a behavioural adjustment to maximize the time spent in high prey density environment. This relationship was weak in model 1a, suggesting that the deeper dives performed during daytime leave less room for such adjustments. As the diving angle in descent could be a way to regulate the horizontal speed it is likely

to respond not only to the prey patch quality but also to the migration stage of the SES [43]. Oblique descent angles have also been suggested to relate to prey location where it could help the SES to combat the camouflage of squids in the downward light [41].

Diving depth had the strongest impact on the diving efficiency, which can be explained by the greater transit duration to reach those greater depths which reduces the amount of time SES could allocate to foraging at the bottom (model 3). The energetic cost of transit to the bottoms of dives is also related to the body buoyancy. Swimming energy expenditure is the lowest at neutral buoyancy allowing the seals to increase their diving efficiency [61]. Seals also tend to adjust their diving efficiency according to the foraging success of the current and the previous dives [28].

The prey encounter rate was positively related to the circular variances of both pitch and heading angles (Figs 1 and 2) which are indicative of the vertical and horizontal sinuosity of the bottom. These diving behaviours also impacted strongly on the horizontal speed at surface, thus increasing the residence time of SES in a given area. This is consistent with observations of Area Restricted Search behaviour in other diving seabirds and pinnipeds or, at larger spatial and temporal scales, with SES [19,68,81,82] alongside side optimal foraging theory which predicts longer residence in high prey density grounds. The heading angle variances at the bottom was detrimental to diving efficiency (model 3, Fig 5), suggesting that increased horizontal sinuosity is associated with prey chasing or handling and to a greater energy expenditure.

The bottom time spent performing wiggles was related to PEE rate at the bottom in day conditions. Its effect displayed a plateau at intermediate-high values ($>$ 30% Fig 1). Wiggles were also found to impact on diving efficiency toward extreme values (Fig 5). Pitch and heading angular variances during the bottom phase of the dive had greater and more consistent effect over the complete range of observed values and appear to be a more reliable indicator of PEE rate. The bottom time spent doing steps related solely to horizontal speed at the surface and displayed contrasting effects (Fig 4), suggesting that this behaviour is employed for multiple purposes. From our perspective, steps may represent short drifting periods or gliding periods allowing horizontal travel at low expense or to locate prey during the bottom phase of the dive.

Della Penna *et al.* ([83]) showed that when foraging dynamic oceanographic mesoscale structures, such as eddies, the horizontal displacements of SES encountering a high PEE rate could be as passive as those of lagrangian drifters. Thus, the SES would keep in contact with the foraging resources by reducing their horizontal displacements. As currents are supposed to contribute significantly to the horizontal movements of SES when they forage intensively [83], the varying current strength encountered by the animal along its trajectory is a source of noise when trying to compute the actual horizontal speed of SES from satellite locations. Despite this methodological limitation, our results highlight that foraging intensive behaviours—increasing of descent and ascent diving angles, but also of horizontal and vertical sinuosity during the bottom phase of their dive—have a negative effect on the horizontal component of their movement. As a consequence they remain within the prey patch, but become more sensitive to current transportation [83,84] and are passively transported with the prey patch by the current. Under such a situation, with a high current velocity the ARS/non ARS behaviour detected from the surface track could result primarily from the current velocity field rather than from the active horizontal movements from the animals. As such, inference of foraging state of the animal using state space models could be erroneous.

Area of the water column targeted by SES

SESs were more successful when foraging closer to the surface (model 1a and 1b). Either in day (Figs 1 & 3) or in night conditions (Fig 2), the greater the bottom depth the lower PEE per

unit of time they were, showing that this observation cannot be explained by diel vertical migrations of SES prey. This negative relationship between the bottom depth and the prey encounter rate at the bottom could indicate a decrease in prey density, a change in prey type/size or a decrease of the ability of SES to catch prey items with increasing depth. Other studies have led to similar results. For example, [85] observed that the occurrence of bioluminescent events detected from light sensors carried by foraging elephant seals was negatively related to their diving depth. Williams & Koslow ([86]) sampled micronekton between the surface and a depth of 900 m with a mid-water trawl and found a decreasing micronekton biomass with depth at night and, in autumn, during daytime as well.

Predators should match their foraging effort to prey distribution. Seventy seven percent of all PEE took place in the bottom phase of a dive. With regards to the accessibility and abundance of resources, the bottom phase is valuable enough to motivate the SES to stop the descent phase and focus on the search of prey at depth. Once the bottom depth is reached, the vertical extent of the bottom phase is expected to provide an indication on the vertical distribution of prey. The PEE rate at the bottom was negatively related to the vertical span of the water column explored during the bottom phase (model 1, Figs 1–3), suggesting that the dispersion of prey along the vertical dimension regulates the prey density encountered at depth by SES. To our knowledge this is the first time that this relationship is highlighted and could be a novel aspect that is worth considering when investigating fine scale prey density underwater.

A range of diving behaviours (e.g. dive depth, descent speed an dive duration) have been associated with mesoscale oceanographic features such as cyclonic eddies, where SES exhibit shallower diving depth compared to anti-cyclonic eddies and other oceanographic domains [82,87]. Water temperature was found to have a direct influence on the diving depth of SES, with SES diving deeper in warmer waters to access their prey [6,82]. Furthermore, bottom depth was shown to be strongly negatively related to light intensity at depth which is attenuated by phytoplankton concentration within the euphotic layers [88]. Characteristics such as a high chlorophyll concentration and cold water at surface are observed in cold-core eddies [89,90], shown to be successful foraging areas where the SES dive depth is close from surface [87]. While underlying determinants leading SES to explore a narrow vertical depth range in their dive bottom phases remain unclear, one could hypothesize that similar bio-physical oceanographic processes could locally constrain prey to aggregate vertically in thinner yet denser prey layers. Future work could try to assess the validity of this hypothesis.

This study could only focus on the vertical dimension of prey distribution because, due to sensor malfunction, we did not have access to the actual swimming velocity when the seal was foraging at the bottom of its dive to allow for a more accurate description of the 3D spatial structure of the prey field. Without that information we could not estimate the volume of water prospected by SES and compare it to the number of PEE in order to get an indication of prey density independent from SES behaviour (in PEE/m^3 instead of PEE per unit of SES bottom time). Additional studies may use 3D dive reconstructions [13,80,91–93] to determine if the effect of the vertical extent of the bottom on the foraging success would be related to the presence/absence of small scale schooling-prey patches (leading to a small vertical extent of the bottom) or conversely, due to changes at a larger scale in the vertical aggregation of prey layers within the water column. We believe that the findings of this study are likely to be generalized to other air breathing divers foraging on small prey items such as mesopelagic fishes or crustaceans, but differences are likely to be found for diving predators foraging on large prey items. Instead, the latter may abort their dive after catching very large preys to return to the surface to feed as observed in Weddell seals (*Leptonychotes weddellii*) feeding on Antarctic toothfish (*Dissostichus mawsoni*) [94].

The prey encounter events detected from acceleration data only provide quantitative information about prey. How the prey species and size relate to the diving behaviour and the decreasing prey encounter rate that we observed along depth remain unknown. Moreover, bio-logging data are collected by free-ranging diving predators which are unlikely to cover the entire range of habitat available to their prey. This makes it difficult to assess the deeper limit of the prey patch on which the SES feed at the bottom of their dives or to test predictions about their foraging behaviour. The development of video camera [34,91,95] and miniaturized sonar loggers [96] may help to overcome these difficulties by providing information about the prey quality and extend our perception range of environment surrounding the SES.

Supporting Information

S1 Appendix. Diving behaviour and device deployment details for the 9 post-breeding female SES.
(PDF)

S2 Appendix. Detection of Prey Encounter Events (PEE).
(PDF)

S3 Appendix. Surface horizontal speed.
(PDF)

S4 Appendix. Influence of vertical speed on swimming effort during transit phases.
(PDF)

Acknowledgments

Thanks to the organizations that provided financial support to this study, Département des Deux-Sèvres and Région Poitou-Charentes, MyctO-3D-MAP and IPSOS-SEAL ANR, Total Foundation, « Éléphant de mer océanographes » CNES research program and Observatoire des Mammifères Explorateurs du Milieu Océanique. Thanks to the people at IPEV and to the field assistants that permitted the field at Kerguelen. Many thanks to Samantha Cox for her numerous relevant comments and her helping with the English revision of the early versions of the paper.

Author Contributions

Conceptualization: YLB CG.

Data curation: BP.

Formal analysis: YLB.

Funding acquisition: CG.

Investigation: YLB JJ BP CG.

Methodology: YLB JJ.

Project administration: CG.

Resources: CG.

Software: YLB.

Supervision: CG.

Validation: YLB JJ BP CG.

Visualization: YLB.

Writing – original draft: YLB JJ CG.

Writing – review & editing: YLB JJ CG.

References

1. Stephens DW, Krebs JR. Foraging Theory. Princeton University Press; 1986.
2. MacArthur RH, Pianka ER. On Optimal Use of a Patchy Environment. Am Nat. 1966; 100: 603–609.
3. Charnov EL. Optimal foraging, the marginal value theorem. Theor Popul Biol. 1976; 9: 129–136. PMID: 1273796
4. McNamara J. Optimal patch use in a stochastic environment. Theor Popul Biol. 1982; 21: 269–288.
5. Kooyman GL. Diverse Divers: Physiology and Behavior. Springer-Verlag; 1989.
6. Guinet C, Vacquié-Garcia J, Picard B, Bessigneul G, Lebras Y, Dragon AC, et al. Southern elephant seal foraging success in relation to temperature and light conditions: insight into prey distribution. Mar Ecol Prog Ser. 2014; 499: 285–301.
7. Bost CA, Cotté C, Terray P, Barbraud C, Bon C, Delord K, et al. Large-scale climatic anomalies affect marine predator foraging behaviour and demography. Nat Commun. 2015; 6: 8220. doi: 10.1038/ncomms9220 PMID: 26506134
8. Viviant M, Trites AW, Rosen DAS, Monestiez P, Guinet C. Prey capture attempts can be detected in Steller sea lions and other marine predators using accelerometers. Polar Biol. 2010; 33: 713–719. -y
9. Naito Y, Bornemann H, Takahashi A, McIntyre T, Plötz J. Fine-scale feeding behavior of Weddell seals revealed by a mandible accelerometer. Polar Sci. 2010; 4: 309–316.
10. Watanabe YY, Takahashi A. Linking animal-borne video to accelerometers reveals prey capture variability. Proc Natl Acad Sci. 2013; 110: 2199–2204. doi: 10.1073/pnas.1216244110 PMID: 23341596
11. Gallon S, Bailleul F, Charrassin J-B, Guinet C, Bost C-A, Handrich Y, et al. Identifying foraging events in deep diving southern elephant seals, Mirounga leonina, using acceleration data loggers. Deep Sea Res Part II Top Stud Oceanogr. 2013; 88–89: 14–22.
12. Foo D, Semmens JM, Arnould JPY, Dorville N, Hoskins AJ, Abernathy K, et al. Testing optimal foraging theory models on benthic divers. Anim Behav. 2016; 112: 127–138.
13. Mitani Y, Andrews RD, Sato K, Kato A, Naito Y, Costa DP. Three-dimensional resting behaviour of northern elephant seals: drifting like a falling leaf. Biol Lett. 2010; 6: 163–166. doi: 10.1098/rsbl.2009.0719 PMID: 19864274
14. Sala JE, Quintana F, Wilson RP, Dignani J, Lewis MN, Campagna C. Pitching a new angle on elephant seal dive patterns. Polar Biol. 2011; 34: 1197–1209.
15. Robinson PW, Tremblay Y, Crocker DE, Kappes MA, Kuhn CE, Shaffer SA, et al. A comparison of indirect measures of feeding behaviour based on ARGOS tracking data. Deep Sea Res Part II Top Stud Oceanogr. 2007; 54: 356–368.
16. Kirkman SP, Yemane DG, Lamont T, Meÿer MA, Pistorius PA. Foraging Behavior of Subantarctic Fur Seals Supports Efficiency of a Marine Reserve's Design. PLoS ONE. 2016; 11: e0152370. doi: 10.1371/journal.pone.0152370 PMID: 27163373
17. Hindell MA, McMahon CR, Bester MN, Boehme L, Costa D, Fedak MA, et al. Circumpolar habitat use in the southern elephant seal: implications for foraging success and population trajectories. Ecosphere. 2016; 7.
18. Lascelles BG, Taylor PR, Miller MGR, Dias MP, Oppel S, Torres L, et al. Applying global criteria to tracking data to define important areas for marine conservation. Divers Distrib. 2016; 22: 422–431.
19. Dragon A, Bar-Hen A, Monestiez P, Guinet C. Horizontal and vertical movements as predictors of foraging success in a marine predator. Mar Ecol Prog Ser. 2012; 447: 243–257. Do
20. Hanuise N, Bost C-A, Huin W, Auber A, Halsey LG, Handrich Y. Measuring foraging activity in a deep-diving bird: comparing wiggles, oesophageal temperatures and beak-opening angles as proxies of feeding. J Exp Biol. 2010; 213: 3874–3880.
21. McIntyre T, Bornemann H, Plötz J, Tosh CA, Bester MN. Water column use and forage strategies of female southern elephant seals from Marion Island. Mar Biol. 2011; 158: 2125–2139.

22. McIntyre T, Stansfield LJ, Bornemann H, Plötz J, Bester MN. Hydrographic influences on the summer dive behaviour of Weddell seals (Leptonychotes weddellii) in Atka Bay, Antarctica. Polar Biol. 2013; 36: 1693–1700.
23. Kareiva P, Odell G. Swarms of predators exhibits "preytaxis" if individual predators use area-restricted search. Am Nat. 1987; 130: 233–270.
24. Parker GA, Stuart RA. Animal Behavior as a Strategy Optimizer: Evolution of Resource Assessment Strategies and Optimal Emigration Thresholds. Am Nat. 1976; 110: 1055–1076.
25. Thompson D, Fedak MA. How long should a dive last? A simple model of foraging decisions by breath-hold divers in a patchy environment. Anim Behav. 2001; 61: 287–296.
26. Sparling CE, Georges J-Y, Gallon SL, Fedak M, Thompson D. How long does a dive last? Foraging decisions by breath-hold divers in a patchy environment: a test of a simple model. Anim Behav. 2007; 74: 207–218.
27. Doniol-Valcroze T, Lesage V, Giard J, Michaud R. Optimal foraging theory predicts diving and feeding strategies of the largest marine predator. Behav Ecol. 2011; arr038.
28. Jouma'a J, Le Bras Y, Richard G, Vacquié-Garcia J, Picard B, Ei Ksabi N, et al. Adjustment of diving behaviour with prey encounters and body condition in a deep diving predator: the Southern Elephant Seal. Funct Ecol. 2015;
29. Cornick LA, Horning M. A test of hypotheses based on optimal foraging considerations for a diving mammal using a novel experimental approach. Can J Zool. 2003; 81: 1799–1807.
30. Tremblay Y, Cherel Y. Benthic and pelagic dives: a new foraging behaviour in rockhopper penguins. Mar Ecol Prog Ser. 2000; 204: 257–267.
31. Viviant M, Jeanniard-du-Dot T, Monestiez P, Authier M, Guinet C. Bottom time does not always predict prey encounter rate in Antarctic fur seals. Funct Ecol. 2016;
32. Hooker SK, Boyd IL, Jessopp M, Cox O, Blackwell J, Boveng PL, et al. Monitoring the Prey-Field of Marine Predators: Combining Digital Imaging with Datalogging Tags. Mar Mammal Sci. 2002; 18: 680–697.
33. Viviant M, Monestiez P, Guinet C. Can We Predict Foraging Success in a Marine Predator from Dive Patterns Only? Validation with Prey Capture Attempt Data. PLoS ONE. 2014; 9: e88503. doi: 10.1371/journal.pone.0088503 PMID: 24603534
34. Naito Y, Costa DP, Adachi T, Robinson PW, Fowler M, Takahashi A. Unravelling the mysteries of a mesopelagic diet: a large apex predator specializes on small prey. Funct Ecol. 2013; 27: 710–717.
35. Austin D, Bowen WD, McMillan JI, Iverson SJ. Linking movement, diving and habitat to foraging success in a large marine predator. Ecology. 2006; 87: 3095–3108. PMID: 17249234
36. Wilson R, Steinfurth A, Ropert-Coudert Y, Kato A, Kurita M. Lip-reading in remote subjects: an attempt to quantify and separate ingestion, breathing and vocalisation in free-living animals using penguins as a model. Mar Biol. 2002; 140: 17–27.
37. Davis RW, Fuiman LA, Williams TM, Horning M, Hagey W. Classification of Weddell seal dives based on 3 dimensional movements and video-recorded observations. Mar Ecol Prog Ser. 2003; 264: 109–122.
38. Fossette S, Gaspar P, Handrich Y, Maho YL, Georges J-Y. Dive and beak movement patterns in leatherback turtles Dermochelys coriacea during internesting intervals in French Guiana. J Anim Ecol. 2008; 77: 236–246. doi: 10.1111/j.1365-2656.2007.01344.x PMID: 18217943
39. Sato K, Charrassin J-B, Bost C-A, Naito Y. Why do macaroni penguins choose shallow body angles that result in longer descent and ascent durations? J Exp Biol. 2004; 207: 4057–4065. doi: 10.1242/jeb.01265 PMID: 15498951
40. Hanuise N, Bost C-A, Handrich Y. Optimization of transit strategies while diving in foraging king penguins. J Zool. 2013; 290: 181–191.
41. Hassrick JL, Crocker DE, Zeno RL, Blackwell SB, Costa DP, Le Boeuf BJ. Swimming speed and foraging strategies of northern elephant seals. Deep Sea Res Part II Top Stud Oceanogr. 2007; 54: 369–383.
42. Ropert-Coudert Y, Kato A, Baudat J, Bost C-A, Maho YL, Naito Y. Time/depth usage of Adélie penguins: an approach based on dive angles. Polar Biol. 2001; 24: 467–470.
43. Miller PJO, Biuw M, Watanabe YY, Thompson D, Fedak MA. Sink fast and swim harder! Round-trip cost-of-transport for buoyant divers. J Exp Biol. 2012; 215: 3622–3630. doi: 10.1242/jeb.070128 PMID: 23014571
44. Hindell M, Burton H, Slip D. Foraging areas of southern elephant seals, Mirounga leonina, as inferred from water temperature data. Mar Freshw Res. 1991; 42: 115–128.

45. McConnell BJ, Chambers C, Fedak MA. Foraging ecology of southern elephant seals in relation to the bathymetry and productivity of the Southern Ocean. Antarct Sci. 1992; 4: 393–398.
46. Schreer JF, Kovacs KM, O'Hara Hines RJ. Comparative diving patterns of pinnipeds and seabirds. Ecol Monogr. 2001; 71: 137–162.
47. Cherel Y, Ducatez S, Fontaine C, Richard P, Guinet C. Stable isotopes reveal the trophic position and mesopelagic fish diet of female southern elephant seals breeding on the Kerguelen Islands. Mar Ecol Prog Ser. 2008; 370: 239–247.
48. Kock K-H. Marine consumers: Fish and squid. Environ Int. 1987; 13: 37–45.
49. Rodhouse PG, White MG. Cephalopods Occupy the Ecological Niche of Epipelagic Fish in the Antarctic Polar Frontal Zone. Biol Bull. 1995; 189: 77–80. doi: 10.2307/1542457 PMID: 27768500
50. Pakhomov EA, Perissinotto R, McQuaid CD. Prey composition and daily rations of myctophid fishes in the Southern Ocean. Mar Ecol Prog Ser. 1996; 134: 1–14.
51. Collins MA, Rodhouse PGK. Southern Ocean Cephalopods. In: Alan J. Southward CMY, and Fuiman Lee A., editor. Advances in Marine Biology. Academic Press; 2006. pp. 191–265. Available: http://www.sciencedirect.com/science/article/pii/S0065288105500038 doi: 10.1016/S0065-2881(05)50003-8 PMID: 16782452
52. Guinet C, Cherel Y, Ridoux V, Jouventin P. Consumption of marine resources by seabirds and seals in Crozet and Kerguelen waters: changes in relation to consumer biomass 1962–85. Antarct Sci. 1996; 8: 23–30.
53. Hindell MA, Bradshaw CJA, Sumner MD, Michael KJ, Burton HR. Dispersal of female southern elephant seals and their prey consumption during the austral summer: relevance to management and oceanographic zones. J Appl Ecol. 2003; 40: 703–715.
54. McIntyre T. Trends in tagging of marine mammals: a review of marine mammal biologging studies. Afr J Mar Sci. 2014; 36: 409–422.
55. Pakhomov E, Yamamura O, Advisory Panel on Micronekton Sampling Inter-calibration Experiment, North Pacific Marine Science Organization. Report of the Advisory Panel on Micronekton Sampling Inter-calibration Experiment [Internet]. Sidney, B.C.: North Pacific Marine Science Organization (PICES); 2010. Available: http://www.pices.int/publications/scientific_reports/Report38/Rep38.pdf
56. McMahon CR, Burton H, Slip D, McLean S, Bester M. Field immobilisation of southern elephant seals with intravenous tiletamine and zolazepam. Vet Rec. 2000; 146: 251–254. PMID: 10737295
57. R Core Team. R: A Language and Environment for Statistical Computing [Internet]. Vienna, Austria: R Foundation for Statistical Computing; 2014. Available: http://www.R-project.org/
58. Le Bras Y. rbl: Biologging tools for diving predators [Internet]. 2016. Available: https://github.com/SESman/rbl
59. Vacquié-Garcia J, Guinet C, Laurent C, Bailleul F. Delineation of the southern elephant seal's main foraging environments defined by temperature and light conditions. Deep Sea Res Part II Top Stud Oceanogr. 2015; 113: 145–153.
60. signal developers. signal: Signal processing [Internet]. 2013. Available: http://r-forge.r-project.org/projects/signal/
61. Richard G, Vacquié-Garcia J, Jouma'a J, Picard B, Génin A, Arnould JPY, et al. Variation in body condition during the post-moult foraging trip of southern elephant seals and its consequences on diving behaviour. J Exp Biol. 2014; 217: 2609–2619. doi: 10.1242/jeb.088542 PMID: 24803471
62. Farrell E, Fuiman L. animalTrack: Animal track reconstruction for high frequency 2-dimensional (2D) or 3-dimensional (3D) movement data. [Internet]. 2013. Available: http://CRAN.R-project.org/package=animalTrack
63. Génin A, Richard G, Jouma'a J, Picard B, Ksabi N El, Vacquié Garcia J, et al. Characterization of post-dive recovery using sound recordings and its relationship to dive duration, exertion, and foraging effort of southern elephant seals (Mirounga leonina). Mar Mammal Sci. 2015; 31: 1452–1470.
64. Sato K, Mitani Y, Cameron MF, Siniff DB, Naito Y. Factors affecting stroking patterns and body angle in diving Weddell seals under natural conditions. J Exp Biol. 2003; 206: 1461–1470. PMID: 12654885
65. Watanabe Y, Baranov EA, Sato K, Naito Y, Miyazaki N. Body density affects stroke patterns in Baikal seals. J Exp Biol. 2006; 209: 3269–3280. doi: 10.1242/jeb.02402 PMID: 16916962
66. Aoki K, Watanabe YY, Crocker DE, Robinson PW, Biuw M, Costa DP, et al. Northern elephant seals adjust gliding and stroking patterns with changes in buoyancy: validation of at-sea metrics of body density. J Exp Biol. 2011; 214: 2973–2987. doi: 10.1242/jeb.055137 PMID: 21832140
67. Halsey LG, Bost C-A, Handrich Y. A thorough and quantified method for classifying seabird diving behaviour. Polar Biol. 2007; 30: 991–1004.

68. Bailleul F, Charrassin J-B, Monestiez P, Roquet F, Biuw M, Guinet C. Successful foraging zones of southern elephant seals from the Kerguelen Islands in relation to oceanographic conditions. Philos Trans R Soc B Biol Sci. 2007; 362: 2169–2181.

69. Robinson PW, Simmons SE, Crocker DE, Costa DP. Measurements of foraging success in a highly pelagic marine predator, the northern elephant seal. J Anim Ecol. 2010; 79: 1146–1156. doi: 10.1111/j.1365-2656.2010.01735.x PMID: 20673236

70. Lund U, Agostinelli C. CircStats: Circular Statistics, from "Topics in circular Statistics" (2001) [Internet]. 2012. Available: http://CRAN.R-project.org/package=CircStats

71. Crocker DE, Boeuf BJL, Costa DP. Drift diving in female northern elephant seals: implications for food processing. Can J Zool. 1997; 75: 27–39.

72. Venables WN, Ripley BD. Modern applied statistics with S. 4. ed., corr. print. New York, NY: Springer; 2007.

73. Pinheiro J, Bates D, DebRoy S, Sarkar D, R Core Team. nlme: Linear and Nonlinear Mixed Effects Models [Internet]. 2015. Available: http://CRAN.R-project.org/package=nlme

74. Cribari-Neto F, Zeileis A. Beta Regression in R. [Internet]. 2010. Available: http://www.jstatsoft.org/v34/i02/

75. Naimi B. usdm: Uncertainty Analysis for Species Distribution Models [Internet]. 2015. Available: http://CRAN.R-project.org/package = usdm

76. Nakagawa S, Schielzeth H. A general and simple method for obtaining R2 from generalized linear mixed-effects models. Methods Ecol Evol. 2013; 4: 133–142.

77. Barton K. MuMIn: Multi-Model Inference [Internet]. 2016. Available: http://CRAN.R-project.org/package=MuMIn

78. Guisan A, Zimmermann NE. Predictive habitat distribution models in ecology. Ecol Model. 2000; 135: 147–186.

79. Kuhn CE, Crocker DE, Tremblay Y, Costa DP. Time to eat: measurements of feeding behaviour in a large marine predator, the northern elephant seal Mirounga angustirostris. J Anim Ecol. 2009; 78: 513–523. doi: 10.1111/j.1365-2656.2008.01509.x PMID: 19040681

80. Iwata T, Sakamoto KQ, Edwards EWJ, Staniland IJ, Trathan PN, Goto Y, et al. The influence of preceding dive cycles on the foraging decisions of Antarctic fur seals. Biol Lett. 2015; 11: 20150227. doi: 10.1098/rsbl.2015.0227 PMID: 26156132

81. Bailleul F, Pinaud D, Hindell M, Charrassin J-B, Guinet C. Assessment of scale-dependent foraging behaviour in southern elephant seals incorporating the vertical dimension: a development of the First Passage Time method. J Anim Ecol. 2008; 77: 948–957. doi: 10.1111/j.1365-2656.2008.01407.x PMID: 18513336

82. Dragon A-C, Monestiez P, Bar-Hen A, Guinet C. Linking foraging behaviour to physical oceanographic structures: Southern elephant seals and mesoscale eddies east of Kerguelen Islands. Prog Oceanogr. 2010; 87: 61–71.

83. Penna A Della, De Monte S, Kestenare E, Guinet C, d'Ovidio F. Quasi-planktonic behavior of foraging top marine predators. Sci Rep. 2015; 5: 18063. doi: 10.1038/srep18063 PMID: 26666350

84. Gaspar P, Georges J-Y, Fossette S, Lenoble A, Ferraroli S, Maho YL. Marine animal behaviour: neglecting ocean currents can lead us up the wrong track. Proc R Soc B Biol Sci. 2006; 273: 2697–2702.

85. Vacquié-Garcia J, Royer F, Dragon A-C, Viviant M, Bailleul F, Guinet C. Foraging in the Darkness of the Southern Ocean: Influence of Bioluminescence on a Deep Diving Predator. PLoS ONE. 2012; 7: e43565. doi: 10.1371/journal.pone.0043565 PMID: 22952706

86. Williams A, Koslow JA. Species composition, biomass and vertical distribution of micronekton over the mid-slope region off southern Tasmania, Australia. Mar Biol. 1997; 130: 259–276.

87. Dragon A-C. Modélisation des stratégies d'approvisionnement des éléphants de mer austraux—influence de la variabilité de la production primaire et des conditions océanographiques physiques [Internet]. phdthesis, Université Pierre et Marie Curie—Paris VI. 2011. Available: https://tel.archives-ouvertes.fr/tel-00660213/document

88. Jaud T, Dragon A-C, Garcia JV, Guinet C. Relationship between Chlorophyll a Concentration, Light Attenuation and Diving Depth of the Southern Elephant Seal Mirounga leonina. PLoS ONE. 2012; 7: e47444. doi: 10.1371/journal.pone.0047444 PMID: 23082166

89. Strass VH, Naveira Garabato AC, Pollard RT, Fischer HI, Hense I, Allen JT, et al. Mesoscale frontal dynamics: shaping the environment of primary production in the Antarctic Circumpolar Current. Deep Sea Res Part II Top Stud Oceanogr. 2002; 49: 3735–3769.

90. Kahru M, Mitchell BG, Gille ST, Hewes CD, Holm-Hansen O. Eddies enhance biological production in the Weddell-Scotia Confluence of the Southern Ocean. Geophys Res Lett. 2007; 34: L14603.

91. Davis RW, Fuiman LA, Williams TM, Collier SO, Hagey WP, Kanatous SB, et al. Hunting Behavior of a Marine Mammal Beneath the Antarctic Fast Ice. Science. 1999; 283: 993–996. PMID: 9974394

92. Johnson MP, Tyack PL. A digital acoustic recording tag for measuring the response of wild marine mammals to sound. IEEE J Ocean Eng. 2003; 28: 3–12.

93. Goldbogen JA, Hazen EL, Friedlaender AS, Calambokidis J, DeRuiter SL, Stimpert AK, et al. Prey density and distribution drive the three-dimensional foraging strategies of the largest filter feeder. Funct Ecol. 2015; 29: 951–961.

94. Ainley DG, Siniff DB. The importance of Antarctic toothfish as prey of Weddell seals in the Ross Sea. Antarct Sci. 2009; 21: 317–327.

95. Takahashi A, Sato K, Naito Y, Dunn MJ, Trathan PN, Croxall JP. Penguin–mounted cameras glimpse underwater group behaviour. Proc R Soc Lond B Biol Sci. 2004; 271: S281–S282.

96. Lawson GL, Hückstädt LA, Lavery AC, Jaffré FM, Wiebe PH, Fincke JR, et al. Development of an animal-borne "sonar tag" for quantifying prey availability: test deployments on northern elephant seals. Anim Biotelemetry. 2015; 3: 22.

ANNEXE E

Acoustic measurements of post-dive cardiac responses in southern elephant seals (*Mirounga leonina*) during surfacing at sea

Day, Louise, Jouma'a, Joffrey, Bonnel, Julien & Guinet Christophe, Acoustic measurements of post-dive cardiac responses in southern elephant seals (*Mirounga leonina*) during surfacing at sea. *Journal of Experimental Biology* (submitted)

Acoustic measurements of post-dive cardiac responses in southern elephant seals (*Mirounga leonina*) during surfacing at sea

Louise DAY, Joffrey JOUMA'A, Julien BONNEL and Christophe GUINET

Centre d'Études Biologiques de Chizé-Centre National de la Recherche Scientifique (CEBC-CNRS), 79360 Villiers-en-bois, France

Running title: Post-dive recovery using acoustic

Key-words: *Mirounga leonina*, heart rate, dive recovery, diving behaviour, passive acoustic monitoring

Corresponding author's email address: louise.day@agrocampus-ouest.fr

Summary statement

This paper demonstrates the reliability of an acoustic method to extract and analyse the cardiac function of free ranging southern elephant seals in order to study post-dive recovery.

Abstract

Measuring physiological data in free-ranging marine mammals remains challenging, owing to their far-ranging foraging habitat. Yet, it is important to understand how these divers recover from effort expended under the water, as marine mammals can perform deep and recurrent dives impacting and being impacted by the whole ecosystem. Among them, southern elephant seals (*Mirounga leonina*) are one of the most extreme divers, diving continuously at great depth and for long duration while travelling over large distances within the Southern Ocean. To determine how they manage post-dive recovery, we deployed hydrophones on four post-breeding female southern elephant seals. Cardiac data were extracted from sound recordings when the animal was at the surface breathing. Mean heart rate at the surface was 102.4 ± 4.9 beats.min^{-1} and seals spent on average 121 ± 20 s breathing. Instantaneous heart rate at the surface increased with surface interval. This finding can be linked to the end of the tachycardia occurring during the ascent towards the surface. Heart rate was unrelated to the duration and swimming effort of the dive prior to the surface interval, and recovery management appears to be predominantly related to the overall number of heart beats performed at the surface, and therefore total surface duration. Hence, surface interval duration is minimized and time allocated to foraging can be extended.

Introduction

Diving marine mammals face a strong dilemma: their food resources are located at depth while they need to restore oxygen supply at the surface. This specificity makes them a particular case of optimal foraging theory with their breath hold capability limiting the time spent submerged. In the marine environment, air-breathing mammals can be reckoned as special central place foragers to the surface (Houston and McNamara, 1985). Hence, surfacing is essential to reconstitute oxygen stores by breathing and restoring oxygen levels in muscles and organs. Besides being conditioned by the distribution and the abundance of prey, the foraging behaviour of these animals is also fundamentally constrained by their physiological abilities, such as oxygen stores and the adaptations of their cardiovascular system (Castellini et al., 1985; Costa et al., 2004). Oxygen stores are higher for diving species than non-diving ones (Butler and Jones, 1997) and are located in the blood and muscles (Hassrick et al., 2010; Kooyman et al., 1983). Two thirds of Phocids' oxygen stores are located in the blood with a lower lung contribution (Meir et al., 2009).

Measures of physiological data are essential to investigate diving mammals foraging behaviour and energy expenditure, an essential information to estimate food consumption (Butler and Jones, 1997). Ideally, physiological parameters should be recorded on free-ranging animals diving voluntarily (Webb et al., 1998). However, accessing physiological data on animals freely ranging in the open ocean remains difficult. Pinnipeds share their time both at sea and on land or ice (Harrison and Kooyman, 1968). This bimodal cycle coupled to their large size makes them a unique system to study diving behaviour, because the deployment and recovery of loggers are eased on land (Costa et al., 2004). Kooyman et al. (1968; 1971; 1973) were the first to access physiological data and calculate metabolic rate using a respiratory chamber on free-ranging Weddell seals, *Leptonychotes weddellii*, with the man-made ice-hole experiments under semi-natural conditions. This technique is not reproducible to species foraging in the open ocean, which is why different methods have been developed to investigate the metabolisms of these animals. The doubly labelled water (DLW) method, which consists of measuring CO_2 production via isotopic analysis (Butler et al., 2004), is a common way to access metabolic rate. In spite of its simple application in the field, this method has been criticized because of its lack of accuracy: it provides the total energy expended over a period with an order of magnitude of some days and it overestimates metabolic rate (Butler et al., 2004; Costa, 1988; Ropert-Coudert et al., 2012).

Previous studies showed that heart rate was a reliable indicator of field metabolic costs (Butler et al., 2004; McPhee et al., 2003; Ropert-Coudert et al., 2012). Weimerskirch et al. (2000) successfully used heart rate as a proxy of energy expenditure and instantaneous effort in flying wandering albatrosses, with the highest heart frequencies observed while albatrosses were walking on land and taking off. This method also provides advantages over DLW in pinnipeds, since it provides an estimation of the metabolic rate of specific activities, such as those occurring during a dive cycle (Butler et al., 2004). The electric approach, which measures the electrical signal of the heart, is the most common way to record heart rate in free-ranging diving mammals (Ropert-Coudert et al., 2012; Webb et al., 1998).

Heart rate studies on elephant seals with an electric method showed that during diving, they exhibited bradycardia. Heart rate rapidly decreased by 50-80% at the beginning of the dive and remained low while the seal was submerged (Andrews et al., 1997). Hindell and Lea (1998) recorded extreme bradycardia with heart rate reaching 2 beats.min^{-1} in 23 dives. Heart rate then increased gradually as the seal rose to the surface (Andrews et al., 1997). Bradycardia, apnoea and vasoconstriction of the peripheral system constitutes the dive response in pinnipeds (Harrison and Kooyman, 1968). However, the electrical method require the fixation of an electrode into the body which can cause complications in the field (Ropert-Coudert et al., 2012).

An acoustic approach provided the first record of a respiratory rate at the surface of translocated northern elephant seals *(Mirounga angustirostris*) in 1996 (Fletcher et al., 1996). Between breaths, putative heart beats were distinguished and cardiac frequency extracted. Several acoustic studies confirmed that this method could provide physiological data such as breath frequency or heart rate at the surface (Burgess et al., 1998; Génin et al., 2015; Le Boeuf et al., 2000).

The aim of this study is to investigate the cardiac response at the surface to active dives in free-ranging southern elephant seals (SES here after). SESs are a major predator in the Southern Ocean. At sea, they dive repeatedly to around 500 m during 20-30 minutes with surface intervals lasting on average 2 minutes but extreme depth records reached over 1,800 m (Hindell et al., 1991; McConnell et al., 1992). They come back on land twice a year for mating during the southern spring and moulting in the summer, and exhibit high site fidelity (Fabiani et al., 2006).

Génin et al (2015) has shown that the number of breaths is tightly related to surfacing time and mainly explained by dive duration and swimming effort made by SESs. Yet, in terms of recovery, the cardiac function might play a major role. In this study, we intend to explore the recovery behaviour of SES through examining variation in heart frequency. First, we investigate how the instantaneous cardiac frequency evolves at the surface. Second, we study the relation between the mean cardiac frequency during the surface interval, and the dive duration and foraging effort performed by SESs during the previous dive.

Materials and methods

Ethics statement

All animals in this study were treated in accordance with the French Polar Institute (IPEV) ethical and Polar Environment Committees guidelines. All scientific procedures conducted on SES had been validated beforehand.

Deployment of devices and data collection

This study is based on data collected on four post-breeding SES females (Table 1): two equipped in October 2011 and another two in October/November 2012 on Kerguelen Islands (49°20’S, 70°20’E). Individuals were captured, then anaesthetized using 1:1 combination of tiletamin and zolazepam (Zoletil 100), which was injected intravenously (0.8 mg/100kg; McMahon et al., 2000). They were then equipped with two devices glued on the head or the back of the individual, using quick-setting epoxy (Araldite AW 2101, Ciba) after cleaning the fur with acetone. First, an Argos-GPS satellite tag (Splash 10-F, Wildlife Computer, USA) was glued to the head of the seals. It

provided real-time position of the seals through the Argos system and also collected GPS location data. Second, an autonomous acoustic/accelerometer/magnetometer and pressure logger named Acousonde^{TM}, model 3A (Acoustimetrics, Greeneridge Scences, Inc, USA) (Burgess, 2000; Burgess et al., 1998) was fixed on the dorsal fur on the longitudinal axis, 10 cm behind the scapula. Acousondes^{TM} recorded at a sampling frequency of 6.3 kHz in 2011 and 12.2 kHz in 2012, with both an acoustic sampling resolution of 16 bits. This difference in sampling rates does not interfere in our study as cardiac and respiratory events occur in a frequency range inferior to 1 kHz. To save battery power and storage space, it was programmed to record sound 3 h every 12 h in 2011 and 4 h every 24 h in 2012. All devices provided measurements of time, location and depth at 1 Hz, as well as the three-dimensional magnetic field strength and acceleration at a 5 Hz frequency. The instruments sampled acoustic data until battery exhaustion, which occurred between 10 and 20 days after deployment. All devices were retrieved once individuals returned ashore to moult after their foraging trip in January/February following deployments. Seals were located on land using their Argos position.

Acoustic data processing

Cardiac occurrences detection

When the animal is surfacing, the water flow noise produced by swimming ceases and most of the sound is due to breathing. Respiratory signals are contained between frequencies within the 0 and 700 Hz range. Between two respirations, spectrograms (time-frequency representation) showed putative cardiac occurrences (Fletcher et al., 1996; Le Boeuf et al., 2000). Heart sounds are expected to be dual due to the closure of mitral and the aortic valves (Burgess et al., 1998). The two sounds are undistinguishable, as they occur too close together in time. Hence, cardiac occurrences (a combination of the two valves' sounds) are brief and regular temporal impulsions at frequencies from 0 to 150 Hz (Burgess et al., 1998).

Acoustic recordings of surface intervals were visualized and analysed using the software Raven (The Cornell Lab of Ornithology – Bioacoustics Research Program) to generate a spectrogram for each surface interval. The same parameters were used for the computation of all spectrograms: a window of Hann type and a size of 512 samples, an overlap of 50 % and a Discrete Fourier Transform (DFT) calculated with 512 samples.

Each cardiac beat was determined using visual and auditory cues (Fig. 1). Hence, each occurrence is characterised by its temporal abscissa. When two beats are consecutive, an instantaneous cardiac frequency (beats.min^{-1}) is calculated using the temporal difference between the two occurrences (Eqn. 1).

Equation 1: **Instantaneous cardiac frequency** $(f_{Hinst}) = \frac{60}{x_{t+1} - x_t}$

Some surface intervals contained high-amplitude noise from external sources (water splashes possibly due to rough weather conditions or due to certain animal behaviours such as grooming). A noisy acoustic environment prevents access to heart data. As such, a surface interval was only kept for further analyses when a minimum of five cardiac beats were measured, so that the cardiac frequency could be estimated with confidence. Cardiac frequency for a surface interval f_H was computed as the average of f_{Hinst} (Eqn. 1) during each surface interval.

Surface interval duration

The beginning, end and duration of each surface interval, to the nearest second, was determined using visual and auditory cues. A surface interval begins with the first respiration and ends with the last one.

Dive cycle

A dive cycle is composed of a dive followed by a surface interval. SESs were considered to be diving when they reached depths greater than 15 m, to avoid considering subsurface movements as dives. A dive can be decomposed into three phases: descent, bottom and ascent. Each phase can be determined using a vertical speed criterion. Vertical speed was modelled with an order four polynomial function adjusted on instantaneous vertical speed using a custom-written Matlab code (Matlab software 8.1, The MathWorks, Natick, MA, USA). Ascent and descent phases were identified as periods before or after surfacing where the modelled vertical speed exceeded 0.75 $m.s^{-1}$. Bottom phases were identified as periods between ascent and descent phases where the modelled vertical speed remained below 0.75 $m.s^{-1}$ (Jouma'a et al., 2016; Vacquié-Garcia et al., 2015).

Dive parameters

For each surface interval where f_H ($beats.min^{-1}$) was measured, data from the previous dive were extracted from the Acousonde™ at a 5 Hz resolution. Statistics on each dive were then calculated to give: maximum depth reached (m), dive duration (min), descent, bottom and ascent duration (min) and the location (latitude and longitude) when the SES reached the surface. Elephant seals perform dives where they passively descend through the water column over a large proportion of time (Crocker et al., 1997). These passive 'drift' dives were identified based on the method designed by Dragon et al., (2012) using the package "rbl" (Le Bras, 2014) in R. A dive was considered as a passive drift dive when passive phases were detected with the following parameters: a minimum duration of 50 s, an absolute roll superior to 90° and a drift rate of between -0.4 and 0.6.

Another important dive parameter is total acceleration. It can be decomposed into two types: static and dynamic. Static acceleration is caused by earth's gravitational pull whereas dynamic acceleration results from the animal's movements (body waves, tail strokes, head motions). The static component corresponds to low frequencies and the dynamic one, to higher frequencies (Génin et al., 2015; Richard et al., 2014).

Mean swimming effort index (SE)

Data provided by accelerometers were used to calculate absolute and mean swimming effort index for each dive phase and for the entire dive (Eqn. 2). The lateral axis of the accelerometer contains information on putative turning and rolling movements (static acceleration) and on flipper stroke (dynamic acceleration) (Richard et al., 2014). Swimming effort was obtained by summing the absolute values of the local extrema of the lateral axis of the acceleration filtered with a band-pass filter which cuts frequencies bellow 0.44 Hz and above 1 Hz (Jouma'a et al., 2016; Richard et al., 2014). Mean swimming effort index was then calculated by dividing the absolute swimming effort by the duration (Δt) of the phase considered.

Equation 2: $$\boldsymbol{Mean\ Swimmind\ Effort\ index} = \frac{\sum|\boldsymbol{peaks}|}{\Delta \boldsymbol{t}}$$

$$\boldsymbol{Mean\ Swimming\ Effort\ index} = \frac{\boldsymbol{\sum|peaks|}}{\boldsymbol{\Delta t}}\ (\boldsymbol{m.s^{-2}})$$

Capture rate

Capture rate (s^{-1}) is the number of Prey Encounter Events (PEE) divided by the bottom duration of a dive. PEE were extracted from the acceleration signal which contained head movements by adapting the method developed by Viviant et al. (2009): on each axis, a high-pass filter with a cut-off frequency of 0.33 Hz was applied. Standard deviation was then calculated with a 1 second-fixed-window and then, a 5 second-moving-window. Significant peaks in this filtered signal were considered as PEE when they were detected simultaneously on all three axes (for details see Vacquié-Garcia et al., 2015).

Data design and statistical analyses

Analyses were conducted at two scales: surface interval level and dive cycle level. At the surface interval scale, the statistical unit is a measure of f_{Hinst} associated with temporal abscissa in seconds (0 corresponding to the beginning of the surface interval). At the dive cycle scale, the statistical unit is a dive cycle. We aimed to explain the mean heart frequency measured at the surface (f_H) using dive and surface interval parameters.

Instantaneous heart frequency at the surface

This part intended to study the evolution of the instantaneous heart frequency within a surface interval. The effect of the time on f_{Hinst} was examined using linear regression (lm function in "stats" R package; R Development Core Team, 2015). The regressions were conducted for each surface interval of each individual. First order effects were selected over second order effects based on an Akaike Information Criterion (AIC) selection (Zuur, 2009). Estimated slopes were used to determine the nature of f_{Hinst} variations. Then, a general model was run on all the surface intervals of the four individuals at the same time to explore the importance of the time on the f_{Hinst} (standardized values; n = 2978). Individual was set as a random factor. To take into account temporal correlation, an auto-correlation structure was included in model, using an auto-regressive correlation structure of order 1 (with the function corAR1 from the package 'nlme'; Pinheiro et al., 2015). The most relevant model, between random effects model, random intercept model or without random effect model, was selected based on AIC (Zuur, 2009).

Mean heart rate and number of beats at the surface

To investigate the contribution of previous dive behaviour on mean heart rate at the surface and on the number of cardiac beats at the surface, we used linear mixed-effects models, also from the package 'nlme'. Values outside the 1.5 interquartile range were removed from the data. All explanatory variables were centred and standardised by dividing by standard deviation at the population scale to keep individual differences and allow comparisons between slope estimates. Time (in days) was included in the model as we assumed a possible impact on the mean heart rate. To test linear and quadratic effects of the time, both variables were included in the model. Individual was set as a random factors, and an auto-regressive correlation structure was included (corAR1). The most parsimonious model, between a random effects model, random intercept model or without random effect model, was selected following Zuur (2009). Same models and same protocol were used to explain the number of beats at the surface.

All statistical analyses were conducted using the software R (R Development Core Team, 2015). Linear mixed-effects models were computed with the 'nlme' package (Pinheiro et al., 2015). For each model, normal distributions of the explained variable and of the residuals, and residuals' homogeneity were checked up. All results are expressed as mean ± standard deviation for single parameters. The significance level was set at $p = 0.05$.

Results

Foraging trips and overall diving behaviour

Each SES travelled eastward of Kerguelen Islands. Acousondes^{TM} provided data for the first days of foraging trips. We obtained 296 hours of sound recorded in 84 files of which 15 (53 hours) were immediately put aside because the animal was still on land or data were too bad to be exploited. Of the 243 hours left, there were 688 dive cycles and we kept the cycles that counted more than 5 heart beats. 284 dive cycles were kept for this study. On average, seals dived for 18.4 ± 3.7 min with a mean depth of 546 ± 159 m. Time spent at the surface recovering averaged 121 ± 19 s (*i.e.* 2 min 1 s; Table 2) with a maximum of 208 s (*i.e.* 3 min 28 s). Consequently, seals were submerged on average 90.1 % of the time, ranging from 89.3 % for ind. 3 to 91.1 % for ind. 4. The four individuals showed differences in their diving strategies. Ind. 1 performed deep long dives whereas ind. 2 performed shallower and shorter dives. Ind. 3 had a greater number of prey event encounters and higher capture rate compared to the three others (Table 3). The longest (33 min 12 s) and the deepest (938.2 m) dives were both performed by ind. 1.

There was a strong negative relationship between dive duration and mean swimming effort index across the four individuals (Pearson's correlation coefficient = -0.74, $p \leq 0.001$; Fig. 2).

Instantaneous cardiac frequency during surface intervals

There was a positive relationship between between f_{Hinst} and time in more than 90 % of the 284 dive. Mean R squared (meaning the percentage of the variance explained by the models) was 0.32 ± 0.26 with a minimum of 6.10^{-5} and a maximum of 0.97. Linear models showed that f_{Hinst} increased significantly with the time spent at the surface (Fig. 3, estimate = 0.009 ± 0.001, t = 7.41, $p \leq 0.001$) with no individual effect.

Mean heart rate at the surface and underwater

At the surface, mean heart rate was 102.4 ± 4.9 beats.min^{-1} with significant differences between seals (Kruskal-Wallis test: $\chi^2_3 = 42.8$, $p \leq 0.001$; Table 2). The mean heart rates for individual seals ranged from 99.0 ± 4.7 (ind. 4) to 105.7 ± 5.2 (ind. 3) beats.min^{-1} while they were breathing at the surface.

In most dives, flow noise generated by seal movements prevented the detection of heart beats. However quiet recording conditions observed during the passive drift phases allowed to detect beats (e.g. short impulse signals), in the frequency range between 0 and 40 Hz, which is likely be

attributed to heart beats. Drift dives were mainly observed in ind. 1 and were present in only 0.08 % of the dives studied here. The low-frequency pattern appeared during the whole passive drift event. A simple calculation of the frequency of occurrence based on drift events exhibited a mean of 20.2 ± 5.1 beats.min^{-1}.

Mean surface heart rate in relation to dive parameters

The most appropriate model in order to explain mean heart rate at the surface with dive parameters and time was the one without individual effect. The mean surface heart rate was found to be positively correlated with both the number of days elapsed since the departure form Kerguelen Island and the prey capture rate (Table 4). The quadratic time term significantly contributed to changes in the relationship. Its estimated coefficient was negative which means that the relation between heart rate and time directed towards a concave shape. Therefore, heart rate increased with time spent at sea, followed by a "plateau" effect (Fig. 4). Dive duration and swimming effort did not influence heart rate at the surface for the seals studied (Table 4).

Total number of heart beats at the surface in relation to dive parameters

To explore the variations of the number of beats counted in surface intervals, we used the same explanatory variables as above. As expected, a strong correlation between number of heart beats and surface duration was found (Pearson's coefficient = 0.96, $p \leq 0.001$). In this case, there were random effects (on the slope and the intercept) across individuals. The total number of heart beats during the surface interval was positively related to both the mean swimming effort index and dive duration. However the total number of cardiac beats at the surface was unrelated to prey capture rate and time (Table 4).

Discussion

Measuring heart rate through acoustic records

This study provides one of the very few datasets of heart rate, simultaneously with breathing rate (Génin et al., 2015) for free ranging post breeding female SESs. Previous studies carried out on heart rate used mainly captive or translocated animals (Andrews et al., 1997; Burgess et al., 1998; Fletcher et al., 1996; 1998; Le Boeuf et al., 2000). Acoustic records offer the possibility to access free-ranging SES heart rates during post-dive surface intervals, although records could contain heart sounds under water only when the flow noise stops (Burgess et al., 1998). This condition of quiet soundscape is satisfied when SESs are passively drifting through the water column. Therefore, heart rate could not be quantified while the seals were actively swimming or gliding underwater due to

associated flow noise. In our study, mean heart rate at the surface measured in the four voluntary diving post-breeding females was 102.4 ± 4.9 beats.min^{-1}. With northern elephant seals, previous acoustic studies recorded a mean heart rate at the surface of 86 beats.min^{-1} for adult males (Le Boeuf et al., 2000) and ranging from 106 to 121 beats.min^{-1} for juveniles (Burgess et al., 1998; Fletcher et al., 1996; Le Boeuf et al., 2000). All these studies demonstrate the reliability of the acoustic method to analyse the cardiovascular system. In our data, heart rate is detected only at the surface. Hindell and Lea (1998), using an electrical approach, extracted heart rate at the surface of one post-breeding SES female over a 50 days period, and found a heart frequency ranging between 65 and 95 beats.min^{-1} while at the surface breathing. They estimated that this number was underestimated by 10-15 % due to the sampling biases. Hence, both measures are in the same order of magnitude.

The electrical method also allowed the detection of heart beats while the SES was swimming underwater. During a dive, an elephant seal exhibits pronounced bradycardia (Elsner et al., 1966), a finding confirmed in free ranging seals (Burgess et al., 1998). Heart rate during diving of free ranging SESs decreases from 40 beats.min^{-1} for dives less than 13 min to 14 beats.min^{-1} for dives lasting between 13 min and 37 min (Hindell and Lea, 1998). In this study, we estimated heart rate during one drift dive and found 20.2 ± 5.1 beats.min^{-1}, which is consistent with the values found by Hindell and Lea, (1998) in their Fig. 3. The high standard deviation calculated here indicates a high variation between inter-beat intervals suggesting that bradycardia is unstable at depth. This is consistent with the hypothesis of Williams et al. (2015b) who found that both depth and exertion garble bradycardia in Weddell seals (*Leptonychotes weddellii*) and bottlenose dolphins (*Tursiops truncates*). However, this diving heart rate obtained by acoustics has to be validated in laboratory condition, using electrocardiogram methods for example.

Post-dive recovery and instantaneous heart rate

During surface interval periods, the instantaneous heart frequency increases with time: it is significantly higher at the end of the surface interval than at the beginning. Additionally, all seals exhibited the same pattern. This result probably represents a part of the dive response of the SES. Indeed, after reaching very low values when the seal chases at the bottom of its dive, heart frequency increases gradually while the seal ascends toward the surface (Harrison and Kooyman, 1968). Andrews et al. (1997) found that the rate of increase of tachycardia was most marked just prior to surfacing, approximately during the last 15 s of ascent. Therefore, increasing heart rate observed through the surface interval in this study is likely to correspond to the decelerating phase of the tachycardia which reaches its maximum value at the end of the surface interval, prior to

diving. Periods of tachycardia enable rapid oxygen loading at the surface, in both blood and muscle stores, and eliminating carbon dioxide accumulated during the previous dive (Reed et al., 1994). Associated with high breathing frequency, high heart rate eases quick gas exchange at the surface and a more efficient recovery (Fedak et al., 1988; Le Boeuf et al., 2000). Hence, surface duration is minimised and submergence times are maximized. Indeed, the four seals studied here spent about 90 % of time under the water, enabling this central place predator to take full advantage of its underwater preys.

Post-dive recovery and physical effort exerted by the SES

The costs associated with diving are a central component of a marine mammal's energy budget (Maresh et al., 2015). This budget can be decomposed into oxygen-consuming additive elements: basal metabolic costs, locomotor costs, feeding costs and thermoregulatory costs (Costa and Williams, 1999). In this study, exertion levels during diving have been evaluated via three parameters: dive duration, mean swimming effort index and capture rate. Contrary to our expectation that, like terrestrial mammals, heart rate should increase with increasing foraging effort no relationship was found between mean heart rate at the surface and dive duration or swimming effort. However a positive relationship was fond with both prey capture rate and the number of days elapsed since Kerguelen Island departure. Dive duration may not reflect the exertion level during a dive as it could be biased as SESs reduce their relative mean swimming effort with increasing dive duration (Fig. 2). Swimming effort *i.e.* movements of the tail, appear to be a reliable indicator of costs due to the locomotion (Williams et al., 2004; Wilson et al., 2006). Capture rate can easily be linked to foraging costs during a dive. Feeding events are responsible for an increase of 44.7 % of the energetic budget in Weddell seals (Williams et al., 2004). Nevertheless, interpretations should be presented with precaution as capture rate is calculated from prey catch attempts and not effective catches. Indeed, around 90 % of the dive cycles analysed in this study had at least one capture attempt.

Our results indicate that SESs manage their recovery by increasing the duration of the post-dive interval and therefore by increasing the total number of cardiac beats (*i.e.* the duration of the tachycardia) rather than acting on heart rate while at the surface. Indeed, the total number of heart beats was highly correlated with the time spent at the surface breathing. Dive duration and mean swimming effort were the two parameters that positively influenced time spent at the surface. Hence, a long dive and/or a dive where the SES gave a high quantity of large tail movements implies a long surface duration. This is in accordance with previous results obtained by Génin et al. (2015) with SES. In Weddell seals, *Leptonychotes weddellii*, the energy expenditure approximated

by the number of flipper strokes taken is highly correlated with the oxygen consumption (Williams et al., 2004). Maresh et al. (2014) showed that with an artificially increased cost of locomotion, northern elephant seals, *Mirounga angustirostris*, spent more time breathing and thus recovering. The relationship between dive duration and surface interval duration had already been demonstrated in several marine mammal species such as northern elephant seals (Andrews et al., 1997; Le Boeuf et al., 2000), grey seals, *Halichoerus grypus* (Thompson and Fedak, 1993) alongside diving birds including thick-billed murres, *Uria lomiva* (Croll et al., 1992).

Capture rate positively influenced mean heart rate at the surface. This result might indicate that seals recover from a foraging dive with a higher heart rate. Hence, the increase of surface mean heart rate after prey capture attempts could be explained by factors unrelated to swimming effort, such as the added energy required for prey warming and digestion. This hypothesis is consistent as prey assimilation affects both resting and diving metabolic rates (Williams et al., 2004).

This study strongly supports that the time spent at the surface and therefore the total number of breaths and heart beats, rather than heart beat frequency, appears to be the main driver of the post-dive recovery behaviour in SES. As such, the cardio-respiratory system as a whole needs to be considered to understand SES recovery strategy. Nonetheless, it is critical to bear in mind the complexity of the cardiac responses observed: cardiac regulation is controlled by neural drivers which themselves react to multiple factors such as the environment or a change in the behaviour (Williams et al., 2015b).

This study also revealed that the mean heart rate at the surface of the four seals varied with the time spent at sea with a non-linear relationship (Fig. 4). In the first 5-10 days of trip, the mean heart rate at the surface increased with time. Then, mean heart rate might decrease (ind. 3) or remain stable (ind. 1, 2 and 4). Females left Kerguelen Island after the breeding season in poor body condition as they lost 25-50 % of their original weight (McCann et al., 1989). Increasing mean heart rate could then reflect the adaptation, or a response to cardio-vascular training during the first few days spent at sea after one month spent on land. By assuming that the higher the heart rate is during surface breathing, the faster the gas exchanges should be, and so, recovery would be more efficient, we suppose that an “optimal” heart rate exists (linked with individual characteristics as body mass or composition) to maximise gas exchange at the surface. Therefore, future analyses with access to larger datasets and more individuals observed over a longer time period should be able to investigate this hypothesis.

Conclusion

This study indicates that SESs manage their post dive recovery by modulating their post dive surface duration, and therefore the number of breaths and heart beats, rather than acting on their breathing rate (Genin et al. 2015) or their heart rate as we found in this study.

Sound recording can be a powerful tool as it provides the simultaneous detection of breathing and heart frequencies, allowing the investigation of the cardio-respiratory system in its entirety (Génin et al., 2015; Le Boeuf et al., 2000). Both physiological data are essential to study post-dive recovery of marine mammals and seabirds. However, the main limitation is that we access the heart rate only when SESs are breathing at surface. A study on harbour seals (*Phoca vitulina*) suggested that the mean heart rate of the complete dive cycle (*i.e.* dive and surface) could be easily explained by the percent of dive time and link to oxygen consumption (Fedak et al., 1988). An improvement indata collection is essential to fully exploit the possibilities of the acoustic method. A major breakthrough would be to trigger audio recording based on external events of interest (e.g. using acceleration data). This would save battery and allow long-term dataset. Examples of interest include recording acoustic data when the animal is at the surface (to study surface heart rate) and/or during drift dive (to study underwater heart rate).

In addition, sound records can also be used to explore others aspects of the elephant seal behaviour and environment. They allow the collection of abiotic sounds, such as those generated by wind and rain, which represent a great interest for oceanographers as the Southern Ocean is difficult to observe. Acoustics offer many possibilities, and non-invasive bio-logging data collection could easily be improved by concertation between the users and the research teams in the future.

Acknowledgements

The authors thank all the fieldworkers for field work at the Kerguelen Islands that helped to collect data and the French Polar Institute (Institut Paul Emile Victor; IPEV) for the financial and logistical support. This study is part Antarctic research program 109 (led by H. Weimerskirch and the observatory Mammifères Explorateurs du Milieu Océanique, MEMO SOERE CTD 02) supported by the French Polar Institute. This work was carried out in the framework of the ANR Blanc MYCTO-3D-MAP, ANR VMC IPSOS-SEAL programs, CNES-TOSCA program (“Éléphants de mer océanographes”), and the DGA/MRIS “PAM Mobile” program. Finally, we wish to thank Samantha Cox for the English support.

Competing interests

No competing interests declared.

Author contribution

Conceptualization: C.G.; Methodology: L.D., J.J. and J.B.; Validation: J.B., J.J.; Formal analysis and investigation: L.D. and J.J.; Writing - original draft preparation: L.D; Writing - review and editing: L.D., J.J., C.G. and J.B.; Resources: C.G. and J.B.; Supervision: C.G. and J.B.; Funding acquisition: C.G.

Funding

The authors thank the Total Foundation and the DGA/MRIS for financial support.

Data availability

Data are available under request.

References

Andrews, R. D., Jones, D. R., Williams, J. D., Thorson, P. H., Oliver, G. W., Costa, D. P. and Boeuf, B. J. L. (1997). Heart rates of northern elephant seals diving at sea and resting on the beach. *Journal of Experimental Biology* **200**, 2083–2095.

Burgess, W. C. (2000). The bioacoustic probe: A general-purpose acoustic recording tag. *The Journal of the Acoustical Society of America* **108**, 2583–2583.

Burgess, W. C., Tyack, P. L., Le Boeuf, B. J. and Costa, D. P. (1998). A programmable acoustic recording tag and first results from free-ranging northern elephant seals. *Deep Sea Research Part II: Topical Studies in Oceanography* **45**, 1327–1351.

Butler, P. J. and Jones, D. R. (1997). Physiology of diving of birds and mammals. *Physiological Reviews* **77**, 837–899.

Butler, P. J., Green, J. A., Boyd, I. L. and Speakman, J. R. (2004). Measuring metabolic rate in the field: the pros and cons of the doubly labelled water and heart rate methods. *Functional Ecology* **18**, 168–183.

Castellini, M. A., Murphy, B. J., Fedak, M., Ronald, K., Gofton, N. and Hochachka, P. W. (1985). Potentially conflicting metabolic demands of diving and exercise in seals. *Journal of Applied Physiology* **58**, 392–399.

Costa, D. P. (1988). Methods for studying the energetics of freely diving animals. *Can. J. Zool.* **66**, 45–52.

Costa, D. P. and Williams, T. M. (1999). Marine mammal energetics. *Biology of marine mammals. Smithsonian Institution Press, Washington, DC* 176–217.

Costa, D. P., Kuhn, C. E., Weise, M. J., Shaffer, S. A. and Arnould, J. P. Y. (2004). When does physiology limit the foraging behaviour of freely diving mammals? *International Congress Series* **1275**, 359–366.

Crocker, D. E., Boeuf, B. J. L. and Costa, D. P. (1997). Drift diving in female northern elephant seals: implications for food processing. *Can. J. Zool.* **75**, 27–39.

Croll, D. A., Gaston, A. J., Burger, A. E. and Konnoff, D. (1992). Foraging Behavior and Physiological Adaptation for Diving in Thick-Billed Murres. *Ecology* **73**, 344–356.

Dragon, A., Bar-Hen, A., Monestiez, P. and Guinet, C. (2012). Horizontal and vertical movements as predictors of foraging success in a marine predator. *Marine Ecology Progress Series* **447**, 243–257.

Elsner, R., Franklin, D. L., Citters, R. L. V. and Kenney, D. W. (1966). Cardiovascular Defense against Asphyxia. *Science* **153**, 941–949.

Fabiani, A., Galimberti, F., Sanvito, S. and Hoelzel, A. R. (2006). Relatedness and site fidelity at the southern elephant seal, Mirounga leonina, breeding colony in the Falkland Islands. *Animal Behaviour* **72**, 617–626.

Fedak, M. A., Pullen, M. R. and Kanwisher, J. (1988). Circulatory responses of seals to periodic breathing: heart rate and breathing during exercise and diving in the laboratory and open sea. *Can. J. Zool.* **66**, 53–60.

Fletcher, S., Boeuf, B. J. L., Costa, D. P., Tyack, P. L. and Blackwell, S. B. (1996). Onboard acoustic recording from diving northern elephant seals. *The Journal of the Acoustical Society of America* **100**, 2531–2539.

Génin, A., Richard, G., Jouma'a, J., Picard, B., El Ksabi, N., Vacquié Garcia, J. and Guinet, C. (2015). Characterization of postdive recovery using sound recordings and its relationship to dive duration, exertion, and foraging effort of southern elephant seals (*Mirounga leonina*). *Marine Mammal Science* **31**, 1452–1470.

Harrison, R. J. and Kooyman, G. L. (1968). General physiology of the pinnipedia. In *The Behavior and physiology of pinnipeds*, pp. 211–296. Appleton-Century-Crofts.

Hassrick, J. L., Crocker, D. E., Teutschel, N. M., McDonald, B. I., Robinson, P. W., Simmons, S. E. and Costa, D. P. (2010). Condition and mass impact oxygen stores and dive duration in adult female northern elephant seals. *Journal of Experimental Biology* **213**, 585–592.

Hindell, M. A. and Lea, M. (1998). Heart Rate, Swimming Speed, and Estimated Oxygen Consumption of a Free-Ranging Southern Elephant Seal. *Physiological Zoology* **71**, 74–84.

Hindell, M., Slip, D. and Burton, H. (1991). The Diving Behavior of Adult Male and Female Southern Elephant Seals, Mirounga-Leonina (Pinnipedia, Phocidae). *Aust. J. Zool.* **39**, 595–619.

Houston, A. I. and McNamara, J. M. (1985). The variability of behaviour and constrained optimization. *Journal of Theoretical Biology* **112**, 265–273.

Jouma'a, J., Le Bras, Y., Richard, G., Vacquié-Garcia, J., Picard, B., El Ksabi, N. and Guinet, C. (2016). Adjustment of diving behaviour with prey encounters and body condition in a deep diving predator: the Southern Elephant Seal. *Functional Ecology* **30**, 636–648.

Kooyman, G. L. (1968). An Analysis of Some Behavioral and Physiological Characteristics Related to Diving in the Weddell Seal. In *Biology of the Antarctic Seas III*, pp. 227–261. American Geophysical Union.

Kooyman, G. L., Kerem, D. H., Campbell, W. B. and Wright, J. J. (1971). Pulmonary function in freely diving Weddell seals, Leptonychotes weddelli. *Respiration Physiology* **12**, 271–282.

Kooyman, G. L., Kerem, D. H., Campbell, W. B. and Wright, J. J. (1973). Pulmonary gas exchange in freely diving weddell seals Leptonychotes weddelli. *Respiration Physiology* **17**, 283–290.

Kooyman, G. L., Castellini, M. A., Davis, R. W. and Maue, R. A. (1983). Aerobic diving limits of immature Weddell seals. *J Comp Physiol B* **151**, 171–174.

Le Boeuf, B. J., Crocker, D. E., Grayson, J., Gedamke, J., Webb, P. M., Blackwell, S. B. and Costa, D. P. (2000). Respiration and heart rate at the surface between dives in northern elephant seals. *Journal of Experimental Biology* **203**, 3265–3274.

Le Bras, Y. (2014). *rbl: Biologging tools in R. R package version 0.1.27. https://github.com/SESman/rbl*.

Maresh, J. L., Simmons, S. E., Crocker, D. E., McDonald, B. I., Williams, T. M. and Costa, D. P. (2014). Free-swimming northern elephant seals have low field metabolic rates that are sensitive to an increased cost of transport. *Journal of Experimental Biology* **217**, 1485–1495.

Maresh, J., Adachi, T., Takahashi, A., Naito, Y., Crocker, D., Horning, M., Williams, T. and Costa, D. (2015). Summing the strokes: energy economy in northern elephant seals during large-scale foraging migrations. *Movement Ecology* **3**, 22.

McCann, T. S., Fedak, M. A. and Harwood, J. (1989). Parental investment in southern elephant seals, Mirounga leonina. *Behav Ecol Sociobiol* **25**, 81–87.

McConnell, B. J., Chambers, C. and Fedak, M. A. (1992). Foraging ecology of southern elephant seals in relation to the bathymetry and productivity of the Southern Ocean. *Antarctic Science* **4**, 393–398.

McMahon, C. R., Burton, H., Slip, D., McLean, S. and Bester, M. (2000). Field immobilisation of southern elephant seals with intravenous tiletamine and zolazepam. *Veterinary Record* **146**, 251–254.

McPhee, J. M., Rosen, D. A. S., Andrews, R. D. and Trites, A. W. (2003). Predicting metabolic rate from heart rate in juvenile Steller sea lions Eumetopias jubatus. *Journal of Experimental Biology* **206**, 1941–1951.

Meir, J. U., Champagne, C. D., Costa, D. P., Williams, C. L. and Ponganis, P. J. (2009). Extreme hypoxemic tolerance and blood oxygen depletion in diving elephant seals. *American Journal of Physiology - Regulatory, Integrative and Comparative Physiology* **297**, R927–R939.

Pinheiro, J., Bates, D., DebRoy, S., Sarkar, D. and R Core Team (2015). Linear and Nonlinear Mixed Effects Models. *R package version 3.1-122*.

R Development Core Team (2015). R: A language and environment for statistical computing. *R Foundation for Statistical Computing, Vienna, Austria.*

Reed, J. Z., Chambers, C., Fedak, M. A. and Butler, P. J. (1994). Gas exchange of captive freely diving grey seals (Halichoerus grypus). *Journal of Experimental Biology* **191**, 1–18.

Richard, G., Vacquié-Garcia, J., Jouma'a, J., Picard, B., Génin, A., Arnould, J. P. Y., Bailleul, F. and Guinet, C. (2014). Variation in body condition during the post-moult foraging trip of southern elephant seals and its consequences on diving behaviour. *Journal of Experimental Biology* **217**, 2609–2619.

Ropert-Coudert, Y., Kato, A., Grémillet, D. and Crenner, F. (2012). Bio-logging: recording the ecophysiology and behaviour of animals moving freely in their environment. In *Sensors for ecology*, pp. 17–41.

Thompson, D. and Fedak, M. A. (1993). Cardiac responses of grey seals during diving at sea. *Journal of Experimental Biology* **174**, 139–154.

Vacquié-Garcia, J., Guinet, C., Dragon, A., Viviant, M., El Ksabi, N. and Bailleul, F. (2015). Predicting prey capture rates of southern elephant seals from track and dive parameters. *Marine Ecology Progress Series* **541**, 265–277.

Viviant, M., Trites, A. W., Rosen, D. A. S., Monestiez, P. and Guinet, C. (2009). Prey capture attempts can be detected in Steller sea lions and other marine predators using accelerometers. *Polar Biol* **33**, 713–719.

Webb, P. M., Costa, D. P., Boeuf, B. J. L. and Andrews, R. D. (1998). Heart Rate and Oxygen Consumption of Northern Elephant Seals during Diving in the Laboratory. *Physiological Zoology* **71**, 116–126.

Weimerskirch, H., Guionnet, T., Martin, J., Shaffer, S. A. and Costa, D. P. (2000). Fast and fuel efficient? Optimal use of wind by flying albatrosses. *Proceedings of the Royal Society of London B: Biological Sciences* **267**, 1869–1874.

Williams, T. M., Fuiman, L. A., Horning, M. and Davis, R. W. (2004). The cost of foraging by a marine predator, the Weddell seal Leptonychotes weddellii: pricing by the stroke. *Journal of Experimental Biology* **207**, 973–982.

Williams, T. M., Fuiman, L. A., Kendall, T., Berry, P., Richter, B., Noren, S. R., Thometz, N., Shattock, M. J., Farrell, E., Stamper, A. M., et al. (2015a). Exercise at depth alters bradycardia and incidence of cardiac anomalies in deep-diving marine mammals. *Nat Commun* **6**, 6055.

Williams, T. M., Bengtson, P., Steller, D. L., Croll, D. A. and Davis, R. W. (2015b). The Healthy Heart: Lessons from Nature's Elite Athletes. *Physiology* **30**, 349–357.

Wilson, R. P., White, C. R., Quintana, F., Halsey, L. G., Liebsch, N., Martin, G. R. and Butler, P. J. (2006). Moving towards acceleration for estimates of activity-specific metabolic rate in free-living animals: the case of the cormorant: Activity-specific metabolic rate in free-living animals. *Journal of Animal Ecology* **75**, 1081–1090.

Zuur, A. F. ed. (2009). *Mixed effects models and extensions in ecology with R*. New York, NY: Springer.

Tables

Table 1: Descriptive information about the four post-breeding female SESs at deployment

Seal ID	Acousonde ID	Body mass (kg)	Size (cm)	Departure day
1	A031	255	254	10 Oct 2011
2	A032	245	238	28 Oct 2011
3	626019	230	232	28 Oct 2012
4	626040	292	225	01 Nov 2012

Table 2: Surface interval parameters (mean ± sd)

Individual	Number of dives	Surface interval	Heart rate

	cycle	(s)	(beats.min^{-1})
1	102	132 ± 19	102.4 ± 4.6
2	85	107 ± 13	101.0 ± 3.7
3	70	122 ± 13	105.7 ± 5.2
4	28	121 ± 18	99.0 ± 4.7

Table 3: Dive parameters of the four female SESs (mean ± sd)

Ind.	Maximum depth (m)	Dive duration (min)	Number of PEE	Capture rate (s^{-1})	Mean swimming effort index ($m.s^{-2}$)
1	611.5 ± 164.4	21.2 ± 3.1	4.9 ± 3.4	0.015 ± 0.023	3.3 ± 0.6
2	434.9 ± 114.9	15.5 ± 2.5	6.4 ± 5.0	0.014 ± 0.011	5.2 ± 0.5
3	575.3 ± 138.5	17.0 ± 2.4	8.9 ± 5.4	0.026 ± 0.020	4.6 ± 0.4
4	579.7 ± 128.2	20.5 ± 2.8	6.6 ± 5.7	0.015 ± 0.015	3.7 ± 0.7

Table 2: Results of linear models looking at mean surface heart rate or at the number of beats in relation to dive parameters and time spent at sea (NS: no statistically significant)

Model	Parameter	Coefficient estimate	p-value
f_H ~	Intercept	94.2 ± 1.5	≤ 0.001
	Mean swimming effort ($m.s^{-2}$)		NS
gls model	Dive duration (min)		NS
corr ~ time (s) | ind	Capture rate (s^{-1})	0.3 ± 0.1	0.02
	Time (days)	1.5 ± 0.4	≤ 0.001
	$Time^2$	-0.05 ± 0.02	0.02
Number of beats ~	Intercept	225.2 ± 22.5	≤ 0.001
	Mean swimming effort ($m.s^{-2}$)	20.4 ± 8.4	0.01
lme model	Dive duration (min)	14.9 ± 7.5	0.04
random ~ slope | ind	Capture rate (s^{-1})		NS
corr ~ time (s) | ind	Time (days)		NS
	$Time^2$		NS

Figure legends

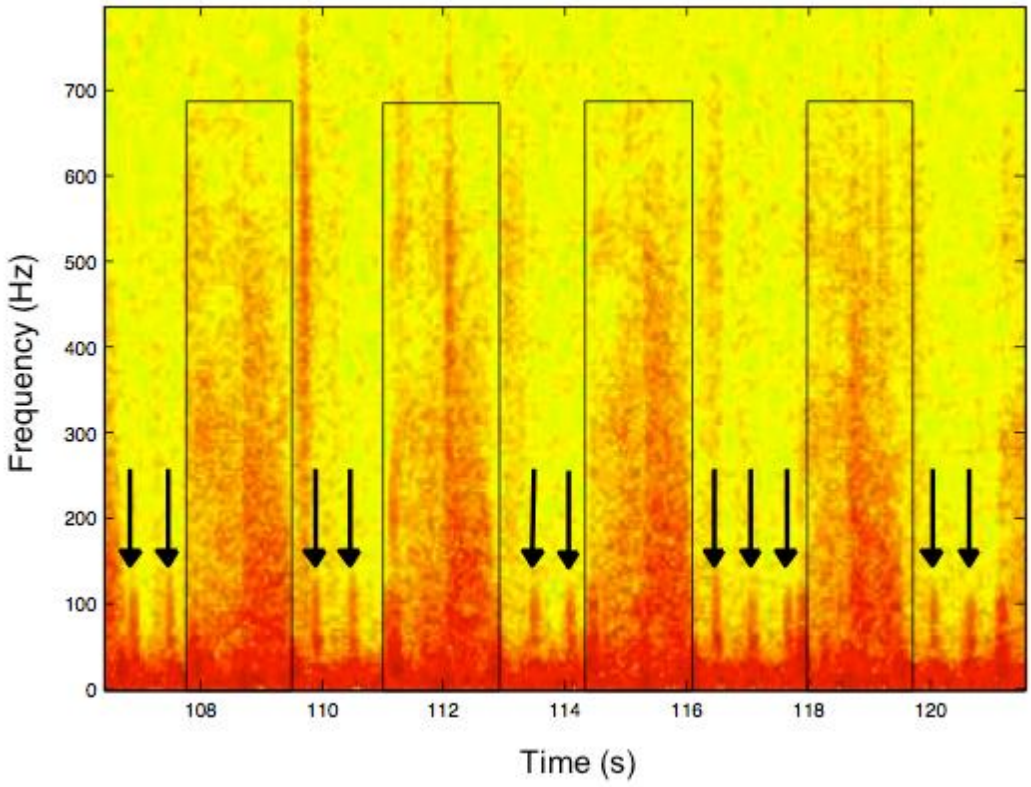

Figure 1: spectrogram of recorded sound performed by ind. 1 during a surface interval showing five respiratory cycles (rectangles in the 0-700 Hz range) with cardiac occurrences between breaths (black arrows in the 0-150 Hz range)

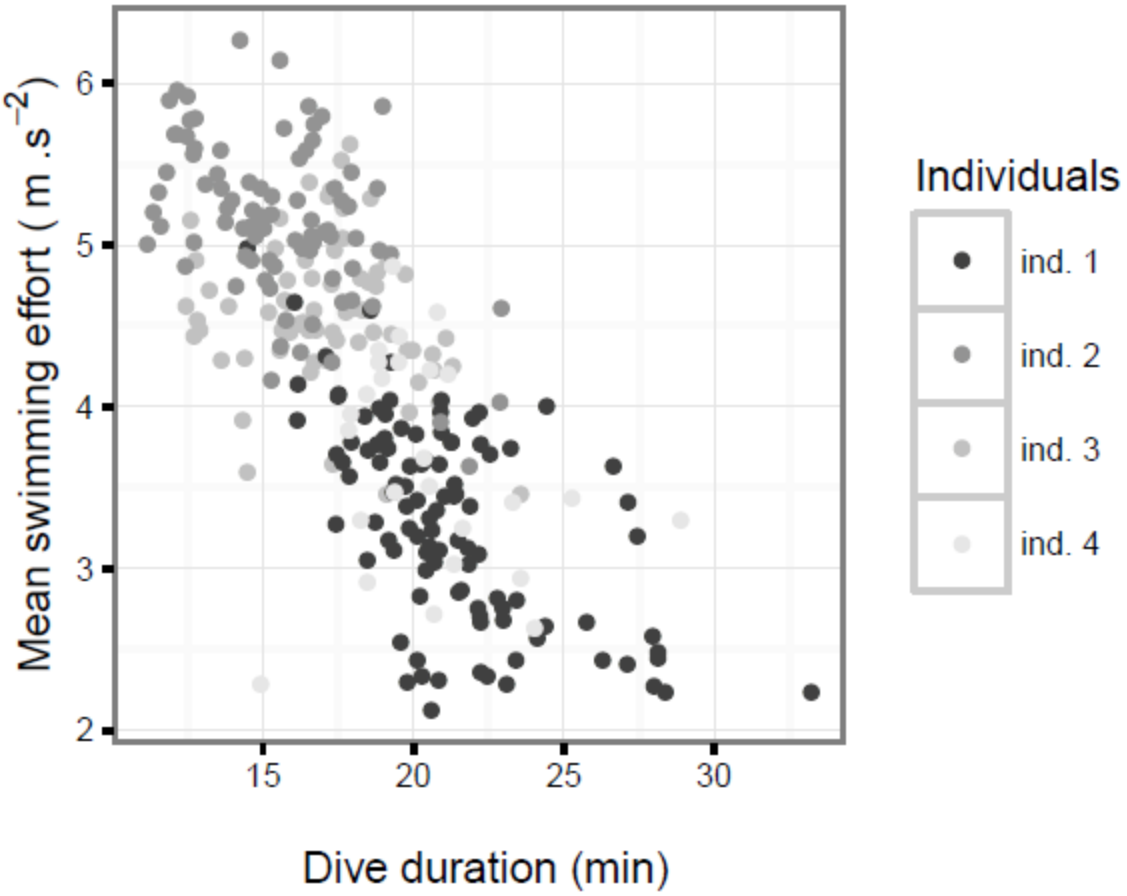

Figure 2: relationship between the dive duration and the mean swimming effort for the four SES studied

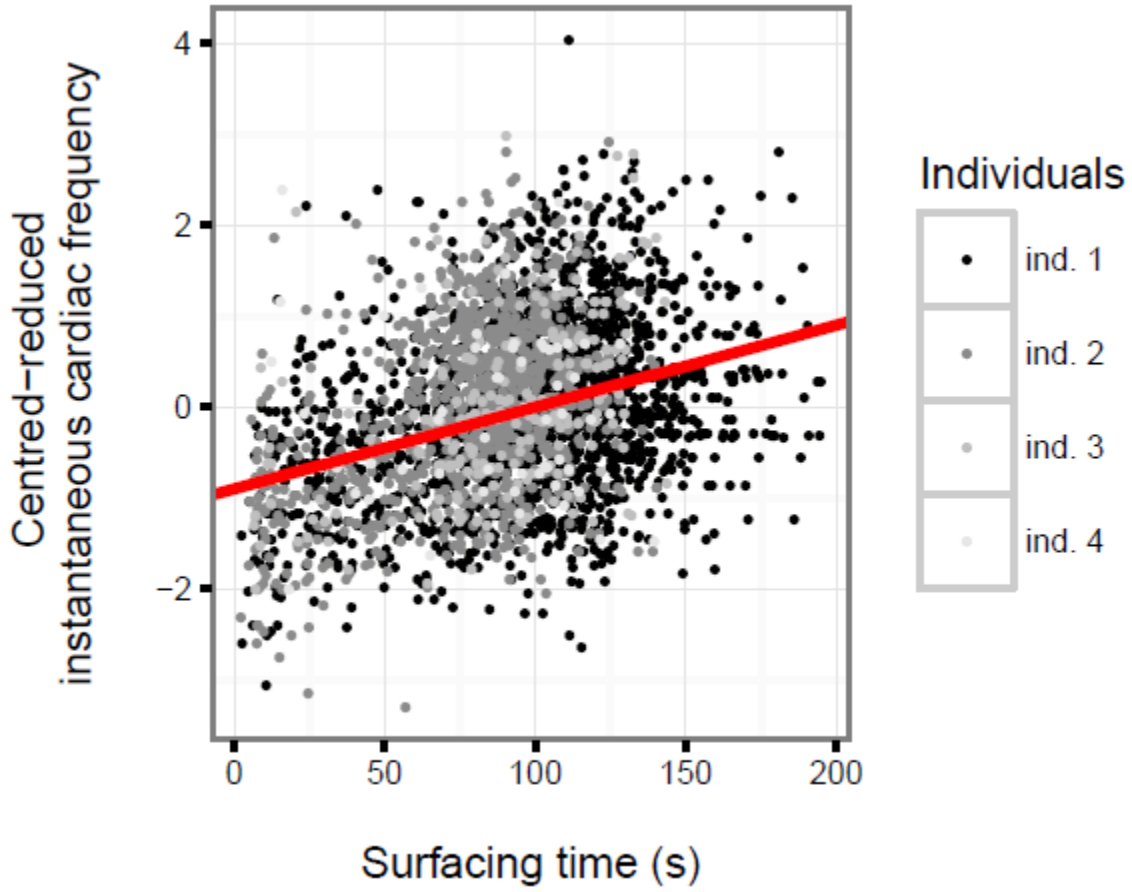

Figure 3: linear relationship between time and f_{Hinst} of the four seals: f_{Hinst} = -0.9 + 0.009*Surfacing time

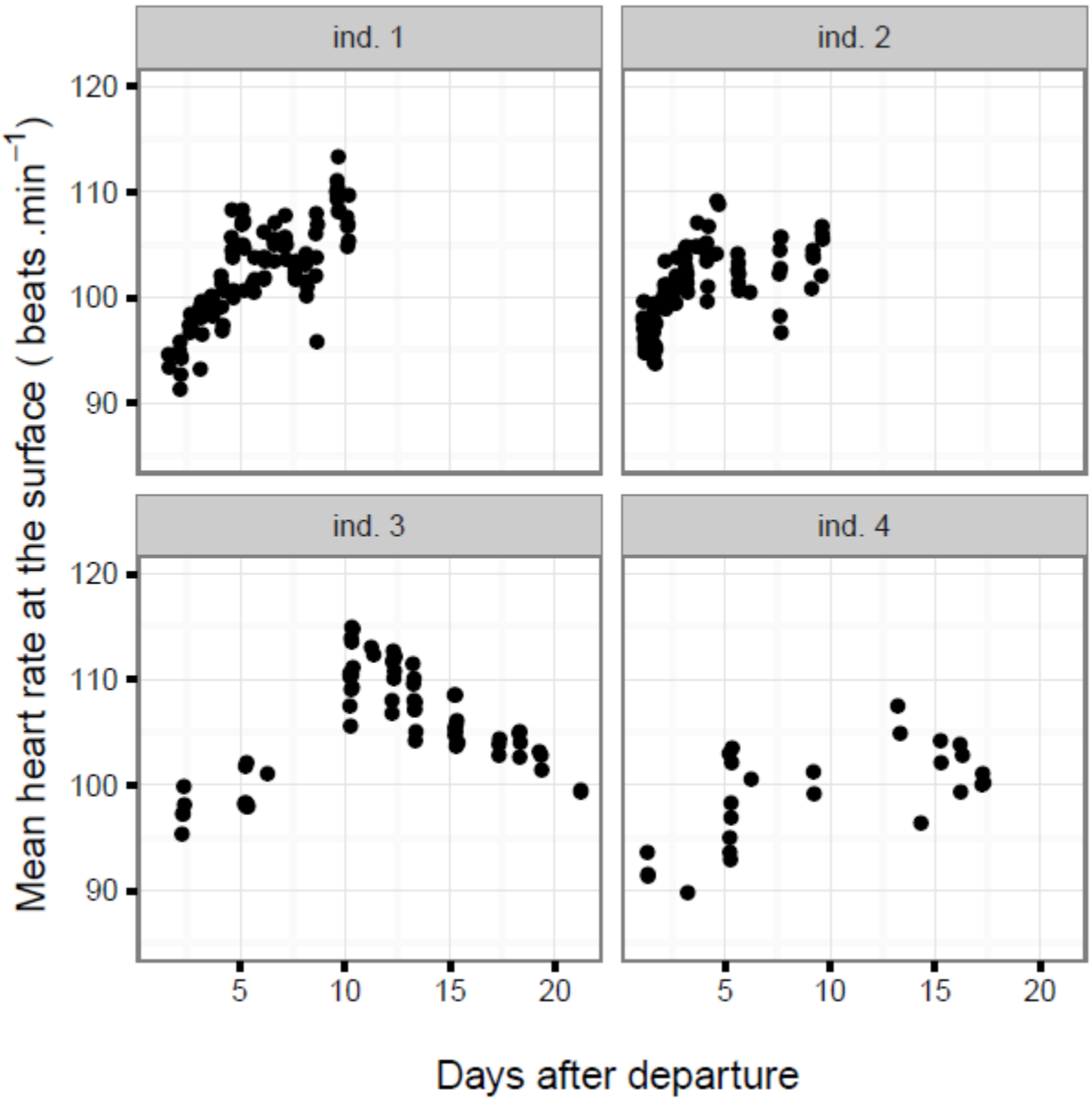

Figure 4: relationship between time spent at sea after breeding season on Kerguelen Island and the mean heart rate measuring during post-dive interval surface for the four female elephant seals

ANNEXE F

Usage of the three-dimensional space at the bottom of the southern elephant seals' dives

Yves, Le Bras, Jouma'a, Joffrey, & Guinet Christophe, Usage of the three-dimensional space at the bottom of the southern elephant seals' dives. *Movement Ecology* (to be submitted)

RESEARCH

Usage of the three-dimensional space at the bottom of the southern elephant seals' dives

Yves Le Bras*, Joffrey Jouma'a and Christophe Guinet

Abstract

Temporary version. To be edited last.

Background: In marine pelagic ecosystems, the spatial distribution of biomass is heterogeneous and dynamic. At large scales, the physical processes are the main driving forces of the distribution. At fine scales, the biotic interactions are likely to be a key determinant however the fine scale spatial interactions between deep diving predators and their prey are still poorly known.

Results: We examined the shape of southern elephant seals path in the bottom of their dives and related it to the estimated prey encounter event density. We found that southern elephant seals track at bottom is strongly dominated by a single horizontal direction allowing the southern elephant seals to explore a large volume of water when foraging at depth. Horizontal deviation across this directional path did not relate to the estimated prey density, suggesting that horizontal exploration is not required in a high prey density environment. However, the extent of the vertical deviations from the main linear component of the track was found to impact negatively on the estimated prey density.

Conclusion: Our results support the hypothesis that southern elephant seals' prey tend to aggregate into discrete schools. As drawn from the shape of the southern elephant seals' trajectories during the bottom phase of their dives, the prey patch are likely to be structured into layers of where prey density is controlled by vertical constraints acting over the spread of the layer. We suggest that, with a limited detection range, this behaviour allows the southern elephant seals to travel great distances and to maximize the volume of water they can prospect for prey items.

Keywords: diving behaviour; three-dimensional reconstruction; prey density; prey distribution; prey patch

Background

The myctophids also called lanternfish are a prime importance resource in most of the world's ocean including the Southern ocean [1]. In the Southern Ocean, these mid-trophic level mesopelagic fish make the connection between macro-zooplankton and top diving predators such as birds (chinstrap penguins [2], king penguins [3]) and marine mammals such as the the antarctic fur seal [4] southern elephant seals

* Correspondence: yveslebras.fr@gmail.com

Centre d'Etude Biologiques de Chizé, UMR 7372, CNRS-ULR, 79360 Villiers-en-bois, France

Full list of author information is available at the end of the article

(*Mirounga leonina*, hereafter SES) [5]. Indeed, SES primarily feed on myctophids [5] and on squids [6]. Because to their large size and abundance, they are likely major consumers of these resources in the Southern Ocean [7, 8]. The otoliths of three common myctophid species (*Electrona antarctica*, *E. carlsbergi* and *Gymnoscopelus nicholsi*) have been found in stomachs of female SES [9, 10]. Despite the key role of the myctophids in pelagic ecosytems, there is a lack of data and knowledge about their ecology, particularly in the remote Southern Ocean [11]. In pelagic ecosystems, dynamic physical processes and ecological interactions lead to a complex and changing spatial distribution of organisms, composed of hierarchically nested patches [12, 13]. Describing this spatial structure for myctophid and understanding the underlying physical and biological processes is a key to be able to understand their ecology and ultimately to anticipate how environmental changes may impact on them [14].

Trawling and acoustic surveys performed in the sectors of South Georgia, Kerguelen and Tasmania have begin to unravel the distribution and schooling patterns of myctophids [11, 15–19]. These surveys provided fundamental data about the myctophid ecology such as their specific richness and their relative abundance, their migration patterns and biologic description (length, weight, and specific structure such as swim bladder). Acoustic survey highlighted large scale relationships between the number of schools and the water temperature and dynamic height [18]. However, collecting data about the fine-scale patterns of the myctophids distribution raises difficulties using these techniques. Accurate sampling of a school with a pelagic trawl is technical and surfacing while avoiding trawl contamination adds a level of complexity. Regarding acoustics, the low-frequency signal required to scan the deep areas inhabited by the myctophids implies a low-resolution and limited ability to distinguish species. Bio-logging allows to track the movements of free-ranging marine predators and to collect the concomitant oceanographic data. Such data allowed bringing light on the foraging habitat of marine predators at large and intermediate scales, highlighting the ecological importance of fronts, eddies and filaments [20–26] but they also provide very fine scale information about the predators behaviour at depth. SES can carry loggers with minimal disturbance [27] making them a data-rich species studied in many bio-logging research projects [28]. At fine-scale, the distribution of their prey is expected to be patchier, more rapidly changing and more susceptible to the impact of biotic interactions [14, 29]. In this study we investigate about how the detailed informations about the diving behaviour of SES could provide insights about this fine-scale distribution.

The distribution of predators and prey are necessarily linked. The optimal foraging theory [30–32] predicts that predator should seek out areas with high prey density while preys should avoid high predator density grounds [33]. The correlation between the spatial distributions of predator and prey depends on the balance between the responses of one to another [34]. In the case of a mobile predator that feed on a prey more static than it, the spatial distributions of the predator and of the prey are expected to be positively correlated [34]. The assumption that movements of predators mimic the spatial pattern of the prey, have received support from many studies on birds and marine mammals: For instance, the diel vertical migrations performed by myctophids [35] translate into the same pattern with the diving depth of elephant seals (*Mirounga angustirostris* and SES) [36]. Another example is the detection of low transit rate or Area-restricted search behaviour [37, 38] (ARS) from GPS tracks which have been widely used to infer the loca-

tion and characteristics of important feeding areas of various marine predators [39–44] .

Ocean is a tri-dimensional (3D) environment. The SES can dive at an average depth of 400 m (up to 2000 m), [45]) and explore a large extent of the water column. Because their foraging strategy can be modified by acting on both horizontal and vertical movements [46–48], it worths examining how the three spatial dimension are involved in the interactions between diving predators and their prey. However, most studies investigating the usage of space by the marine predators have either analysed the animals' behaviour from their GPS track (2D approach), or from time-depth data (uni-dimensional approach). Some efforts have been made to combine these two approaches in order to examine the foraging strategies according horizontal and vertical dimensions (pseudo 3D approach) [49–51]. However, a detailed understanding of how the diving predators use their 3D spatial environment and interact with prey schools requires the actual reconstruction of their 3D path underwater. The 3D path analysis has started to bring new insights into the behaviour of elephant seals [52, 53] and other diving predators [46, 54–58] but also into the fine scale patterns of their prey distribution [59]. To study the fine-scale patterns in the prey distribution and their mechanistic relationships with the behaviour of their predator, we focused on the scale of a dive bottom phase which represents a fundamental organization unit of the foraging strategy where most feeding occurs for many of diving predators [48, 60–65].

In this study six datasets with three-axial acceleration and magnetometry and acoustic recording, sampled at high frequency, allowed us to reconstruct the three-dimensional underwater path of SES using the well established dead-reckoning method [66]. We examine the shape of SES path during the bottom phase of their dives and related it to the estimated prey encounter event density in a attempt to describe the spatial structure of the SES prey at depth.

Methods

Deployment of devices and data collection

During the breeding seasons (October and November) of 2011 and 2012, a total of six SES females of the Kerguelen Islands (49°21′0″ S, 70°13′0″ E), with an average lengths of 2.37 m and an average weights of 278 kg, were equipped with an acoustic tag (Acousondes^{TM} model 3A, manufactured by Acoustimetrics, Greeneridge Sciences, Inc, USA) and a Time-Temperature-Depth Fastloc GPS data logger (SPLASH10-F^{TM} manufactured by Wildlife Computers, USA) to collect locations while animal are at sea. Acousondes^{TM} were programmed to sample depth, light and temperature at 1 Hz, tri-axial (longitudinal, lateral and vertical axes of the logger) body acceleration and tri-axial earth magnetic field at 5 Hz and sound. Animals were captured with a canvas headbag and anesthetized using a 1:1 combination of Tiletamine and Zolazepam (Zoletil 100) injected intravenously [67]. The Acousondes^{TM} were then glued on the seal's back and the SPLASH10-F^{TM} on their head using quick-setting Araldite (Araldite AW 2101), aligning the longitudinal axes of the animals and of the loggers. Details about the length and weight of the equipped animals are provided in Table 1. The sound recording implies high energy consumption. To extend the recording duration we programmed the Acousondes^{TM} to record sound at a frequency of 6 kHz for three hours every 12 hours in 2011 and at a frequency of 12.2 kHz for three hours every 24 hours for the four individuals equipped in 2012.

Table 1 should be inserted here.

Dive analysis

Unless otherwise specified, the data processing and the analysis described in this section were performed using

the R statistical software [68]. The custom code used for the archive data processing is available online as a R package called `rbl` [69].

Dives and dive phases

We defined dives as periods where animals were continuously deeper than 15 m under the surface. This conservative threshold avoids considering brief subsurface excursions as actual dives. Because there is a drift in the pressure readings of the tags over time, a zero offset correction of depth time sequence was applied prior to the delimitation of dives. Each dive was then divided into three phases - descent, bottom and ascent - using the method described in [70]. The bottom phase is defined as the period of a dive where the vertical speed signal, simplified using a polynomial of degree 4, stays under a threshold of 0.75 $\mathrm{m\,s^{-1}}$. Simplifying the vertical speed signal using a polynomial fit allows the method to be sensitive to the overall shape of the time-depth trajectory but not to small scale anomalies such as steps performed in the middle of the descent and ascent phases. The fourth degrees provide enough freedom for the model to handle V-shaped and squared dives. Eventually, the vertical speed threshold was chosen after a blind experiment minimizing the difference between the automatic and the visual delineation of the bottom phases.

The drift dives are specific dives where SES are resting and/or digesting [71] and not expected to react when encountering prey items. Since our focus is on spatial patterns related to predator-prey interactions, we identified and removed these dives from our dataset prior to the analysis.

Prey encounter events

To identify prey encounter event we implemented the method described in [26, 70, 72] (but see [72] for details). The dynamic acceleration resulting from rapid head movements was extracted from the three axes with an order 3 high-pass digital Butterworth filter with a normalized cut-off frequency of 2.4 Hz (performed with `butter` and `filtflit` functions from the `signal` package [73]). For each axis, a one-second fixed window was used to calculate the standard deviation every second. Signals were then processed using a moving standard deviation with a window size of five seconds. Finally, a two-mean clustering was performed for each signal to distinguish "high state" from "low state". These successive operations are performed using the `prey_catch_attempts` function from the `rbl` package. A prey encounter event (hereafter PEE) is occurring when the three axes are simultaneously in "high state". A continuous succession of "high state" is considered as a single PEE.

Three-dimensional path reconstruction

Three-dimensional reconstruction by dead-reckoning (also called path integration) consists in cumulating the successive speed-vectors of the animal (in our case, every second) starting from a known location (in our case, a GPS location collected in the surface period preceding the dive). When arrival point is known, the reconstructed track can be scaled to match the observed locations at departure and arrival (GPS location collected in the surface period following the dive) and reduce the positional uncertainties [66].

Pitch, roll and heading angles describe the body posture of SES with respect to the direction of the earth gravity vector (pitch and roll angles) and earth magnetic vector (heading angle). Assuming that the animals always move in the direction of their longitudinal axis, pitch and heading angles provide all the necessary directional information for the 3D reconstruction. The static acceleration is the gravity based acceleration component. It can be obtained by applying the appropriate low-frequency filter to the acceleration signal. As [74], we used an order 3 low-pass digital Butterworth filter with a normalized cut-off frequency of

0.20 Hz applied to the three axes. The direction of the gravity vector according to the accelerometer provides a reference to calculate the pitch and roll angles of the SES (we used the `pitch` and `roll` functions from the `animalTrack` package [75]). The low-pass filter was applied to the magnetic data as well. The resulting signal, combined with pitch and roll information allows to calculate the heading angle (performed using `tilt_compensate` function from the `animalTrack` package).

Then, to fulfil the missing information about the speed-vectors prior to the dead-reckoning 3D reconstruction, we had to calculate the swimming speed of SES. The swimming speed of SES relatively to surrounding water was assessed using sound [76] which was recorded by the Acousondes^{TM}. This task was performed in MATLAB using custom code which is available on request. The principle of the method is to calibrate the relationship between the water flow noise level and the swimming speed of SES in the few parts of the dataset where it could be calculated reliably from acceleration data and then, to extrapolate swimming speed over the entire dive periods from the noise level using this relationship. In a first step, the low-frequency noise was extracted with a 110 Hz low-pass filter. In a second step, we selected segments of the descent phases of dives where SES had a steep pitch angle and a steady trajectory and computed the swimming speed (v_{seal}) using the vertical speed (v_z) and the pitch angle (α): $v_{seal} = v_z/sin(\alpha)$. These segments were defined as the periods of descents where SES were deeper than 200 m depth, continuously diving with pitch angle steeper than -75 degrees. These two thresholds ensure that residual air in the lung of the SES will not affect the seal's buoyancy [74, 77, 78] and that trigonometry formulas would be accurate.

Eventually we performed the 3D path reconstruction (Figure 2), forcing the departure and arrival points to match the observed GPS locations collected during the surface period preceding and following the dives (`dead_reckoning` function of the [75] package applied on the body posture angles, swimming speed and GPS data), Because the Acousondes^{TM} were programmed to record acoustic data at specific hour of the day, we could not predict the swimming speed at night. As a consequence, all the 3D dives of our dataset occurred during daytime.

Figure 2 should be inserted here.

Shape of bottom phase trajectories

To describe how the SES used the 3D space during the bottom of their dives, we extracted the main components of the animals path during the bottom phases. This was achieved by computing the eigenvalues and eigenvectors of the variance–covariance matrix of SES locations during the bottom phases. Then, we used these locations, the eigenvectors and the eigenvalues to compute a range of metrics describing the shape of the SES trajectories:

Mean depth The mean depth is the depth of the gravity center of the SES positions at bottom.

Total inertia The total inertia is defined as the sum of the eigenvalues. It quantifies the amount of movement performed by the SES during the dives' bottom.

First main component inertia It is the inertia of the first main component (expressed relatively to the total inertia). This variable provide a measure of the dominance of movements parallel to the direction of the first component in comparison to the movements orthogonal to this direction. Because the trajectories were largely dominated by this component, we studied its characteristics in details. Then we chose to describe the remaining variability in the shape of the trajectories according to the horizontal and vertical dimensions rather than according to the others main

components. Indeed, this opposition reflects the fact that horizontal and vertical movements are submitted to different constraints: the time or oxygen depletion for vertical movements, the will to move toward a new prey patch or to move away from colony for horizontal movement. This opposition between vertical and horizontal dimension offers a meaningful framework to interpret the results.

First main component vertical and horizontal extent They quantifies the horizontal and vertical extent covered by SES along the first main component. These two variables allow us to describe the extent of SES exploration along the path of the first main component using a classical horizontal *versus* vertical opposition. To compute these statistics, we calculated the coordinates of SES bottom positions in the frame of reference determined by the eigenvectors (called scores). With the scores of data point according to for the first eigenvector, we selected the two points the closest to the 10% and 90% quantiles. Eventuality, we computed the horizontal and vertical distances between these points using the coordinates of the corresponding SES positions.

Vertical and horizontal width These are two measures of the horizontal and vertical distance covered by the SES across the first main component (not to be confounded with movement along the first main component). These variables allow us to describe the amount of vertical and horizontal spread of the SES deviations from to the first main component path. The horizontal width is defined by the difference between the 10% and 90% quantiles of the distances of SES positions to the plane (noted plane A, blue plane on figure 1) passing through the gravity center of the trajectory and encompassing the first eigenvector and the gravity vector. The vertical width is defined by the difference between the 10% and 90% quantiles of the distances of SES positions to the plane (noted plane B, orange plane on figure 1) passing through the gravity center of the trajectory, encompassing the first eigenvector and a vector orthogonal to plane A.

Swimming speed variability A low swimming speed variability can indicate a drifting or gliding behaviour [79] which is believed to be related to low foraging effort (rather to resting/digesting [71] or reducing locomotion costs [80]) while a strong variability is expected to be related to prey chasing [81]. Besides the shape-description variables, we used the standard deviation of the swimming speed during the bottom phase as a foraging effort proxy able to discriminate these behaviours.

Volume of water prospected by SES at the bottom of their dives

We estimated the volume of water prospected by SES that is to say, the volume of water where SES would have been able to detect a prey at the bottom phase of a dive. To achieve this task, we assumed that SES could see in any direction around their current position within a given radius. The prospected volume could then be assessed using Monte Carlo integration: we sampled random points uniformly distributed in the cuboid that encompass the bottom phase more or less the chosen radius (to account for the spheres located at extreme track locations); distances of these points to each SES position were then computed; the prospected volume is obtained by multiplying the volume of the cuboid by the proportion of sampled points found at least once within the given radius of the trajectory.

We tested three "detection-distance" scenarios for the sphere radius: a short distance of 1.5 m to simulate the case where prey catches would be opportunistic events as well as 9 and 18 m according to the foraging scale highlighted by [59] on the northern elephant seals. The samples were constituted of one mil-

lion points for the 1.5 m radius and half a million for the 9 and 18 m radius (yielding a 1% measurement error, additional file 1) Once this volume was computed we used it to compute a proxy of the prey encounters density at the bottom of SES dives define as the ratio between the number of PEE and the prospected water volume (expressed in µPEE/m^3 units).

Statistical analysis

We modelled the prey density proxy (PEE per unit of water prospected at bottom) according the descriptors of bottom trajectory previously described (namely, the mean depth, the total inertia, the first main component inertia, the first main component extent on the horizontal and vertical dimensions, the horizontal and vertical widths and variability of the swimming speed) using Generalized Linear Models (GLM). We fitted three models, one for each detection radius.

We started the model selection with Poisson family GLMs to predict the number of PEE at bottom. The link function was set to logarithm (the standard link function for these GLMs) and the log-transformed volume of prospected water was included in the model as an offset term. With these settings, we could model the PEE per unit of water prospected at bottom as response variable while using the appropriate count family distribution to predict the number of PEE at bottom.

These Poisson models indicated over-dispersion ($\theta = \sigma^2/\mu$, $\theta_{0.5m} = 2.93$, $\theta_{9m} = 2.68$, $\theta_{18m} = 2.73$) so we switched to the more flexible Negative Binomial distribution (using `glm.nb` from the `MASS` package [82]) which allows for higher variance/mean ratio. We observed a large proportion of zeros in our data (27.44%) incorrectly predicted by the GLMs. Hence, we tested the zero-inflated variants of Poisson and Negative Binomial models (using `zeroinfl` from the `pscl` package [83]). These models led to very significant improvement of Akaïke Information Criterion (AIC) (Vuong's test p-values were < 0.01 for all models).

The explanatory variables considered for selection in the count part of the zero-inflated model are identical to the Poisson and Negative Binomial models. Because the 3D behaviour of SES is not well known, the choice of explanatory variable for the zero excess part was restricted to the non shape-description variables (namely, the individual identity, the mean depth and the swimming speed variability and the log-transformed bottom duration which is not included in the count part). The seal identity captures the variability due to differences of accelerometer sensitivity and individuals' foraging behaviour, the swimming speed variability can account for the shift between drifting/gliding and active swimming behaviour in terms of foraging effort, the mean depth provides basic information about the environment (which is a likely source of excess zeros) and the log-transformed bottom duration has an obvious link to the probability of PEE.

We tested all the possible combinations of explanatory variables and selected the best candidates according to AIC. Many explanatory variables could arguably have a log-scale effect on the response variable (e.g the bottom duration in the Binomial GLM). However, because of collinearity between the raw variable and its log-transformed variant we tested for log-scale effect one explanatory variable at a time, replacing its raw version by its log-transformed version.

Results

Shape of SES trajectories at the bottom of their dives

On average, the first main component explained 94% of the total inertia (Figure 3). This contribution increases along with the total inertia of the bottom phase trajectory (Figure 3). Moreover, the first main component is almost exclusively orientated on a horizontal plane (Figure 4). The dive on the left of the figure 2

displays a typical example of a 3D dive of our dataset with the characteristics detailed in figures 3 (high directional anisotropy) and 4 (most of the SES movements actually occur in the horizontal dimensions). No bi-modality pattern is really noticeable of figure 4 but the vertical component of the first main component range between 17 % to 76 % in a few bottom phases (5 %) which correspond to deep diving depths (680 m vs. 481 m, t-test p-value = 1.40×10^{-13}). All dives confounded, the SES travelled average horizontal distances of 429 m in their descent phases, 706 m in bottom phases and 393 m in ascent phases (the respectives variation coefficients are 92%, 77% and 90%). Because the first main component is horizontally orientated, first main component inerta and the length of the first main component according to the horizontal plane (first main component horizontal extent) were very correlated. As a result, when checking for multicollinearity before model selection, the Variance Inflation Factor indicated issues. The first main component horizontal extent was removed prior to the model selection.

Figure 3 should be inserted here.

Figure 4 should be inserted here.

Table 2 should be inserted here.

Prey field density at the bottom of SES dives

We found an average prey encounter density[1] of $1.37 \times 10^4 \pm 1.05 \times 10^3$ µPEE/m^3 with the 0.5 m radius ($SD = 1.66 \times 10^4$ µPEE/m^3), $1.61 \times 10^1 \pm 1.24$ µPEE/m^3 with the 9 m radius ($SD = 2.00 \times 10^1$ µPEE/m^3) and $4.17 \pm 3.29 \times 10^{-1}$ µPEE/m^3 with the 18 m radius ($SD = 5.27$ µPEE/m^3).

[1] values are given in the following format: mean ± bootstrap confidence interval at 95%. The standard deviation is given later in brakets

Prey density model

The sign of the estimated effects were consistent across the different radius that we tested (Table 3). The bottom depth has a positive influence on the probability of catching at least one prey item but a negative effect on the amount of PEE per unit of prospected water volume (Table 3). The same results arise with the amount of total inertia explained by the first main component and the vertical extent covered across the first main component but the effect of total inertia explained by the first main component on the absence of PEE event at bottom is not significant for the 0.5 m radius model while the effect of the vertical extent covered across the first main component on the absence of PEE event at bottom is not significant for the 9 m radius model (Table 3).

An increase of the total inertia of the vertical extent covered across the first main component is related to lower PEE in both the count and zero models (Table 3). The variability of SES swimming speed (both absolute and vertical) is associated to higher PEE per unit of prospected water volume (Table 3). The dispersion parameter (θ) increases with the chosen detection radius (Table 3). The probability of not encountering prey strongly decrease with the bottom phase duration (Table 3). The horizontal distance covered across the first main component was not selected as explanatory variable.

Table 3 should be inserted here.

Discussion

Schooling behaviour

The principal component analysis revealed that SES trajectories of at the bottom of their dives is strongly anisotropic with a path strongly dominated by single direction (Figure 3) as it was noted by [84] on northern elephant seals. A spherical first passage time (SFPT, [85]) analysis performed on our dataset revealed that ARS could be detected in the bottom of SES dives

and could account for 67.4% of PEE in the bottom phases. In the periods of the bottom phase with hight SFPT (ARS), 95% of the SES positions where enclosed within a spheres of radius $45.3 \pm SD = 28.9$ m [86], *in review*). In these ARS the increase of SFPT was related to a decrease of the SES swimming speed and greater sinuosity but the SES trajectories remained fairly anisotropic (Jouma'a personal communication). Our observations support the hypothesis that SES prey do not aggregate in large discrete schools having a radius ranging between 40 m (ARS scale) and 400 m (bottom phase scale). Indeed, in such a situation the predator is expected to adopt an overall sinuous and isotropic trajectory. The schooling behaviour is unlikely to explain prey density variations encountered by the SES from a bottom phase to another but it is possible that prey aggregate in discrete schools of a few individuals at smaller scales. Our results suggest that the deep scattering layer is rather constituted of scattered solitary prey or small group of individuals. The seals' movement at bottom scale would correspond to an intermediate level of aggregation in the hierarchical patch system [13] such as suggested by the patterns highlighted by [59] with northern elephant seal.

PEE density along depth

The dominant direction in the trajectories of SES at dives' bottom was preponderantly horizontal (Figure 4). This indicates that SES target specific layers of the water column during their bottom. The shallower is this layer, the less time and energy is required to reach it and the more accessible and the more profitable it is. Performing dives' bottom phase a greater depth was found to be associated with smaller prey encounter density (Table 3). While the SES and their prey perform diel vertical migrations [35, 36, 87], this process cannot explain our result because all the 3D dives in our dataset occurred during daytime. A previous study, based on likelihood of detecting bioluminescence [88] highlighted a similar pattern. The impact of the changes in the size or species composition of the mesopelagic fish community in relation with this decreasing prey encounter density could not be examined with the tools available to us but they could have a substantial importance. Assuming that the energy content of a prey item does not vary with depth, the deep dives would imply smaller energy income (because of reduced encounter rates) but larger expenditure (because of the longer transit between surface and bottom). Thus, these dives would be be doubly detrimental to the SES energy balance. However, the probability that no PEE occur decreased with the SES diving depth (Table 3), suggesting that a better resource predictability in the deep environment might compensate to some extent for this bad energy balance. An alternative explanation is that SES could extend their diet to other prey types or size to compensate for the long transit duration.

We distinguished between two sources of vertical exploration in the explanatory variables. The first is the depth range covered by SES by moving along the first main component. The second is the range of depth covered by moving orthogonally to this component. An increase in any of these was associated to a decrease of the prey density proxy (Table 3). However, the amount of horizontal exploration orthogonally the main direction of the bottom trajectory was not significantly related to the prey encounter density. Not only the SES target specific layers, but the prey density in this layer is shaped according to the vertical dimension. This result suggest that local prey density could by driven by vertical constraints that delineate the vertical extent of the deep scattering layer. The nature of these constraints could be biotic (e.g. predation risk, aggregation into reproductive swarms) or abiotic (e.g. habitat preferences regarding temperature, light intensity or oxygen concentration). In addition to the effect

of oceanographic parameters on the prey abundance, such conditions could impact locally on the foraging success of SES by controlling the prey density and, consequently, on the foraging efficiency at the bottom of dives.

A trade-off between feeding resources richness (primary production taking place in the well lighted subsurface water) and predation risk (expected to be greater in luminous environment) is responsible for the diel vertical migration pattern phenomenon [89]. The light level intensity, decreasing with depth, delineate the upper boundary of many pelagic species and, consequently, relates with the diving depth of SES [87]. Using bio-logging data collected by free-ranging SES, the sampled environment totally rely on the animals' decisions [90]. Because they are constrained to return at surface in order to breathe, the diving predators do not benefit from pursuing deeper when an exploitable prey patch is encountered. The presence-only data collected using bio-logging makes it difficult to assess the deeper limit of the prey patch on which the SES forage. Therefore, the relationship between the PEE density and the vertical extent of the SES path underwater conveys more of a qualitative than quantitative information about the link between thickness of the deep scattering layer and its corresponding density.

Foraging behaviour

The prey density proxy was negatively related to an increase of the overall travel distance in the bottom phase (total inertia, Table 3). In hight density patches, the SES would travel shorter overall distances which could be explained by a greater locomotion cost forcing them to end the bottom phase early. The prey density proxy positively related to the dominance of the first main component (first main component inertia, Table 3) which corresponds predominantly to horizontal movements. This is consistent with the hypothesis of thin and dense resource layers. However, the amount of horizontal movements covered orthogonally to this dominant direction in the bottom phases was not significantly related to prey encounter density. This indicates that horizontal exploration mainly takes place moving forward according to the first main component. Based on their observation of the behaviour of *Thunnus maccoyii*, [91] suggested that feeding during periods of straight movement could be more common than expected from the optimal foraging theory. At the scale of a complete foraging trip at sea, SES feeds to a large extent during the transit part of their trip [Refs?] but this pattern seems to be observable within the dives' bottom phase where foraging is expected to be the primary objective of the diving predator. Such an extensive search behaviour is expected when prey are well dispersed in the environment [92] which seems consistent with the suspected non-schooling behaviour of SES prey that we have previously discussed. The notion of prey dispersion is relative to the sensory detection range of the predator. If the spread of prey items largely exceeds the perception range of the predator a straight path is an efficient sampling strategy to scan large volumes of water. Besides the hypothesis of a behaviour driven by the prey distribution, [91] hypothesize that a successful feeding during travel could result from the evolution of migratory opportunistic predators, allowing to meet the energetic requirements while moving rapidly. Given the very wide range of oceanographic conditions the elephant seal explore [72], the opportunistic behaviour may a be relevant point. However, SES do not really fulfil the criterion of a migratory predator as the primary goal of their trip at sea is believed to be foraging.

Our estimates of the prey density changed very quickly according to the chosen detection radius ranging in five order of magnitude from a tenth of µPEE/m^3 (18 m radius) to a few ten of thousands µPEE/m^3 (0.5 m radius). Sampling micronekton with

a large midwater trawl, [17] found an average micronekton biomass of 2.5 mg m^{-3} during the day. Assuming a similar avoidance for the net and the SES, and an average fish weight of 10 g this would translate into a really coarse estimation of 2.50×10^5 µPEE/m^3. Among the detection radius we tested, the 0.5 m radius seems the most realistic ($1.37 \times 10^4 \pm 1.05 \times 10^3$ µPEE/m^3). Our estimation of the prey density rely on the idea that SES do attempt to catch a prey when they detect one. The prey avoidance as well as the probability of multiple simultaneous prey encounters could not be taken into account. These special cases however seem less likely in a short detection distances scenario such as the 0.5 m radius that we tested. Despite the good correspondence between the amount of PEE detected from head-mounted and back-mounted acceleration data (Additional file), the latter have a tendency to miss some events. As a result we expect our estimation of the prey encounter density to be underestimated. We suggest that the hunting behaviour of SES may be opportunistic in the sense that prey item would be detected at short distances and suddenly be captured but the SES without a substantial race between the prey and the predator.

Limitations of the study

Each method used to assess the micronekton resources of the pelagic ecosystem have their own weaknesses. Trawl sampling is costly, requires good weather operating conditions and net avoidance of the different species are is unknown. Bio-logging implies a bias sampling due to different range of habitat available to the predators and prey (a typical example the diving predators is the depth range) and difficulties to distinguish between what is related to animal behaviour and to the environment. For instance, the predator decision to attack a prey can involve many parameters such as the type of prey, its size, its energetic content, its handling time, and abundance. Eventually, bio-logging studies are also limited by the number of individuals that could be equipped (six in this studies). Acoustic surveys depend on presence/absence of a swim bladder as well as on its composition (gas or lipid) which, for some species, is known to change according to the stage of development. Distinguishing between species and estimating biomass is thus difficult with communities of mixed species and/or mixed ages. Spatial resolution of the data also decrease with depth as lower signal frequencies are required.

Due to the limited Acousondes^{TM} battery life, we could only sample the first part of the SES foraging trips. As the SES tend to adopt a faster horizontal transit rate in these periods, this sampling bias is likely to magnify the dominance of linear horizontal paths that we highlighted at the bottom of dives. Further studies could analyse the shape of underwater 3D trajectories of SES during other part of the trip to overcome this issue. In particular, the Area-restricted search appear like interesting periods to focus on the habitat of prey and the foraging strategy according to horizontal and vertical dimensions.

The 3D reconstruction of the SES path underwater by dead-reckoning assumes that the direction of travel of the animal is always parallel to the body orientation. More sophisticated methods such as the one developed by [93] which is free of this assumption, attest that this approximation can have substantial impact on the reconstructed tracks. However, such methods imply large computation time which is not practicable with dataset constituted with hundreds of dives. It has to be noted that dead-reckoning is submitted to cumulative errors and conversely to other methods ([66, 93]) they were not estimated with our method. Uncertainties reach a maximum in the bottom part of the dive as it is the most distant of the known GPS locations collected at surface. As a consequence, some precautions need to be taken when studying the spatial patterns of

dead-reckoning reconstructed trajectories at the bottom of their dives, especially at fine-scale. The last discussion point about the 3D reconstruction method implemented in this study relates to the assessment of SES swimming speed. The water-flow noise to water-flow speed relationship in the descent phase that we extrapolated to entire dives presuppose that flow behaves similarly throughout the dives which is yet to be vetted.

Perspectives

The straightness of the SES underwater path has been reported by [84] who highlight its consistency from one dive to another. It is not clear how SES orientate themselves and how migratory objectives contribute to this pattern. Examining this pattern in relation to currents [94] would be interesting to examine in order to study the navigation skill of SES.

We could only focus on the quantitative aspect of prey field because acceleration data do not provide information about the nature of the PEE. Thus, it is unclear if the results mainly concern one type of prey such as a specific myctophid species more abundant in the study area – the eastern edge of the Kerguelen shelf – or partially apply to the different prey types targeted by SES (myctophids and squids). We could not test for the role of the quality of prey items (size and species) which could imply distinct types of predator-prey spatial interaction due to different detectability, aggregative behaviour or predator-escaping abilities (responsiveness, speed, manoeuvrability). To address these issues a camera is needed in order to identify the species and size of the prey items [60, 62, 95]. However, the high power consumption of these devices and the very dark environment the SES forage in are still technical constraints to their usage. Miniaturized sonar [96] could bring the power of high-frequency acoustic signals to identify species to new depths. In quantitative terms it is also promising tool: by extending the perception range of bio-logging outside of the very intimate sphere surrounding the animals it could allow to examine thoroughly the fine-scale prey distribution, the range and mechanisms of the prey detection and hunting strategies of the SES.

Conclusion

The usage of the 3D space made by the SES at the bottom of their dives suggest that their prey do not tend to form large discrete schools but rather adopt a scattered distribution structured within specific layers of the water column. The prey encounter density in these layers decreased with depth but then, the SES tend to perform prey encounter event on a more regular basis. However, it is not clear how to interpret this tendency given that qualitative information such as the species and size of the prey that SES encountered unavailable to us. We suggest that the prey abundance decrease with depth but that their distribution in a hierarchical patch structure lessens. The extent of the vertical exploration performed by the SES during their bottom phases related negatively to the prey encounter density, seemingly indicating that the thickness of the layers targeted by SES mechanically impacts the micronekton density. These results underline the primary importance of the vertical dimension into the spatial organization of the micronekton.

The 3D trajectories in our dataset were essentially linear path. While the vertical deviations from this path were of the the same order of magnitude than the horizontal ones, they better related to the prey encounter density. Under such circumstances, the widely used Time-Depth Recorders can be considered as an effective simplification of the SES movements at scales of few-hundreds meters. The adaptive mechanisms underlying this behaviour, such as a trade-off between the travel speed and energetic requirements or an unbalanced ratio between SES sensory perception range and prey distribution and avoidance, remain unclear.

We suggest that these observations could be related to a number of environmental conditions: a prey field organized in layers, a short prey detection distance, external constraint such as the purpose for SES to move away from their breeding site.

We believe that this study highlights the importance of knowledge about the 3three-dimensional predator-prey interactions and gives support to the usage of biologging to unravel and monitor fine-scale micronekton distribution, particularly in remote areas such as the deep pelagic ecosystems of the Southern ocean.

List of abbreviations

ARS: Area-restricted search; SES: southern elephant seals; PEE: prey encounter event; AIC: Akaïke Information Criterion; GPS: Global Positionning System. 2D,3D: bi-dimensional, tri-deminesional. SD: Stadard deviation. SE: Standard error. CI: Confidence interval

Ethics approval

Our study on elephant seals was approved and authorized by the ethics committee of the French Polar Institute (Institut Paul Emile Victor – IPEV) in May 2008. Animals were handled and cared for in total accordance with the guidelines of this committee (dirpol@ipev.fr).

Availability of data and materials

The dataset(s) supporting the conclusions of this article is available in the [repository name] repository, [unique persistent identifier and hyperlink to dataset(s) in http:// format].

Competing interests

The authors declare that they have no competing interests

Authors' contributions

YLB analysed and interpreted the data. YLB and CG designed the study. YLB, CG and JJ made major contributions in writing the manuscript. All authors read and approved the final manuscript.

Funding

The "Département des Deux-Sèvres" and the "Région Poitou-Charentes", the "MyctO-3D-MAP" and "IPSOS-SEAL" ANR, the Total Foundation, the "Éléphant de mer océanographes" CNES research program and the "Observatoire des Mammifères Explorateurs du Milieu Océanique" provided financial support to this study.

Acknowledgements

We would like to thanks David Nerini for helpful discussions, the IPEV team and the field assistants that made the field work at Kerguelen possible.

References

1. J Gjosaeter. A Review Of The World Resources Of Mesopelagic Fish Fao Fisheries Technical Paper No 193. Food And Agriculture Organization Of The United Nations; 1980. 00000.
2. Jansen JK, Boveng PL, Bengtson JL. Foraging modes of chinstrap penguins: contrasts between day and night. Marine Ecology Progress Series. 1998 May;165:161–172. 00036.
3. Kooyman GL, Cherel Y, Maho YL, Croxall JP, Thorson PH, Ridoux V, et al. Diving Behavior and Energetics During Foraging Cycles in King Penguins. Ecological Monographs. 1992 Mar;62(1):143–163. 00244.
4. Casaux R, Baroni A, Carlini A. The diet of the Antarctic fur seal Arctocephalus gazella at Harmony Point, Nelson Island, South Shetland Islands. Polar Biology. 1998 Nov;20(6):424–428. 00041.
5. Cherel Y, Ducatez S, Fontaine C, Richard P, Guinet C. Stable isotopes reveal the trophic position and mesopelagic fish diet of female southern elephant seals breeding on the Kerguelen Islands. Marine Ecology Progress Series. 2008 Oct;370:239–247. 00076.
6. Cherel Y, Duhamel G, Gasco N. Cephalopod fauna of subantarctic islands: new information from predators. Marine Ecology Progress Series. 2004 Jan;266:143–156. 00051.
7. Guinet C, Cherel Y, Ridoux V, Jouventin P. Consumption of marine resources by seabirds and seals in Crozet and Kerguelen waters: changes in relation to consumer biomass 1962–85. Antarctic Science. 1996 Mar;8(01):23–30.
8. Hindell MA, Bradshaw CJA, Sumner MD, Michael KJ, Burton HR. Dispersal of female southern elephant seals and their prey consumption during the austral summer: relevance to management and oceanographic zones. Journal of Applied Ecology. 2003 Aug;40(4):703–715. 00096.
9. Slip DJ. The diet of southern elephant seals (Mirounga leonina) from Heard Island. Canadian Journal of Zoology. 1995 Aug;73(8):1519–1528.
10. Daneri G, Carlini A. Fish prey of southern elephant seals, Mirounga leonina, at King George Island. Polar Biology. 2002 Oct;25(10):739–743. 00042.
11. Saunders RA, Fielding S, Thorpe SE, Tarling GA. School characteristics of mesopelagic fish at South Georgia. Deep Sea Research Part I: Oceanographic Research Papers. 2013 Nov;81:62–77. 00003.
12. Kotliar NB, Wiens JA. Multiple Scales of Patchiness and Patch Structure: A Hierarchical Framework for the Study of Heterogeneity. Oikos. 1990;59(2):253–260.
13. Fauchald P. Foraging in a Hierarchical Patch System. The American Naturalist. 1999 Jun;153(6):603–613.
14. Levin SA. The Problem of Pattern and Scale in Ecology: The Robert H. MacArthur Award Lecture. Ecology. 1992 Dec;73(6):1943–1967.
15. Pakhomov EA, Perissinotto R, McQuaid CD. Prey composition and daily rations of myctophid fishes in the Southern Ocean. Marine Ecology Progress Series. 1996 Apr;134:1–14.
16. Gauthier S, Oeffner J, ODriscoll RL. Species composition and acoustic signatures of mesopelagic organisms in a subtropical convergence zone, the New Zealand Chatham Rise. Marine Ecology Progress Series. 2014 Apr;503:23–40. 00003.
17. Williams A, Koslow JA. Species composition, biomass and vertical distribution of micronekton over the mid-slope region off southern

Tasmania, Australia. Marine Biology. 1997 Dec;130(2):259–276. 00057.

18. Fielding S, Watkins JL, Collins MA, Enderlein P, Venables HJ. Acoustic determination of the distribution of fish and krill across the Scotia Sea in spring 2006, summer 2008 and autumn 2009. Deep Sea Research Part II: Topical Studies in Oceanography. 2012 Jan;59–60:173–188. 00024.
19. Koubbi P, Moteki M, Duhamel G, Goarant A, Hulley PA, O'Driscoll R, et al. Ecoregionalization of myctophid fish in the Indian sector of the Southern Ocean: Results from generalized dissimilarity models. Deep Sea Research Part II: Topical Studies in Oceanography. 2011 Jan;58(1–2):170–180.
20. Bost CA, Cotté C, Bailleul F, Cherel Y, Charrassin JB, Guinet C, et al. The importance of oceanographic fronts to marine birds and mammals of the southern oceans. Journal of Marine Systems. 2009 Oct;78(3):363–376. 00160.
21. Nordstrom CA, Battaile BC, Cotté C, Trites AW. Foraging habitats of lactating northern fur seals are structured by thermocline depths and submesoscale fronts in the eastern Bering Sea. Deep Sea Research Part II: Topical Studies in Oceanography. 2013 Apr;88–89:78–96.
22. Monte SD, Cotté C, d'Ovidio F, Lévy M, Corre ML, Weimerskirch H. Frigatebird behaviour at the ocean–atmosphere interface: integrating animal behaviour with multi-satellite data. Journal of The Royal Society Interface. 2012 Jul;9(77):3351–3358.
23. Cotté C, Park YH, Guinet C, Bost CA. Movements of foraging king penguins through marine mesoscale eddies. Proceedings of the Royal Society B: Biological Sciences. 2007 Jul;274(1624):2385–2391. 00070.
24. Dragon AC, Monestiez P, Bar-Hen A, Guinet C. Linking foraging behaviour to physical oceanographic structures: Southern elephant seals and mesoscale eddies east of Kerguelen Islands. Progress in Oceanography. 2010 Oct;87(1–4):61–71.
25. Strass VH, Naveira Garabato AC, Pollard RT, Fischer HI, Hense I, Allen JT, et al. Mesoscale frontal dynamics: shaping the environment of primary production in the Antarctic Circumpolar Current. Deep Sea Research Part II: Topical Studies in Oceanography. 2002;49(18):3735–3769.
26. Guinet C, VacquiGarcia J, Picard B, Bessigneul G, Lebras Y, Dragon AC, et al. Southern elephant seal foraging success in relation to temperature and light conditions: insight into prey distribution. Marine Ecology Progress Series. 2014 Mar;499:285–301.
27. McMahon CR, Field IC, Bradshaw CJA, White GC, Hindell MA. Tracking and data–logging devices attached to elephant seals do not affect individual mass gain or survival. Journal of Experimental Marine Biology and Ecology. 2008 Jun;360(2):71–77. 00032.
28. McIntyre T. Trends in tagging of marine mammals: a review of marine mammal biologging studies. African Journal of Marine Science. 2014 Oct;36(4):409–422. 00002.
29. Hunt GL, Mehlum F, Russell RW, Irons D, Decker MB, Becker PH. Physical processes, prey abundance, and the foraging ecology of seabirds. Proceedings of the 22nd International Ornithological Congress, Durban, South Africa BirdLife South Africa. 1999;p. 2040–2056.
30. MacArthur RH, Pianka ER. On Optimal Use of a Patchy Environment. The American Naturalist. 1966 Nov;100(916):603–609.
31. Pyke G. Optimal Foraging Theory - a Critical-Review. Annual Review of Ecology and Systematics. 1984;15:523–575.
32. Stephens DW, Krebs JR. Foraging Theory. Princeton University Press; 1986.
33. Sih A. Predator-prey space use as an emergent outcome of a behavioral response race. In: Ecology of Predator-Prey Interactions. oxford university press, usa ed.; 2005. p. 240–255.
34. Sih A. The Behavioral Response Race Between Predator and Prey. The American Naturalist. 1984;123(1):143–150.
35. Catul V, Gauns M, Karuppasamy PK. A review on mesopelagic fishes belonging to family Myctophidae. Reviews in Fish Biology and Fisheries. 2010 Oct;21(3):339–354. 00041.
36. Leboeuf B, Costa D, Huntley A, Feldkamp S. Continuous, Deep Diving in Female Northern Elephant Seals, Mirounga-Angustirostris. Canadian Journal of Zoology. 1988 Feb;66(2):446–458. 00000 WOS:A1988M613400024.
37. Kareiva P, Odell G. Swarms of predators exhibits "preytaxis" if individual predators use area-restricted search. The American Naturalist. 1987 Aug;130(2):233–270.
38. Fauchald P, Tveraa T. Using First-Passage Time in the analysis of Area-Retricted Search and habitat selection. Ecology. 2003 Feb;84(2):282–288.
39. Robinson PW, Tremblay Y, Crocker DE, Kappes MA, Kuhn CE, Shaffer SA, et al. A comparison of indirect measures of feeding behaviour based on ARGOS tracking data. Deep Sea Research Part II: Topical Studies in Oceanography. 2007 Feb;54(3–4):356–368. 00046.
40. Scheffer A, Trathan PN, Collins M. Foraging behaviour of King Penguins (Aptenodytes patagonicus) in relation to predictable mesoscale oceanographic features in the Polar Front Zone to the north of South Georgia. Progress in Oceanography. 2010 Jul;86(1–2):232–245.
41. Robinson PW, Simmons SE, Crocker DE, Costa DP. Measurements of foraging success in a highly pelagic marine predator, the northern elephant seal. Journal of Animal Ecology. 2010;79(6):1146–1156. 00031.
42. Lascelles BG, Taylor PR, Miller MGR, Dias MP, Oppel S, Torres L, et al. Applying global criteria to tracking data to define important areas for marine conservation. Diversity and Distributions. 2016 Apr;22(4):422–431. 00006.
43. Hindell MA, McMahon CR, Bester MN, Boehme L, Costa D, Fedak MA, et al. Circumpolar habitat use in the southern elephant seal: implications for foraging success and population trajectories. Ecosphere. 2016 May;7(5):n/a–n/a. 00003.
44. Kirkman SP, Yemane DG, Lamont T, Meÿer MA, Pistorius PA. Foraging Behavior of Subantarctic Fur Seals Supports Efficiency of a Marine Reserve's Design. PLOS ONE. 2016 May;11(5):e0152370. 00001.

45. McConnell BJ, Chambers C, Fedak MA. Foraging ecology of southern elephant seals in relation to the bathymetry and productivity of the Southern Ocean. Antarctic Science. 1992;4(04):393–398.
46. Davis RW, Fuiman LA, Williams TM, Collier SO, Hagey WP, Kanatous SB, et al. Hunting Behavior of a Marine Mammal Beneath the Antarctic Fast Ice. Science. 1999 Feb;283(5404):993–996. 00266.
47. Simpkins MA, Kelly BP, Wartzok D. Three-dimensional analysis of search behaviour by ringed seals. Animal Behaviour. 2001 Jul;62(1):67–72. 00021.
48. Austin D, Bowen WD, McMillan JI, Iverson SJ. Linking movement, diving and habitat to foraging success in a large marine predator. Ecology. 2006 Dec;87(12):3095–3108. 00095.
49. Bailleul F, Pinaud D, Hindell M, Charrassin JB, Guinet C. Assessment of scale-dependent foraging behaviour in southern elephant seals incorporating the vertical dimension: a development of the First Passage Time method. Journal of Animal Ecology. 2008;77(5):948–957. 00055.
50. Bestley S, Jonsen ID, Hindell MA, Harcourt RG, Gales NJ. Taking animal tracking to new depths: synthesizing horizontal–vertical movement relationships for four marine predators. Ecology. 2015 Feb;96(2):417–427. 00013.
51. Virginie Ramasco, Barraquand F, Biuw M, McConnell B, Nilssen KT. The intensity of horizontal and vertical search in a diving forager: the harbour seal. Movement Ecology. 2015 May;3(1):15.
52. Mitani Y, Andrews RD, Sato K, Kato A, Naito Y, Costa DP. Three-dimensional resting behaviour of northern elephant seals: drifting like a falling leaf. Biology Letters. 2010 Apr;6(2):163–166. 00039.
53. Matsumura M, Watanabe YY, Robinson PW, Miller PJO, Costa DP, Miyazaki N. Underwater and surface behavior of homing juvenile northern elephant seals. Journal of Experimental Biology. 2011 Feb;214(4):629–636. 00007.
54. Mitani Y, Watanabe Y, Sato K, Cameron MF, Naito Y. 3D diving behavior of Weddell seals with respect to prey accessibility and abundance. Marine Ecology Progress Series. 2004 Nov;281:275–281.
55. Shiomi K, Sato K, Mitamura H, Arai N, Naito Y, Ponganis PJ. Effect of ocean current on the dead-reckoning estimation of 3-D dive paths of emperor penguins. Aquatic Biology. 2008 Sep;3(3):265–270. 00025.
56. Wilson RP, Shepard ELC, Liebsch N. Prying into the intimate details of animal lives: use of a daily diary on animals. Endangered Species Research. 2008;v4:123–137. 00000.
57. Narazaki T, Sato K, Abernathy KJ, Marshall GJ, Miyazaki N. Sea turtles compensate deflection of heading at the sea surface during directional travel. Journal of Experimental Biology. 2009 Dec;212(24):4019–4026. 00018.
58. BenoitBird KJ, Battaile BC, Nordstrom CA, Trites AW. Foraging behavior of northern fur seals closely matches the hierarchical patch scales of prey. Marine Ecology Progress Series. 2013 Apr;479:283–302. 00000.
59. Adachi T, Costa DP, Robinson PW, Peterson SH, Yamamichi M, Naito Y, et al. Searching for prey in a three-dimensional environment: hierarchical movements enhance foraging success in northern elephant seals. Functional Ecology. 2016 May;p. n/a–n/a. 00000.
60. Hooker SK, Boyd IL, Jessopp M, Cox O, Blackwell J, Boveng PL, et al. Monitoring the Prey-Field of Marine Predators: Combining Digital Imaging with Datalogging Tags. Marine Mammal Science. 2002 Jul;18(3):680–697. 00060.
61. Viviant M, Monestiez P, Guinet C. Can We Predict Foraging Success in a Marine Predator from Dive Patterns Only? Validation with Prey Capture Attempt Data. PLoS ONE. 2014 Mar;9(3):e88503.
62. Naito Y, Costa DP, Adachi T, Robinson PW, Fowler M, Takahashi A. Unravelling the mysteries of a mesopelagic diet: a large apex predator specializes on small prey. Functional Ecology. 2013 Jun;27(3):710–717. 00032.
63. Wilson R, Steinfurth A, Ropert-Coudert Y, Kato A, Kurita M. Lip-reading in remote subjects: an attempt to quantify and separate ingestion, breathing and vocalisation in free-living animals using penguins as a model. Marine Biology. 2002 Jan;140(1):17–27. 00115.
64. Davis RW, Fuiman LA, Williams TM, Horning M, Hagey W. Classification of Weddell seal dives based on 3 dimensional movements and video-recorded observations. Marine Ecology Progress Series. 2003 Dec;264:109–122. 00062.
65. Fossette S, Gaspar P, Handrich Y, Maho YL, Georges JY. Dive and beak movement patterns in leatherback turtles Dermochelys coriacea during internesting intervals in French Guiana. Journal of Animal Ecology. 2008 Mar;77(2):236–246. 00046.
66. Wensveen PJ, Thomas L, Miller PJO. A path reconstruction method integrating dead-reckoning and position fixes applied to humpback whales. Movement Ecology. 2015 Sep;3(1):1–16. 00000.
67. McMahon CR, Burton H, Slip D, McLean S, Bester M. Field immobilisation of southern elephant seals with intravenous tiletamine and zolazepam. Veterinary Record. 2000 Feb;146(9):251–254.
68. R Core Team. R: A Language and Environment for Statistical Computing. Vienna, Austria: R Foundation for Statistical Computing; 2014.
69. Le Bras Y. rbl: Biologging tools for diving predators; 2016. 00000 R package version 0.1.28.
70. Jouma'a J, Le Bras Y, Richard G, Vacquié-Garcia J, Picard B, Ei Ksabi N, et al. Adjustment of diving behaviour with prey encounters and body condition in a deep diving predator: the Southern Elephant Seal. Functional Ecology. 2015 Jul;p. n/a–n/a. 00000.
71. Crocker DE, Boeuf BJL, Costa DP. Drift diving in female northern elephant seals: implications for food processing. Canadian Journal of Zoology. 1997 Jan;75(1):27–39. 00125.
72. Vacquié-Garcia J, Guinet C, Laurent C, Bailleul F. Delineation of the southern elephant seal's main foraging environments defined by temperature and light conditions. Deep Sea Research Part II: Topical Studies in Oceanography. 2015 Mar;113:145–153.
73. signal developers. signal: Signal processing; 2013.
74. Richard G, Vacquié-Garcia J, Jouma'a J, Picard B, Génin A, Arnould JPY, et al. Variation in body condition during the post-moult foraging trip of southern elephant seals and its consequences on diving behaviour. The Journal of Experimental Biology. 2014

Jul;217(14):2609–2619.
75. Farrell E, Fuiman L. animalTrack: Animal track reconstruction for high frequency 2-dimensional (2D) or 3-dimensional (3D) movement data.; 2013. 00000.
76. Burgess WC, Tyack PL, Le Boeuf BJ, Costa DP. A programmable acoustic recording tag and first results from free-ranging northern elephant seals. Deep Sea Research Part II: Topical Studies in Oceanography. 1998 Jul;45(7):1327–1351. 00089.
77. Kooyman GL, Sinnett EE. Pulmonary Shunts in Harbor Seals and Sea Lions during Simulated Dives to Depth. Physiological Zoology. 1982 Jan;55(1):105–111. 00077.
78. Falke KJ, Hill RD, Qvist J, Schneider RC, Guppy M, Liggins GC, et al. Seal lungs collapse during free diving: evidence from arterial nitrogen tensions. Science. 1985 Aug;229(4713):556–558. 00117.
79. Dragon A, Bar-Hen A, Monestiez P, Guinet C. Comparative analysis of methods for inferring successful foraging areas from Argos and GPS tracking data. Marine Ecology Progress Series. 2012 Apr;452:253–267.
80. Aoki K, Watanabe YY, Crocker DE, Robinson PW, Biuw M, Costa DP, et al. Northern elephant seals adjust gliding and stroking patterns with changes in buoyancy: validation of at-sea metrics of body density. The Journal of Experimental Biology. 2011 Jan;214(17):2973–2987. 00028.
81. Hassrick JL, Crocker DE, Zeno RL, Blackwell SB, Costa DP, Le Boeuf BJ. Swimming speed and foraging strategies of northern elephant seals. Deep Sea Research Part II: Topical Studies in Oceanography. 2007 Feb;54(3–4):369–383.
82. Venables WN, Ripley BD. Modern applied statistics with S. 4th ed. Statistics and computing. New York, NY: Springer; 2007.
83. Zeileis A, Kleiber C, Jackman S. Regression Models for Count Data in R. Journal of Statistical Software. 2008;27(8). 00000.
84. Davis RW, Fuiman LA, Williams TM, Le Boeuf BJ. Three-dimensional movements and swimming activity of a northern elephant seal. Comparative Biochemistry and Physiology Part A: Molecular & Integrative Physiology. 2001 Jul;129(4):759–770. 00086.
85. Bailleul F, Lesage V, Hammill MO. Spherical First Passage Time: A tool to investigate area-restricted search in three-dimensional movements. Ecological Modelling. 2010 Jul;221(13–14):1665–1673. 00012.
86. Jouma'a J, Le Bras Y, Picard B, Guinet C. Three-dimensional assessment of hunting strategies in a deep diving predator. Marine Ecology Progress Series. in review;.
87. Jaud T, Dragon AC, Garcia JV, Guinet C. Relationship between Chlorophyll a Concentration, Light Attenuation and Diving Depth of the Southern Elephant Seal Mirounga leonina. PLoS ONE. 2012 Oct;7(10):e47444.
88. Vacquié-Garcia J, Royer F, Dragon AC, Viviant M, Bailleul F, Guinet C. Foraging in the Darkness of the Southern Ocean: Influence of Bioluminescence on a Deep Diving Predator. PLoS ONE. 2012 Aug;7(8):e43565.
89. Iwasa Y. Vertical Migration of Zooplankton: A Game Between Predator and Prey. The American Naturalist. 1982 Aug;120(2):171–180. 00114.
90. Ropert-Coudert Y, Wilson RP. Trends and perspectives in animal-attached remote sensing. Frontiers in Ecology and the Environment. 2005 Oct;3(8):437–444.
91. Bestley S, Patterson TA, Hindell MA, Gunn JS. Predicting feeding success in a migratory predator: integrating telemetry, environment, and modeling techniques. Ecology. 2010 Aug;91(8):2373–2384. 00043.
92. Hill S, Burrows MT, Hughes RN. Adaptive search in juvenile plaice foraging for aggregated and dispersed prey. Journal of Fish Biology. 2002 Nov;61(5):1255–1267. 00019.
93. Laplanche C, Marques TA, Thomas L. Tracking marine mammals in 3D using electronic tag data. Methods in Ecology and Evolution. 2015 Apr;p. n/a–n/a.
94. Chapman JW, Klaassen RHG, Drake VA, Fossette S, Hays GC, Metcalfe JD, et al. Animal Orientation Strategies for Movement in Flows. Current Biology. 2011 Oct;21(20):R861–R870. 00065.
95. Watanabe YY, Takahashi A. Linking animal-borne video to accelerometers reveals prey capture variability. Proceedings of the National Academy of Sciences. 2013 May;110(6):2199–2204.
96. Lawson GL, Hückstädt LA, Lavery AC, Jaffré FM, Wiebe PH, Fincke JR, et al. Development of an animal-borne "sonar tag" for quantifying prey availability: test deployments on northern elephant seals. Animal Biotelemetry. 2015 Jul;3(1):22. 00000.

Figures

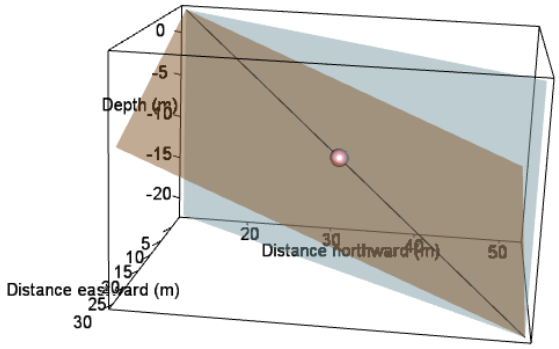

Figure 1 Reference planes for the calculation of vertical and horizontal width. The first main component is represented by the thick black line in the middle. The blue (respectively orange) plane stands for plane A (respectively plane B). The pink sphere indicates the position of the gravity center.

Tables

Table 1 Deployment details. All indviduals are post-breeding females.

Individual name	Length (m)	Weight (kg)	Number of 3D dives / dives	Recording duration (days)
2011-16	2.54	255	144 / 822	13
2011-18	2.28	245	238 / 1081	13
2012-01	2.32	230	248 / 1945	24
2012-02	2.35	362	68 / 409	12
2012-04	2.48	282	50 / 289	4
2012-08	2.25	292	244 / 1777	29

Additional Files

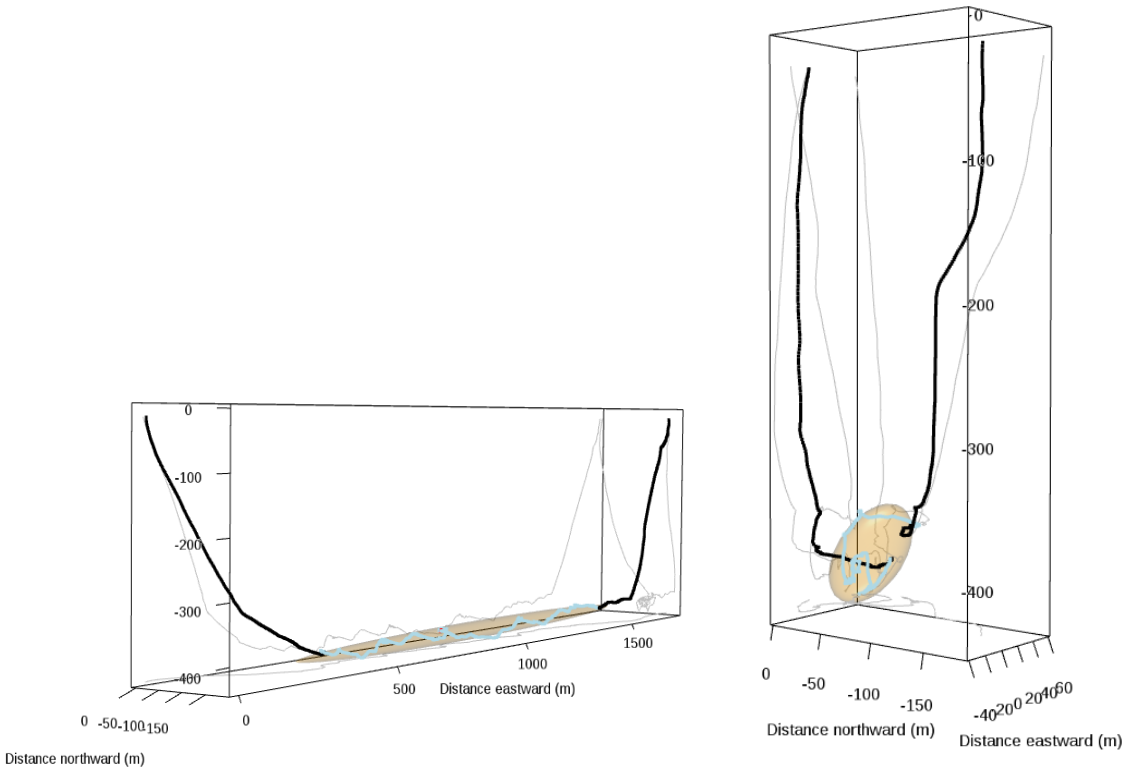

Figure 2 Two 3D dives examples. These dives have about the same depth but show two constrasting situations: on the left the first main component explains a very large part of the total inertia while on the right, the inertia explained by the first main component is particularly low. The blue part represents the dive's bottom phase. The axis of the orange ellispoid displays the three main components. To reflect the actual dive shape, the scale is even across all axis of a dive but they are different for each dive. The thin grey lines display the projections of SES path in 2D spaces.

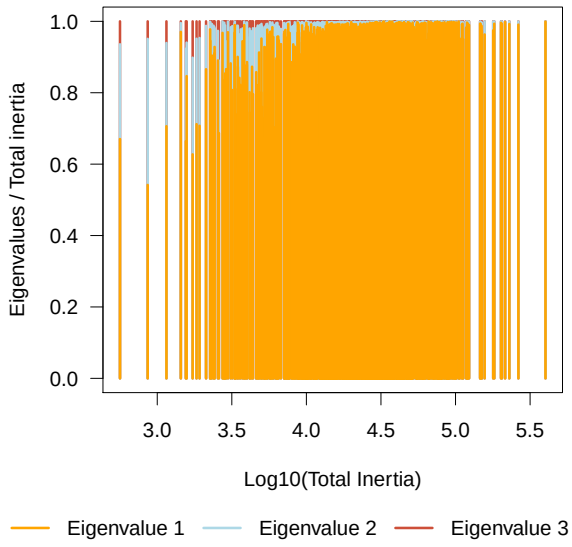

Figure 3 Contribution of the main components to total inertia. The bottom trajectory describes a sphere when all eigenvalues are equal and thus contribute to the same extent to total inertia. The bottom trajectory describes a line when the first eigenvalue is represents 100% of total inertia. In our data the first main component explained on average (grey line) 94% of total inertia

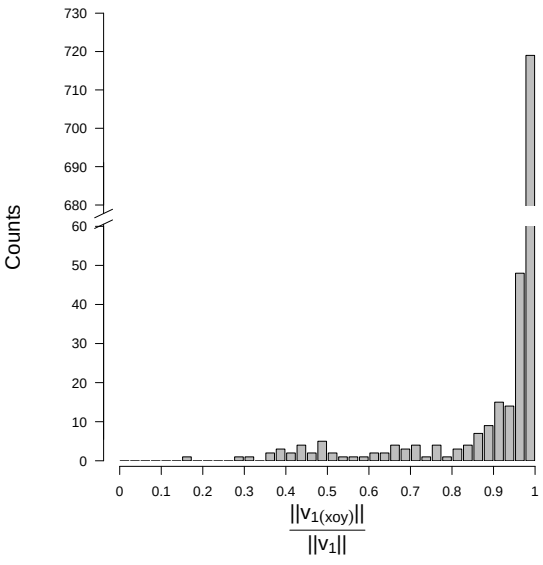

Figure 4 Length ratio between the first eigenvector projected on the horizontal plane ($v_{1(xoy)}$) and the first eigenvector in 3D space (v_1). A ratio of 0 indicates that the first main component of movement is vertical while a ratio of 1 indicate that the first main component is included in the horizontal plane.

Table 2 Descriptive statistics of the shape parameters of bottom trajectories. $n = 866$ 3D dives. Refer to methods for detailed explanation about what these variables represent and how they were computed.

	Nb PEE at bottom	Bottom duration (s)	Mean bottom depth (m)	Horizontal width (m)
Min	0.00	5.40×10^{1}	5.36×10^{1}	3.50×10^{-1}
Max	2.80×10^{1}	1.73×10^{3}	8.48×10^{2}	1.39×10^{2}
Median	2.00	4.51×10^{2}	4.36×10^{2}	2.04×10^{1}
Mean	3.37	5.00×10^{2}	4.42×10^{2}	2.32×10^{1}
SE mean	1.30×10^{-1}	6.67	5.25	4.50×10^{-1}
$CI_{95\%}$ mean	2.50×10^{-1}	1.31×10^{1}	1.03×10^{1}	8.80×10^{-1}
Variance	1.38×10^{1}	3.86×10^{4}	2.38×10^{4}	1.76×10^{2}
SD	3.71	1.96×10^{2}	1.54×10^{2}	1.33×10^{1}
	First main component vertical width (m)	First main component horizontal width (m)	Total inertia (m^2)	First main component inertia (%)
Min	4×10^{-2}	3.68×10^{1}	5.63×10^{2}	5.33×10^{1}
Max	3.84×10^{2}	1.78×10^{3}	4.01×10^{5}	10.00×10^{1}
Median	2.68×10^{1}	4.09×10^{2}	2.41×10^{4}	9.72×10^{1}
Mean	4.87×10^{1}	4.31×10^{2}	3.26×10^{4}	9.37×10^{1}
SE mean	2.16	7.25	1.11×10^{3}	2.84×10^{-1}
$CI_{95\%}$ mean	4.23	1.42×10^{1}	2.18×10^{3}	5.56×10^{-1}
Variance	4.02×10^{3}	4.55×10^{4}	1.07×10^{9}	6.96×10^{1}
SD	6.34×10^{1}	2.13×10^{2}	3.27×10^{4}	8.34
	Vertical width (m)	Bottom speed SD ($m\,s^{-1}$)	Bottom vertical speed SD ($m\,s^{-1}$)	
Min	2.10	1.10×10^{-1}	1.60×10^{-1}	
Max	1.54×10^{2}	1.15	2.01	
Median	2.32×10^{1}	3.20×10^{-1}	7.90×10^{-1}	
Mean	3.15×10^{1}	3.50×10^{-1}	8.50×10^{-1}	
SE mean	8.00×10^{-1}	1×10^{-2}	1×10^{-2}	
$CI_{95\%}$ mean	1.57	1×10^{-2}	2×10^{-2}	
Variance	5.57×10^{2}	3×10^{-2}	9×10^{-2}	
SD	2.36×10^{1}	1.70×10^{-1}	3.00×10^{-1}	

Table 3 Results of the three zero-inflated models. Please notice that (for historical reasons) the binomial part of zero-inflated models (rows labelled "Zero") predicts the absence of PEE instead of presence. For better readability, the coefficient estimates of the intercept and of SES identities are not included in this table. Please refer to the additional file for complete summary tables.

		Radius 0.5 m		**Radius 9 m**		**Radius 18 m**	
Variable	**Model**	Coefficient	p-value	Coefficient	p-value	Coefficient	p-value
Mean depth	Count	-1.76×10^{-1}	4.57×10^{-5}	-2.21×10^{-1}	4.97×10^{-8}	-2.44×10^{-1}	1.97×10^{-9}
	Zero	-2.05	9.62×10^{-3}	-1.95	5.07×10^{-3}	-1.87	9.37×10^{-3}
Total inertia	Count	-3.08×10^{-1}	1.66×10^{-8}	-4.69×10^{-1}	$< 2 \times 10^{-16}$	-5.09×10^{-1}	$< 2 \times 10^{-16}$
	Zero	6.48×10^{-1}†	2.18×10^{-2}	1.55	3.32×10^{-3}	5.78×10^{-1}†	2.40×10^{-2}
First main component inertia	Count	1.36×10^{-1}†	7.88×10^{-3}	1.68×10^{-1}†	6.01×10^{-4}	1.85×10^{-1}†	1.17×10^{-4}
	Zero	–	–	-1.22	1.50×10^{-2}	–	–
Vertical extent along first main component	Count	-8.51×10^{-2}†	3.45×10^{-2}	-1.00×10^{-1}†	8.49×10^{-3}	-1.01×10^{-1}†	8.52×10^{-3}
	Zero	-5.43×10^{-1}†	3.91×10^{-1}	–	–	-5.03×10^{-1}†	4.00×10^{-1}
Vertical width across first main component	Count	-3.08×10^{-1}	2.23×10^{-6}	-2.94×10^{-1}	1.16×10^{-6}	-2.99×10^{-1}	8.64×10^{-7}
	Zero	3.29	1.38×10^{-3}	2.62	2.52×10^{-4}	3.12	9.38×10^{-4}
Vertical speed variability	Count	5.01×10^{-1}	2.01×10^{-14}	3.17×10^{-1}	6.26×10^{-7}	3.22×10^{-1}	4.75×10^{-7}
	Zero	-3.97	1.21×10^{-3}	-3.71	5.74×10^{-5}	-3.97	1.99×10^{-4}
Absolute speed variability	Count	–	–	8.74×10^{-2}	4.17×10^{-2}	8.45×10^{-2}	4.92×10^{-2}
	Zero	-1.98	1.99×10^{-2}	-1.50	1.05×10^{-2}	-1.57	2.32×10^{-2}
$log(\theta)$	Count	1.13†	7.95×10^{-16}	1.41†	$< 2 \times 10^{-16}$	1.37†	$< 2 \times 10^{-16}$
Bottom duration	Zero	-5.71	1.35×10^{-3}	-7.19	3.30×10^{-4}	-5.84	3.81×10^{-4}

† indicates that the coefficient refer a to variable that was not log-transformed.

Additional file 1 — Assessment of prospected water volume

Description The Monte Carlo integration provided an easy-to-implement method in order to estimate the volume of water surrounding the trajectory of southern elephant seals. However this numeric method is sensitive to the sampling effort as well as to the ratio between the "volume of the encompassing cuboid" and the "prospected volume". Here, we present the code and results of a simple experiment to quantify the uncertainty of water volume estimates with the settings used in the paper. Because, the computation increases rapidly with the number of points we limited the sampling effort to 500000 random points which yields coefficient of variation of $CV_{0.5m} = 2\%$, $CV_{9m} < 1\%$ and $CV_{18m} < 1\%$.

annexe G

Chapitre 3

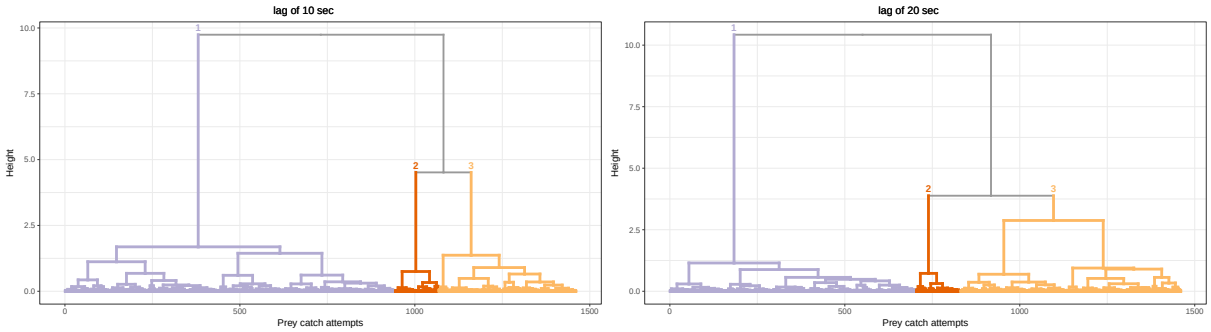

Σ VeDBA (m.s^{-2})	Σ effort (m.s^{-2})	μ speed (m.s^{-1})	σ^2_c roll (°)	μ_c pitch (°)	σ^2_c heading (°)	PCA rate attempts/min	n
27.68±18.32	23.33±16	1.65±0.36	2.9±0.21	−12.18±3.93	5.82±0.78	0.08±0.69	454
72.19±22.13	67.34±20.59	1.78±0.34	6.24±0.79	51.61±1.77	6.71±0.83	0.05±0.53	127
70.17±26.86	40.77±15.76	1.56±0.29	26.8±1.5	−1.06±3.79	31.27±1.52	1.39±2.92	879

Σ VeDBA (m.s^{-2})	Σ effort (m.s^{-2})	μ speed (m.s^{-1})	σ^2_c roll (°)	μ_c pitch (°)	σ^2_c heading (°)	PCA rate attempts/min	n
54.77±30.46	45.57±27.76	1.64±0.34	5.06±0.48	−12.04±2.97	9.65±1.03	0.04±0.41	479
132.13±38.83	124.31±33.14	1.76±0.3	8.68±1.04	41.76±1.92	12.56±1.39	0.08±0.48	155
138.15±45.94	80.44±26.03	1.6±0.26	32.49±1.14	−1.47±2.02	37.61±1.08	1.39±2.19	826

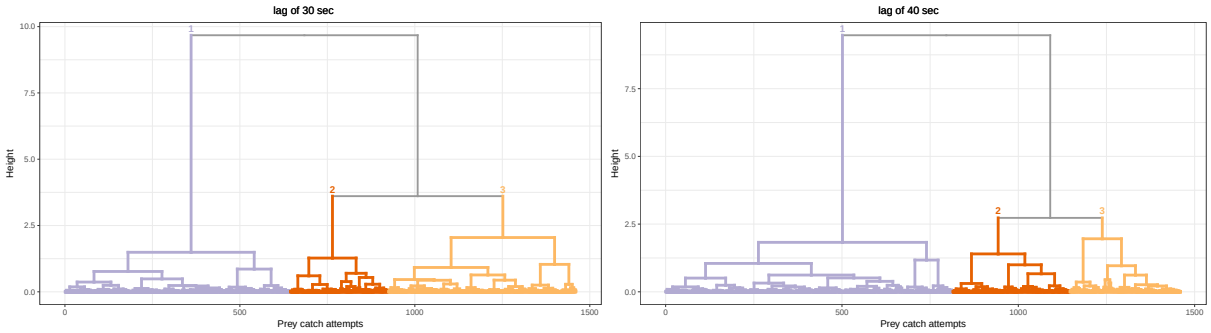

Σ VeDBA (m.s^{-2})	Σ effort (m.s^{-2})	μ speed (m.s^{-1})	σ^2_c roll (°)	μ_c pitch (°)	σ^2_c heading (°)	PCA rate attempts/min	n
76.19±40.89	61.34±35.78	1.63±0.33	5.62±0.43	−14.64±2.09	10.68±0.94	0.08±0.43	411
170.36±59.04	156.29±51.19	1.71±0.29	9.94±0.93	26.22±3.06	15.34±1.34	0.14±0.71	262
199.24±66.04	117.72±37.14	1.62±0.26	32.4±1.08	−2.31±1.65	38.47±0.94	1.3±1.77	787

Σ VeDBA (m.s^{-2})	Σ effort (m.s^{-2})	μ speed (m.s^{-1})	σ^2_c roll (°)	μ_c pitch (°)	σ^2_c heading (°)	PCA rate attempts/min	n
99±52.31	78.88±45.14	1.62±0.32	5.63±0.37	−15.34±1.82	11.44±0.82	0.11±0.41	375
213.52±77.92	194.15±66.51	1.7±0.29	8.95±0.64	21.24±2.97	15.17±1.05	0.15±0.54	268
250.53±84.13	152.77±48.25	1.63±0.25	30.3±1.06	−2.19±1.56	37.4±0.97	1.19±1.52	817

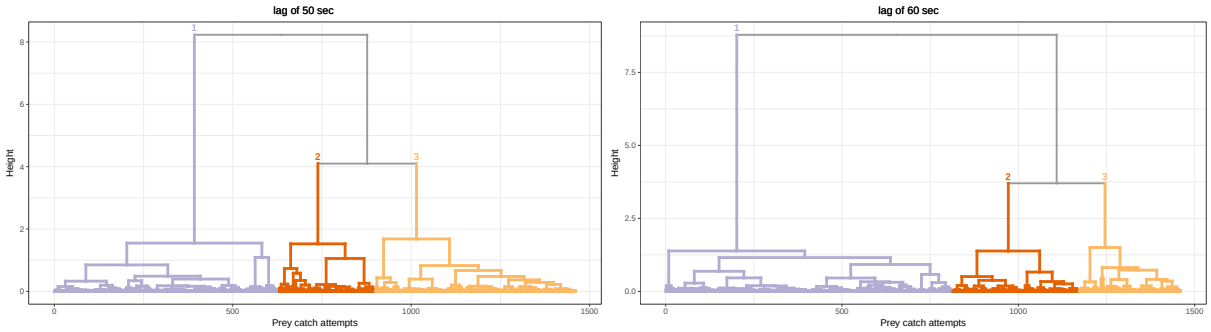

Σ VeDBA (m.s^{-2})	Σ effort (m.s^{-2})	μ speed (m.s^{-1})	σ^2_c roll (°)	μ_c pitch (°)	σ^2_c heading (°)	PCA rate attempts/min	n
100.46±53.16	80.79±50.26	1.61±0.33	4.13±0.27	−17.95±1.59	9.79±0.63	0.05±0.25	249
232.03±90.66	204.88±79.9	1.67±0.28	8.86±0.46	9.88±3.04	16.13±0.95	0.2±0.52	397
298.87±99.18	185.37±60.99	1.64±0.25	28.82±0.96	−2.98±1.63	36.32±0.94	1.12±1.29	814

Σ VeDBA (m.s^{-2})	Σ effort (m.s^{-2})	μ speed (m.s^{-1})	σ^2_c roll (°)	μ_c pitch (°)	σ^2_c heading (°)	PCA rate attempts/min	n
126.06±66.04	100.75±61.11	1.6±0.33	4.6±0.23	−17.31±1.49	10.78±0.57	0.07±0.25	273
277.28±103.28	246.54±88.45	1.68±0.27	8.69±0.43	9.65±2.42	16.11±0.9	0.19±0.5	374
345.09±111.79	218.23±71.88	1.65±0.24	27.03±0.87	−3±1.61	35.18±0.92	1.03±1.13	813

FIGURE G.1 – Hierarchical clustering of prey catch attempts (PCA) performed by six southern elephant seals (*Mirounga leonina*) within area restricted search region based on their behavioural features at the bottom before a PCA considering different time windows ranging from 10 to 60 s. Beyond 40 s, up to 60 s, the classification was still the same except that the proportion of PCA in each cluster was different.

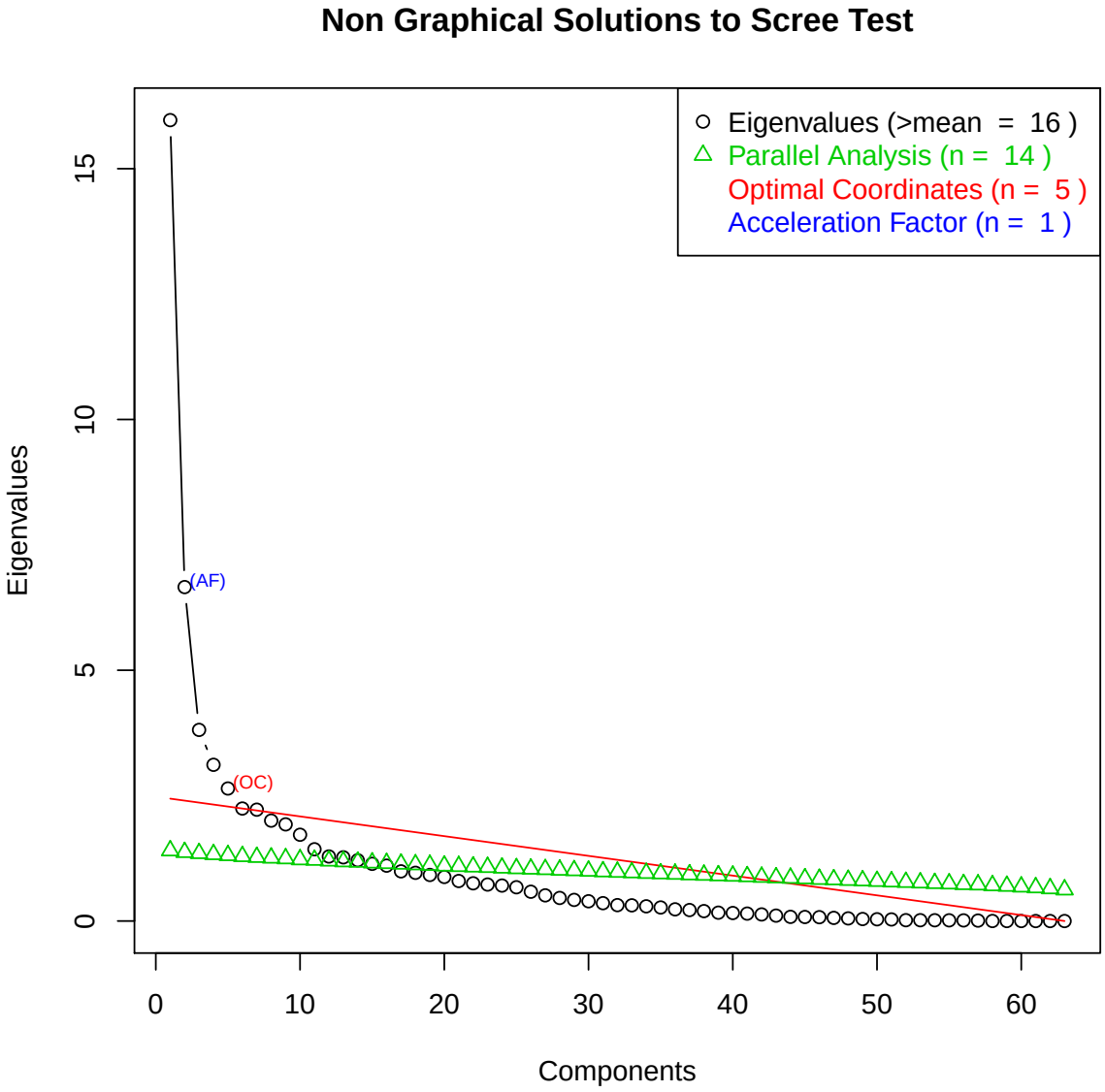

FIGURE G.2 – Determination of the number of scores to keep from the principal component analysis for the unsupervised classification of prey catch attempts performed by six post-breeding female southern elephant seals (*Mirounga leonina*).

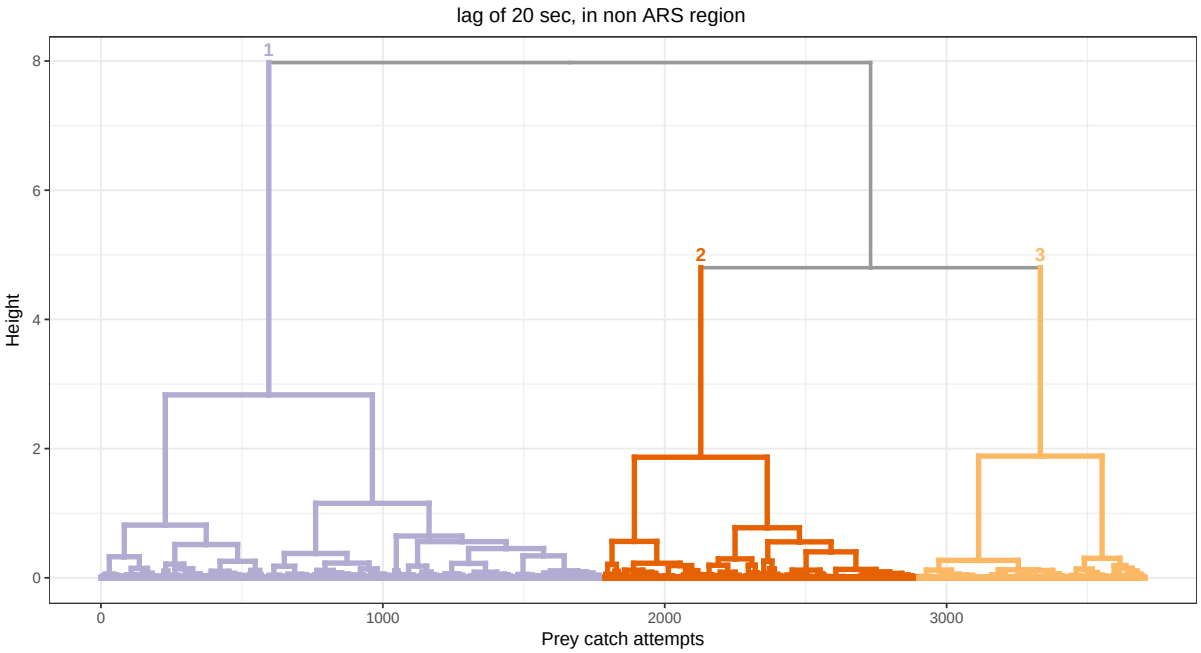

Σ VeDBA ($m.s^{-2}$)	Σ effort ($m.s^{-2}$)	μ speed ($m.s^{-1}$)	σ_c^2 roll (°)	μ_c pitch (°)	σ_c^2 heading (°)	**PCA rate attempts/min**	n
66.27±34.02	53.25±30.73	1.84±0.37	3.44±0.32	−12.27±3.82	7.06±0.63	0.08±0.48	1659
142.54±37.21	131.29±33.25	1.9±0.3	5.75±0.54	41.19±2.25	9.42±0.99	0.15±0.7	732
133.13±46.87	78.25±28.15	1.66±0.37	27.63±1.48	−1.05±3.63	32.5±1.51	1.31±2.06	1312

FIGURE G.3 – Hierarchical clustering of prey catch attempts performed by six southern elephant seals (*Mirounga leonina*) inside and outside area restricted search (ARS) during the bottom of dives, based on their behavioural features before a prey catch attempts considering a 20 s time windows.

annexe H

Chapitre 4

Table S1: List of the top five ranked linear mixed-effects models by AIC of bottom time (bttmTime) as the response variable explained by dive duration (diveTime) ascent and descent angles (ascntAngl, dscntAngl), ascent and descent effort (ascntEffrt, dscntEffrt), body density (bdDnsty) and maximum depth (mxDpth). For each model, the number of parameters (df), maximum log-likelihood (logLik), Akaike's information criterion (AIC), the difference in AIC (ΔAIC) and the model weight (wAIC), were calculated. Three data sets have been considered: a) with all dives, b) only dives with captures and c) only dives without capture.

Situation	Models	df	logLik	AIC	ΔAIC	wAIC
a) All dives	bttmTime ~ diveTime + ascntAngl + ascntEffrt + bdDnsty + dscntAngl + dscntEffrt + mxDpth + 1	11	-129246.9	258515.7	0	0.94
	bttmTime ~ diveTime + ascntAngl + ascntEffrt +dscntAngl+ dscntEffrt + mxDpth + 1	10	-129253.0	258526.0	10.3	0.05
	bttmTime ~ diveTime + ascntAngl + ascntEffrt + bdDnsty + dscntAngl + mxDpth + 1	10	-129284.8	258589.6	73.8	<0.01
	bttmTime ~ diveTime + ascntAngl + ascntEffrt + dscntAngl + mxDpth + 1	9	-129289.0	258596.1	80.4	<0.01
	bttmTime ~ diveTime + ascntAngl + bdDnsty + dscntAngl + dscntEffrt + mxDpth + 1	10	-129433.8	258887.7	372.0	<0.01
b) Dives with PCA	bttmTime ~ diveTime + ascntAngl + ascntEffrt + bdDnsty + dscntAngl + dscntEffrt + mxDpth + 1	11	-114748.2	229518.5	0.00	0.99
	bttmTime ~ diveTime + ascntAngl + ascntEffrt + dscntAngl + dscntEffrt + mxDpth + 1	10	-114753.7	229527.3	6.89	<0.01
	bttmTime ~ diveTime + ascntAngl + ascntEffrt + bdDnsty + dscntAngl + mxDpth + 1	10	-114784.3	229588.7	16.45	<0.01
	bttmTime ~ diveTime + ascntAngl + ascntEffrt + dscntAngl + mxDpth + 1	9	-114788.2	229594.5	21.49	<0.01
	bttmTime ~ diveTime + ascntAngl + bdDnsty + dscntAngl + dscntEffrt + mxDpth + 1	10	-114885.2	229790.4	220.11	<0.01
c) Dives without PCA	bttmTime ~ diveTime + ascntAngl + ascntEffrt + bdDnsty + dscntAngl + dscntEffrt + mxDpth + 1	11	-13835.6	27693.1	0.00	0.62
	bttmTime ~ diveTime + ascntAngl + ascntEffrt + bdDnsty + dscntAngl + mxDpth + 1	10	-13837.7	27695.4	2.26	0.20
	bttmTime ~ diveTime + ascntAngl + ascntEffrt + dscntAngl + dscntEffrt + mxDpth + 1	10	-13838.1	27696.1	3.01	0.13
	bttmTime ~ diveTime + ascntAngl + ascntEffrt + dscntAngl + mxDpth + 1	9	-13840.2	27698.3	5.17	0.04
	bttmTime ~ diveTime + ascntAngl + bdDnsty + dscntAngl + dscntEffrt + mxDpth + 1	10	-13873.0	27764.0	72.81	<0.01

Table S2: List of the top five ranked linear mixed-effects models by AIC of bottom swimming effort (bttmEffrt) as the response variable explained by bottom time (bttmTime), body density (bdDnsty) and maximum depth (mxDpth). For each model, the number of parameters (df), maximum log-likelihood (logLik), Akaike's information criterion (AIC), the difference in AIC (ΔAIC) and the model weight (wAIC), were calculated. Two data sets have been considered: a) with all dives and b) only dives with PCA. Presence of PCA during the bottom phase was added in the first model and the number of these PCA in the second.

Situation	Models	df	logLik	AIC	ΔAIC	wAIC
a) All Dives	bttmEffrt ~ bdDnsty +PCA + diveTime + mxDpth + 1	8	12274,35	-24532,70	0	0,99
	bttmEffrt ~ PCA + diveTime + mxDpth + 1	7	12261,21	-24508,41	24,28	<0.01
	bttmEffrt ~ bdDnsty + diveTime + mxDpth + 1	7	12183,89	-24353,78	178,92	<0.01
	bttmEffrt ~ diveTime + mxDpth + 1	6	12173,37	-24334,73	197,96	<0.01
	bttmEffrt ~ bdDnsty + PCA + diveTime + 1	7	9302,85	-18591,70	5941,00	<0.01
b) Dives with PCA	bttmEffrt ~ bdDnsty + bttmTime + mxDpth + PCA Nb+ 1	8	13587,90	-27159,81	0	0.99
	bttmEffrt ~ bdDnsty + bttmTime + PCA Nb + 1	7	13500,23	-26986,45	173,35	<0.01
	bttmEffrt ~ bttmTime + mxDpth + PCA Nb + 1	7	13441,39	-26868,78	291,03	<0.01
	bttmEffrt ~ bttmTime + PCA Nb + 1	6	13355,86	-26699,76	460,08	<0.01
	bttmEffrt ~ bdDnsty + bttmTime + 1	6	12681,54	-25351,08	1808,72	<0.01

Table S3: List of the top five ranked linear mixed-effects models by AIC of surface time (surfTime) as the response variable explained by total swimming effort provided during the last dive (diveEffrt) and the prey capture attempts availability (PCA). For each model, the number of parameters (df), maximum log-likelihood (logLik), Akaike's information criterion (AIC), the difference in AIC (ΔAIC) and the model weight (wAIC) were calculated.

Models	df	logLik	AIC	ΔAIC	wAIC
surfTime ~ diveEffrt + diveTime + 1	6	-84733.65	169479.30	0	0.78
surfTime ~ PCA + diveEffrt + diveTime + 1	7	-84733.88	169481.76	2.45	0.23
surfTime ~ diveEffrt + 1	5	-84978.81	169967.62	488.32	<0.01
surfTime ~ PCA + diveEffrt + 1	6	-84977.92	169967.83	488.53	<0.01
surfTime ~ PCA + diveTime + 1	6	-85702.37	171416.73	1937.43	<0.01

Table S4: Estimates and confidence intervals for prey availability (PCA), number of prey (PCA Range) and the body density in each linear mixed effects models associated to box plot. With the maximum depth (maxDepth), these variables were used to explain the bottom duration (bottomTime), the bottom swimming effort (bottomEffort) and the total bottom swimming effort (bottomEffortTOT).

	Figure 1			Figure 2			Figure 3			Figure 4			Figure 5		
	bottomTime~PCA+maxDepth			bottomTime~PCARange+maxDepth			bottomTime~bodyDensity+maxDepth			bottomEffortTOT~bodyDensity+maxDepth			bottomEffort~PCA+maxDepth		
Depth	lower	estimate PCA:presence	upper	lower	estimate PCARange	upper	lower	estimate bodyDensity	upper	lower	estimate bodyDensity	upper	lower	estimate PCA:presence	upper
]50,100]	195.67	226.85	258.02	-27.26	14.74	56.74	-47.19	11.29	69.77	-8.07	20.56	49.19	-0.05	-0.01	0.03
]100,150]	229.83	256.15	282.47	-42.70	-23.12	-3.54	-3.30	39.69	82.67	-0.32	17.77	35.86	-0.02	0.02	0.05
]150,200]	170.90	193.02	215.14	-5.50	6.18	17.85	-27.57	-7.78	12.01	-27.71	-13.73	0.25	0.06	0.10	0.13
]200,250]	102.86	121.82	140.77	-2.28	6.16	14.60	-9.85	5.80	21.45	-28.42	-12.61	3.20	0.07	0.10	0.14
]250,300]	88.16	105.58	123.00	10.25	19.14	28.03	-39.28	-26.08	-12.88	-23.65	-10.43	2.80	0.04	0.07	0.10
]300,350]	52.23	68.01	83.78	21.02	30.03	39.03	-39.31	-23.52	-7.72	10.17	20.12	30.08	0.12	0.14	0.17
]350,400]	-40.06	-26.60	-13.15	16.10	23.88	31.66	-54.65	-40.97	-27.28	15.99	25.44	34.89	0.15	0.17	0.19
]400,450]	-107.66	-93.04	-78.43	10.50	21.03	31.57	-38.43	-22.03	-5.62	19.16	29.26	39.36	0.17	0.19	0.22
]450,500]	-155.77	-140.44	-125.11	14.72	28.03	41.34	-34.37	-13.83	6.73	14.09	24.71	35.34	0.18	0.20	0.23
]500,550]	-183.80	-168.57	-153.34	8.99	21.27	33.55	-30.76	-10.61	9.54	2.10	11.98	21.85	0.15	0.18	0.20
]550,600]	-112.18	-92.92	-73.66	23.47	35.54	47.61	-10.38	9.83	30.05	14.51	23.95	33.39	0.06	0.08	0.11
]600,650]	-153.93	-131.62	-109.32	37.49	50.02	62.55	-34.71	-13.83	7.04	25.05	34.47	43.88	0.05	0.08	0.10
]650,700]	-62.56	-40.04	-17.51	35.95	46.49	57.03	-47.35	-29.37	-11.40	30.52	39.36	48.19	-0.01	0.02	0.04
]700,750]	38.48	59.67	80.87	49.84	60.67	71.50	-72.38	-57.21	-42.04	17.43	24.96	32.49	-0.03	-0.01	0.02
]750,800]	60.00	73.34	86.68	40.34	47.33	54.32	-65.50	-53.51	-41.52	19.77	26.65	33.53	-0.05	-0.03	-0.01
]800,850]	32.22	46.56	60.91	28.65	36.95	45.26	-58.82	-45.71	-32.60	18.82	25.86	32.91	-0.04	-0.02	0.01
]850,900]	61.26	76.79	92.31	21.80	31.72	41.63	-60.13	-45.64	-31.15	20.22	29.30	38.39	-0.05	-0.02	0.02
]900,950]	20.08	54.20	88.33	18.47	37.75	57.02	-66.20	-44.26	-22.31	2.98	16.12	29.27	-0.06	-0.02	0.01
]950,1000]	41.34	90.92	140.49	-13.23	19.30	51.84	-63.63	-33.17	-2.71	-2.68	16.69	36.05	-0.08	-0.03	0.03
]1000,1050]	12.57	49.47	86.36	-42.46	-4.99	32.48	-	-12.03	-	-13.37	16.85	47.07	-0.13	-0.03	0.07

Figure S1: Evolution of the relation between total bottom swimming effort and total transit swimming effort according to depth and animal's body density. The histogram represents the number of dives per boxplots. The dashed line indicates when the ratio of total transit swimming effort to total transit swimming effort is equal to 1. In most depth ranges, this ratio is negatively related to animal's body density (estimate PCA:presence<0).

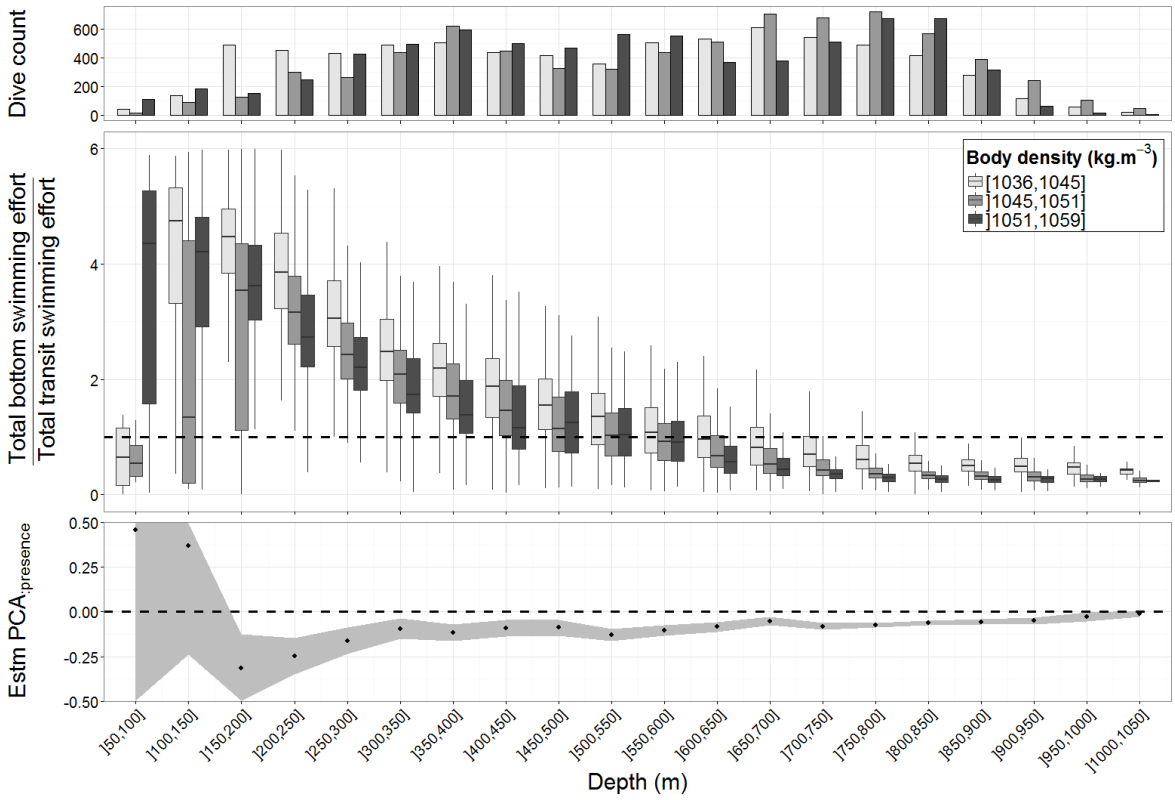

ANNEXE I

CHAPITRE 5

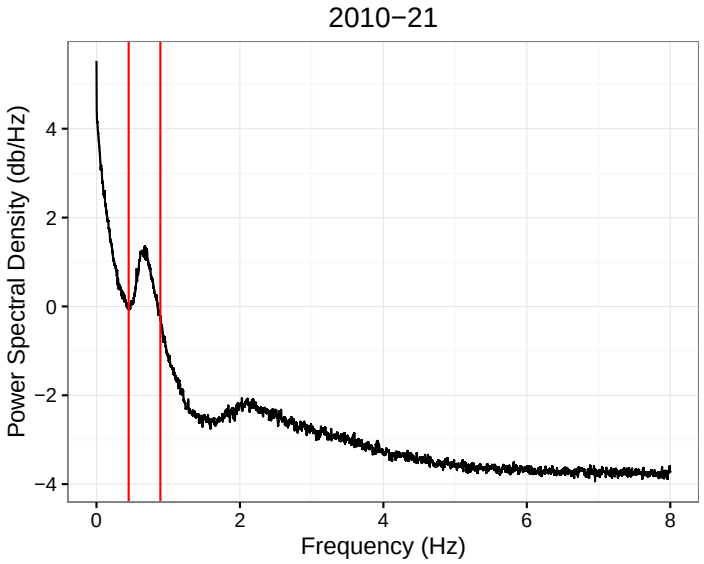

FIGURE I.1 – Power Spectral Density realized on 50 randomly chosen dives of the post-breeding female elephant seal 2010-21. Using the lavielle's method the low and high cut-off frequencies used in the band pass filter to isolate frequencies due to animal's flipper stroke were respectively 0.45 and 0.89 Hz.

Table I.1 - Overall information on post moulting animals with the associated energy expenditure (FMR) calculated from the predicted values of the number of stroke. Mean values are given with ± sd.

id	sex	*n* days	*n* dives	Date departure	Dive duration (s)	Surface intervals (s)	Maximum depth (m)	FMR
2004-10	F	158	5165	2/29/2004 11:42:58	1212.88 ± 694.98	129.02 ± 37.67	318.25 ± 182.78	103.65 ± 140.85
2004-2	M	133	3691	2/27/2004 20:02:15	1222.62 ± 506.98	120.34 ± 39.98	380.1 ± 172.89	118.87 ± 211.72
2004-8	M	156	5241	2/29/2004 12:47:43	920.77 ± 480.12	109.87 ± 39.61	311.37 ± 211.63	125.23 ± 184.08
2004-9	F	143	2498	2/23/2004 19:50:49	2044.69 ± 749.55	152.21 ± 35.06	492.72 ± 179.14	67.22 ± 85.35
2004-3	F	134	3499	3/1/2004 15:36:00	1396.98 ± 673.22	129.4 ± 31.12	404.51 ± 152.94	83.82 ± 77.54
2004-5	M	155	4154	3/2/2004 12:34:27	1343.9 ± 689.35	136.02 ± 51.44	350.19 ± 183.13	151.68 ± 287.19
2004-6	F	151	2866	3/6/2004 18:04:23	1746.88 ± 654.55	118.26 ± 32.58	353.17 ± 203.45	80.58 ± 124.99
2004-7	F	148	4106	3/7/2004 14:33:30	1394.21 ± 567.98	109.82 ± 23.91	378.36 ± 175.82	86.29 ± 82.17
2005-5	F	251	1277	1/25/2005 7:18:16	1791.16 ± 629.49	115.66 ± 30.27	333.64 ± 200.55	64.52 ± 56.06
2005-11	F	207	1462	2/23/2005 9:18:23	1511.45 ± 565.37	135.56 ± 29.46	422.74 ± 197.12	68 ± 19.29
2005-13	F	211	1897	2/17/2005 11:39:28	1649.78 ± 641.41	129.55 ± 35.39	380.8 ± 199.71	72.64 ± 80.77
2005-2	M	142	1873	2/14/2005 9:34:56	997.88 ± 533.84	112.53 ± 51.45	295.1 ± 198.27	141.1 ± 212.28
2005-3	M	132	2205	2/6/2005 1:57:49	914 ± 504.4	118.92 ± 50.37	263.24 ± 163.78	164.9 ± 247.99
2005-7	F	209	1255	2/24/2005 16:13:30	2116.78 ± 665.73	145.64 ± 36.07	523.56 ± 180.1	57.99 ± 41.38
2006-10	F	126	1338	2/13/2006 11:26:00	1360.18 ± 496.92	103.82 ± 21.19	377.25 ± 126.39	79.13 ± 70.84
2006-7	M	103	379	2/6/2006 19:32:44	1106.36 ± 446.6	62.07 ± 53.02	191.42 ± 69.1	120.33 ± 218.13
2007-5	M	159	1068	12/17/2006 7:25:19	985.18 ± 498.8	120.1 ± 49.26	317.47 ± 219.45	155.56 ± 280.29
2007-7	M	180	1782	12/31/2006 9:02:38	1104.93 ± 852.07	107.67 ± 50.05	333.14 ± 267.92	179.94 ± 278.02
2007-9	F	208	1404	12/19/2006 0:09:53	1519.23 ± 696.79	126.34 ± 39.99	375.61 ± 208.69	115.85 ± 240.3
2007-1	F	228	3309	5/5/2007 13:55:49	1847.01 ± 564.3	131.99 ± 27.22	416.28 ± 171.93	62.32 ± 33.23
2007-15	F	128	1467	5/5/2007 3:05:52	1372.04 ± 318.57	136.6 ± 25.19	642.11 ± 195.4	73.8 ± 23.58
2007-16	F	199	3733	5/23/2007 0:03:00	1516 ± 479.77	110.65 ± 23.21	419.77 ± 204.01	75.59 ± 83.34
2007-13	F	180	2139	6/4/2007 17:54:04	1766.13 ± 443.33	116.47 ± 22.45	547.95 ± 228.87	65.36 ± 32.82
2007-2	F	190	2880	6/2/2007 18:21:48	1663.67 ± 429.83	123.7 ± 20.3	575.07 ± 211.72	65.55 ± 35.28
2007-4	M	116	1975	6/7/2007 12:53:30	1788.87 ± 518.58	130.49 ± 26.47	642.23 ± 217.91	67.43 ± 30.69
2008-2	F	155	3822	12/24/2007 15:33:59	1223.41 ± 527.73	115.08 ± 26.66	371.33 ± 199.3	80.13 ± 34.52
2008-3	M	277	3913	12/26/2007 0:13:39	2060.55 ± 611.91	136.49 ± 27	508.05 ± 139.44	67.4 ± 13.69
2008-1	M	248	4157	1/4/2008 8:47:43	1437.97 ± 757.14	124.98 ± 37.45	388.89 ± 202.73	87.05 ± 63.27
2008-6	F	193	3780	2/3/2008 8:53:44	1717.83 ± 642.02	126.91 ± 28.04	391.3 ± 140.53	68.93 ± 18.53
2008-7	F	159	3303	2/2/2008 12:35:43	1549.68 ± 563.49	127.96 ± 29.21	368.08 ± 176.2	69.69 ± 17.51
2009-12	M	157	2078	12/26/2008 17:57:49	1426.67 ± 450.92	123.63 ± 24.3	549.16 ± 155.29	73.33 ± 53.1
2009-16	M	152	4699	1/1/2009 17:19:44	1054.18 ± 538.86	111.71 ± 31.25	357.75 ± 167.57	99.2 ± 125.95
2009-17	F	169	2480	1/23/2009 19:57:30	1793.93 ± 591.96	121.91 ± 20.63	453.11 ± 153.72	64.16 ± 29.47
2009-20	M	242	3218	1/14/2009 13:43:30	1777.13 ± 535.66	135.75 ± 27.82	581.57 ± 202.09	73.75 ± 97.41
2009-21	F	181	3576	1/18/2009 8:36:48	1562.06 ± 604.4	143.53 ± 25.48	512.4 ± 176.18	67.91 ± 25.23
2009-23	F	203	2743	1/29/2009 16:18:09	1740.45 ± 742.25	153.62 ± 30.71	489.14 ± 184.61	65.82 ± 13.87
2009-24	F	111	1797	1/26/2009 6:14:18	1633.92 ± 607.91	120.91 ± 25.98	431.13 ± 160.93	71.16 ± 13.05
2009-25	F	234	3700	1/29/2009 16:59:03	1470.77 ± 427.93	118.99 ± 26.16	427.67 ± 207.71	77.06 ± 83.52
2009-28	F	133	1940	1/27/2009 10:49:50	1951.17 ± 716.22	127.8 ± 20.26	441.53 ± 141.56	67.67 ± 16.35
2009-27	F	117	3386	2/8/2009 17:17:38	1140.92 ± 710.37	105.66 ± 38.33	295.99 ± 136.1	144.88 ± 269.91
2009-32	M	121	1289	2/2/2009 8:38:30	1665.03 ± 617.49	134.16 ± 31.56	290.88 ± 119.69	73.58 ± 99.85
2009-33	M	241	4339	2/8/2009 3:18:58	1816.39 ± 773.39	154.4 ± 51.28	373.53 ± 171.14	74.31 ± 61.73
2009-35	M	108	2513	2/8/2009 12:47:48	1367.23 ± 607.42	124.13 ± 43.03	481.01 ± 357.83	83.99 ± 52.81
2010-16	M	350	1127	2/24/2010 0:49:14	1623.94 ± 503.91	125.75 ± 24.69	318.35 ± 104.33	65 ± 41.97
2010-17	F	233	4762	2/14/2010 15:15:16	1977.36 ± 727.56	127.51 ± 23.84	387.01 ± 130.24	64.32 ± 39.28
2011-4	M	105	3049	1/31/2011 18:31:50	1431.35 ± 463.07	127.56 ± 34.05	414.88 ± 173.61	87.96 ± 131.02
2011-9	M	109	2260	1/27/2011 8:56:49	1419.92 ± 581.49	138.88 ± 44.59	420.23 ± 199.43	93.46 ± 140.88
2012-23	F	229	5385	2/11/2012 20:12:29	1675.33 ± 678.24	118.05 ± 30.63	473.36 ± 234.39	73.93 ± 76.89
2012-24	F	215	5243	2/12/2012 8:00:43	1787.16 ± 595.55	145.68 ± 25.32	460.22 ± 168.73	62.53 ± 12.21
2013-20	F	238	4688	2/20/2013 15:34:02	1883.69 ± 626.57	143.37 ± 30.03	485.95 ± 216.85	69.48 ± 91.1
2013-21	F	234	6332	2/27/2013 19:23:45	1770.74 ± 598.75	137.52 ± 33	474.18 ± 199.12	74.4 ± 115.83
2013-25	M	222	1679	2/11/2013 16:35:00	2129.1 ± 650.96	149.2 ± 28.85	465.05 ± 168.32	61.38 ± 63.34
2013-30	F	295	8987	2/24/2013 15:28:36	1405.18 ± 711.04	122.67 ± 40.13	351.59 ± 221.58	136.29 ± 278.38
2013-33	F	322	4896	2/23/2013 15:04:41	578.67 ± 578.71	38.87 ± 43.11	101.72 ± 114.05	354.63 ± 425.87
2013-34	F	228	7293	2/27/2013 15:43:35	1529.06 ± 685.52	154.77 ± 45.99	368.49 ± 194.28	119.9 ± 264.89
2013-36	F	230	4045	2/28/2013 20:08:27	1384.82 ± 536.61	58.01 ± 53.25	335.2 ± 174.82	98.11 ± 180.32
2013-38	F	236	4117	2/10/2013 9:02:42	2258.09 ± 656.4	145.58 ± 26.29	527.05 ± 189.21	60.8 ± 46.01
2013-39	M	229	6521	2/21/2013 7:24:51	1324.08 ± 572.77	130.2 ± 44.32	305.36 ± 156.03	111.41 ± 226.86
2013-40	F	202	2557	2/25/2013 5:50:31	1702.89 ± 302.16	153.12 ± 32.35	664.64 ± 245.95	66.95 ± 28.97
2013-41	F	222	5897	2/27/2013 15:00:54	1933.41 ± 618.78	119.67 ± 31.2	398.54 ± 167.23	70.65 ± 110.49
2013-44	F	228	6501	2/13/2013 12:28:04	1780.55 ± 571	138.87 ± 33.57	422.83 ± 210.51	73.83 ± 134.91
2013-45	F	165	4599	2/19/2013 17:15:38	1599.03 ± 564.49	138.05 ± 26.68	472.08 ± 161.65	66.79 ± 33.58
2013-46	F	230	5446	2/26/2013 19:28:36	1964.87 ± 714.11	129.66 ± 28.92	398.54 ± 144.17	69.97 ± 133.33
2013-47	F	220	6170	2/20/2013 22:46:46	1668.37 ± 568.33	137.01 ± 28.26	396.65 ± 161.11	69.48 ± 87.7
2013-48	F	167	5626	2/17/2013 10:01:14	1567.88 ± 575.46	111.47 ± 23.96	384.27 ± 163.31	77.85 ± 136.5
2013-23	M	232	3942	3/15/2013 3:54:46	1668.66 ± 693.45	142.55 ± 40.81	328.8 ± 164.11	101.35 ± 247.39
2013-27	M	185	4506	3/6/2013 19:55:07	1858.87 ± 831.43	146.28 ± 51.49	410.43 ± 204.4	105.41 ± 244.91
2013-28	F	214	3658	3/6/2013 5:03:12	1753.15 ± 695.82	128.11 ± 34.75	516.93 ± 214.07	109.19 ± 236.81

2013-29	M	113	2017	3/4/2013 0:45:11	2019.32 ± 521.11	194.15 ± 50.13	831.22 ± 362.7	63.63 ± 46.47
2013-35	M	132	2472	3/31/2013 18:30:48	2202.02 ± 569.71	145.58 ± 23.48	455.58 ± 93.79	57.06 ± 74.66
2013-19	M	123	1433	4/3/2013 15:25:48	2184.92 ± 462.73	188.21 ± 35.71	444.79 ± 99.86	64.37 ± 162.87
2013-43	M	233	5692	4/5/2013 0:12:00	1329.83 ± 690.23	132.8 ± 55.76	244.96 ± 155.91	222.58 ± 491.55
2014-13	M	300	7893	12/26/2013 14:47:36	1169.13 ± 801.18	110.16 ± 56.32	343.44 ± 254.24	220.52 ± 424.89
2014-15	M	256	2845	12/29/2013 14:27:44	2199.45 ± 807.63	153.87 ± 40.78	557.84 ± 330.62	72.01 ± 155.11
2014-17	M	273	5262	12/27/2013 13:38:30	1516.36 ± 740.9	137.74 ± 45.34	462.8 ± 272.05	117.2 ± 250.54
2014-1	F	232	6422	1/31/2014 19:15:18	1594.94 ± 491.31	129.93 ± 23.18	482.09 ± 182.2	67.4 ± 40.76
2014-11	F	236	6214	1/29/2014 14:19:14	1767.11 ± 556	133.93 ± 25.67	441.94 ± 169.26	72.02 ± 102.41
2014-12	F	244	6494	1/28/2014 16:51:39	1696.49 ± 588.4	120.47 ± 26.59	411.11 ± 186.33	77.56 ± 150.47
2014-14	F	232	5908	1/31/2014 19:49:52	1869.7 ± 682.04	130.33 ± 33.37	420.25 ± 145.39	85.48 ± 179.5
2014-20	F	221	3657	1/31/2014 17:40:31	1879.2 ± 732.55	133.55 ± 26.42	448.52 ± 195.75	65.64 ± 71.17
2014-21	F	231	6587	1/29/2014 17:05:00	1506.87 ± 692.61	125.81 ± 40.22	415.81 ± 195.41	121.21 ± 288.79
2014-3	M	300	4068	1/5/2014 13:31:30	1728.18 ± 608.92	123.93 ± 24.39	293.31 ± 127.88	71.83 ± 127.32
2014-4	M	266	3286	1/28/2014 6:36:24	1923.26 ± 688.98	161.9 ± 35.93	513.45 ± 277.15	102.06 ± 293.83
2014-6	M	243	3125	1/19/2014 15:17:38	2076.66 ± 676.51	166.37 ± 34.51	649.81 ± 205	72.74 ± 152.25
2014-7	M	282	5153	1/12/2014 15:39:07	1806.47 ± 579.52	129.92 ± 27.37	404.79 ± 144.62	65.62 ± 107.08
2014-8	F	251	5036	1/25/2014 15:46:23	2069.68 ± 731.79	136.06 ± 33.36	413.37 ± 134.26	65.28 ± 75.9
2015-12	M	281	6650	12/15/2014 16:56:24	1106.61 ± 733.07	102.72 ± 42.13	290.66 ± 179.96	204.88 ± 437.52
2015-13	M	132	1296	12/18/2014 20:27:30	1153.43 ± 530.07	122.59 ± 42.32	418.95 ± 200.3	112.49 ± 177.27
2015-16	M	279	1732	12/28/2014 18:05:17	1723.88 ± 627.45	113.21 ± 20.7	298.36 ± 85.53	67.56 ± 41.59
2015-17	M	126	5250	12/16/2014 14:26:01	730.27 ± 304.39	103.95 ± 30.61	180.87 ± 101.57	144.11 ± 247.33
2015-2	M	201	2821	12/16/2014 18:17:26	1962.1 ± 760.49	164.36 ± 43.92	697.83 ± 326.38	83.92 ± 210.06
2015-22	M	146	2359	12/19/2014 7:10:10	1316.5 ± 679.78	137.45 ± 46.32	420.52 ± 223.71	125.36 ± 271.99
2015-1	M	242	2255	1/9/2015 4:46:46	1859.84 ± 657.21	146.72 ± 41.5	698.26 ± 365.8	78.02 ± 149.67
2015-10	F	169	2583	1/31/2015 14:55:06	1786.32 ± 690.51	125.36 ± 25.72	436.1 ± 142.8	75.85 ± 166.4
2015-11	F	244	4590	1/24/2015 13:38:37	1941.59 ± 640.88	139.82 ± 28.81	410.27 ± 156.62	63.2 ± 58.67
2015-14	F	248	6047	1/24/2015 8:50:31	1644.54 ± 588.48	123.55 ± 25.89	420.09 ± 186.5	72.36 ± 98.05
2015-19	F	239	6008	1/22/2015 5:36:22	1772.45 ± 620.43	131.23 ± 25.76	420.92 ± 164.62	65.93 ± 49.87
2015-20	F	239	4292	1/22/2015 20:46:24	1964.2 ± 575.97	135.4 ± 22.79	522.78 ± 147.23	61.71 ± 30.19
2015-23	M	286	1177	1/1/2015 13:52:02	1505.07 ± 641.29	32.37 ± 35.81	293.74 ± 149.61	98.86 ± 203.95
2015-24	F	278	5850	1/20/2015 19:49:38	1881.57 ± 632.57	134.96 ± 26.81	458.22 ± 150.22	64.48 ± 73.88
2015-5	F	238	5120	1/25/2015 14:42:52	1924.53 ± 549.91	125.04 ± 25.23	451.59 ± 142.92	65.7 ± 88.03
2015-6	F	251	6210	1/22/2015 21:27:55	1768.56 ± 673.48	117.53 ± 27.33	407.65 ± 170.67	80.9 ± 153.25
2015-9	F	287	3602	1/26/2015 22:57:45	2243.46 ± 812.28	126.13 ± 24.66	439.03 ± 175.12	60.78 ± 63.44
2015-25	F	233	4305	2/2/2015 20:28:17	1627.11 ± 599.41	123.69 ± 26.22	447.85 ± 170.41	65.28 ± 33.52
2015-4	F	233	5152	2/1/2015 13:27:58	1845.52 ± 586.68	139.6 ± 23.01	508.26 ± 178.87	65.36 ± 53.18
2015-7	F	229	4795	2/3/2015 5:41:05	1842.29 ± 629.01	133.71 ± 32.37	466.01 ± 185.05	73.33 ± 127.71
2015-8	F	240	5191	2/3/2015 19:23:00	2025.86 ± 842.04	143.08 ± 36.55	391.98 ± 160.39	86.56 ± 193.84

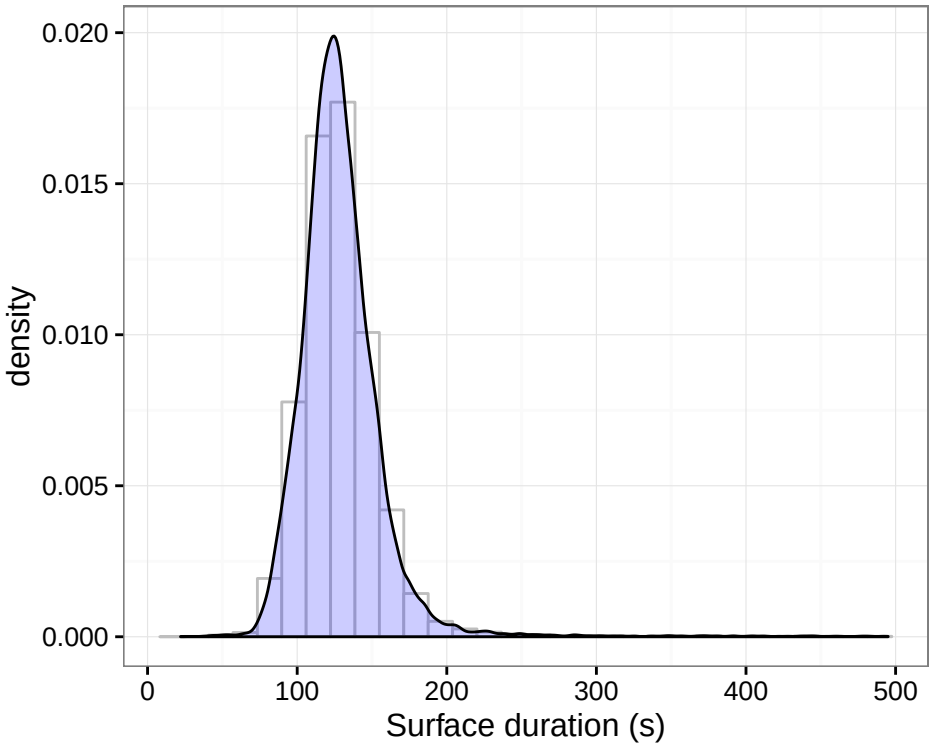

FIGURE I.2 – Density distribution of the surface duration for all post-breeding dives. To avoid the presence of extended surface interval we only kept surface duration below 350 s.

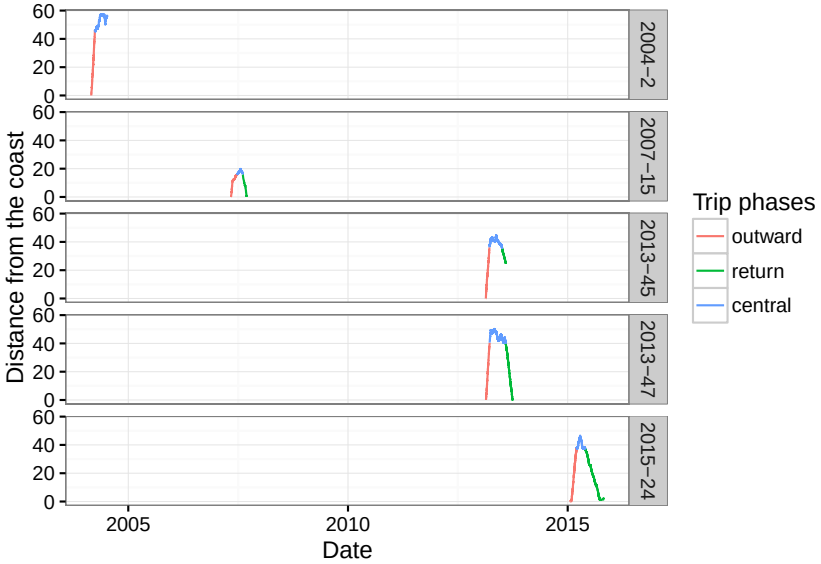

FIGURE I.3 – Distance from the coast of Kerguelen vs. time spent at sea for five randomly chosen post-moulting southern elephant seal. The colour code is for the different trip phases identified, using a threshold of 80 % of the maximum distance from the departure location to defined the central phase.

Stratégies d'acquisition des ressources en proies et coût du transport chez l'éléphant de mer austral

Résumé :

L'océan austral est un écosystème fragile dont la dynamique est influencée par des variations climatiques qui vont structurer la distribution spatio-temporelle des ressources. L'objectif de cette thèse était d'étudier les stratégies d'acquisition des ressources en proies mises en place par l'éléphant de mer austral face aux contraintes énergétiques (coûts du transport et coûts d'accès à la ressource) et temporelles (temps passé au fond d'une plongée et limite de plongée aérobie) auxquelles il est soumis. L'utilisation d'un ensemble d'enregistreurs de données déployés sur ces animaux a permis de reconstruire en trois dimensions leur plongée, mais également de calculer leur effort de nage, le nombre de proies rencontrées ainsi que leur dépense énergétique. Notre étude montre qu'à l'échelle d'une plongée, les éléphants de mer adaptent leur trajectoire, mais également le temps qu'ils passent au fond, en fonction du nombre de proies rencontrées. Pour des densités locales de proie importantes, ils passent plus de temps au fond, et concentrent leur recherche en zone restreinte, caractérisée par une diminution de la vitesse et une augmentation de la sinuosité horizontale. Au-delà de 550 m, le coût d'accès aux ressources devient supérieur aux coûts d'acquisition; ils doivent alors faire face à un compromis entre l'accessibilité et la disponibilité en proies. À mesure qu'ils s'alimentent, ces phoques augmentent leur flottabilité, diminuant de surcroît leur dépense énergétique. Cette étude démontre également une structuration spatio-temporelle de cette dépense énergétique qui semble être liée au succès d'alimentation et donc à la distribution des ressources en proies.

Mots clés : *Mirounga leonina*, comportement de plongée, comportement d'alimentaion, stratégie de chasse, limite de plongées aérobie, effort de nage, condition corporelle, dépense énergétique

Resource Acquisition Strategies and Cost of Transport in Southern Elephant Seal

Summary:

The Southern Ocean is a fragile ecosystem whose dynamics are influenced by climate change that will structure the spatio-temporal distribution of resources. The objective of this PhD was to investigate the foraging strategies used by the southern elephant seal, under energetic (cost of transport and costs of access to the resource) and temporal (time at the bottom of a dive and aerobic dive limit) constraints. Using a set of animal-borne data loggers allowed us to reconstruct their three-dimensional path underwater, but also to calculate their swimming effort, the number of prey encountered and their energy expenditure. At the dive level, our study shows that elephant seals adapt their path, but also the time spent at the bottom, depending on the number of prey encountered. For high local prey density, they spent more time at the bottom, and concentrated their foraging effort in areas restricted search, characterized by a decrease in speed and an increase in horizontal sinuosity. Beyond 550 m, the cost of access to resources becomes greater than the cost of acquisition; they must therefore deal with a trade-off between prey accessibility and availability. While feeding, these seals increase their buoyancy, reducing furthermore their energy expenditure. This study also shows a spatio-temporal structure of the energy expenditure that appears to be related to feeding success and therefore to prey resources distribution.

Keywords: *Mirounga leonina*, diving behaviour, foraging behaviour, hunting strategy, aerobic dive limit, swimming effort, body condition, energy expenditure

Centre d'Études Biologiques de Chizé
U.M.R. 7372 - CNRS
Université de La Rochelle

79360 Villiers-en-Bois